Étude du rôle des cellules musculaires lisses vasculaires (CMLV) et des anticorps anti-CMLV dans la pathogénie de l'artérite à cellules géantes (maladie de Horton)

Alexis Régent

UNIVERSITÉ PARIS DESCARTES
FACULTÉ DE MÉDECINE

UNIVERSITÉ PARIS DESCARTES

Ecole Doctorale : biologie et biotechnologie

Discipline : pathologie cardiovasculaire

Alexis REGENT

THÈSE pour obtenir le grade de DOCTEUR

Sciences de la Vie et de la Santé

Étude du rôle des cellules musculaires lisses vasculaires (CMLV) et des anticorps anti-CMLV dans la pathogénie de l'artérite à cellules géantes (maladie de Horton)

Dirigée par Luc Mouthon

présentée et soutenue publiquement le 10 novembre 2014

Jury :

Pr. Frédéric BATTEUX	Président
Pr. Luc MOUTHON	Directeur de thèse
Dr. Sylvia COHEN-KAMINSKY	Rapporteur
Pr. Bernard BONNOTTE	Rapporteur
Pr. Thierry MARTIN	Examinateur

Remerciements

Je tiens à exprimer mes sincères remerciements à M. le Pr Frédéric Batteux pour avoir accepté d'être le président de mon jury de thèse. Les rares discussions que nous avons eues au laboratoire ont nourri le début de ma réflexion scientifique.

Je tiens à exprimer ma gratitude à Mme le Dr Sylvia Cohen Kaminsky pour avoir accepté d'être rapporteur de ce travail. C'est un honneur de pouvoir bénéficier de son expertise sur la physiopathologie de l'hypertension artérielle pulmonaire et du remodelage vasculaire.

Je tiens à remercier spécialement M. le Pr Bernard Bonnotte pour avoir accepté d'être rapporteur de ce travail. C'est un plaisir de pouvoir envisager des travaux collaboratifs clinques ou fondamentaux autour de l'artérite à cellules géantes.

Je remercie M. le Pr Thierry Martin d'avoir accepté d'être examinateur de ce travail. Son expérience et ses compétences dans le domaine de l'immunologie clinique vont enrichir la discussion sur ce travail.

J'exprime mes sincères remerciements à M. le Pr Luc Mouthon pour la confiance qu'il m'a accordée depuis mon arrivée au laboratoire et le soutien indéfectible durant toute cette période de thèse. La volonté d'effectuer des travaux ambitieux et l'étendue de ses connaissances scientifiques ont permis de mener à bien cette recherche. Travailler à partir de cette collection de cellules musculaires lisses vasculaires de patients atteints d'artérite à cellules géantes était un défi. Merci d'avoir apporté votre énergie pour le relever.

Je remercie M. le Pr Loïc Guillevin pour le soutien qu'il m'a apporté et pour avoir eu le plaisir et l'honneur d'être chef de clinique dans son service.

Je remercie MM. les Pr Gérald Simonneau et Marc Humbert pour avoir mis à ma disposition des échantillons biologiques et des explants pulmonaires de patients atteints d'hypertension pulmonaire.

Je remercie Mme le Dr Véronique Witko-Sarsat pour sa participation scientifique à mon travail.

Je tiens à remercier Mathieu Tamby pour avoir participé à ma formation pendant toute ma période de thèse. Les échanges quotidiens et son esprit critique ont été l'occasion de remettre en cause les dogmes et de prendre le recul nécessaire à la réflexion. Le laboratoire doit beaucoup à ses connaissances en culture cellulaire et en immunologie.

Je tiens à remercier Kim Ly, bouillonnant d'idées, qui a démarré la collection de cellules musculaires lisses vasculaires avec Mathieu. Malgré les mésaventures de la culture cellulaire, notre travail commun a su être constructif et collaboratif. J'espère pouvoir le poursuivre et profiter de sa bonne humeur légendaire.

Merci à toute l'équipe "neutrophiles et vascularites" et aux anciens de l'UPRES EA 4058. Je tiens plus spécifiquement à remercier Tiana pour sa bonne humeur, Nicolas qui a toujours une solution bricolée, Sébastien pour son efficacité, Nada, Aurélie, Céline, Julie, Magali, Alessia et Arnaud. Merci à vous.

Merci à Carole et Christiane qui m'ont aidé et ont contribué à faire de ces années de thèse des moments agréables.

Merci aux Pr Loïc Gullevin, Pr Claire Le-Jeunne, Pr Antoine Brézin, Pr Gilles Renard, Pr Elisabeth Vidal, Pr Pierre-Yves Robert et aux médecins de leurs services respectifs qui ont permis la constitution de cette collection biologique. Sans vous, ces travaux de recherche n'auraient pas pu voir le jour. Je remercie en particulier le Dr Pascal Cohen et le Dr Marion Casadevall qui m'ont laissé le temps nécessaire pour finaliser l'écriture de la thèse et les infirmières et aides-soignants qui m'ont soutenu.

Je remercie les plates formes de protéomique et de génomique de l'Institut Cochin pour leur aide dévouée, en particulier Guilhem Clary, Philippe Chafey, Cédric Broussard, Christian Fédérici, Florent Dumont et Sébastien Jacques.

Je remercie enfin la Société Nationale Française de Médecine Interne, le Groupe Pasteur Mutualité et l'Association pour la Recherche en Médecine Interne et en Immunologie clinique pour leur soutien financier

Je remercie enfin chaleureusement ma famille et mes amis, qui m'ont toujours soutenu et à qui je dédie cette thèse. Si le sujet vous a souvent paru obscur, vous avez eu la délicatesse de prendre régulièrement des nouvelles de « mes petites cellules ». Merci !
En particulier, je tiens à remercier mes filles Clémence et Victoria qui sont mes bonheurs quotidiens et Christine, ma femme, soutien de tous les instants. Votre amour est mon énergie.

Résumé

Rationnel : L'artérite à cellules géantes (ACG) est une vascularite primitive des gros vaisseaux dont le diagnostic repose sur la mise en évidence d'un infiltrat inflammatoire et de cellules géantes à la biopsie d'artère temporale (BAT). On note également un remodelage de la paroi vasculaire lié à une prolifération des cellules musculaires lisses vasculaires (CMLV) pouvant aboutir à une occlusion artérielle.

Objectif : Caractériser les auto-anticorps dirigés contre les cellules endothéliales (CE) et les CMLV au cours de l'ACG et préciser le rôle des CMLV dans le remodelage pariétal.

Méthodes : La recherche d'auto-anticorps a reposé sur un immunoblot 2D couplé à la spectrométrie de masse. Les protéomes des CMLV d'artère ombilicale, d'artère pulmonaire et d'aorte humaines normales a été comparés par protéomique différentielle (2D-DIGE). Nous avons utilisé la 2D-DIGE et des puces d'expression pan-génomiques pour comparer les CMLV issues de BAT de patients suspects d'ACG (avec un diagnostic final d'ACG ou non), afin d'identifier les mécanismes contribuant à la prolifération des CMLV.

Résultats : Chez 15 patients atteints d'ACG, nous avons notamment identifié la lamine, la vinculine et l'annexine A5 comme cible des auto-anticorps anti-CMLV. Les antigènes cibles identifiés sont liés à Grb2, une protéine adaptatrice impliquée dans la prolifération des CMLV. Nous avons mis en évidence des protéomes différents au sein des CMLV humaines normales selon leur origine vasculaire et avons principalement identifié des protéines du cytosquelette et du métabolisme énergétique.A partir des CMLV isolées des BAT et à l'aide d'Ingenuity®, nous avons identifié l'endothéline 1 (ET-1) et la paxilline comme des molécules impliquées dans le remodelage vasculaire. En immunohistochimie et par qPCR, nous avons confirmé l'expression de l'ET-1 et de ses récepteurs ET_AR et ET_BR au sein des artères temporales de patients atteints d'ACG. Enfin, nous avons inhibé la prolifération des CMLV avec du macitentan, un inhibiteur d'ET_AR et en particulier avec son métabolite actif, mais pas avec d'autres inhibiteurs des récepteurs de l'ET-1.

Conclusion : Nous avons identifié chez les patients atteints d'ACG des anticorps anti-CMLV dont le rôle pathogéne potentiel reste à définir. Les différences protéiques observées à partir des CMLV humaines normales pourraient correspondre à des phénotypes différents. A partir d'un matériel biologique unique, nous avons pu montrer que la prolifération excessive des CMLV au cours de l'ACG pouvait être inhibée par le macitentan ce qui permet d'envisager un usage thérapeutique de cette molécule.

Mots clés : artérite à cellules géantes, cellule musculaire lisse vasculaire, endothéline 1, hypertension artérielle pulmonaire, paxilline

Abstract :

Background : Giant cell arteritis (GCA) is a large vessel vasculitis and its diagnosis usually relies on the identification of an inflammatory infiltrate made of mononuclear cells and giant cells upon temporal artery biopsy. There is also a remodeling process in the arterial wall due to an excessive proliferation of vascular smooth muscle cells (VSMC) which can sometimes lead to arterial occlusion.

Purpose: Identify auto-antibodies targeting either endothelial cells (EC) and/or VSMC during GCA and better understand the role of VSMC in the remodeling process.

Methods : Auto-antibodies were detected by a 2-dimensionnal immunoblot and their target antigens were identified by mass spectrometry. Proteoms of umbilical artery, pulmonary artery and aorta VSMC were compared by 2 dimension differential in gel electrophoresis (2D-DIGE). In order to identify mechanisms involved in VSMC proliferation in GCA, we used both 2D-DIGE and pan genomic chips in order to compare VSMC isolated at the time of temporal artery biopsy (TAB) from patients with a final diagnosis of GCA or another diagnosis.

Results : In 15 patients with GCA, we identified lamin, vinculin and Annexin A5 as target antigens of anti-VSMC antibodies. Target antigens were linked with Grb2, an adaptator protein involved in VSMC proliferation. Normal VSMC originating from different vascular beds have differ in protein contents with differential expression of cytoskeleton and energy metabolism proteins. We compared VSMC from TAB with Ingenuity software and identified endothelin-1 (ET-1) and paxillin as proteins involved in vessel remodeling. We confirmed by immunohistichemistry and qPCR that ET-1 and its receptor ET_AR and ET_BR were expressed in temporal arteries from patients with GCA. Last, we reduced VSMC proliferation with Macitentan, an ET_AR and ET_BR antagonist and significantly inhibited VSMC proliferation with its active metabolite whereas other ET-1 inhibitors had no effect.

Conclusion : We identified anti-VSMC auto-antibodies in patients with GCA. Their pathogenic role remains to be determined. Normal VSMC from different vascular locations differ in protein conten which might reflect different phenotypes and different properties. The escessive proliferation of VSMC from patients with GCA was inhibited by Macitentan. This drug might constitute a future therapeutic option.

Key words: giant cell arteritis, vascular smooth muscle cells, endothelin-1, pulmonary arterial hypertension, paxillin

Table des matières

1. Introduction 10
1.1. Artérite à cellules géantes (ACG) ou maladie de Horton : aspects cliniques 11
1.1.1. Généralités 11
1.1.2. Epidémiologie 11
1.1.3. Présentation clinique 12
1.1.4. Biologie 15
1.1.5. Apports et limites de la biopsie d'artère temporale (BAT) 16
1.1.6. Apport de l'imagerie 18
1.1.7. Traitement 20
1.1.8. Surveillance, évolution à long terme 23
1.2. Physiopathologie de l'ACG 24
1.2.1. Prédisposition génétique 26
1.2.2. Hypothèse infectieuse 27
1.2.3. Dysrégulation du système immunitaire 28
1.3. Les cellules musculaires lisses vasculaires (CMLV) en contexte physiologique et pathologique 33
1.3.1. Caractérisation des CMLV normales 33
1.3.2. Fonctions des CMLV normales 34
1.3.3. Mécanismes de régulation des CMLV 35
1.3.4. Etude des CMLV in vitro 37
1.3.5. Les CMLV en condition pathologique 37
1.4. L'hypertension artérielle pulmonaire 39
1.4.1. Données cliniques 39
1.4.2. Physiopathologie de l'HTAP, les données du remodelage vasculaire 40
1.4.3. Thérapeutiques ciblées au cours de l'hypertension artérielle pulmonaire (HTAP) 42
1.5. L'endothéline et ses récepteurs 44
2. Objectifs 46
3. Résultats 48
3.1. Identification des cibles antigéniques des anticorps anti cellules musculaires lisses vasculaires et anti-cellules endothéliales au cours de l'artérite à cellule géante 49
3.2. Analyse protéomique des cellules musculaires lisses vasculaires en condition physiologique et pathologique: d'un phénotype contractile à un phénotype synthétique 92
3.3. Analyse moléculaire des cellules musculaires lisses de patients atteints d'artérite à cellules géantes : contrôle de la prolifération par l'inhibition de l'endothéline-1 172
4. Discussion 232
4.1. Identification d'auto-anticorps au cours de l'ACG, intérêt et signification 233
4.1.1. Les AECA et anti-CMLV au cours des pathologies vasculaires 233
4.1.2. Analyse des auto-Ac dirigés contre les CE et les CMLV au cours de l'ACG 236
4.1.3. Les auto-Ac, bio-marqueurs potentiels au cours de l'ACG 238
4.1.4. Limites de l'approche utilisée pour identifier un auto-Ac 240
4.1.5. La modification du répertoire, conséquence du remodelage vasculaire ? 241
4.2. Mise en évidence de l'hétérogénéité des CMLV en condition physiologique et pathologique. 243
4.2.1. Analyse du protéome des CMLV humaines normales 244
4.2.2. Les CMLV dans le contexte de l'HTAP 245
4.2.3. Implication clinique 246
4.2.4. Limites de cette étude 247
4.3. Modification des caractéristiques des CMLV au cours de l'ACG : identification de pistes thérapeutiques 249

4.3.1 Analyse comparative des protéomes et des profils d'expressions géniques 249
4.3.2. Modulation du remodelage, une cible thérapeutique innovante au cours de l'ACG 251
4.3.3. Forces et faiblesses de cette étude 252
5. Conclusion et perspectives 255
6. Références bibliographiques 258
7. Annexes 278

Abréviations :

AAN : anticorps-antinucléaires

ACG : artérite à cellules géantes

Ac : anticorps

ACR : « American College of Rheumatology » pour Collège des Rhumatologues Américains

ADN : acide désoxyribonucléique

ANCA : anticorps anti-cytoplasme des polynucléaires neutrophiles

Anti-CCP : anticorps anti-peptide cyclique citruliné

BAT : biopsie d'artère temporale

CC : chémokine

CCL : « chemokine ligand » pour ligand des chemokines

CCR : « chemokine receptor » pour récepteur des chémokines

CD : cluster de différenciation

CE : cellule endothéliale

CMLV : cellules musculaires lisses vasculaires

CRP : C-réactive protéine

DC : cellule dendritique

ELISA : « enzyme-linked immunosorbent assay »

ET-1 : endothéline 1

ET_AR : récepteur de type A à l'endothéline 1

ET_BR : récepteur de type B à l'endothéline 1

HAoSMC : « human aortic smooth muscle cell » pour cellule musculaire lisse d'aorte humaine

HLA : « human leukocyte antigen » pour complexe majeur d'histocompatibilité

HTAP : hypertension artérielle pulmonaire

HTP : hypertension pulmonaire

HPASMC : « human pulmonary artery smooth muscle cell » pour cellule musculaire lisse d'artère pulmonaire humaine

HUASMC : « human umbilical artery smooth muscle cell » pour cellule musculaire lisse d'artère ombilicale humaine

HUVEC : « human umbilical vein endothelial cell » pour cellule endothéliale de veine ombilicale humaine

Ig : immunoglobuline

IL : interleukine

IRM : imagerie par résonance magnétique

LB : lymphocyte B

LT : lymphocyte T

MMP : « matrix métalloproteinase » pour métalloprotéase matricielle

MS : spectrométrie de masse

NOIAA : neuropathie optique ischémique antérieure aigue

NORB : neuropathie optique rétro-bulbaire

PAPm : pression artérielle pulmonaire moyenne

PDE5 : phosphodiestérase de type 5

PDGF : « platelet derived growth factor » pour facteur de croissance dérivé des plaquettes

PET-scan : « positron emission tomography » pour scintigraphie au glucose marqué

PPR : pseudo-polyarthrite rhizomélique

SMA : « smooth muscle actin » pour actine du muscle lisse

SNP : single nucleotide peptide

TNF : « tumor necrosis factor » pour facteur de nécrose tumorale

VEGF : « vascular endothelium growth factor » pour facteur de croissance endothelial

VIH : virus de l'immunodéficience humaine

Vs : vitesse de sédimentation

2D-DIGE : « Two dimension-differential in gel electrophoresis » pour électrophorèse différentielle bi-dimensionnelle en gel

1. Introduction

1.1. Artérite à cellules géantes (ACG) ou maladie de Horton : aspects cliniques

1.1.1. Généralités

L'artérite à cellules géantes (ACG) ou maladie de Horton est une panartérite giganto-cellulaire segmentaire et focale non nécrosante qui touche les vaisseaux de gros calibre et en particulier ceux à destinée céphalique (aorte, troncs brachio-céphaliques, artères carotides externes mais aussi artères vertébrales…) (1)(Tableau 1). Elle doit être distinguée des autres vascularites, en particulier des vascularites associées aux anticorps (Ac) anti-cytoplasme des polynucléaires neutrophiles (ANCA) qui peuvent également intéresser l'artère temporale, avec une sémiologie céphalique identique à celle de l'ACG (2).

Tableau 1 : Critères de classification de l'artérite à cellules géantes de l'ACR

- Âge au début de la maladie ≥ 50 ans
- Céphalées d'apparition récente (début ou nouveau type de céphalées)
- Anomalie de l'artère temporale à la palpation (induration ou diminution du pouls non due à l'artériosclérose des artères cervicales)
- Vitesse de sédimentation supérieure à 50 mm à la première heure (méthode Westergren)
- Biopsie d'artère temporale anormale montrant une vascularite caractérisée par la prédominance d'une infiltration par des cellules mononucléées ou par un granulome inflammatoire, habituellement avec des cellules géantes

La présence d'au moins trois critères parmi les cinq précédents permet de classer la maladie avec une sensibilité à 93,5% et une spécificité à 91,2%.

ACR : American College of Rheumatology (Collège des Rhumatologues Américains)

1.1.2. Epidémiologie

L'ACG est exclusivement observée chez des sujets de plus de 50 ans, avec un âge moyen de début de la maladie entre 70 et 80 ans. Il existe une prédominance féminine avec un sexe ratio de l'ordre de 2 (3). La prévalence de l'ACG chez les patients de plus de 50 ans établit un

gradient nord-sud (4) (5) et varie de 278/100 000 dans le comté d'Olmsted dans le Minnesota aux Etats Unis (6), à 25/100 000 en Allemagne (7)ou 1,47/100 000 au Japon (8) et son incidence est plus élevée chez les caucasiens même si cette pathologie a été rapportée chez les sujets d'origine asiatique, noire ou arabe (9). Les facteurs de risque cardiovasculaires et le tabagisme pourraient favoriser la maladie (risque relatif de 4,5 et 6,3 respectivement) (10) ainsi qu'une ménopause précoce (risque relatif de 3,5) (11). La prévalence de l'ACG varie au cours du temps avec des « épidémies » bien que la périodicité soit inconstante dans les études, ce qui a fait évoquer l'hypothèse d'un facteur infectieux inaugural (12 , 13).

1.1.3. Présentation clinique

Les manifestations initiales sont peu spécifiques et inconstantes, de début insidieux ou brutal ce qui rend parfois le diagnostic difficile. Les patients peuvent présenter des signes généraux : fièvre le plus souvent modérée, amaigrissement ou asthénie.

- Les céphalées (80% des patients) récentes et inhabituelles par leur intensité sont parfois plus spécifiquement localisées à la région temporale ou de façon plus trompeuse à la région occipitale. Elles s'accompagnent fréquemment d'une hyperesthésie du cuir chevelu (signe du peigne). A l'examen, on peut retrouver une artère temporale indurée, épaissie avec une diminution ou une abolition du pouls (Figure 1). Présente chez 1/3 des patients, la claudication de la mâchoire, liée à une ischémie des muscles masticateurs qui cède au repos, est fortement évocatrice du diagnostic (14 , 15).

Figure 1 : Exemple d'aspect inflammatoire et tortueux d'une artère temporale chez une patiente atteinte d'ACG prouvée histologiquement.

- La pseudopolyarthrite rhizomélique (PPR), présente chez 40 % des patients, n'entraine en règle jamais de destruction articulaire. Les douleurs articulaires des ceintures, de type inflammatoire se traduisent par un enraidissement douloureux et symétrique des épaules et des hanches s'estompant progressivement dans la journée. Parfois, les patients présentent des cervicalgies inflammatoires (torticolis fébrile). Plus rarement, ils peuvent avoir une oligo-arthrite ou une polyarthrite non destructrice (16).

- Les signes ophtalmiques, présents chez 25% des patients, peuvent être transitoires ou évoluer vers une atteinte irréversible chez 10 à 15% d'entre eux. L'amaurose définitive est fréquemment annoncée par des signes transitoires : diplopie, amaurose fugace, flou ou brouillard visuel ou encore amputation du champ visuel. Ces signes surviennent en règle dans un contexte d'artérite temporale dont les signes ont été négligés. Moins de 5% des patients présentent une cécité inaugurale irréversible. Classiquement, on retrouve une neuropathie optique ischémique antérieure aiguë (NOIAA), plus rarement une ischémie rétinienne ou une neuropathie optique rétrobulbaire (NORB). Si la cécité peut être inaugurale chez 10% des

patients, elle survient parfois paradoxalement après l'instauration de la corticothérapie (17). D'après Cid et al., la présence d'un syndrome inflammatoire marqué au moment du diagnostic est associée à un risque plus faible de complication ischémique céphalique (18). En cas de signe oculaire survenant dans un contexte inflammatoire, une ACG doit être recherchée et un traitement doit être débuté en urgence en raison du risque de bilatéralisation des symptômes, ce d'autant que le traitement permet rarement une récupération visuelle.

- Tous les territoires vasculaires peuvent être atteints au cours de l'ACG, ce qui conduit à une grande diversité des signes cliniques et à une symptomatologie parfois peu évocatrice. On citera les signes ORL (otalgie, dysphagie, dysphonie, douleur dentaire, douleur ou beaucoup plus rarement nécrose de langue) (19), neurologiques (accidents vasculaires cérébraux, localisés préférentiellement dans le territoire cérébral postérieur) (20), cardiaques (21 , 22) et pulmonaires (toux sèche, infarctus du myocarde lié à une atteinte spécifique des artères coronaires), cutanés (nécrose du scalp)(23).

Aucune manifestation clinique n'est constante et aucune des manifestations cliniques rencontrées au cours de l'ACG ne permet d'affirmer avec certitude le diagnostic. Certains signes cliniques sont plus fortement évocateurs et plus souvent associés à une positivité de la biopsie d'artère temporale (BAT): la claudication intermittente des mâchoires, un épisode de diplopie, une artère temporale indurée à la palpation et l'abolition d'un pouls temporal doivent conduire à la réalisation d'une BAT (24). Dans près de 70% des cas, les patients présentent des signes céphaliques, rhumatologiques et visuels et le diagnostic est alors aisé. Cependant, chez 5 à 10 % des patients, l'atteinte ophtalmique est inaugurale, ce qui fait la gravité de la maladie à la phase aigüe (25). Devant une NOIAA, un bilan inflammatoire à la recherche d'arguments en faveur d'une ACG doit donc être réalisé en urgence. Enfin, plus rarement, les patients ne présentent que des signes généraux peu ou pas spécifiques. Dans

cette situation, la réalisation d'un PET-scanner à la recherche d'une fixation de l'aorte (aortite), des artères humérales ou sous-clavières a tout son intérêt, ne dispensant bien sûr pas de pratiquer une BAT. Rarement, c'est la découverte fortuite d'un épaississement de l'aorte thoracique, d'un syndrome de l'arc aortique (26), d'une dilatation fusiforme de l'aorte ou d'une dissection mise en évidence sur une tomodensitométrie ou d'une insuffisance aortique avec dilatation anévrysmale de l'aorte en échographie qui oriente vers le diagnostic. En l'absence de signes évocateurs, la BAT est proposée si le bilan étiologique est négatif chez les patients de plus de 50 ans qui ont un syndrome inflammatoire prolongé inexpliqué.

1.1.4. Biologie

Il n'existe pas de marqueur sanguin spécifique présentant un intérêt diagnostique dans l'ACG et la biologie montre une inflammation non spécifique (augmentation de la vitesse de sédimentation (VS) et de la protéine C réactive (CRP), anémie inflammatoire, hyperleucocytose à polynucléaires neutrophiles, thrombocytose) et parfois une cholestase non ictérique. La VS supérieure à 50 mm à la première heure constitue un des critères de classification établi parle Collège des Rhumatologues Américains (ACR) (Tableau 1). Son intérêt en pratique, comparé à la CRP, est discutable. Les autres marqueurs classiques de l'inflammation (fibrinogène, orosomucoïde, haptoglobine) sont élevés mais ne constituent pas des éléments diagnostiques. Certains patients ont un syndrome inflammatoire peu marqué et pourraient avoir un risque de complication ophtalmologique plus important (retard diagnostique ou forme particulière de la maladie). La VS tend à se normaliser plus tardivement que la CRP et son élévation aspécifique fait courir le risque de sur-traiter les patients. De nombreux auto-Ac ont été identifiés au cours de l'ACG. Cependant aucun d'entre eux n'a démontré à ce jour son intérêt à visée diagnostique ou pronostique. Des Ac anti-cardiolipine ont été détectés et leur présence a été associée aux poussées et rechutes de la maladie (27). Par ailleurs, des Ac anti-cellule endothéliale (AECA) ont été détectés par

« enzyme linked immuno sorbant assay » (ELISA) cellulaire (28) mais la présence de ces auto-Ac n'a pas été confirmée par immunofluorescence indirecte (29) et leur intérêt pour le diagnostic et le suivi des patients n'est pas démontré. Enfin, des Ac anti-ferritine ont été identifiés à l'aide d'une approche de type puce protéique (30). Selon la présentation clinique peuvent être recherché des Ac anti-peptide cyclique citrulliné (CCP) ou un facteur rhumatoïde, des ANCA ou des Ac anti-nucléaires (AAN). Ces différents Ac sont négatifs au cours de l'ACG. Ainsi, la présence d'ANCA au cours d'une vascularite temporale oriente très fortement vers le diagnostic de vascularite associée aux ANCA de localisation temporale et devra amener à demander une relecture de la BAT (31).

1.1.5. Apports et limites de la biopsie d'artère temporale (BAT)

Le diagnostic de certitude repose sur la positivité de la BAT qui met en évidence un infiltrat fait de cellules mononuclées au niveau de la média, des macrophages et des cellules géantes qui se localisent le plus souvent au contact de la limitante élastique interne qui est fragmentée. L'intima est épaissie avec une prolifération sous-endothéliale constituant une néo-intima. Enfin, une néovascularisation de la média et de la néointima peut se rencontrer. Au niveau adventitiel, on retrouve souvent un infiltrat inflammatoire en regard des *vasa vasorum (Figure 2).* Enfin, la lumière vasculaire peut être thrombosée. L'atteinte histologique est segmentaire ce qui rend nécessaire l'analyse d'un fragment de taille suffisante sur toute sa longueur. Si une biopsie de 2 à 3 centimètres est optimale, une longueur supérieure à 5 mm après fixation semble suffisante pour interpréter les résultats (32 , 33). En effet, il a été montré que 15,1% des biopsies étaient positive au dessus de 5 mm alors que ce pourcentage baisse à 3% en dessous de ce seuil. Par précaution, il est recommandé d'obtenir un fragment de 10 mm au minimum, ce d'autant que la fixation dans le formol rétracte le prélèvement de 8% environ. La bilatéralisation de la biopsie ne doit pas être proposée systématiquement en pratique courante, car elle ne modifie le résultat histologique que dans 3,3 % des cas et prive de la

possibilité ultérieure de réaliser une nouvelle biopsie en cas de suspicion de rechute (34). Il persiste souvent sur la BAT des signes évocateurs d'ACG pendant plusieurs semaines même si la spécificité des anomalies observées décroit après une semaine de traitement (35). L'initiation de la corticothérapie ne doit donc pas être différée du fait de la réalisation de la biopsie. Dans 10 à 20 % des cas, alors que la biopsie est négative, le diagnostic est alors posé du fait d'une symptomatologie clinique très évocatrice (céphalées ou trouble visuel et syndrome inflammatoire chez un patient de plus de 50 ans) et d'une amélioration spectaculaire des symptômes à l'instauration de la corticothérapie (36). Cependant, les critères de l'ACR sont des critères de classification et non de diagnostic de l'ACG. Des anomalies histologiques similaires à celles identifiées au cours de l'ACG sont retrouvées au cours d'une autre vascularite intéressant les vaisseaux de gros calibre, la maladie de Takayasu. Schématiquement, le diagnostic d'artérite de Takayasu est volontiers retenu chez une femme jeune alors que le diagnostic d'ACG est retenu chez les patients de plus de 50 ans.

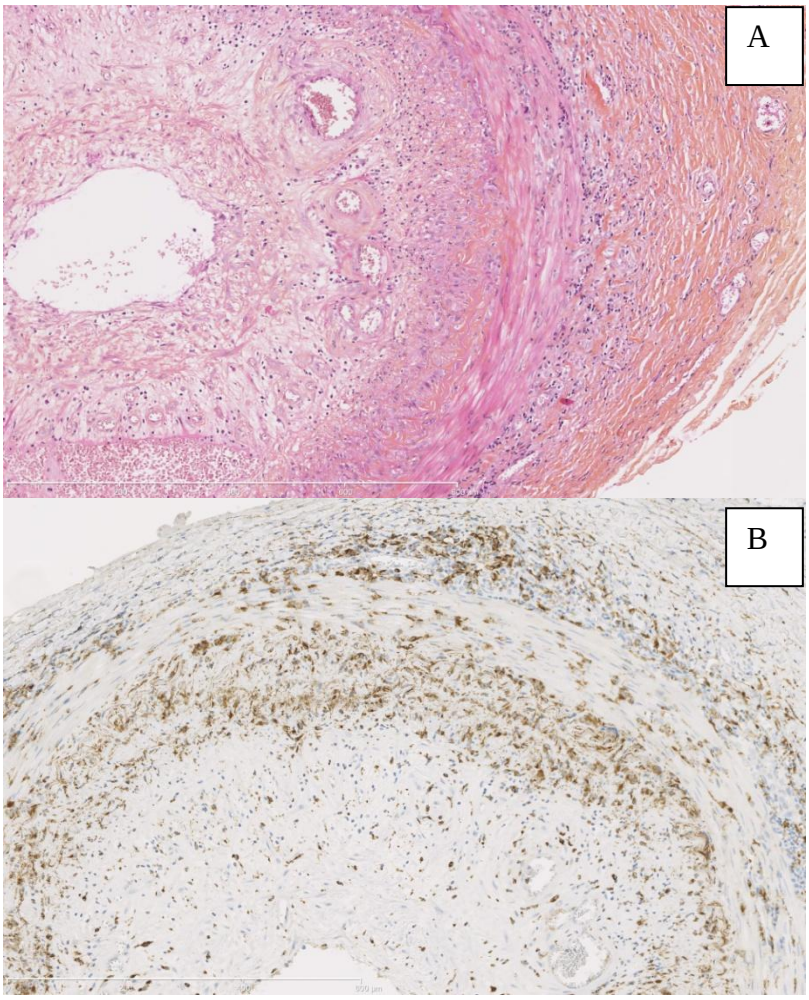

Figure 2 : Histologie d'une artère temporale de patient atteint ACG (grossissement 12X).(Courtesy Dr Depinay). On retrouve sur la coloration Hémalun-Erythrosine-Safran (panneau A) une infiltration lymphocytaire des trois tuniques de la paroi artérielle, un épaississement de la media avec constitution d'une néo-intima au sein de laquelle on distingue des néo-vaisseaux. La limitante élastique interne apparaît fragmentée. L'immunohistochimie, réalisée avec un marquage par un anticorps anti-CD68 (panneau B) confirme la présence de macrophages au contact des limitantes élastiques

1.1.6. Apport de l'imagerie

Le signe du halo (témoin d'un œdème pariétal) ou une sténose/occlusion lors de l'échographie-doppler des artères temporales ont montré une sensibilité de 87 % et une spécificité de 96 % pour le diagnostique d'ACG dans une méta-analyse (37). Néanmoins, l'échographie de l'artère temporale ne s'est pas encore imposée en France pour le diagnostic

d'ACG compte-tenu de l'expérience requise de l'opérateur qui doit être importante, de l'utilisation de sondes échographiques adaptées ainsi que de la difficulté d'explorer par ailleurs les vaisseaux intra-thoraciques (38). Enfin, la scintigraphie au glucose marqué (PET-Scan) permet une bonne exploration des gros troncs intra-thoraciques. Une fixation des vaisseaux thoraciques est présente chez 83 % des patients au diagnostic et l'intensité de la fixation diminue à 3 et 6 mois parallèlement à l'inflammation sans se négativer (39) (Figure 3). Cela pourrait être lié à un remodelage vasculaire persistant à distance. Après introduction de la corticothérapie, l'interprétation de ces examens d'imagerie est délicate. Par ailleurs, aucun de ces examens ne permet d'obtenir un diagnostic de certitude et d'éliminer une autre cause d'artérite temporale. A ce jour, ils n'ont pas permis de remplacer la BAT qui reste l'élément clé du diagnostic.

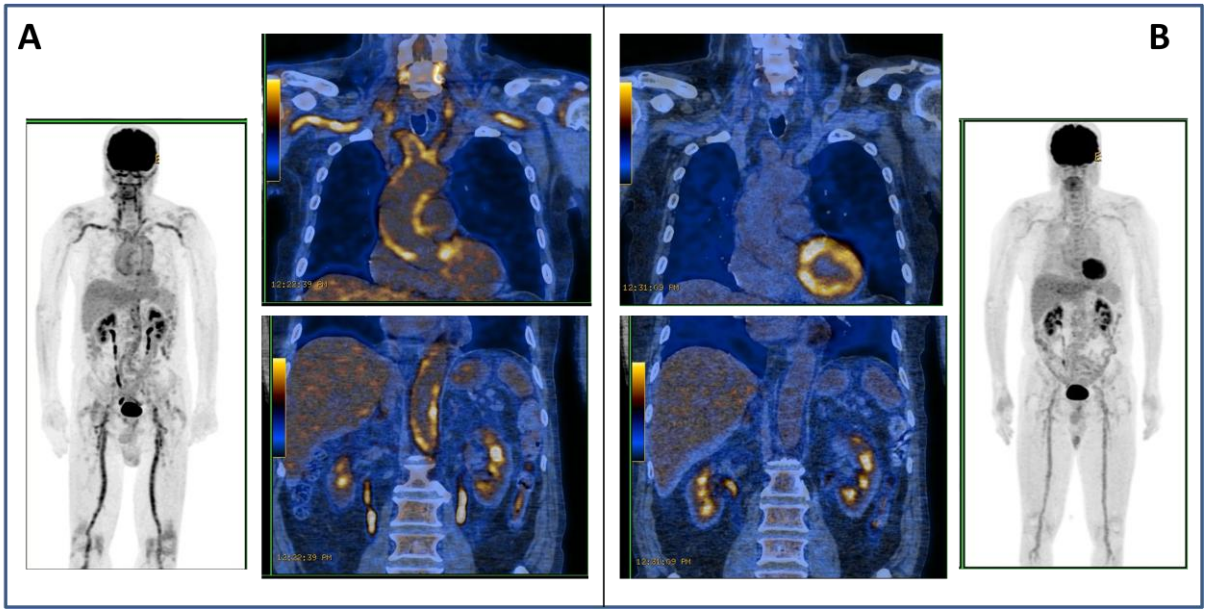

Figure 3 : Scintigraphie au fluoro-désoxy-glucose marqué d'un patient atteint d'ACG histologiquement prouvée. La captation du traceur au niveau de la paroi de l'aorte, des artères sous-clavières, des troncs supra-aortiques, des artères fémorales à la phase initiale (panneau A) est nettement diminuée après 6 mois de traitement par corticothérapie (panneau B).

1.1.7. Traitement

Le traitement de l'ACG repose, en l'absence de manifestation oculaire, sur une corticothérapie orale à la dose initiale de 0,5 à 0,7 mg/kg de prednisone durant 4 semaines avec une décroissance progressive guidée par la réponse clinique et biologique. En cas de trouble visuel, bien que l'intérêt de cette approche n'ait pas été démontré dans une étude prospective randomisée, il est recommandé d'administrer un bolus intraveineux de méthylprednisolone, relayé par une corticothérapie à 1 mg/kg de prednisone. La durée de la corticothérapie n'est pas clairement définie, d'une durée d'un an minimum à 7-8 ans voire plus prolongée encore pour certains patients ce qui conduit à des doses cumulées de corticoïdes pouvant aller de 3 à 8 grammes. Les modalités de décroissance de la corticothérapie reposent sur les signes cliniques et les marqueurs biologiques de l'inflammation et en particulier la CRP. L'objectif est d'être à la dose minimale efficace afin de minimiser les effets indésirables de la corticothérapie.

De nombreux immunosuppresseurs (méthotrexate, azathioprine, cyclophosphamide, mycofénolate mofétil) ont été proposés, à visée d'épargne cortisonique en association à la corticothérapie. Si les essais cliniques ont parfois été réalisés en traitement d'attaque (40 , 41 , 42), ils sont souvent réservés en pratique clinique au situation de corticodépendance ou de rechute. Parmi eux, le méthotrexate (7,5 à 15 mg/semaine) a montré son intérêt dans une étude randomisée contrôlée contre placebo réalisée chez 42 patients tant sur la dose cumulée de corticoïdes que sur le nombre de rechute (40)alors que deux autres études réalisées chez 21 patients (41)et 98 patients (42), également randomisées, contrôlées contre placebo n'ont pas montré de bénéfice respectivement sur la dose cumulée de corticoïdes et la fréquence des rechutes. Néanmoins, dans une méta-analyse, la dose cumulée de corticoïdes est inférieure de 842 mg à 48 semaines dans le groupe méthotrexate comparativement au groupe sans méthotrexate. De même, le risque de première et de deuxième rechute est abaissé sous

méthotrexate ($p \leq 0.05$) (43). Il est donc licite, en l'absence de contre-indication, et en particulier chez les patients à risque élevé de complications de la corticothérapie, de le proposer lors des rechutes, en association à la corticothérapie. Les résultats obtenus avec le cyclophophamide (44) ou l'azathioprine (45) sont difficiles à évaluer en l'absence d'étude contrôlée de bonne qualité, ce qui conduit à peu les utiliser en pratique. D'autres traitements adjuvants ont été proposés en association à la corticothérapie à visée d'épargne cortisonique mais ont tendance à être abandonnés. Ainsi, la dapsone entraine un risque accru de survenue d'une agranulocytose (46) et l'hydroxychloroquine n'a pas d'efficacité démontrée dans un essai randomisé contrôlé avec une fréquence inattendue d'éruptions cutanées (47).

Les traitements biologiques ont également été testés, en particulier les biothérapies antagonistes du « tumor necrosis factor »-α (TNF-α). Cependant, dans une étude prospective randomisée en double aveugle contre placebo réalisée chez 44 patients inclus en phase de rémission (traitement préalable par corticoïdes seuls), il n'a pas été mis en évidence de diminution du nombre de rechutes avec un traitement par un Ac monoclonal anti-TNFα chimérique, l'infliximab pendant 22 semaines (48). De même, dans un essai randomisé contrôlé contre placebo réalisé chez 70 patients et évaluant un Ac monoclonal anti-TNFα humanisé, l'adalimumab en association à la corticothérapie, la proportion de patients en rémission à 26 semaines sous moins de 0.1mg/kg de corticoïdes n'était pas différente dans les 2 groupes (49). D'autres biothérapies antagonistes du récepteur de l'interleukine (IL)1 (IL1-Ra) (50) ou un Ac monoclonal dirigé contre le récepteur de l'IL6 (51)) comme le tocilizumab ont été rapportés comme pouvant permettre d'obtenir des résultats intéressants en termes de contrôle de la maladie et de diminution de la corticothérapie. Cependant, ces traitements n'ont pas encore été évalués dans des essais prospectifs et ne peuvent donc pas être proposés actuellement faute de démonstration suffisante de leur efficacité disponible dans la littérature, excepté dans le cadre des essais thérapeutiques actuellement en cours. Ces traitements, s'ils

semblent efficaces par inhibition directe des cytokines impliquées dans la réponse inflammatoire systémique et l'amélioration des symptômes, pourraient avoir un effet purement suspensif. Les biothérapies peuvent aussi être discutées dans des formes ne répondant pas à une combinaison de traitements corticoïdes et immunosuppresseurs.

Une anti-agrégation plaquettaire par aspirine à faible dose doit être associée à la phase aigüe en prévention des complications cardio-vasculaires. En effet, les patients ayant une ACG ont un risque plus élevé que la population générale de faire un infarctus du myocarde et/ou un accident vasculaire cérébral. La durée optimale de cette anti-agrégation n'est pas définie mais dans une cohorte de 432 patients atteint d'ACG inclus prospectivement et appariés à une cohorte contrôle, le risque relatif d'évènements cardio-vasculaires était de 2,42 à 24 mois ce qui soutient l'idée d'une anti-agrégation prolongée (52). L'intérêt d'une anticoagulation à dose efficace n'a pas été démontré mais elle peut être proposée transitoirement à la phase aigüe de la maladie en particulier en cas d'évènement ischémique oculaire avéré.

Enfin, il ne faut pas oublier de prévenir les complications de la corticothérapie au long cours (≥ 7,5 mg pendant 3 mois) responsable d'une morbidité importante (ostéoporose, infections, athérome accéléré…) en proposant un traitement par bisphosphonates et des vaccinations contre la grippe et le pneumocoque (53). Lorsque la dose de corticoïdes est de 5 mg/jour et que l'on envisage de diminuer en dessous de cette dose dans le but d'interrompre la corticothérapie, il convient de rechercher une insuffisance surrénalienne par un test au synacthène. De façon importante, 49% des patients présentent un défaut de réponse qui régresse dans la majorité des cas dans les 3 ans (54).

Les rechutes sont marquées par une ascension de la CRP et des autres marqueurs de l'inflammation et la réapparition des signes cliniques initiaux. Ils imposent souvent une

augmentation de la corticothérapie au palier précédent, dose maintenue quelques semaines avant de reprendre la décroissance. C'est dans ce contexte qu'il faudra envisager, si cela n'a pas encore été fait, un traitement par methotrexate ou un autre traitement d'épargne cortisonique.

1.1.8. Surveillance, évolution à long terme

Au cours du suivi, la cause principale de morbidité est liée à la corticothérapie. Ainsi, dans une cohorte de 120 patients suivis en moyenne 10 ans, 86% des patients présentent des effets indésirables de la corticothérapie : ostéoporose fracturaire, infection, cataracte sous capsulaire postérieure…Sur les 120 patients, 23 sont décédés dont 3 du fait de l'ACG (53). A plus long terme, la morbidité et la mortalité de l'ACG sont associées à la formation d'anévrysmes de l'aorte dont la rupture à long terme constitue une cause de décès. L'évolution anévrysmale de l'aorte thoracique (risque relatif de 17) et de l'aorte abdominale (risque relatif de 2,4) est imprévisible, mal corrélée à l'activité de la maladie et survient avec un délai moyen de 5,8 ans pour l'aorte thoracique et de 2,5 ans pour l'aorte abdominale (55). La fixation de l'aorte au PET-scanner pourrait permettre d'identifier un sous-groupe de patients qui vont présenter une dilatation de l'aorte au cours du suivi (56). Les modalités de dépistage d'une dilatation anévrysmale au diagnostic ou lors du cours évolutif de l'ACG ne sont pas codifiées. Ce risque évolutif pourrait justifier selon certains auteurs une surveillance annuelle de l'échographie abdominale, d'une échographie trans-thoracique et d'une radiographie de thorax. Au moindre doute ou en cas d'évolution anévrysmale, l'imagerie par résonnance magnétique (IRM) avec injection de gadolinium ou tomodensitométrie seraient alors justifiés (57).

Dans les études, la mortalité des patients atteints d'ACG semble peu différente de la population générale. Les principales causes de mortalité sont les accidents cardiovasculaires, les infections ou les cancers avec des résultats parfois discordants (58). Cependant, le sous-

groupe de patients qui présentent une aortite ou une dilatation anévrysmale de l'aorte pourrait avoir un risque accru de mortalité.

1.2. Physiopathologie de l'ACG

Malgré des progrès récents concernant la physiopathologie de l'ACG, celle-ci reste encore largement méconnue. En effet, de nombreuses composantes interviennent probablement ce qui explique la complexité des études. Ainsi, les connaissances actuellement disponibles sur la physiopathologie de l'ACG sont résumées dans la figure 4. De nombreuses composantes interviennent : susceptibilité génétique, environnement, facteur déclenchant possiblement infectieux, perturbation du système immunitaire, participation des cellules de la paroi artérielle. Les raisons qui contribuent à la pérennisation de l'inflammation restent obscures. (59). Une autre limite importante à la compréhension de la physiopathologie est l'absence de modèle animal (spontané ou induit) permettant de reproduire la maladie. A ce jour, le seul modèle d'ACG est le modèle chimérique développé par Cornelia Weyand. Un fragment d'artère temporale humaine est isolé au moment de la BAT réalisée à visée diagnostique. Il est ensuite implanté dans le tissu sous-cutané d'une souris NOD.CB17 Prkdc présentant un déficit immunitaire combiné sévère. Ce modèle de xénogreffe peut être manipulé avec, par exemple, l'injection aux souris receveuses de LPS ou de corticoïdes (60) (61), la déplétion en cellules dendritiques (DC) préalable à la xénogreffe (62) … Il a ainsi permis de nombreux progrès dans la compréhension de la physiopathologie de l'ACG.

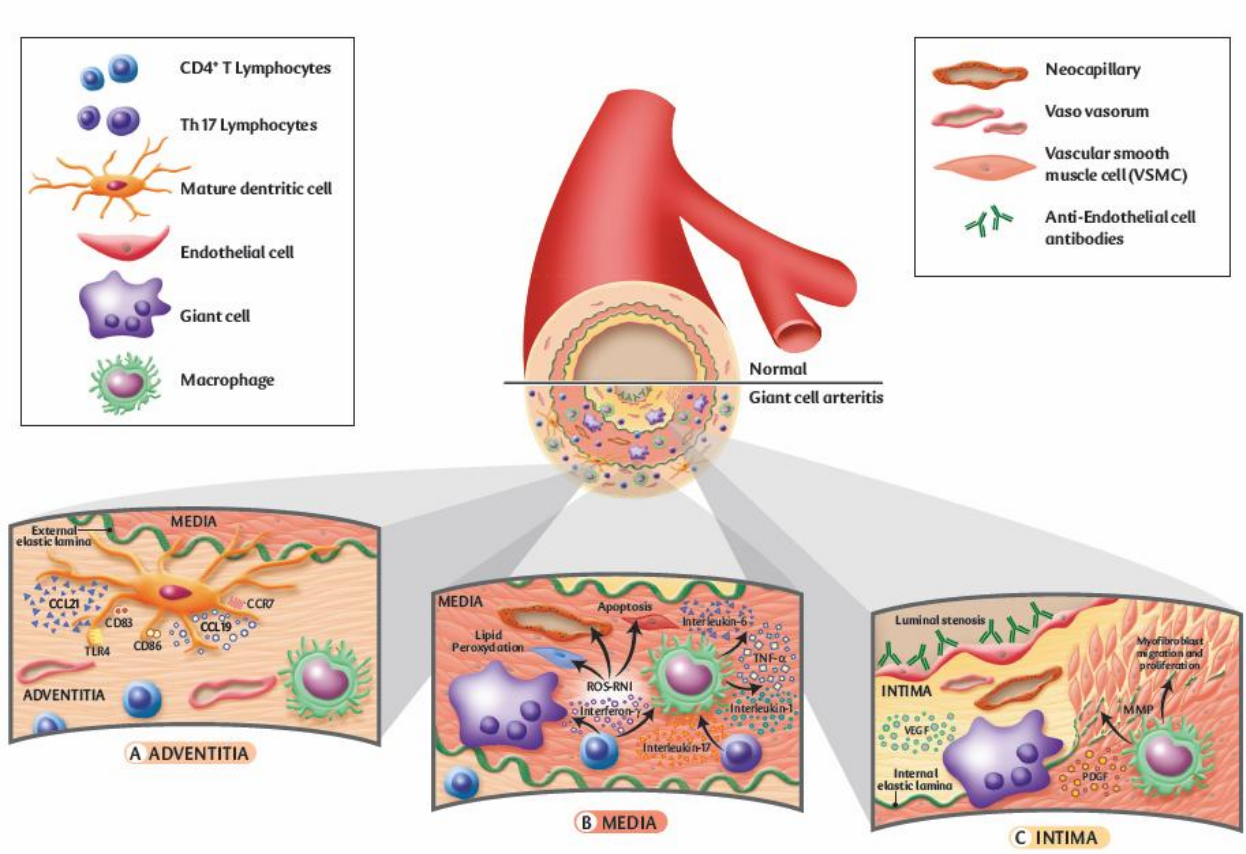

Figure 4: Physiopathologie de l'artérite à cellules géantes, d'après Ly et al. Autoimmunity Reviews 2010(59) **(A)** En l'absence de signaux d'activation, les DC adventitielles immatures expriment à leur surface principalement les TLR, la protéine S100 et le CCR6. Après activation par un stimulus inconnu, ces DC vont exprimer des marqueurs d'activation (CD83) et des molécules de co-stimulation (CD86) et vont produire des cytokines (IL-6, IL-12 et IL-18) et des chémokines (CCL18, CCL19, CCL20 CCL21) et leurs récepteurs (CCR7). Ainsi, elles vont rester piégées dans la paroi artérielle et agir comme des cellules présentatrices de l'antigène, en recrutant et activant les LT $CD4^+$. Les LT $CD4^+$vont infiltrer la paroi artérielle via les vasa vasorum et se positionner au niveau de la LEE et de la jonction intima-média. **(B)** Les LT $CD4^+$ vont ensuite subir une expansion clonale et se polariser selon un profil Th1 ou Th17 en fonction des cytokines et chémokines produites par les DC. Les LTh1 producteurs d'IFN-γ vont recruter et activer des macrophages qui peuvent fusionner pour former des cellules géantes et participer à la formation de granulomes. Les Th17 produisant l'IL-17 comme les Th1 vont favoriser la production de cytokines pro-inflammatoires (TNF-α, IL-1 et IL-6) par les macrophages ce qui va engendrer une inflammation locale et systémique. Les cellules géantes et les macrophages, situés à proximité de la limitante élastique interne à la jonction intima-média, vont également libérer des ROS, du NO et des MMP, qui vont contribuer à la peroxydation des lipides membranaires et à l'apoptose des CMLV et des CE. **(C)** Les macrophages et les cellules géantes produisent également le PDGF et le VEGF. Sous l'action combinée des MMP, du PDGF et du VEGF, la LEI est détruite et un remodelage vasculaire apparaît. Les myofibroblastes vont proliférer et migrer vers l'intima. Il se constitue une hyperplasie intimale et une sténose luminale associées parallèlement à des phénomènes d'angiogénèse.
Abréviations: ACG: artérite à cellules géantes, CCL: chémokines (C-C motif) ligand, CCR: récepteur de chémokine (C-C motif), CD: cluster de différenciation, CE: cellules

endothéliales, CMLV: cellules musculaires lisses vasculaires, DC: cellules dendritiques, IFN-γ: interféron-γ, IL: interleukine, LEE: limitante élastique externe, LEI: limitante élastique interne, LT: lymphocytes T, MMP: métalloprotéases matricielles, NO: monocyte d'azote, PDGF: facteur de croissance dérivé des plaquettes, ROS: espèces oxygénées réactives, Th1: lymphocytes T helper 1, Th17: lymphocytes T helper 17 , TLR: Toll-like receptor, TNF-α: tumor necrosis factor-α, VEGF: vascular endothelial growth factor

1.2.1. Prédisposition génétique

Une prédisposition génétique a été suggérée par la survenue de cas d'ACG chez des apparentés au premier degré (63). De nombreux gènes de susceptibilité ont été identifiés au cours de l'ACG. En particulier, les haplotypes du complexe majeur d'histocompatibilité (« Human Leucocyte Antigen » (HLA)) de classe II HLA-DRB1*04 sont associés à l'ACG et leur portage pourrait également être associé à un risque ophtalmologique accru (64) et favoriser la cortico-résistance (65). Des associations plus faibles ont également été rapportées entre l'ACR et le HLA de classe I en particulier HLA-B15 et MICA (MHC class I polypeptide-related sequence A) (66). Des microsatellites ou « single nucleotide peptide » (SNP) relatifs à des cytokines (IL18, TNF-α, interféron (IFN)-γ, IL10, IL17…), à des marqueurs de l'endothélium vasculaire (« intercellular adhesion molecule » (ICAM)-1, « vascular endothelial growth factor » (VEGF), « endothelial nitric oxyde synthase » (eNOS), « matrix metalloprotease » (MMP)-9…) ou à des composants de l'immunité innée (« toll like receptor » (TLR)-4 ou encore «Nucleotide-binding oligomerization domain like receptor pyrin containing domain » (NLRP)-1) ont été associés à un risque accru d'ACG (67 , 68 , 69 , 70 , 71 , 72 , 73 , 74 , 75 , 76) ou à la sévérité de la maladie (77 , 78). Cependant, ces résultats n'ont pas été validés dans des cohortes de réplication ou n'ont pas été confirmés dans de larges populations. Une étude génétique européenne de type GWAS (genome-wide association study) réalisée à partir d'une large cohorte de patients atteints d'ACG est

actuellement en cours en Espagne. L'objectif est d'identifier des gènes de prédisposition et/ou pronostiques dans cette maladie.

1.2.2. Hypothèse infectieuse

Le fait que le CMH de classe I ou II soit associé à l'ACG (64 , 65), l'évolution de la maladie sur un mode épidémique et enfin l'oligoclonalité des lymphocytes T (LT) issus de l'artère temporale (79 , 80)ont fait envisager qu'un antigène extérieur ou de la paroi artérielle active les DC adventitielles. De nombreuses études ont eu comme objectif d'identifier un possible agent infectieux inaugural en recherchant de l'ADN bactérien ou viral. Ainsi, l'ADN de parvovirus B19 (81 , 82) ou herpès simplex virus (HSV)(83) ont été identifiés. Cependant, ces résultats n'ont pas pu être confirmés dans d'autres études (84 , 85). Par ailleurs, les résultats de la recherche d'herpès virus humain (HHV)-6 (82), HHV-7 (86), virus varicelle zona (VZV) (87), cytomégalovirus (CMV) (86) ou de virus Epstein-Barr (EBV) (86) étaient négatifs. Enfin, des immunoglobulines (Ig) M sériques dirigées contre le virus parainfluenzae de type 1 ont été détectées de façon plus fréquente dans une population de patients atteints d'ACG histologiquement prouvée que dans une population contrôle (88). Cependant, ce résultat n'a pas été confirmé depuis. L'ADN de *Chlamydia pneumoniae* a été mis en évidence par amplification génique (« polymerase chain reaction ») (PCR) au sein de lésions d'ACG (89). Cependant, ces résultats n'ont pas non plus été confirmés depuis (90 , 91). Plus récemment, il a été rapporté en communication orale au congrès de l'ACR en 2012, qu'une bactérie avait été identifiée au sein d'artères temporales à l'aide d'une PCR de l'ARN 16s chez 9/10 patients atteints d'ACG alors que 0/11 patients indemne d'ACG n'avait d'ARN bactérien. Il s'agissait de *Burkholderia pseudomallei-like.* L'identification de cette bactérie avait été faite par biologie moléculaire et sa présence avait été confirmée au sein des BAT par immunofluorescence avec un Ac spécifique du LPS de *Burkholderia pseudomallei-like.* Cultivée à partir d'une artère temporale, son injection à des souris déclenchait une vascularite

des vaisseaux pulmonaires. (92). Cependant, cette étude n'a jamais été publiée car les résultats ont été contestés et les biais méthodologiques mis à jour ont finalement conduit les auteurs à interrompre au moins temporairement le processus de publication.

1.2.3. Dysrégulation du système immunitaire

Activation lymphocytaire T

Il existe de façon physiologique des DC immatures de phénotype $S100^{+}CD11c^{+}CCR6^{+}CD83^{-}CMH\text{-}II^{low}$ au niveau adventitiel. Suite à la présentation d'un antigène de nature indéterminée (possiblement d'origine infectieuse ou de la paroi vasculaire), ces DC vont alors acquérir un phénotype mature et exprimer les cluster de différenciation (CD)80/86 et CMH-II (62). L'expression des TLR par les DC de la paroi artérielle dépend du territoire vasculaire. Ainsi, les TLR 2,4 et 8 sont fortement exprimés au niveau temporal alors que les TLR 1, 5 et 6 le sont peu. Le pattern d'expression des TLR est proche entre les artères carotides et l'aorte ce qui pourrait expliquer le tropisme vasculaire de l'ACG (61). Les DC vont sécréter des chémokines : CC chémokine ligand (CCL)18, CCL19, CCL20 et CCL21 et exprimer le CC chémokine receptor (CCR)7, un ligand de CCL19 et CCL21, ce qui conduit à une activation autocrine (62, 93). Le défaut de migration de ces DC vers le ganglion de drainage conduit à un recrutement et à une stimulation des LT $CD4^{+}$ dans la paroi artérielle. Dans un modèle de greffe de BAT chez des souris atteintes de déficit immunitaire combiné sévère (SCID), l'ajout d'adjuvant complet de Freund, un agoniste du TLR2 et en particulier du LPS, agoniste du TLR 4, permet la maturation des DC alors que le TNFα ne permet ni l'expression du CD83 ni la synthèse de CCL21 par les DC (62). La déplétion en DC ou en LT réduit notablement les lésions de vascularite ce qui témoigne de l'importance de ces populations cellulaires dans le processus pathologique (62).

Absents des artères saines, les LT vont être recrutés via les vasa vasorum qui expriment intracellular adhesion molecule-1 (ICAM-1) et vascular cell adhesion molecule-1 (VCAM-1), nécessaires à la diapédèse (94). Les LT vont subirent une expansion oligoclonale (95) et peuvent proliférer en présence d'extraits d'artère temporale (96). De façon intéressante, la stimulation des DC par du LPS conduit à une synthèse de CCL20 et au recrutement de LT $CD4^+CCR6^+$ responsables d'une pan artérite alors que la stimulation par de la flagelline permet le recrutement de cellules $CD4^+CCR6^-$ et induit une périartérite (97). L'environnement cytokinique au sein des artères temporales va polariser les LT. Ainsi, sous l'influence de l'IL12 et IL18, les LT-Helper (LTh) 1 générés vont produire de l'IFN-γ et sous l'influence d'IL6, d'IL1β et d'IL23, les LTh17 générés vont produire de l'IL17. Ces LTh1 et LTh17 ont une sensibilité différente à la corticothérapie. En effet, alors que la production des cytokines Th17 (IL-1β, IL-6 et IL-23) est diminuée, la production de cytokines Th1 (IL-12) par les monocytes circulants et infiltrant les artères de sujets atteints d'ACG n'est que peu atteinte, suggérant 2 voies d'activation lymphocytaire (98). Cependant, plus récemment, Samson et al. ont rapportés que des précurseurs des Th17, les LT $CD4^+CD161^+CCR6^+$ infiltrent de façon massive les lésions d'artérite temporale et que les LTh1 expriment CD161 (spécifique des Th17) ce qui pourraient témoigner de la différenciation des Th17 en Th1 par plasticité (99). Il a été mis en évidence une expansion de la population des LT $CD4^+$ producteurs d'IL21 et que cette population pourrait participer à la différenciation préférentielle Th1/Th17 au détriment de la voie Treg (100). Le blocage de la voie NOTCH pourrait permettre de diminuer l'infiltrat lymphocytaire des lésions vasculaires dans un modèle expérimental (101). Il existe parallèlement un déficit quantitatif en LT régulateurs sanguins de phénotype $CD4^+CD25^{high}foxp3^+$, population lymphocytaire quasi absente des lésions vasculaires qui ne peuvent pas contrebalancer l'effet pro-inflammatoire Th1/Th17 (99 , 100).

Réponse humorale

Peu d'études se sont intéressées à l'immunité humorale. En effet, l'analyse histologique des BAT montre des lymphocytes B (LB) épars, localisés préférentiellement au niveau adventitiel. Il s'y associe parfois des plasmocytes dans 7 à 24 % des cas et leur présence serait significativement associée à une cécité définitive mais le rôle précis de ces plasmocytes n'est pas élucidé (102). Récemment, l'étude des populations lymphocytaires B a montré une diminution des populations de LB effecteurs TNF-α^+, une conservation des LB régulateurs IL10$^+$ en phase d'activité de l'ACG et une synthèse d'IL6 par les LB qui pourrait participer à la pathogénie de la maladie (103).

Une étude s'est intéressée à rechercher un auto-Ac de type IgG à partir d'une librairie de cDNA issue de testicule humain au cours de l'ACG et de la PPR. Des réactivités fortes vis-à-vis de la lamine C, de la cytokératine 15 et du cytochrome C ont ainsi pu être mises en évidence (104).Par ailleurs, d'autres auto-Ac ont également été décrits. Trente trois pourcents des patients atteints d'ACG ont des Ac dirigés contre des cellules endothéliales (CE) de veine ombilicale humaine (HUVEC) (« enzyme-linked immunosorbent assay » (ELISA) cellulaire sur cellules fixées) et leur présence semble corrélée à l'activité de la maladie. Cependant, ceux-ci ne sont pas spécifiques de l'ACG et leur caractère pathogène au cours de cette maladie n'est pas démontré (28). La présence de ces Ac dans le sérum a été remise en cause par une technique d'immunofluorescence (29). Des Ac anti-cardiolipine (aCL) ont été mis en évidence chez 31 à 50 % des patients atteints d'ACG non traitée. Jamais associés aux Ac anti-β2gp1 (105), leur présence serait corrélée à une positivité de la BAT et à un taux d'hémoglobine bas mais pas aux complications ischémiques (106 , 107). Sous traitement, ils se négativent généralement dans les 3 mois et la persistance ou la réascension des aCL serait associée à une rechute de la maladie (27). La présence d'Ac dirigés contre les anti-phospholipides (recherche d'anti-coagulant circulant, aCL ou anti-β2gp1) n'est pas associé à

un risque accru d'évènement thrombotique (108). D'autres auto-anticorps ont été rapportés dirigés notamment contre la molécule HSP 60 (109). Plus récemment des anticorps dirigés contre des peptides de la ferritine ont été rapportés chez 92% des patients atteints d'ACG active (30). L'utilisation de plusieurs épitopes pourrait permettre de sensibiliser ce test et de s'en servir au dépistage dans une population suspecte d'ACG (110). Enfin, des anticorps dirigés contre la progranuline, protéine ayant la capacité de se lier au récepteur du TNF, ont également été rapportés aux cours des vascularites systémiques et en particulier chez 14/65 patients ayant une ACG et/ou une PPR (111). La signification de ces auto-anticorps au cours de l'ACG est encore inconnue.

Remodelage vasculaire

L'activation des LT CD4+ de profil Th1 conduit à la production d'IL-2 et d'IFN-γ et Th17 responsable de la synthèse d'IL17. La chémokine CCL2, ligand de CCR2, produite par les leucocytes de la paroi et par les CMLV semble avoir un rôle important dans la stimulation des macrophages. Le niveau d'expression de CCL2 au sein de l'artère temporale par PCR quantitative a été corrélé aux rechutes de la maladie dans la première année (112). Les macrophages activés sécrètent alors de l'IL6 et de l'IL1β à l'origine des manifestations cliniques de la maladie. Ces macrophages présentent une hétérogénéité fonctionnelle et tous ne sécrètent pas l'IL6, l'IL1β ou la collagénase. La stimulation chronique conduit à la formation de granulomes caractéristiques de la maladie au niveau de la limitante élastique interne et de la media. Les macrophages de la media produisent des formes réactives de l'oxygène dont la cible principale semble être la CMLV (93). On constate une désorganisation de la media ainsi qu'une apoptose des CMLV. Ces dérivés de l'oxygène agissent également sur le métabolisme cellulaire comme en témoigne la production accrue d'aldolase réductase (113). Les macrophages et les cellules géantes produisent également du « platelet derived growth factor » (PDGF) et du VEGF, responsables de la néo-vascularisation de la media et

dont l'expression est corrélée à l'épaississement intimal responsable des phénomènes ischémiques de la maladie (114 , 115). L'action conjuguée des formes réactives de l'oxygène et du NO synthétisé par les CE des néovaisseaux pourrait contribuer à recruter des lymphocytes et des macrophages et à pérenniser l'inflammation (116). Enfin, le déséquilibre de la balance entre les métalloprotéases matricielles (MMP)-2, MMP-9 et MMP14 et les inhibiteurs tissulaires de métalloprotéases TIMP1 et TIMP2 participe également au remodelage de la paroi des vaisseaux (117).

Plusieurs éléments mettent en évidence un rôle non univoque de la CMLV dans la pathogénie de la maladie. La CMLV est une cible des formes réactives de l'oxygène qui conduisent à leur apoptose ou à la modification de leur phénotype avec différenciation myofibroblastique et prolifération sous-intimale. Des taux élevés de MMP9, en partie sécrétée par les CMLV, ont été associés à la destruction de la limitante élastique interne, à l'hyperplasie intimale et au rétrécissement de la lumière artérielle (118). Ces éléments associés à l'activation de la voie de l'endothéline-1 (ET-1) pourraient participer aux manifestations ischémiques de la maladie (119). A contrario, la production d'aldolase réductase participe à la neutralisation des effets de la peroxydation des lipides (113).

Enfin, les CE présentes au niveau des vasa vasorum et des néo-vaisseaux vont exprimer les molécules d'adhésion ICAM-1, ICAM-2, P-selectin, E-selectin et VCAM-1 et participer au recrutement leucocytaire (120). Les patients qui présentent les complications ischémiques de la maladie ont significativement moins de néovaisseaux au niveau de l'artère temporale et la tubulogenèse d'HUVEC cultivées sur un matrigel en présence de leur sérums est diminuée comparativement aux patients indemnes d'évènements ischémiques (121).

1.3. Les cellules musculaires lisses vasculaires (CMLV) en contexte physiologique et pathologique

Les CMLV sont des cellules hautement spécialisées de la média qui régulent le tonus vasculaire et participent au remodelage de la paroi en condition physiologique ou pathologique.

1.3.1. Caractérisation des CMLV normales

Une population cellulaire hétérogène

Contrairement aux cellules musculaires striées et aux cardiomyocytes, les CMLV ne sont pas des cellules en différenciation terminale et ont donc une plasticité en réponse aux stimuli locaux. Les CMLV peuvent être identifiées par la détection des nombreuses protéines contractiles qu'elles expriments telle que l'α-SMA, la caldesmone, la smootheline, la « smooth muscle myosin heavy chain » (SM-MHC) (122). Cependant, ces protéines sont des marqueurs de différenciation cellulaire et non des marqueurs de lignée cellulaire dont la présence permettrait de discriminer entre les CMLV et tous les autres types cellulaires. A titre d'exemple, l'α-SMA est une protéine abondante (jusqu'à 40 % du contenu protéique des CMLV) qui joue un rôle majeur dans la contraction cellulaire. Cependant, l'α-SMA peut également être exprimée transitoirement par les cardiomyocytes (123), par des fibroblastes (124), par des CE (125) et par des cellules tumorales (126). L'identification des CMLV repose donc sur de multiples marqueurs. Par ailleurs, au sein du vaisseau à l'état basal, les CMLV pourraient constituer une population hétérogène. Ainsi, Frid et al. ont analysés les gros vaisseaux d'embryon et de veau adulte d'un point de vue morphologique et par immunohistochimie à l'aide d'un panel d'anticorps dirigés notamment contre l'α-SMA, la myosine et la desmine. Selon la morphologie cellulaire (cellules irrégulières ou allongées), la présence ou non de fibres élastiques en amas autour de ces cellules et l'expression protéique, ils distinguent schématiquement 4 types de CMLV différentes ce qui soutient l'idée de

populations différentes sans que les conséquences de cette hétérogénéité ne soient abordées (127). Par ailleurs, des populations de CMLV de rat d'origine embryonnaire ou adulte ont des profils distincts d'expression de l'α-SMA, de « cellular retinol binding protein » et de « smooth muscle-myosin heavy chain ». Transférées dans des artères carotides dénudées d'autres rats, ces cellules conservent leur expression phénotypique initiale ce qui suggére une certaine stabilité de leur phénotype (128). Cependant, si on note des populations hétérogènes dans l'expression protéique, il ne s'agit pas pour autant de lignées distinctes et ces variations phénotypiques sont source d'une grande complexité dans l'analyse des données de la littérature.

Origine embryologique

D'un point de vue embryologique, de nombreux précurseurs des CMLV ont été identifiés. Ainsi, certaines CMLV pourraient être d'origine ectodermique (129) alors que d'autres sont d'origine mésodermiques (130 , 131). Il a également été évoqué qu'au cours de l'embryogenèse, certaines CMLV pourraient provenir de la dédifférenciation de CE suite à la perte d'expression du facteur von Willebrand et à la synthèse d'α-SMA (132). D'autres encore pourraient provenir de cellules souches pluripotentes d'origine médullaire (133).

1.3.2. Fonctions des CMLV normales

Au plan fonctionnel, on distingue des CMLV de phénotype « contractile » qui expriment des protéines du cytosquelette telles que la vimentine, la gelsoline, la vinculine, l'α-smooth muscle actin (SMA), la smooth muscle-myosin heavy chain (SM-MHC)(134 , 135 , 136) et des CMLV de phénotype « synthétique » qui prolifèrent, migrent et synthétisent la matrice extracellulaire et perdent en partie les marqueurs de différenciation précédemment décrits. Cette dichotomie schématique n'est pas figée et on observe une modulation phénotypique avec le passage actif d'un phénotype à l'autre au cours d'un processus dynamique complexe

(122). Dans certaines conditions, les CMLV perdent leurs caractéristiques contractiles et prolifèrent peu ce qui témoigne des limites de cette dichotomie (137).

La principale fonction des CMLV à l'état physiologique est d'assurer le tonus vasculaire qui permet de maintenir une pression artérielle systémique. La contraction est assurée par l'interaction entre la myosine et l'actine en présence d'ATP. Cette contraction est finement régulée via des étapes de phosphorylatin/déphosphorylation de la myosine et par de nombreuses protéines telles que la calmoduline, caldesmone…(138). Au cours du développement vasculaire et dans les suites d'un traumatisme ou d'une plaie vasculaire, les CMLV sont capables de proliférer et de migrer. Les protéines de la MEC impliquées dans l'ancrage des CMLV et la nature des facteurs de croissance présents dans le milieu extra-cellulaire vont contribuer à réguler cette prolifération (139). L'apoptose des CMLV, contre-partie de la prolifération cellulaire intervient également dans l'homéostasie de la paroi (140)(141). Enfin, les CMLV participent au maintien de la matrice extra-cellulaire par des mécanismes opposés de dégradation par les métalloprotéases (MMP-2, 9, 7 ou 13 notamment) et par la synthèse de collagène, d'élastine et de la matrice nouvellement synthétisée qui permet de maintenir la résistance aux contraintes mécaniques et de servir de soutien au CMLV(142 , 143).

1.3.3. Mécanismes de régulation des CMLV

Les CMLV vont intégrer de nombreux signaux contribuant à réguler leur fonction. Ainsi, les CE vont notamment sécréter de l'ET-1, des prostacyclines ou du NO en réponse aux contraintes mécaniques (144), ce qui va conduire à une adaptation du tonus vasculaire. Dans un système de coculture de CE et de CMLV, la prolifération des CMLV est également diminuée par contact direct avec les CE ce qui souligne que les facteurs solubles ne sont pas les seuls éléments qui contribuent à la régulation des CMLV (145). Par ailleurs, d'autres cellules vont pouvoir interagir avec les CMLV et ces échanges ont notamment été décrit dans

le contexte de l'athérosclérose : plaquettes, lymphocytes, macrophages (146). Les CMLV vont également répondre à des composants de la matrice extra-celulaire (147), aux facteurs de croissance qu'elle contient (148) et aux MMP (149), à des facteurs neuronaux (150), à la thrombine (151) ou encore aux formes réactives de l'oxygène et au potentiel redox local (152). Parmi les facteurs solubles, on retiendra principalement le PDGF et en particulier l'isoforme BB-PDGF qui induit la prolifération et la migration des CMLV (153), le TGF-β qui est un inhibiteur de la prolifération des CMLV chez l'homme (154) ou le facteur de réponse sérique (155).

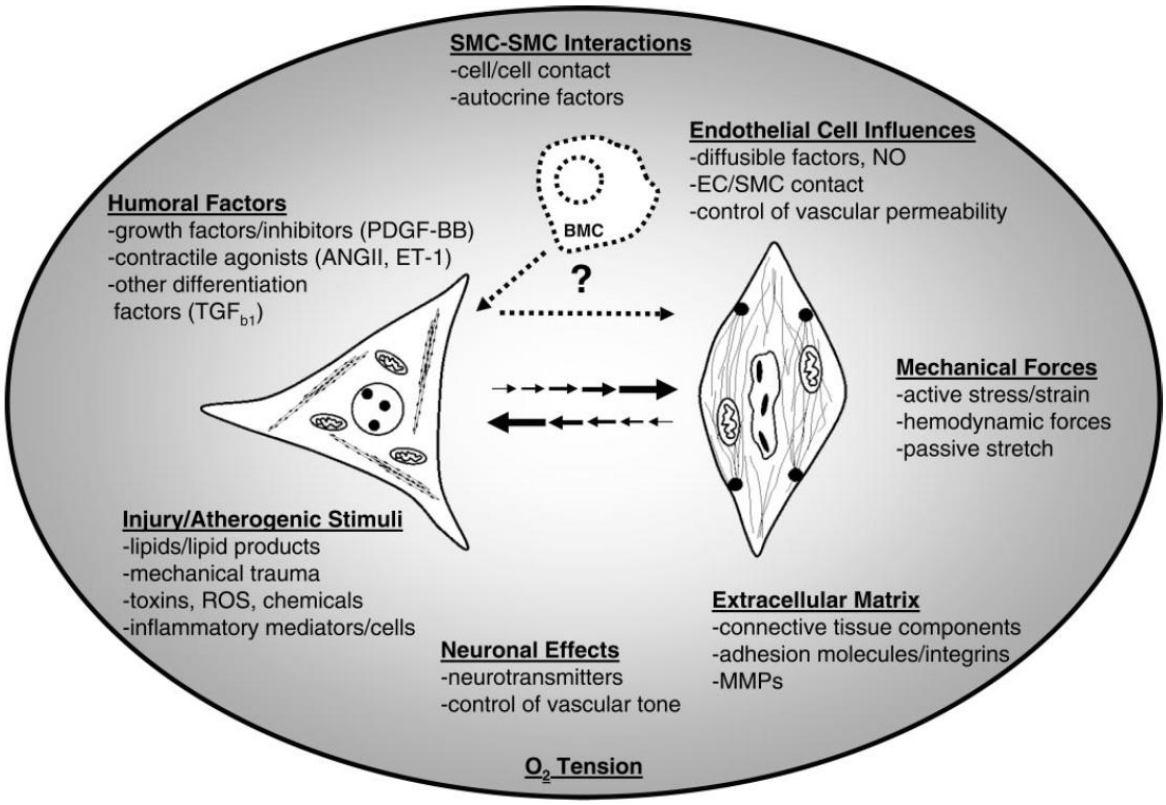

Figure 5: Représentation schématique des facteurs intervenant dans la différenciation des CMLV, d'après (122).

Les CMLV sont des cellules hautement plastiques qui vont pouvoir intégrer de nombreux signaux environnementaux. Ces signaux vont permettrent la différenciation cellulaire en phénotype synthétique (à gauche de la figure) et contractile (à droite de la figure). Cette transition n'est pas définitive et des changements phénotypiques sont possibles. Ces CMLV pourraient également provenir de progéniteurs médullaires, représentés en haut dans le schéma.

ANG: angiotensine ; BMC: cellules dérivées de la moelle osseuse ; EC: cellules endothéliales ; ET: endothéline ; MMP: métalloprotéases matricielles ; NO: monoxide d'azote

; PDGF: “platelet-derived growth factor” ; ROS:” formes réactives de l’oxygène” ; SMC : cellules musculaires lisses vasculaires ; TGF : “transforming growth factor”

L’ensemble de ces stimuli va conduire à une activation des MAP kinases, en particulier de JNK (c-jun amino-terminal protein kinase) et ERK (extracellular signal-regulated kinase), à modifier le profil d’expression des micro-RNA ou va encore moduler l’épigénétique même si les mécanismes sous-jacents restent parfois méconnus (156 , 157). L’ensemble participe à la régulation du phénotype et des caractéristiques des CMLV.

1.3.4. Etude des CMLV in vitro

Compte-tenu de la grande variabilité des CMLV, les recherches sont effectuées sur des cellules en culture primaire. Leur capacité proliférative permet habituellement de les utiliser jusqu’au 6 ou 7ème passage. Cependant, on observe des phénomènes de dédifférenciation et il a ainsi été mis en évidence que les CMLV de rats isolées de différents vaisseaux présentaient une baisse progressive de la rigidité cellulaire et une baisse du contenu en collagène lors des passages successifs (158). A notre connaissance, la seule lignée disponible a été établie à partir de CMLV d’artère mammaire humaine immortalisées après transduction séquentielle lentivirale de la sous-unité catalytique de l’holoenzyme humaine Telomerase Reverse Transcriptase et de l’antigène T du polyomavirus SV40 (Simian Virus 40) (159). C’est à partir de ces CMLV que nous avons pu identifier des auto-AC au cours de la sclérodermie systémique (ScS) et/ou de l’hypertension artérielle pulmonaire (HTAP) (160).

1.3.5. Les CMLV en condition pathologique

Les CMLV sont impliquées dans des pathologies aussi diverses et fréquentes que l’athérome, l’hypertension artérielle (HTA), le diabète mais également au cours de maladies rares telles que la ScS ou l’HTAP. Bien que les métastases soient hétérogènes et que la vascularisation repose parfois sur des capillaires dépourvus de CMLV, elles peuvent

également participer au développement des métastases (161). Au cours de ces différentes pathologies, les CMLV vont intégrer de très nombreux signaux liés aux interactions cellulaires, aux facteurs endothéliaux (146), aux forces mécaniques (162), aux facteurs de croissance humoraux (155)… La modulation phénotypique qui en résulte va alors conduire à un remodelage de la paroi artérielle parfois caractéristique d'une maladie : remodelage eutrophique ou hypertrophique au cours de l'HTA (163), lésions plexiformes au cours de l'HTAP (164) ou encore lésion en bulbe d'oignon au cours de la ScS (165)… D'autres cellules vont exprimer des marqueurs de différenciation des CMLV et participer au remodelage vasculaire et à l'épaississement pariétal ce qui souligne la compléxité des phénomènes de remodelage. Ainsi, les CE de microcirculation identifiées par leur expression de facteur VIII, de lectine et de LDL peuvent acquérir l'expression d'α-SMA en réponse à l'inhibition du récepteur au VEGF (166). Par ailleurs, les fibroblastes adventitiels peuvent également se différencier en myofibroblastes en condition hypoxique (167). Enfin, les cellules souches mésenchymateuses cocultivées avec des fibroblastes adventitiels ou des cellules endothéliales aquièrent également l'expression d'α-SMA (168) (169). L'ensemble de ces cellules participent donc au remodelage vasculaire et peuvent acquérir un phénotype VSMC like ou myofibroblastique. C'est également au cours de ces processus pathologiques et notamment au cours de l'athérome que les CMLV vont acquérir des marqeurs d'autres types cellulaires. Ainsi, les CMLV peuvent exprimer le « Bone morphogenetic protein endothelial cell precursor-derived regulator » ce qui entraîne la perte d'expression d'α-SMA, la synthèse des phosphatases alcalines et une minéralisation qui témoigne d'une différenciation ostéoblastique (170). La place des CMLV en pathologie sera abordée plus en détail au cours de l'HTAP, pathologie marquée par un remodelage vasculaire qui présente certaines similitudes avec celui observé au cours de l'ACG.

1.4. L'hypertension artérielle pulmonaire

L'HTAP est une maladie cardiovasculaire rare et grave conduisant à la dysfonction cardiaque droite et au décès (171). La prévalence est de l'ordre de 15 cas par million d'habitant en France avec cependant des variations régionales (172). L'hypertension pulmonaire (HTP) se définit par une pression moyenne dans l'artère pulmonaire ≥ 25 mm Hg lors du cathétérisme cardiaque droit. Une classification clinique a été effectuée et a permis d'identifier 5 groupes d'HTP partageant des mécanismes physiopathologiques, des données hémodynamiques et une prise en charge commune. On distingue ainsi l'HTAP (groupe 1), l'HTP secondaire à une insuffisance ventriculaire gauche (groupe 2), l'HTP secondaire à une hypoxie ou à une maladie pulmonaire (groupe 3), l'HTP chronique post-embolique (groupe 4) et l'HTP de mécanisme multiple et mal identifié (groupe 5) (173).

Au sein du groupe 1 (HTAP), on distingue (1) l'HTAP idiopathique ; (2) l'HTAP héritable au cours de laquelle de nombreuses mutations ont été rapportées ; (3) l'HTAP liée aux toxiques et anorexigènes ; (4) l'HTAP associée aux connectivites, au virus de l'immunodéficience humaine (VIH), à l'hypertension portale, aux schistosomiases et aux maladies cardiaques congénitales (173).

1.4.1. Données cliniques

Les symptômes, principalement l'asthénie et la dyspnée, sont peu spécifiques ce qui conduit à un délai diagnostic et 75% des patients au diagnostic ont une classe fonctionnelle de dyspnée de la New York Heart Association (NYHA) III ou IV (172). Le diagnostic formel repose sur le cathétérisme cardiaque droit avec mise en évidence d'une pression artérielle pulmonaire moyenne (PAPm) de repos ≥25 mm Hg, une pression capillaire <15 mm Hg. Au cours des 15 dernières années, 3 classes médicamenteuses à savoir les inhibiteurs des récepteurs de l'endothéline A et/ou B, les inhibiteurs des phosphodiestérases de type 5 (PDE5) et les analogues des prostacyclines ont été développées et sont utilisées seules ou en

association. Ces thérapies spécifiques ont permis une amélioration de la survie par rapport aux cohortes historiques (171, 174).

1.4.2. Physiopathologie de l'HTAP, les données du remodelage vasculaire

De nombreuses mutations ont été rapportées au cours de l'HTAP héritable et participent à la pathogénie. On décrit ainsi des mutations du « bone morphogenic protein receptor type 2 » (BMPR2), de l'« activin-like receptor kinase-1» (ALK1) (175), de l'« endoglin » (ENG) (176), de « mothers against decapentaplegic » (Smad) (177 , 178), de la cavéoline (179) et du canal potassique KCNK3 (180). Au-delà de ces mutations fréquentes, des mutations survenant au sein de familles restreintes ont permis d'identifier d'autres mécanismes impliqués dans la pathogénie et les recherches actuelles portent également sur la régulation de l'expression génique (181).

Les anomalies endothéliales sont précoces et pourraient précéder la muscularisation des artérioles pulmonaires distales (182). L'étude de l'inactivation du chromosome X sur les CE plaide en faveur d'une prolifération clonale des CE au cours de l'HTAP idiopathique alors qu'elle n'est pas retrouvée au cours des HTAP associée à une cardiopathie congénitale ou à la ScS (183). Par ailleurs, on retrouve au sein des lésions plexiformes une instabilité des microsatellites, des mutations sur le gène codant pour le transforming growth factor (TGF)-βRII (184), ainsi que de multiples mutations somatiques dans les CE ou les CMLV cultivées à partir d'explants pulmonaires de patients (185). Ces éléments sont en faveur d'une prolifération clonale avec des similitudes avec le cancer (186). Les CE ont des capacités prolifératives accrues et une résistance à l'apoptose induites par une sécrétion autocrine de fibroblast growth factor (FGF) (187) alors que la perte de fonction de BMPR2 conduit à une apoptose accrue de ces CE (188). Ces CE modifient leur métabolisme énergétique qui dépend de façon marquée de la glycolyse, ce qui témoigne d'altérations du métabolisme mitochondrial (189). Une augmentation de l'expression du récepteur de l'endothelium-

specific tyrosine kinase-2 (Tie 2) dans sa forme phosphorylée sur les CE va conduire à une augmentation de la production de sérotonine et induire la prolifération des CMLV (190). Par ailleurs, l'augmentation de l'activité de l'arginase 2 au sein des CE contribue à diminuer l'arginase, substrat de la NO synthase ce qui réduit l'effet vasodilatateur et anti-prolifératif du NO (191).

De nombreux autres éléments de la physiopathologie de l'HTAP impliquent les CMLV. Ainsi, la sérotonine et son transporteur pourraient contribuer à une activation de la voie du PDGF, élément majeur de la prolifération des CMLV (192). Par ailleurs, la sérotonine conduit à une augmentation de la protéine S100A4 qui induit la prolifération des CMLV (193). Alors que la signalisation via BMPR2 inhibe en condition physiologique le PDGF et l'EGF, son défaut conduit à une prolifération des CMLV en réponse à l'EGF et au BMP2. Par ailleurs, BMP2 régule l'activité transcriptionnelle de PPAR-γ et des gènes cibles APOE et adiponectine conduisant à une prolifération accrue des CMLV (194). Enfin le défaut de BMPR2 conduit également à une production accrue d'ostéoprotégérine et de tenascine-C (195, 196).

Au niveau de l'interstitium, les protéines de la matrice extra-cellulaire comme la fibronectine ou la tenascine-C et des médiateurs inflammatoires comme S100A4 ou fractalkine contribuent à l'hypertrophie pariétale (197 , 198).Enfin, des niveaux élevés d'élastase ont été documentés dans des modèles animaux d'HTAP et il a été mis en évidence que l'élastase leucocytaire humaine induisait le relargage du basic FGF (bFGF) stocké dans la matrice extracellulaire (199), ce qui conduit à la synthèse de MMP et de tenascine-C. L'inhibition de l'élastase dans un modèle murin d'HTAP permet la régression des lésions d'HTAP (200).

L'HTAP peut survenir dans un contexte infectieux (VIH, schistosomiase, HHV8…) ou dysimmunitaire (ScS, lupus érythémateux systémique…) ce qui est en faveur d'une

participation inflammatoire et immunitaire. L'accumulation adventitielle de monocytes/macrophages ayant des caractéristiques de fibroblastes (production de collagène ou d'α-SMA) est un élément du remodelage vasculaire dans un modèle d'HTAP hypoxique. Leur déplétion contribue à diminuer la production de tenascine-C ou de pro-collagène (201). Des cytokines pro-inflammatoires telles que l'IL1 ou l'IL6, MCP1 ainsi que leurs récepteurs ont été identifiées au sein d'explants pulmonaires de patients atteints d'HTAP subissant une transplantation pulmonaire (202). Par ailleurs, des auto-Ac dirigés contre les CE, les CMLV et les fibroblastes ont également été rapportés au cours de l'HTAP (160, 203 , 204) qui pourraient participer à la physiopathologie de la maladie (160). Enfin, la présence de follicules lymphoïdes tertiaires au sein de l'adventice des artérioles pulmonaires sur des explants pulmonaires de patients atteints d'HTAP idiopathique témoigne de la participation du système immunitaire adaptatif (205).

L'ensemble de ces éléments contribue, au cours de l'HTAP, au remodelage vasculaire, conduisant à une extension en distalité de la muscularisation des artères pulmonaires, à un épaississement des vaisseaux proximaux avec constitution d'une néo-intima et à une oblitération liée à l'épaississement néo-intimal observé.

1.4.3. Thérapeutiques ciblées au cours de l'hypertension artérielle pulmonaire (HTAP)

Les 3 classes thérapeutiques actuellement disponibles visent à cibler la dysfonction endothéliale. Celle-ci se caractérise par une diminution de la production de prostacyclines (PGI2), de NO et par l'augmentation de la synthèse d'ET-1. L'effet anti-proliférant sur les CMLV de la prostacycline délivrée par voie intra-veineuse continue ou de ses analogues stables a permis de réduire la mortalité de l'HTAP (206). Cependant, les difficultés de manipulation et de tolérance de ces traitements ont conduit à développer le selexipag, un agoniste des récepteurs de la prostacycline disponible par voie orale. L'évaluation de ce médicament montre des résultats encourageants (207). L'ET-1 a un rôle vasoconstricteur

puissant et des inhibiteurs du récepteur de l'endothéline de type A (ET_AR) ou B (ET_BR) ont été développés. Le bosentan, l'ambrisentan et le macitentan ont tous trois une efficacité démontrée au cours de l'HTAP (208-210). L'inhibition de la phosphodiestérase de type 5 entraîne une augmentation de la guanosine monophosphate cyclique (GMPc), avec pour conséquence une relaxation des CMLV et une inhibition de leur prolifération. Le sildénafil et le tadalafil ont tous deux une efficacité démontrée sur la distance parcourue lors du test de marche de 6 minutes (211, 212). Le riociguat, est une molécule activatrice de la guanylate cyclase soluble et contribue à la relaxation musculaire. Ce traitement a une efficacité sur la distance parcourue lors du test de marche de 6 minutes et a récemment obtenu une AMM dans le traitement de l'HTAP (213). D'autres thérapeutiques ont également été proposées dans l'HTAP, comprenant les antagonistes des récepteurs de la sérotonine ou les inhibiteurs de tyrosine kinase. Les premiers n'ont pas d'efficacité démontrée, tandis que les seconds avaient un certain degré d'efficacité sur le critère principal qui était le test de marche mais entrainaient des effets secondaires importants (213), ce qui a amené le laboratoire à renoncer à une demande d'AMM.

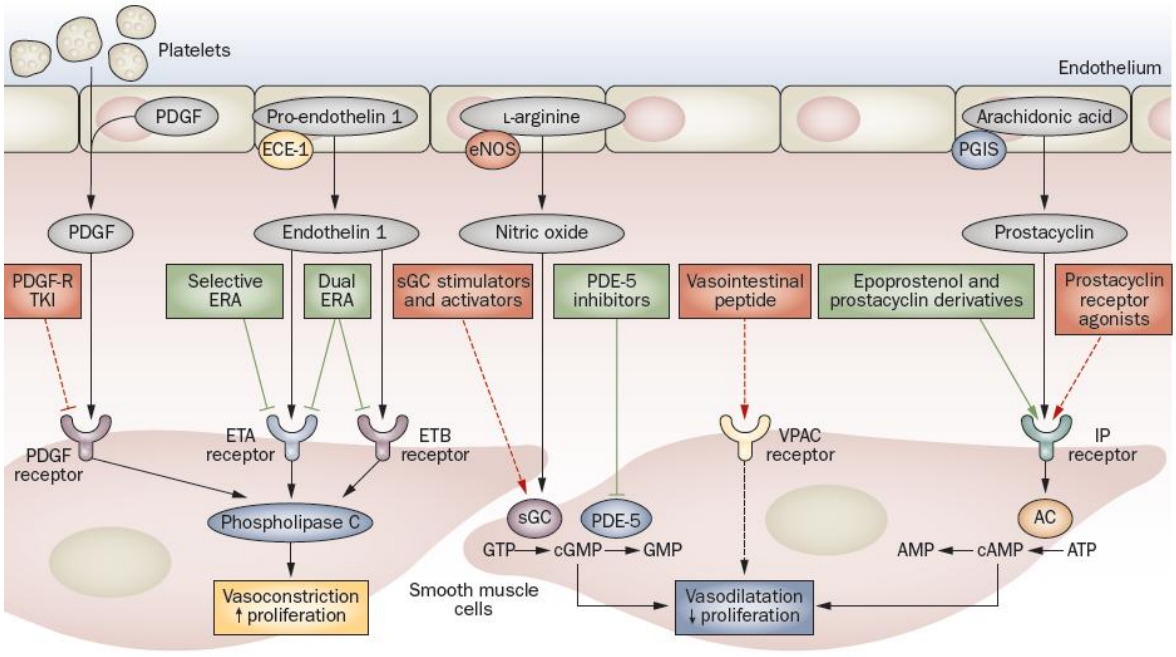

Figure 6 : Cibles thérapeutique actuelles et à venir au cours de l'HTAP. D'après (214).

Les cibles thérapeutiques de l'HTAP identifiées sur les CMLV d'artère pulmonaire et les médicaments correspondant sont représentées, dans des carrés verts pour les traitements reconnus et rouges pour les médicaments à l'étude. Les flèches indiquent une stimulation et les lignes terminées une inhibition.
Abréviations: AC : adénylate cyclase; cAMP : AMP cyclique; cGMP : GMP cyclique; ECE-1 : enzyme de conversion de l'endothéline 1; eNOS : NO synthase endothéliale ; ETA : récepteur de l'endothéline de type A; ETB : récepteur de l'endothéline de type B; ERA : antagonistes des récepteurs de l'endothéline; IP : prostaglandine I2; PDE-5 : phosphodiestérase de type 5; PDGF : facteur de croissance dérivé des plaquettes; PDGF-R TKI : inhibiteur de tyrosine kinase du récepteur au PDGF; PGIS : prostaglandine I synthase; sGC : guanylate cyclase soluble; VPAC : récepteur du peptide vasointestinal.

1.5. L'endothéline et ses récepteurs

L'ET-1 appartient à une famille de peptides de 21 acides aminés ayant un effet vasoconstricteur puissant (215). L'ET-1 est principalement sécrétée par l'endothélium vasculaire mais également par les CMLV et les macrophages (146). Deux récepteurs de l'endothéline, ET_AR et ET_BR, ont été identifiés : (i) l'ET_BR, principalement exprimé par les CE, a un rôle de vasodilatation transitoire en réponse au NO et prévient l'apoptose (216)(ii) l'ET_AR exprimé par les CMLV est responsable de la vasoconstriction (217), de la prolifération cellulaire (218 , 219) et de la migration cellulaire (220). Cependant, l'ET_BR a également été identifiée sur les CMLV avec des rôles similaires à l'ET_AR et pourrait amplifier les réponses à l'ET-1 (217). Près de 80% de l'ET-1 est synthétisée dans le compartiment baso-latéral des CE vers les CMLV et au sein de l'interstitium où la concentration peut être plus de 10 fois celle du plasma (221). Ainsi, l'ET-1 agit de façon autocrine et paracrine.

Divers stimuli modulent l'expression et la sécrétion de l'ET-1 parmi lesquelles le TGF-β1, l'IL1, l'angiotensine II ou les forces mécaniques liées au flux sanguin (222 , 223 , 224). L'ET-1 a des effets chémotactiques sur les macrophages (225), stimule l'adhésion des polynucléaires neutrophiles (226) et l'agrégation plaquettaire (227). Enfin, l'ET-1 stimule la production du TNF-α, du VEGF et du « basic-fibroblast growth factor-2 » (bFGF) (228 , 229) (223, 230) et potentialise l'effet du TGF-β et du PDGF (231).

Au cours de l'ACG, des taux élevés d'ET-1, ET_AR et ET_BR ont été retrouvés au niveau protéique au sein des artères temporales alors que les mRNA étaient diminués par rapport à une population contrôle (119). En immuno histochimie, des taux élevés d'ET_BR n'ont pas été confirmés (232). Au niveau plasmatique, un taux élevé d'ET-1 pourrait être associé à un risque visuel accru (119, 233).

2. Objectifs

Dans un premier temps, nous avons voulu identifier des auto-Ac dirigés contre les CE et les CMLV dans le sérum de patients atteints d'ACG. Ces auto-Ac pourraient être utilisés en pratique clinique comme marqueur diagnostique ou pronostique au cours de l'ACG. Nous avons identifié leurs cibles par immunoblot bi-dimensionnel couplé à la spectrométrie de masse (MS).

La modification du répertoire d'auto-Ac au cours de l'ACG, pourrait être un élément participant à la pathogénie de la maladie ou être le reflet du remodelage vasculaire intervenant dans l'artère temporale, les deux possibilités n'étant pas mutuellement exclusives. C'est dans cette optique que nous avons cherché à aborder les mécanismes du remodelage vasculaire au cours de l'ACG. Nous avons tout d'abord cherché à étudier la variabilité de CMLV en condition physiologique (à l'aide d'HAoSMC, HPASMC et HUASMC) et en condition pathologique, avec des CMLV isolées au moment d'une transplantation pulmonaire d'explants pulmonaires de patients atteints d'HTAP, maladie marquée par un remodelage vasculaire. Nous avons étudié cette variabilité à l'aide d'une approche protéomique par électrophorèse différentielle bi-dimensionnelle en gel (2D-DIGE). Enfin, nous avons isolé les CMLV à partir de BAT réalisées pour suspicion d'ACG et confirmé leur phénotype par immunofluorescence. A partir de cette collection unique, nous avons étudié le contenu protéique et le profil d'expression transcriptomique des CMLV en fonction du diagnostic final: ACG histologiquement prouvée, ACG sans preuve histologique ou autre diagnostique. Deux approches complémentaires ont été utilisées avec la 2D-DIGE et des puces d'expression pan génomique. A terme, le but est d'identifier les éléments qui contribuent au remodelage vasculaire afin de proposer de cibler les molécules clés à l'aide de thérapeutiques innovantes qui pourraient permettre de prévenir la survenue de complications ischémiques chez les patients atteints d'ACG.

3. Résultats

3.1. Identification des cibles antigéniques des anticorps anti cellules musculaires lisses vasculaires et anti-cellules endothéliales au cours de l'artérite à cellule géante

Alexis Régent, Hanadi Dib, Kim H Ly, Christian Agard, Mathieu C Tamby, Nicolas Tamas, Babette Weksler, Christian Federici, Cédric Broussard, Loïc Guillevin et Luc Mouthon

Régent et al. Arthritis Research & Therapy 2011, 13:R107

Les études immunologiques réalisées au cours de l'artérite à cellules géantes suggèrent qu'un antigène d'origine inconnue déclenche une réaction immunitaire spécifique. La recherche d'un agent infectieux qui agirait comme facteur déclenchant n'a pas aboutie. Nous avons donc décidé de rechercher des auto-Ac dirigés contre les CE et les CMLV dans le sérum des patients atteints d'ACG afin de rechercher un biomarqueur qui pourrait avoir un intérêt diagnostique ou pronostique.

Pour cela, les sérums de 15 patients atteints d'ACG ont été testés en 5 pools de 3 patients et comparés à un pool de 12 sujets sains. Les réactivités IgG ont été recherchées par immunoblot-2D à partir d'extraits protéiques d'HUVEC et de CMLV et les antigènes cibles ont été identifiés par MS.

Nous avons pu mettre en évidence que les IgG sériques de patients atteints d'ACG reconnaissaient 162±3 (moyenne±déviation standard (SD)) et 100±17 (moyenne±SD) spots protéiques d'HUVEC et de CMLV respectivement alors que les sujets sains reconnaissaient 79 et 94 spots protéiques respectivement. Au total, 30 spots d'HUVEC et 19 spots de CMLV ont été reconnus par au moins 2/3 et 3/5 respectivement des pools de sérums de patients atteints d'ACG et pas par les sujets sains. Parmi les protéines identifiées, on trouve la vinculine, la lamine A/C, la protéine « voltage-dependent anion-selective channel protein 2 »,

l'annexine 5 et d'autres protéines impliquées dans le métabolisme énergétique et dans des processus cellulaires clés. L'analyse à l'aide du logiciel Ingenuity® a montré que beaucoup d'antigènes identifiés comme cible d'auto-Ac interagissaient avec la protéine « growth factor receptor-bound protein 2 » (Grb2), une protéine impliquée dans la réponse aux facteurs de croissance.

Au total, des Ac de type IgG sont présents dans le sérum des patients atteints d'ACG et reconnaissent des antigènes de CE et de CMLV. Ces antigènes participent à des fonctions cellulaires clés mais leur rôle pathogène nécessite d'être déterminé.

Régent et al. Arthritis Research & Therapy 2011, 13:R107
http://arthritis-research.com/content/13/3/R107

arthritis research&therapy

RESEARCH ARTICLE Open Access

Identification of target antigens of anti-endothelial cell and anti-vascular smooth muscle cell antibodies in patients with giant cell arteritis: a proteomic approach

Alexis Régent[1,2,3], Hanadi Dib[1,2], Kim H Ly[1,2,4†], Christian Agard[5†], Mathieu C Tamby[1,2], Nicolas Tamas[1,2], Babette Weksler[6], Christian Federici[1,2], Cédric Broussard[7], Loïc Guillevin[2,3] and Luc Mouthon[1,2,3*]

Abstract

Introduction: Immunological studies of giant cell arteritis (GCA) suggest that a triggering antigen of unknown nature could generate a specific immune response. We thus decided to detect autoantibodies directed against endothelial cells (ECs) and vascular smooth muscle cells (VSMCs) in the serum of GCA patients and to identify their target antigens.

Methods: Sera from 15 GCA patients were tested in 5 pools of 3 patients' sera and compared to a sera pool from 12 healthy controls (HCs). Serum immunoglobulin G (IgG) reactivity was analysed by 2-D electrophoresis and immunoblotting with antigens from human umbilical vein ECs (HUVECs) and mammary artery VSMCs. Target antigens were identified by mass spectrometry.

Results: Serum IgG from GCA patients recognised 162 ± 3 (mean ± SD) and 100 ± 17 (mean ± SD) protein spots from HUVECs and VSMCs, respectively, and that from HCs recognised 79 and 94 protein spots, respectively. In total, 30 spots from HUVECs and 19 from VSMCs were recognised by at least two-thirds and three-fifths, respectively, of the pools of sera from GCA patients and not by sera from HCs. Among identified proteins, we found vinculin, lamin A/C, voltage-dependent anion-selective channel protein 2, annexin V and other proteins involved in cell energy metabolism and key cellular pathways. Ingenuity pathway analysis revealed that most identified target antigens interacted with growth factor receptor-bound protein 2.

Conclusions: IgG antibodies to proteins in the proteome of ECs and VSMCs are present in the sera of GCA patients and recognise cellular targets that play key roles in cell biology and maintenance of homeostasis. Their potential pathogenic role remains to be determined.

Introduction

Giant cell arteritis (GCA), also known as temporal arteritis, is a primary systemic vasculitis involving large- and medium-sized vessels. GCA commonly causes bitemporal headaches, jaw claudication, scalp tenderness and/or abnormal temporal arteries (tender, nodular, swollen and thickened arteries with decreased pulses) detected during physical examinations. GCA does not occur in people younger than 50 years old, and its incidence increases with age and peaks in Caucasians older than 70 years of age [1,2]. Ocular ischaemic complications occur in 25% of the patients and leads to irreversible visual loss in 15% [3]. No definite immunological marker has been identified in GCA, and patients usually present with increased erythrocyte sedimentation rates and/or C-reactive protein levels. Diagnosing GCA can be difficult, and temporal artery biopsy is the gold standard for making the diagnosis [4]. However, in 10% to 20% of patients with GCA, the biopsy shows no specific change [5].

* Correspondence: luc.mouthon@cch.aphp.fr
† Contributed equally
[1]Inserm U1016, Institut Cochin, CNRS UMR 8104, 8 rue Méchain, F-75014 Paris, France
Full list of author information is available at the end of the article

GCA is an inflammatory condition of unknown origin characterised by the presence of giant cells and a remodelling process in the arterial wall [6]. In patients with GCA, an immune-mediated reaction is suspected to be triggered by an antigen of unknown origin, either microbial or a self-antigen, that could be presented to T cells by dendritic cells [7]. Thus, macrophages and giant cells stimulated by interferon-γ (IFN-γ) play a major role in the disruption of the elastic lamina and the remodelling of vessel walls. In addition, in the adventitia, macrophages produce proinflammatory cytokines such as interleukin 1 (IL-1) and IL-6, whereas in the media and intima they contribute to arterial injury by producing metalloproteinases and nitric oxide [6,8,9].

Anti-endothelial cell (anti-EC) antibodies (AECAs) have been detected in a wide range of systemic inflammatory and/or autoimmune diseases, including primary and/or secondary systemic vasculitis [10]. Although the pathogenic role of AECAs remains controversial [11,12], these antibodies may be responsible for EC activation [13] and induction of antibody-dependent, cell-mediated cytotoxicity and apoptosis [14]. In GCA, AECAs were detected in 33% of sera by performing ELISA on fixed human umbilical vein ECs (HUVECs) [15], but their presence was not confirmed by indirect immunofluorescence [16]. Anti-vascular smooth muscle cell (anti-VSMC) antibodies have been detected in an experimental rat model of vasculitis [17]; however, to our knowledge, these antibodies have not been investigated in patients with primary systemic vasculitis.

We used 1-D and 2-D immunoblotting, followed by mass spectrometry (MS), to investigate the presence of autoantibodies directed against ECs and VSMCs and identify their target antigens in patients with GCA.

Materials and methods

Patients

Serum samples were obtained from 15 patients who fulfilled the American College of Rheumatology (ACR) criteria for GCA [4] and 33 patients with anti-neutrophil cytoplasm antibody (ANCA)-associated vasculitis who fulfilled the ACR and the Chapel Hill criteria used as vasculitis controls, with the control group comprising 15 patients with Wegener's granulomatosis (WG), 9 with Churg-Strauss syndrome (CSS) and 9 with microscopic polyangiitis (MPA) [18]. In each group of patients with ANCA-associated vasculitis, two-thirds of the patients had active disease as assessed by a Birmingham Vasculitis Activity Score (BVAS) >3 in the absence of treatment, and one-third of the patients had inactive disease as assessed by a BVAS <3. Some patients in both groups either received corticosteroids and/or immunsuppressants at the time of blood sampling. Sera from 12 healthy blood donors were used as healthy controls (HCs). Serum samples were collected from patients and HCs, aliquoted and stored at -80°C until use. Serum samples were used individually for 1-D immunoblotting and pooled for 2-D immunoblotting (five pools of sera from three patients with GCA each, and one pool of sera from twelve HCs). All patients and healthy controls gave their written informed consent to participate in the study. Serum samples were collected with the approval of the ethics committee of the groupe hospitalier Pitié-Salpêtrière, and the study conformed to the principles outlined in the Declaration of Helsinki.

Cell culture

Human internal mammary artery VSMCs were obtained from patients undergoing aortocoronary bypass surgery. All patients gave their written consent, and the protocol for waste surgical tissue was approved by the ethics committee of groupe hospitalier Pitié-Salpêtrière. These cells were immortalised by transduction of a lentiviral vector incorporating the catalytic subunit of the human holoenzyme telomerase RT and T antigen of simian virus 40 in a primary culture of VSMCs as previously described [19]. Immortalised VSMCs were cultured in Smooth Muscle Cell Basal Medium (PromoCell, Heidelberg, Germany) supplemented with decomplemented FCS (5%), insulin (5 μg/mL), basic fibroblast growth factor (bFGF) (2 ng/mL), epidermal growth factor (EGF) (0.5 ng/ml), streptomycin/penicillin (1%) and ciprofloxacin (1%) at 37°C in 5% CO_2. The VSMC phenotype was confirmed by using smooth muscle myosin heavy chains 1 and 2 and sm22α antibodies (Abcam, Cambridge, UK) (data not shown).

HUVECs were isolated from sterile, freshly obtained umbilical cords at the time of a normal delivery by using 15 mg/mL collagenase type I digestion as previously described [20,21]. All donors gave their written consent. HUVECs were cultured with EC medium (PromoCell) supplemented with decomplemented FCS (2%), bFGF (1 ng/mL), EGF (0.1 ng/mL), EC growth supplement/heparin (0.4%), hydrocortisone (1 μg/mL), streptomycin/penicillin (1%) and ciprofloxacin (1%) at 37°C in 5% CO_2. HUVECs from four donors were harvested after the third passage to perform protein extraction.

One-dimensional immunoblotting

Confluent VSMCs were detached with the use of 0.05% trypsin and 0.53 mM ethylenediaminetetraacetic acid. Protein extract was obtained by use of a 125 mM Tris, pH 6.8, solution containing 4% SDS, 1.45 M β-mercaptoethanol, 1 μg/mL aprotinin, 1 μg/mL leupeptin, 1 μg/mL pepstatin and 1 mM phenylmethylsulphonyl fluoride (PMSF). Protein extract was then sonicated four times for 30 seconds each and boiled. In total, 120 μL of solubilised proteins were separated by electrophoresis on

10% SDS-PAGE gels (Bio-Rad Laboratories, Hercules, CA, USA), transferred onto nitrocellulose membranes by using a semidry electroblotter (model A; Ancos, Hojby, Denmark) and incubated with sera from patients with GCA, WG, CSS and MPA or from healthy donors at a 1:100 dilution overnight at 4°C with the Cassette Miniblot System (Immunetics Inc., Cambridge, MA, USA). Detection of IgG reactivity was carried out as previously reported [22-24] (Additional file 1) with the use of a γ-chain-specific secondary rabbit anti-human IgG antibody coupled to alkaline phosphatase. Immunoreactivity was revealed by Nitro Blue Tetrazolium/5-bromo-4-chloro-3-indolyl phosphate staining (Sigma-Aldrich, St. Louis, MO, USA) as previously reported [23,24] (Additional file 1) and quantified by densitometry in reflective mode (Epson Perfection 1200 S densitometer; Seiko Epson Corp., Nagano-ken, Japan) and scanned again to quantify transferred proteins [23,24].

Two-dimensional immunoblotting

Protein extracts

HUVECs and VSMCs were stored at -80°C in 1 mM PMSF and protease inhibitors (Complete Mini; Roche Diagnostics, Meylan, France). Protein extraction was performed as described previously [25] (Additional file 1). Briefly, cells were suspended at 1×10^6/mL in a sample solution extraction kit (Kit 3; Bio-Rad Laboratories). Cell samples were sonicated, and the supernatant was collected after ultracentrifugation (Optima L90-K ultracentrifuge; Beckman Coulter, Fullerton, CA, USA) at 150,000 × *g* for 25 minutes at 4°C. Protein quantification was carried out using the Lowry method [26]. The supernatant was aliquoted and stored at -80°C.

Two-dimensional electrophoresis

Two-dimensional electrophoresis (2-DE), 2-D immunoblotting and protein identification by MS were performed as previously reported [27] and are detailed in Additional file 1.

Modelling with the use of ingenuity pathway analysis software

To gain insight into the biological pathways and networks that were significantly represented in our proteomic data sets, we used ingenuity pathway analysis software (IPA; Ingenuity Systems, Redwood City, CA, USA). IPA selects 'focus proteins' to be used for generating biological networks. Focus proteins are the proteins from data sets that are mapped to corresponding gene objects in the Ingenuity Pathway Knowledgebase (IPKB) and are known to interact with other proteins on the basis of published, peer-reviewed content in the IPKB. From these interactions, IPA builds networks with a size of no more than 35 genes or proteins. A *P* value for each network is calculated according to the fit of the user's set of significant genes and/or proteins. IPA computes a score for each network from the *P* value that indicates the likelihood of the focus proteins in a network being found together by chance. We selected only networks scoring ≥ 2 with $P < 0.01$ of not being generated by chance. Biological functions were assigned to each network by use of annotations from the scientific literature and stored in the IPKB. Fisher's exact test was used to calculate the *P* value to determine the probability of each biological function and/or disease or pathway being assigned by chance. We used $P \leq 0.05$ to select highly significant biological functions and pathways represented in our proteomic data sets. The build function of IPA allows the generation of pathways that can complete the data analysis by showing interactions of identified proteins with a specific group of molecules [28,29].

Results

The clinical and histological characteristics of patients with GCA are summarised in Additional file 2, Supplemental Table S1. The mean age (± SD) of the patients with GCA was 74.8 ± 8.15 years. Among the 15 patients (5 men), 13 had histological evidence of GCA. All the 15 patients had active disease at the time of blood sampling: twelve were included at the time of diagnosis, two experienced a disease relapse and another one had an acute flare while being treated with prednisone. None of the other 14 patients were taking corticosteroids at the time of blood sampling.

One-dimensional immunoblotting of IgG reactivity against VSMC protein extracts

One-dimensional immunoblots of IgG reactivity were analysed with VSMC protein extracts in sera from patients with GCA; control patients with ANCA-associated vasculitis, including those with WG, MPA and CSS; and HCs. All subjects tested expressed an IgG reactivity band directed against a 45-kDa protein. In patients with GCA, a number of IgG reactivities were expressed that were not identified in patients with ANCA-associated vasculitis or in HCs, including reactivities directed against protein bands of 85 kDa (Additional file 3).

Two-dimensional immunoblotting of IgG reactivity against VSMC protein extracts

The proteome of VSMCs contained 1,427 different proteins ranging from 3 to 10 isoelectrofocalisation points (IPs) and from 10 to 250 kDa. Among those, a mean (± SD) of 679 ± 258 protein spots were detected after being transferred onto polyvinylidene fluoride (PVDF) membranes. Serum IgG from the HC pool recognised 94 protein spots, whereas IgG from the 5 pools from

GCA patients recognised a mean (± SD) of 100 ± 17 protein spots corresponding to a total of 268 different protein spots. Most of these 268 protein spots were recognised from only 1 or 2 pools from patients with GCA and/or from the HC pool. Among these protein spots, 29 were recognised by at least three-fifths of the pools from GCA patients, including 19 not recognised by the HC pool (Additional file 4, Supplemental Table S2). These 19 protein spots were identified by MS as detailed in Table 1 and Additional file 5. The localisations of identified protein spots in the analytical gel are depicted in Figure 1. Among these proteins, only one, the far upstream element-binding protein 2 (FUBP2) (Figure 2), was recognised in all five pools of sera from

Table 1 Mass spectrometry data of vascular smooth muscle cell protein spots identified as specific target antigen[a]

Spot ID	Protein	SwissProt accession number	Theoretical/ estimated MW, kDa	Theoretical/ estimated pI	Number of unique identified peptides[c, d]	Total ion score[d]	Best ion score[d]	Sequence coverage, %[d]
173	Vinculin	[Swiss Prot: VINC_HUMAN]	124/122	5.5/6.4	3/14	39	19	19
294	Putative heat shock protein HSP90, subunit α_2[b]	[Swiss Prot: HS902_HUMAN]	39/94	4.6/5.6	1/5	40	40	22
340	Far upstream element-binding protein 2	[Swiss Prot: FUBP2_HUMAN]	73/88	6.8/7.2	4-2/10-9	67-46	24-32	21-16
341	Far upstream element-binding protein 2	[Swiss Prot: FUBP2_HUMAN]	73/88	6.8/7.4	5-5/12-11	84-119	24-35	25-19
344	Far upstream element-binding protein 2	[Swiss Prot: FUBP2_HUMAN]	73/88	6.8/7.8	4/11	85	37	22
580	Lamin A/C[b]	[Swiss Prot: LMNA_HUMAN]	74/67	6.6/6.5	1/10	24	24	16
	Coatomer subunit α[b]	[Swiss Prot: COPA_HUMAN]	138/67	7.7/6.5	1/3	37	37	3
598	UDP-glucose 6-dehydrogenase[b]	[Swiss Prot: UGDH_HUMAN]	55/66	6.6/6.7	2/4	46	39	11
609	No identified protein		/66	/5.9				
683	No identified protein		/60	/5.8				
686	Protein disulphide-isomerase A3	[Swiss Prot: PDIA3_HUMAN]	57/59	6.0/6.1	11-11/16-17	1,048-804	140-106	42-44
694	Protein disulphide-isomerase A3	[Swiss Prot: PDIA3_HUMAN]	57/59	6.0/6.3	8-8/14-13	460-362	86-63	38-35
702	No identified protein		/59	/7.6				
734	T-complex protein 1, subunit β	[Swiss Prot: TCPB_HUMAN]	57/57	6.0/6.5	8-12/14-14	503-519	121-121	39-40
852	No identified protein		/51	/5.2				
877	No identified protein		/49	/7.0				
918	ANKRD26-like family C member 1A	[Swiss Prot: A26CA_HUMAN]	121/47	5.8/5.7	3-4/6-6	242-251	97-107	9-7
	Actin cytoplasmic 1	[Swiss Prot: ACTB_HUMAN]	42/47	5.3/5.7	5/10	390	131	53
	Actin cytoplasmic 2	[Swiss Prot: ACTG_HUMAN]	42/47	5.3/5.7	7/9	418	107	38
953	26S protease regulatory subunit 8	[Swiss Prot: PRS8_HUMAN]	46/46	7.1/7.6	9-2/15-7	180-53	41-31	45-21
	Mitochondrial import receptor subunit TOMM40 homolog	[Swiss Prot: TOM40_HUMAN]	38/46	6.8/7.6	1-1/2-4	48-66	48-38	7-15
	Fumarate hydratase mitochondrial precursor[b]	[Swiss Prot: FUMH_HUMAN]	55/46	8.9/7.6	1/3	61	61	7
1108	Nucleophosmin	[Swiss Prot: NPM_HUMAN]	33/39	4.6/5.1	3-4/5-5	83-203	39-65	24-25
1216	Annexin A2	[Swiss Prot: ANXA2_HUMAN]	39/35	7.6/8.0	11-13/8-10	650-265	99-51	45-38

[a]MW: molecular weight, pI: isoelectric point, ANKRD26: ankyrin repeat domain-containing protein 26, TOMM40: translocase of outer mitochondrial membrane 40 homolog (yeast). [b]Only one peptide of the protein was recognised by matrix-assisted laser desorption ionization time-of-flight/time-of-flight mass spectrometry; identification spectrum for each protein spot is given in Additional file 5;[c]indicate number of unique identified peptides in MSMS and in MS+MSMS searches; [d]identification was performed twice. When available, both values are given.

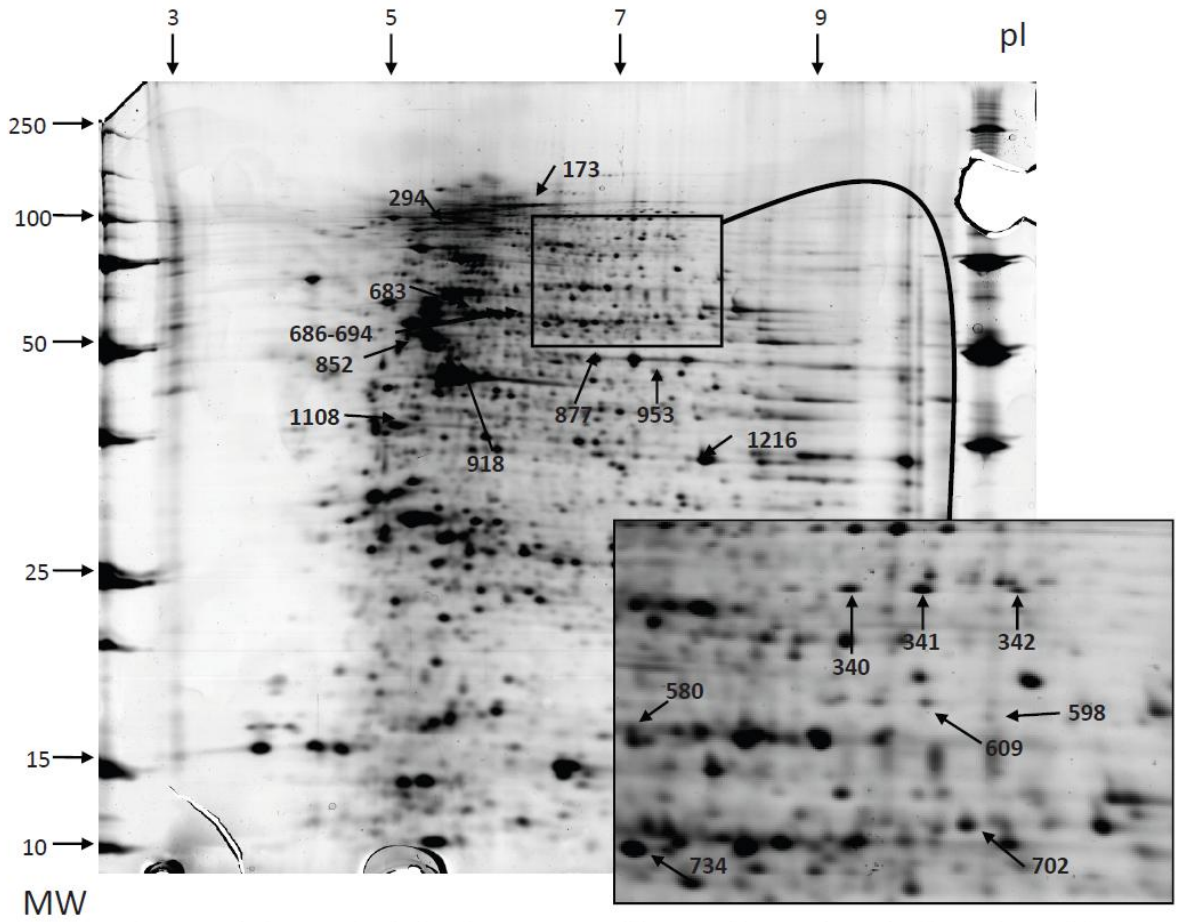

Figure 1 Two-dimensional silver-stained gel of total protein extracted from vascular smooth muscle cells. Localisation of the 19 IgG-reactive spots recognised by three-fifths of the pools of sera from giant cell arteritis patients. Numbers were arbitrarily assigned by a computer program. Inset: Enlarged area ranging from 6.5 to 8.2 isoelectric points and 50 to 110 kDa. MW: molecular weight, pI: isoelectric points.

GCA patients, whereas three different proteins were identified in four pools of sera from GCA patients: actin cytoplasmic 1, actin cytoplasmic 2 and ANKRD26-like family C member 1A (Additional file 4, Supplemental Table S2). Interestingly, IgG from pools of sera from each of three GCA patients recognised lamin A/C (Figure 3) and vinculin (Additional file 6).

IgG reactivity against HUVEC protein extracts

The proteome of HUVECs contains 820 different proteins ranging from 3 to 10 IP and from 10 to 250 kDa. Among these, a mean (± SD) of 515 ± 73 protein spots were successfully detected after transfer onto PVDF membranes. Serum IgG from the HC pool recognised 79 protein spots, whereas IgG from the 3 pools of GCA patients recognised a mean (± SD) of 162 ± 3 protein spots corresponding to 191 different protein spots. Most of these 191 protein spots were recognised in only 1 pool of IgG from GCA patients and/or were also recognised in the HC pool. Among these protein spots, 45 were recognised in at least two-thirds of pools from GCA patients, including 30 that were not recognised in the HC pool (Additional file 7, Supplemental Table S3). Of these 30 proteins, 22 were identified by matrix-assisted laser desorption ionization time-of-flight/time-of-flight MS. Complete MS data are shown in Table 2. Localisations of identified protein spots in the analytical gel are depicted in Figure 4. Overall, three proteins were recognised by IgG in sera from GCA patients in HUVEC and VSMC protein extracts: mitochondrial fumarate hydratase, lamin A/C and vinculin. IgG reactivity against vinculin and lamin A/C in sera from GCA patients and the HC pool are depicted in Figure 5 and Additional file 8 respectively.

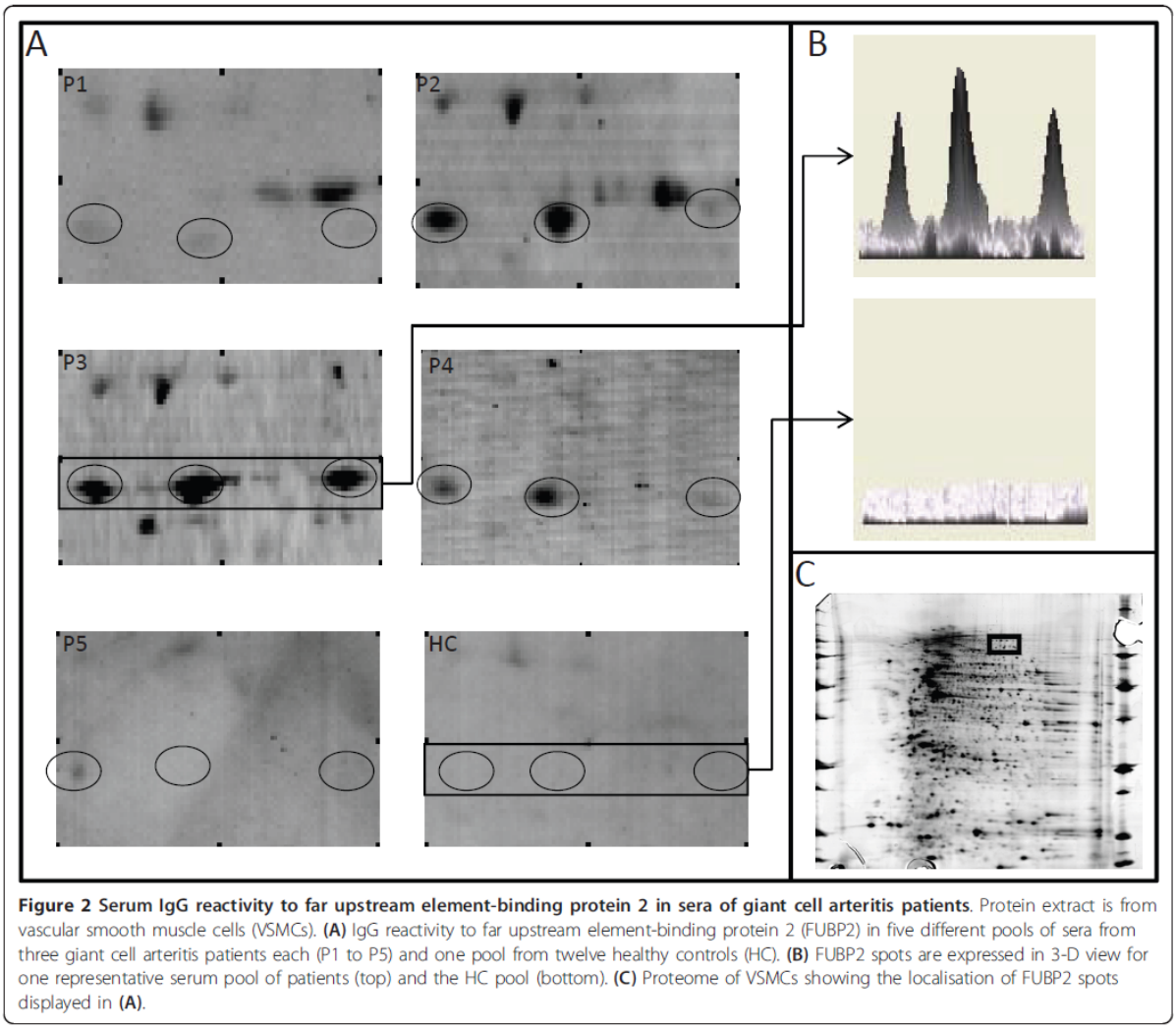

Figure 2 Serum IgG reactivity to far upstream element-binding protein 2 in sera of giant cell arteritis patients. Protein extract is from vascular smooth muscle cells (VSMCs). **(A)** IgG reactivity to far upstream element-binding protein 2 (FUBP2) in five different pools of sera from three giant cell arteritis patients each (P1 to P5) and one pool from twelve healthy controls (HC). **(B)** FUBP2 spots are expressed in 3-D view for one representative serum pool of patients (top) and the HC pool (bottom). **(C)** Proteome of VSMCs showing the localisation of FUBP2 spots displayed in **(A)**.

Biological network analysis of identified autoantibody specificities

Lists of VSMC and HUVEC proteins specifically recognised and/or recognised with high intensity by IgG in sera from GCA patients were analysed with IPA. Interestingly, most of the VSMC and HUVEC proteins specifically recognised and/or recognised with high intensity interacted with growth factor receptor-bound protein 2 (Grb2), a protein involved in VSMC proliferation. Therefore, we could depict the signalling network between HUVEC and VSMC proteins identified as major targets of autoantibodies in patients with GCA (Figure 6). Interestingly, TNF-α, IL-4 (Figure 6) and other molecules such as platelet-derived growth factor and IFN-γ (Additional file 9) were also involved in this signalling network.

Discussion

In the present work, we detected IgG antibodies directed against the proteome of VSMCs and HUVECs in the sera of patients with GCA and identified their target antigens by using a 2-D immunoblotting technique and MS.

Few studies have focused on perturbations of the humoral immune system in patients with GCA. Few B lymphocytes are detected in temporal artery biopsies from patients with GCA [30]. When present, they are mainly found in the adventitial layer [31]. Moreover, plasma cells can be found in the adventitia in 7% to 24% of temporal artery biopsies from patients with GCA [32]. Plasma cells might localise in adventitia because of an infectious agent initiating vascular inflammation. However, a number of studies failed to identify an

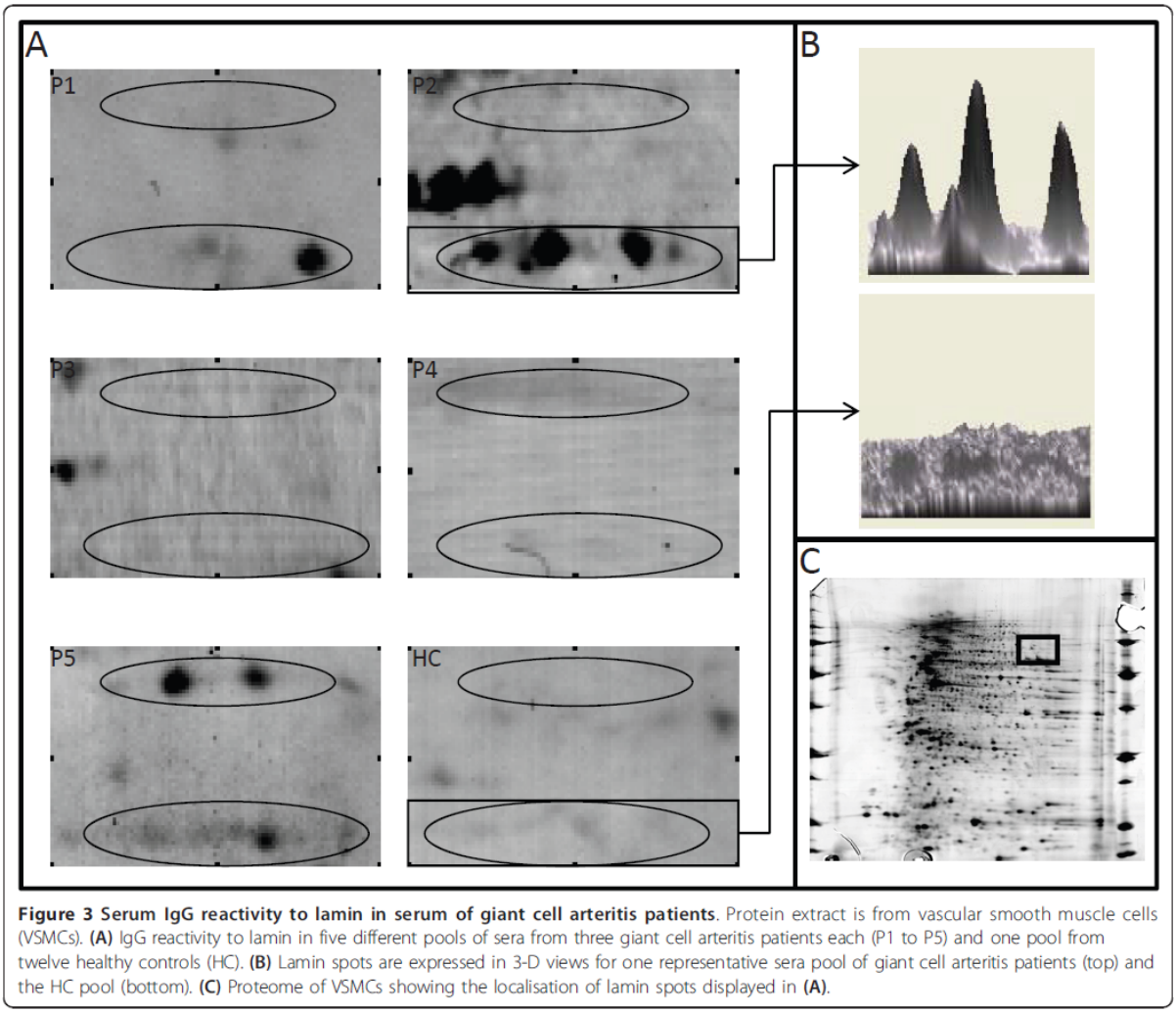

Figure 3 Serum IgG reactivity to lamin in serum of giant cell arteritis patients. Protein extract is from vascular smooth muscle cells (VSMCs). **(A)** IgG reactivity to lamin in five different pools of sera from three giant cell arteritis patients each (P1 to P5) and one pool from twelve healthy controls (HC). **(B)** Lamin spots are expressed in 3-D views for one representative sera pool of giant cell arteritis patients (top) and the HC pool (bottom). **(C)** Proteome of VSMCs showing the localisation of lamin spots displayed in **(A)**.

infectious agent, either a virus or bacteria, in the arterial wall by immunohistochemistry or PCR [33]. Alternatively, an autoantigen present in the arterial wall might trigger a specific immune response in GCA.

AECAs have been detected in healthy individuals [34] and in a number of systemic autoimmune diseases [10,35]. AECAs have been associated with disease activity in patients with vasculitis, particularly in those with anti-ANCA-associated vasculitis, Takayasu's arteritis or GCA [15], although these data remain controversial [36]. In addition, AECA could induce EC apoptosis in patients with systemic sclerosis [37]. However, the pathogenic role of AECAs has not yet been documented in GCA, and further investigations are necessary in this clinical setting.

Although to our knowledge anti-VSMC antibodies have not yet been reported in a human disease, such antibodies have been identified in a mouse model of vasculitis. Baiu *et al*. [17] showed that splenic mouse lymphocytes cultured with syngenic VSMCs induced vasculitic lesions after adoptive transfer into these mice. Serum collected from mice with vasculitis contained antibodies directed against VSMCs. Both wild-type and B-cell-deficient mice showed vascular inflammation after serum transfer, but mice deficient in both B and T cells ($Rag2^{-/-}$) Yes it should did not, which suggests that immunoglobulin and cell-mediated pathways, particularly T cells, work in concert to contribute to the vasculitis lesions in this model. Thus, autoantibodies targeting proteins in the proteome of VSMCs might play a role in the pathogenesis of GCA, and their function needs to be further explored.

Few studies have been conducted to identify the potential targets of autoantibodies in GCA. Screening antigens in a cDNA library derived from normal human testis revealed high-intensity serum IgG reactivity

Table 2 Mass spectrometry data of the endothelial cell protein spots identified as specific target antigens[a]

Spot ID	Protein	SwissProt accession number	Theoretical/ estimated MW, kDa	Theoretical/ estimated pI	Number of unique identified peptides[c]	Total ion score	Best ion score	Sequence coverage, %
228	Vinculin	[Swiss Prot: VINC_HUMAN]	124/116	5.5/6.6	3/13	53	34	15
461	Lamin A/C	[Swiss Prot: LMNA_HUMAN]	74/80	6.6/7.3	11/23	573	82	39
	Semaphorin-4D precursor	[Swiss Prot: SEM4D_HUMAN]	96/80	8.3/7.3	2/2	44	29	2
476	Ezrin	[Swiss Prot: EZRI_HUMAN]	69/79	5.9/7.0	2/8	92	58	13
	Moesin	[Swiss Prot: MOES_HUMAN]	67/79	6.1/7.0	3/12	186	96	19
	Lamin A/C	[Swiss Prot: LMNA_HUMAN]	74/79	6.6/7.0	8/21	314	70	37
	Radixin	[Swiss Prot: RADI_HUMAN]	68/79	6.0/7.0	2/6	92	58	10
	Semaphorin-4D precursor	[Swiss Prot: SEM4D_HUMAN]	96/79	8.3/7.0	2/2	35	20	2
557	Far upstream element-binding protein 1	[Swiss Prot: FUBP1_HUMAN]	67/75	7.2/7.2	3/7	114	47	13
631	Lamin A/C	[Swiss Prot: LMNA_HUMAN]	74/71	6.6/6.9	6/10	184	48	15
646	Lamin A/C	[Swiss Prot: LMNA_HUMAN]	74/70	6.6/7.0	12/28	482	71	46
680	No protein identified		/66	/8.0				
681	No protein identified		/66	/8.2				
683	No protein identified		/66	/8.6				
703	No protein identified		/65	/5.9				
768	No protein identified		/60	/7.9				
784	Dihydrolipoyl dehydrogenase, mitochondrial precursor	[Swiss Prot: DLDH_HUMAN]	54/59	7.6/7.3	2/2	42	22	5
789	Inosine 5'-monophosphate dehydrogenase 2	[Swiss Prot: IMDH2_HUMAN]	56/58	6.4/7.1	4/7	169	94	17
853	No protein identified		/54	/6				
908	α-enolase	[Swiss Prot: ENOA_HUMAN]	47/50	7.0/8.3	7/12	450	143	47
950	Tripeptidyl peptidase 1 precursor	[Swiss Prot: TPP1_HUMAN]	61/50	6.0/6.4	3/5	89	34	15
1017	Fumarate hydratase, mitochondrial precursor	[Swiss Prot: FUMH_HUMAN]	55/48	8.9/8.0	6/7	243	71	24
1085	Heterogeneous nuclear ribonucleoprotein D0	[Swiss Prot: HNRPD_HUMAN]	38/43	7.6/7.8	3/3	122	69	11
1214	PDZ and LIM domain protein 1	[Swiss Prot: PDLI1_HUMAN]	36/37	6.6/7.4	5/10	269	62	44
1249	60S acidic ribosomal protein P0	[Swiss Prot: RLA0_HUMAN]	34/37	5.7/6.0	2/5	56	35	21
1352	Voltage-dependent anion-selective channel protein 2	[Swiss Prot: VDAC2_HUMAN]	32/33	7.5/7.4	4/4	155	75	18
1359	Annexin A5	[Swiss Prot: ANXA5_HUMAN]	36/33	4.9/5.3	10/12	538	86	52
1376	No protein identified		/32	/7.5				
1440	Heat shock protein β1	[Swiss Prot: HSPB1_HUMAN]	23/29	6.0/6.2	5/8	382	138	47
	NADH dehydrogenase [ubiquinone] iron-sulphur protein 3, mitochondrial precursor	[Swiss Prot: NDUS3_HUMAN]	30/29	7.0/6.2	2/6	70	38	26
1614	Protein DJ-1	[Swiss Prot: PARK7_HUMAN]	20/25	6.3/6.6	5/5	202	75	51

Table 2 Mass spectrometry data of the endothelial cell protein spots identified as specific target antigens[a] *(Continued)*

1632	No protein identified		/23	/5.3				
1734	Peptidyl-prolyl *cis-trans* isomerase A	[Swiss Prot: PPIA_HUMAN]	18/18	7.7/8	3/5	78	48	36
1817	Thioredoxin-dependent peroxide reductase, mitochondrial precursor	[Swiss Prot: PRDX3_HUMAN]	28/15	7.7/6.8	5/6	211	61	44
1821	Fatty acid-binding protein, epidermal[b]	[Swiss Prot: FABP5_HUMAN]	15/15	6.6/6.7	1/5	26	26	47
2120	Elongation factor Tu, mitochondrial precursor	[Swiss Prot: EFTU_HUMAN]	50/45	7.3/6.9	5/6	120	58	15
	Poly(rC)-binding protein 1[b]	[Swiss Prot: PCBP1_HUMAN]	37/46	6.7/6.9	1/2	36	36	6
	Heterogeneous nuclear ribonucleoprotein D0[b]	[Swiss Prot: HNRPD_HUMAN]	38/45	7.6/6.9	1/4	39	36	10

[a]MW: molecular weight, PDZ and LIM domain protein 1: postsynaptic density 95 (PSD95), pI: isoelectric point. [b]Only one peptide of the protein was recognized by matrix-assisted laser desorption ionization time-of-flight/time-of-flight mass spectrometry; identification spectrum for each protein spot is given in Additional file 5. [c]indicate number of unique identified peptides in MSMS and in MS+MSMS searches.

directed against a number of ubiquitous autoantigens, including human lamin C, cytokeratin and mitochondrial cytochrome oxidase subunit II in the sera of patients with GCA [38]. Interestingly, we identified vinculin, lamin A/C and mitochondrial fumarate hydratase as target antigens of antibodies to proteins in the proteome of VSMCs and HUVECs. Vinculin is a cytoskeleton protein involved in extracellular matrix adhesion and intercellular junctions by binding to actin filaments. This protein has several interaction sites with numerous

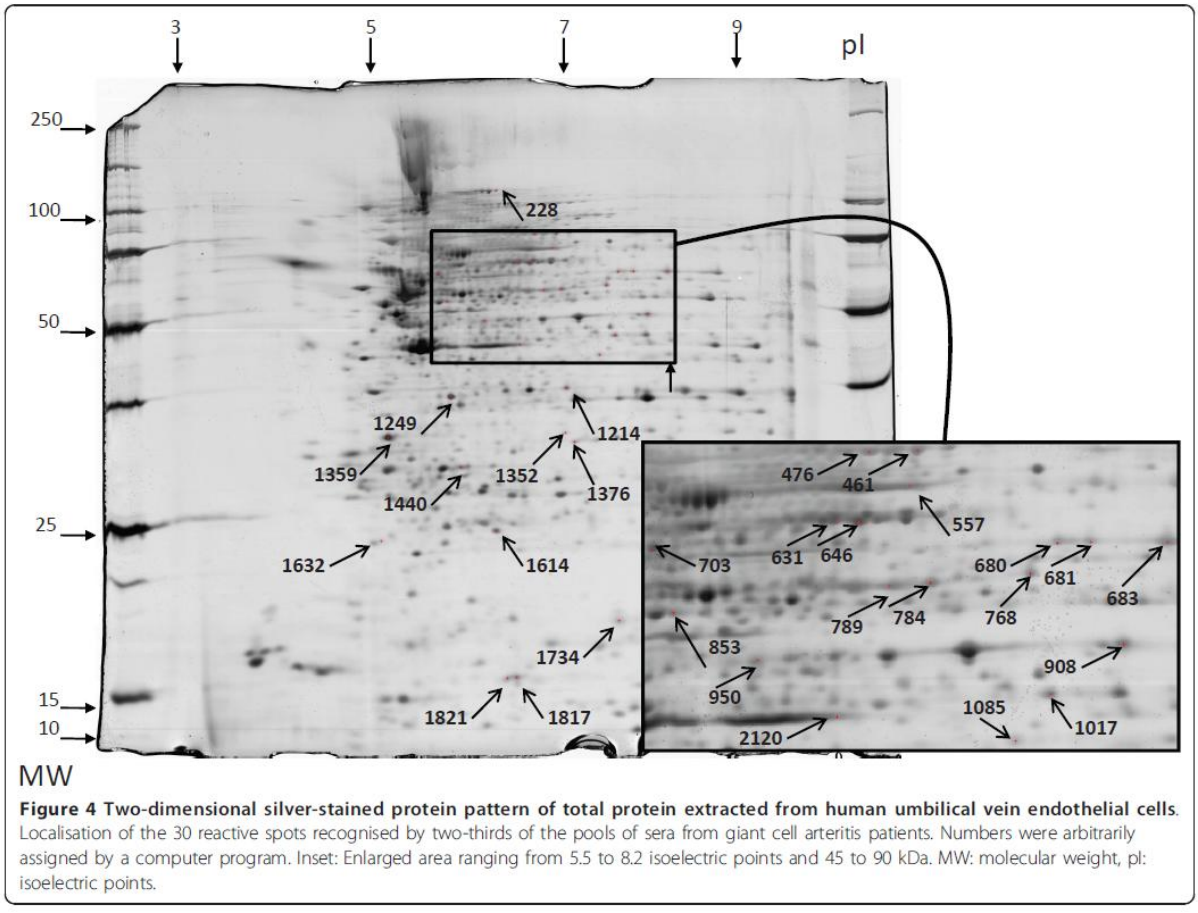

Figure 4 Two-dimensional silver-stained protein pattern of total protein extracted from human umbilical vein endothelial cells. Localisation of the 30 reactive spots recognised by two-thirds of the pools of sera from giant cell arteritis patients. Numbers were arbitrarily assigned by a computer program. Inset: Enlarged area ranging from 5.5 to 8.2 isoelectric points and 45 to 90 kDa. MW: molecular weight, pI: isoelectric points.

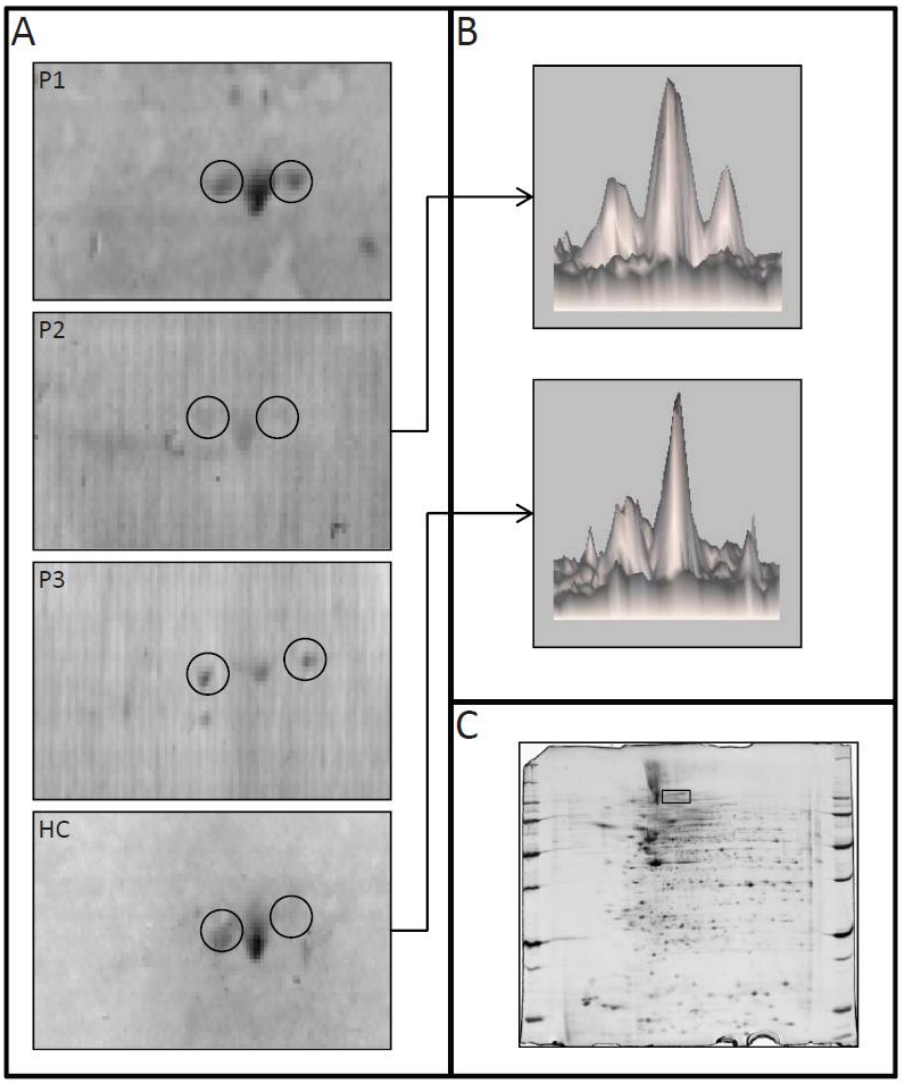

Figure 5 Serum IgG reactivity to vinculin in serum of patients with giant cell arteritis. **(A)** IgG reactivities to vinculin in three different pools of sera from three GCA patients each (P1 to P3) and one pool from twelve healthy controls (HC). **(B)** Vinculin spots are expressed in 3-D views for one representative sera pool of patients (top) and the pool of HCs (bottom). **(C)** Proteome of human umbilical vein endothelial cells showing the localisation of vinculin spots displayed in **(A)**.

binding partners, including α-actin [39]. Changes in the relative content of vinculin and α-actin have been reported in the human aortic intima of patients with atherosclerosis [40]. Because vascular remodelling may occur in atherosclerosis, this type of change could be associated with vascular remodelling in GCA. Lamin A and C are both encoded by the *LMNA* gene and represent major constituents of the inner nuclear membrane. Mutations in the *LMNA* gene have been identified in a number of conditions, including Hutchinson-Gilford progeria syndrome [41]. The most frequent mutation responsible for progeria creates a truncated progeria mutant lamin A (progerin), which accumulates within the nuclei of human vascular cells and may be directly responsible for vascular involvement in progeria [42]. Other *LMNA* gene mutations, such as Dunnigan-type familial partial lipodystrophy (FPLD2), can lead to proatherogenic metabolic disturbances such as dyslipidemia, hyperinsulinemia, hypertension and diabetes. Premature atherosclerosis-induced FPLD2 seems to be associated with monogenic insulin resistance syndrome [43]. Identification of lamin A/C as target antigens in

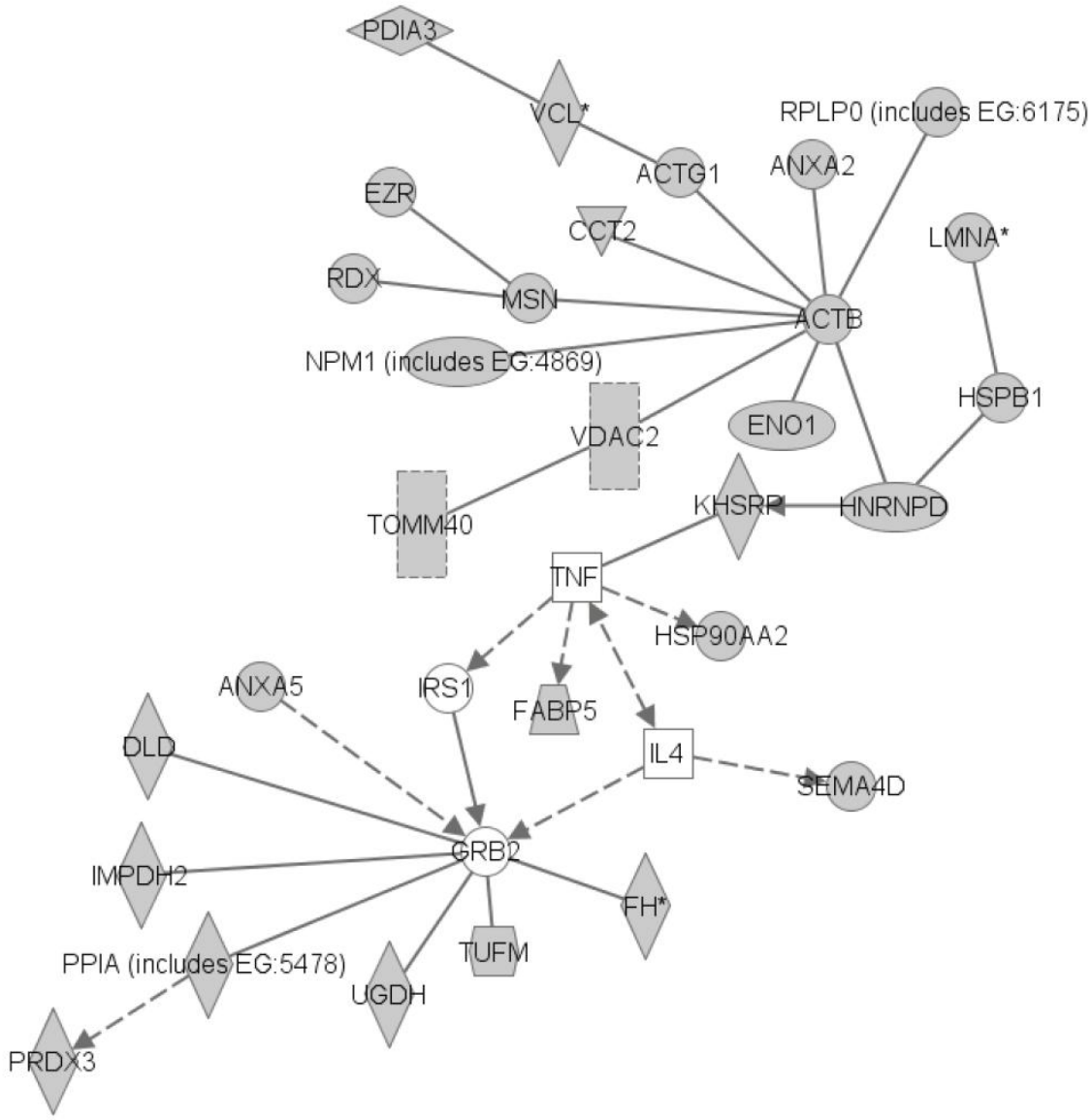

Figure 6 Pathway generated by ingenuity pathway analysis with proteins identified as specific target antigens. Solid lines indicate direct interactions. Dashed lines indicate indirect interactions. Arrows indicate stimulation. Mass spectrometry-identified proteins are depicted in grey. ACTB: actin, β; ACTG1: actin, γ1; ANXA2: annexin A2; ANXA5: annexin A5; CCT2: chaperonin containing TCP1, subunit 2 (β); DLD: dihydrolipoamide dehydrogenase; ENO1: enolase 1, α; EZR: ezrin; FABP5: fatty acid-binding protein 5; FH: fumarate hydratase; GRB2: growth factor receptor-bound protein 2; HNRNPD: heterogeneous nuclear ribonucleoprotein D; HSP90AA2: heat shock protein 90 α (cytosolic), class A member 2; HSPB1: HSPB1: heat shock 27-kDa protein 1; IL4: interleukin 4; IMPDH2: IMP (inosine 5'-monophosphate) dehydrogenase; IRS1: insulin receptor substrate 1; KHSRP: KH-type splicing regulatory protein = FUBP2; LMNA: lamin A/C; MSN: moesin; NPM1: nucleophosmin (nuclear phosphoprotein B23, numatrin); PDIA3: protein disulphide isomerase, family A, member 3; PPIA: peptidylpropyl isomerase A; PRDX3: peroxiredoxin 3; RDX: radixin; RPLPO: ribosomal protein, large, P0; SEMA4D: Sema domain, immunoglobulin domain (Ig), transmembrane domain (TM) and short cytosolic domain (semaphorin) 4D; TNF: tumour necrosis factor; TOMM40: translocase of outer mitochondrial membrane 40 homolog (yeast); TUFM: Tu translation elongation factor, mitochondrial; UGDH: UDP-glucose 6-dehydrogenase; VCL: vinculin; VDAC2: voltage-dependent anion channel 2.

sera from patients with GCA seems interesting. Further investigations are necessary to characterise the implications of lamin A/C in vascular remodelling in this condition.

We found another antigen, far upstream element-binding protein 2 (FUBP = KHSRP), to be recognised by all five pools of sera from GCA patients in VSMC protein extracts. This protein, which binds to a DNA region called far-upstream element (FUSE), is a transcriptional activator of c-*myc*, a proto-oncogene that plays a key role in the regulation of cell growth, proliferation and differentiation. The FUSE-binding protein (FUBP) regulates FUSE activity [44]. Anti-FUBP antibodies were identified in synoviocytes in patients with rheumatoid arthritis, a condition marked by a proliferation of synovial tissue [45]. However, the potential pathogenic role of these antibodies has not yet been identified.

By using IPA, we found that most of the VSMC and HUVEC proteins specifically recognised and/or recognised with high intensity by IgG in sera from GCA patients interacted with Grb2. Grb2 is an intracellular linker protein that facilitates the activation of the small GTPase Ras by receptor tyrosine kinases and is involved in VSMC proliferation. Zhang and colleagues [46] reported that Grb2 is required for the development of neointima in response to vascular injury. Thus, Grb2 might be overexpressed and/or activated in ECs and VSMCs of patients with GCA and might stimulate the remodelling process. Moreover, proteins overexpressed in the remodelling process in the presence of activated Grb2 might trigger a specific immune response, possibly through structural antigen modifications occurring in the presence of metalloproteases and/or reactive oxygen species. A number of the VSMC and HUVEC proteins specifically recognised and/or recognised with high intensity by IgG in sera from GCA patients interacted with TNF-α. This result is in agreement with the pathophysiology of GCA and the ongoing inflammatory process in the arterial wall.

The combined use of 2-DE and immunoblotting offers an interesting approach to the identification of target antigens of autoantibodies [25]. However, our work has several limitations. Fewer than 1,500 protein spots were stained in the reference gel of VSMC and HUVEC protein extracts, which is less than the total number of proteins contained in these cells. Therefore, a number of proteins were probably lost at each step of the technique, depending on their charge, molecular weight, subcellular localisation and/or abundance in the cell. In addition, as expected, none of the identified antigens represented cell surface proteins, because protein extraction for 2-DE does not permit identification of membrane proteins. Finally, our pools of sera were from three patients each because this number was sufficiently low to allow the detection of strong reactivity that would be present in the serum of a single individual [25]. However, we cannot rule out the possibility that a low-intensity reactivity specific to a given individual might not be detected by using this pooling approach.

Conclusions

We provide evidence that IgG antibodies directed toward the proteome of VSMCs and HUVECs are present in the sera of patients with GCA. These antibodies recognise cellular targets that play key roles in cell biology and the maintenance of homeostasis. The potential pathogenic role of these antibodies should be further investigated.

Additional material

Additional file 1: Supplemental file. Detailed data concerning 2-D electrophoresis technique and mass spectrometry identification [47-49].

Additional file 2: Supplemental Table S1. Clinical and histological characteristics of 15 patients with giant cell arteritis.

Additional file 3: Supplemental Figure S1. One-dimensional immunoblot IgG reactivity from giant cell arteritis patients with vascular smooth muscle cell proteins. Serum samples from three patients with GCA were tested, and sera from four patients with Wegener's granulomatosis (WG), two with Churg-Strauss syndrome (CSS) and two with microscopic polyangeitis (MPA) used as vasculitis controls, intravenous immunoglobulin (IVIg) as a positive control and PBS and sera from two healthy controls (HCs) as negative controls were immunoblotted at a dilution of 1:100 with a soluble extract of immortalised human mammary artery VSMCs.

Additional file 4: Supplemental Table S2. Antigens specifically recognised by IgG of three-fifths of the pools of sera from giant cell arteritis patients.

Additional file 5: Mass spectrometry data of target antigens recognised by only one peptide.

Additional file 6: Supplemental Figure S2. 2-D immunoblots of IgG reactivity to vinculin in sera from patients with giant cell arteritis. Protein extract is from vascular smooth muscle cells (VSMCs). **(A)** IgG reactivities of five different pools of sera from three giant cell arteritis patients each (P1 to P5) and one pool from twelve healthy controls (HCs). **(B)** Vinculin spots are expressed in 3-D views for one representative sera pool of patients (top) and the HC pool (bottom). **(C)** Proteome of VSMCs showing the localisation of vinculin spots displayed in **(A)**.

Additional file 7: Supplemental Table S3. Antigens specifically recognised by IgG of two-thirds of the pools of sera from giant cell arteritis patients.

Additional file 8: Supplemental Figure S3. Two-dimensional immunoblots of IgG reactivity to lamin in sera of patients with giant cell arteritis. Protein extract is from human umbilical vein endothelial cells (HUVECs). **(A)** IgG reactivities to lamin of three different pools of sera from three giant cell arteritis patients each (P1 to P3) and one pool from twelve healthy controls (HCs). **(B)** Lamin spots are expressed in 3-D views for one representative sera pool from patients (top) and the HC pool (bottom). **(C)** Proteome of HUVECs showing the localisation of lamin spots displayed in **(A)**.

Additional file 9: Supplement Figure S4. Protein network generated by merging the two pathways involved in target antigens. Protein extracts are from human umbilical vein endothelial cells and vascular smooth muscle cells. Solid lines indicate direct interactions. Dashed lines indicate indirect interactions. Arrows indicate stimulation. ABCA2: ATP-binding cassette, subfamily A, (ABC1), member 2; ACTB: actin, β; ACTG1:

actin, γ1; ANXA2: annexin A2; ANXA5: annexin A5; CCND2: cyclin D2; CCT2: chaperonin containing TCP1, subunit 2 (β); COPA: coatomer protein complex, subunit α; CPOX: coproporphyrinogen oxidase; DLD: dihydrolipoamide dehydrogenase; ENO1: enolase 1, α; EZR: ezrin; FABP5: fatty acid-binding protein 5; FH: fumarate hydratase; FUBP1: far upstream element (FUSE)-binding protein 1; GRB2: growth factor receptor-bound protein 2; HNRNPD: heterogeneous nuclear ribonucleoprotein D; HSP90AA2: heat shock protein 90 kDa α (cytosolic), class A, member 2; HSPB1: heat shock 27-kDa protein 1; IFNG: interferon γ; IKBKG: inhibitor of κ light polypeptide gene enhancer in B cells, kinase γ; IL4: interleukin 4; IMPDH2: IMP (inosine 5'-monophosphate) dehydrogenase; IRS1: insulin receptor substrate 1; KHSRP: KH-type splicing regulatory protein; LMNA: lamin A/C; MSN: moesin; NDUFS3: NADH dehydrogenase (ubiquinone) iron-sulphur protein 3, 30 kDa (NADH coenzyme Q reductase); NPM1: nucleophosmin (nuclear phosphoprotein B23, numatrin); PARK7: Parkinson's disease (autosomal recessive early onset) 7; PDGF BB: platelet-derived growth factor B dimer; PDIA3: protein disulphide isomerase, family A, member 3; PHB: prohibitin; PPIA: peptidylpropyl-isomerase A; PRDX3: peroxiredoxin 3; PSMC5: proteasome 26S subunit, ATPase, 5; RDX: radixin; RPLPO: ribosomal protein, large, P0; SEMA4D: Sema domain, immunoglobulin domain (Ig), transmembrane domain (TM) and short cytosolic domain (semaphorin) 4D; TNF: tumour necrosis factor; TOMM40: translocase of outer mitochondrial membrane 40 homolog (yeast); TP53: tumour protein P53; TPP1: tripeptidyl 1 peptidase; TUFM: Tu translation elongation factor, mitochondrial; UGDH: UDP-glucose 6-dehydrogenase; VCL: vinculin; VDAC2: voltage-dependent anion channel 2.

Abbreviations

ACR: American College of Rheumatology; AECA: anti-endothelial cell antibody; ANCA: antineutrophil cytoplasm antibody; bFGF: basic fibroblast growth factor; CSS: Churg-Strauss syndrome; EC: endothelial cell; EGF: epidermal growth factor; ELISA: enzyme-linked immunosorbent assay; FCS: foetal calf serum; FUBP2: far upstream element-binding protein 2; FUSE: far upstream element; GCA: giant cell arteritis; Grb2: growth factor receptor-bound protein 2; HC: healthy control; HUVEC: human umbilical vein endothelial cell; IFN-γ: interferon-γ; IL: interleukin; IP: isoelectrofocalisation point; IPA: ingenuity pathway analysis; IPKB: Ingenuity Pathway Knowledgebase; MPA: microscopic polyangiitis; MS: mass spectrometry; PMSF: phenylmethylsulphonyl fluoride; PVDF: polyvinylidene fluoride; RT: reverse transcriptase; TNF-α: tumour necrosis factor α; VSMC: vascular smooth muscle cell; WG: Wegener's granulomatosis.

Acknowledgements

AR received financial support from the Direction Régionale et départementale de Champagne-Ardennes et de la Marne and the Société Nationale Française de Médecine Interne (SNFMI). HD received financial support from Avenir Mutualiste des Professions Libérales & Indépendantes (AMPLI) and Association pour la Recherche en Médecine Interne et en Immunologie Clinique (ARMIIC). KHL received financial support from Limoges Hospital. MCT received a grant from Pfizer and the Direction de la Recherche Clinique (PHRC National Auto-HTAP). We also thank the Unité de Recherche Clinique Cochin-Necker. We also thank CSL Behring for financial support. None of the funding bodies had a role in the study design; the collection, analysis or interpretation of data; the writing of the manuscript; or the decision to submit the manuscript for publication.

Author details

[1]Inserm U1016, Institut Cochin, CNRS UMR 8104, 8 rue Méchain, F-75014 Paris, France. [2]Université Paris Descartes, 12 rue de l'Ecole de Médecine, F-75270 Paris, France. [3]Pôle de Médecine Interne, Centre de Référence pour les vascularites nécrosantes et la sclérodermie systémique, Hôpital Cochin, Assistance Publique Hôpitaux de Paris, 27 rue du Faubourg Saint-Jacques, F-75679 Paris Cedex 14 Paris, France. [4]Service de Médecine Interne A, CHU Dupuytren, 2 avenue Martin Luther King, F-87042 Limoges cedex 1, France. [5]Service de Médecine Interne, hôpital Hôtel Dieu, Place Alexis Ricordeau, F-44093 Nantes cedex 1, France. [6]Weill Medical College of Cornell University, 1300 York Avenue, New York, NY 10065, USA. [7]Institut Cochin, Plate-forme Protéomique de l'Université Paris Descartes, CNRS UMR 8104, 8 rue Méchain, F-75014 Paris, France.

Authors' contributions

AR carried out the immunoblotting and proteomic experiments, analysed the results and drafted the manuscript. HD carried out immunoblotting and proteomic experiments with AR, participated in the analysis of the results and edited the manuscript. KHL carried out 1-D immunoblotting experiments and participated in the drafting of the manuscript. CA conducted the inclusion of patients into the study, analysed the results and edited the manuscript. MCT participated in the study design and the analysis of the results and also edited the manuscript. NT participated in immunoblotting and proteomic experiments, participated in the analysis of the results and edited the manuscript. CF performed ingenuity pathway analysis, participated in the analysis of the results and edited the manuscript. CB performed proteomic analysis, participated in the analysis of the results and edited the manuscript. BW provided immortalised VSMCs, participated in the analysis of the results and edited the manuscript. LG provided sera from patients, participated in the study design and analysis of the results and also edited the manuscript. LM provided sera from patients, designed the experiments, analysed the results and drafted the manuscript. All authors read and approved the final manuscript.

Competing interests

AR, HD and LM have applied for a patent related to the content of this article (Patent Procédé de diagnostic d'une vascularite FR0951205).

Received: 25 February 2011 Revised: 15 May 2011
Accepted: 28 June 2011 Published: 28 June 2011

References

1. Hunder GG: **Epidemiology of giant-cell arteritis.** *Cleve Clin J Med* 2002, **69(Suppl 2)**:SII79-SII82.
2. Gonzalez-Gay MA, Vazquez-Rodriguez TR, Lopez-Diaz MJ, Miranda-Filloy JA, Gonzalez-Juanatey C, Martin J, Llorca J: **Epidemiology of giant cell arteritis and polymyalgia rheumatica.** *Arthritis Rheum* 2009, **61**:1454-1461.
3. González-Gay MA, Blanco R, Rodríguez-Valverde V, Martínez-Taboada VM, Delgado-Rodriguez M, Figueroa M, Uriarte E: **Permanent visual loss and cerebrovascular accidents in giant cell arteritis: predictors and response to treatment.** *Arthritis Rheum* 1998, **41**:1497-1504.
4. Hunder GG, Bloch DA, Michel BA, Stevens MB, Arend WP, Calabrese LH, Edworthy SM, Fauci AS, Leavitt RY, Lie JT, Lightfoot RW Jr, Masi AT, McShane DJ, Mills JA, Wallace SL, Zvaifler NJ: **The American College of Rheumatology 1990 criteria for the classification of giant cell arteritis.** *Arthritis Rheum* 1990, **33**:1122-1128.
5. Hall S, Persellin S, Lie JT, O'Brien PC, Kurland LT, Hunder GG: **The therapeutic impact of temporal artery biopsy.** *Lancet* 1983, **2**:1217-1220.
6. Ly KH, Regent A, Tamby MC, Mouthon L: **Pathogenesis of giant cell arteritis: more than just an inflammatory condition?** *Autoimmun Rev* 2010, **9**:635-645.
7. Brack A, Geisler A, Martinez-Taboada VM, Younge BR, Goronzy JJ, Weyand CM: **Giant cell vasculitis is a T cell-dependent disease.** *Mol Med* 1997, **3**:530-543.
8. Rittner HL, Kaiser M, Brack A, Szweda LI, Goronzy JJ, Weyand CM: **Tissue-destructive macrophages in giant cell arteritis.** *Circ Res* 1999, **84**:1050-1058.
9. Rodríguez-Pla A, Bosch-Gil JA, Rosselló-Urgell J, Huguet-Redecilla P, Stone JH, Vilardell-Tarres M: **Metalloproteinase-2 and -9 in giant cell arteritis: involvement in vascular remodeling.** *Circulation* 2005, **112**:264-269.
10. Guilpain P, Mouthon L: **Antiendothelial cells autoantibodies in vasculitis-associated systemic diseases.** *Clin Rev Allergy Immunol* 2008, **35**:59-65.
11. Hu N, Westra J, Huitema MG, Stegeman CA, Limburg PC, Kallenberg CG: **Autoantibodies against glomerular endothelial cells in anti-neutrophil cytoplasmic autoantibody-associated systemic vasculitis.** *Nephrology (Carlton)* 2009, **14**:11-15.
12. Holmén C, Christensson M, Pettersson E, Bratt J, Stjärne P, Karrar A, Sumitran-Holgersson S: **Wegener's granulomatosis is associated with organ-specific antiendothelial cell antibodies.** *Kidney Int* 2004, **66**:1049-1060.

13. Holmén C, Elsheikh E, Christensson M, Liu J, Johansson AS, Qureshi AR, Jalkanen S, Sumitran-Holgersson S: **Anti endothelial cell autoantibodies selectively activate SAPK/JNK signalling in Wegener's granulomatosis.** *J Am Soc Nephrol* 2007, **18**:2497-2508.
14. van Paassen P, Duijvestijn A, Debrus-Palmans L, Damoiseaux J, Vroomen M, Tervaert JW: **Induction of endothelial cell apoptosis by IgG antibodies from SLE patients with nephropathy: a potential role for anti-endothelial cell antibodies.** *Ann N Y Acad Sci* 2007, **1108**:147-156.
15. Navarro M, Cervera R, Font J, Reverter JC, Monteagudo J, Escolar G, López-Soto A, Ordinas A, Ingelmo M: **Anti-endothelial cell antibodies in systemic autoimmune diseases: prevalence and clinical significance.** *Lupus* 1997, **6**:521-526.
16. Amor-Dorado JC, García-Porrua C, Gonzalez-Gay MA: **Anti-endothelial cell antibodies and biopsy-proven temporal arteritis.** *Lupus* 2002, **11**:134.
17. Baiu DC, Barger B, Sandor M, Fabry Z, Hart MN: **Autoantibodies to vascular smooth muscle are pathogenic for vasculitis.** *Am J Pathol* 2005, **166**:1851-1860.
18. Jennette JC, Falk RJ, Andrassy K, Bacon PA, Churg J, Gross WL, Hagen EC, Hoffman GS, Hunder GG, Kallenberg CGM, McCluskey RT, Sinico RA, Rees AJ, Van Es LA, Waldherr R, Wiik A: **Nomenclature of systemic vasculitides: proposal of an international consensus conference.** *Arthritis Rheum* 1994, **37**:187-192.
19. Weksler BB, Subileau EA, Perrière N, Charneau P, Holloway K, Leveque M, Tricoire-Leignel H, Nicotra A, Bourdoulous S, Turowski P, Male DK, Roux F, Greenwood J, Romero IA, Couraud PO: **Blood-brain barrier-specific properties of a human adult brain endothelial cell line.** *FASEB J* 2005, **19**:1872-1874.
20. Ronda N, Leonardi S, Orlandini G, Gatti R, Bellosta S, Bernini F, Borghetti A: **Natural anti-endothelial cell antibodies (AECA).** *J Autoimmun* 1999, **13**:121-127.
21. Tamby MC, Chanseaud Y, Humbert M, Fermanian J, Guilpain P, Garcia-de-la-Peña-Lefebvre P, Brunet S, Servettaz A, Weill B, Simonneau G, Guillevin L, Boissier MC, Mouthon L: **Anti-endothelial cell antibodies in idiopathic and systemic sclerosis associated pulmonary arterial hypertension.** *Thorax* 2005, **60**:765-772.
22. García de la Peña-Lefebvre P, Chanseaud Y, Tamby MC, Reinbolt J, Batteux F, Allanore Y, Kahan A, Meyer O, Benveniste O, Boyer O, Guillevin L, Boissier MC, Mouthon L: **IgG reactivity with a 100-kDa tissue and endothelial cell antigen identified as topoisomerase 1 distinguishes between limited and diffuse systemic sclerosis patients.** *Clin Immunol* 2004, **111**:241-251.
23. Tamby MC, Bussone G, Mouthon L: **Antitopoisomerase 1 antibodies in systemic sclerosis: how to improve the detection?** *Ann N Y Acad Sci* 2007, **1109**:221-228.
24. Chanseaud Y, García de la Peña-Lefebvre P, Guilpain P, Mahr A, Tamby MC, Uzan M, Guillevin L, Boissier MC, Mouthon L: **IgM and IgG autoantibodies from microscopic polyangiitis patients but not those with other small- and medium-sized vessel vasculitides recognize multiple endothelial cell antigens.** *Clin Immunol* 2003, **109**:165-178.
25. Terrier B, Tamby MC, Camoin L, Guilpain P, Broussard C, Bussone G, Yaïci A, Hotellier F, Simonneau G, Guillevin L, Humbert M, Mouthon L: **Identification of target antigens of antifibroblast antibodies in pulmonary arterial hypertension.** *Am J Respir Crit Care Med* 2008, **177**:1128-1134.
26. Lowry OH, Rosebrough NJ, Farr AL, Randall RJ: **Protein measurement with the Folin phenol reagent.** *J Biol Chem* 1951, **193**:265-275.
27. Guilpain P, Servettaz A, Tamby MC, Chanseaud Y, Tamas N, Garcia de la Pena-Lefebvre P, Broussard C, Guillevin L, Camoin L, Mouthon L: **A combined SDS-PAGE and proteomics approach to identify target autoantigens in healthy individuals and patients with autoimmune diseases.** *Ann N Y Acad Sci* 2007, **1109**:538-549.
28. Bussone G, Dib H, Tamby MC, Broussard C, Federici C, Woimant G, Camoin L, Guillevin L, Mouthon L: **Identification of new autoantibody specificities directed at proteins involved in the transforming growth factor β pathway in patients with systemic sclerosis.** *Arthritis Res Ther* 2011, **13**:R74.
29. Qi YX, Jiang J, Jiang XH, Wang XD, Ji SY, Han Y, Long DK, Shen BR, Yan ZQ, Chien S, Jiang ZL: **PDGF-BB and TGF-β1 on cross-talk between endothelial and smooth muscle cells in vascular remodeling induced by low shear stress.** *Proc Natl Acad Sci USA* 2011, **108**:1908-1913.
30. Banks PM, Cohen MD, Ginsburg WW, Hunder GG: **Immunohistologic and cytochemical studies of temporal arteritis.** *Arthritis Rheum* 1983, **26**:1201-1207.
31. Lavignac C, Jauberteau-Marchan MO, Liozon E, Vidal E, Catanzano G, Liozon F: **Immunohistochemical study of lesions in Horton's temporal arteritis before and during corticotherapy in French.** *Rev Med Interne* 1996, **17**:814-820.
32. Chatelain D, Duhaut P, Loire R, Bosshard S, Pellet H, Piette JC, Sevestre H, Ducroix JP: **Small-vessel vasculitis surrounding an uninflamed temporal artery: a new diagnostic criterion for polymyalgia rheumatica?** *Arthritis Rheum* 2008, **58**:2565-2573.
33. Duhaut P, Bosshard S, Ducroix JP: **Is giant cell arteritis an infectious disease? Biological and epidemiological evidence.** *Presse Med* 2004, **33**:1403-1408.
34. Servettaz A, Guilpain P, Camoin L, Mayeux P, Broussard C, Tamby MC, Tamas N, Kaveri SV, Guillevin L, Mouthon L: **Identification of target antigens of antiendothelial cell antibodies in healthy individuals: a proteomic approach.** *Proteomics* 2008, **8**:1000-1008.
35. Domiciano DS, Carvalho JF, Shoenfeld Y: **Pathogenic role of anti-endothelial cell antibodies in autoimmune rheumatic diseases.** *Lupus* 2009, **18**:1233-1238.
36. Del Papa N, Guidali L, Sironi M, Shoenfeld Y, Mantovani A, Tincani A, Balestrieri G, Radice A, Sinico RA, Meroni PL: **Anti-endothelial cell IgG antibodies from patients with Wegener's granulomatosis bind to human endothelial cells in vitro and induce adhesion molecule expression and cytokine secretion.** *Arthritis Rheum* 1996, **39**:758-766.
37. Bordron A, Dueymes M, Levy Y, Jamin C, Leroy JP, Piette JC, Shoenfeld Y, Youinou PY: **The binding of some human antiendothelial cell antibodies induces endothelial cell apoptosis.** *J Clin Invest* 1998, **101**:2029-2035.
38. Schmits R, Kubuschok B, Schuster S, Preuss KD, Pfreundschuh M: **Analysis of the B cell repertoire against autoantigens in patients with giant cell arteritis and polymyalgia rheumatica.** *Clin Exp Immunol* 2002, **127**:379-385.
39. Ziegler WH, Liddington RC, Critchley DR: **The structure and regulation of vinculin.** *Trends Cell Biol* 2006, **16**:453-460.
40. Glukhova MA, Kabakov AE, Frid MG, Ornatsky OI, Belkin AM, Mukhin DN, Orekhov AN, Koteliansky VE, Smirnov VN: **Modulation of human aorta smooth muscle cell phenotype: a study of muscle-specific variants of vinculin, caldesmon, and actin expression.** *Proc Natl Acad Sci USA* 1988, **85**:9542-9546.
41. Eriksson M, Brown WT, Gordon LB, Glynn MW, Singer J, Scott L, Erdos MR, Robbins CM, Moses TY, Berglund P, Dutra A, Pak E, Durkin S, Csoka AB, Boehnke M, Glover TW, Collins FS: **Recurrent *de novo* point mutations in lamin A cause Hutchinson-Gilford progeria syndrome.** *Nature* 2003, **423**:293-298.
42. McClintock D, Gordon LB, Djabali K: **Hutchinson-Gilford progeria mutant lamin A primarily targets human vascular cells as detected by an anti-lamin A G608G antibody.** *Proc Natl Acad Sci USA* 2006, **103**:2154-2159.
43. Hegele RA: **Premature atherosclerosis associated with monogenic insulin resistance.** *Circulation* 2001, **103**:2225-2229.
44. Duncan R, Bazar L, Michelotti G, Tomonaga T, Krutzsch H, Avigan M, Levens D: **A sequence-specific, single-strand binding protein activates the far upstream element of *c-myc* and defines a new DNA-binding motif.** *Genes Dev* 1994, **8**:465-480.
45. Goëb V, Thomas-L'Otellier M, Daveau R, Charlionet R, Fardellone P, Le Loët X, Tron F, Gilbert D, Vittecoq O: **Candidate autoantigens identified by mass spectrometry in early rheumatoid arthritis are chaperones and citrullinated glycolytic enzymes.** *Arthritis Res Ther* 2009, **11**:R38.
46. Zhang S, Ren J, Khan MF, Cheng AM, Abendschein D, Muslin AJ: **Grb2 is required for the development of neointima in response to vascular injury.** *Arterioscler Thromb Vasc Biol* 2003, **23**:1788-1793.
47. García de la Peña-Lefebvre P, Chanseaud Y, Tamby MC, Reinbolt J, Batteux F, Allanore Y, Kahan A, Meyer O, Benveniste O, Boyer O, Guillevin L, Boissier MC, Mouthon L: **IgG reactivity with a 100-kDa tissue and endothelial cell antigen identified as topoisomerase 1 distinguishes between limited and diffuse systemic sclerosis patients.** *Clin Immunol* 2004, **111**:241-251.
48. Shevchenko A, Wilm M, Vorm O, Mann M: **Mass spectrometric sequencing of proteins silver-stained polyacrylamide gels.** *Anal Chem* 1996, **68**:850-858.

49. Perkins DN, Pappin DJ, Creasy DM, Cottrell JS: **Probability-based protein identification by searching sequence databases using mass spectrometry data.** *Electrophoresis* 1999, **20**:3551-3567.

doi:10.1186/ar3388
Cite this article as: Régent *et al.*: Identification of target antigens of anti-endothelial cell and anti-vascular smooth muscle cell antibodies in patients with giant cell arteritis: a proteomic approach. *Arthritis Research & Therapy* 2011 **13**:R107.

Identification of target antigens of anti-endothelial-cell and anti-vascular-smooth-muscle-cell antibodies in patients with giant cell arteritis: a proteomic approach

Alexis Régent[1,2,3,] Hanadi Dib[1,2], Kim H. Ly[1,2,4*], Christian Agard[5*], Mathieu C. Tamby[1,2], Nicolas Tamas[1,2], Babette Weksler[6], Christian Federici[1,2], Cédric Broussard[7], Loïc Guillevin[2,3], Luc Mouthon[1,2,3].

*Both authors contributed equally to the work.

Supplemental data

Material and Methods

1-D Immunoblotting

Confluent cells were detached with use of 0.05% trypsin, 0.53 mM EDTA. Protein extract was obtained by use of a 125-mM Tris, pH 6.8, solution containing 4% sodium dodecyl sulfate (SDS), 1.45 M β-mercaptoethanol, 1 µg/ml aprotinin, 1 µg/ml leupeptin, 1 µg/ml pepstatin and 1 mM of PMSF. Protein extract was then sonicated 4 x 30 s and boiled. Aliquots of 120 µl solubilised proteins were separated by polyacrylamide gel electrophoresis on 10% gels (Bio-Rad, Hercules, CA), transferred onto nitrocellulose membranes by use of a semi-dry electroblotter (Model A, Ancos, Hojby, Denmark) and incubated with sera from patients (GCA, WG, MPA, CSS) or healthy donors at 1:100 dilution or with IVIg solution at 1:100 dilution overnight at 4°C by use of a Cassette Miniblot System (Immunetics Inc., Cambridge, MA, USA). Detection of IgG reactivity was as previously reported (234) with a γ-chain-specific secondary rabbit anti-human IgG antibody coupled to alkaline phosphatase. Immunoreactivities were revealed by use of nitroblue tetrazolium/5-bromo-4-chloro-3-indolyl-phosphate (NBT/BCIP) (Sigma-Aldrich, St. Louis, MO, USA). Quantification of immunoreactivities involved densitometry in reflective mode (Epson Perfection 1200S densitometer, Seiko Epson Corp., Nagano-ken, Japan). The membranes were then stained with colloidal gold (Protogold, Biocell, Cardiff, UK) and scanned again to quantify transferred proteins.

2-D Electrophoresis

Proteins were isoelectrofocused with pH range IPG strips on the Protean IEF Cell Isoelectric Focusing System (Bio-Rad). Frozen samples were thawed and diluted, to a final volume of 400 µl each, into IPG sample buffer containing 7 M

ultrapure urea (VWR, Fontenay-Sous-Bois, France), 2 M thiourea (Sigma), 4% (v/v) Chaps (Sigma), 7.5% (v/v) Triton X100 (Sigma),0.04% (v/v) carrier ampholyte mixture matching the pH range 3–10 (Pharmalytes 3–10; Amersham Biosciences, Uppsala, Sweden) and Bromophenol Blue (Sigma). IPG strips were rehydrated and focused in an automated run in the ceramic strip holders with 9-h rehydration at 20◦C, the 12 h at 50 V, 1 h at 200V, 1 h at 1000 V, then 6 h at 10,000 V and 1 h at 10,000 V.

Before running the second dimension, the strips were equilibrated for 15 min in 10 mL of the first equilibration solution (51 mM Tris [Amersham Biosciences], 6 mM urea, 40% [v/v] glycerol, 52 mM SDS, 32.4 mM DTT), then for 20 min in the second equilibration solution (51 mM Tris, 6 mM urea, 40% [v/v] glycerol, 52 mM SDS, 86.5 mM iodoacetamide). The second dimension electrophoresis was carried out in a Laemmli system on 7–18% polycrylamide linear gradient gels (20 cm × 20 cm × 1.5 mm) with a 18.5% buffer solution containing 2.5 M acrylamide (Amersham Biosciences), 24.7 mM piperazine diacrylyl (PDA) (Bio-Rad), 0.375 M Tris-HCl (Amersham Biosciences), pH 8.8, 15% (v/v) glycerol (Sigma), 3.5 mM SDS (Amersham Biosciences), 0.05% (v/v) TEMED (BioRad), 1.6 mM APS (BioRad), and a 7.5% buffer solution containing 1.0 M acrylamide, 10 mM PDA, 0.375 M Tris-HCl pH 8.8, 3.5 mM SDS, bi-distilled water, 0.06% (v/v) TEMED, and 2.4 mM APS were mixed. The equilibrated IPG gels were sealed on top of the 2-D gel with 1% agarose containing 50 mM Tris-Cl (pH 6.8), 2% (w/v) SDS, 30% (v/v) glycerol, and bromophenol blue and cathode-running buffer (24.8 mM Tris, 192 mM glycine, and 0.1% (w/v) SDS) was added. Gels were run at 40 V constant for 1 h, then 80 V constant for 1 h and then at 120V for 21 h 15 min.

The gels were transferred onto a polyvinylidene fluoride (PVDF) (Millipore,Bedford, MA) membrane by semidry transfer (BioRad) at 320 mA for 1 h 30 min. After blocking the membranes with PBS-0.2% (v/v) Tween for 90 min, each membrane was incubated overnight at +4°C with one pool of sera (3 sera for patients and 12 sera for healthy controls) diluted 1:100. Membranes were then extensively washed before being incubated with a secondary rabbit anti-human Fc-γ specific antibody coupled to alkaline phosphatase (Dako) for 90 min at room temperature. Immunoreactivities were revealed by use of the NBT–BCIP substrate (Sigma). Specific reactivities were determined by densitometrically scanning the membranes (densitometer GS-800, Bio-Rad) with use of Quantity one software (Bio-Rad). The membranes were then stained with colloidal gold (Protogold; British Biocell International, Cardiff, UK) and subjected to a second densitometric analysis to record labelled protein spots for each gel.

Gel Staining

Analytical gels were stained with ammoniacal silver nitrate. Images of both the gels and the 2-D blots were acquired by use of a densitometer (GS-800; Bio-Rad) and the images were exported to the Image Master 2D Platinum 6 software (Amersham). The number of spots was determined. A stack of the 2-D blot images before and after colloidal gold staining was acquired by the matching algorithm according to the manufacturer's recommendations. Specific labels were then manually linked to the protein spots probed by serum IgG on both images. The algorithm automatically propagated these labels from the image of the colloidal gold-stained 2-D blot to the images of both reference silver-stained and preparative gels.

Protein Identification

For preparative 2-D gels, 100 µg of proteins were loaded onto IPG strips. Gels were stained after electrophoresis with 0.2% (w/v) Coomassie Blue R-250 in 50% (v/v) methanol and 10% (v/v) acetic acid, and destained in 50% (v/v) methanol and 2% (v/v) acetic acid. The relevant spots were selected by comparing the 2-D blots with the silver-stained analytical gels and colloidal Coomassie blue-stained preparative gels. The spots were then excised, and in-gel trypsin digestion was performed as described (235) with slight modification.

In-gel trypsin digestion

In-gel digestion was carried out with trypsin as described by Shevchenko (235) with minor modifications and involved for all steps a Freedom EVO 100 digester/spotter robot (Tecan, Männedorf, CH). Spots were first de-stained two times with a mixture of 100 mM ammonium bicarbonate (ABC) and 50% acetonitrile (ACN) for 45 min at 22°C and then dried with use of 100% ACN for 15 min. Protein spots were then treated with 25 mM ABC containing 10 mM DTT for 1 h at 60°C and then alkylated by use of 55 mM iodoacetamide in 25 mM ABC for 30 min in the dark at 22°C. Gel pieces were washed twice with 25 mM ABC and finally shrunk two times with 100% ACN for 15 min and dried with 100% ACN for 10 min. Bands were completely dehydrated after 1 h at 60°C. Gel pieces were incubated with 13 µL Sequencing Grade Modified Trypsin (Promega, WI; 12.5 µg/mL in 40 mMABC-10% ACN pH 8.0) overnight at 40°C. After digestion, peptides were washed with 30 µL of 25 mM ABC, shrunk with 100% (v/v) ACN and extracted twice with a mixture of 50% (v/v) ACN-5% (v/v) formic acid (FA). Extracts were then dried by vacuum centrifuge (Eppendorf, Hamburg, Germany). Finally, peptides were desalted using C18-ZipTips

(Millipore) and two elutions, first with 50% (v/v) ACN-5% (v/v) FA and then 80% (v/v) ACN-5% (v/v) FA. Pooled elutions were allowed to dry at room temperature.

Protein identification by mass spectrometry

For mass spectrometry (MS) and MS/MS analysis, peptides were redissolved in 4 µL CHCA (5 mg/mL in 50% (v/v) ACN-0.1% (v/v) TFA). One microliter and a half of each sample was spotted directly onto a MALDI plate (Applied Biosystems, Foster City, CA). Droplets were allowed to dry at room temperature. The sample analysis involved a MALDI-TOF-TOF 4800 mass spectrometer (Applied Biosystems). Spectra acquisition and processing involved use of the 4000 series explorer software (Applied Biosystems) version 3.5.28193 in positive reflectron mode at fixed laser fluency with low mass gate and delayed extraction. External plate calibration was by four calibration points spotted onto the four corners of the plate with a mixture of five external standards (PepMix 1, LaserBio Labs, Sophia Antipolis, France). Peptide masses were acquired by steps of 50 spectra for 900 to 4000 Da. MS spectra were summed from 1000 laser shots by an Nd-YAG laser operating at 355 nm and 200 Hz. After filtering tryptic-, keratin- and matrix-contaminant peaks, up to 15 parent ions were selected for subsequent MS/MS fragmentation according to mass range, signal intensity, S/N, and absence of neighboring masses in the MS spectrum. MS/MS spectra were acquired in 1-kV positive mode, and 1000 shots were summed in increments of 50. Database searching involved MASCOT 2.2 (MatrixScience, London, UK) (236) *via* GPS explorer software (Applied Biosystems) version 3.6 combining MS and MS/MS interrogations on human proteins from Swiss-Prot databank release 54.5, 17 253 entries (www.expasy.org). The search parameters were as follows: carbamidomethylation as a variable modification for cysteins and

oxidation as a variable modification for methionines. Up to one missed tryptic cleavage was permitted and mass accuracy tolerance of 30 ppm for precursors and 0.3 Da for fragments were used for all tryptic mass searches. Positive identification was based on a MASCOT score above the significance level (*i.e*.< 5%). In the case of peptides match to multiple members of a protein family, the reported protein is the one with the highest number of peptide matches.

Abbreviation :

CSS : Churg-Strauss syndrome

EC : endothelial cells

GCA : giant cell arteritis

MPA : microscopic polyangiitis

MS : mass spectrometry

NBT/BCIP : nitroblue tetrazolium/5-bromo-4-chloro-3-indolyl-phosphate

PDA : piperazine diacrylyl

PMSF : phenylmethanesulfonylfluoride

PVDF : polyvinylidene fluoride

SDS : sodium dodecyl sulfate

WG : Wegener's granulomatosis

Supplemental table S1: Clinical and histological characteristics of 15 patients with giant cell arteritis.

	Pool 1			Pool 2			Pool 3			Pool 4			Pool 5		
Patient	1	2	3	4	5	6	7	8	9	10	11	12	13	14	15
Histology of TAB	+	+	+	+	+	+	+	+	+	-	+	-	+	+	+
Disease evolution*	D	D	D	D	D	D	D	D	D	D	Rel	Rel	D	Fl	D
steroid dosage (mg/d)*	0	0	0	0	0	0	0	0	0	0	0	0	0	25	0

* at the time of blood sampling.

D: Diagnosis; F: Female; Fl: Flare; M: Male; Rel: Relapse; +: Evidence of giant cell arteritis; -: Normal or fibrous endarteritis; TAB: Temporal artery biopsy

Supplemental Figure S1. One-dimensional immunoblot IgG reactivity from giant cell arteritis patients with vascular smooth muscle cell proteins. Serum samples from three patients with GCA were tested, and sera from four patients with Wegener's granulomatosis (WG), two with Churg-Strauss syndrome (CSS) and two with microscopic polyangeitis (MPA) used as vasculitis controls, intravenous immunoglobulin (IVIg) as a positive control and PBS and sera from two healthy controls (HCs) as negative controls were immunoblotted at a dilution of 1:100 with a soluble extract of immortalised human mammary artery VSMCs.

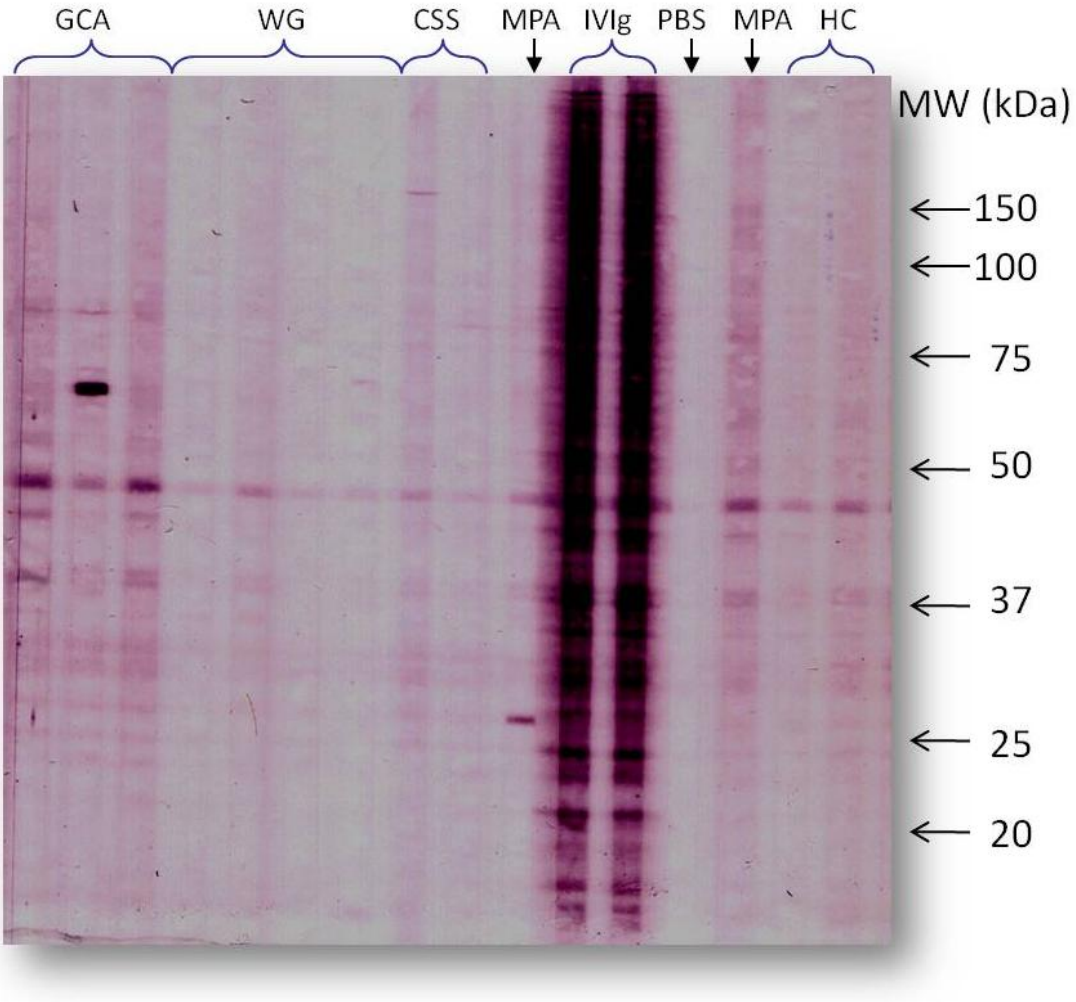

<u>Supplemental table S2</u>. Antigens specifically recognized by IgG of three-fifths pools of sera from giant cell arteritis patients. Protein extract is from vascular smooth muscle cell.

Spot ID	Protein	GCA pool 1	GCA pool 2	GCA pool 3	GCA pool 4	GCA pool 5
173	Vinculin		+	+		+
294	Putative HSP 90-alpha A2	+			+	+
340	Far upstream element-binding protein 2	+	+	+	+	+
341	Far upstream element-binding protein 2	+	+	+	+	
344	Far upstream element-binding protein 2		+	+	+	
580	Lamin A/C		+	+		+
	Coatomer subunit alpha		+	+		+
598	UDP-glucose 6-dehydrogenase	+	+	+		
609	No protein identified	+	+	+		
683	No protein identified		+		+	+
686	Protein disulfide-isomerase A3	+	+	+		
694	Protein disulfide-isomerase A3	+	+	+		
702	No protein identified	+	+		+	+
734	T-complex protein 1 subunit beta	+	+		+	
852	No protein identified	+			+	+
877	No protein identified	+	+	+	+	
918	ANKRD26-like family C member 1A	+	+	+		+
	Actin cytoplasmic 1	+	+	+		+
	Actin cytoplasmic 2	+	+	+		+
953	26S protease regulatory subunit 8	+			+	+
	Mitochondrial Import receptor subunit TOM40 homolog	+			+	+
	Fumarate hydratase mitochondrial	+			+	+
1108	Nucleophosmin	+	+	+		
1216	Annexin A2	+	+	+		

ANKRD26: Ankyrin repeat domain-containing protein 26; GCA: giant cell arteritis; HSP: heat shock protein; ID: identity; UDP: Uridine diphosphate; TOM40 : Translocase of outer membrane 40kDa

Supplemental File 2. Mass Spectrometry Data. The following information is given to highlight the MS/MS spectra for the 8 proteins identified with a single peptide showed in Tables 2 and 4.

Precursor 1348.667Da MS/MS results (protein ID 294 - putative HSP90lamine A/C)

Mascot Search Results

Match to: H90B3_HUMAN Score: 40

Putative heat shock protein HSP 90-beta-3 OS=Homo sapiens GN=HSP90AB3P PE=5 SV=1

1 MPEEVHHGEE EVETFAFQAE IAQLISLIIN TFYSNEEIFL QELISNASDA

51 LDKIRYESLT DPSKLDSGKE LKIDIIPNPQ ERTLALVDTG IGMTKADLIN

101 NLRTIAKSGT KACMEALQAE KLVVITKHND DEQYAWESSA GGSFTVHADH

151 GEPIGRGTKV ILHLKEDQTE YLEERRVKEV VKKHSQFIGY PITLYLEKEQ

201 DKEISDDEAE EEKGEKEEED KDDEEKPKIK DVGSDEEDDS KEYGEFYKSL

251 TSDWEDHLAV KHFSVEGQLE FRALLFSPRR APFDLFENKK KKNNIKLYVR

301 RVFIMDSCDE LIPEYLNFIH GVVDSEDLPL NISREMLQQS KILKYVSHMK

351 ETQKSTYYIT GESKEQVANS AFVERVRKQG FEVVYMTEPI DEYCVQQLKE

401 FDGKSLVSVT KEGLELPEDE EEKKKMEESK EKFENLCKLM KEILDKKVEK

451 VTISNRLVSS PCCIVTSTYG WTANMEQIMK AQALRDNSTM GYMMAKKHLE

501 INPDHPIMET LRQKAEADKN DKAVKDLVVL LFETALLSSG FSLEDPQTHS

551 NHIYHMIKLG LGTDEDEVAA EEPSDAVPDE IPPLEGDEDA SRMEEVD

Start - End	Observed	Mr(expt)	Mr(calc)	ppm	Miss	Sequence
262 - 272	1348.667	1347.659	1347.657	2	0	K.HFSVEGQLEFR.A

(Ions score 40)

MS/MS Fragmentation of HFSVEGQLEFR

Found in H90B3_HUMAN, Putative heat shock protein HSP 90-beta-3 OS=Homo sapiens GN=HSP90AB3P PE=5 SV=1

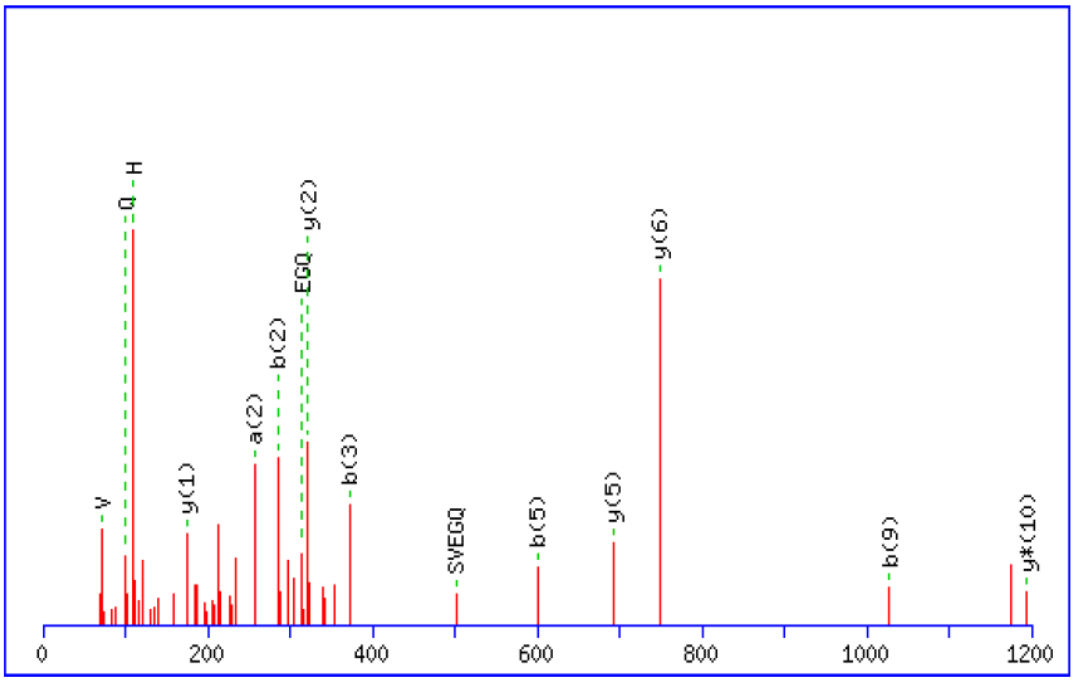

#	b	Seq.	y	#
1	138.066	H		11
2	285.135	F	1211.606	10
3	372.167	S	1064.537	9
4	471.235	V	977.505	8
5	600.278	E	878.437	7
6	657.299	G	749.394	6
7	785.358	Q	692.373	5
8	898.442	L	564.314	4
9	1027.484	E	451.23	3
10	1174.553	F	322.187	2
11		R	175.119	1

Precursor 1023.503Da MS/MS results (protein ID 580 - lamine A/C)

Mascot Search Results

Match to: LMNA_HUMAN Score: 38 Expect: 3.6

Lamin-A/C OS=Homo sapiens GN=LMNA PE=1 SV=1

1 METPSQRRAT RSGAQASSTP LSPTRITRLQ EKEDLQELND

RLAVYIDRVR

51 SLETENAGLR LRITESEEVV SREVSGIKAA YEAELGDARK TLDSVAKERA

101 RLQLELSKVR EEFKELKARN TKKEGDLIAA QARLKDLEAL LNSKEAALST

151 ALSEKRTLEG ELHDLRGQVA KLEAALGEAK KQLQDEMLRR VDAENRLQTM

201 KEELDFQKNI YSEELRETKR RHETRLVEID NGKQREFESR LADALQELRA

251 QHEDQVEQYK KELEKTYSAK LDNARQSAER NSNLVGAAHE ELQQSRIRID

301 SLSAQLSQLQ KQLAAKEAKL RDLEDSLARE RDTSRRLLAE KEREMAEMRA

351 RMQQQLDEYQ ELLDIKLALD MEIHAYRKLL EGEEERLRLS PSPTSQRSRG

401 RASSHSSQTQ GGGSVTKKRK LESTESRSSF SQHARTSGRV AVEEVDEEGK

451 FVRLRNKSNE DQSMGNWQIK RQNGDDPLLT YRFPPKFTLK AGQVVTIWAA

501 GAGATHSPPT DLVWKAQNTW GCGNSLRTAL INSTGEEVAM RKLVRSVTVV

551 EDDEDEDGDD LLHHHHGSHC SSSGDPAEYN LRSRTVLCGT CGQPADKASA

601 SGSGAQVGGP ISSGSSASSV TVTRSYRSVG GSGGGSFGDN LVTRSYLLGN

651 SSPRTQSPQN CSIM

Start - End	Observed	Mr(expt)	Mr(calc)	ppm	Miss	Sequence	
209 - 216	1023.503	1022.496	1022.503	-7	0	K.NIYSEELR.E	(Ions score 24)

MS/MS Fragmentation of **NIYSEELR**
Found in **LMNA_HUMAN**, Lamin-A/C OS=Homo sapiens GN=LMNA PE=1 SV=1

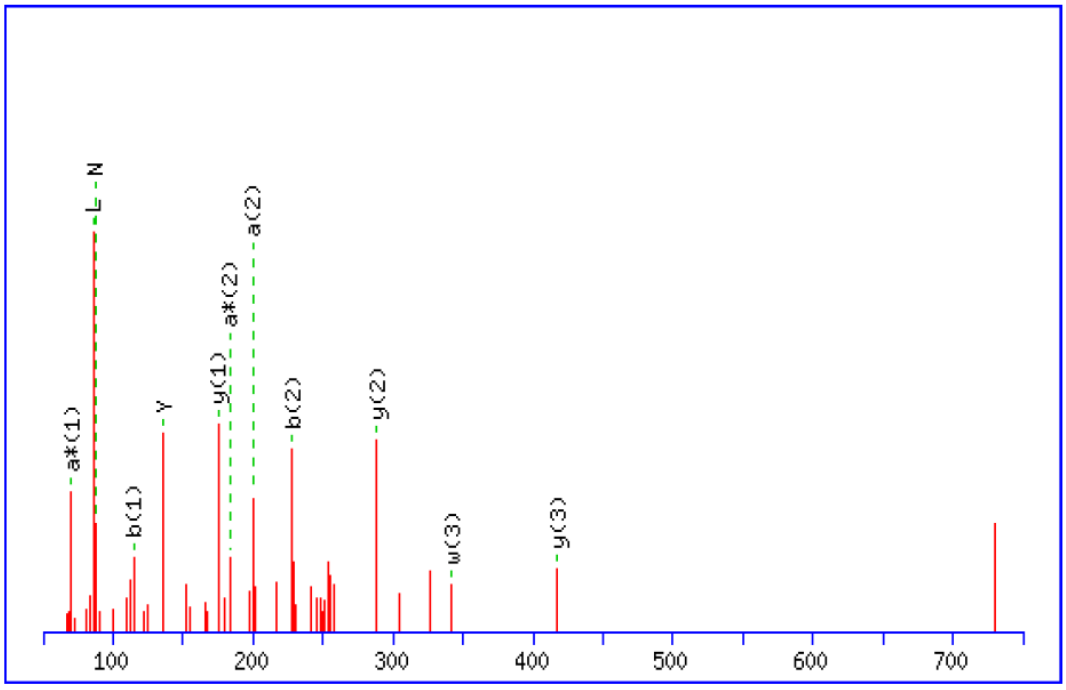

#	b	Seq.	y	#
1	115.05	N		8
2	228.134	I	909.468	7
3	391.198	Y	796.384	6
4	478.23	S	633.32	5
5	607.272	E	546.288	4
6	736.315	E	417.246	3
7	849.399	L	288.203	2
8		R	175.119	1

Precursor 1023.503Da MS/MS results (protein ID 580 - coatamer subunit-alapha)

Mascot Search Results

Match to: COPA_HUMAN Score: 37

Coatomer subunit alpha OS=Homo sapiens GN=COPA PE=1 SV=2

1 MLTKFETKSA RVKGLSFHPK RPWILTSLHN GVIQLWDYRM
CTLIDKFDEH
51 DGPVRGIDFH KQQPLFVSGG DDYKIKVWNY KLRRCLFTLL GHLDYIRTTF
101 FHHEYPWILS ASDDQTIRVW NWQSRTCVCV LTGHNHYVMC
AQFHPTEDLV
151 VSASLDQTVR VWDISGLRKK NLSPGAVESD VRGITGVDLF GTTDAVVKHV
201 LEGHDRGVNW AAFHPTMPLI VSGADDRQVK IWRMNESKAW
EVDTCRGHYN
251 NVSCAVFHPR QELILSNSED KSIRVWDMSK RTGVQTFRRD
HDRFWVLAAH
301 PNLNLFAAGH DGGMIVFKLE RERPAYAVHG NMLHYVKDRF
LRQLDFNSSK
351 DVAVMQLRSG SKFPVFNMSY NPAENAVLLC TRASNLENST YDLYTIPKDA
401 DSQNPDAPEG KRSSGLTAVW VARNRFAVLD RMHSLLIKNL
KNEITKKVQV
451 PNCDEIFYAG TGNLLLRDAD SITLFDVQQK RTLASVKISK VKYVIWSADM
501 SHVALLAKHA IVICNRKLDA LCNIHENIRV KSGAWDESGV
FIYTTSNHIK
551 YAVTTGDHGI IRTLDLPIYV TRVKGNNVYC LDRECRPRVL TIDPTEFKFK
601 LALINRKYDE VLHMVRNAKL VGQSIIAYLQ KKGYPEVALH FVKDEKTRFS
651 LALECGNIEI ALEAAKALDD KNCWEKLGEV ALLQGNHQIV EMCYQRTKNF
701 DKLSFLYLIT GNLEKLRKMM KIAEIRKDMS GHYQNALYLG DVSERVRILK
751 NCGQKSLAYL TAATHGLDEE AESLKETFDP EKETIPDIDP NAKLLQPPAP
801 IMPLDTNWPL LTVSKGFFEG TIASKGKGGA LAADIDIDTV GTEGWGEDAE

851 LQLDEDGFVE ATEGLGDDAL GKGQEEGGGW DVEEDLELPP
ELDISPGAAG
901 GAEDGFFVPP TKGTSPTQIW CNNSQLPVDH ILAGSFETAM RLLHDQVGVI
951 QFGPYKQLFL QTYARGRTTY QALPCLPSMY GYPNRNWKDA
GLKNGVPAVG
1001 LKLNDLIQRL QLCYQLTTVG KFEEAVEKFR SILLSVPLLV VDNKQEIAEA
1051 QQLITICREY IVGLSVETER KKLPKETLEQ QKRICEMAAY FTHSNLQPVH
1101 MILVLRTALN LFFKLKNFKT AATFARRLLE LGPKPEVAQQ TRKILSACEK
1151 NPTDAYQLNY DMHNPFDICA ASYRPIYRGK PVEKCPLSGA
CYSPEFKGQI
1201 CRVTTVTEIG KDVIGLRISP LQFR

Start - End	Observed	Mr(expt)	Mr(calc)	ppm	Miss	Sequence
719 - 726	1023.503	1022.496	1022.525	-29	1	K.MMKIAEIR.K 2 __Oxidation (M) (Ions score 37)

MS/MS Fragmentation of **MMKIAEIR**
Found in **COPA_HUMAN**, Coatomer subunit alpha OS=Homo sapiens GN=COPA PE=1 SV=2

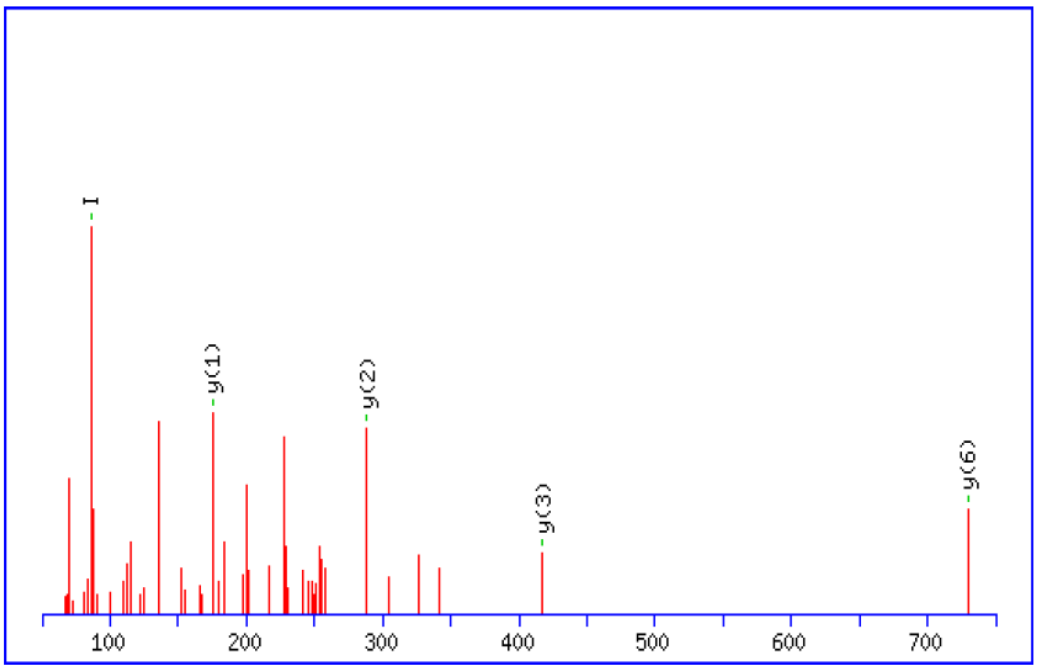

#	b	Seq.	y	#
1	84.044	M		8
2	167.082	M	812.499	7
3	295.176	K	729.462	6
4	408.261	I	601.367	5
5	479.298	A	488.283	4
6	608.34	E	417.246	3
7	721.424	I	288.203	2
8		R	175.119	1

Precursor 1370.688Da MS/MS results (protein ID 598 - UDP glucose 6 deshydrogenase)

Mascot Search Results

Match to: UGDH_HUMAN Score: 39

UDP-glucose 6-dehydrogenase OS=Homo sapiens GN=UGDH PE=1 SV=1

Matched peptides shown in Bold Red

1 MFEIKKICCI GAGYVGGPTC SVIAHMCPEI RVTVVDVNES
RINAWNSPTL
51 PIYEPGLKEV VESCRGKNLF FSTNIDDAIK EADLVFISVN TPTKTYGMGK
101 GRAADLKYIE ACARRIVQNS NGYKIVTEKS TVPVRAAESI RRIFDANTKP
151 NLNLQVLSNP EFLAEGTAIK DLKNPDRVLI GGDETPEGQR AVQALCAVYE
201 HWVPREKILT TNTWSSELSK LAANAFLAQR ISSINSISAL CEATGADVEE
251 VATAIGMDQR IGNKFLKASV GFGGSCFQKD VLNLVYLCEA
LNLPEVARYW
301 QQVIDMNDYQ RRRFASRIID SLFNTVTDKK IAILGFAFKK DTGDTRESSS
351 IYISKYLMDE GAHLHIYDPK VPREQIVVDL SHPGVSEDDQ VSRLVTISKD
401 PYEACDGAHA VVICTEWDMF KELDYERIHK KMLKPAFIFD GRRVLDGLHN
451 ELQTIGFQIE TIGKKVSSKR IPYAPSGEIP KFSLQDPPNK KPKV

Start - End	Observed	Mr(expt)	Mr(calc)	ppm	Miss	Sequence
178 - 190	1370.688	1369.681	1369.684	-2	0	R.VLIGGDETPEGQR.A (Ions score 39)

MS/MS Fragmentation of VLIGGDETPEGQR
Found in UGDH_HUMAN, UDP-glucose 6-dehydrogenase OS=Homo sapiens GN=UGDH PE=1 SV=1

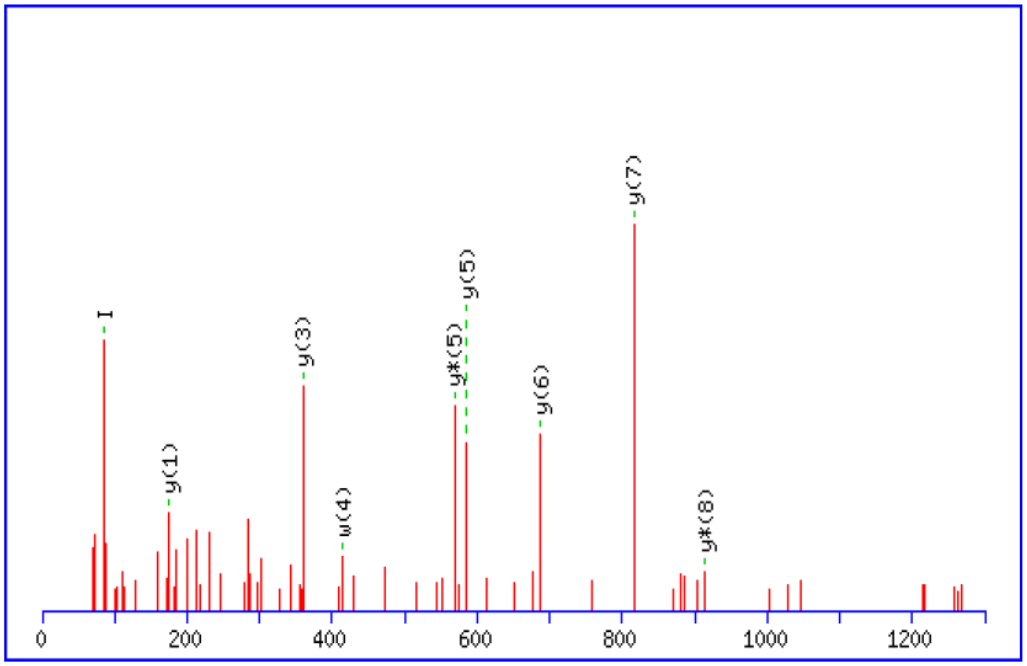

#	b	Seq.	y	#
1	100.076	V		13
2	213.16	L	1271.623	12
3	326.244	I	1158.539	11
4	383.265	G	1045.454	10
5	440.287	G	988.433	9
6	555.314	D	931.412	8
7	684.356	E	816.385	7
8	785.404	T	687.342	6
9	882.457	P	586.294	5
10	1011.499	E	489.242	4
11	1068.521	G	360.199	3
12	1196.579	Q	303.178	2
13		R	175.119	1

Precursor 1214.597Da MS/MS results (protein ID 953 - fumarate hydratase mitochondriale)

Mascot Search Results

Match to: FUMH_HUMAN Score: 61

Fumarate hydratase, mitochondrial OS=Homo sapiens GN=FH PE=1 SV=3

Matched peptides shown in Bold Red

1 MYRALRLLAR SRPLVRAPAA ALASAPGLGG AAVPSFWPPN

AARMASQNSF

51 RIEYDTFGEL KVPNDKYYGA QTVRSTMNFK IGGVTERMPT PVIKAFGILK

101 RAAAEVNQDY GLDPKIANAI MKAADEVAEG KLNDHFPLVV

WQTGSGTQTN

151 MNVNEVISNR AIEMLGGELG SKIPVHPNDH VNKSQSSNDT FPTAMHIAAA

201 IEVHEVLLPG LQKLHDALDA KSKEFAQIIK IGRTHTQDAV PLTLGQEFSG

251 YVQQVKYAMT RIKAAMPRIY ELAAGGTAVG TGLNTRIGFA EKVAAKVAAL

301 TGLPFVTAPN KFEALAAHDA LVELSGAMNT TACSLMKIAN DIRFLGSGPR

351 SGLGELILPE NEPGSSIMPG KVNPTQCEAM TMVAAQVMGN

HVAVTVGGSN

401 GHFELNVFKP MMIKNVLHSA RLLGDASVSF TENCVVGIQA NTERINKLMN

451 ESLMLVTALN PHIGYDKAAK IAKTAHKNGS TLKETAIELG YLTAEQFDEW

501 VKPKDMLGPK

Start - End	Observed	Mr(expt)	Mr(calc)	ppm	Miss	Sequence
52 - 61	1214.597	1213.590	1213.587	3	0	R.IEYDTFGELK.V

(Ions score 61)

MS/MS Fragmentation of **IEYDTFGELK**

Found in **FUMH_HUMAN**, Fumarate hydratase, mitochondrial OS=Homo sapiens GN=FH PE=1 SV=3

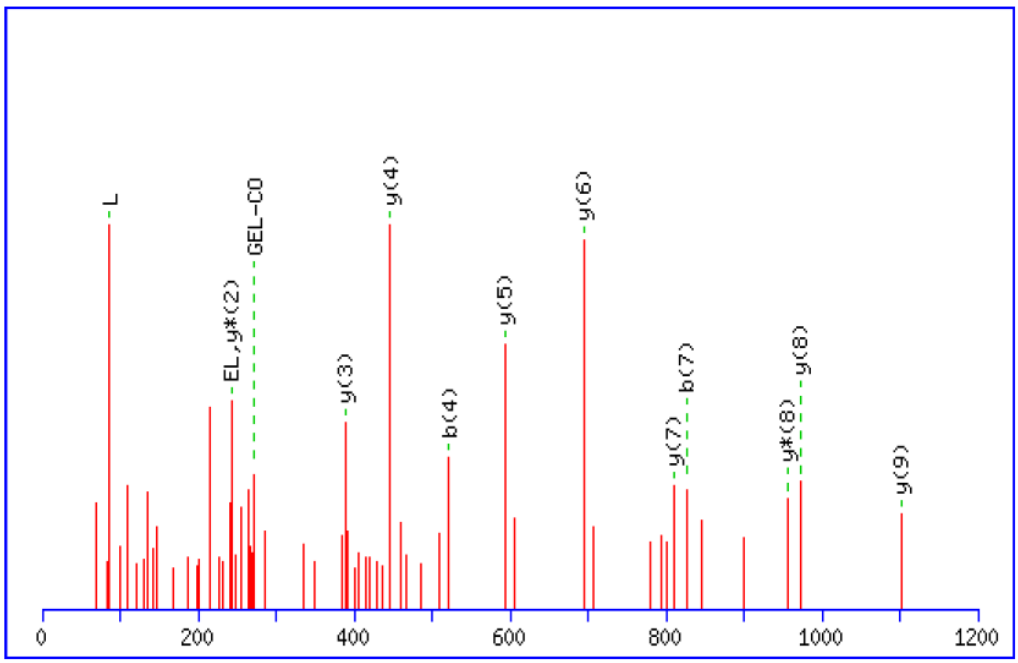

#	b	Seq.	y	#
1	114.091	I		10
2	243.134	E	1101.51	9
3	406.197	Y	972.467	8
4	521.224	D	809.404	7
5	622.272	T	694.377	6
6	769.34	F	593.329	5
7	826.362	G	446.261	4
8	955.404	E	389.239	3
9	1068.488	L	260.197	2
10		K	147.113	1

Precursor 927.552Da MS/MS results (protein ID 1821 - Fatty acid-binding protein, epidermal)

Mascot Search Results

Match to: FABP5_HUMAN Score: 26

Fatty acid-binding protein, epidermal - Homo sapiens (Human)

Matched peptides shown in Bold Red

1 MATVQQLEGR WRLVDSKGFD EYMKELGVGI ALRKMGAMAK PDCIITCDGK

51 NLTIKTESTL KTTQFSCTLG EKFEETTADG RKTQTVCNFT DGALVQHQEW

101 DGKESTITRK LKDGKLVVEC VMNNVTCTRI YEKVE

Start - End	Observed	Mr(expt)	Mr(calc)	ppm	Miss	Sequence
25 - 33	927.552	926.545	926.555	-11	0	K.ELGVGIALR.K (Ions score 26)

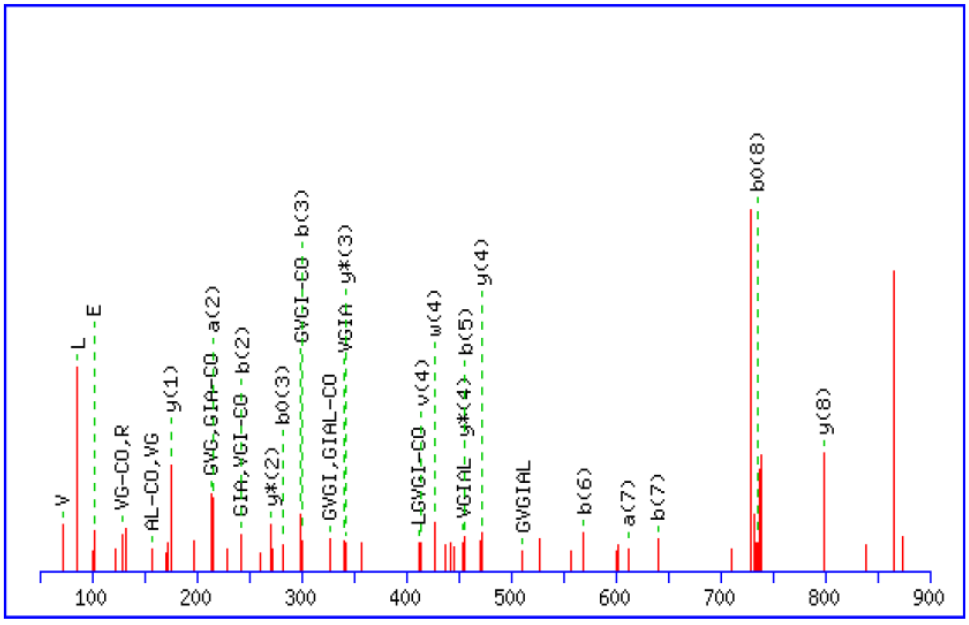

#	b	Seq.	y	#
1	130.05	E		9
2	243.134	L	798.52	8
3	300.155	G	685.436	7
4	399.224	V	628.414	6
5	456.245	G	529.346	5
6	569.329	I	472.324	4
7	640.366	A	359.24	3
8	753.451	L	288.203	2
9		R	175.119	1

Precursor 1388.841Da MS/MS results (protein ID 2120 - Poly(rC)-binding protein 1)

Mascot Search Results

Match to: PCBP1_HUMAN Score: 36

Poly(rC)-binding protein 1 - Homo sapiens (Human)

1 MDAGVTESGL NVTLTIRLLM HGKEVGSIIG KKGESVKRIR
EESGARINIS
51 EGNCPERIIT LTGPTNAIFK AFAMIIDKLE EDINSSMTNS TAASRPPVTL
101 RLVVPATQCG SLIGKGGCKI KEIRESTGAQ VQVAGDMLPN STERAITIAG
151 VPQSVTECVK QICLVMLETL SQSPQGRVMT IPYQPMPASS
PVICAGGQDR
201 CSDAAGYPHA THDLEGPPLD AYSIQGQHTI SPLDLAKLNQ
VARQQSHFAM
251 MHGGTGFAGI DSSSPEVKGY WASLDASTQT THELTIPNNL IGCIIGRQGA
301 NINEIRQMSG AQIKIANPVE GSSGRQVTIT GSAASISLAQ
YLINARLSSE
351 KGMGCS

Start - End	Observed	Mr(expt)	Mr(calc)	ppm	Miss	Sequence
58 - 70	1388.841	1387.833	1387.807	19	0	R.IITLTGPTNAIFK.A

(Ions score 36)

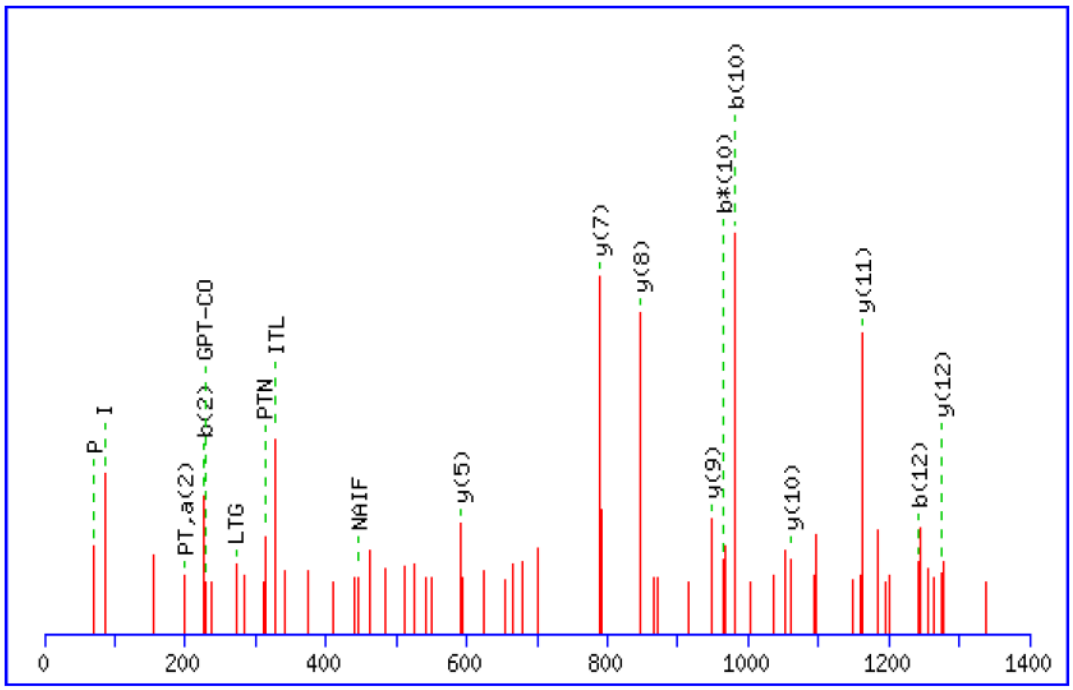

#	b	Seq.	y	#
1	114.091	I		13
2	227.175	I	1275.731	12
3	328.223	T	1162.647	11
4	441.307	L	1061.599	10
5	542.355	T	948.515	9
6	599.376	G	847.467	8
7	696.429	P	790.446	7
8	797.477	T	693.393	6
9	911.52	N	592.345	5
10	982.557	A	478.302	4
11	1095.641	I	407.265	3
12	1242.709	F	294.181	2
13		K	147.113	1

Precursor 914.507Da MS/MS results (protein ID 2120 - Heterogeneous nuclear ribonucleoprotein D0)

Mascot Search Results

Match to: HNRPD_HUMAN Score: 44 Expect:
0.77

Heterogeneous nuclear ribonucleoprotein D0 - Homo sapiens (Human)

Matched peptides shown in Bold Red

1 MEVPPRLSHV PPPLFPSAPA TLASRSLSHW RPRPPRQLAP LLPSLAPSSA
51 RQGARRAQRH VTAQQPSRLA GGAAIKGGRR RRPDLFRRHF
KSSSIQRSAA
101 AAAATRTARQ HPPADSSVTM EDMNEYSNIE EFAEGSKINA
SKNQQDDGKM
151 FIGGLSWDTS KKDLTEYLSR FGEVVDCTIK TDPVTGRSRG FGFVLFKDAA
201 SVDKVLELKE HKLDGKLIDP KRAKALKGKE PPKKVFVGGL SPDTSEEQIK
251 EYFGAFGEIE NIELPMDTKT NERRGFCFIT YTDEEPVKKL LESRYHQIGS
301 GKCEIKVAQP KEVYRQQQQQ QKGGRGAAAG GRGGTRGRGR
GQGQNWNQGF
351 NNYYDQGYGN YNSAYGGDQN YSGYGGYDYT GYNYGNYGYG
QGYADYSGQQ
401 STYGKASRGG GNHQNNYQPY

Start - End	Observed	Mr(expt)	Mr(calc)	ppm	Miss	Sequence
190 - 197	914.507	913.500	913.506	-7	0	R.GFGFVLFK.D (Ions score 36)

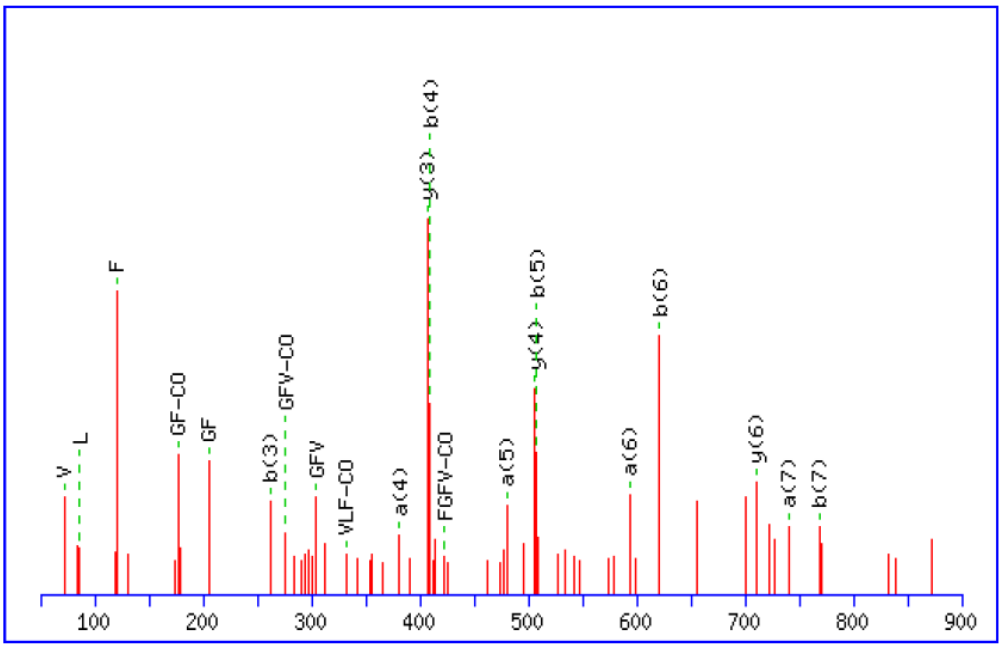

#	b	Seq.	y	#
1	58.029	G		8
2	205.097	F	857.492	7
3	262.119	G	710.424	6
4	409.187	F	653.402	5
5	508.255	V	506.334	4
6	621.34	L	407.265	3
7	768.408	F	294.181	2
8		K	147.113	1

Supplemental Figure S3. Two-dimensional immunoblots of IgG reactivity to lamin in sera of patients with giant cell arteritis. Protein extract is from human umbilical vein endothelial cells (HUVECs). **(A)** IgG reactivities to lamin of three different pools of sera from three giant cell arteritis patients each (P1 to P3) and one pool from twelve healthy controls (HCs). **(B)** Lamin spots are expressed in 3-D views for one representative sera pool from patients (top) and the HC pool (bottom). **(C)** Proteome of HUVECs showing the localisation of lamin spots displayed in **(A)**.

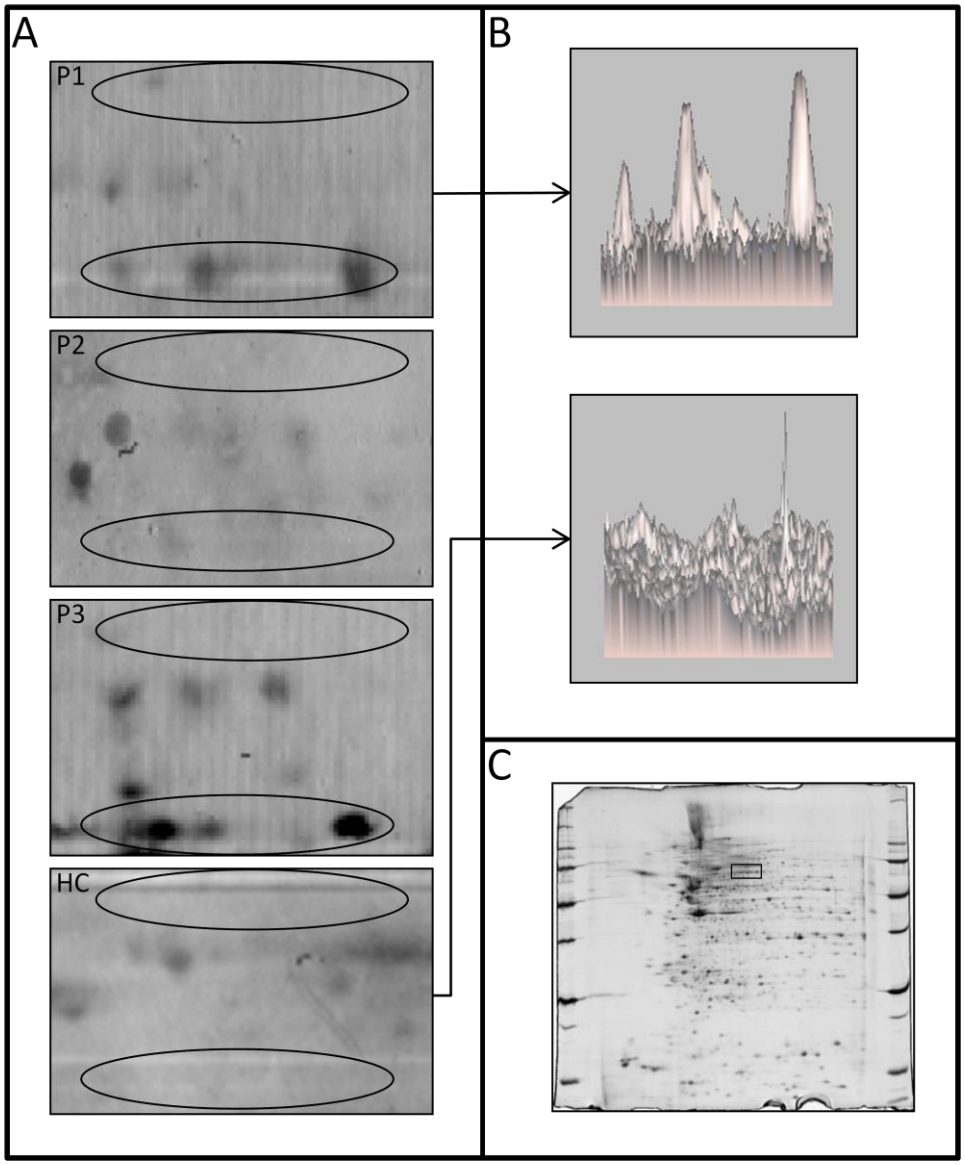

Supplemental Figure S4. Protein network generated by merging the two pathways involved in target antigens. Protein extracts are from human umbilical vein endothelial cells and vascular smooth muscle cells. Solid lines indicate direct interactions. Dashed lines indicate indirect interactions. Arrows indicate stimulation. ABCA2: ATP-binding cassette, subfamily A, (ABC1), member 2; ACTB: actin, β; ACTG1: actin, γ1; ANXA2: annexin A2; ANXA5: annexin A5; CCND2: cyclin D2; CCT2: chaperonin containing TCP1, subunit 2 (β); COPA: coatomer protein complex, subunit α; CPOX: coproporphyrinogen oxidase; DLD: dihydrolipoamide dehydrogenase; ENO1: enolase 1, α; EZR: ezrin; FABP5: fatty acid-binding protein 5; FH: fumarate hydratase; FUBP1: far upstream element (FUSE)-binding protein 1; GRB2: growth factor receptor-bound protein 2; HNRNPD: heterogeneous nuclear ribonucleoprotein D; HSP90AA2: heat shock protein 90 kDa α (cytosolic), class A, member 2; HSPB1: heat shock 27-kDa protein 1; IFNG: interferon γ; IKBKG: inhibitor of κ light polypeptide gene enhancer in B cells, kinase γ; IL4: interleukin 4; IMPDH2: IMP (inosine 5'-monophosphate) dehydrogenase; IRS1: insulin receptor substrate 1; KHSRP: KH-type splicing regulatory protein; LMNA: lamin A/C; MSN: moesin; NDUFS3: NADH dehydrogenase (ubiquinone) iron-sulphur protein 3, 30 kDa (NADH coenzyme Q reductase); NPM1: nucleophosmin (nuclear phosphoprotein B23, numatrin); PARK7: Parkinson's disease (autosomal recessive early onset) 7; PDGF BB: platelet-derived growth factor B dimer; PDIA3: protein disulphide isomerase, family A, member 3; PHB: prohibitin; PPIA: peptidylpropyl-isomerase A; PRDX3: peroxiredoxin 3; PSMC5: proteasome 26S subunit, ATPase, 5; RDX: radixin; RPLPO: ribosomal protein, large, P0; SEMA4D: Sema domain, immunoglobulin domain (Ig), transmembrane domain (TM) and short cytosolic domain (semaphorin) 4D; TNF: tumour necrosis factor; TOMM40: translocase of outer mitochondrial membrane 40 homolog (yeast); TP53: tumour protein P53; TPP1: tripeptidyl 1

peptidase; TUFM: Tu translation elongation factor, mitochondrial; UGDH: UDP-glucose 6-dehydrogenase; VCL: vinculin; VDAC2: voltage-dependent anion channel 2.

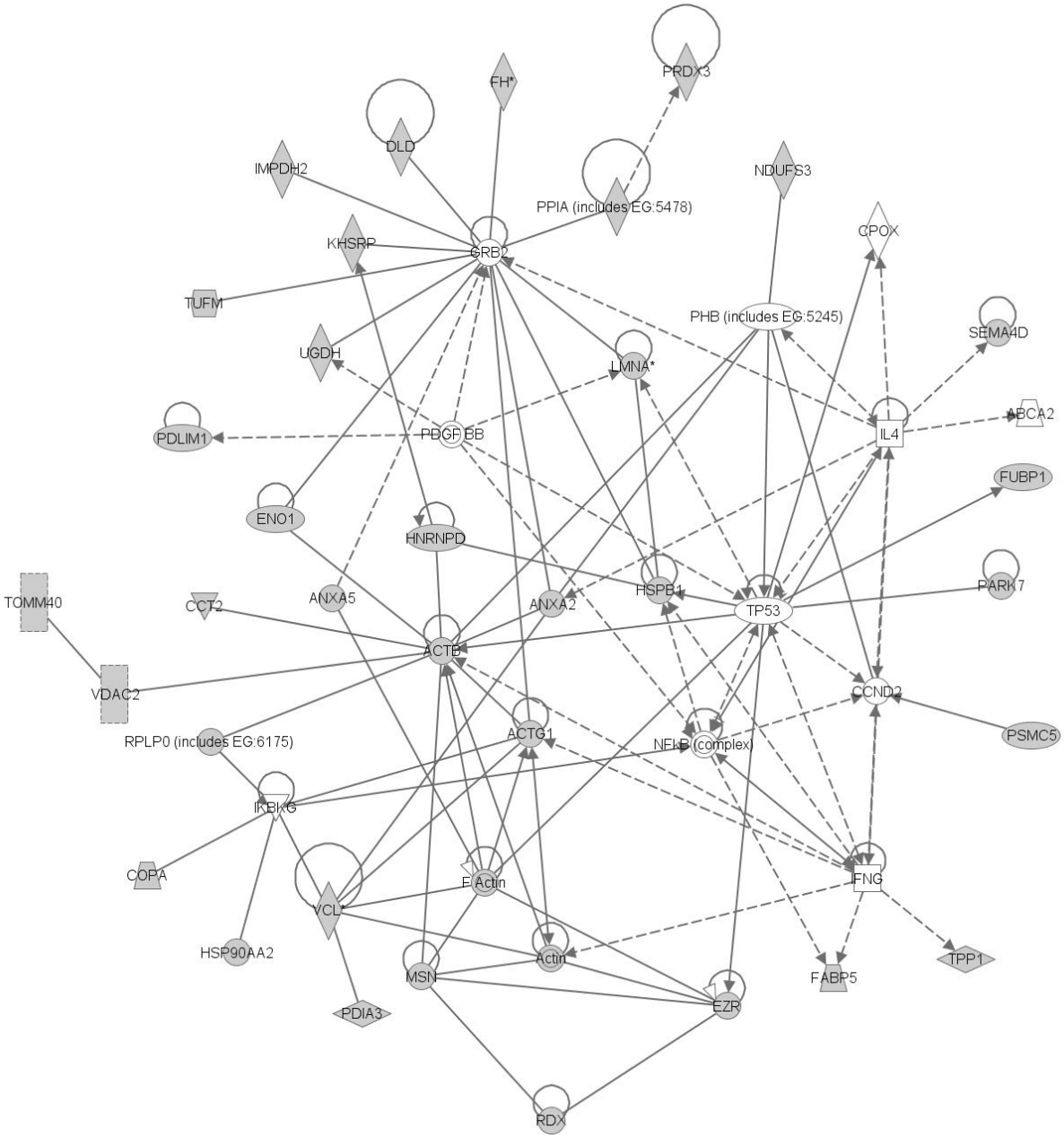

3.2. Analyse protéomique des cellules musculaires lisses vasculaires en condition physiologique et pathologique: d'un phénotype contractile à un phénotype synthétique

Alexis Régent, Kim Heang Ly, Guilhem Clary, Sébastien Lofek, Matthieu Tamby, Nicolas Tamas, Christian Federici, Cédric Broussard, Philippe Chafey, Marc Humbert, Frédéric Perros, Luc Mouthon

Les CMLV sont des cellules hautement spécialisées qui régulent le tonus vasculaire et participent au remodelage vasculaire au cours de processus physiologiques ou pathologiques. La comparaison des CMLV issues de vaisseaux différents n'a jamais été réalisée et cela pourrait permettre de comprendre pourquoi certaines maladies touchent un type de vaisseau alors qu'un autre est épargné.

Notre objectif est de comparer le contenu protéique de cellules humaines normales provenant d'aorte (HAoSMC), d'artère ombilicale (HUASMC) et d'artère pulmonaire (HPASMC) avec des cellules provenant d'artère pulmonaire de patients présentant une HTAP (PAH-SMC), pathologie marquée par un remodelage vasculaire. Les protéomes ont été comparés par 2D-DIGE et les protéines d'intérêt ont été identifiées par MS. Seulement 19 spots protéiques étaient différemment exprimés entre HAoSMC et HPASMC alors que 132 et 124 étaient exprimées différemment entre HUASMC et HAoSMC et HPASMC respectivement (rapport d'expression 1.5, $p<0.05$). Parmi les 336 spots protéiques qui étaient exprimés différemment entre HPASMC et PAH-SMC, nous avons identifié que la calponine, une protéine impliquée dans la régulation de la contraction des CMLV était plus exprimée au sein des PAH-SMC et que la protéine « uveal antigen with coiled-coil domains and ankyrin repeats »(UACA), impliquée dans la régulation de l'apoptose induite par le stress était

surexprimée dans les CMLV de donneurs sains. L'analyse à l'aide du logiciel Ingenuity a permis d'identifier que la paxilline était une protéine qui interagissait avec de nombreuses protéines d'intérêt. De façon notable, la prolifération des PAH-SMC était augmentée comparativement aux HPASMC. L'inhibition de la paxilline à l'aide d'un siRNA a permis d'inhiber ce phénotype. Ainsi, les CMLV ont des contenus protéiques très différents d'un site à l'autre en condition physiologique avec une variation encore plus grande en condition pathologique. La paxilline pourrait être une cible thérapeutique d'avenir au cours de l'HTAP.

Proteomic analysis of vascular smooth muscle cells in physiological condition and in pulmonary arterial hypertension: toward contractile versus synthetic phenotypes.

Alexis Régent[1,2], Kim Heang Ly[3], Guilhem Clary[1,4], Sébastien Lofek[1], Mathieu Tamby[1], Nicolas Tamas[1], Christian Federici[1,4], Cédric Broussard[1,4], Philippe Chafey[1,4], Marc Humbert[5], Frédéric Perros[5], Luc Mouthon[1,2]

[1]Institut Cochin, INSERM U1016, CNRS UMR 8104, LabEx INFLAMEX, Université Paris Descartes, Paris France ;

[2]Service de Médecine Interne, Centre de Référence pour les vascularites nécrosantes et la sclérodermie systémique, Hôpital Cochin, Assistance Publique-Hôpitaux de Paris, Paris, France;

[4]Plate-forme Protéomique 3P5, Université Paris Descartes, Sorbonne Paris Cité, Paris, France.

[5]Université Paris-Sud, Faculté de Médecine, Le Kremlin-Bicêtre, France; INSERM UMR-S 999, Hypertension Artérielle Pulmonaire: Physiopathologie et Innovation Thérapeutique, LabEx LERMIT, Le Plessis-Robinson, France; Centre Chirurgical Marie Lannelongue, Département de recherche Médicale, Le Plessis-Robinson, France

AR: alexisregent@hotmail.com ; KHL: kim.ly@chu-limoges.fr ; GC: guilhem.clary@inserm.fr ; SL : sebastien.lofek@gmail.com ; MT : mtamby@gmail.com; NT: nicolas.tamas@parisdescartes.fr ; CF: christian.federici@inserm.fr ; CB: cedric.broussard@inserm.fr ; PC :

philippe.chafey@inserm.fr; MH: marc.humbert@u-psud.fr; FP : frederic.perros@gmail.com; LM: luc.mouthon@cch.aphp.fr

Correspondance: Dr Luc Mouthon, INSERM U1016, CNRS UMR 8104, 8 rue Mechain, 75014 Paris, France.

Tel: +33 (0) 1 58 41 20 31 / Fax: +33 (0) 1 58 41 14 50

e-mail: luc.mouthon@cch.aphp.fr

Key words: Cell biology, vascular smooth muscle cell, pulmonary hypertension, paxillin

ABSTRACT

Vascular smooth muscle cells (VSMC) are highly specialized cells that regulate vascular tone and participate in vessel remodelling in physiological and pathological conditions. It is unclear why certain diseases involve one type of vessel and spare others. Our objective was to compare the proteomes of normal human VSMC from aorta (HAoSMC), umbilical artery (HUASMC), pulmonary artery (HPASMC) and pulmonary artery VSMC from patients with pulmonary arterial hypertension (PAH-SMC). Proteomes of VSMC were compared by 2D DIGE and MS. Only 19 proteins where differentially expressed between HAoSMC and HPASMC while 132 and 124 were differentially expressed between HUASMC and HAoSMC or HPASC, respectively (fold change 1.5, $p<0.05$). Among the 336 proteins that were differentially expressed between HPASMC and PAH-SMC (fold change 1.5, $p<0.05$), calponin, a protein involved in regulation of VSMC contraction was overexpressed in PAH-SMC and uveal antigen with coiled-coil domains and ankyrin repeats (UACA), a protein involved in the regulation of stress-induced apoptosis was overexpressed in VSMC from healthy donors . Analysis with Ingenuity® identified paxillin as a molecule interacting with a lot of proteins differentially expressed between HPASMC and PAH-SMC. Interestingly, proliferation of PAH-SMC was increased compared to HPASMC. Inhibition of paxillin with si-RNA reversed this phenotype. Thus, VSMC have very diverse protein content regarding their vascular origin. Paxillin targeting may be a promising treatment of PAH.

ABBREVIATIONS:

α-SMA: α-smooth muscle actin

BMPR2: Bone morphogenetic protein receptor type II

CD: cluster of differentiation

CREB: C-AMP Response Element-binding protein

EC: endothelial cell

HAoSMC: human aortic smooth muscle cells

HPASMC: human pulmonary artery smooth muscle cells

HUASMC: human umbilical artery smooth muscle cells

PAH: pulmonary arterial hypertension

PDGF: platelet derived growth factor

SMA: α-smooth muscle actin

SM-MHC: smooth muscle-myosin heavy chain

STAT: signal transducer and activator of transcription

TGF-β: transforming growth factor β

TP53: tumor protein 53

VSMCs: vascular smooth muscle cells

vWF: von Willebrand Factor

INTRODUCTION

Vascular smooth muscle cells (VSMCs) are highly specialized cells that regulate vascular tone and participate in vascular remodelling in physiological and pathological conditions [1]. VSMC have been separated on a functional basis in a “synthetic” phenotype which is responsible for proliferation, synthesis of extracellular matrix and a fully differentiated “contractile” phenotype that express high level of contractile protein such as smooth muscle-myosin heavy chain (SM-MHC), α-smooth muscle actin (SMA) and calponin [2-4]. However, phenotypic modulations and reversible transitions between these phenotypes occur in a complex and dynamic process [1]. VSMC can modify their expression pattern in response to acute stimuli such as PDGF, TGF-β and serum responsive factor [5]. Epigenetic regulation and microRNA expression profile might also contribute to this phenotypic modulation even though underlying mechanisms remain unclear [6, 7].

Many disorders are associated with VSMC dysfunction [8]. In pulmonary arterial hypertension (PAH), a severe condition defined by an elevated mean pulmonary arterial pressure above 25 mmHg at rest [9], there is distal extension of VSMC to normally non muscularized pulmonary arterioles which are also reduced in numbers [10]. There is also a thickening of the vascular wall due to increased migration and proliferation of VSMC. These elements contribute to intimal hyperplasia and neointimal formation with plexiform hyperplasia [10]. However, very scarce studies have compared VSMC [11, 12] and it is unclear why certain diseases involve pulmonary arteries whereas others involve the aorta. One of the reasons might be that the properties of VSMC are not the same in the different locations. In this view, to our knowledge, extensive studies of VSMC in different locations are lacking. In addition, we recently reported that IgG from patients with PAH and/or systemic

sclerosis bind to VSMCs and induce VSMC contraction [13]. However, we do not know if this is the consequence of the recognition of modified antigens corresponding to the disease process or antigens that are expressed in higher amounts than in VSMC from healthy controls. In order to better assess VSMC heterogeneity, we decided to use a proteomic approach to compare normal human VSMCs originating from different vascular beds and VSMC cultured from pulmonary arteries from patients with PAH.

2. PATIENTS AND METHODS

2.1. CELLS:

VSMC from patients with PAH were isolated from sterile, freshly obtained surgical explants from four different Caucasian donors undergoing pulmonary transplantation (3 patients had mutation in Bone morphogenetic protein receptor type II (BMPR2) gene). Briefly, pulmonary arteries were dissected and small vessels were digested by collagenase and elastase during 90 minutes before seeding in cell culture flasks (Falcon, Becton Dickinson, Franklin Lakes, New Jersey, USA). Smooth muscle cell origin was assessed by a positive α-SMA staining and a negative CD90 staining upon indirect immunofluorescence. Normal human VSMC were obtained from pulmonary artery, aorta and umbilical artery from four different healthy Caucasian donors each (Promocell GmbH, Heidelberg, Germany).

2.2 VSMCs culture and sample preparation

Normal human VSMC from aorta (HAoSMC), umbilical artery (HUSMC), pulmonary artery (HPASMC) and VSMC from patients with PAH (PAH-SMC) were cultured in smooth muscle cell growth medium 2 (Promocell GmbH) until harvesting after the fourth passage and proteins were extracted as previsouly described [14]**.**

2.3 2D DIGE and image analyses, in-gel trypsin digestion, and protein identification by MS.

The samples of different VSMC types were labeled with fluorescent dyes and separated by 2DE, then gels were analyzed and protein spots differentially expressed between VSMC types were excised and in-gel trypsin digested and

identified using MS. 2D DIGE, in-gel trypsin digestion, and MS protein identification procedures where adaptated from [14] and are detailed in Supporting Information.

2.4 Generation of biological networks

Generation of biological networks using Ingenuity pathway analysis (IPA) and Pathway Studio) were used to gain insights into the biological pathways and networks that were significantly represented in our proteomic data sets, (IPA; Ingenuity Systems, Redwood City, CA, USA) (Pathway Studio, Elsevier, Amsterdam, Netherlands). After uploading lists of differentially expressed protein to the IPA server, pathway networks with significant p-values ($p<0.05$) were generated.

2.5 SiRNA transfection and proliferation assay

Paxillin-siRNA and non targeting -siRNA were diluted with *trans*IT-X2 in opti-MEMI medium and transfection was performed according to manufacturer's instructions (Mirus bio LLC, Madison, Wisconsin, USA). Paxillin silencing was confirmed with an immunoblot with a rabbit anti-human paxillin antibody (Abcam, Cambridge, United Kingdom). Proliferation assay was performed with cells at 4^{th} passage with Cell Prolifération ELISA BrdU (Roche Diagnostics, Mannheim, Germany). Briefly, cells were serum starved for 24 hours and then stimulated during 72 hours with Paxillin-siRNA and non targeting-siRNA in a 96 well plate. After incubation, 10 µL of BrdU labelling solution was added to each well for 24 hours and BrdU incorporation was measured according to manufacturer's instructions with a spectrophotometer at 370 nm (FusionTM Universal Microplate Analyser, PerkinElmer, Waltham, Massachussetts, EU).

3. RESULTS

3.1 Comparison of proteins differentially expressed between VSMCs from pulmonary artery, aorta and umbilical artery

Using DeCyder Image Analysis software, a mean of 3293±250 different protein spots were detected in each gel. Among these, 2733±352 could be matched to the reference gel and were used for the comparative analysis.

A total of 198 and 79 distinct protein spots were identified as differentially expressed between VSMC from pulmonary artery, aorta and umbilical artery (fold change ≥ 1.5 and 2 respectively and a Student's t test p-value≤0.05) (Table1 A). Interestingly, there were huge differences between HUASMC and either HAoSMC or HPASMC with 132 and 124 proteins spots differentially expressed respectively whereas only 19 protein spots were differentially expressed between HPASMC and HAoSMC (fold change≥1.5 and p-value<0.05). Principal component analysis (PCA) was performed on the spots of interest (fold change≥1.5 and p-value<0.05). Interestingly, the two first components contributed to 76.9% of the variance of the analysis (Figure 1A).

Due to spot size and the different staining used for protein identification, 145 protein spots out of the 198 protein spots of interest (fold change ≥ 1.5 and a Student's t test p-value≤0.05), could be picked up for mass spectrometry identification.

Comparison of proteins differentially expressed between HUASMC and HAoSMC

One hundred and thirty two proteins were significantly differentially expressed between HUASMC and HAoSMC. These proteins were involved in glycolysis and gluconeogenesis as well as in 14-3-3 mediated signalling pathway (Additional Figure 1). Several proteins showed a high fold change of expression: vimentin, a

cytoskeleton protein involved in cell shape was overexpressed in HAoSMC in three different spots (fold change 3.0; 2.1; 2.1 respectively) while it was underexpressed in three other spots (fold change 2.7; 3.7; 6.4 respectively). Myosin, involved in contraction and cell motility was overexpressed in HAoSMC compared to HUASMC in two different spots (fold change 2.5; 2.5) and protein disulfide isomerase, a protein involved in disulfide bonds rearrangement was overexpressed in HUASMC compared to HAoSMC (fold change 8.2) (Table2 and supplemental Table 1).

Comparison of proteins differentially expressed between HUASMC and HPASMC

One hundred and twenty four proteins spots were differentially expressed between HUASMC and HPASMC. These proteins were involved in 14-3-3 mediated signalling pathway as well as in actin signalling (Additional Figure 2). Several proteins showed a high difference in fold change of expression: Protein S100 A4 and A6, which are involved in calcium signalling, were over expressed in HPASMC compared to HUASMC (fold change 3.7 and 3.4 respectively). Cathepsin D, a lyzozomal protein known to be expressed in extracellular space in aorta, was also overexpressed in HPASMC (fold change 2.8 and 1.8) (Figure 2). Protein disulfide isomerase 1 was overexpressed in HUAMSC (fold change 1.9 and 19) (Table 3 and Supplemental Table 2) compared to HPASMC.

Comparison of proteins differentially expressed between HPASMC and HAoSMC

Nineteen protein spots were differentially expressed between HPASMC and HAoSMC including proteins involved in cytoskeleton and cell interaction such as

myosine (fold change 2.2 and 1.8), collagen (fold change 2.2 and 4.9) and caldesmon (fold change 2.1) (Table 4 and Supplemental Table 3) that were overexpressed in aorta.

Biological network analysis of identified proteins

Using data on the 145 protein spots that were differentially expressed between HPASMC, HAoSMC, HUASMC (fold change ≥1.5 and $p<0.05$), we used IPA to generate a user-built pathway. Interestingly, Akt, NF-kB, and other protein and complexes involved in cellular response or proliferation such as c-AMP Response Element-binding protein (Creb) or tumor protein (TP53) were associated with a large number of identified proteins (Figure 3).

3.2 Identification of proteins differentially expressed between VSMC from pulmonary artery from healthy individuals and patients with PAH

Three hundred and thirty six and 259 protein spots were differentially expressed between HPASMC and PAH-SMC (fold change ≥ 1.5 and 2 respectively and a Student's t test p-value<0.05) (Table 5 and supplemental Table 4). PCA was performed with the 145 previously identified spots of interest and with the 207 new protein spots that were identified (fold change ≥ 1.5 and a Student's t test p-value<0.05) and the 2 first components contributed to 73.6% of the variance (Figure 1B). Interestingly, there was a greater number of differentially expressed proteins between PAH-SMC and HPASMC than between normal VSMC from different vessels and there was as much as 568 protein spots differentially expressed between PAH-SMC and HUASMC (Table1 B).

Identified proteins are involved in glycolysis, gluconeogenesis and mitochondrial dysfunction (Additional Figure 3). Interstingly, calponin a protein involved in regulation of VSMC contraction was overexpressed in PAH-SMC (Fold change 8.9) (Figure 4). Peroxiredoxin, a protein that mediates signal transduction was identified in two different protein spots and was overexpressed in PAH-SMC (fold change 6.8 and 5.5). On the opposite, uveal antigen with coiled-coil domains and ankyrin repeats (UACA), a protein involved in the regulation of stress-induced apoptosis was overexpressed in VSMC from healthy donors (fold change 10.1). Vigilin was also overexpressed as identified in two different spots in PASMC (fold change 8.8 and 9.4) (Table 5) (Figure 5).

Biological network analysis of identified proteins

A biological network was generated with IPA software using proteins differentially expressed between VSMC from patients with PAH and HPASMC. Interestingly, paxillin and signal transducers and activators of transcription (STAT) 3 were identified as proteins that interact with a large number of identified proteins (Figure 6).

Proliferation of VSMC with paxillin inhibition

Proliferation of PAH-SMC and HPASMC were compared in the presence of paxillin-siRNA and non targeting si-RNA. Proliferation of PAH-SMC was increased compared to HPASMC and inhibited by paxillin-siRNA whereas no effect was observed on HPASMC (Figure 7).

4. DISCUSSION

By using 2D DIGE, we compared the protein expression profiles of VSMC from different normal human arteries (HUASMC, HPASMC and HAoSMC) and found major differences between the proteomes of HUASMC and either HAoSMC or HPASMC. We also compared cells obtained in physiological conditions (HPASMC) and VSMC from patients with PAH.

Interestingly, 14-3-3 mediated signalling pathway was one of the major pathways that contributed to differentiate HUASM from either HPASMC or HAoSMC. This pathway is involved in a wide range of vital regulatory processes, such as mitogenic signal transduction, apoptotic cell death, cell cycle control and cell growth control. In VSMC, it has been shown that ζ 14-3-3-protein was localized in SMA^+-cells in atherosclerotic plaques [15]. In addition, it was shown that γ14-3-3-protein expression was increased in the context of coronary artery vasculopathy or in experimental models of arterial injury [16] and that γ14-3-3-protein was phosphorylated after PDGF stimulation [17]. At a protein level, we identified filamin and vimentin as differentially expressed between HUASMC and HPASMC or HAoSMC. Interestingly, filamin, gelsolin, vimentin and vinculin expression was reported to be diminished in medial atherosclerotic coronary VSMC [18] and vimentin and calponin expression was also diminished in VSMC from dissected aorta [2]. Taken together, these results suggest that the observed modification of protein content might be the consequence a switch between synthetic and contractile phenotypic state.

Calponin is a protein that is implicated in the regulation and modulation of smooth muscle contraction. It has been shown that calponin was overexpressed in HPASMC in response to incubation with MicroRNA-206 [19] and that mice treated with an adenovirus containing the full length cDNA of protein kinase G Iα had a diminished

calponin downregulation [20]. UACA has a documented role in the regulation of apoptosis. Interestingly, it has been found that this protein was down regulated in non small cell lung cancer [21]. The downregulation of this protein in PAH-SMC might contribute to explain the increased proliferation and decreased apoptosis documented in patients with PAH [22]. Proteins that were differentially expressed between HPASMC and PAH-SMC were involved in the “mitochondrial dysfunction” pathway as identified with IPA. Interestingly, energy metabolism abnormalities such as lower oxygen consumption of mitochondria and significantly higher glycolytic rate have been described during PAH [23]. This effect, called the Warburg effect was first described in cancer and is one of the hallmarks of PAH [10]. Taken together, we bring new information regarding the modification of the VSMC protein content occurring in VSMC from patients with PAH. In addition, we identified with IPA that a huge number of proteins differentially expressed between HPASMC and PAH-SMC were linked with paxillin. Our data thus confirms previous results from Veith and colleagues who identified paxillin as a regulator of VSMC growth in the setting of PAH [24]. To our knowledge, there is no currently available paxillin inhibitor. However, it has been shown that saracatinib, a Src inhibitor evaluated in cancer, could down regulate paxillin phosphorylation [25]. We confirmed in the present work that paxillin-siRNA could inhibit the excessive growth of PAH-SMC. Thus, targeting paxillin in patients with PAH might represent a future therapeutic option.

Another regulatory protein, STAT3, was also identified by Ingenuity analysis. This protein is a key mediator in PAH and is considered as a new possible therapeutic target [26].

Interestingly, few data were reported on the heterogeneity of VSMC and the underlying mechanisms of this heterogeneity [6, 7]. We recently demonstrated that,

according to their origin, endothelial cells (EC) have very distinct protein content and that it could reflect different biological properties and influence immune recognition [14]. The unique protein content observed in PAH-SMC might be the cause or the consequence of the pathological process and it might modify cell recognition by auto-antibodies. In this context, we reported that serum IgG from patients with PAH could induce the contraction of VSMC [13]. Our data could also contribute to explain why some arteries are involved and some other are spared in vascular diseases such as PAH, giant cell arteritis and other vascular diseases. In this view, specific TLR profiles were identified in dendritic cells of the adventitial layer of different vessels that might contribute to explain the vascular tropism of large vessel vasculitis [27].

However, our study has some limitations. We could only identify a mean of 3293 different protein spots and some proteins were lost at each step of the 2DIGE experiments and during protein identification process. In addition, the proliferation assay was performed with only 4 distinct donors in each group and additional experiments in larger groups of patients might be necessary to confirm our results.

In conclusion, we have demonstrated that proteome profiles of VSMC differ between HPASM, HAoSMC, HUASMC and PAH-SMC. It might reflect distinct biological properties, with a rather contractile phenotype in fully differentiated HPASMC and HAoSMC and a synthetic phenotype in HUAMSC. We confirm that paxillin targeting might be a therapeutic target in the context of PAH.

Acknowledgements

This work was performed within the Département Hospitalo-Universitaire (DHU) autoimmune and hormonal diseases. AR received financial support from the Société Nationale Française de Médecine Interne (SNFMI), ARMIIC (Association pour la

Recherche en Médecine Interne et en Immunologie Clinique) and GPM (Groupe Pasteur Mutualité). SL received a financial support from the DRCD of Assistance Publique-Hôpitaux de Paris.

REFERENCES

[1] Owens, G. K., Kumar, M. S., Wamhoff, B. R., Molecular regulation of vascular smooth muscle cell differentiation in development and disease. *Physiol Rev* 2004, *84*, 767-801.

[2] Zhang, J., Wang, L., Fu, W., Wang, C., *et al.*, Smooth muscle cell phenotypic diversity between dissected and unaffected thoracic aortic media. *J Cardiovasc Surg (Torino)* 2013, *54*, 511-521.

[3] Rensen, S. S., Doevendans, P. A., van Eys, G. J., Regulation and characteristics of vascular smooth muscle cell phenotypic diversity. *Neth Heart J* 2007, *15*, 100-108.

[4] Ailawadi, G., Moehle, C. W., Pei, H., Walton, S. P., *et al.*, Smooth muscle phenotypic modulation is an early event in aortic aneurysms. *J Thorac Cardiovasc Surg* 2009, *138*, 1392-1399.

[5] Werth, D., Grassi, G., Konjer, N., Dapas, B., *et al.*, Proliferation of human primary vascular smooth muscle cells depends on serum response factor. *Eur J Cell Biol* 2010, *89*, 216-224.

[6] Liu, R., Leslie, K. L., Martin, K. A., Epigenetic regulation of smooth muscle cell plasticity. *Biochim Biophys Acta* 2014.

[7] Madrigal-Matute, J., Rotllan, N., Aranda, J. F., Fernandez-Hernando, C., MicroRNAs and atherosclerosis. *Curr Atheroscler Rep* 2013, *15*, 322.

[8] Lacolley, P., Regnault, V., Nicoletti, A., Li, Z., Michel, J. B., The vascular smooth muscle cell in arterial pathology: a cell that can take on multiple roles. *Cardiovasc Res* 2012, *95*, 194-204.

[9] Hoeper, M. M., Bogaard, H. J., Condliffe, R., Frantz, R., *et al.*, Definitions and diagnosis of pulmonary hypertension. *J Am Coll Cardiol* 2013, *62*, D42-50.

[10] Rabinovitch, M., Molecular pathogenesis of pulmonary arterial hypertension. *J Clin Invest* 2012, *122*, 4306-4313.

[11] Choi, H. Y., Rahmani, M., Wong, B. W., Allahverdian, S., *et al.*, ATP-binding cassette transporter A1 expression and apolipoprotein A-I binding are impaired in intima-type arterial smooth muscle cells. *Circulation* 2009, *119*, 3223-3231.

[12] VanderLaan, P. A., Reardon, C. A., Getz, G. S., Site specificity of atherosclerosis: site-selective responses to atherosclerotic modulators. *Arterioscler Thromb Vasc Biol* 2004, *24*, 12-22.

[13] Bussone, G., Tamby, M. C., Calzas, C., Kherbeck, N., *et al.*, IgG from patients with pulmonary arterial hypertension and/or systemic sclerosis binds to vascular smooth muscle cells and induces cell contraction. *Ann Rheum Dis* 2012, *71*, 596-605.

[14] Dib, H., Chafey, P., Clary, G., Federici, C., *et al.*, Proteomes of umbilical vein and microvascular endothelial cells reflect distinct biological properties and influence immune recognition. *Proteomics* 2012, *12*, 2547-2555.

[15] Umahara, T., Uchihara, T., Koyama, S., Hashimoto, T., *et al.*, Isoform-specific immunolocalization of 14-3-3 proteins in atherosclerotic lesions of human carotid and main cerebral arteries. *J Neurol Sci* 2012, *317*, 106-111.

[16] Autieri, M. V., Inducible expression of the signal transduction protein 14-3-3gamma in injured arteries and stimulated human vascular smooth muscle cells. *Exp Mol Pathol* 2004, *76*, 99-107.

[17] Autieri, M. V., Carbone, C. J., 14-3-3Gamma interacts with and is phosphorylated by multiple protein kinase C isoforms in PDGF-stimulated human vascular smooth muscle cells. *DNA Cell Biol* 1999, *18*, 555-564.

[18] de la Cuesta, F., Zubiri, I., Maroto, A. S., Posada, M., *et al.*, Deregulation of smooth muscle cell cytoskeleton within the human atherosclerotic coronary media layer. *J Proteomics* 2013, *82*, 155-165.

[19] Jalali, S., Ramanathan, G. K., Parthasarathy, P. T., Aljubran, S., *et al.*, Mir-206 regulates pulmonary artery smooth muscle cell proliferation and differentiation. *PLoS One* 2012, *7*, e46808.
[20] Yi, B., Cui, J., Ning, J. N., Wang, G. S., *et al.*, Over-expression of PKGIalpha inhibits hypoxia-induced proliferation, Akt activation, and phenotype modulation of human PASMCs: the role of phenotype modulation of PASMCs in pulmonary vascular remodeling. *Gene* 2012, *492*, 354-360.
[21] Moravcikova, E., Krepela, E., Prochazka, J., Rousalova, I., *et al.*, Down-regulated expression of apoptosis-associated genes APIP and UACA in non-small cell lung carcinoma. *Int J Oncol* 2012, *40*, 2111-2121.
[22] Nasim, M. T., Ogo, T., Chowdhury, H. M., Zhao, L., *et al.*, BMPR-II deficiency elicits pro-proliferative and anti-apoptotic responses through the activation of TGFbeta-TAK1-MAPK pathways in PAH. *Hum Mol Genet* 2012, *21*, 2548-2558.
[23] Xu, W., Koeck, T., Lara, A. R., Neumann, D., *et al.*, Alterations of cellular bioenergetics in pulmonary artery endothelial cells. *Proc Natl Acad Sci U S A* 2007, *104*, 1342-1347.
[24] Veith, C., Marsh, L. M., Wygrecka, M., Rutschmann, K., *et al.*, Paxillin regulates pulmonary arterial smooth muscle cell function in pulmonary hypertension. *Am J Pathol* 20012, *181*, 1621-1633.
[25] Jones, R. J., Young, O., Renshaw, L., Jacobs, V., *et al.*, Src inhibitors in early breast cancer: a methodology, feasibility and variability study. *Breast Cancer Res Treat* 2009, *114*, 211-221.
[26] Paulin, R., Meloche, J., Bonnet, S., STAT3 signaling in pulmonary arterial hypertension. *JAKSTAT* 2012, *1*, 223-233.
[27] Pryshchep, O., Ma-Krupa, W., Younge, B. R., Goronzy, J. J., Weyand, C. M., Vessel-specific Toll-like receptor profiles in human medium and large arteries. *Circulation* 2008, *118*, 1276-1284.
[28] Shevchenko, A., Loboda, A., Ens, W., Schraven, B., Standing, K. G., Archived polyacrylamide gels as a resource for proteome characterization by mass spectrometry. *Electrophoresis* 2001, *22*, 1194-1203.

Figure 1. Comparison of proteomes of HUASMC, HAoSMC and HPASMC donors and PAH-SMC.

Principal component analysis (PCA) of the protein spots differentially expressed between HUASMC, HAoSMC and HPASMC with variance attributed to the two first components of the analysis. A hierarchical clustering of protein spots displayed as a heat map was also generated (A.) Addition of the protein spots of interest in the PAH-SMC versus HPASMC comparison to the PCA analysis and hierarchical clustering (B). The color scale goes from green (decreased protein expression) to black (no change in protein expression) to red (increased protein expression). White color represents a spot which is not detected or not matched. (C).

HUASMC : human umbilical artery smooth muscle cell; HAoSMC : human aorta smooth muscle cell; HPASMC : human pulmonary artery smooth muscle cell; PAH-SMC : pulmonary arterial hypertension smooth muscle cell

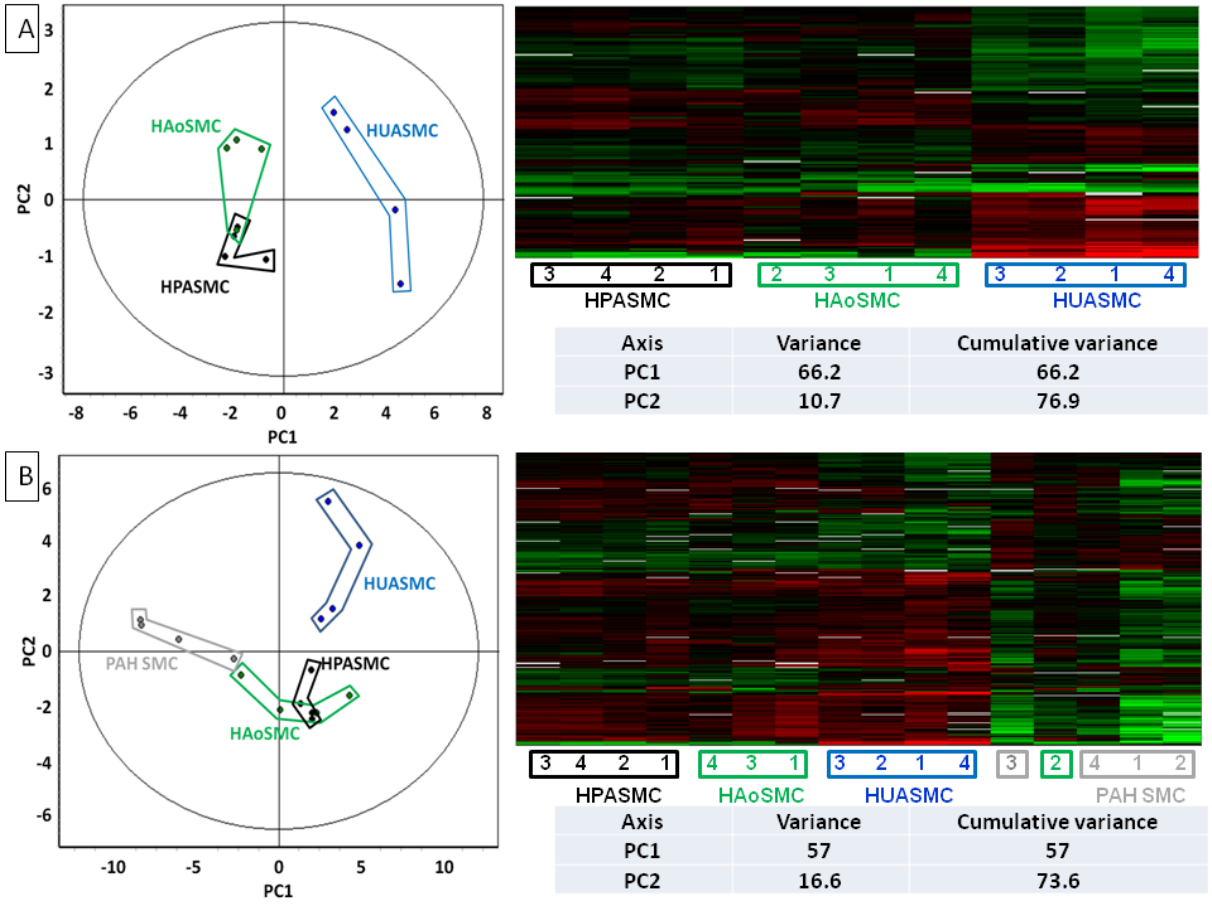

Figure 2: Differential expression of cathepsin D in smooth muscle cells from aorta, umbilical artery, pulmonary artery and SMC from patients with pulmonary arterial hypertension.

(A) 2D gel images of proteomes of HUASMC, HPASMC, HAoSMC and PAH-SMC from four individual donors each. The spot corresponding to cathepsin D protein is outlined in black. (B) Cathepsin D protein spots are expressed in 3D view in one single donor HUASMC (upper panel) and one HPASMC (lower panel) representative protein extract. (C) An internal standard proteome from a representative gel: the selected area of the gel contains the cathepsin D protein spot depicted in panel A. HUASMC : human umbilical artery smooth muscle cell; HAoSMC : human aorta smooth muscle cell; HPASMC : human pulmonary artery smooth muscle cell; PAH-SMC : Pulmonary artery hypertension smooth muscle cell

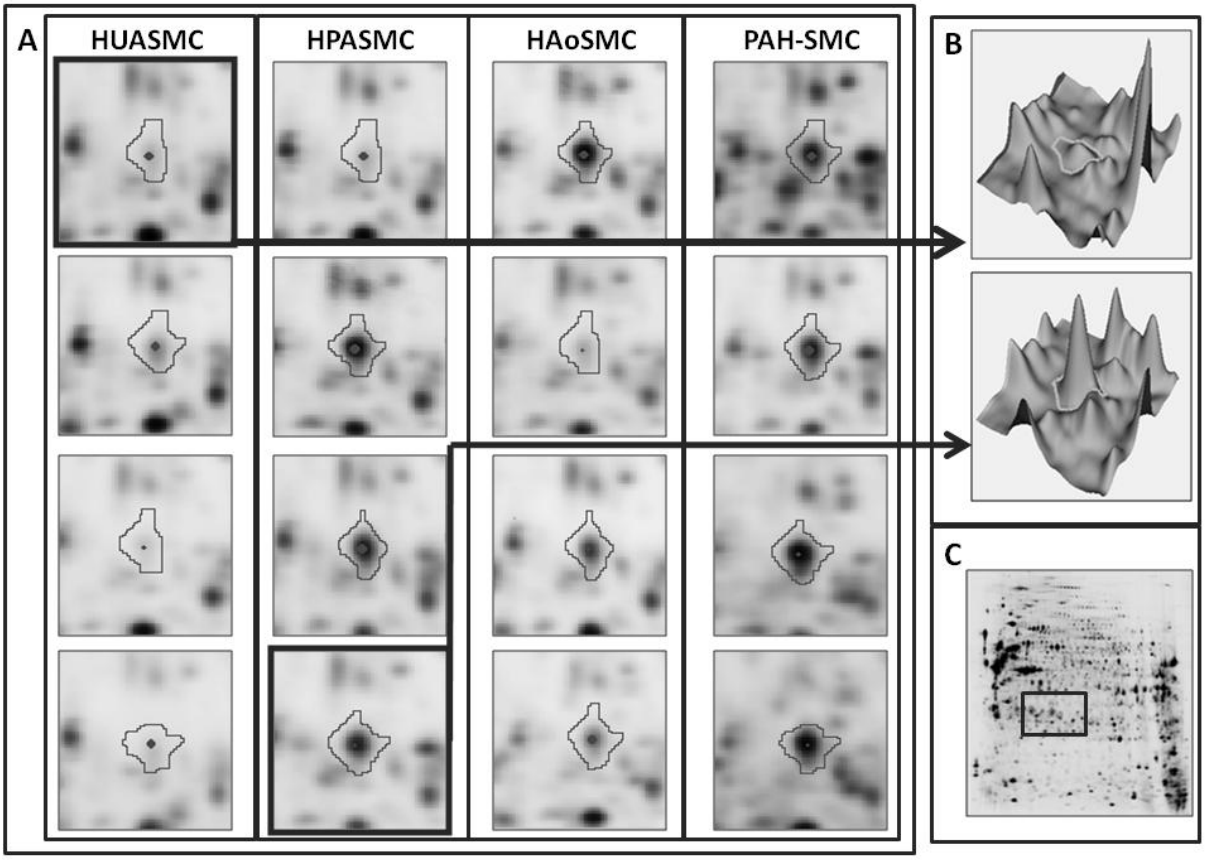

Figure 3: Biological network analysis with normal vascular smooth muscle cells.

An ingenuity user-built network was generated by ingenuity pathway analysis (IPA) with identified proteins showing major differences in expression between normal vascular smooth muscle cells groups (HUASMC, HPASMC and HAoSMC). Solid lines indicate direct interactions. Dashed lines indicate indirect interactions. Arrows indicate stimulation.

AMPK : AMP-activated kinase; ATP5C1: ATP synthase, H+ transporting, mitochondrial F1 complex, gamma polypeptide 1; C1QBP: complement component 1, q subcomponent binding protein; Creb: Cyclic AMP response element binding; DLD: dihydrolipoamide dehydrogenase; EEF1A1: eukaryotic translation elongation factor 1 alpha 1; HNRNPA1: heterogeneous nuclear ribonucleoprotein A1; HSP90AB1: heat shock protein 90kDa alpha (cytosolic), class B member 1; Hsp70: Hsp70gene; Jnk: JUN kinase; LDHB: lactate dehydrogenase B; LMNA:lamin A/C; MAPK1: mitogen-activated protein kinase 1; MYH9: myosin, heavy chain 9, non-muscle; NFkB (complex): NF-Kappa B; P4HB: prolyl 4-hydroxylase, beta polypeptide; PPIA: peptidylprolyl isomerase A (cyclophilin A); SERPINE1: serpin peptidase inhibitor, clade E (nexin, plasminogen activator inhibitor type 1), member 1; TP53: tumor protein p53; YWHAQ: tyrosine 3-monooxygenase/tryptophan 5-monooxygenase activation protein, theta

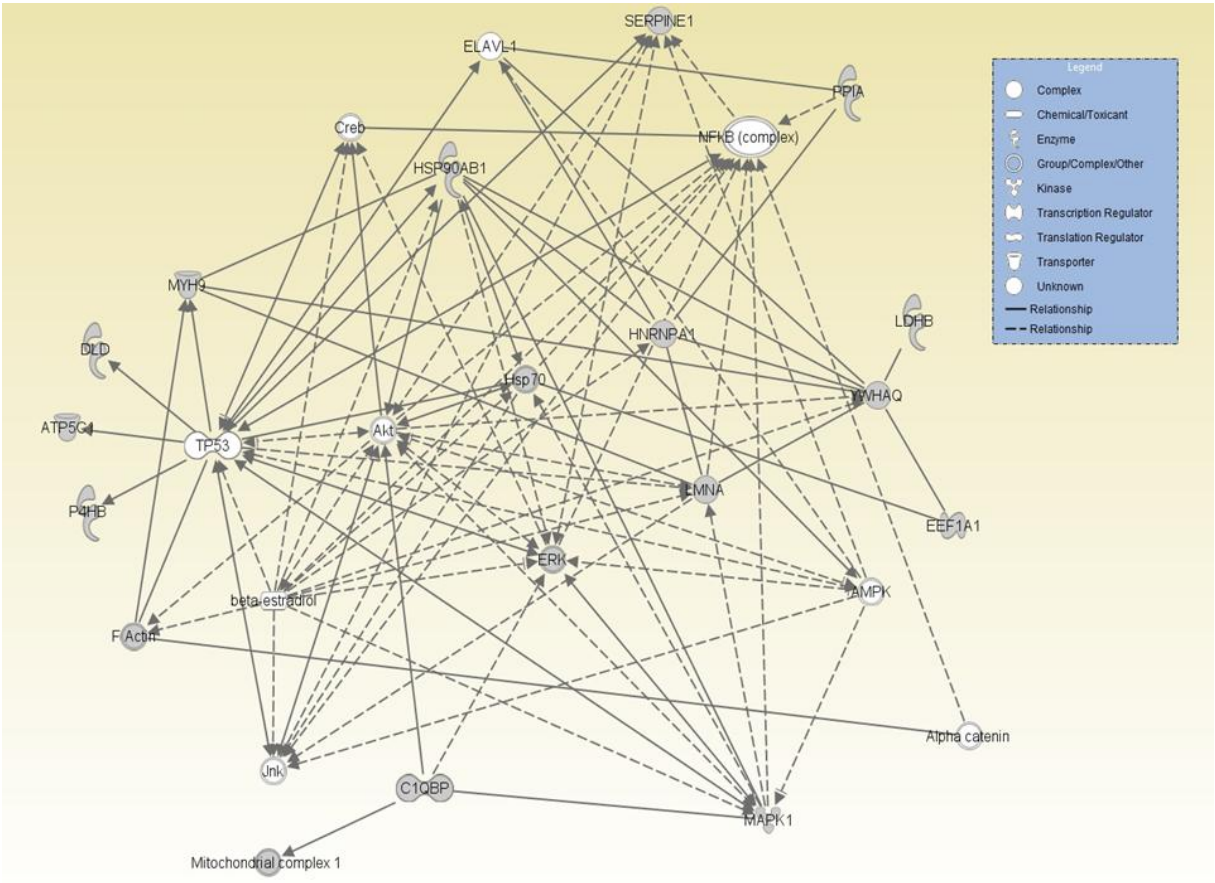
SERPINE1
ELAVL1
PPIA
Creb
NFkB (complex)
HSP90AB1
MYH9
LDHB
HNRNPA1
DLD
Hsp70
YWHAQ
ATP5G1
TP53
Akt
EMNA
P4HB
EEF1A1
ERK
AMPK
beta-estradiol
F Actin
Alpha catenin
Jnk
C1QBP
MAPK1
Mitochondrial complex 1
Legend
Complex
Chemical/Toxicant
Enzyme
Group/Complex/Other
Kinase
Transcription Regulator
Translation Regulator
Transporter
Unknown
Relationship
Relationship

Figure 4: Differential expression of calponin in smooth muscle cells from aorta, umbilical artery, pulmonary artery and SMC from patients with pulmonary hypertension.

(A) 2D gel images of proteomes of HUASMC, HPASMC, HAoSMC and PAH-SMC from four individual donors each. The spot corresponding to calponin protein is outlined in black. (B) Calponin protein spots are expressed in 3D view in one single donor of PAH-SMC (upper panel) and one HPASMC (lower panel) representative protein extract. (C) An internal standard proteome from a representative gel: the selected area of the gel contains the calponin protein spot depicted in panel A. HUASMC : human umbilical artery smooth muscle cell; HAoSMC : human aorta smooth muscle cell; HPASMC : human pulmonary artery smooth muscle cell; PAH-SMC : Pulmonary artery hypertension smooth muscle cell

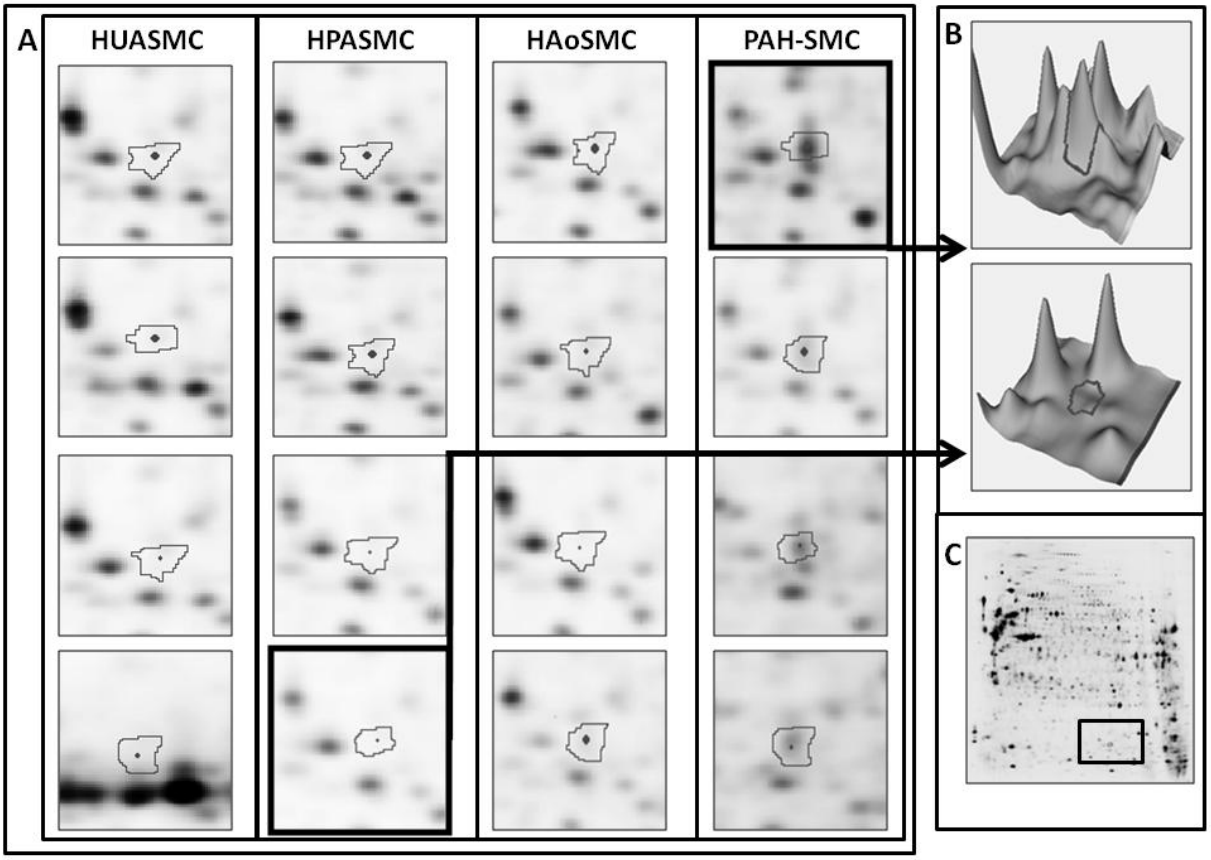

Figure 5: Differential expression of vigilin in smooth muscle cells from aorta, umbilical artery, pulmonary artery and SMC from patients with pulmonary hypertension.

(A) 2D gel images of proteomes of HUASMC, HPASMC, HAoSMC and PAH-SMC from four individual donors each. The spot corresponding to vigilin protein is outlined in black. (B) Vigilin protein spots are expressed in 3D view in one single donor of PAH-SMC (upper panel) and one HPASMC (lower panel) representative protein extract. (C) An internal standard proteome from a representative gel: the selected area of the gel contains the vigilin protein spot depicted in panel A.

HUASMC : human umbilical artery smooth muscle cell; HAoSMC : human aorta smooth muscle cell; HPASMC : human pulmonary artery smooth muscle cell; PAH-SMC : Pulmonary artery hypertension smooth muscle cell

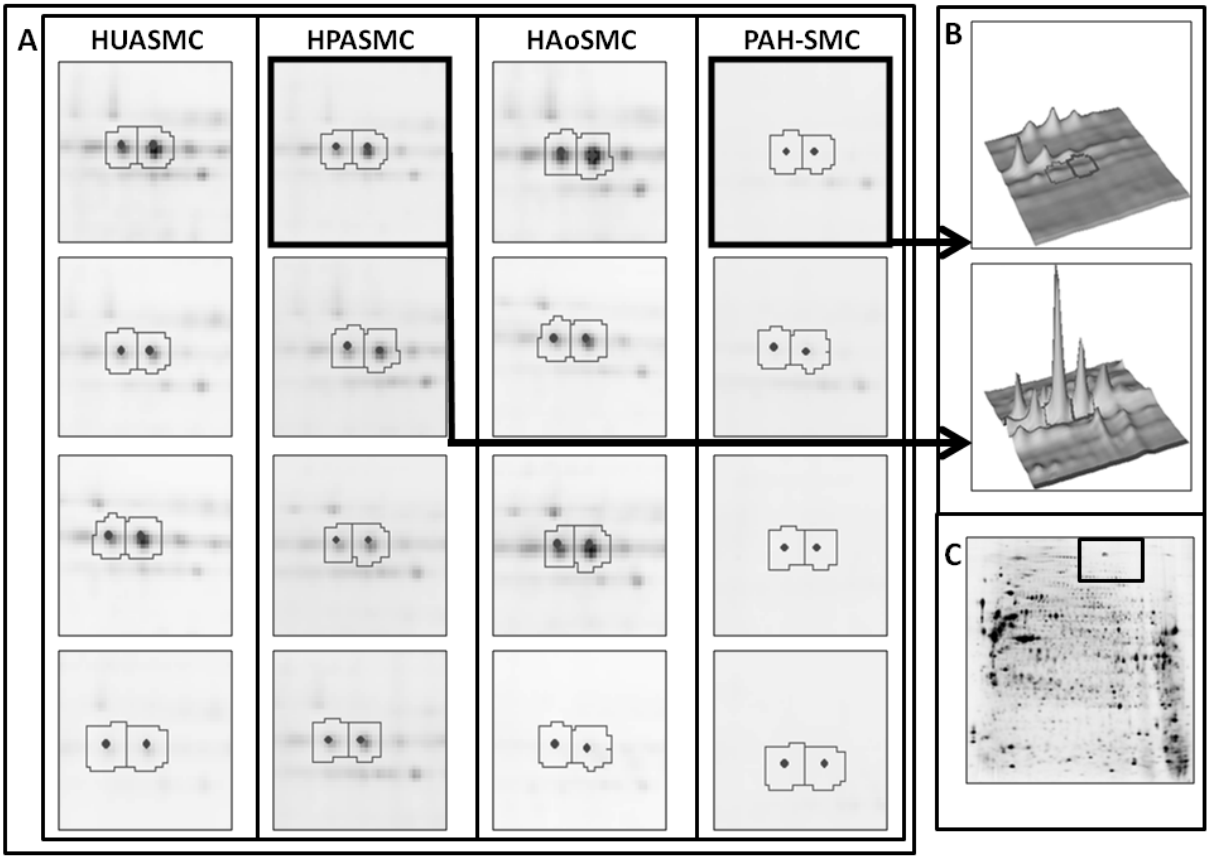

Figure 6: Biological network analysis with pulmonary artery vascular smooth muscle cells from patients with PAH and healthy controls

An ingenuity user-built network was generated by ingenuity pathway analysis (IPA) with identified proteins showing major differences in expression between pulmonary artery vascular smooth muscle cells from patients with pulmonary artery hypertension (PAH) and healthy controls. Solid lines indicate direct interactions. Dashed lines indicate indirect interactions. Arrows indicate stimulation. The intensity of green and red molecule colors indicates the degree of up- or downregulation, respectively. If normalized ratio, fold-change, or log ratio/log fold-change is chosen as expression value type, a greater intensity of green represents a higher degree of downregulation, and a greater intensity of red represents a higher degree of upregulation.

ACTB: actin, beta; AK4: adenylate kinase 4; ALDH1A3: aldehyde dehydrogenase 1 family, member A3; ANXA2: annexin A2; ARHGAP: Rho GTPase activating protein 1; CKAP4: cytoskeleton-associated protein 4; COL1A1: collagen, type I, alpha 1; COL6A1: collagen, type VI, alpha 1; COTL1: coactosin-like F-actin binding protein 1; CTSB: cathepsin B; DBT: dihydrolipoamide branched chain transacylase E2; DDX1: DEAD (Asp-Glu-Ala-Asp) box helicase 1; DNAJB11: DnaJ (Hsp40) homolog, subfamily B, member 11; DPYSL2: dihydropyrimidinase-like 2; ELAVL1: ELAV like RNA binding protein 1; ENO1: enolase 1, (alpha); ERP44; endoplasmic reticulum protein 44; EZR: ezrin; FLNA: filamin A, alpha; GFPT1: glutamine--fructose-6-phosphate transaminase 1; NHNRNPC: heterogeneous nuclear ribonucleoprotein C (C1/C2); HNRNPF: heterogeneous nuclear ribonucleoprotein F; HNRNPH1: heterogeneous nuclear ribonucleoprotein H1 (H); HNRNPL: heterogeneous nuclear ribonucleoprotein; HNRNPK: heterogeneous nuclear ribonucleoprotein K; HNRNPM: heterogeneous nuclear ribonucleoprotein M; HSPA5: heat shock 70kDa protein 5

(glucose-regulated protein, 78kDa); HSPA8: heat shock 70kDa protein 8; HSP90AB1: heat shock protein 90kDa alpha (cytosolic), class B member 1; KHSRP: KH-type splicing regulatory protein; LAMTOR1: late endosomal/lysosomal adaptor, MAPK and MTOR activator 1; LGLS1: lectin, galactoside-binding, soluble, 1; MYL6: myosin, light chain 6, alkali, smooth muscle and non-muscle; LMNA: lamin A/C; LMNB2: lamin B2; LMSN: moesin; LRPAP1: low density lipoprotein receptor-related protein associated protein 1; NONO: non-POU domain containing, octamer-binding; NR3C1: NR3C1: nuclear receptor subfamily 3, group C, member 1; PDIA3: protein disulfide isomerase family A, member 3; PDIA4: protein disulfide isomerase family A, member 4; NCL: nucleolin; P4HB: prolyl 4-hydroxylase, beta polypeptide; PFN1: profilin 1; PCBP1: poly(rC) binding protein 1; PDCD6IP: programmed cell death 6 interacting protein; PDIA3: protein disulfide isomerase family A, member 3; PKM: pyruvate kinase, musclePTBP1: polypyrimidine tract binding protein 1; PRDX1: peroxiredoxin 1; PTK2: protein tyrosine kinase 2; PXN: paxillin; RAB1A: RAB1A, member RAS oncogene family; RPL11: ribosomal protein L11; RPL22: ribosomal protein L22; RPS7: ribosomal protein S7; RPS14: ribosomal protein S14; RRBP1: ribosome binding protein 1; RSU1: Ras suppressor protein 1; SSB: Sjogren syndrome antigen B (autoantigen La); SEPINH1: serpin peptidase inhibitor, clade H (heat shock protein 47), member 1, (collagen binding protein 1); STAT3: Signal transducer and activator of transcription 3; TGM2: transglutaminase 2; TOR1A: torsin family 1, member A (torsin A); TRIOBP: TRIO and F-actin binding protein; TUBB: tubulin, beta class I; UCHL1: ubiquitin carboxyl-terminal esterase L1 (ubiquitin thiolesterase); UGDH: UDP-glucose 6-dehydrogenase; VIM: vimentin; VCL: vinculin; XRCC5: X-ray repair complementing defective repair in Chinese hamster cells 5 (double-strand-break rejoining); XRCC6: X-ray repair complementing defective repair

in Chinese hamster cells 6; YWHAG: tyrosine 3-monooxygenase/tryptophan 5-monooxygenase activation protein, gamma; YWHAH: tyrosine 3-monooxygenase/tryptophan 5-monooxygenase activation protein, eta; YWHAQ: 3-monooxygenase/tryptophan 5-monooxygenase activation protein, theta; YWHAZ: tyrosine 3-monooxygenase/tryptophan 5-monooxygenase activation protein, zeta; ZYC: zyxin

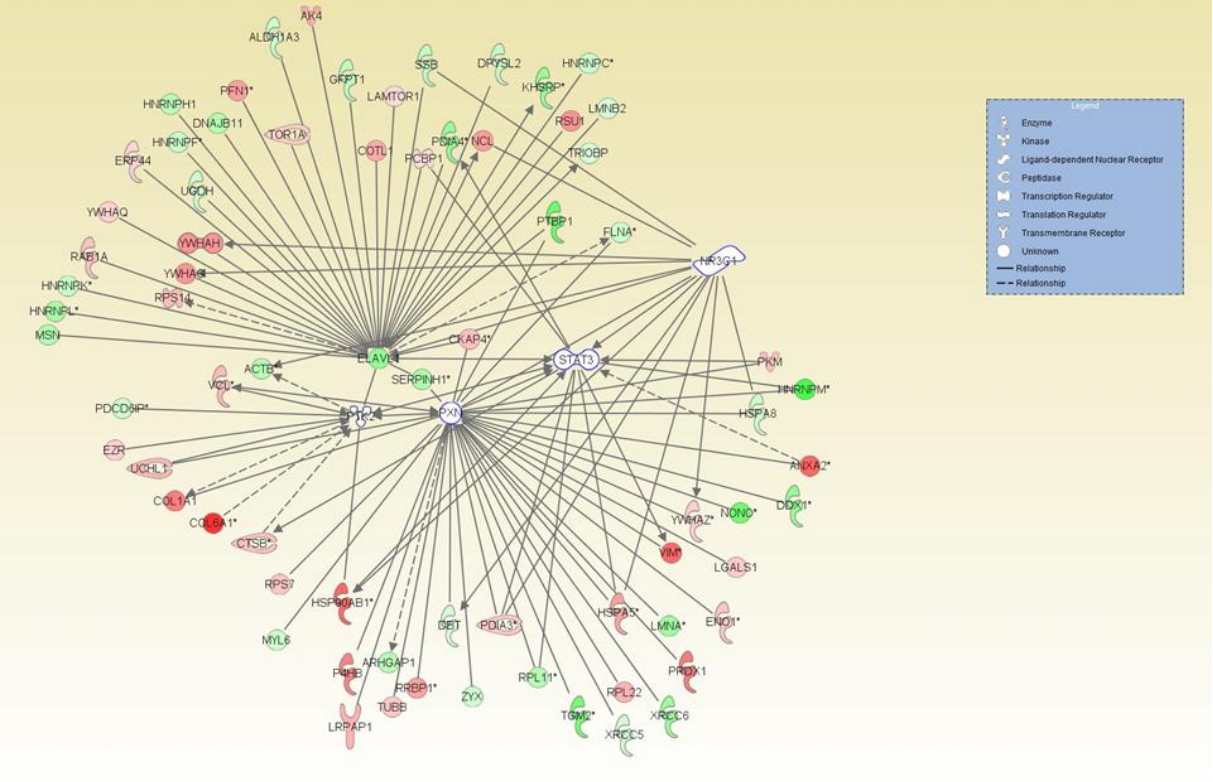

Figure 7: Proliferation of PAH-SMC and HPASMC with paxillin inhibition.

Proliferation of PAH-SMC and HPASMC was measured with a cell proliferation ELISA BrdU kit with paxillin-siRNA and non targeting paxillin si-RNA. Proliferation evaluated by BrdU incorporation was measured with a spectrophotometer at 370 nm.

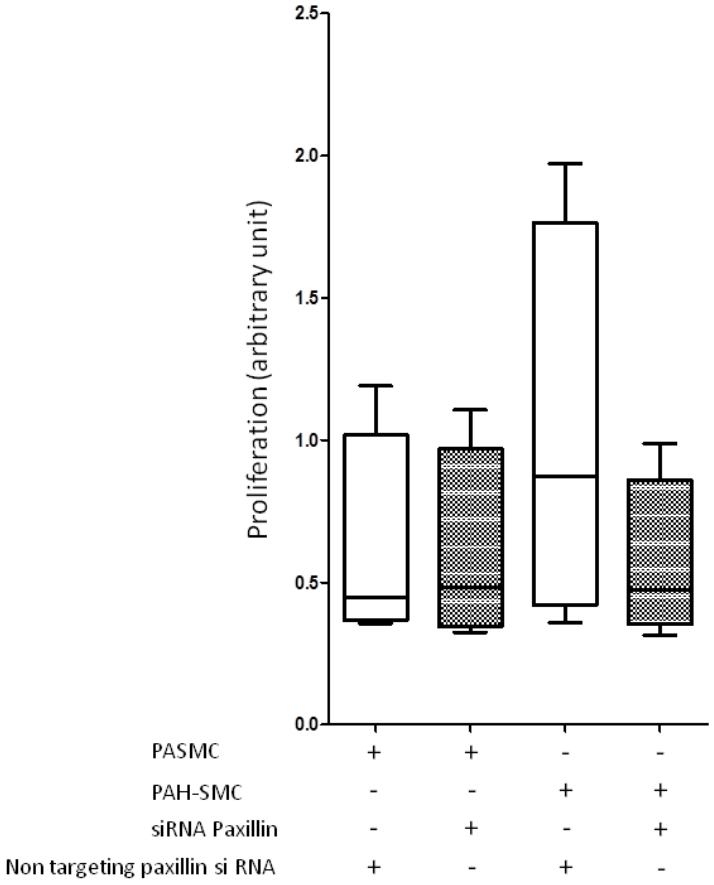

Table 1. Number of protein spots differentially expressed [a)] between all normal smooth muscle cells from umbilical, pulmonary and aorta artery (panel A) and between smooth muscle cells from PAH and normal cells (panel B)

A	HUASMC vs HAoSMC	HUASMC vs HPASMC	HPASMC vs HAoSMC	All comparisons
Number of proteins differentially expressed (fold change 1.5)	132	124	19	198
overexpressed [b)]	61	52	14	
underexpressed [b)]	71	72	5	
Number of proteins differentially expressed (fold change 2.0)	48	52	7	79
overexpressed [b)]	22	30	6	
underexpressed [b)]	26	22	1	
B	PAH-SMC vs HPASMC	PAH-SMC vs HAoSMC	PAH-SMC vs HUASMC	All comparisons
Number of proteins differentially expressed (fold change 1.5)	208	405	568	737
overexpressed [b)]	117	226	264	
underexpressed [b)]	91	179	304	
Number of proteins differentially expressed (fold change 2.0)	150	299	459	583
overexpressed [b)]	82	170	212	
underexperssed [b)]	68	129	247	

a) Differentially expressed protein spots detected (Student's t-test p-value ≤ 0.05) using DeCyder biological variation analysis (BVA) module
b) Over- and underexpressed proteins in HUASMC versus HAoSMC and HUASMC versus HPASMC comparisons or in HPASMC versus HAoSMC comparison (panel A) and over- and underexpressed proteins in PAH-SMC versus HPASMC, HAoSMC and HUASMC respectively
HUASMC: human umbilical artery smooth muscle cells, HPASMC: human pulmonary artery smooth muscle cells, HAoSMC: human aorta smooth muscle cells, PAH-SMC: pulmonary artery smooth muscle cells

Table 2. Differentially expressed proteins between vascular smooth muscle cells from umbilical artery and aorta artery (fold change ≥2.0, p≤0.05)

SPOT	IDENTIFIED PROTEIN	NAME	T-test	Fold change	Exp pI	Exp MM	Theo pI	Theo MM	Total ion Score	Best ion Score	Number of identified peptides
354	Alpha-actinin-1	ACTN1	3,6E-02	-2.2	5.6	106	5.3	103	1280	106	26
632	Programmed cell death 6-interacting protein & Procollagen-lysine,2-oxoglutarate 5-dioxygenase 2 & Filamin-A	PDC6I & PLOD2 & FLNA	3,2E-02	2.6	7.0	89	6.1 & 6.2 & 5.7	96 & 82 & 281	886 & 567 & 530	87 & 92 & 86	20 & 11 & 11
645	Procollagen-lysine,2-oxoglutarate 5-dioxygenase 2 & Filamin-A	PLOD2 & FLNA	2,8E-02	2.7	6.8	89	6.2 & 5.7	82 & 281	783 & 581	86 & 82	15 & 12
728	Myosin-9 & Src substrate cortactin	MYH9 & SRC8	1,8E-02	-2.5	5.5	84	8.8 & 5.2	354 & 62	1420 & 172	113 & 41	27 & 5
731	Myosin-9 & Src substrate cortactin	MYH9 & SRC8	1,7E-02	-2.5	5.6	84	8.8 & 5.2	354 & 62	2165 & 643	112 & 95	36 & 12
826	TATA-binding protein-associated factor 2N	RBP56	5,7E-03	-2.2	8.8	80	8	62	136	57	3
841	Collagen alpha-3(VI) chain & Vimentin	CO6A3 & VIME	1,4E-03	-2.1	5.8	78	6.2 & 5.1	341 & 54	1662 & 744	90 & 70	29 & 16
981	Trifunctional enzyme subunit alpha	ECHA	4,4E-02	2.6	10.0	72	9	79	1665	99	29
1300	UDP-glucose 6-dehydrogenase	UGDH	2,6E-02	-2.4	8.3	59	6.7	55	1061	90	21
1372	Glucose-6-phosphate 1-dehydrogenase & D-3-phosphoglycerate dehydrogenase	G6PD & SERA	3,9E-03	-2.0	7.6	57	6.4 & 6.3	59 & 57	1068 & 494	104 & 93	21 & 10
1386	Vimentin & Tubulin beta chain	VIME & TBB5	3,0E-03	-2.1	5.1	56	5.1 & 4.8	54 & 50	1761 & 1123	114 & 110	33 & 17
1420	V-type proton ATPase subunit B, brain isoform	VATB2	1,7E-04	36.7	6.0	55	5.6	57	1498	113	23
1435	Histidine--tRNA ligase, cytoplasmic	SYHC	1,9E-02	3.5	6.2	55	5.7	57	998	96	18
1474	Collagen alpha-3(VI) & Vimentin & NAD-dependent malic enzyme, mitochondrial	CO6A3 & VIME & MAOM	2,8E-02	3.7	5.7	53	6.2 & 5.1 & 6.6	341 & 54 & 63	625 & 475 & 404	87 & 57 & 92	11 & 8 & 8
1565	Alpha-enolase	ENOA	2,0E-02	-2.1	8.7	50	7	47	999	107	16
1576	Heterogeneous nuclear ribonucleoprotein F & Cartilage-associated protein & Eukaryotic	HNRPF & CRTAP & IF4A1	4,6E-02	2.3	5.6	50	5.4 & 5.3 & 5.3	46 & 44 & 46	636 & 490 & 926	95 & 82 &110	10 & 10 &18

	initiation factor 4A-I										
1624	Eukaryotic initiation factor 4A-I & Vimentin	IF4A1 & VIME	**2,1E-02**	**2.7**	**7.8**	**48**	**5.3 & 5.1**	**46 & 54**	**1022 & 668**	**103 & 81**	**19 & 14**
1641	No identified protein		**6,0E-05**	**2.9**	**6.5**	**47**					
1645	Vimentin & Interleukin enhancer-binding factor 2 & Myoferlin	VIME & ILF2 & MYOF	**6,0E-05**	**6.4**	**6.7**	**47**	**5.1 & 5.2 & 5**	**54 & 43 & 83**	**465 & 780 & 746**	**66 & 79 & 92**	**11 & 15 & 13**
1657	Calcium-binding mitochondrial carrier protein SCaMC-1 & Ornithine aminotransferase, mitochondrial & Synaptic vesicle membrane protein VAT-1 homolog	SCMC1 & OAT & VAT1	**1,1E-02**	**2.1**	**9.6**	**44**	**6 & 6 & 5.9**	**53 & 46 & 42**	**629 & 422 & 253**	**72 & 81 & 94**	**14 & 7 & 4**
1756	Interleukin enhancer-binding factor 2 & Protein disulfide-isomerase	ILF2 & PDIA1	**2,4E-04**	**8.2**	**5.7**	**44**	**5.2 & 4.7**	**43 & 55**	**283 & 477**	**89 & 80**	**5 & 10**
1924	Vimentin & Tropomyosin alpha-4 chain	VIME & TPM4	**2,3E-02**	**-3.0**	**7.4**	**38**	**5.1 & 4.7**	**54 & 28**	**703 & 519**	**89 & 60**	**15 & 12**
2045	Annexin A2 & Fructose-bisphosphate aldolase A & Glyceraldehyde-3-phosphate dehydrogenase	ANXA2 & ALDOA & G3P	**2,9E-02**	**-2.1**	**8.7**	**36**	**7.6 & 8.4 & 8.6**	**38 & 39 & 36**	**528 & 322 & 174**	**78 & 66 & 75**	**10 & 7 & 3**
2328	Cathepsin B & Chloride intracellular channel protein 1	CATB & CLIC1	**2,1E-02**	**3.2**	**4.8**	**29**	**5.2 & 5.1**	**28 & 27**	**531 & 366**	**106 & 72**	**8 & 7**
2349	14-3-3 protein theta & 14-3-3 protein zeta/delta	1433T & 1433Z	**9,9E-03**	**-2.3**	**4.9**	**29**	**4.7 & 4.7**	**28 & 28**	**666 & 641**	**91 & 90**	**12 & 13**
2378	Galectin-3 & Voltage-dependent anion-selective channel protein 3 & Surfeit locus protein 1	LEG3 & VDAC3 & SURF1	**6,9E-03**	**-2.2**	**5.8**	**29**	**8.6 & 8.9 & 9.6**	**26 & 31 & 33**	**501 & 348 & 157**	**88 & 108 & 65**	**9 & 6 & 3**
2392	Proteasome activator complex subunit 1	PSME1	**1,2E-03**	**-2.5**	**5.7**	**28**	**5.8**	**29**	**563**	**76**	**10**
2467	Annexin A1	ANXA1	**1,3E-02**	**-2.1**	**10.2**	**26**	**6.6**	**39**	**615**	**112**	**9**
2570	Ubiquitin carboxyl-terminal hydrolase isozyme L1 & Peroxiredoxin-4 & T-complex protein 1 subunit	UCHL1 & PRDX4 & TCPB	**2,4E-03**	**2.1**	**8.3**	**25**	**5.2 & 5.5 & 6**	**25 & 27 & 57**	**270 & 203 & 370**	**86 & 78 & 81**	**5 & 4 & 7**
3104	Peptidyl-prolyl cis-trans isomerase A	PPIA	**2,2E-02**	**-2.3**	**8.8**	**16**	**7.7**	**18**	**483**	**69**	**11**
3300	Hemoglobin subunit alpha	HBA	**2,5E-02**	**3.4**	**8.5**	**14**	**8.7**	**15**	**64**	**37**	**2**
3344	Cystatin-B	CYTB	**4,9E-02**	**12.0**	**8.0**	**13**	**7**	**11**	**104**	**62**	**2**
3528	Hemoglobin subunit beta	HBB	**1,3E-02**	**-2.1**	**5.0**	**11**	**6.8**	**16**	**100**	**56**	**2**
3529	Protein S100-A6 & Hemoglobin subunit alpha	S10A6 & HBA	**2,1E-02**	**-4.2**	**5.3**	**10**	**5.3 & 8.7**	**10 & 15**	**249 & 109**	**49 & 56**	**7 & 2**

Exp: experimental; MM: molecular mass; pI: isoelectrofocalisation point; Theo: theoretical. Relative quantification and statistical evaluation were carried out with DeCyderTM 2D software (GE Healthcare, version 7.0). Down or up-expressed proteins between groups were retained if protein spot fold change was larger than +1.5 or smaller than –1.5 and

a Student’s t-test p-value less than 0.05

Table 3 Differentially expressed proteins between vascular smooth muscle cells from umbilical artery and pulmonary artery (fold change ≥2.0, p≤0.05)

SPOT	IDENTIFIED PROTEIN	NAME	T-test	Fold change	Exp pI	Exp MM	Theo pI	Theo MM	Total ion Score	Best ion Score	Number of identified peptides
113	Collagen alpha-3(VI)	CO6A3	**6,0E-03**	**5.5**	**6.7**	**122**	**6.2**	**341**	**255**	**79**	**5**
278	Collagen alpha-2(VI) chain	CO6A1	**1,5E-02**	**-2.7**	**6.4**	**110**	**5.2**	**106**	**595**	**86**	**12**
279	Collagen alpha-2(VI) chain	CO6A1	**1,8E-02**	**-2.5**	**6.5**	**110**	**5.2**	**106**	**212**	**67**	**5**
281	Collagen alpha-2(VI) chain	CO6A1	**1,3E-02**	**-2.1**	**6.5**	**110**	**5.2**	**106**	**792**	**86**	**15**
285	Myosin-9 & Collagen alpha-1(VI) chain	MYH9 & CO6A1	**2,3E-02**	**-2.3**	**5.2**	**110**	**5.5 & 5.2**	**226 & 106**	**2305 &1498**	**103 & 103**	**40 & 25**
354	Alpha-actinin-1	ACTN1	**3,0E-06**	**-3.0**	**5.6**	**106**	**5.3**	**103**	**1280**	**106**	**26**
404	Myosin-9 & Collagen alpha-1(VI) chain	MYH9 & CO6A1	**2,5E-02**	**2.4**	**5.1**	**102**	**5.5 & 5.2**	**226 & 106**	**1418 & 1265**	**109 &87**	**40 & 25**
626	Programmed cell death 6-interacting protein & Procollagen-lysine,2-oxoglutarate 5-dioxygenase 2	PDC6I & PLOD2	**1,4E-02**	**2.8**	**7.1**	**89**	**6.1 & 6.2**	**96 & 82**	**1712 & 561**	**89 & 82**	**35 & 11**
632	Programmed cell death 6-interacting protein & Procollagen-lysine,2-oxoglutarate 5-dioxygenase 2 & Filamin-A	PDC6I & PLOD2 & FLNA	**9,6E-03**	**3.2**	**7.0**	**89**	**6.1 & 6.2 & 5.7**	**96 & 82 & 281**	**917 & 567 & 662**	**100 & 92 &80**	**18 & 11 & 15**
633	Procollagen-lysine,2-oxoglutarate 5-dioxygenase 2	PLOD2	**8,4E-03**	**2.8**	**7.3**	**89**	**6.2**	**82**	**874**	**72**	**17**
640	Procollagen-lysine,2-oxoglutarate 5-dioxygenase 2	PLOD2	**7,5E-03**	**3.2**	**7.2**	**89**	**6.2**	**82**	**806**	**86**	**16**
645	Procollagen-lysine,2-oxoglutarate 5-dioxygenase 2 & Filamin-A	PLOD2 & FLNA	**1,5E-02**	**3.0**	**6.8**	**89**	**6.2 & 5.7**	**82 & 281**	**783 & 581**	**86 & 82**	**15 & 12**
676	2-oxoglutarate dehydrogenase, mitochondrial & Procollagen-lysine,2-oxoglutarate 5-dioxygenase 2	ODO1 & PLOD2	**4,8E-02**	**3.1**	**6.8**	**88**	**6.1 & 6.2**	**111 & 82**	**785**	**64**	**17**
838	TATA-binding protein-associated factor 2N	RBP56	**1,2E-02**	**-2.4**	**9.1**	**79**	**8**	**62**	**248**	**78**	**6**
933	Prelamin-A/C & Moesin	LMNA & MOES	**2,3E-03**	**-2.1**	**7.3**	**74**	**6.6 & 6.1**	**74 & 68**	**1594 & 1372**	**104 & 94**	**31 & 26**
1145	Cytoskeleton-associated protein 4 &	CKAP4 &	**1,0E-02**	**2.5**	**5.9**	**65**	**5.6 & 5.4**	**66 & 52**	**1143 & 588**	**117 & 88**	**20 & 12**

	ERO1-like protein alpha	ERO1A									
1232	Prolyl 4-hydroxylase subunit alpha-1	P4HA1	**5,8E-04**	**2.3**	**6.4**	**62**	**5.7**	**59**	**860**	**106**	**15**
1254	EH domain-containing protein 3	EHD3	**2,2E-02**	**-2.1**	**7.3**	**61**	**6.1**	**61**	**709**	**79**	**14**
1300	UDP-glucose 6-dehydrogenase	UGDH	**3,4E-02**	**-2.3**	**8.3**	**59**	**6.7**	**55**	**1061**	**90**	**21**
1420	V-type proton ATPase subunit B, brain isoform	VATB2	**2,1E-05**	**55.6**	**6.0**	**55**	**5.6**	**57**	**1498**	**113**	**23**
1435	Histidine--tRNA ligase, cytoplasmic	SYHC	**2,3E-02**	**3.2**	**6.2**	**55**	**5.7**	**57**	**998**	**96**	**18**
1474	Collagen alpha-3(VI) & Vimentin & NAD-dependent malic enzyme, mitochondrial	CO6A3 & VIME & MAOM	**2,8E-02**	**3.7**	**5.7**	**53**	**6.2 & 5.1 & 6.6**	**341 & 54 & 63**	**625 & 475 & 404**	**87 & 57 & 92**	**11 & 8 & 8**
1624	Eukaryotic initiation factor 4A-I & Vimentin	IF4A1 & VIME	**1,9E-02**	**2.9**	**5.6**	**48**	**5.3 & 5.1**	**46 & 54**	**1022 & 668**	**103 & 81**	**19 & 14**
1641	No identified protein		**1,1E-04**	**2.8**							
1645	Vimentin & Interleukin enhancer-binding factor 2 & Myoferlin	VIME & ILF2 & MYOF	**5,2E-05**	**6.6**	**5.7**	**47**	**5.1 & 5.2 & 5**	**54 & 43 & 83**	**465 & 780 & 746**	**66 & 79 & 92**	**11 & 15 & 13**
1756	Interleukin enhancer-binding factor 2 & Protein disulfide-isomerase	ILF2 & PDIA1	**4,6E-05**	**19.1**	**5.2**	**44**	**5.2 & 4.7**	**43 & 55**	**283 & 477**	**89 & 80**	**5 & 10**
1830	Vimentin	VIME	**4,0E-03**	**-2.1**	**4.8**	**42**	**5.1**	**54**	**1662**	**128**	**32**
1924	Vimentin & Tropomyosin alpha-4 chain	VIME & TPM4	**1,2E-02**	**-2.6**	**4.8**	**40**	**5.1 & 4.7**	**54 & 28**	**703 & 519**	**89 & 60**	**15 & 12**
2343	Cathepsin D	CATD	**4,7E-02**	**-2.8**	**6.1**	**29**	**5.6**	**38**	**602**	**117**	**9**
2570	Ubiquitin carboxyl-terminal hydrolase isozyme L1 & Peroxiredoxin-4 & T-complex protein 1 subunit	UCHL1 & PRDX4 & TCPB	**1,5E-03**	**2.1**	**5.7**	**25**	**5.2 & 5.5 & 6**	**25 & 27 & 57**	**270 & 203 & 370**	**86 & 78 & 81**	**5 & 4 & 7**
2573	Ubiquitin carboxyl-terminal hydrolase isozyme L1 & Vacuolar protein sorting-associated protein 28 homolog	UCHL1 & VPS28	**7,7E-03**	**2.7**	**5.5**	**25**	**5.2 & 5.4**	**25 & 25**	**360 & 150**	**75 & 68**	**7 & 3**
2831	Myosin regulatory light polypeptide 9	MYL9	**1,1E-03**	**-2.2**	**4.9**	**21**	**4.8**	**20**	**253**	**84**	**5**
2978	Cofilin-1 & Transgelin	COF1 & TAGL	**7,9E-03**	**2.4**	**7.1**	**18**	**8.3 & 8.9**	**18 & 22**	**353 & 157**	**120 & 68**	**5 & 3**
3193	Coactosin-like protein	COTL1	**2,7E-04**	**2.1**	**5.5**	**15**	**5.5**	**16**	**364**	**57**	**9**
3250	NADH dehydrogenase [ubiquinone] 1 alpha subcomplex subunit 5 & 60S ribosomal protein L22	NDUA5 & RL22	**2,1E-02**	**-2.4**	**6.0**	**14**	**5.8 & 9.2**	**13 & 15**	**122 & 176**	**46 & 68**	**3 & 3**
3462	Protein S100-A4 & Dolichyl-diphosphooligosaccharide--protein glycosyltransferase subunit 1	S10A4 & RPN1	**1,5E-03**	**-3.7**	**5.9**	**12**	**5.9 & 6**	**12 & 66**	**110 & 226**	**43 & 62**	**3 & 4**

3529	Protein S100-A6 & Hemoglobin subunit alpha	S10A6 & HBA	**3,1E-02**	**-3.4**	**5.3**	**10**	**5.3 & 8.7**	**10 & 15**	**249 & 109**	**49 & 56**	**7 & 2**

Exp: experimental; MM: molecular mass; pI: isoelectrofocalisation point; Theo: theoretical. Relative quantification and statistical evaluation were carried out with DeCyderTM 2D software (GE Healthcare, version 7.0). Down or up-expressed proteins between groups were retained if protein spot fold change was larger than +1.5 or smaller than –1.5 and a Student's t-test p-value less than 0.05

Table 4 Differentially expressed proteins between vascular smooth muscle cells from pulmonary artery and aorta artery (fold change ≥2.0, p≤0.05)

SPOT	IDENTIFIED PROTEIN	NAME	T-test	Fold change	Exp pI	Exp MM	Theo pI	Theo MM	Total ion Score	Best ion Score	Number of identified peptides
113	Collagen alpha-3(VI)	CO6A3	**7,2E-03**	**-4.9**	**6.7**	**122**	**6,3**	**34**	**255**	**79**	**5**
404	Myosin-9 & Collagen alpha-1(VI) chain	MYH9 & CO6A1	**3,2E-02**	**-2.2**	**5.1**	**102**	**5.5 & 5.3**	**227 & 109**	**1418 & 1265**	**109 & 87**	**27 & 21**
872	Caldesmon	CALD1	**4,3E-02**	**-2.1**	**7.2**	**78**	**5,6**	**93**	**1122**	**98**	**22**
1756	Interleukin enhancer-binding factor 2 & Protein disulfide-isomerase	ILF2 & PDIA1	**3,8E-02**	**-2.3**	**5.2**	**44**	**5.2 & 4.8**	**43 & 57**	**283& 498**	**89 & 80**	**5 & 10**

Exp: experimental; MM: molecular mass; pI: isoelectrofocalisation point; Theo: theoretical. Relative quantification and statistical evaluation were carried out with DeCyderTM 2D software (GE Healthcare, version 7.0). Down or up-expressed proteins between groups were retained if protein spot fold change was larger than +1.5 or smaller than –1.5 and a Student's t-test p-value less than 0.05

Table 5. Differentially expressed proteins between pulmonary artery vascular smooth muscle cells from patients with PAH and healthy controls (fold change ≥2.0, p≤0.05)

SPOT	IDENTIFIED PROTEIN	NAME	T-test	Fold Change	Exp pI	Exp MM	Theo pI	Theo MM	Total ion Score	Best ion Score	Number of identified peptides
152	Collagen alpha-1(I) chain	CO1A1	**3.7E-03**	**5.4**	**6.1**	**119**	**5,6**	**139**	**433**	**72**	**8**
220	Uveal autoantigen with coiled-coil domains and ankyrin repeats	UACA	**1.1E-03**	**-10.1**	**8.0**	**114**	**6.6**	**163**	**57**	**32**	**2**
222	Vigilin	VIGLN	**1.3E-04**	**-8.8**	**7.6**	**114**	**6.4**	**141**	**476**	**65**	**11**
223	Vigilin	VIGLN	**1.6E-04**	**-9.4**	**7.7**	**113**	**6.4**	**141**	**1123**	**95**	**23**
404	Myosin-9 & Collagen alpha-1(VI) chain	MYH9 & CO6A1	**2.3E-03**	**8.5**	**5.1**	**102**	**5.5 & 5.3**	**227 & 109**	**1418 & 1265**	**109 & 87**	**40 & 25**
408	Collagen alpha-1(VI) chain & Dipeptidyl peptidase 4	CO6A1 & DPP4	**4.7E-03**	**5.2**	**5.2**	**102**	**5.2 & 5.7**	**106 & 88**	**868 & 438**	**86 & 67**	**15 & 11**
458	Kinesin-1 heavy chain	KINH	**2.0E-02**	**-2.7**	**7.1**	**99**	**6.1**	**110**	**1444**	**100**	**28**
461	Kinesin-1 heavy chain	KINH	**4.2E-03**	**-3.7**	**7.0**	**99**	**6.1**	**110**	**395**	**89**	**8**
500	Collagen alpha-3(VI) chain & vinculin	CO6A3 & VINC	**6.9E-03**	**2.8**	**6.1**	**96**	**6.2 & 5.5**	**341 & 118**	**1758 & 1336**	**91 & 87**	**32 & 29**
501	Vinculin	VINC	**1.4E-02**	**2.2**	**6.2**	**96**	**5.5**	**124**	**2033**	**105**	**41**
545	Staphylococcal nuclease domain-containing protein 1 & Elongation factor 2	SND1 & EF2	**4.9E-02**	**-2.7**	**8.0**	**94**	**6.8 & 6.2**	**102 & 82**	**1115 & 520**	**79 & 96**	**22 & 11**
552	Staphylococcal nuclease domain-containing protein 1	SND1	**1.8E-02**	**-3.6**	**8.1**	**94**	**6.8**	**102**	**1531**	**98**	**28**
620	Endoplasmin	ENPL	**3.5E-02**	**-4.2**	**5.0**	**91**	**4.7**	**90**	**2230**	**105**	**44**
632	Programmed cell death 6-interacting protein & Procollagen-lysine,2-oxoglutarate 5-dioxygenase 2 & Filamin-A	PDC6I & PLOD2 & FLNA	**1.9E-02**	**-2.1**	**7.0**	**89**	**6.1 & 6.2 & 5.7**	**96 & 82 & 281**	**917 & 567 & 662**	**100 & 92 & 80**	**18 & 11 & 15**
633	Procollagen-lysine,2-oxoglutarate 5-dioxygenase 2	PLOD2	**4.0E-02**	**-2.1**	**7.3**	**89**	**6.2**	**82**	**874**	**72**	**17**
640	Procollagen-lysine,2-oxoglutarate 5-dioxygenase 2	PLOD2	**4.6E-02**	**-2.3**	**7.2**	**89**	**6.2**	**82**	**806**	**86**	**16**
644	Mitochondrial 10-formyltetrahydrofolate dehydrogenase	AL1L2	**2.5E-03**	**-2.3**	**6.3**	**89**	**6.1**	**102**	**1303**	**100**	**24**
648	Mitochondrial 10-formyltetrahydrofolate dehydrogenase	AL1L2	**1.0E-02**	**-2.8**	**6.4**	**89**	**6.1**	**102**	**1326**	**89**	**25**
677	Hypoxia up-regulated protein 1	HYOU1	**2.5E-03**	**-2.2**	**4.9**	**88**	**4.6**	**61**	**904**	**96**	**15**
686	Ribosome-binding protein 1 & Heat shock protein HSP 90-beta & Prolyl 3-hydroxylase 1	RRBP1 & HS90B & P3H1	**1.3E-03**	**-2.2**	**5.2**	**87**	**8.8 & 5 & 5**	**354 & 83 & 81**	**1690 & 942 & 723**	**111 & 76 & 78**	**27 & 19 & 15**
706	Prolyl 3-hydroxylase 3	P3H3	**1.0E-02**	**-2.8**	**6.8**	**86**	**5.8**	**80**	**244**	**84**	**4**

747	Putative pre-mRNA-splicing factor ATP-dependent RNA helicase DHX15	DHX15	**1.0E-02**	**-4.9**	**8.5**	**84**	**7.1**	**91**	**663**	**69**	**14**
783	ATP-dependent RNA helicase DDX1 & Aconitate hydratase & DnaJ homolog subfamily C member 10	DDX1 & ACON & DJC10	**4.1E-02**	**-2.7**	**8.2**	**81**	**6.8 & 6.9 & 6.7**	**82 & 82 & 87**	**860 & 724 &513**	**88 & 85 & 54**	**17 & 13 & 12**
787	Far upstream element-binding protein 2	FUBP2	**7.5E-03**	**-2.9**	**7.9**	**81**	**6.8**	**73**	**588**	**75**	**11**
788	ATP-dependent RNA helicase DDX1 & Far upstream element-binding protein 2 & Aconitate hydratase	DDX1 & FUBP2 & ACON	**1.2E-02**	**-4.3**	**8.1**	**81**	**6.8 & 6.8 & 6.9**	**82 & 73 & 82**	**643 & 657 & 514**	**63 & 90 & 79**	**14 & 13 & 10**
805	Protein-glutamine gamma-glutamyltransferase 2	TGM2	**1.1E-02**	**-5.7**	**5.3**	**80**	**5.1**	**77**	**1229**	**95**	**23**
809	Protein Hook homolog 3 & Protein-glutamine gamma-glutamyltransferase 2	HOOK3 & TGM2	**2.6E-02**	**-3.5**	**5.3**	**80**	**5.1 & 5.1**	**83 & 77**	**879 & 813**	**90 & 86**	**16 & 17**
810	Protein-glutamine gamma-glutamyltransferase 2 & Protein disulfide-isomerase A4	TGM2 & PDIA4	**2.9E-02**	**-4.5**	**5.3**	**80**	**5.1 & 4.9**	**77 & 71**	**1074 & 883**	**82 & 93**	**20 & 16**
823	Delta-1-pyrroline-5-carboxylate synthase & Procollagen-lysine,2-oxoglutarate 5-dioxygenase 1	P5CS & PLOD1	**1.0E-02**	**-2.9**	**7.5**	**80**	**6.7 & 6.5**	**87 & 82**	**993 & 398**	**90 & 59**	**19 & 10**
826	TATA-binding protein-associated factor 2N	RBP56	**3.4E-02**	**-2.3**	**8.8**	**80**	**8**	**62**	**19**	**57**	**3**
851	Procollagen-lysine,2-oxoglutarate 5-dioxygenase 1 & Glucosamine--fructose-6-phosphate aminotransferase	PLOD1 & GFPT1	**5.6E-03**	**-2.7**	**7.6**	**78**	**6.5 & 6.7**	**82 & 79**	**908 & 344**	**85 & 91**	**18 & 6**
858	Ribosome-binding protein 1 & Heat shock 70 kDa protein 4 & 78 kDa glucose-regulated protein	RRBP1 & HSP74 & GRP78	**6.9E-03**	**3.9**	**5.0**	**78**	**8.7 & 5.1 & 5**	**152 & 94 & 70**	**621 & 546 & 273**	**83 & 79 & 77**	**13 & 12 & 5**
871	Caldesmon & Methylmalonyl-CoA mutase, mitochondrial	CALD1 & MUTA	**4.1E-03**	**-4.4**	**6.9**	**77**	**5.6 & 6**	**93 & 79**	**1223 & 753**	**135 & 96**	**23 & 12**
872	Caldesmon	CALD1	**2.8E-03**	**-2.6**	**7.2**	**78**	**5.6**	**93**	**1122**	**98**	**22**
903	Peptidyl-prolyl cis-trans isomerase & Protein disulfide-isomerase A4 & 78 kDa glucose-regulated protein	FKB10 & PDIA4 & GRP78	**1.3E-02**	**-2.1**	**5.4**	**75**	**5.3 & 4.9 & 5**	**61 & 71 & 70**	**1022 & 656 & 984**	**96 & 79 & 94**	**19 & 13 & 18**
933	Prelamin-A/C & Moesin	LMNA & MOES	**2.3E-02**	**-3.3**	**7.3**	**74**	**6.6 & 6.1**	**74 & 68**	**1594 & 1372**	**104 & 94**	**31 & 26**
939	Prelamin-A/C	LMNA	**2.2E-03**	**-3.2**	**8.0**	**74**	**6.6**	**74**	**1732**	**117**	**30**
944	Prelamin-A/C	LMNA	**7.0E-03**	**-4.0**	**7.7**	**74**	**6.6**	**74**	**1831**	**110**	**32**
946	78 kDa glucose-regulated protein & Protein disulfide-isomerase A4	GRP78 & PDIA4	**3.0E-03**	**-2.3**	**5.2**	**74**	**5 & 4.9**	**70 & 71**	**2261 & 699**	**112 & 100**	**35 & 13**
956	Peptidyl-prolyl cis-trans isomerase & Stress-70 protein, mitochondrial	FKB10 & GRP75	**1.7E-04**	**-2.0**	**5.5**	**73**	**5.3 & 5.4**	**61 & 69**	**1134 & 726**	**93 & 81**	**19 &13**
981	Trifunctional enzyme subunit alpha	ECHA	**1.2E-02**	**-6.5**	**10.0**	**72**	**9**	**79**	**1665**	**99**	**29**
1010	Trifunctional enzyme subunit alpha & Heterogeneous nuclear ribonucleoprotein M	ECHA & HNRPM	**3.1E-03**	**-4.2**	**9.9**	**71**	**9 & 9.2**	**79 & 30**	**1251 & 1158**	**85 & 100**	**22 & 18**
1020	Glycerol-3-phosphate dehydrogenase &	GPDM & TOM70	**6.2E-03**	**-3.2**	**7.5**	**71**	**6.3 &**	**76 & 67**	**464 &**	**73 & 63 &**	**10 & 10 &**

	Mitochondrial import receptor subunit TOM70 & Prelamin-A/C	& LMNA					**6.8 & 6.6**	**& 74**	**433 & 432**	**83**	**8**
1021	Heterogeneous nuclear ribonucleoprotein M & Trifunctional enzymz subunit alpha	HNRPM & ECHA	**3.0E-03**	**-7.7**	**10.0**	**71**	**9.2 & 9**	**30 & 79**	**1074 & 532**	**99 & 89**	**20 & 10**
1027	Heat shock protein 75 kDa, mitochondrial & Prelamin-A/C & X-ray repair cross-complementing protein 6	TRAP1 & LMNA & XRCC6	**8.7E-03**	**-4.2**	**7.3**	**71**	**8.5 & 6.6 & 6.2**	**49 & 74 & 70**	**772 & 708 & 1101**	**94 & 79 & 89**	**16 & 14 & 21**
1049	Heterogeneous nuclear ribonucleoprotein M & Calcium-binding mitochondrial carrier protein Aralar2	HNRPM & CMC2	**8.9E-03**	**-2.5**	**9.8**	**69**	**9.2 & 8.8**	**30 & 74**	**1048 & 863**	**108 & 90**	**18 & 15**
1054	Calcium-binding mitochondrial carrier protein Aralar2 & Heterogeneous nuclear ribonucleoprotein M	CMC2 & HNRPM	**5.0E-04**	**-6.7**	**9.9**	**69**	**8.8 & 9.2**	**74 & 30**	**369 & 1126**	**77 & 113**	**8 & 20**
1060	Phosphoenolpyruvate carboxykinase [GTP], mitochondrial	PCKGM	**1.2E-02**	**-2.4**	**8.1**	**69**	**6.6**	**67**	**877**	**84**	**18**
1075	Plastin 3 & Heat shock cognate 71 kDa	PLST & HSP7C	**4.0E-03**	**2.7**	**5.9**	**68**	**5.4 & 5.4**	**71 & 70**	**1113 & 1098**	**87 & 100**	**22 & 21**
1097	Heterogeneous nuclear ribonucleoprotein Q	HNRPQ	**1.5E-02**	**-3.3**	**8.3**	**68**	**8.7**	**69**	**612**	**74**	**13**
1101	Heterogeneous nuclear ribonucleoprotein Q	HNRPQ	**4.2E-04**	**-6.5**	**8.5**	**68**	**8.7**	**69**	**561**	**74**	**12**
1141	Heterogeneous nuclear ribonucleoprotein L	HNRPL	**6.0E-03**	**-3.7**	**8.1**	**65**	**8.5**	**64**	**707**	**106**	**14**
1146	Cytoskeleton-associated protein 4	CKAP4	**7.1E-04**	**-2.4**	**6.2**	**65**	**5.6**	**66**	**1748**	**147**	**26**
1147	Heterogeneous nuclear ribonucleoprotein L & ATP-dependent Clp protease ATP-binding subunit clpX-like & NAD-dependent malic enzyme	HNRPL & CLPX & MAOM	**9.1E-03**	**-2.8**	**7.9**	**65**	**8.5 & 6.3 & 6.6**	**64 & 63 & 63**	**558 & 472 & 332**	**102 & 68 & 91**	**10 & 10 & 8**
1156	78 kDa glucose-regulated protein & Heterogeneous nuclear ribonucleoprotein K & Heat shock cognate 71 kDa protein	GRP78 & HNRPK & HSP7C	**1.0E-02**	**-2.1**	**5.6**	**65**	**5 & 5.4 & 5.4**	**70 & 51 & 71**	**901 & 683 & 446**	**93 & 90 & 74**	**15 & 12 &7**
1159	78 kDa glucose-regulated & Heterogeneous nuclear ribonucleoprotein K & Cytoskeleton-associated protein 4	GRP78 & HNRPK & CKAP4	**3.2E-03**	**-2.4**	**5.4**	**64**	**5 & 5.4 & 5.6**	**70 & 51 & 66**	**926 & 688 & 504**	**106 & 107 & 76**	**15 & 12 & 10**
1164	Prelamin-A/C & Dihydropyrimidinase-related protein 2 & T-complex protein 1 subunit gamma	LMNA & DPYL2 & TCPG	**3.3E-02**	**-2.4**	**7.0**	**65**	**6.6 & 6 & 6.1**	**74 & 62 & 61**	**1616 & 1056 & 904**	**82 & 117 & 81**	**31 & 17 & 18**
1233	Dihydropyrimidinase-related protein 3 & Carnitine O-palmitoyltransferase 1, liver isoform &	DPYL3 & CPT1A	**2.7E-02**	**-2.8**	**7.2**	**62**	**6 & 8.9**	**62 & 88**	**878 & 387**	**98 & 81**	**14 & 7**
1298	Non-POU domain-containing octamer-binding protein & Elongation factor 1-alpha 1 & Polypyrimidine tract-binding protein 1	NONO & EF1A1 & PTBP1	**7.7E-04**	**-6.2**	**10.1**	**59**	**9 & 9.1 & 9.2**	**54 & 50 & 57**	**545 & 171 & 289**	**72 & 48 & 121**	**11 & 5 & 5**
1302	Non-POU domain-containing octamer-binding protein	NONO	**5.1E-04**	**-4.9**	**10.0**	**59**	**9**	**54**	**204**	**71**	**4**

1309	tRNA-splicing ligase RtcB homolog & UDP-glucose 6-dehydrogenase & Aldehyde dehydrogenase family 1 member A3 & Pyruvate kinase isozymes M1/M2	RTCB & UGDH & AL1A3 & KPYM	**4.4E-02**	**-2.0**	**8.1**	**58**	**6.8 & 6.7 & 7.1**	**55 & 55 & 56**	**820 & 459 & 362 & 325**	**92 & 67 & 55 & 64**	**15 & 11 & 9 & 7**
1361	Prelamin-A/C	LMNA	**3.7E-03**	**2.1**	**8.9**	**57**	**6.6**	**74**	**1710**	**116**	**32**
1421	Dihydrolipoyllysine-residue succinyltransferase component of 2-oxoglutarate dehydrogenase complex & Heterogeneous nuclear ribonucleoprotein H & Rho GTPase-activating protein 1	ODO2 & HNRH1 & RHG01	**8.3E-03**	**-2.9**	**6.4**	**55**	**5.9 & 5.9 & 5.9**	**41 & 49 & 50**	**501 & 413 & 220**	**93 & 84 & 53**	**9 & 8 & 5**
1427	Mitochondrial-processing peptidase subunit alpha & Aldehyde dehydrogenase X & Aspartate--tRNA ligase & T-complex protein 1 subunit beta	MPPA & AL1B1 & SYDC & TCPB	**7.3E-03**	**-2.3**	**6.9**	**55**	**5.9 & 6 & 6.1**	**55 & 55 & 57**	**261 & 260 & 259 & 212**	**68 & 78 & 67 & 70**	**6 & 5 & 5 & 4**
1447	ATP synthase subunit alpha, mitochondrial & Annexin A2	ATPA & ANXA2	**4.5E-02**	**-2.3**	**8.8**	**54**	**8.3 & 7.6**	**55 & 38**	**974 & 500**	**108 & 83**	**16 & 9**
1468	ATP synthase subunit alpha, mitochondrial & Hypoxia up-regulated protein 1 & Serine hydroxymethyltransferase, mitochondrial	ATPA & HYOU1 & GLYM	**1.7E-03**	**-4.1**	**9.4**	**53**	**8.3 & 5.1 & 8.1**	**55 & 108 & 53**	**1090 & 513 & 614**	**112 & 115 & 82**	**16 & 9 & 12**
1527	Actin, cytoplasmic 1 & Thioredoxin domain-containing protein 5	ACTB & TXND5	**6.4E-03**	**-3.1**	**5.5**	**51**	**5.3 & 5.4**	**42 & 44**	**967 & 707**	**118 & 101**	**15 & 14**
1560	Vimentin & Cytoskeleton-associated protein 4 & Gamma-enolase	VIME & CKAP4 & ENOG	**9.0E-03**	**2.7**	**5.0**	**50**	**5.1 & 5.6 & 4.9**	**54 & 66 & 47**	**1612 & 1124 & 980**	**127 & 117 & 106**	**31 & 18 & 14**
1574	Lupus La protein	LA	**2.9E-05**	**-2.4**	**7.4**	**50**	**6.7**	**47**	**722**	**106**	**12**
1576	Heterogeneous nuclear ribonucleoprotein F & Cartilage-associated protein & Eukaryotic initiation factor 4A-I & Heterogeneous nuclear ribonucleoprotein F	HNRPF & CRTAP & IF4A1	**8.5E-04**	**-2.3**	**5.6**	**50**	**5.4 & 5.3 & 5.3**	**46 & 44 & 46**	**636 & 490 & 926**	**95 & 82 &110**	**10 & 10 &18**
1604	No identified protein		**9.6E-03**	**-2.1**	**9.1**	**49**			**-**	**-**	**-**
1611	Prelamin-A/C & Fumarate hydratase, mitochondrial	LMNA & FUMH	**1.3E-02**	**3.9**	**8.0**	**49**	**6.6 & 7**	**74 & 50**	**1172 & 357**	**80 & 92**	**23 & 5**
1618	Serpin H1	SERPH	**1.2E-02**	**-2.7**	**9.5**	**48**	**8.8**	**45**	**355**	**74**	**6**
1622	Serpin H1 & Vimentin	SERPH & VIME	**2.5E-03**	**-3.6**	**9.7**	**48**	**8.8 & 5.1**	**45 & 54**	**700 & 365**	**80 & 58**	**12 & 9**
1651	Vimentin & Heat shock protein HSP 90-beta	VIME & HS90B	**2.9E-04**	**6.2**	**5.0**	**47**	**5.1 & 5**	**54 & 83**	**1774 & 679**	**99 & 91**	**34 & 12**
1659	Vimentin	VIME	**1.2E-02**	**2.8**	**4.9**	**47**	**5.1**	**54**	**2439**	**118**	**12**
1736	Alpha-enolase & Fumarylacetoacetase & Myosin-9	ENOA & FAAA & MYH9	**2.2E-03**	**2.3**	**7.5**	**45**	**7 & 6.5 & 5.5**	**47 & 46 & 226**	**632 & 110 & 682**	**132 & 64 & 92**	**9 & 2 & 11**

1744	Vimentin	VIME	**5.6E-03**	**5.2**	**4.8**	**44**	**5.1**	**54**	**1895**	**97**	**37**
1745	DnaJ homolog subfamily B member 11	DJB11	**4.3E-03**	**-3.2**	**6.8**	**44**	**5.8**	**38**	**721**	**105**	**13**
1756	Interleukin enhancer-binding factor 2 & Protein disulfide-isomerase	ILF2 & PDIA1	**3.2E-03**	**5.1**	**5.2**	**44**	**5.2 & 4.7**	**43 & 55**	**283 & 477**	**89 & 80**	**5 & 10**
1772	Trifunctional enzyme subunit alpha & 26S protease regulatory subunit 10B & 26S protease regulatory subunit 10B & Alpha-2-macroglobulin receptor-associated	ECHA & PRS10 & AMRP	**1.2E-04**	**3.2**	**8.5**	**44**	**9 & 7.1 & 6.9**	**79 & 44 & 38**	**1073 & 536 &377**	**102 & 68 & 56**	**19 & 12 & 10**
1830	Vimentin	VIME	**4.8E-02**	**2.1**	**4.8**	**42**	**5.1**	**54**	**1662**	**128**	**32**
1831	Heterogeneous nuclear ribonucleoproteins C1/C2 & Suppressor of G2 allele of SKP1 homolog	HNRPC & SUGT1	**8.6E-04**	**-2.3**	**5.1**	**42**	**5 & 5.1**	**34 & 41**	**154 & 132**	**60 & 61**	**3 & 3**
1848	Tubulin beta-2A chain & Short/branched chain specific acyl-CoA dehydrogenase, mitochondrial & Arfaptin-2	TBB2A & ACDSB & ARFP2	**8.8E-03**	**2.2**	**6.2**	**41**	**4.8 & 5.7 & 5.7**	**50 & 44 & 38**	**680 & 475 & 167**	**90 & 94 & 85**	**12 & 9 & 3**
1898	Caldesmon	CALD1	**1.1E-03**	**-3.3**	**10.4**	**40**	**5.6**	**93**	**469**	**60**	**11**
1909	Phosphoglycerate kinase 1 & Alpha-enolase	PGK1 & ENOA	**2.5E-02**	**2.0**	**6.6**	**40**	**8.3 & 7**	**44 & 47**	**701 & 715**	**104 & 116**	**12 & 11**
1910	Phosphotriesterase-related protein & Biliverdin reductase A	PTER & BIEA	**2.7E-02**	**2.1**	**7.1**	**40**	**6.1 & 6.1**	**39 & 33**	**210 & 128**	**64 & 59**	**4 & 3**
1924	Vimentin & Tropomyosin alpha-4 chain	VIME & TPM4	**1.2E-02**	**-2.5**	**4.8**	**40**	**5.1 & 4.7**	**54 & 28**	**703 & 519**	**89 & 60**	**15 & 12**
1930	Nucleophosmin & V-type proton ATPase subunit d 1	NPM & VA0D1	**2.1E-03**	**-9.0**	**4.9**	**39**	**4.6 & 4.9**	**33 & 40**	**464 & 448**	**98 & 77**	**8 & 8**
1933	Vimentin & Nucleophosmin & V-type proton ATPase subunit d 1	VIME & NPM & VA0D1	**6.0E-05**	**-4.0**	**5.0**	**38**	**5.1 & 4.6 & 4.9**	**54 & 33 & 40**	**482 & 411 & 324**	**85 & 92 & 81**	**9 & 7 & 6**
1947	Glyoxylate reductase/hydroxypyruvate reductase	GRHPR_HUMAN	**5.6E-05**	**2.0**	**8.3**	**39**	**7**	**36**	**376**	**72**	**8**
1964	Pyruvate kinase isozymes M1/M2 & Annexin A1	KPYM & ANXA1	**9.4E-03**	**2.8**	**7.4**	**38**	**8 & 6.6**	**58 & 39**	**944 & 579**	**92 & 117**	**15 & 8**
2035	Alpha-enolase & Torsin-1A	ENOA & TOR1A	**1.7E-03**	**2.1**	**7.3**	**37**	**7 & 6.2**	**47 & 36**	**396 & 264**	**97 & 75**	**6 & 5**
2051	Tubulin beta chain	TBB5	**9.5E-03**	**2.2**	**5.7**	**36**	**4.8**	**50**	**732**	**116**	**12**
2087	Glyceraldehyde-3-phosphate dehydrogenase	G3P	**1.1E-02**	**3.7**	**8.3**	**36**	**8.6**	**36**	**669**	**88**	**12**
2128	39S ribosomal protein L44, mitochondrial & Glyceraldehyde-3-phosphate dehydrogenase	RM44 & G3P	**1.1E-03**	**2.5**	**8.4**	**34**	**7 & 8.6**	**34 & 36**	**426 & 177**	**78 & 88**	**9 & 3**
2161	Heterogeneous nuclear ribonucleoprotein A1 & ELAV-like protein 1	ROA1 & ELAV1	**8.9E-04**	**-4.5**	**10.3**	**34**	**9.2 & 9.2**	**39 & 36**	**671 & 308**	**109 & 84**	**11 & 6**
2225	Elongation factor Tu, mitochondrial	EFTU	**4.7E-02**	**3.1**	**6.8**	**32**	**6.3**	**45**	**822**	**81**	**16**
2280	Cathepsin B & Alpha-soluble NSF attachment protein	CATB & SNAA	**7.7E-03**	**2.6**	**5.4**	**31**	**5.2 & 5.2**	**28 & 33**	**533 & 109**	**92 & 74**	**9 & 2**
2316	Cathepsin D & Annexin A5 & 14-3-3 protein epsilon	CATD & ANXA5 & 1433E	**2.4E-02**	**-5.5**	**5.1**	**30**	**5.6 & 4.9 &**	**38 & 36 & 29**	**571 & 532 &**	**91 & 88 & 52**	**10 & 9 & 3**

							4.6		118		
2324	Cathepsin D	CATD	4.3E-04	-3.7	5.5	30	5.6	38	501	70	9
2328	Cathepsin B & Chloride intracellular channel protein 1	CATB & CLIC1	1.5E-02	2.5	5.4	30	5.2 & 5.1	28 & 27	531 & 366	106 & 72	8 & 7
2356	Glutathione S-transferase omega-1	GSTO1	3.5E-02	2.9	6.8	29	6.2	27	323	66	7
2364	Protein disulfide-isomerase A3 & Triosephosphate isomerase	PDIA3 & TPIS	3.0E-02	2.3	7.5	29	5.6 & 5.7	54 & 31	304 & 117	107 & 59	5 & 2
2365	Hydroxyacyl-coenzyme A dehydrogenase, mitochondrial	HCDH	3.2E-03	4.8	8.2	29	8.4	33	457	59	10
2426	Ras suppressor protein 1 & Probable fructose-2,6-bisphosphatase TIGAR	RSU1 & TIGAR	3.0E-04	4.5	8.1	28	8.6 & 7.6	31 & 30	425 & 185	62 & 84	10 & 3
2438	6-phosphogluconolactonase & Actin-related protein 2/3 complex subunit 2	6PGL & ARPC2	2.5E-02	4.3	6.3	28	5.7 & 6.8	27 & 34	491 & 344	77 & 57	9 & 8
2478	Serpin H1 & Abhydrolase domain-containing protein 11	SERPH & ABHDB	1.2E-04	2.7	8.2	27	8.8 & 9.5	45 & 35	218 & 167	74 & 75	4 & 3
2505	3-hydroxybutyrate dehydrogenase type 2 & Trifunctional enzyme subunit beta, mitochondrial & 3-hydroxybutyrate dehydrogenase type 2 & Heterogeneous nuclear ribonucleoprotein A1	BDH2 & RA1L2 & ECHB & ROA1	1.8E-04	2.6	9.1	26	7.6 & 9.1 & 9.2	27 & 34 & 47	356 & 238 & 373 & 339	87 & 69 & 69 & 89	6 & 5 & 7 & 7
2517	Succinate dehydrogenase [ubiquinone] iron-sulfur subunit, mitochondrial & 40S ribosomal protein S3a & Peptidyl-prolyl cis-trans isomerase B & Transforming growth factor-beta-induced protein ig-h3	DHSB & RS3A & PPIB & BGH3	4.9E-03	2.8	10.3	27	8.8 & 9.8 & 9.3	29 & 30 & 20	466 & 276 & 209 & 446	60 & 77 & 78 & 65	11 & 7 & 4 & 9
2522	Annexin A1 & Cathepsin B & Inorganic pyrophosphatase	ANXA1 & CATB & IPYR	1.4E-02	2.3	5.2	26	6.6 & 5.2 & 5.5	39 & 28 & 33	587 & 309 & 56	101 & 90 & 30	9 & 5 & 2
2532	Adenylate kinase isoenzyme 4, mitochondrial	KAD4	3.7E-03	3.5	8.6	26	8.5	25	177	48	4
2555	14-3-3 protein gamma & Calpain small subunit 1 & 14-3-3 protein eta	1433G & CPNS1 & 1433F	3.7E-04	4.4	5.1	26	4.8 & 5.1 & 4.8	28 & 28 & 28	126 & 125 & 73	53 & 67 & 45	3 & 2 & 2
2573	Ubiquitin carboxyl-terminal hydrolase isozyme L1 & Vacuolar protein sorting-associated protein 28 homolog	UCHL1 & VPS28	1.5E-02	2.9	5.5	25	5.2 & 5.4	25 & 25	360 & 150	75 & 68	7 & 3
2591	Uncharacterized protein C2orf47, mitochondrial	CB047	1.1E-02	-2.4	8.3	25	7	22	40	40	1
2602	No identified protein		3.2E-03	2.3	7.0	25					
2610	NADH dehydrogenase [ubiquinone] iron-sulfur protein 8 & Actin, cytoplasmic 1 & Plasma membrane calcium-transporting ATPase 4	NDUS8 & ACTB & ATPG	2.9E-03	2.7	5.3	24	5.1 & 5.3 & 9	20 & 42 & 30	192 & 139 & 122	58 & 62 & 66	4 & 3 & 3
2561	Glyceraldehyde-3-phosphate dehydrogenase & Prohibitin-2	G3P & PHB2	3.3E-03	5.7	10.4	24	8.6 & 9.8	36 & 33	364 & 307	88 & 69	6 & 6
2713	Transgelin & Peptidyl-prolyl cis-trans isomerase B	TAGL & PPIB &	2.4E-03	5.1	10.2	22	8.9 &	22 & 20	265 &	72 & 73 &	5 & 5 & 5

	& Glyceraldehyde-3-phosphate dehydrogenase	G3P					**9.3 & 8.6**	**& 36**	**249 & 276**	**76**	
2737	Transgelin & NADH dehydrogenase [ubiquinone] 1 beta subcomplex subunit 10	TAGL & NDUBA	**5.9E-04**	**-2.9**	**10.0**	**22**	**8.9 & 8.7**	**22 & 21**	**646 & 156**	**75 & 52**	**13 & 4**
2754	ATP synthase subunit alpha, mitochondrial & 40S ribosomal protein S7	ATPA & RS7	**8.0E-03**	**2.4**	**7.0**	**22**	**8.3 & 10.1**	**55 & 22**	**115 & 60**	**62 & 33**	**3 & 2**
2763	ATP synthase subunit O, mitochondrial	ATPO	**4.4E-03**	**-2.3**	**10.8**	**22**	**9.8**	**21**	**507**	**107**	**8**
2773	Transgelin	TAGL	**3.4E-03**	**-2.1**	**8.8**	**22**	**8.9**	**22**	**365**	**66**	**7**
2486	Transgelin-2	TAGL2	**3.8E-03**	**-2.4**	**9.8**	**22**	**8.5**	**22**	**704**	**104**	**13**
2804	Programmed cell death protein 6 & F-actin-capping protein subunit beta & Deoxyribonucleoside 5'-monophosphate N-glycosidase	PDCD6 & CAPZB & RCL	**2.5E-03**	**4.5**	**5.0**	**21**	**5.2 & 5.4 & 5**	**22 & 31 & 19**	**152 & 208 & 312**	**68 & 67 & 90**	**3 & 4 & 6**
2805	Ras-related protein Rab-1A & Sorcin	RAB1A & SORCN	**1.9E-02**	**2.5**	**5.2**	**21**	**5.9 & 5.3**	**23 & 22**	**344 & 219**	**116 & 59**	**5 & 5**
2857	60S ribosomal protein L11	RL11	**2.5E-03**	**-3.1**	**10.8**	**20**	**9.6**	**20**	**110**	**59**	**2**
2858	Myosin regulatory light chain 12A	ML12A	**1.5E-02**	**-2.3**	**4.8**	**20**	**4.7**	**20**	**386**	**86**	**6**
2894	Nucleolin	NUCL	**7.7E-03**	**4.1**	**5.4**	**20**	**4.6**	**76**	**452**	**90**	**9**
2912	Myosin regulatory light chain 12A & Protein canopy homolog 2	ML12A & CNPY2	**8.6E-03**	**-2.1**	**4.9**	**19**	**4.7 & 4.7**	**20 & 19**	**379 & 225**	**79 & 71**	**7 & 5**
2976	Translocon-associated protein subunit delta & Annexin A2	SSRD & ANXA2	**1.7E-03**	**6.4**	**5.6**	**18**	**5.5 & 7.6**	**17 & 38**	**148 & 500**	**67 & 83**	**3 & 8**
2980	Tubulin beta-2A chain	TBB2A	**3.2E-04**	**3.3**	**4.7**	**18**	**4.8**	**50**	**337**	**106**	**5**
2991	Nucleophosmin & Tubulin beta-2A chain	NPM & TBB2A	**2.0E-04**	**5.1**	**4.6**	**18**	**4.6 & 4.8**	**33 & 50**	**278 & 158**	**69 & 59**	**5 & 3**
2999	Transgelin & Destrin	TAGL & DEST	**1.2E-04**	**3.0**	**7.6**	**18**	**8.9 & 8.1**	**22 & 18**	**314 & 163**	**68 & 98**	**6 & 3**
3089	Transgelin & Peroxiredoxin-1	TAGL & PRDX1	**1.5E-02**	**5.5**	**7.6**	**17**	**8.9 & 8.3**	**22 & 22**	**153 & 70**	**63 & 44**	**3 & 2**
3131	Protein mago nashi homolog	MGN	**2.8E-03**	**2.0**	**6.1**	**16**	**5.7**	**17**	**253**	**60**	**6**
3152	Myosin light polypeptide 6	MYL6	**1.9E-03**	**-2.1**	**4.7**	**16**	**4.6**	**17**	**683**	**85**	**12**
3193	Coactosin-like protein	COTL1	**4.2E-06**	**3.5**	**5.5**	**15**	**5.5**	**16**	**364**	**57**	**9**
3233	Profilin-1 & 60S ribosomal protein L22	PROF1 & RL22	**9.9E-03**	**3.1**	**10.0**	**15**	**8.5 & 9.2**	**15 & 15**	**151 & 102**	**77 & 58**	**3 & 2**
3263	Calponin-3	CNN3	**1.2E-04**	**8.9**	**7.8**	**14**	**5.7**	**36**	**74**	**43**	**2**
3292	ATP synthase subunit alpha, mitochondrial & Galectin-1	ATPA & LEG1	**2.1E-04**	**2.2**	**5.0**	**14**	**8.3 & 5.3**	**55 & 15**	**523 & 269**	**105 & 99**	**7 & 5**
3300	Hemoglobin subunit alpha	HBA	**3.6E-04**	**2.9**	**8.5**	**14**	**8.7**	**15**	**64**	**37**	**2**
3330	NADH dehydrogenase [ubiquinone] iron-sulfur protein 5 & 60S ribosomal protein L11	NDUS5 & RL11	**3.3E-04**	**2.4**	**10.7**	**14**	**9.3 & 9.6**	**12 & 20**	**98 & 74**	**71 & 37**	**2 & 2**
3347	Profilin-1 & Ribonuclease UK114 & Cofilin-1	PROF1 & UK114 & COF1	**3.8E-02**	**2.2**	**9.9**	**13**	**8.5 & 8.7 &**	**15 & 14 & 18**	**423 & 313 &**	**78 & 104 & 102**	**8 & 5 & 5**

							.8.3		**272**		
3388	40S ribosomal protein S3	RS3	**5.5E-05**	**4.1**	**10.7**	**13**	**9.7**	**27**	**289**	**67**	**5**
3413	40S ribosomal protein S3	RS3	**5.9E-05**	**4.0**	**10.4**	**13**	**9.7**	**27**	**310**	**68**	**5**
3464	40S ribosomal protein S14	RS14	**4.7E-03**	**2.7**	**9.3**	**12**	**10.1**	**16**	**151**	**71**	**3**
3536	Profilin-1 & Guanine nucleotide-binding protein G(I)/G(S)/G(O) subunit gamma-12 & Histone H2B type 1-B	PROF1 & GBG12 & H2B1B	**1.8E-03**	**4.0**	**10.7**	**11**	**8.5 & 9.1 & 10.3**	**15 & 8 & 14**	**232 & 209 & 155**	**72 & 67 & 64**	**5 & 4 & 4**
3545	Peroxiredoxin-5, mitochondrial	PRDX5	**3.3E-03**	**6.8**	**9.1**	**11**	**6.7**	**17**	**353**	**94**	**7**
3557	Peptidyl-prolyl cis-trans isomerase B	PPIB	**7.4E-03**	**3.0**	**10.4**	**11**	**9.3**	**20**	**90**	**63**	**2**

Exp: experimental; MM: molecular mass; pI: isoelectrofocalisation point; Theo: theoretical. Relative quantification and statistical evaluation were carried out with DeCyderTM 2D software (GE Healthcare, version 7.0). Down or up-expressed proteins between groups were retained if protein spot fold change was larger than +1.5 or smaller than –1.5 and a Student's t-test p-value less than 0.05

Additional file 1: Detailed data concerning 2-D electrophoresis technique and mass spectrometry identification

Proteomic analysis of vascular smooth muscle cells in physiological condition and in pulmonary arterial hypertension: toward contractile versus synthetic phenotypes.

Alexis Régent[1,2], Kim Heang Ly[3], Guilhem Clary[1,4], Sébastien Lofek[1], Mathieu Tamby[1], Nicolas Tamas[1], Christian Federici[1,4], Cédric Broussard[1,4], Philippe Chafey[1,4], Marc Humbert[5], Frédéric Peros[5], Luc Mouthon[1,2]

Protein extraction

Vascular smooth muscle cells (VSMC) from patients with pulmonary artery hypertension (PAH) and cells from pulmonary artery, aorta and umbilical artery (4 patients each) were used for proteomic experiments. Cells pellet (stored at -80°C) were lysed in lysis buffer (8M urea, 2M thiourea, 4% CHAPS, 60mM dithiothreitrol DTT). Then the protein extracts were clarified by ultra-centrifugation at 100.000g for 1 hour at 4°C. The separated supernatants were then treated with the 2D Clean-Up kit (GE Healthcare, Vélizy-Villacoublay, France) according to the manufacturer's instructions. The resultant dry pellets were resuspended into lysis buffer without DTT and centrifuged at 20,000g for 10 min at 4°C. Protein concentration was determined by the Quick Sart Bradford assay (Biorad, Hercules, California). Protein quantification and the quality of sample preparation were controlled by 1D SDS-PAGE performed using Bio-Rad mini-Protean III electrophoresis system. Samples were diluted 1:1

(v/v) with 2 x SDS sample buffer and run on SDS-PAGE (T=12%) with 5µg protein per lane. The gels were visualized by staining using Bio-Safe Coomassie (Bio-Rad).

Protein labelling with CyDye DIGE fluor

DIGE Minimal labeling of protein samples was performed according to the manufacturer's instruction (GE Healthcare, Orsay, France). Briefly, samples (50µg) were labeled for 30 min on ice in the dark with 400 pmol Cy3 or Cy5 Fluor minimal dyes. Internal Standard, a pool of equal portions of each of the samples used for this study, was labeled with cy2. The reaction was stopped by adding 10 nmol lysine followed by incubation on ice for 10 min in the dark.

Two dimension in gel electrophoresis

Fifty µg of labelled samples (Cy3 or Cy5) and internal standard (Cy2) were mixed. Each mixed Cy-dye labelled protein extract (150µg) was added to rehydration buffer (8 M urea, 2 M thiourea, 2% (w/v) CHAPS, 1.2% (v/v) DeStreak Reagent (GE Healthcare), 0.5% (v/v) IPG buffer pH 3-11 NL (GE Healthcare) and bromophenol blue) in a final volume of 350µL and used to rehydrated pH 3-11NL IPG strips 18 cm (GE Healthcare) 24h at room temperature under low-viscosity paraffin oil.

Isoelectrofocusing was performed at 20°C using IPGphor3 (GE Healthcare) for a total of 40 kVh. At the end of focalisation, IPG strips were incubated consecutively for 15 min each in equilibration buffer I and II (Buffer I: 50 mM Tris-HCl (pH 6.8), 6 M urea, 2% Sodium Dodecyl Sulphate, 30% glycerol and 1% DTT; Buffer II: 50 mM Tris-HCl (pH 6.8), 6 M urea, 2% Sodium Dodecyl Sulphate, 30% glycerol and 2.5% iodoacetamide) with gentle agitation.

Equilibrated strips were placed onto homemade polyacrylamide gels (8-18%) and overlaid with agarose solution (0.5% low-melting agarose and trace of bromophenol blue in running buffer) and electrophoresis was performed simultaneously in a Ettan-DALT II system (GE Healthcare) at 2.5W/gel at 15°C until the bromophenol blue dye reached the bottom of the gels.

Gels Analysis

Gels were scanned using a Typhoon 9400 (GE Healthcare) with a resolution set at 100µm and using optimal excitation/emission wavelength for each DIGE fluor dye (Cy2 488/520 nm; Cy3 532/580 nm; Cy5 633/670 nm). Image analysis, relative quantification and statistical evaluation and PCA (Principal Component Analysis) were carried out with DeCyderTM 2D software (GE Healthcare, version 7.0). Down or up-expressed proteins, of the different group-to-group comparisons, were retained if protein spot fold change was larger than +1.5 or smaller than –1.5 and a Student's t-test p-value less than 0.05.

For mass spectrometry analysis, 2 semi-preparative 2D-gels were prepared as analytical gels. One 2D gels loaded with 400 µg of mix containing equal amount of HAoSMC, HUASMC and HPASMC samples, and the other containing 400 µg protein mix of PAH-SMC and VSMC samples.

After electrophoresis, 2D-gels were fixed in 30% (v/v) ethanol, 2% (v/v) phosphoric acid (two changes, 30 min each), and then stained for 72h in 0.01% (w/v) Coomassie Brilliant Blue G-250, 12% (w/v) ammonium sulfate, 18% (v/v) ethanol and 2% (v/v) phosphoric acid. Spots of interest were manually excised from Coomassie blue-stained semi-preparative gels.

Protein Identification by Mass Spectrometry (MS) and Database Searching.

Spots excised from gels were placed into 96-well microtiter plates. Then, in-gel digestion was carried out with trypsin as described by Shevchenko et al. [28] with minor modifications and using for all steps a Freedom EVO 100 digester/spotter robot (Tecan, Switzerland). Spots were first destained two times with a mixture of 100 mM ammonium bicarbonate (ABC) and 50% (v/v) acetonitrile (ACN) for 45 min at 22°C and then dehydrated using 100% ACN for 15 min. Protein spots were then reduced with 25 mM ABC containing 10 mM DTT for 1 h at 60°C and then alkylated with 55 mM iodoacetamide in 25 mM ABC for 30 min in the dark at 22°C. Gel pieces were washed twice with 25 mM ABC and finally dried using 100% ACN for 10 min. Bands were finally completely dehydrated after 1 h at 60°C. Gel pieces were incubated with 13 µL of sequencing grade modified trypsin (Promega, USA; 12.5 µg/mL in 40 mM ABC with 10% ACN, pH 8.0) overnight at 40°C.

After digestion, peptides were washed with 30 µL of 25 mM ABC, dried with 100% ACN and extracted twice with a mixture of 50% ACN–5% formic acid. Extracts were dried using a vacuum centrifuge Concentrator plus (Eppendorf).

For MS and tandem Mass Spectrometry (MS/MS) analyses, peptides were dissolved in 4 µL of alpha-CHCA (2.5 mg/mL in 70% ACN–0.1% trifluoroacetic acid). One microliter and a half of each sample were spotted directly onto a MALDI plate (ABSciex, USA). Droplets were allowed to dry at room temperature. Samples analyses were performed using a MALDI TOF-TOF 4800 mass spectrometer (ABSciex). Spectra acquisition and processing were performed using the 4000 series explorer software (ABI) version 3.5.28193 in positive reflectron mode at fixed laser fluency with a low mass gate and delayed extraction. External plate calibration was

performed using 4 calibration points spotted onto the 4 corners of the plate using a mixture of five external standards (PepMix 1; LaserBio Labs, France). Peptide masses were acquired by steps of 50 spectra in the range of 900 to 4000 Da. MS spectra were summed from 500 laser shots from an Nd-YAG laser operating at 355 nm and 200 Hz. After filtering tryptic, keratin and matrix contaminant peaks up to 15 parent ions were selected for subsequent MS/MS fragmentation according to mass range, signal intensity, signal to noise ratio, and absence of neighboring masses in the MS spectrum. MS/MS spectra were acquired in 1 kV positive mode and 1000 shots were summed by steps of 50. Database searches were carried out using Mascot version 2.2 (MatrixScience, London, UK) via GPS explorer software (ABSciex) version 3.6 combining MS and MS/MS inquiries on *human* proteins from SwissProt databank (20321 sequences, March 2012, www.expasy.org).

The search parameters were as follows: carbamidomethylation as a variable modification for cysteins and oxidation as a variable modification for methionines. Up to 1 missed tryptic cleavage was tolerated and mass accuracy tolerance of 30 ppm for precursors and 0.3 Da for fragments were used for all tryptic mass searches. Positive identification was based on a Mascot score above the significance level (i.e. < 5%).The reported proteins were always those with the highest number of peptide matches. Under our identification criteria, no result was found to match to multiple members of a protein family.

For MS and MS/MS ORBITRAP analyses, analyses were realized using an Ultimate 3000 Rapid Separation Liquid Chromatographic (RSLC) system (Thermo Fisher Scientific) online with a hybrid LTQ-Orbitrap-Velos mass spectrometer (Thermo

Fisher Scientific). Briefly, peptides were loaded and washed on a C_{18} reverse phase precolumn (3 µm particle size, 100 Å pore size, 150 µm i.d., 1 cm length). The loading buffer contains 98% H_2O, 2% ACN and 0.1% TFA. Peptides were then separated on a C_{18} reverse phase resin (2 µm particle size, 100 Å pore size, 75 µm i.d., 15 cm length) with a 4 min "effective gradient" from 100% A (0.1% FA and 100% H_2O) to 50% B (80% ACN, 0.085% FA and 20% H_2O).

The Linear Trap Quadrupole Orbitrap mass spectrometer acquired data throughout the elution process and operated in a data dependent scheme with full MS scans acquired with the Orbitrap, followed by up to 20 LTQ MS/MS CID spectra on the most abundant ions detected in the MS scan. Mass spectrometer settings were: full MS (AGC: $1*10^6$, resolution: $6*10^4$, m/z range 400-2000, maximum ion injection time: 500 ms); MS/MS (AGC: $5*10^3$, maximum injection time: 50 ms, minimum signal threshold: 500, isolation width: 2Da, dynamic exclusion time setting: 15 s). The fragmentation was permitted of precursor with a charge state of 2, 3, 4 and up. For the spectral processing, the software used to generate .mgf files is Proteome discoverer 1.2. The threshold of Signal to Noise for extraction values is 3. For database searching, all the search parameters were the same as MALDI search except the precursor mass tolerance which was set to 10 ppm and the fragment mass tolerance to 0.45 Da.

Supplemental figure 1: Canonical pathways proposed by ingenuity with protein differentially expressed between HUASMC and HAoSMC (fold change ≥1.5 and p<0.05).Blue bars scale represents – log (p-value) and p-value is the probability that the canonical pathway was generated by chance. Threshold was established at 1.3 corresponding to a 0.05 p-value. Ratio is the percentage of protein of the selective pathway that was identified with proteomic experiments.

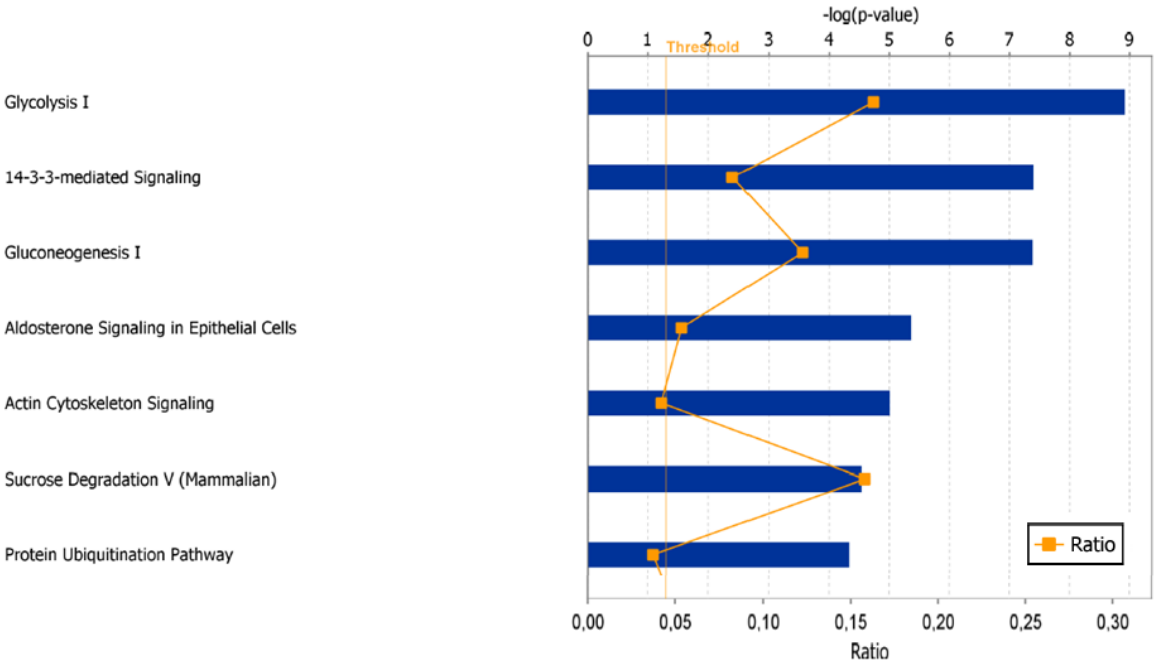

Supplemental figure 2: Canonical pathways proposed by ingenuity with protein differentially expressed between HUASMC and HPASMC (fold change ≥1.5 and p<0.05). Blue bars scale represents – log (p-value) and p-value is the probability that the canonical pathway was generated by chance. Threshold was established at 1.3 corresponding to a 0.05 p-value. Ratio is the percentage of protein of the selective pathway that was identified with proteomic experiments.

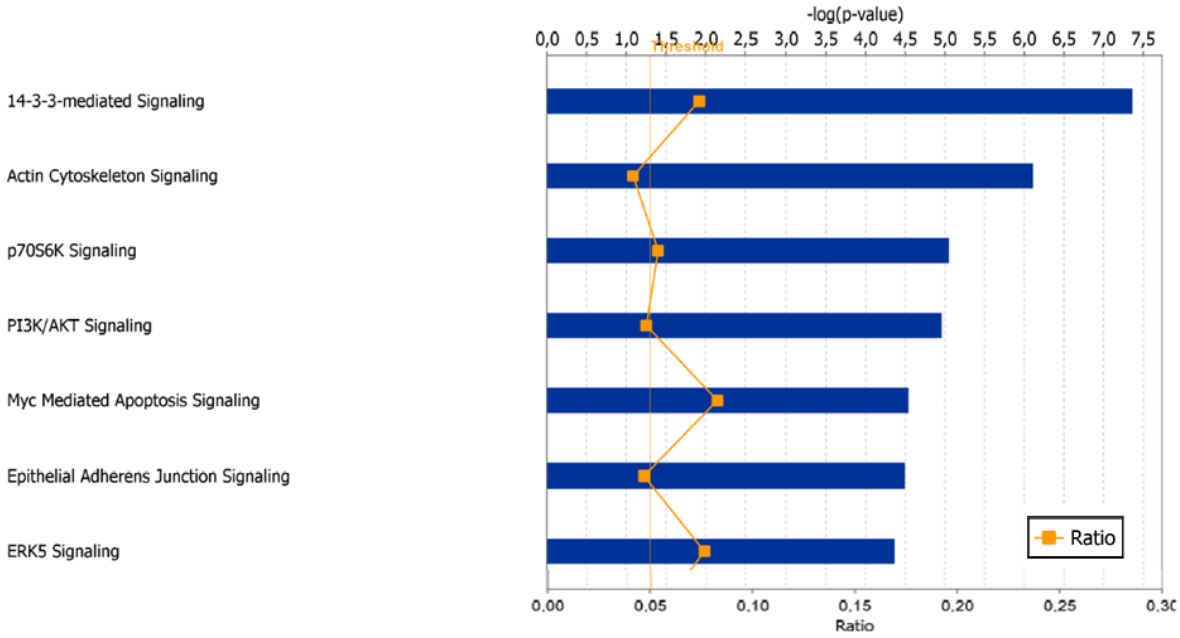

Supplemental figure 3: Canonical pathways proposed by ingenuity with protein differentially expressed between HPASMC and PAH-SMC (fold change ≥1.5 and p<0.05). Blue bars scale represents – log (p-value) and p-value is the probability that the canonical pathway was generated by chance. Threshold was established at 1.3 corresponding to a 0.05 p-value. Ratio is the percentage of protein of the selective pathway that was identified with proteomic experiments.

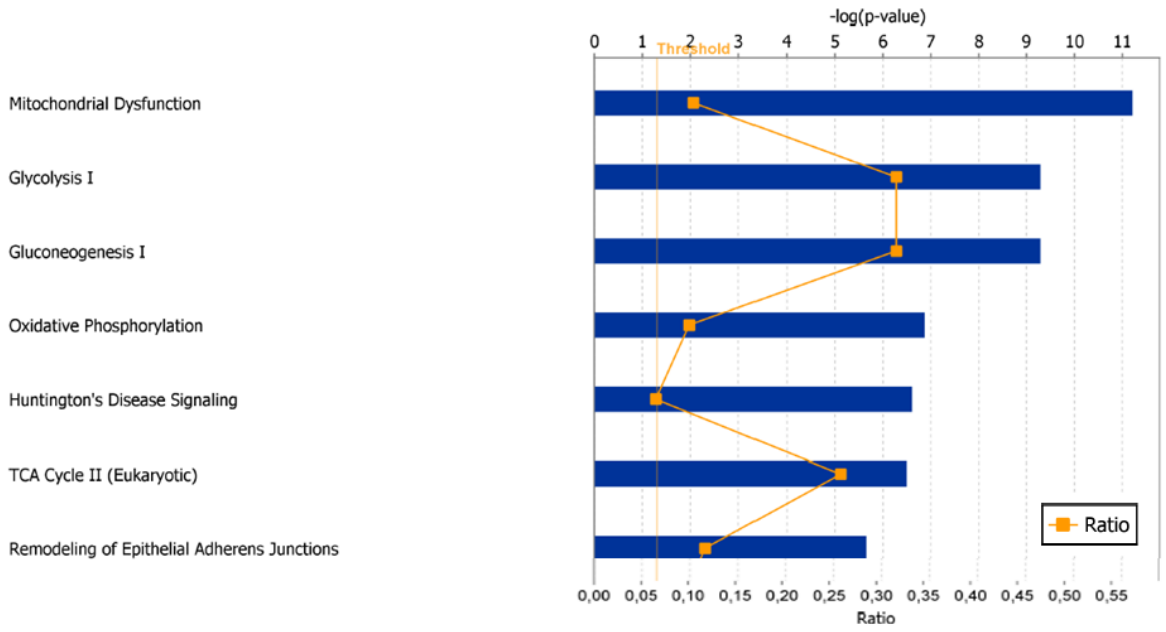

Supplemental table 1 Differentially expressed proteins between VSMC from umbilical artery and aorta (fold change ≥1.5, p≤0.05).

SPOT	IDENTIFIED PROTEIN	NAME	T-test	Fold change	Exp pI	Exp MM	Theo pI	Theo MM	Total ion Score	Best ion Score	Number of identified peptides
354	Alpha-actinin-1	ACTN1	**0.036**	**-2.17**	**5.62**	**105.674**	**5.3**	**103**	**1280**	**106**	**26**
617	Alpha-actinin-4	ACTN4	**0.046**	**-1.59**	**5.58**	**90.653**	**5.3**	**105**	**2390**	**98**	**40**
632	Programmed cell death 6-interacting protein & Procollagen-lysine.2-oxoglutarate 5-dioxygenase 2 & Filamin-A	PDC6I & PLOD2 & FLNA	**0.032**	**2.62**	**6.95**	**89.41**	**6.1 & 6.2 & 5.7**	**96 & 82 & 281**	**886 & 567 & 530**	**87 & 92 & 86**	**20 & 11 & 11**
640	Procollagen-lysine.2-oxoglutarate 5-dioxygenase 2	PLOD2	**0.045**	**1.97**	**7.19**	**88.863**	**6.2**	**82**	**806**	**86**	**16**
645	Procollagen-lysine.2-oxoglutarate 5-dioxygenase 2 & Filamin-A	PLOD2 & FLNA	**0.028**	**2.69**	**6.84**	**88.591**	**6.2 & 5.7**	**82 & 281**	**783 & 581**	**86 & 82**	**15 & 12**
728	Myosin-9 & Src substrate cortactin	MYH9 & SRC8	**0.018**	**-2.5**	**5.54**	**84.35**	**8.8 & 5.2**	**354 & 62**	**1420 & 172**	**113 & 41**	**27 & 5**
731	Myosin-9 & Src substrate cortactin	MYH9 & SRC8	**0.017**	**-2.48**	**5.59**	**84.479**	**8.8 & 5.2**	**354 & 62**	**2165 & 643**	**112 & 95**	**36 & 12**
826	TATA-binding protein-associated factor 2N	RBP56	**0.0057**	**-2.23**	**8.8**	**79.82**	**8**	**62**	**136**	**57**	**3**
838	TATA-binding protein-associated factor 2N	RBP56	**0.0069**	**-1.9**	**9.08**	**78.606**	**8**	**62**	**248**	**78**	**6**
841	Collagen alpha-3(VI) chain & Vimentin	CO6A3 & VIME	**0.0014**	**-2.1**	**5.79**	**78.365**	**6.2 & 5.1**	**341 & 54**	**1662 & 744**	**90 & 70**	**29 & 16**
933	Prelamin-A/C & Moesin	LMNA & MOES	**0.049**	**-1.83**	**7.26**	**74.157**	**6.6 & 6.1**	**74 & 68**	**1594 & 1372**	**104 & 94**	**31 & 26**
960	Stress-70 protein	GRP75	**0.013**	**1.69**	**5.76**	**72.471**	**5.4**	**69**	**1928**	**107**	**33**
981	Trifunctional enzyme subunit alpha	ECHA	**0.044**	**2.55**	**10.04**	**72.028**	**9**	**79**	**1665**	**99**	**29**
1146	Cytoskeleton-associated protein 4	CKAP4	**0.037**	**1.5**	**6.23**	**65.195**	**5.6**	**66**	**1748**	**147**	**26**
1164	Prelamin-A/C & Dihydropyrimidinase-related protein 2 & T-complex protein 1 subunit gamma	LMNA & DPYL2 & TCPG	**0.048**	**-1.78**	**7.02**	**64.697**	**6.6 & 6 & 6.1**	**74 & 62 & 61**	**1616 & 1056 & 904**	**82 & 117 & 81**	**31 & 17 & 18**
1246	60 kDa heat shock protein	CH60	**0.042**	**1.55**	**5.42**	**60.663**	**5.2**	**58**	**1937**	**114**	**29**
1300	UDP-glucose 6-dehydrogenase	UGDH	**0.026**	**-2.44**	**8.25**	**58.831**	**6.7**	**55**	**1061**	**90**	**21**

1313	Dihydrolipoyl dehydrogenase. mitochondrial	DLDH	**0.03**	**1.91**	**7.69**	**58.381**	**6.5**	**50**	**819**	**88**	**16**
1314	Protein disulfide-isomerase A3 & Lamin-B2 & Vimentin	PDIA3 & LMNB2 & VIME	**0.015**	**1.77**	**5.96**	**58.381**	**5.6 & 5.3 & 5.1**	**54 & 67 & 54**	**964 & 560 & 892**	**110 & 84 & 80**	**16 & 14 & 19**
1317	Dihydrolipoyl dehydrogenase. mitochondrial & tRNA-splicing ligase RtcB homolog & Bifunctional 3'-phosphoadenosine 5'-phosphosulfate synthase 2	DLDH & RTCB &PAPS2	**0.027**	**1.62**	**7.91**	**58.381**	**6.5 & 6.8 & 8.2**	**50 & 55 & 70**	**1073 & 346 & 339**	**102 & 55 & 68**	**20 & 9 & 8**
1372	Glucose-6-phosphate 1-dehydrogenase & D-3-phosphoglycerate dehydrogenase	G6PD & SERA	**0.0039**	**-2.03**	**7.56**	**56.967**	**6.4 & 6.3**	**59 & 57**	**1068 & 494**	**104 & 93**	**21 & 10**
1386	Vimentin & Tubulin beta chain	VIME & TBB5	**0.003**	**-2.05**	**5.07**	**56.014**	**5.1 & 4.8**	**54 & 50**	**1761 & 1123**	**114 & 110**	**33 & 17**
1403	Vimentin	VIME	**0.026**	**1.8**	**5.32**	**55.331**	**5.1**	**54**	**2111**	**115**	**40**
1420	V-type proton ATPase subunit B. brain isoform	VATB2	**0.00017**	**36.7**	**5.99**	**55.246**	**5.6**	**57**	**1498**	**113**	**23**
1421	Dihydrolipoyllysine-residue succinyltransferase component of 2-oxoglutarate dehydrogenase complex & Heterogeneous nuclear ribonucleoprotein H & Rho GTPase-activating protein 1	ODO2 & HNRH1 & RHG01	**0.0099**	**1.81**	**6.39**	**54.993**	**5.9 & 5.9 & 5.9**	**41 & 49 & 50**	**501 & 413 & 220**	**93 & 84 & 53**	**9 & 8 & 5**
1422	Selenium-binding protein 1 & Mitochondrial-processing peptidase subunit alpha & Pyruvate dehydrogenase protein X component. mitochondrial	SBP1 & MPPA & ODPX	**0.03**	**1.67**	**6.66**	**55.077**	**5.9 & 5.9 & 6**	**52 & 55 & 48**	**561 & 552 & 446**	**78 & 80 & 85**	**11 & 10 & 8**
1431	Reticulocalbin-2 & Vimentin	RCN2 & VIME	**0.0029**	**1.52**	**4.52**	**54.656**	**4.2 & 5.1**	**35 & 54**	**614 & 477**	**106 & 66**	**10 & 10**
1435	Histidine--tRNA ligase. cytoplasmic	SYHC	**0.019**	**3.53**	**6.16**	**54.908**	**5.7**	**57**	**998**	**96**	**18**
1474	Collagen alpha-3(VI) & Vimentin & NAD-dependent malic enzyme. mitochondrial	CO6A3 & VIME & MAOM	**0.028**	**3.74**	**5.72**	**52.844**	**6.2 & 5.1 & 6.6**	**341 & 54 & 63**	**625 & 475 & 404**	**87 & 57 & 92**	**11 & 8 & 8**
1543	Rab GDP dissociation inhibitor beta & Alpha-elonase	GDIB & ENOA	**0.00088**	**-1.84**	**6.95**	**50.623**	**6.1 & 7**	**51 & 47**	**1119 & 498**	**98 & 118**	**21 & 8**
1548	Alpha-enolase	ENOA	**0.021**	**-1.77**	**7.67**	**50.391**	**7**	**47**	**984**	**109**	**16**
1555	Alpha-enolase	ENOA	**0.025**	**-1.9**	**8.09**	**50.159**	**7**	**47**	**1450**	**124**	**23**
1565	Alpha-enolase	ENOA	**0.02**	**-2.07**	**8.74**	**50.236**	**7**	**47**	**999**	**107**	**16**
1576	Heterogeneous nuclear ribonucleoprotein F & Cartilage-associated protein & Eukaryotic initiation factor 4A-I	HNRPF & CRTAP & IF4A1	**0.046**	**2.3**	**5.58**	**49.7**	**5.4 & 5.3 & 5.3**	**46 & 44 & 46**	**636 & 490 & 926**	**95 & 82 &110**	**10 & 10 &18**
1589	Vimentin & Calumenin	VIME & CALU	**0.024**	**1.59**	**4.63**	**49.396**	**5.1 & 4.5**	**54 & 35**	**1057 & 764**	**106 & 81**	**24 & 14**
1604	No identified protein		**0.016**	**1.96**	**9.46**	**48.199**					

1618	Serpin H1	SERPH	**0.0059**	**1.77**	**5.6**	**47.685**	**8.8**	**45**	**355**	**74**	**6**
1624	Eukaryotic initiation factor 4A-I & Vimentin	IF4A1 & VIME	**0.021**	**2.69**	**7.79**	**48.052**	**5.3 & 5.1**	**46 & 54**	**1022 & 668**	**103 & 81**	**19 & 14**
1630	Plasminogen activator inhibitor 1	PAI1	**0.018**	**1.89**	**5.67**	**47.176**	**7**	**43**	**558**	**99**	**10**
1641	No identified protein		**0.00006**	**2.94**	**6.46**	**47.32**					
1645	Vimentin & Interleukin enhancer-binding factor 2 & Myoferlin	VIME & ILF2 & MYOF	**0.00006**	**6.39**	**6.7**	**47.176**	**5.1 & 5.2 & 5**	**54 & 43 & 83**	**465 & 780 & 746**	**66 & 79 & 92**	**11 & 15 & 13**
1656	Calcium-binding mitochondrial carrier protein SCaMC-1 & Prelamin-A/C & Protein disulfide-isomerase A3	SCMC1 & LMNA & PDIA3	**0.013**	**1.94**	**7.87**	**46.887**	**6 & 6.6 & 5.6**	**53 & 74 & 54**	**706 & 389 & 503**	**74 & 83 & 102**	**16 & 8 & 9**
1657	Calcium-binding mitochondrial carrier protein SCaMC-1 & Ornithine aminotransferase. mitochondrial & Synaptic vesicle membrane protein VAT-1 homolog	SCMC1 & OAT & VAT1	**0.011**	**2.07**	**9.63**	**44.166**	**6 & 6 & 5.9**	**53 & 46 & 42**	**629 & 422 & 253**	**72 & 81 & 94**	**14 & 7 & 4**
1665	26S protease regulatory subunit 8 & Pyruvate dehydrogenase E1 component subunit alpha. somatic form. mitochondrial	PRS8 & ODPA	**0.00021**	**1.57**	**5.18**	**43.627**	**7.3 & 6.5**	**45 & 40**	**475 & 312**	**83 & 60**	**8 & 7**
1753	Phosphoglycerate kinase 1	PGK1	**0.0062**	**-1.6**	**7.32**	**43.828**	**8.3**	**44**	**1187**	**95**	**21**
1756	Interleukin enhancer-binding factor 2 & Protein disulfide-isomerase	ILF2 & PDIA1	**0.00024**	**8.19**	**5.69**	**43.56**	**5.2 & 4.7**	**43 & 55**	**283 & 477**	**89 & 80**	**5 & 10**
1759	Dihydrolipoyl dehydrogenase. mitochondrial & Poly(rC)-binding protein 2	DLDH & PCBP2	**0.011**	**-1.72**	**7.72**	**42.701**	**6.5 & 6.3**	**50 & 39**	**140 & 129**	**56 & 58**	**3 & 3**
1774	Stomatin-like protein 2 & Actin. cytoplasmic 1	STML2 & ACTB	**0.00097**	**1.56**	**9.73**	**42.963**	**5.4 & 5.3**	**36 & 42**	**609 & 411**	**90 & 109**	**9 & 8**
1794	Mitogen-activated protein kinase 1	MK01	**0.02**	**-1.62**	**7.91**	**42.57**	**6.5**	**41**	**805**	**85**	**15**
1804	Alpha-enolase & Fructose-bisphosphate aldolase A & Glyceraldehyde-3-phosphate dehydrogenase	ENOA & ALDOA & G3P	**0.015**	**-1.61**	**10.23**	**41.987**	**7 & 8.4 & 8.6**	**47 & 39 & 36**	**307 & 949 & 523**	**79 & 113 & 77**	**5 & 16 & 10**
1813	Poly(rC)-binding protein 1 & Fructose-bisphosphate aldolase & Acyl-coenzyme A thioesterase 9	PCBP1 & ALDOC & ACOT9	**0.0036**	**-1.76**	**8.81**	**40.284**	**6.7 & 6.5 & 7.8**	**37 & 39 & 48**	**650 & 425 & 375**	**100 & 86 & 76**	**11 & 8 & 8**
1829	Aspartate aminotransferase. mitochondrial & Heterogeneous nuclear ribonucleoprotein A3	AATM & ROA3	**0.0039**	**1.56**	**4.81**	**39.61**	**9 & 9.1**	**45 & 40**	**884 & 486**	**119 & 106**	**15 & 7**
1886	Heat shock cognate 71 kDa protein & Alcohol dehydrogenase class-3 & Phosphoserine aminotransferase	HSP7C & ADHX & SERC	**0.0074**	**-1.72**	**4.97**	**38.169**	**5.4 & 7.6 & 7.6**	**71 & 40 & 40**	**767 & 411 & 213**	**104 & 101 & 78**	**12 & 8 & 4**

1924	Vimentin & Tropomyosin alpha-4 chain	VIME & TPM4	**0.023**	**-3.02**	**7.35**	**38.355**	**5.1 & 4.7**	**54 & 28**	**703 & 519**	**89 & 60**	**15 & 12**
1964	Pyruvate kinase isozymes M1/M2 & Annexin A1	KPYM & ANXA1	**0.002**	**-1.92**	**8.7**	**37.656**	**8 & 6.6**	**58 & 39**	**396 & 264**	**97 & 75**	**6 & 5**
2004	Annexin A2	ANXA2	**0.024**	**-1.52**	**7.66**	**37.083**	**7.6**	**38**	**1037**	**97**	**18**
2016	Annexin A2 & LIM and SH3 domain protein 1	ANXA2 & LASP1	**0.046**	**-1.62**	**9.25**	**36.407**	**7.6 & 6.6**	**38 & 30**	**421 & 575**	**93 & 66**	**7 & 12**
2045	Annexin A2 & Fructose-bisphosphate aldolase A & Glyceraldehyde-3-phosphate dehydrogenase	ANXA2 & ALDOA & G3P	**0.029**	**-2.08**	**8.71**	**36.351**	**7.6 & 8.4 & 8.6**	**38 & 39 & 36**	**528 & 322 & 174**	**78 & 66 & 75**	**10 & 7 & 3**
2048	Annexin A2	ANXA2	**0.041**	**-1.55**	**6.22**	**36.351**	**7.6**	**38**	**1843**	**90**	**32**
2060	L-lactate dehydrogenase B chain & Pyruvate kinase isozymes M1/M2	LDHB & KPYM	**0.021**	**-1.99**	**6.59**	**34.611**	**5.7 & 8**	**37 & 58**	**800 & 699**	**83 & 76**	**15 & 14**
2119	Inorganic pyrophosphatase 2. mitochondrial	IPYR2	**0.041**	**1.59**	**7.74**	**33.72**	**6**	**35**	**533**	**83**	**11**
2153	S-formylglutathione hydrolase	ESTD	**0.00087**	**-1.78**	**7.04**	**33.411**	**6.5**	**31**	**494**	**87**	**9**
2165	Tetratricopeptide repeat protein 35 & Complex I intermediate-associated protein 30. mitochondrial	TTC35 & CIA30	**0.031**	**1.63**	**5.06**	**32.602**	**6.2 & 5.9**	**35 & 35**	**458 & 216**	**76 & 56**	**8 & 5**
2198	Annexin A5	ANXA5	**0.00026**	**-1.89**	**10,0**	**32.502**	**4.9**	**36**	**1136**	**128**	**17**
2204	2.4-dienoyl-CoA reductase. mitochondrial & ATP synthase subunit gamma. mitochondrial & Voltage-dependent anion-selective channel protein 3	DECR & ATPG & VDAC3	**0.028**	**1.79**	**4.6**	**30.615**	**8.8 & 9 & 8.9**	**32 & 30 & 31**	**539 & 323 & 364**	**87 & 86 & 83**	**10 & 5 & 6**
2294	Complement component 1 Q subcomponent-binding protein. mitochondrial	C1QBP	**0.0066**	**1.7**	**9.96**	**30.335**	**4.3**	**24**	**318**	**75**	**5**
2301	Carbonyl reductase [NADPH] 1 & Heterogeneous nuclear ribonucleoprotein A1 & Voltage-dependent anion-selective channel protein 3 & NAD(P)H dehydrogenase [quinone] 1	CBR1 & ROA1 & VDAC3 & NQO1	**0.024**	**-1.52**	**5.41**	**29.736**	**8.6 & 9.2 & 8.9**	**30 & 39 & 31**	**520 & 400 & 465 & 359**	**97 & 109 & 97 & 75**	**9 & 7 & 7 & 7**
2328	Cathepsin B & Chloride intracellular channel protein 1	CATB & CLIC1	**0.021**	**3.17**	**4.83**	**29.239**	**5.2 & 5.1**	**28 & 27**	**531 & 366**	**106 & 72**	**8 & 7**
2349	14-3-3 protein theta & 14-3-3 protein zeta/delta	1433T & 1433Z	**0.0099**	**-2.32**	**4.87**	**28.618**	**4.7 & 4.7**	**28 & 28**	**666 & 641**	**91 & 90**	**12 & 13**
2375	14-3-3 protein gamma	1433G	**0.01**	**-1.69**	**9.74**	**28.662**	**4.8**	**28**	**728**	**85**	**14**
2378	Galectin-3 & Voltage-dependent anion-selective channel protein 3 & Surfeit locus protein 1	LEG3 & VDAC3 & SURF1	**0.0069**	**-2.15**	**5.78**	**28.706**	**8.6 & 8.9 & 9.6**	**26 & 31 & 33**	**501 & 348 & 157**	**88 & 108 & 65**	**9 & 6 & 3**

2381	Beta-hexosaminidase subunit beta & Nicotinamide N-methyltransferase & Chloride intracellular channel protein 4	HEXB & NNMT & CLIC4	**0.0087**	**-1.57**	**5.13**	**28.618**	**5.9 & 5.6 & 5.5**	**50 & 30 & 29**	**576 & 284 & 156**	**72 & 60 & 93**	**11 & 6 & 3**
2386	78 kDa glucose-regulated protein & Heterogeneous nuclear ribonucleoprotein Q	GRP78 & HNRPQ	**0.0053**	**-1.86**	**4.79**	**28.356**	**5 & 8.7**	**70 & 69**	**639 & 296**	**111 & 78**	**11 & 6**
2390	14-3-3 protein theta	1433T	**0.0017**	**-1.93**	**6.22**	**28.487**	**4.7**	**28**	**868**	**98**	**15**
2392	Proteasome activator complex subunit 1	PSME1	**0.0012**	**-2.45**	**5.71**	**28.053**	**5.8**	**29**	**563**	**76**	**10**
2413	Beta-hexosaminidase subunit beta & Nicotinamide N-methyltransferase & Chloride intracellular channel protein 4	HEXB & NNMT & CLIC4	**0.012**	**-1.73**	**4.82**	**27.882**	**5.9 & 5.6 & 5.5**	**50 & 30 & 29**	**430 & 214 & 259**	**75 & 82 & 83**	**9 & 4 & 5**
2424	14-3-3 protein zeta/delta	1433Z	**0.012**	**-1.78**	**4.87**	**27.754**	**4.7**	**28**	**954**	**94**	**17**
2431	14-3-3 protein beta/alpha	1433B	**0.0049**	**-1.81**	**5.19**	**27.164**	**4.8**	**28**	**878**	**107**	**16**
2467	Annexin A1	ANXA1	**0.013**	**-2.08**	**10.15**	**26.385**	**6.6**	**39**	**615**	**112**	**9**
2516	Protein NipSnap homolog 1 & Calponin-3 & Elongation factor 1-alpha 1	NIPS1 & CNN3 & EF1A1	**0.028**	**1.88**	**7.94**	**25.627**	**9.4 & 5.7 & 9.1**	**33 & 36 & 50**	**360 & 292 & 163**	**73 & 63 & 57**	**8 & 7 & 4**
2548	Triosephosphate isomerase	TPIS	**0.026**	**-1.66**	**5.72**	**25.315**	**5.7**	**31**	**901**	**100**	**14**
2570	Ubiquitin carboxyl-terminal hydrolase isozyme L1 & Peroxiredoxin-4 & T-complex protein 1 subunit	UCHL1 & PRDX4 & TCPB	**0.0024**	**2.11**	**8.25**	**25.006**	**5.2 & 5.5 & 6**	**25 & 27 & 57**	**270 & 203 & 370**	**86 & 78 & 81**	**5 & 4 & 7**
2591	Uncharacterized protein C2orf47. mitochondrial	CB047	**0.029**	**1.51**	**6.52**	**23.772**	**7**	**22**	**40**	**40**	**1**
2663	Flavin reductase (NADPH)	BLVRB	**0.016**	**-1.93**	**8.58**	**23.591**	**7.3**	**22**	**287**	**102**	**5**
2820	Ferritin light chain	FRIL	**0.0053**	**1.5**	**5.84**	**20.867**	**5.5**	**20**	**542**	**94**	**8**
2831	Myosin regulatory light polypeptide 9	MYL9	**0.004**	**-1.62**	**4.92**	**20.613**	**4.8**	**20**	**253**	**84**	**5**
3029	Eukaryotic translation initiation factor 5A-1	IF5A1	**0.029**	**-1.78**	**5.25**	**17.334**	**5.1**	**17**	**416**	**85**	**8**
3104	Peptidyl-prolyl cis-trans isomerase A	PPIA	**0.022**	**-2.27**	**8.81**	**16.353**	**7.7**	**18**	**483**	**69**	**11**
3115	Peptidyl-prolyl cis-trans isomerase A	PPIA	**0.02**	**-1.97**	**9.1**	**16.203**	**7.7**	**18**	**315**	**69**	**6**
3157	Peroxiredoxin-5. mitochondrial	PRDX5	**0.048**	**1.72**	**8.44**	**15.666**	**6.7**	**17**	**479**	**102**	**8**
3172	ATP synthase subunit delta. mitochondrial & Protein CutA	ATPD & CUTA	**0.0054**	**-1.53**	**4.8**	**15.404**	**4.5 & 5.2**	**15 & 16**	**131 & 120**	**59 & 78**	**3 & 2**

3175	Heat shock protein beta-6 & Actin-related protein 2/3 complex subunit 5-like protein	HSPB6 & ARP5L	**0.014**	**1.63**	**6.96**	**15.263**	**6 & 6.2**	**17 & 17**	**172 & 151**	**54 & 61**	**4 & 3**
3193	Coactosin-like protein	COTL1	**0.043**	**1.5**	**5.53**	**15.123**	**5.5**	**16**	**364**	**57**	**9**
3300	Hemoglobin subunit alpha	HBA	**0.025**	**3.37**	**8.5**	**13.964**	**8.7**	**15**	**64**	**37**	**2**
3344	Cystatin-B	CYTB	**0.049**	**11.97**	**8.01**	**13.439**	**7**	**11**	**104**	**62**	**2**
3383	Profilin-1	PROF1	**0.014**	**-1.96**	**5.21**	**12.835**	**5.3**	**13**	**126**	**72**	**2**
3387	Myotrophin	MTPN	**0.012**	**-1.58**	**5.94**	**12.053**	**5.9 & 6**	**12 & 66**	**243**	**91**	**4**
3467	10 kDa heat shock protein. mitochondrial	CH10	**0.025**	**1.54**	**9.64**	**13.04**	**8.9**	**11**	**294**	**115**	**6**
3503	Dynein light chain 1. cytoplasmic & Isovaleryl-CoA dehydrogenase. mitochondrial	DYL1 & IVD	**0.023**	**-1.55**	**7.69**	**11.724**	**6.9 & 6.9**	**10 & 43**	**99 & 80**	**99 & 46**	**1 & 2**
3528	Hemoglobin subunit beta	HBB	**0.013**	**-2.1**	**5,0**	**11.458**	**6.8**	**16**	**100**	**56**	**2**
3529	Protein S100-A6 & Hemoglobin subunit alpha	S10A6 & HBA	**0.021**	**-4.16**	**5.3**	**10**	**5.3 & 8.7**	**10 & 15**	**249 & 109**	**49 & 56**	**7 & 2**
3550	Hemoglobin subunit beta	HBB	**0.017**	**1.77**	**4.8**	**11.249**	**6.8**	**16**	**201**	**103**	**7**

Exp: experimental; MM: molecular mass; pI: isoelectrofocalisation point; Theo: theoretical. Relative quantification and statistical evaluation were carried out with DeCyderTM 2D software (GE Healthcare, version 7.0). Down or up-expressed proteins between groups were retained if protein spot fold change was larger than +1.5 or smaller than –1.5 and a Student's t-test p-value less than 0.05

Supplemental table 2 Differentially expressed proteins between VSMC from umbilical artery and pulmonary artery (fold change ≥1.5, p≤0.05)

SPOT	IDENTIFIED PROTEIN	NAME	T-test	Fold change	Exp pI	Exp MM	Theo pI	Theo MM	Total ion Score	Best ion Score	Number of identified peptides
113	Collagen alpha-3(VI)	CO6A3	0.006	5.53	6.74	122	6.2	341	255	79	5
278	Collagen alpha-2(VI) chain	CO6A1	0.015	-2.72	6.35	110	5.2	106	595	86	12
279	Collagen alpha-2(VI) chain	CO6A1	0.018	-2.45	6.45	110	5.2	106	212	67	5
281	Collagen alpha-2(VI) chain	CO6A1	0.013	-2.12	6.54	110	5.2	106	792	86	15
285	Myosin-9 & Collagen alpha-1(VI) chain	MYH9 & CO6A1	0.023	-2.28	5.19	110	5.5 & 5.2	226 & 106	2305 &1498	103 & 103	40 & 25
290	Collagen alpha-1(VI) chain & Spectrin alpha chain,	CO6A1 & SPTA2	0.041	-1.97	5.27	109	5.2 & 5.2	106 & 285	1152 & 497	110 & 67	19 & 13
292	Myosin-9 & Collagen alpha-1(VI) chain & Hypoxia up-regulated protein 1	MYH9 & CO6A1 & HYOU1	0.035	-1.78	5.39	109	5.5 & 5.2 & 5.1	226 & 106 & 108	1523 & 1164 & 879	109 & 95 & 76	27 & 19 & 18
354	Alpha-actinin-1	ACTN1	0.000003	-2.99	5.62	106	5.3	103	1280	106	26
363	Collagen alpha-3(VI)	CO6A3	0.045	-1.53	6.01	105	6.2	341	2331	99	42
404	Myosin-9 & Collagen alpha-1(VI) chain	MYH9 & CO6A1	0.025	2.37	5.11	102	5.5 & 5.2	226 & 106	1418 & 1265	109 &87	40 & 25
534	Kinesin-1 heavy chain	KINH	0.0012	-1.91	6.05	95	6.1	110	1194	106	24
626	Programmed cell death 6-interacting protein & Procollagen-lysine,2-oxoglutarate 5-dioxygenase 2	PDC6I & PLOD2	0.014	2.77	7.1	89	6.1 & 6.2	96 & 82	1712 & 561	89 & 82	35 & 11
632	Programmed cell death 6-interacting protein & Procollagen-lysine,2-oxoglutarate 5-dioxygenase 2 & Filamin-A	PDC6I & PLOD2 & FLNA	0.0096	3.24	6.95	89	6.1 & 6.2 & 5.7	96 & 82 & 281	917 & 567 & 662	100 & 92 &80	18 & 11 & 15
633	Procollagen-lysine,2-oxoglutarate 5-dioxygenase 2	PLOD2	0.0084	2.82	7.29	89	6.2	82	874	72	17
640	Procollagen-lysine,2-oxoglutarate 5-dioxygenase 2	PLOD2	0.0075	3.23	7.19	89	6.2	82	806	86	16
645	Procollagen-lysine,2-oxoglutarate 5-dioxygenase 2 & Filamin-A	PLOD2 & FLNA	0.015	2.96	6.84	89	6.2 & 5.7	82 & 281	783 & 581	86 & 82	15 & 12
672	Elongation factor 2	EF2	0.01	-1.56	8,0	88	6.4	95	1554	88	29
676	2-oxoglutarate dehydrogenase, mitochondrial & Procollagen-lysine,2-oxoglutarate 5-dioxygenase 2	ODO1 & PLOD2	0.048	3.08	6.76	88	6.1 & 6.2	111 & 82	785	64	17
706	Prolyl 3-hydroxylase 3	P3H3	0.029	1.76	6.82	86	5.8	80	244	84	4
826	TATA-binding protein-associated factor 2N	RBP56	0.00086	-1.94	8.8	80	8	62	136	57	3

838	TATA-binding protein-associated factor 2N	RBP56	0.012	-2.37	9.08	79	8	62	248	78	6
841	Collagen alpha-3(VI) chain & Vimentin	CO6A3 & VIME	0.019	-1.66	5.79	78	6.2 & 5.1	341 & 54	1662 & 744	90 & 70	29 & 16
932	Moesin & Prelamin-A/C	MOES & LMNA	0.0054	-1.97	7.11	74	6.1 & 6.6	68 & 74	1130 & 1015	96 & 87	24 & 20
933	Prelamin-A/C & Moesin	LMNA & MOES	0.0023	-2.07	7.26	74	6.6 & 6.1	74 & 68	1594 & 1372	104 & 94	31 & 26
1051	Plastin-3 & Heat shock cognate 71 kDa protein	PLST & HSP7C	0.036	-1.61	5.83	69	5.4 & 5.4	71 & 71	1903 & 893	97 & 87	34 & 16
1145	Cytoskeleton-associated protein 4 & ERO1-like protein alpha	CKAP4 & ERO1A	0.01	2.51	5.91	65	5.6 & 5.4	66 & 52	1143 & 588	117 & 88	20 & 12
1146	Cytoskeleton-associated protein 4	CKAP4	0.0075	1.65	6.23	65	5.6	66	1748	147	26
1164	Prelamin-A/C & Dihydropyrimidinase-related protein 2 & T-complex protein 1 subunit gamma	LMNA & DPYL2 & TCPG	0.026	-1.62	7.02	65	6.6 & 6 & 6.1	74 & 62 & 61	1616 & 1056 & 904	82 & 117 & 81	31 & 17 & 18
1232	Prolyl 4-hydroxylase subunit alpha-1	P4HA1	0.00058	2.25	6.37	62	5.7	59	860	106	15
1237	Prolyl 4-hydroxylase subunit alpha-2 & Staphylococcal nuclease domain-containing protein 1	P4HA2 & SND1	0.015	1.91	5.97	62	5.4 & 6.8	59 & 102	838 & 807	95 & 85	15 & 14
1254	EH domain-containing protein 3	EHD3	0.022	-2.08	7.25	61	6.1	61	709	79	14
1300	UDP-glucose 6-dehydrogenase	UGDH	0.034	-2.31	8.25	59	6.7	55	1061	90	21
1314	Protein disulfide-isomerase A3 & Lamin-B2 & Vimentin	PDIA3 & LMNB2 & VIME	0.019	1.64	5.96	58	5.6 & 5.3 & 5.1	54 & 67 & 54	964 & 560 & 892	110 & 84 & 80	16 & 14 & 19
1372	Glucose-6-phosphate 1-dehydrogenase & D-3-phosphoglycerate dehydrogenase	G6PD & SERA	0.00044	-1.77	7.56	57	6.4 & 6.3	59 & 57	1068 & 494	104 & 93	21 & 10
1386	Vimentin & Tubulin beta chain	VIME & TBB5	0.0044	-1.83	5.07	56	5.1 & 4.8	54 & 50	1761 & 1123	114 & 110	33 & 17
1420	V-type proton ATPase subunit B, brain isoform	VATB2	0.000021	55.56	5.99	55	5.6	57	1498	113	23
1422	Selenium-binding protein 1 & Mitochondrial-processing peptidase subunit alpha & Pyruvate dehydrogenase protein X component, mitochondrial	SBP1 & MPPA & ODPX	0.049	1.53	6.66	55	5.9 & 5.9 & 6	52 & 55 & 48	561 & 552 & 446	78 & 80 & 85	11 & 10 & 8
1431	Reticulocalbin-2 & Vimentin	RCN2 & VIME	0.0039	1.61	4.52	55	4.2 & 5.1	35 & 54	614 & 477	106 & 66	10 & 10
1435	Histidine--tRNA ligase, cytoplasmic	SYHC	0.023	3.16	6.16	55	5.7	57	998	96	18
1474	Collagen alpha-3(VI) & Vimentin & NAD-dependent malic enzyme, mitochondrial	CO6A3 & VIME & MAOM	0.028	3.7	5.72	53	6.2 & 5.1 & 6.6	341 & 54 & 63	625 & 475 & 404	87 & 57 & 92	11 & 8 & 8
1543	Rab GDP dissociation inhibitor beta & Alpha-elonase	GDIB & ENOA	0.0092	-1.51	6.95	51	6.1 & 7	51 & 47	1119 & 498	98 & 118	21 & 8
1548	Alpha-enolase	ENOA	0.03	-1.51	7.67	50	7	47	984	109	16

1555	Alpha-enolase	ENOA	0.032	-1.71	8.09	50	7	47	1450	124	23
1597	78 kDa glucose-regulated protein & Vimentin & Thioredoxin domain-containing protein 5	GRP78 & VIME & TXND5	0.039	1.71	5.17	49	5 & 5.1 & 5.4	70 & 54 & 44	688 & 997 & 519	96 & 77 & 99	10 & 20 & 10
1624	Eukaryotic initiation factor 4A-I & Vimentin	IF4A1 & VIME	0.019	2.85	5.6	48	5.3 & 5.1	46 & 54	1022 & 668	103 & 81	19 & 14
1641	No identified protein		0.00011	2.83							
1645	Vimentin & Interleukin enhancer-binding factor 2 & Myoferlin	VIME & ILF2 & MYOF	0.000052	6.63	5.67	47	5.1 & 5.2 & 5	54 & 43 & 83	465 & 780 & 746	66 & 79 & 92	11 & 15 & 13
1657	Calcium-binding mitochondrial carrier protein SCaMC-1 & Ornithine aminotransferase, mitochondrial & Synaptic vesicle membrane protein VAT-1 homolog	SCMC1 & OAT & VAT1	0.05	1.66	6.7	47	6 & 6 & 5.9	53 & 46 & 42	629 & 422 & 253	72 & 81 & 94	14 & 7 & 4
1756	Interleukin enhancer-binding factor 2 & Protein disulfide-isomerase	ILF2 & PDIA1	0.000046	19.14	5.18	44	5.2 & 4.7	43 & 55	283 & 477	89 & 80	5 & 10
1830	Vimentin	VIME	0.004	-2.12	4.82	42	5.1	54	1662	128	32
1855	Protein disulfide-isomerase & Collagen alpha-3(VI) & Endoplasmin	PDIA1 & CO6A3 & ENPL	0.017	1.91	5.28	41	4.7 & 6.2 & 4.7	55 & 341 & 90	529 & 343 & 352	65 & 76 & 67	11 & 7 & 7
1924	Vimentin & Tropomyosin alpha-4 chain	VIME & TPM4	0.012	-2.55	4.81	40	5.1 & 4.7	54 & 28	703 & 519	89 & 60	15 & 12
1964	Pyruvate kinase isozymes M1/M2 & Annexin A1	KPYM & ANXA1	0.031	-1.57	7.35	38	8 & 6.6	58 & 39	944 & 579	92 & 117	15 & 8
2051	Tubulin beta chain	TBB5	0.021	-1.82	5.71	36	4.8	50	732	116	12
2060	L-lactate dehydrogenase B chain & Pyruvate kinase isozymes M1/M2	LDHB & KPYM	0.05	-1.73	6.22	36	5.7 & 8	37 & 58	800 & 699	83 & 76	15 & 14
2153	S-formylglutathione hydrolase	ESTD	0.00036	-1.83	7.74	34	6.5	31	494	87	9
2198	Annexin A5	ANXA5	0.0033	-1.63	5.06	33	4.9	36	1136	128	17
2324	Cathepsin D	CATD	0.027	-1.78	5.52	30	5.6	38	501	70	9
2343	Cathepsin D	CATD	0.047	-2.82	6.11	29	5.6	38	602	117	9
2349	14-3-3 protein theta & 14-3-3 protein zeta/delta	1433T & 1433Z	0.0076	-1.96	4.83	29	4.7 & 4.7	28 & 28	666 & 641	91 & 90	12 & 13
2375	14-3-3 protein gamma	1433G	0.017	-1.58	4.87	29	4.8	28	728	85	14
2381	Beta-hexosaminidase subunit beta & Nicotinamide N-methyltransferase & Chloride intracellular channel protein 4	HEXB & NNMT & CLIC4	0.015	-1.56	5.78	29	5.9 & 5.6 & 5.5	50 & 30 & 29	576 & 284 & 156	72 & 60 & 93	11 & 6 & 3
2386	78 kDa glucose-regulated protein & Heterogeneous nuclear ribonucleoprotein Q	GRP78 & HNRPQ	0.003	-1.93	5.13	29	5 & 8.7	70 & 69	639 & 296	111 & 78	11 & 6
2390	14-3-3 protein theta	1433T	0.0039	-1.84	4.79	28	4.7	28	868	98	15

2392	Proteasome activator complex subunit 1	PSME1	0.0027	-1.96	6.22	28	5.8	29	563	76	10
2424	14-3-3 protein zeta/delta	1433Z	0.013	-1.74	4.82	28	4.7	28	954	94	17
2431	14-3-3 protein beta/alpha	1433B	0.0079	-1.78	4.87	28	4.8	28	878	107	16
2467	Annexin A1	ANXA1	0.034	-1.74	5.19	27	6.6	39	615	112	9
2476	Adenylate kinase 2, mitochondrial	KAD2	0.034	-1.72	9.22	27	7.7	26	683	87	13
2548	Triosephosphate isomerase	TPIS	0.027	-1.52	7.94	26	5.7	31	901	100	14
2570	Ubiquitin carboxyl-terminal hydrolase isozyme L1 & Peroxiredoxin-4 & T-complex protein 1 subunit	UCHL1 & PRDX4 & TCPB	0.0015	2.11	5.72	25	5.2 & 5.5 & 6	25 & 27 & 57	270 & 203 & 370	86 & 78 & 81	5 & 4 & 7
2573	Ubiquitin carboxyl-terminal hydrolase isozyme L1 & Vacuolar protein sorting-associated protein 28 homolog	UCHL1 & VPS28	0.0077	2.65	5.49	25	5.2 & 5.4	25 & 25	360 & 150	75 & 68	7 & 3
2663	Flavin reductase (NADPH)	BLVRB	0.012	-1.66	8.58	24	7.3	22	287	102	5
2831	Myosin regulatory light polypeptide 9	MYL9	0.0011	-2.22	4.92	21	4.8	20	253	84	5
2858	Myosin regulatory light chain 12A	ML12A	0.00011	-1.77	4.82	20	4.7	20	386	86	6
2912	Myosin regulatory light chain 12A & Protein canopy homolog 2	ML12A & CNPY2	0.000083	-1.58	4.85	19	4.7 & 4.7	20 & 19	379 & 225	79 & 71	7 & 5
2978	Cofilin-1 & Transgelin	COF1 & TAGL	0.0079	2.36	7.12	18	8.3 & 8.9	18 & 22	353 & 157	120 & 68	5 & 3
3029	Eukaryotic translation initiation factor 5A-1	IF5A1	0.03	-1.66	5.25	17	5.1	17	416	85	8
3104	Peptidyl-prolyl cis-trans isomerase A	PPIA	0.031	-1.99	8.81	16	7.7	18	483	69	11
3115	Peptidyl-prolyl cis-trans isomerase A	PPIA	0.05	-1.63	9.1	16	7.7	18	315	69	6
3152	Myosin light polypeptide 6	MYL6	0.00052	-1.64	4.69	16	4.6	17	683	85	12
3172	ATP synthase subunit delta, mitochondrial & Protein CutA	ATPD & CUTA	0.0043	-1.57	4.8	15	4.5 & 5.2	15 & 16	131 & 120	59 & 78	3 & 2
3175	Heat shock protein beta-6 & Actin-related protein 2/3 complex subunit 5-like protein	HSPB6 & ARP5L	0.0014	1.82	6.96	15	6 & 6.2	17 & 17	172 & 151	54 & 61	4 & 3
3187	UPF0556 protein C19orf10	CS010	0.018	1.7	7.46	15	6.2	16	305	69	6
3193	Coactosin-like protein	COTL1	0.00027	2.1	5.53	15	5.5	16	364	57	9
3250	NADH dehydrogenase [ubiquinone] 1 alpha subcomplex subunit 5 & 60S ribosomal protein L22	NDUA5 & RL22	0.021	-2.38	6.02	14	5.8 & 9.2	13 & 15	122 & 176	46 & 68	3 & 3
3462	Protein S100-A4 & Dolichyl-diphosphooligosaccharide--protein glycosyltransferase subunit 1	S10A4 & RPN1	0.0015	-3.68	5.94	12	5.9 & 6	12 & 66	110 & 226	43 & 62	3 & 4
3528	Hemoglobin subunit beta	HBB	0.0074	-1.85	5,0	11	6.8	16	100	56	2
3529	Protein S100-A6 & Hemoglobin subunit alpha	S10A6 &	0.031	-3.42	5.3	10	5.3 & 8.7	10 & 15	249 & 109	49 & 56	7 & 2

		HBA									

Exp: experimental; MM: molecular mass; pI: isoelectrofocalisation point; Theo: theoretical. Relative quantification and statistical evaluation were carried out with DeCyderTM 2D software (GE Healthcare, version 7.0). Down or up-expressed proteins between groups were retained if protein spot fold change was larger than +1.5 or smaller than –1.5 and a Student's t-test p-value less than 0.05

Supplemental table 3 Differentially expressed proteins between vascular smooth muscle cells from pulmonary artery and aorta artery (fold change ≥1.5, p≤0.05)

SPOT	IDENTIFIED PROTEIN	NAME	T-test	Fold change	Exp pI	Exp MM	Theo pI	Theo MM	Total ion Score	Best ion Score	Number of identified peptides
113	Collagen alpha-3(VI)	CO6A3	**0.0072**	**-4.9**	**6.74**	**122**	**6.3**	**34**	**255**	**79**	**5**
404	Myosin-9 & Collagen alpha-1(VI) chain	MYH9 & CO6A1	**0.032**	**-2.15**	**5.11**	**102**	**5.5 & 5.3**	**227 & 109**	**1418 & 1265**	**109 & 87**	**27 & 21**
728	Myosin-9 & Src substrate cortactin	MYH9 & SRC8	**0.022**	**-1.77**	**5.54**	**84**	**5.2 & 5.2**	**43 & 62**	**1420**	**113**	**27**
1060	Phosphoenolpyruvate carboxykinase [GTP], mitochondrial	PCKGM	**0.05**	**1.5**	**8.13**	**69**	**7.6**	**71**	**877**	**84**	**18**
872	Caldesmon	CALD1	**0.043**	**-2.12**	**7.15**	**78**	**5.6**	**93**	**1122**	**98**	**22**
1468	ATP synthase subunit alpha, mitochondrial & Hypoxia up-regulated protein 1 & Serine hydroxymethyltransferase, mitochondrial	ATPA & HYOU1 & GLYM	**0.022**	**1.51**	**9.43**	**53**	**9.2 & 5.2 & 8.8**	**60 & 111 & 56**	**538 &513 & 402**	**74 & 115 &64**	**10 & 9 & 10**
1756	Interleukin enhancer-binding factor 2 & Protein disulfide-isomerase	ILF2 & PDIA1	**0.038**	**-2.34**	**5.18**	**44**	**5.2 & 4.8**	**43 & 57**	**283& 498**	**89 & 80**	**5 & 10**
1682	Elongation factor 2 & T-complex protein 1 subunit eta	EF2 & TCPH	**0.034**	**-1.52**	**8.06**	**46**	**6.4 & 7.6**	**95 & 59**	**401 & 373**	**82 &71**	**8 & 7**
1759	Dihydrolipoyl dehydrogenase, mitochondrial & Poly(rC)-binding protein 2	DLDH & PCBP2	**0.006**	**-1.57**	**7.32**	**44**	**8.0 & 6.3**	**54 & 39**	**140 & 129**	**56 & 58**	**3 & 3**
2378	Galectin-3 & Voltage-dependent anion-selective channel protein 3 & Surfeit locus protein 1	LEG3 & VDAC3 & SURF1	**0.006**	**-1.6**	**9.74**	**29**	**8.6 & 8.8 & 9.6**	**26 & 31 & 33**	**501 & 245 & 157**	**88 & 61 & 65**	**9 & 5 & 3**
3501	Protein S100-A10	S10AA	**0.017**	**-1.53**	**8.62**	**12**	**6.8**	**112**	**75**	**44**	**2**
2682	Calcium-binding protein p22 & Proteasome subunit beta type-6	CHP1 & PSB6	**0.011**	**1.68**	**5.05**	**23**	**5.0 & 4.8**	**225 & 25**	**526 & 175**	**103 & 66**	**9 & 3**
2150	Ubiquitin thioesterase OTUB1 & HCLS1-associated protein X-1 & Tropomyosin alpha-1 chain	OTUB1 & HAX1 & TPM1	**0.0079**	**1.91**	**4.91**	**34**	**4.9 & 4.8 & 4.7**	**31 & 32 & 33**	**409 &400 & 304**	**82 & 98 &74**	**7 & 6 & 7**

Exp: experimental; MM: molecular mass; pI: isoelectrofocalisation point; Theo: theoretical. Relative quantification and statistical evaluation were carried out with DeCyderTM 2D software (GE Healthcare, version 7.0). Down or up-expressed proteins between groups were retained if protein spot fold change was larger than +1.5 or smaller than –1.5 and a Student's t-test p-value less than 0.05

Supplemental table 4 Differentially expressed proteins between pulmonary artery vascular smooth muscle cells from patients with PAH and healthy controls (fold change ≥1.5, p≤0.05)

SPOT	IDENTIFIED PROTEIN	NAME	T-test	Fold change	Exp pI	Exp MM	Theo pI	Theo MM	Total ion Score	Best ion Score	Number of identified peptides
152	Collagen alpha-1(I) chain	CO1A1	0.0037	5.4	6.06	119	5,6	139	433	72	8
220	Uveal autoantigen with coiled-coil domains and ankyrin repeats	UACA	0.0011	-10.11	7.99	114	6.6	163	57	32	2
222	Vigilin	VIGLN	0.00013	-8.81	7.62	114	6.4	141	476	65	11
223	Vigilin	VIGLN	0.00016	-9.42	7.69	113	6.4	141	1123	95	23
354	Alpha-actinin-1	ACTN1	0.013	-1.88	5.62	106	5.3	103	1280	106	26
404	Myosin-9 & Collagen alpha-1(VI) chain	MYH9 & CO6A1	0.0023	8.48	5.11	102	5.5 & 5.3	227 & 109	1418 & 1265	109 &87	40 & 25
408	Collagen alpha-1(VI) chain & Dipeptidyl peptidase 4	CO6A1 & DPP4	0.0047	5.21	5.15	102	5.2 & 5.7	106 & 88	868 & 438	86 & 67	15 & 11
458	Kinesin-1 heavy chain	KINH	0.02	-2.71	7.06	99	6.1	110	1444	100	28
461	Kinesin-1 heavy chain	KINH	0.0042	-3.71	6.97	99	6.1	110	395	89	8
500	Collagen alpha-3(VI) chain & vinculin	CO6A3 & VINC	0.0069	2.75	6.09	96	6.2 & 5.5	341 & 118	1758 & 1336	91 & 87	32 & 29
501	Vinculin	VINC	0.014	2.2	6.19	96	5.5	124	2033	105	41
545	Staphylococcal nuclease domain-containing protein 1 & Elongation factor 2	SND1 & EF2	0.049	-2.7	8,0	94	6.8 & 6.2	102 & 82	1115 & 520	79 & 96	22 & 11
552	Staphylococcal nuclease domain-containing protein 1	SND1	0.018	-3.59	8.12	94	6.8	102	1531	98	28
568	Ribosome-binding protein 1	RRBP1	0.0014	1.88	5.44	93	8.7	152	1947	107	34
573	Neutral alpha-glucosidase AB	GANAB	0.0087	-1.94	6.36	93	5.6	104	1260	95	28
620	Endoplasmin	ENPL	0.035	-4.24	4.97	91	4.7	90	2230	105	44
626	Programmed cell death 6-interacting protein & Procollagen-lysine,2-oxoglutarate 5-dioxygenase 2	PDC6I & PLOD2	0.027	-1.97	7.1	89	6.1 & 6.2	96 & 82	1712 & 561	89 & 82	35 & 11
632	Programmed cell death 6-interacting protein & Procollagen-lysine,2-oxoglutarate 5-dioxygenase	PDC6I & PLOD2 &	0.019	-2.11	6.95	89	6.1 & 6.2 & 5.7	96 & 82 & 281	917 & 567 & 662	100 & 92 &80	18 & 11 & 15

	2 & Filamin-A	FLNA									
633	Procollagen-lysine,2-oxoglutarate 5-dioxygenase 2	PLOD2	**0.04**	**-2.14**	**7.29**	**89**	**6.2**	**82**	**874**	**72**	**17**
640	Procollagen-lysine,2-oxoglutarate 5-dioxygenase 2	PLOD2	**0.046**	**-2.28**	**7.19**	**89**	**6.2**	**82**	**806**	**86**	**16**
644	Mitochondrial 10-formyltetrahydrofolate dehydrogenase	AL1L2	**0.0025**	**-2.28**	**6.34**	**89**	**6.1**	**102**	**1303**	**100**	**24**
645	Procollagen-lysine,2-oxoglutarate 5-dioxygenase 2 & Filamin-A	PLOD2 & FLNA	**0.047**	**-1.97**	**6.84**	**89**	**6.2 & 5.7**	**82 & 281**	**783 & 581**	**86 & 82**	**15 & 12**
648	Mitochondrial 10-formyltetrahydrofolate dehydrogenase	AL1L2	**0.01**	**-2.81**	**6.44**	**89**	**6.1**	**102**	**1326**	**89**	**25**
677	Hypoxia up-regulated protein 1	HYOU1	**0.0025**	**-2.16**	**4.9**	**88**	**4.6**	**61**	**904**	**96**	**15**
686	Ribosome-binding protein 1 & Heat shock protein HSP 90-beta & Prolyl 3-hydroxylase 1	RRBP1 & HS90B & P3H1	**0.0013**	**-2.16**	**5.16**	**87**	**8.8 & 5 & 5**	**354 & 83 & 81**	**1690 & 942 & 723**	**111 & 76 & 78**	**27 & 19 & 15**
706	Prolyl 3-hydroxylase 3	P3H3	**0.01**	**-2.77**	**6.82**	**86**	**5.8**	**80**	**244**	**84**	**4**
725	Protein NOXP20	NXP20	**0.0065**	**-1.54**	**4.79**	**84**	**4.6**	**61**	**698**	**85**	**12**
747	Putative pre-mRNA-splicing factor ATP-dependent RNA helicase DHX15	DHX15	**0.01**	**-4.88**	**8.47**	**84**	**7.1**	**91**	**663**	**69**	**14**
783	ATP-dependent RNA helicase DDX1 & Aconitate hydratase & DnaJ homolog subfamily C member 10	DDX1 & ACON & DJC10	**0.041**	**-2.66**	**8.15**	**81**	**6.8 & 6.9 & 6.7**	**82 & 82 & 87**	**860 & 724 &513**	**88 & 85 & 54**	**17 & 13 & 12**
787	Far upstream element-binding protein 2	FUBP2	**0.0075**	**-2.87**	**7.86**	**81**	**6.8**	**73**	**588**	**75**	**11**
788	ATP-dependent RNA helicase DDX1 & Far upstream element-binding protein 2 & Aconitate hydratase	DDX1 & FUBP2 & ACON	**0.012**	**-4.31**	**8.09**	**81**	**6.8 & 6.8 & 6.9**	**82 & 73 & 82**	**643 & 657 & 514**	**63 & 90 & 79**	**14 & 13 & 10**
793	Elongation factor G, mitochondrial	EFGM	**0.004**	**-1.54**	**6.93**	**80**	**5.9**	**80**	**676**	**90**	**13**
802	Procollagen-lysine,2-oxoglutarate 5-dioxygenase 3 & X-ray repair cross-complementing protein 5	PLOD3 & XRCC5	**0.044**	**-1.92**	**6.22**	**81**	**5.6 & 5.6**	**82 & 83**	**591 & 292**	**98 & 78**	**10 & 6**
805	Protein-glutamine gamma-glutamyltransferase 2	TGM2	**0.011**	**-5.67**	**5.34**	**80**	**5.1**	**77**	**1229**	**95**	**23**
809	Protein Hook homolog 3 & Protein-glutamine gamma-glutamyltransferase 2	HOOK3 & TGM2	**0.026**	**-3.54**	**5.25**	**80**	**5.1 & 5.1**	**83 & 77**	**879 & 813**	**90 & 86**	**16 & 17**
810	Protein-glutamine gamma-glutamyltransferase 2 & Protein disulfide-isomerase A4	TGM2 & PDIA4	**0.029**	**-4.47**	**5.3**	**80**	**5.1 & 4.9**	**77 & 71**	**1074 & 883**	**82 & 93**	**20 & 16**
819	Procollagen-lysine,2-oxoglutarate 5-dioxygenase 3 & Mitotic spindle assembly checkpoint protein MAD1	PLOD3 & MD1L1	**0.015**	**-1.72**	**6.32**	**80**	**5.6 & 5.7**	**82 & 83**	**950 & 432**	**113 & 71**	**16 & 10**

823	Delta-1-pyrroline-5-carboxylate synthase & Procollagen-lysine,2-oxoglutarate 5-dioxygenase 1	P5CS & PLOD1	**0.01**	**-2.92**	**7.49**	**80**	**6.7 & 6.5**	**87 & 82**	**993 & 398**	**90 & 59**	**19 & 10**
825	Threonine--tRNA ligase & Delta-1-pyrroline-5-carboxylate synthase & Zyxin & Caldesmon	SYTC & P5CS & ZYX & CALD1	**0.0086**	**-1.95**	**7.28**	**80**	**6.2 & 6.7 & 6.2**	**83 & 87 & 61**	**698 & 484 & 355 & 271**	**64 & 73 & 135 & 77**	**15 & 10 & 6 &5**
826	TATA-binding protein-associated factor 2N	RBP56	**0.034**	**-2.31**	**8.8**	**80**	**8**	**62**	**19**	**57**	**3**
851	Procollagen-lysine,2-oxoglutarate 5-dioxygenase 1 & Glucosamine--fructose-6-phosphate aminotransferase	PLOD1 & GFPT1	**0.0056**	**-2.74**	**7.64**	**78**	**6.5 & 6.7**	**82 & 79**	**908 & 344**	**85 & 91**	**18 & 6**
858	Ribosome-binding protein 1 & Heat shock 70 kDa protein 4 & 78 kDa glucose-regulated protein	RRBP1 & HSP74 & GRP78	**0.0069**	**3.86**	**5,0**	**78**	**8.7 & 5.1 & 5**	**152 & 94 & 70**	**621 & 546 & 273**	**83 & 79 & 77**	**13 & 12 & 5**
871	Caldesmon & Methylmalonyl-CoA mutase, mitochondrial	CALD1 & MUTA	**0.0041**	**-4.35**	**6.93**	**77**	**5.6 & 6**	**93 & 79**	**1223 & 753**	**135 & 96**	**23 & 12**
872	Caldesmon	CALD1	**0.0028**	**-2.58**	**7.15**	**78**	**5.6**	**93**	**1122**	**98**	**22**
879	Cytoplasmic dynein 1 intermediate chain 2 & Peptidyl-prolyl cis-trans isomerase FKBP10	DC1I2 & FKB10	**0.0077**	**-1.77**	**5.44**	**77**	**5.1 & 5.3**	**71 & 61**	**689 & 237**	**124 & 63**	**11 & 6**
903	Peptidyl-prolyl cis-trans isomerase & Protein disulfide-isomerase A4 & 78 kDa glucose-regulated protein	FKB10 & PDIA4 & GRP78	**0.013**	**-2.06**	**5.38**	**75**	**5.3 & 4.9 & 5**	**61 & 71 & 70**	**1022 & 656 & 984**	**96 & 79 & 94**	**19 & 13 & 18**
933	Prelamin-A/C & Moesin	LMNA & MOES	**0.023**	**-3.26**	**7.26**	**74**	**6.6 & 6.1**	**74 & 68**	**1594 & 1372**	**104 & 94**	**31 & 26**
939	Prelamin-A/C	LMNA	**0.0022**	**-3.15**	**7.99**	**74**	**6.6**	**74**	**1732**	**117**	**30**
944	Prelamin-A/C	LMNA	**0.007**	**-4.02**	**7.69**	**74**	**6.6**	**74**	**1831**	**110**	**32**
946	78 kDa glucose-regulated protein & Protein disulfide-isomerase A4	GRP78 & PDIA4	**0.003**	**-2.25**	**5.19**	**74**	**5 & 4.9**	**70 & 71**	**2261 & 699**	**112 & 100**	**35 & 13**
956	Peptidyl-prolyl cis-trans isomerase & Stress-70 protein, mitochondrial	FKB10 & GRP75	**0.00017**	**-2.01**	**5.46**	**73**	**5.3 & 5.4**	**61 & 69**	**1134 & 726**	**93 & 81**	**19 &13**
957	78 kDa glucose-regulated protein & Peptidyl-prolyl cis-trans isomerase	GRP78 & FKB10	**0.047**	**-1.74**	**5.38**	**73**	**5 & 5.3**	**70 & 61**	**905 & 1145**	**109 & 96**	**17 & 21**
981	Trifunctional enzyme subunit alpha	ECHA	**0.012**	**-6.53**	**10.04**	**72**	**9**	**79**	**1665**	**99**	**29**
987	TRIO and F-actin-binding protein	TARA	**0.029**	**-1.64**	**6.54**	**71**	**8.9**	**261**	**1042**	**86**	**20**
1010	Trifunctional enzyme subunit alpha & Heterogeneous nuclear ribonucleoprotein M	ECHA & HNRPM	**0.0031**	**-4.17**	**9.85**	**71**	**9 & 9.2**	**79 & 30**	**1251 & 1158**	**85 & 100**	**22 & 18**

1019	Annexin A6 & Dihydrolipoyllysine-residue acetyltransferase component of pyruvate dehydrogenase complex, mitochondrial	ANXA6 & ODP2	**0.0055**	**1.61**	**5.87**	**70**	**5.4 & 5.5**	**76 & 60**	**1658 & 1073**	**101 & 85**	**28 & 20**
1020	Glycerol-3-phosphate dehydrogenase & Mitochondrial import receptor subunit TOM70 & Prelamin-A/C	GPDM & TOM70 & LMNA	**0.0062**	**-3.21**	**7.52**	**71**	**6.3 & 6.8 & 6.6**	**76 & 67 & 74**	**464 & 433 & 432**	**73 & 63 & 83**	**10 & 10 & 8**
1021	Heterogeneous nuclear ribonucleoprotein M & Trifunctional enzymz subunit alpha	HNRPM & ECHA	**0.003**	**-7.67**	**9.95**	**71**	**9.2 & 9**	**30 & 79**	**1074 & 532**	**99 & 89**	**20 & 10**
1027	Heat shock protein 75 kDa, mitochondrial & Prelamin-A/C & X-ray repair cross-complementing protein 6	TRAP1 & LMNA & XRCC6	**0.0087**	**-4.2**	**7.34**	**71**	**8.5 & 6.6 & 6.2**	**49 & 74 & 70**	**772 & 708 & 1101**	**94 & 79 & 89**	**16 & 14 & 21**
1049	Heterogeneous nuclear ribonucleoprotein M & Calcium-binding mitochondrial carrier protein Aralar2	HNRPM & CMC2	**0.0089**	**-2.47**	**9.78**	**69**	**9.2 & 8.8**	**30 & 74**	**1048 & 863**	**108 & 90**	**18 & 15**
1054	Calcium-binding mitochondrial carrier protein Aralar2 & Heterogeneous nuclear ribonucleoprotein M	CMC2 & HNRPM	**0.0005**	**-6.67**	**9.94**	**69**	**8.8 & 9.2**	**74 & 30**	**369 & 1126**	**77 & 113**	**8 & 20**
1060	Phosphoenolpyruvate carboxykinase [GTP], mitochondrial	PCKGM	**0.012**	**-2.38**	**8.13**	**69**	**6.6**	**67**	**877**	**84**	**18**
1075	Plastin 3 & Heat shock cognate 71 kDa	PLST & HSP7C	**0.004**	**2.71**	**5.93**	**68**	**5.4 & 5.4**	**71 & 70**	**1113 & 1098**	**87 & 100**	**22 & 21**
1097	Heterogeneous nuclear ribonucleoprotein Q	HNRPQ	**0.015**	**-3.3**	**8.25**	**68**	**8.7**	**69**	**612**	**74**	**13**
1101	Heterogeneous nuclear ribonucleoprotein Q	HNRPQ	**0.00042**	**-6.54**	**8.49**	**68**	**8.7**	**69**	**561**	**74**	**12**
1141	Heterogeneous nuclear ribonucleoprotein L	HNRPL	**0.006**	**-3.67**	**8.12**	**65**	**8.5**	**64**	**707**	**106**	**14**
1146	Cytoskeleton-associated protein 4	CKAP4	**0.00071**	**-2.4**	**6.23**	**65**	**5.6**	**66**	**1748**	**147**	**26**
1147	Heterogeneous nuclear ribonucleoprotein L & ATP-dependent Clp protease ATP-binding subunit clpX-like & NAD-dependent malic enzyme	HNRPL & CLPX & MAOM	**0.0091**	**-2.84**	**7.86**	**65**	**8.5 & 6.3 & 6.6**	**64 & 63 & 63**	**558 & 472 & 332**	**102 & 68 & 91**	**10 & 10 & 8**
1156	78 kDa glucose-regulated protein & Heterogeneous nuclear ribonucleoprotein K & Heat shock cognate 71 kDa protein	GRP78 & HNRPK & HSP7C	**0.01**	**-2.09**	**5.63**	**65**	**5 & 5.4 & 5.4**	**70 & 51 & 71**	**901 & 683 & 446**	**93 & 90 & 74**	**15 & 12 &7**
1159	78 kDa glucose-regulated & Heterogeneous nuclear ribonucleoprotein K & Cytoskeleton-associated protein 4	GRP78 & HNRPK & CKAP4	**0.0032**	**-2.41**	**5.43**	**64**	**5 & 5.4 & 5.6**	**70 & 51 & 66**	**926 & 688 & 504**	**106 & 107 & 76**	**15 & 12 & 10**
1164	Prelamin-A/C & Dihydropyrimidinase-related protein 2 & T-complex protein 1 subunit gamma	LMNA & DPYL2 & TCPG	**0.033**	**-2.35**	**7.02**	**65**	**6.6 & 6 & 6.1**	**74 & 62 & 61**	**1616 & 1056 & 904**	**82 & 117 & 81**	**31 & 17 & 18**

1165	Very long-chain specific acyl-CoA dehydrogenase, mitochondrial & Transketolase	ACADV & TKT	**0.01**	**-1.87**	**8.57**	**65**	**7.7 & 7.6**	**66 & 68**	**868 & 462**	**74 & 70**	**18 & 11**
1233	Dihydropyrimidinase-related protein 3 & Carnitine O-palmitoyltransferase 1, liver isoform &	DPYL3 & CPT1A	**0.027**	**-2.75**	**7.19**	**62**	**6 & 8.9**	**62 & 88**	**878 & 387**	**98 & 81**	**14 & 7**
1254	EH domain-containing protein 3	EHD3	**0.022**	**-1.92**	**7.25**	**61**	**6.1**	**61**	**709**	**79**	**14**
1298	Non-POU domain-containing octamer-binding protein & Elongation factor 1-alpha 1 & Polypyrimidine tract-binding protein 1	NONO & EF1A1 & PTBP1	**0.00077**	**-6.15**	**10.08**	**59**	**9 & 9.1 & 9.2**	**54 & 50 & 57**	**545 & 171 & 289**	**72 & 48 & 121**	**11 & 5 & 5**
1302	Non-POU domain-containing octamer-binding protein	NONO	**0.00051**	**-4.88**	**9.95**	**59**	**9**	**54**	**204**	**71**	**4**
1309	tRNA-splicing ligase RtcB homolog & UDP-glucose 6-dehydrogenase & Aldehyde dehydrogenase family 1 member A3 & Pyruvate kinase isozymes M1/M2	RTCB & UGDH & AL1A3 & KPYM	**0.044**	**-2.02**	**8.13**	**58**	**6.8 & 6.7 & 7.1**	**55 & 55 & 56**	**820 & 459 & 362 & 325**	**92 & 67 & 55 & 64**	**15 & 11 & 9 & 7**
1314	Protein disulfide-isomerase A3 & Lamin-B2 & Vimentin	PDIA3 & LMNB2 & VIME	**0.013**	**-1.59**	**5.96**	**58**	**5.6 & 5.3 & 5.1**	**54 & 67 & 54**	**964 & 560 & 892**	**110 & 84 & 80**	**16 & 14 & 19**
1321	Protein disulfide-isomerase A3	PDIA3	**0.0042**	**-1.83**	**6.1**	**58**	**5.6**	**54**	**1143**	**109**	**21**
1361	Prelamin-A/C	LMNA	**0.0037**	**2.13**	**8.87**	**57**	**6.6**	**74**	**1710**	**116**	**32**
1421	Dihydrolipoyllysine-residue succinyltransferase component of 2-oxoglutarate dehydrogenase complex & Heterogeneous nuclear ribonucleoprotein H & Rho GTPase-activating protein 1	ODO2 & HNRH1 & RHG01	**0.0083**	**-2.88**	**6.39**	**55**	**5.9 & 5.9 & 5.9**	**41 & 49 & 50**	**501 & 413 & 220**	**93 & 84 & 53**	**9 & 8 & 5**
1422	Selenium-binding protein 1 & Mitochondrial-processing peptidase subunit alpha & Pyruvate dehydrogenase protein X component, mitochondrial	SBP1 & MPPA & ODPX	**0.0036**	**-1.89**	**6.66**	**55**	**5.9 & 5.9 & 6**	**52 & 55 & 48**	**561 & 552 & 446**	**78 & 80 & 85**	**11 & 10 & 8**
1423	Pyruvate kinase isozymes M1/M2 & Aldehyde dehydrogenase X, mitochondrial	KPYM & AL1B1	**0.035**	**-1.67**	**7.09**	**55**	**8.0 & 6.0**	**58 & 55**	**797 & 656**	**88 & 86**	**15 & 12**
1427	Mitochondrial-processing peptidase subunit alpha & Aldehyde dehydrogenase X & Aspartate--tRNA ligase & T-complex protein 1 subunit beta	MPPA & AL1B1 & SYDC & TCPB	**0.0073**	**-2.3**	**6.85**	**55**	**5.9 & 6 & 6.1**	**55 & 55 & 57**	**261 & 260 & 259 & 212**	**68 & 78 & 67 & 70**	**6 & 5 & 5 & 4**
1447	ATP synthase subunit alpha, mitochondrial & Annexin A2	ATPA & ANXA2	**0.045**	**-2.3**	**8.8**	**54**	**8.3 & 7.6**	**55 & 38**	**974 & 500**	**108 & 83**	**16 & 9**
1450	Lipoamide acyltransferase component of branched-chain alpha-keto acid dehydrogenase complex	ODB2	**0.0055**	**-1.57**	**7.24**	**54**	**6.2**	**46**	**561**	**88**	**13**

1468	ATP synthase subunit alpha, mitochondrial & Hypoxia up-regulated protein 1 & Serine hydroxymethyltransferase, mitochondrial	ATPA & HYOU1 & GLYM	**0.0017**	**-4.08**	**9.43**	**53**	**8.3 & 5.1 & 8.1**	**55 & 108 & 53**	**1090 & 513 & 614**	**112 & 115 & 82**	**16 & 9 & 12**
1510	ATP synthase subunit beta & Protein disulfide-isomerase A6 & Vimentin & Dynactin subunit	ATPB & PDIA6 & VIME &DCTN2	**0.0044**	**-1.87**	**5.22**	**52**	**5 & 5 & 5.1**	**52 & 46 & 54**	**1233 & 1121 & 990 & 709**	**102 & 105 & 89 & 103**	**19 & 17 & 20 & 103**
1524	Vimentin & Actin, cytoplasmic 1	VIME & ACTB	**0.013**	**-1.96**	**5.38**	**52**	**5.1 & 5.3**	**54 & 42**	**921 & 655**	**134 & 85**	**18 & 12**
1527	Actin, cytoplasmic 1 & Thioredoxin domain-containing protein 5	ACTB & TXND5	**0.0064**	**-3.12**	**5.48**	**51**	**5.3 & 5.4**	**42 & 44**	**967 & 707**	**118 & 101**	**15 & 14**
1560	Vimentin & Cytoskeleton-associated protein 4 & Gamma-enolase	VIME & CKAP4 & ENOG	**0.009**	**2.65**	**5.01**	**50**	**5.1 & 5.6 & 4.9**	**54 & 66 & 47**	**1612 & 1124 & 980**	**127 & 117 & 106**	**31 & 18 & 14**
1574	Lupus La protein	LA	**0.000029**	**-2.37**	**7.41**	**50**	**6.7**	**47**	**722**	**106**	**12**
1576	Heterogeneous nuclear ribonucleoprotein F & Cartilage-associated protein & Eukaryotic initiation factor 4A-I & Heterogeneous nuclear ribonucleoprotein F	HNRPF & CRTAP & IF4A1 & HNRPF	**0.00085**	**-2.32**	**5.58**	**50**	**5.4 & 5.3 & 5.3**	**46 & 44 & 46**	**636 & 490 & 926**	**95 & 82 &110**	**10 & 10 &18**
1604	No identified protein		**0.0096**	**-2.13**	**9.08**	**49**			**-**	**-**	**-**
1609	CCA tRNA nucleotidyltransferase 1, mitochondrial & Prelamin-A/C & Alpha-enolase	TRNT1 & LMNA & ENOA	**0.028**	**1.61**	**7.64**	**49**	**6.3 & 6.6 & 7**	**45 & 74 & 47**	**379 & 814 & 374**	**58 & 83 & 92**	**9 & 16 & 5**
1611	Prelamin-A/C & Fumarate hydratase, mitochondrial	LMNA & FUMH	**0.013**	**3.86**	**7.95**	**49**	**6.6 & 7**	**74 & 50**	**1172 & 357**	**80 & 92**	**23 & 5**
1618	Serpin H1	SERPH	**0.012**	**-2.72**	**9.46**	**48**	**8.8**	**45**	**355**	**74**	**6**
1622	Serpin H1 & Vimentin	SERPH & VIME	**0.0025**	**-3.56**	**9.69**	**48**	**8.8 & 5.1**	**45 & 54**	**700 & 365**	**80 & 58**	**12 & 9**
1628	Fumarate hydratase	FUMH	**0.0042**	**-1.52**	**8.39**	**48**	**7**	**50**	**729**	**118**	**13**
1651	Vimentin & Heat shock protein HSP 90-beta	VIME & HS90B	**0.00029**	**6.21**	**4.97**	**47**	**5.1 & 5**	**54 & 83**	**1774 & 679**	**99 & 91**	**34 & 12**
1658	Ornithine aminotransferase, mitochondria & Beta-centractin	OAT & ACTY	**0.0089**	**-1.55**	**6.91**	**47**	**6 & 6**	**46 & 42**	**880 & 468**	**109 & 100**	**15 & 10**
1659	Vimentin	VIME	**0.012**	**2.84**	**4.86**	**47**	**5.1**	**54**	**2439**	**118**	**12**

1665	26S protease regulatory subunit 8 & Pyruvate dehydrogenase E1 component subunit alpha, somatic form, mitochondrial	PRS8 & ODPA	**0.003**	**-1.78**	**7.87**	**47**	**7.3 & 6.5**	**45 & 40**	**475 & 312**	**83 & 60**	**8 & 7**
1684	Annexin A2 & Citrate synthase, mitochondrial & Phosphoglycerate kinase 1	ANXA2 & CISY & PGK1	**0.007**	**-1.57**	**8.72**	**46**	**7.6 & 7.4 & 8.3**	**38 & 49 & 44**	**565 & 549 & 510**	**96 & 85 & 93**	**10 & 12 & 10**
1716	Cytochrome b-c1 complex subunit 2 & Citrate synthase & Alpha-enolase	QCR2 & CISY & ENOA	**0.01**	**1.71**	**8.45**	**46**	**7.7 & 7.4 & 7**	**47 & 49 & 47**	**432 & 332 & 529**	**95 & 68 & 97**	**8 & 8 & 7**
1723	No identified protein		**0.033**	**-1.58**	**7.39**	**45**					
1730	2',3'-cyclic-nucleotide 3'-phosphodiesterase & Elongation factor 1-alpha 1 & Glucose-6-phosphate isomerase & Aspartate aminotransferase, mitochondrial	CN37 & EF1A1 & G6PI & AATM	**0.0039**	**1.86**	**9.9**	**45**	**9.2 & 9.1 & 8.4**	**47 & 50 & 63**	**432 & 416 & 306 & 248**	**61 & 98 & 82 & 90**	**11 & 8 & 6 & 3**
1736	Alpha-enolase & Fumarylacetoacetase & Myosin-9	ENOA & FAAA & MYH9	**0.0022**	**2.33**	**7.5**	**45**	**7 & 6.5 & 5.5**	**47 & 46 & 226**	**632 & 110 & 682**	**132 & 64 & 92**	**9 & 2 & 11**
1744	Vimentin	VIME	**0.0056**	**5.22**	**4.84**	**44**	**5.1**	**54**	**1895**	**97**	**37**
1745	DnaJ homolog subfamily B member 11	DJB11	**0.0043**	**-3.24**	**6.83**	**44**	**5.8**	**38**	**721**	**105**	**13**
1756	Interleukin enhancer-binding factor 2 & Protein disulfide-isomerase	ILF2 & PDIA1	**0.0032**	**5.1**	**5.18**	**44**	**5.2 & 4.7**	**43 & 55**	**283 & 477**	**89 & 80**	**5 & 10**
1771	Mitochondrial import receptor subunit TOM40 & UTP--glucose-1-phosphate uridylyltransferase & Isovaleryl-CoA dehydrogenase	TOM40 & UGPA & IVD	**0.025**	**-1.72**	**8.21**	**43**	**6.8 & 8.2 & 6.9**	**38 & 57 & 43**	**563 & 368 & 314**	**94 & 77 & 69**	**9 & 8 & 7**
1772	Trifunctional enzyme subunit alpha & 26S protease regulatory subunit 10B & 26S protease regulatory subunit 10B & Alpha-2-macroglobulin receptor-associated	ECHA & PRS10 & AMRP	**0.00012**	**3.17**	**8.45**	**44**	**9 & 7.1 & 6.9**	**79 & 44 & 38**	**1073 & 536 &377**	**102 & 68 & 56**	**19 & 12 & 10**
1813	Poly(rC)-binding protein 1 & Fructose-bisphosphate aldolase & Acyl-coenzyme A thioesterase 9	PCBP1 & ALDOC & ACOT9	**0.018**	**1.53**	**7.91**	**43**	**6.7 & 6.5 & 7.8**	**37 & 39 & 48**	**650 & 425 & 375**	**100 & 86 & 76**	**11 & 8 & 8**
1829	Aspartate aminotransferase, mitochondrial & Heterogeneous nuclear ribonucleoprotein A3	AATM & ROA3	**0.029**	**-1.59**	**10.23**	**42**	**9 & 9.1**	**45 & 40**	**884 & 486**	**119 & 106**	**15 & 7**
1830	Vimentin	VIME	**0.048**	**2.12**	**4.82**	**42**	**5.1**	**54**	**1662**	**128**	**32**

1831	Heterogeneous nuclear ribonucleoproteins C1/C2 & Suppressor of G2 allele of SKP1 homolog	HNRPC & SUGT1	**0.00086**	**-2.28**	**5.09**	**42**	**5 & 5.1**	**34 & 41**	**154 & 132**	**60 & 61**	**3 & 3**
1848	Tubulin beta-2A chain & Short/branched chain specific acyl-CoA dehydrogenase, mitochondrial & Arfaptin-2	TBB2A & ACDSB & ARFP2	**0.0088**	**2.17**	**6.24**	**41**	**4.8 & 5.7 & 5.7**	**50 & 44 & 38**	**680 & 475 & 167**	**90 & 94 & 85**	**12 & 9 & 3**
1870	Serine-threonine kinase receptor-associated protein & Heterogeneous nuclear ribonucleoproteins C1/C2	STRAP & VIME & HNRPC	**0.0023**	**-1.79**	**5.13**	**41**	**5 & 5.1 & 5**	**38 & 54 & 34**	**645 & 426 & 787**	**87 & 57 & 105**	**12 & 10 & 15**
1898	Caldesmon	CALD1	**0.0011**	**-3.33**	**10.4**	**40**	**5.6**	**93**	**469**	**60**	**11**
1909	Phosphoglycerate kinase 1 & Alpha-enolase	PGK1 & ENOA	**0.025**	**2.03**	**6.64**	**40**	**8.3 & 7**	**44 & 47**	**701 & 715**	**104 & 116**	**12 & 11**
1910	Phosphotriesterase-related protein & Biliverdin reductase A	PTER & BIEA	**0.027**	**2.09**	**7.05**	**40**	**6.1 & 6.1**	**39 & 33**	**210 & 128**	**64 & 59**	**4 & 3**
1924	Vimentin & Tropomyosin alpha-4 chain	VIME & TPM4	**0.012**	**-2.52**	**4.81**	**40**	**5.1 & 4.7**	**54 & 28**	**703 & 519**	**89 & 60**	**15 & 12**
1930	Nucleophosmin & V-type proton ATPase subunit d 1	NPM & VA0D1	**0.0021**	**-9.01**	**4.92**	**39**	**4.6 & 4.9**	**33 & 40**	**464 & 448**	**98 & 77**	**8 & 8**
1933	Vimentin & Nucleophosmin & V-type proton ATPase subunit d 1	VIME & NPM & VA0D1	**0.00006**	**-3.96**	**4.97**	**38**	**5.1 & 4.6 & 4.9**	**54 & 33 & 40**	**482 & 411 & 324**	**85 & 92 & 81**	**9 & 7 & 6**
1947	Glyoxylate reductase/hydroxypyruvate reductase	GRHPR_HUMAN	**0.000056**	**2.03**	**8.3**	**39**	**7**	**36**	**376**	**72**	**8**
1964	Pyruvate kinase isozymes M1/M2 & Annexin A1	KPYM & ANXA1	**0.0094**	**2.79**	**7.35**	**38**	**8 & 6.6**	**58 & 39**	**944 & 579**	**92 & 117**	**15 & 8**
2035	Alpha-enolase & Torsin-1A	ENOA & TOR1A	**0.0017**	**2.1**	**7.29**	**37**	**7 & 6.2**	**47 & 36**	**396 & 264**	**97 & 75**	**6 & 5**
2042	Elongation factor 1-delta & Thioredoxin-like protein 1	EF1D & TXNL1	**0.0031**	**-1.93**	**5.08**	**36**	**4.9 & 4.8**	**31 & 32**	**606 & 267**	**100 & 77**	**9 & 5**
2051	Tubulin beta chain	TBB5	**0.0095**	**2.24**	**5.71**	**36**	**4.8**	**50**	**732**	**116**	**12**
2085	Heterogeneous nuclear ribonucleoproteins A2/B1 & Malate dehydrogenase, mitochondrial & L-lactate dehydrogenase A chain & Voltage-dependent anion-selective channel protein 1	ROA2 & MDHM & LDHA & VDAC1	**0.038**	**-1.51**	**9.79**	**36**	**9 & 8.5 & 8.5**	**37 & 33 & 37**	**707 & 693 & 495 & 378**	**121 & 93 & 102 & 88**	**12 & 11 & 10 & 7**
2087	Glyceraldehyde-3-phosphate dehydrogenase	G3P	**0.011**	**3.67**	**8.26**	**36**	**8.6**	**36**	**669**	**88**	**12**

2096	L-lactate dehydrogenase B chain	LDHB	**0.039**	**1.53**	**6.21**	**35**	**5.7**	**37**	**793**	**104**	**14**
2128	39S ribosomal protein L44, mitochondrial & Glyceraldehyde-3-phosphate dehydrogenase	RM44 & G3P	**0.0011**	**2.54**	**8.37**	**34**	**7 & 8.6**	**34 & 36**	**426 & 177**	**78 & 88**	**9 & 3**
2134	Endoplasmic reticulum resident protein 44 & Inorganic pyrophosphatase	ERP44 & IPYR	**0.0045**	**1.71**	**5.72**	**34**	**5 & 5.5**	**44 & 33**	**347 & 327**	**88 & 76**	**7 & 6**
2161	Heterogeneous nuclear ribonucleoprotein A1 & ELAV-like protein 1	ROA1 & ELAV1	**0.00089**	**-4.53**	**10.33**	**34**	**9.2 & 9.2**	**39 & 36**	**671 & 308**	**109 & 84**	**11 & 6**
2170	Phosphatidylinositol transfer protein alpha isoform & Fumarylacetoacetate hydrolase domain-containing protein 2B & Dynamin-1-like protein	PIPNA & FAH2B & DNM1L	**0.035**	**1.5**	**7.25**	**33**	**6.1 & 7.6 & 6.4**	**32 & 35 & 82**	**281 & 319 & 98**	**97 & 56 & 55**	**6 & 7 & 2**
2198	Annexin A5	ANXA5	**0.0089**	**1.65**	**5.06**	**33**	**4.9**	**36**	**1136**	**128**	**17**
2225	Elongation factor Tu, mitochondrial	EFTU	**0.047**	**3.07**	**6.75**	**32**	**6.3**	**45**	**822**	**81**	**16**
2276	Heterogeneous nuclear ribonucleoprotein A1 & Erzin & Voltage-dependent anion-selective channel protein 1 & 14-3-3 protein zeta/delta & Trifunctional enzyme subunit beta, mitochondrial	ROA1 & EZRI & VDAC1 & 1433Z & ECHB	**0.0044**	**1.83**	**9.75**	**31**	**9.2 & 6 & 8.6**	**39 & 69 & 31**	**336 & 415 & 250 & 244 & 250**	**72 & 64 & 75 & 86 & 76**	**7 & 10 & 4 & 4 & 6**
2280	Cathepsin B & Alpha-soluble NSF attachment protein	CATB & SNAA	**0.0077**	**2.61**	**5.41**	**31**	**5.2 & 5.2**	**28 & 33**	**533 & 109**	**92 & 74**	**9 & 2**
2291	Heterogeneous nuclear ribonucleoprotein A1-like 2 & Heterogeneous nuclear ribonucleoprotein A1 & Serpin H1	RA1L2 & ROA1 & SERPH	**0.000061**	**1.97**	**9.03**	**31**	**9.1 & 9.2 & 8.8**	**34 & 39 & 45**	**238 & 385 & 191**	**96 & 81 &66**	**4 & 8 & 3**
2316	Cathepsin D & Annexin A5 & 14-3-3 protein epsilon	CATD & ANXA5 & 1433E	**0.024**	**-5.49**	**5.08**	**30**	**5.6 & 4.9 & 4.6**	**38 & 36 & 29**	**571 & 532 & 118**	**91 & 88 & 52**	**10 & 9 & 3**
2324	Cathepsin D	CATD	**0.00043**	**-3.69**	**5.52**	**30**	**5.6**	**38**	**501**	**70**	**9**
2328	Cathepsin B & Chloride intracellular channel protein 1	CATB & CLIC1	**0.015**	**2.48**	**5.41**	**30**	**5.2 & 5.1**	**28 & 27**	**531 & 366**	**106 & 72**	**8 & 7**
2349	14-3-3 protein theta & 14-3-3 protein zeta/delta	1433T & 1433Z	**0.027**	**1.89**	**4.83**	**29**	**4.7 & 4.7**	**28 & 28**	**666 & 641**	**91 & 90**	**12 & 13**
2356	Glutathione S-transferase omega-1	GSTO1	**0.035**	**2.93**	**6.81**	**29**	**6.2**	**27**	**323**	**66**	**7**
2364	Protein disulfide-isomerase A3 & Triosephosphate isomerase	PDIA3 & TPIS	**0.03**	**2.29**	**7.53**	**29**	**5.6 & 5.7**	**54 & 31**	**304 & 117**	**107 & 59**	**5 & 2**

2365	Hydroxyacyl-coenzyme A dehydrogenase, mitochondrial	HCDH	**0.0032**	**4.75**	**8.24**	**29**	**8.4**	**33**	**457**	**59**	**10**
2392	Proteasome activator complex subunit 1	PSME1	**0.016**	**1.58**	**6.22**	**28**	**5.8**	**29**	**563**	**76**	**10**
2426	Ras suppressor protein 1 & Probable fructose-2,6-bisphosphatase TIGAR	RSU1 & TIGAR	**0.0003**	**4.49**	**8.06**	**28**	**8.6 & 7.6**	**31 & 30**	**425 & 185**	**62 & 84**	**10 & 3**
2438	6-phosphogluconolactonase & Actin-related protein 2/3 complex subunit 2	6PGL & ARPC2	**0.025**	**4.28**	**6.26**	**28**	**5.7 & 6.8**	**27 & 34**	**491 & 344**	**77 & 57**	**9 & 8**
2478	Serpin H1 & Abhydrolase domain-containing protein 11	SERPH & ABHDB	**0.00012**	**2.66**	**8.21**	**27**	**8.8 & 9.5**	**45 & 35**	**218 & 167**	**74 & 75**	**4 & 3**
2491	Actin, cytoplasmic 1	ACTB	**0.05**	**1.97**	**5.72**	**27**	**5.3**	**42**	**517**	**98**	**8**
2505	3-hydroxybutyrate dehydrogenase type 2 & Trifunctional enzyme subunit beta, mitochondrial & 3-hydroxybutyrate dehydrogenase type 2 & Heterogeneous nuclear ribonucleoprotein A1	BDH2 & RA1L2 & ECHB & ROA1	**0.00018**	**2.64**	**9.1**	**26**	**7.6 & 9.1 & 9.2**	**27 & 34 & 47**	**356 & 238 & 373 & 339**	**87 & 69 & 69 & 89**	**6 & 5 & 7 & 7**
2517	Succinate dehydrogenase [ubiquinone] iron-sulfur subunit, mitochondrial & 40S ribosomal protein S3a & Peptidyl-prolyl cis-trans isomerase B & Transforming growth factor-beta-induced protein ig-h3	DHSB & RS3A & PPIB & BGH3	**0.0049**	**2.81**	**10.32**	**27**	**8.8 & 9.8 & 9.3**	**29 & 30 & 20**	**466 & 276 & 209 & 446**	**60 & 77 & 78 & 65**	**11 & 7 & 4 & 9**
2522	Annexin A1 & Cathepsin B & Inorganic pyrophosphatase	ANXA1 & CATB & IPYR	**0.014**	**2.28**	**5.19**	**26**	**6.6 & 5.2 & 5.5**	**39 & 28 & 33**	**587 & 309 & 56**	**101 & 90 & 30**	**9 & 5 & 2**
2532	Adenylate kinase isoenzyme 4, mitochondrial	KAD4	**0.0037**	**3.5**	**8.58**	**26**	**8.5**	**25**	**177**	**48**	**4**
2555	14-3-3 protein gamma & Calpain small subunit 1 & 14-3-3 protein eta	1433G & CPNS1 & 1433F	**0.00037**	**4.4**	**5.06**	**26**	**4.8 & 5.1 & 4.8**	**28 & 28 & 28**	**126 & 125 & 73**	**53 & 67 & 45**	**3 & 2 & 2**
2565	Triosephosphate isomerase & Dihydropteridine reductase	TPIS & DHPR	**0.00042**	**1.81**	**7.81**	**25**	**5.7 & 7.1**	**31 & 26**	**875 & 266**	**100 & 65**	**14 & 4**
2573	Ubiquitin carboxyl-terminal hydrolase isozyme L1 & Vacuolar protein sorting-associated protein 28 homolog	UCHL1 & VPS28	**0.015**	**2.87**	**5.49**	**25**	**5.2 & 5.4**	**25 & 25**	**360 & 150**	**75 & 68**	**7 & 3**
2591	Uncharacterized protein C2orf47, mitochondrial	CB047	**0.011**	**-2.44**	**8.25**	**25**	**7**	**22**	**40**	**40**	**1**
2602	No identified protein		**0.0032**	**2.32**	**6.98**	**25**					

2610	NADH dehydrogenase [ubiquinone] iron-sulfur protein 8 & Actin, cytoplasmic 1 & Plasma membrane calcium-transporting ATPase 4	NDUS8 & ACTB & ATPG	**0.0029**	**2.73**	**5.25**	**24**	**5.1 & 5.3 & 9**	**20 & 42 & 30**	**192 & 139 & 122**	**58 & 62 & 66**	**4 & 3 & 3**
2633	26S proteasome non-ATPase regulatory subunit 10 & Thioredoxin-dependent peroxide reductase, mitochondrial	PSD10 & PRDX3	**0.0028**	**1.53**	**6.19**	**24**	**5.7 & 5.8**	**24 & 21**	**106 & 73**	**74 & 44**	**2 & 2**
2651	Glyceraldehyde-3-phosphate dehydrogenase & Prohibitin-2	G3P & PHB2	**0.0033**	**5.73**	**10.36**	**24**	**8.6 & 9.8**	**36 & 33**	**364 & 307**	**88 & 69**	**6 & 6**
2713	Transgelin & Peptidyl-prolyl cis-trans isomerase B & Glyceraldehyde-3-phosphate dehydrogenase	TAGL & PPIB & G3P	**0.0024**	**5.11**	**10.24**	**22**	**8.9 & 9.3 & 8.6**	**22 & 20 & 36**	**265 & 249 & 276**	**72 & 73 & 76**	**5 & 5 & 5**
2737	Transgelin & NADH dehydrogenase [ubiquinone] 1 beta subcomplex subunit 10	TAGL & NDUBA	**0.00059**	**-2.89**	**10,0**	**22**	**8.9 & 8.7**	**22 & 21**	**646 & 156**	**75 & 52**	**13 & 4**
2754	ATP synthase subunit alpha, mitochondrial & 40S ribosomal protein S7	ATPA & RS7	**0.008**	**2.35**	**7.03**	**22**	**8.3 & 10.1**	**55 & 22**	**115 & 60**	**62 & 33**	**3 & 2**
2763	ATP synthase subunit O, mitochondrial	ATPO	**0.0044**	**-2.33**	**10.78**	**22**	**9.8**	**21**	**507**	**107**	**8**
2773	Transgelin	TAGL	**0.0034**	**-2.12**	**8.8**	**22**	**8.9**	**22**	**365**	**66**	**7**
2786	Transgelin-2	TAGL2	**0.0038**	**-2.38**	**9.82**	**22**	**8.5**	**22**	**704**	**104**	**13**
2804	Programmed cell death protein 6 & F-actin-capping protein subunit beta & Deoxyribonucleoside 5'-monophosphate N-glycosidase	PDCD6 & CAPZB & RCL	**0.0025**	**4.45**	**5.04**	**21**	**5.2 & 5.4 & 5**	**22 & 31 & 19**	**152 & 208 & 312**	**68 & 67 & 90**	**3 & 4 & 6**
2805	Ras-related protein Rab-1A & Sorcin	RAB1A & SORCN	**0.019**	**2.48**	**5.21**	**21**	**5.9 & 5.3**	**23 & 22**	**344 & 219**	**116 & 59**	**5 & 5**
2857	60S ribosomal protein L11	RL11	**0.0025**	**-3.09**	**10.82**	**20**	**9.6**	**20**	**110**	**59**	**2**
2858	Myosin regulatory light chain 12A	ML12A	**0.015**	**-2.27**	**4.82**	**20**	**4.7**	**20**	**386**	**86**	**6**
2894	Nucleolin	NUCL	**0.0077**	**4.09**	**5.43**	**20**	**4.6**	**76**	**452**	**90**	**9**
2912	Myosin regulatory light chain 12A & Protein canopy homolog 2	ML12A & CNPY2	**0.0086**	**-2.05**	**4.85**	**19**	**4.7 & 4.7**	**20 & 19**	**379 & 225**	**79 & 71**	**7 & 5**
2930	Peptidyl-prolyl cis-trans isomerase B & N-alpha-acetyltransferase 50 & NADH dehydrogenase [ubiquinone] iron-sulfur protein 4, mitochondrial	PPIB & NAA50 & NDUS4	**0.0074**	**-1.81**	**10.2**	**19**	**9.3 & 9 & 9.4**	**20 & 19 & 15**	**696 & 87 & 66**	**81 & 44 & 38**	**13 & 2 & 2**
2944	Protein canopy homolog 2 & Trafficking protein particle complex subunit 3	CNPY2 & TPPC3	**0.0075**	**-1.86**	**4.94**	**19**	**4.8 & 4.9**	**20 & 21**	**408 & 301**	**69 & 63**	**8 & 7**

2976	Translocon-associated protein subunit delta & Annexin A2	SSRD & ANXA2	**0.0017**	**6.35**	**5.59**	**18**	**5.5 & 7.6**	**17 & 38**	**148 & 500**	**67 & 83**	**3 & 8**
2980	Tubulin beta-2A chain	TBB2A	**0.00032**	**3.33**	**4.74**	**18**	**4.8**	**50**	**337**	**106**	**5**
2986	60S ribosomal protein L12	RL12	**0.0093**	**-1.92**	**10.75**	**18**	**9.5**	**18**	**178**	**89**	**3**
2991	Nucleophosmin & Tubulin beta-2A chain	NPM & TBB2A	**0.0002**	**5.06**	**4.64**	**18**	**4.6 & 4.8**	**33 & 50**	**278 & 158**	**69 & 59**	**5 & 3**
2999	Transgelin & Destrin	TAGL & DEST	**0.00012**	**3.04**	**7.57**	**18**	**8.9 & 8.1**	**22 & 18**	**314 & 163**	**68 & 98**	**6 & 3**
3066	Ragulator complex protein LAMTOR1	LTOR1	**0.042**	**1.57**	**4.96**	**17**	**5**	**18**	**161**	**93**	**3**
3089	Transgelin & Peroxiredoxin-1	TAGL & PRDX1	**0.015**	**5.51**	**7.57**	**17**	**8.9 & 8.3**	**22 & 22**	**153 & 70**	**63 & 44**	**3 & 2**
3131	Protein mago nashi homolog	MGN	**0.0028**	**2,0**	**6.1**	**16**	**5.7**	**17**	**253**	**60**	**6**
3152	Myosin light polypeptide 6	MYL6	**0.0019**	**-2.07**	**4.69**	**16**	**4.6**	**17**	**683**	**85**	**12**
3171	60S acidic ribosomal protein P2 & ATP synthase subunit delta, mitochondrial	RLA2 & ATPD	**0.00011**	**-1.75**	**4.59**	**15**	**4.4 & 4.5**	**12 & 15**	**286 & 114**	**89 & 69**	**4 & 2**
3193	Coactosin-like protein	COTL1	**0.0000042**	**3.47**	**5.53**	**15**	**5.5**	**16**	**364**	**57**	**9**
3233	Profilin-1 & 60S ribosomal protein L22	PROF1 & RL22	**0.0099**	**3.08**	**9.99**	**15**	**8.5 & 9.2**	**15 & 15**	**151 & 102**	**77 & 58**	**3 & 2**
3263	Calponin-3	CNN3	**0.00012**	**8.88**	**7.83**	**14**	**5.7**	**36**	**74**	**43**	**2**
3292	ATP synthase subunit alpha, mitochondrial & Galectin-1	ATPA & LEG1	**0.00021**	**2.18**	**4.98**	**14**	**8.3 & 5.3**	**55 & 15**	**523 & 269**	**105 & 99**	**7 & 5**
3300	Hemoglobin subunit alpha	HBA	**0.00036**	**2.87**	**8.5**	**14**	**8.7**	**15**	**64**	**37**	**2**
3309	Profilin-1	PROF1	**0.00044**	**1.68**	**9.85**	**14**	**8.5**	**15**	**481**	**82**	**9**
3330	NADH dehydrogenase [ubiquinone] iron-sulfur protein 5 & 60S ribosomal protein L11	NDUS5 & RL11	**0.00033**	**2.38**	**10.67**	**14**	**9.3 & 9.6**	**12 & 20**	**98 & 74**	**71 & 37**	**2 & 2**
3347	Profilin-1 & Ribonuclease UK114 & Cofilin-1	PROF1 & UK114 & COF1	**0.038**	**2.18**	**9.85**	**13**	**8.5 & 8.7 & 8.3**	**15 & 14 & 18**	**423 & 313 & 272**	**78 & 104 & 102**	**8 & 5 & 5**
3388	40S ribosomal protein S3	RS3	**0.000055**	**4.13**	**10.68**	**13**	**9.7**	**27**	**289**	**67**	**5**
3413	40S ribosomal protein S3	RS3	**0.000059**	**3.97**	**10.39**	**13**	**9.7**	**27**	**310**	**68**	**5**
3464	40S ribosomal protein S14	RS14	**0.0047**	**2.67**	**9.3**	**12**	**10.1**	**16**	**151**	**71**	**3**

3501	Protein S100-A10	S10AA	**0.0017**	**1.53**	**8.62**	**12**	**7.3**	**11**	**75**	**44**	**2**
3528	Hemoglobin subunit beta	HBB	**0.015**	**1.88**	**5,0**	**11**	**6.8**	**16**	**100**	**56**	**2**
3529	Protein S100-A6 & Hemoglobin subunit alpha	S10A6 & HBA	**0.028**	**1.8**	**5.3**	**10**	**5.3 & 8.7**	**10 & 15**	**249 & 109**	**49 & 56**	**7 & 2**
3535	No identified protein		**0.0054**	**1.6**	**7.44**	**11**					
3536	Profilin-1 & Guanine nucleotide-binding protein G(I)/G(S)/G(O) subunit gamma-12 & Histone H2B type 1-B	PROF1 & GBG12 & H2B1B	**0.0018**	**3.96**	**10.67**	**11**	**8.5 & 9.1 & 10.3**	**15 & 8 & 14**	**232 & 209 & 155**	**72 & 67 & 64**	**5 & 4 & 4**
3545	Peroxiredoxin-5, mitochondrial	PRDX5	**0.0033**	**6.82**	**9.11**	**11**	**6.7**	**17**	**353**	**94**	**7**
3557	Peptidyl-prolyl cis-trans isomerase B	PPIB	**0.0074**	**2.99**	**10.39**	**11**	**9.3**	**20**	**90**	**63**	**2**

Exp: experimental; MM: molecular mass; pI: isoelectrofocalisation point; Theo: theoretical. Relative quantification and statistical evaluation were carried out with DeCyderTM 2D software (GE Healthcare, version 7.0). Down or up-expressed proteins between groups were retained if protein spot fold change was larger than +1.5 or smaller than –1.5 and a Student's t-test p-value less than 0.05

3.3. Analyse moléculaire des cellules musculaires lisses de patients atteints d'artérite à cellules géantes : contrôle de la prolifération par l'inhibition de l'endothéline-1

Alexis Régent†, Kim Heang Ly†, Matthieu Groh, Chabha Khifer, Sébastien Lofek, Mathieu Tamby, Guilhem Clary, Philippe Chaffey, Veronique Baud, Cédric Broussard, Christian Federici, François Labrousse, Laura Mesturoux, Claire Le-Jeunne, Elisabeth Vidal, Antoine Brezin, Véronique Witko-Sarsat, Loïc Guillevin, Luc Mouthon

L'étude de la physiopathologie de l'ACG a porté, avant tout, sur le dysfonctionnement du système immunitaire. Les mécanismes qui conduisent au remodelage artériel et à son éventuelle occlusion restent mal connus.

Nous avons donc cultivé des CMLV issues d'artère temporale de patients suspects d'ACG. Nous avons retenus les CMLV de 4 patients avec ACG prouvée histologiquement (TAB^+-ACG), de 4 patients avec ACG sans preuve histologique (TAB^--ACG) et de 4 patients ayant un autre diagnostic que l'ACG (GCA-controls) et avons analysé les protéomes par 2D-DIGE à pH 3-11. Les CMLV d'aorte normale (HAoSMC) ont été utilisé comme contrôle. Par ailleurs, nous avons fait une analyse du profil d'expression génique à l'aide de puces Affymetrix®. La prolifération des CMLV a été étudiée à l'aide d'un kit ELISA BrdU.

Nous avons identifié que 16, 30 et 2 protéines de CMLV respectivement étaient différemment exprimées entre les groupes TAB^+-GCA et GCA-control, entre les groupes TAB^+-GCA et TAB^--GCA et entre les groupes TAB^--GCA et GCA-control (rapport d'expression≥1.5 et p≤0.05). Nous avons pu montrer que parmi les 153

protéines différemment exprimées entre les CMLV du groupe TAB^{+}-GCA et HAoSMC, de nombreuses étaient liées à la paxilline ou à l'ET-1. De nombreux gènes parmi ceux différemment exprimés entre les groupes TAB^{+}-GCA et GCA-control sont impliqués dans la prolifération cellulaire. La paxilline et l'ET-1 ont de nouveau été identifiées comme des liens entre les gènes d'intérêt. La prolifération des CMLV du groupe TAB^{+}-GCA en présence de macitentan, un inhibiteur des récepteurs de l'ET-1 et en particulier de son métabolite actif était diminuée.

Les CMLV du groupe TAB^{+}-GCA ont un contenu protéique et un profil d'expression génomique qui témoigne d'une capacité de prolifération accrue. L'inhibition via le macitentan pourrait représenter une nouvelle approche thérapeutique du remodelage au cours de l'ACG.

Molecular analysis of vascular smooth muscle cells from patients with giant cell arteritis: targeting endothelin-1 receptor to control proliferation

Alexis Régent[1,2†], Kim Heang Ly[3,4†], Matthieu Groh[1,2], Chabha Khifer[1], Sébastien Lofek[1], Mathieu Tamby[1], Guilhem Clary[1], Philippe Chafey[1], Veronique Baud[1], Cédric Broussard[1], Christian Federici[1], François Labrousse[5], Laura Mesturoux[5], Claire Le-Jeunne[2], Elisabeth Vidal[3,4], Antoine Brezin[6], Véronique Witko-Sarsat[1], Loïc Guillevin[2], Luc Mouthon[1,2]

[†]both authors contributed equally to the work

[1]Institut Cochin, INSERM U1016, CNRS UMR 8104, LabEx INFLAMEX, Université Paris Descartes, Paris, France;

[2]Pôle de Médecine Interne, Centre de Référence pour les vascularites nécrosantes et la sclérodermie systémique, Hôpital Cochin, Assistance Publique Hôpitaux de Paris (AP-HP), Paris ;

[3]Service de Médecine Interne A, CHU Dupuytren, Limoges, France

[4]Laboratoire d'immunologie, EA3842, Faculté de médecine, Limoges;

[5]Laboratoire d'anatomie pathologie, CHU Limoges, Limoges

[6]Service d'ophtalmologie, hôpital Cochin, AP-HP, Paris.

AR: alexisregent@hotmail.com ; KHL: kim.ly@chu-limoges.fr ; MG : matthieu.groh@cch.aphp.fr; CK : Ckiefer@yahoo.fr; SL : sebastien.lofek@inserm.fr; MT : mtamby@gmail.com; GC: guilhem.clary@inserm.fr; PC : philippe.chafey@inserm.fr; VB : veronique.baud@inserm.fr; CB :

cedric.broussard@inserm.fr ; CF : christian.federici@inserm.fr ; FL : francois.labrousse@unilim.fr ; LM : laura.mesturoux@chu-limoges.fr; CLJ : claire.le-jeunne@cch.aphp.fr; EV : elisabeth.vidal@unilim.fr; AB : antoine.brezin@cch;aphp.fr; VWS : veronique.witko@inserm.fr; LG : loic.guillevin@cch.aphp.fr; LM: luc.mouthon@cch.aphp.fr

Correspondance: Dr Luc Mouthon, INSERM U1016, CNRS UMR 8104, 8 rue Mechain, 75014 Paris, France.

Tel: +33 (0) 1 / Fax: +33 (0) 1

e-mail: luc.mouthon@cch.aphp.fr

Key words: giant cell arteritis; vascular smooth muscle cells; proliferation; paxillin; endothelin-1

ABSTRACT

Background. The pathophysiology of giant cell arteritis (GCA) and the mechanisms underlying vascular remodeling are poorly understood.

Patients and Methods. Vascular smooth muscle cells (VSMC) were cultured from temporal artery biopsies (TAB) obtained from consecutive patients suspected of GCA: four patients with biopsy proven GCA (TAB^+-GCA), four patients with biopsy-negative GCA (TAB^--GCA), and four patients with another diagnosis than GCA (GCA-control). Two-dimension DIGE (2D-DIGE) at pH range of 3-11 and affymetrix chips were used in order to analyze proteomes and gene expression profile of VSMC from the different groups. Normal human aorta VSMC (HAoSMC) were used as control in proteomic experiments. Proliferation of VSMC was analysed using a BrdU proliferation assay ELISA kit.

Results. We identified 16, 30 and 2 protein spots that were differentially expressed between VSMC from TAB^+-GCA and GCA-control patients, between TAB^+-GCA and TAB^--GCA patients and between TAB^--GCA and GCA-control patients, respectively (fold change≥1.5 and p≤0.05). One hundred and fifty three protein spots were differentially expressed between VSMC from TAB^+-GCA and HAoSMC, which were linked with paxillin and endothelin-1.

Genes differentially expressed between VSMC from patients with TAB^+-GCA, TAB^--GCA and GCA-control were mostly involved in proliferation. Paxillin and endothelin-1 were also identified as potential links between genes of interest. Proliferation of VSMC from TAB^+-GCA patients was reduced in the presence of macitentan, an endothelin receptor antagonist.

Conclusion. VSMC from patients with GCA expressed proteins that confer an increased proliferation potential. Inhibition of the increased proliferation of VSMC

during GCA with macitentan might represent a promising therapeutic approach in patients with GCA, in combination with glucocorticoids.

ABBREVIATIONS:

α-SMA: α-smooth muscle actin

2DE: Two dimension electrophoresis

CD: cluster of differentiation

DIGE: differential in gel electrophoresis

EC: endothelial cell

ET-1: endothelin 1

GCA: giant cell arteritis

Grb2: growth factor receptor-bound protein 2 HAoSMC: human aortic smooth muscle cells

MS: mass spectrometry

PCA: principal component analysis

PDGF: platelet derived growth factor

Pparγ: Peroxisome proliferator-activated receptor gamma

PPIA: peptidylpropyl isomerase A

TA: temporal artery

TAB: temporal artery biopsy

VEGF: vascular endothelial growth factor

VSMC: vascular smooth muscle cells

vWF: von Willebrand Factor

1. **INTRODUCTION**

Giant cell arteritis (GCA) is a primary vasculitis that occurs in patients aged over 50 [1]. It specifically involves aorta and external carotid arteries and their branches, with intimal hyperplasia and luminal obstruction leading to ischemic manifestations such as temporal headaches, jaw claudication, scalp tenderness and temporal artery involvement. Initial prognosis relies on visual impairment with blurry vision, transient or permanent sight loss in as much as 20% of patients [2, 3]. Urgent diagnosis is required in order to initiate glucocorticoid treatment even though it has a limited efficacy on vision if already impaired [4]. Pathological examination of temporal arteries identifies a mononuclear Th-1 and Th-17 infiltrate of the adventitia, an internal elastic lamina disruption with macrophages and multinucleated cells and an intimal hyperplasia [5]. Macrophages produce platelet derived growth factor (PDGF) and vascular endothelial growth factor (VEGF) that are responsible for the thickening of the vessel wall [6, 7] and also produce high level of reactive oxygen species which target vascular smooth muscle cells (VSMC) [8]. The imbalance between Matrix Metalloprotease (MMP) and the Tissue Inhibitors of Matrix Metalloprotease (TIMP) [9] contribute to the remodeling of the vessel wall [10]. In this context, it has been demonstrated that endothelin 1 (ET-1), a powerfull vasocontrictor and the endothelin receptor ET_AR and ET_BR were expressed in vascular lesions from GCA patients [11, 12] and that high plasmatic levels of ET-1 were associated with an increased risk of visual impairment [12, 13].

This is why we decided to isolate vascular smooth muscle cells (VSMC) by culturing them from temporal artery biopsies (TAB) from patients with GCA and from patients with negative TAB and other conditions. We identified that genes differentially expressed between VSMC from these patients were mostly involved in proliferation.

Proteomic and transcriptomic analyses identified paxillin and endothelin-1 as key activation pathways in VSMC from patients with biopsy proven GCA as compared to controls. Proliferation of VSMC from patients with biopsy proven GCA was reduced in the presence of macitentan, an endothelin receptor antagonist.

2. PATIENTS AND METHODS

2.1 Patients

Between January 2010 and June 2012, we included 122 consecutive patients suspected of GCA at the time of TAB in two different centers (Limoges and Paris) including 40 with biopsy-proven GCA (TAB^+GCA), 29 with biopsy-negative GCA (TAB^-GCA), 6 with polymyalgia rheumatica without GCA and 47 with another diagnosis than GCA (GCA-controls) (collection dc-2010-1079). VSMC from patients with GCA were isolated from sterile, freshly obtained surgical TAB of patients suspected of GCA. We selected 12 consecutive patients for whom we were able to isolate and culture VSMC: four patients with biopsy proven GCA (TAB^+-GCA), four patients fulfilling ACR criteria for the diagnosis of GCA without histological evidence of GCA (TAB^--GCA), and four patients with another diagnosis than GCA (GCA-control). Clinical and biological data were recorded at the time of TAB and updated with the TAB results and final diagnosis. Clinical data are detailed in Supplemental Table 1. All patients and controls gave their written informed consent to participate. The study was approved by the ethics committee of Cochin hospital.

2.2 Vascular smooth muscle cells

Briefly, temporal arteries were dissected and adventice and media were mechanically separated. Media was digested by collagenase and elastase during 90 minutes before seeding in cell culture flasks (Falcon, Becton Dickinson, Franklin Lakes, New Jersey, USA). Smooth muscle cell origin was assessed by a positive α-SMA staining and a negative CD90 staining upon indirect immunofluorescence experiments. Normal human aorta VSMC (HAoSMC) from four different healthy Caucasian donors older than 50 were used as control (Promocell GmbH, Heidelberg, Germany).

HAoSMC and VSMC from TAB were cultured in smooth muscle cell growth medium 2 (Promocell GmbH) until harvesting after the fourth passage and proteins were extracted as previsouly described [14].

2.3 Two-dimensional differential in gel electrophoresis and protein identification by mass spectrometry.

The samples of different VSMC types were labelled with fluorescent dyes and separated by two-dimensional electrophoresis, then gels were analyzed and protein spots differentially expressed between VSMC types were excised and in-gel trypsin digested and identified using mass spectrometry (MS). Two-dimensional differential in gel electrophoresis (2D-DIGE), in-gel trypsin digestion, and mass spectrometry protein identification procedures where adaptated from [14] and are detailed in Additional file 1.

2.4 RNA extraction in culture cells and chip analysis

For chip experiments, RNA extraction was performed with trizol method [15]. Cell pellets (passage 4) were resuspended in 1 mL trizol with 0.2 mL of chloroform (Merck) and centrifugated at 12000 rpm during 15 minutes at 4°C. Supernatants were incubated with isopropanol (Normapur) thus inducing RNA precipitation and centrifugated at 12000 rpm during 10 minutes at 4°C. Then, pellets were washed twice with ethanol 75% (Normapur) and resuspended in sterile water and stored at -80°C. After quality control, pangenomic affymetrix genechips (Affymetrix, Santa Clara, CA, USA) were used according to manufacturer instructions. For RNA analysis, data were normalized using Robust Multi-array Average (RMA) algorithm in Bioconductor with the ENSG custom CDF vs 15 [16]. Statistical analysis ware carried

out with the use of Partek® GS. First, variations in gene expression were analyzed using unsupervised hierarchical clustering and principal component analysis (PCA) to assess data from technical bias and outlier samples. To find differentially expressed genes, we applied a two way ANOVA for each gene and made pair wise post hoc tests between groups (contrasts).

For PCR experiments, total RNAs were extracted from cells at passage 6 with Qiagen RNeasy Isolation Kit (Qiagen, Venlo, Netherlands) treated with RNase-free DNase I (Qiagen). cDNA synthesis was performed with a High-Capacity cDNA Reverse Transcription Kit (Applied Biosystems, Carlsbad, California, USA), as recommended by the manufacturer. Real-time PCR was performed by predesigned primer/probe TaqMan gene expression assays (Applied biosystems) and normalized to HPRT housekeeping gene as previsously described [17]. Experiments were assessed in triplicate. The comparative ΔCt method was used for relative quantification of gene expression on duplicate of each reaction.

2.5 Generation of biological networks

Ingenuity pathway analysis (IPA) and Pathway Studio were used for the generation of biological networks to gain insights into the biological pathways and networks that prevailed in our proteomic and genomic data sets, (IPA; Ingenuity Systems, Redwood City, CA, USA and Pathway Studio, Elsevier, Amsterdam, Netherlands). After uploading lists of differentially expressed protein and genes to the IPA server, pathway networks with significant p-values ($p<0.05$) were generated.

2.6 Immunohistochemistry

Immunohistochemistry was performed on paraffin-embedded sections of temporal arteries (TA) deparaffinised in 22 biopsy-proven GCA patients and 21 GCA-controls. Sections of TA were rehydrated and subjected to steam-heat antigen retrieval in citrate buffer in a microwave oven (750 W). Endogenous peroxidases were inhibited with 5% H2O2 in methanol and non-specific sites were blocked with PBS-3% bovine serum albumin. Anti-ET-1 (Thermo Fisher Scientific, Waltham, MA, USA) anti-ET_AR and anti-ET_BR (Abcam, Cambridge, UK) were incubated at a 1/100 dilution overnight at 4°C and revealed with the anti-rabbit HRP Envision™ (Dako, Glostrup, Denmark). After counter staining, the slides were studied with a Leica microscope (×200 magnification).

2.7 Proliferation assay

Cell proliferation was analysed using VSMC at the 6th passage with Cell Proliferation ELISA BrdU (Roche Diagnostics, Mannheim, Germany) [18]. Briefly, cells were serum starved for 24 hours and then stimulated during 72 hours with 100mM ET-1 (Sigma-Aldrich, Saint Quentin Fallavier, France), macitentan and its active metabolite (kindly provided by Actelion Pharmaceuticals, Allschwil, Swiss) in a 96 well plate. After incubation, 10 µL of BrdU labelling solution was added to each well for 24 hours and BrdU incorporation was measured according to manufacturer's instructions with a spectrophotometer at 370 nm (FusionTM Universal Microplate Analyser, PerkinElmer, Waltham, Massachussetts, EU).

2.8 SiRNA transfection

Paxillin-siRNA and non targeting-siRNA were diluted with *trans*IT-X2 in opti-MEMI medium and transfection was performed according to manufacturer's instructions

(Mirus bio LLC, Madison, Wisconsin, USA). Paxillin silencing was confirmed with an immunoblot with a rabbit anti-human paxillin antibody (Abcam, Cambridge, United Kingdom).

3. RESULTS

3.1. Protein analysis

Using DeCyder Image Analysis software, a mean of 3293±250 different protein spots were detected in each gel. Among these, 2733±352 could be matched to the reference gel and were used for the comparative analysis.

A total of 39 distinct protein spots were identified as differentially expressed between VSMC from TAB^+-GCA, TAB^--GCA and GCA-controls (fold change ≥ 1.5 and a Student's t test p-value<0.05) (Table1). PCA was performed on the spots of interest (fold change≥1.5 and p-value<0.05). Interestingly, the two first components contributed to 59.4% of the variance of the analysis (Figure 1A).

Due to protein spot size and the different staining used for protein identification, 26 protein spots out of the 39 protein spots of interest (fold change ≥ 1.5 and a Student's t test p-value<0.05) could be picked up for MS identification (supplemental Table 2, 3 and 4). Only 4 and 6 different proteins spots were differentially expressed between VSMC from TAB^+-GCA compared to GCA-controls or TAB^--GCA respectively (fold change ≥ 2.0 and a Student's t test p-value<0.05) and results of MS are detailed in Table 2 and 3 respectively. Among identified proteins we found myosin and cytoskeleton proteins. Interestingly, peptidylpropyl isomerase A (PPIA), an enzyme involved in the folding of proteins which is expressed during inflammatory condition and annexin A5, an anticoagulant protein were overexpressed in VSMC from GCA-controls compared to VSMC from TAB^+-GCA (fold change 2.0, p=0.022

and fold change 1.6, p=0.04 respectively) (Figure 2). No protein with a fold change ≥ 2.0 and a Student's t test p-value<0.05 was identified in the comparison between VSMC from TAB$^-$-GCA and GCA-controls.

In order to compare cells from TAB with VSMC obtained in more physiological conditions, TAB$^+$-GCA were compared with HAoSMC and as much as 153 and 108 protein spots were differentially expressed (fold change ≥ 1.5 and ≥ 2.0 and a Student's t test p-value<0.05) respectively (Table 4 and supplemental Table 5). The 153 spots of interest and the 39 previously identified spots of interest were used for a PCA and results of the PCA reveal a huge difference between normal cell and cell obtained in pathological condition (Figure 1B). Among the 153 spots of interest, a huge number were involved in cytoskeleton (vimentin, tropomyosin, tubulin...) and in cell energy metabolism (glucose phosphate deshydrogenase, malate deshydrogenase, pyruvate kinase...). Using IPA software, TGF-β, NF-κB as well as ET-1 and paxillin were identified as links between proteins differentially expressed in VSMC from patients with TAB$^+$-GCA and HAoSMC (Figure 3).

3.2. Genomic analysis

Additional analysis was performed with RNA extracted from VSMC from TAB$^+$-GCA, TAB$^-$-GCA and GCA-controls. All data have been deposited in NCBI's Gene Expression Omnibus [19] and are accessible through GEO Series accession number GSExxx (http://www.ncbi.nlm.nih.gov/geo/query/acc.cgi?acc=GSExxx). Interestingly, a heatmap was generated with genes that were significantly differentially expressed between groups (three different comparisons, p≤0.05 and fold change ≥1.5) and we observe that all Pearson dissimilarity between groups was superior to dissimilarity within one group (Figure 4A). We then focused on genes that were differentially

expressed between VSMC from TAB^+-GCA and GCA-controls. Among the 166 genes, a number of them were involved in proliferation, contraction and migration (Figure 4B). Interstingly, tenascin, a protein involved in vascular remodelling was among the gene with the most increased ratio of expression in VSMC from TAB^+-GCA compared to GCA-controls. In addition, ET_AR and ET_BR expression was increased (fold change 1.93 and 2.83) in VSMC from TAB^+-GCA compared to GCA-controls even though it didn't reach statistical significance. Using IPA software, paxillin and ET-1 as well as growth factor receptor-bound protein 2 (Grb2) and Peroxisome proliferator-activated receptor gamma (Pparγ) were identified as potential link between genes of interest (Figure 5).

3.3. Endothelin-1 in vascular lesion of GCA

The previous results support the idea that paxillin and ET-1 might be involved in the proliferation of VSMC in GCA lesions. In order to assess the role of the endothelin system, we performed immunochemistry experiments in temporal artery lesions of patients with biopsy-proven GCA. As shown in Figure 6A, there is a huge expression of ET-1 and its receptor ET_BR and to a less extent of ET_AR in temporal lesions of GCA. ET-1 and ET_BR mRNA were overexpressed in VSMC from patients with TAB^+-GCA compared to GCA-controls while this was not the case for ET_AR (Figure 6B).

3.4. Inhibition of the excessive proliferation of VSMC from patients with biopsy-proven giant cell arteritis

Cell proliferation was increased in VSMC from patients with TAB^+-GCA as compared to HAoSMC. Paxillin inhibition using siRNA reduced HAoSMC proliferation whereas

no significant effect was observed with VSMC from patients with TAB^+-GCA (Figure 7A). Stimulation of VSMC with ET-1 alone did not modify the proliferation rate of either HAoSMC or VSMC from patients with TAB^+-GCA. Macitentan, an ET_AR and ET_BR inhibitor, tended to decreased the proliferation of VSMC from patients with GCA^+-ACG and HAoSMC and the active metabolite of macitentan (ACT) significantly reduced proliferation of VSMC from patients with TAB^+-GCA (Figure 7B). Our results suggest that ET-1 inhibition might represent an interesting perspective in the treatment of patients with GCA, which is probably not the case of paxillin targeting.

4. DISCUSSION

In the present work, by culturing VSMC form TAB from patients with GCA and controls, we were able to identify that genes differentially expressed between VSMC from patients with proven GCA and controls were mostly involved in cell proliferation. We also found that β-catenin expression was increased in VSMC from patients with TAB^+-GCA at an mRNA level compared to VSMC from GCA-control. Translocation of this protein in the nucleus is associated with an increased expression of cyclin D1 and induces VSMC proliferation [20]. It has been shown that VSMC proliferation was mediated by β-catenin after MMP 9 and 12 exposures [21] and after stimulation by PDGF [22]. In addition, tenascin mRNA was also found elevated in VSMC from patients with TAB^+-GCA compared to VSMC from GCA-control. This extracellular protein synthesized by VSMC regulates proliferation, migration, differentiation, and survival in response to developmental and environmental cues [23]. It may regulate VSMC proliferation and favour neo-intimal hyperplasia in a mice model of arterial graft [24] and tenascin is elevated in familial forms of pulmonary artery hypertension [25]. In addition, annexin A5 protein was down regulated in VSMC from TAB^+-GCA compared to GCA control. This protein exerts anticoagulant properties and the role of anti-annexin A5 antibodies has been suggested to explain the thrombotic events during Behcet disease [26] and Takayasu arteritis [27]. In addition, we identified that myosin, a protein involved in cellular movement [28] is overexpressed in VSMC from patients with TAB^+-GCA. Altogether, the proteomic and genomic data suggest that VSMC in the arterial lesion of GCA have increased proliferative properties and that downregulation of annexin A5 might contribute to the occurrence of thrombotic events. Interestingly, the role of PPIA in the constitution of aortic aneurysm in a mice model has been demonstrated [29] and its down regulation at a protein level in VSMC from TAB^+-GCA

patients compared to GCA control might have protective properties. However, although our results might help to better understand the mechanisms underlying arterial occlusion and ischemic complication occurring in patients with GCA, additional work will be needed to precisely document these mechanisms.

Finally, FTH1 mRNA was increased in VSMC from TAB^{+}-GCA. This result suggests an increased production of ferritin although it was not confirmed in our proteomic experiments. FTH1 has been reported to be the target of auto-antibodies in GCA [30, 31]. Whereas increased of protein expression might contribute to trigger autoantibodies production either directed against FTH1 or other VSMC antigens remains however controversial [32].

Both proteomic and transcriptomic analyses identified paxillin and ET-1 as key activation pathways in VSMC from patients with biopsy proven GCA as compared to controls. Paxillin has already been found to be a regulator of VSMC growth in the context of pulmonary arterial hypertension [33]. However, in our preliminary experiments, we could not confirm its role in regulating VSMC proliferation in GCA. Additional experiments will be required in larger groups of patients in order to better evaluate the potential interest of targeting this molecule. As previously reported by Lozano and colleagues, we observed that ET-1, ET_AR and ET_BR expression was increased in TAB from patients with GCA as compared to controls, leading to the interpretation that ET-1 might be involved in the pathogenesis of GCA [12] and that ET-1 targeting might be a promising therapy to inhibit VSMC proliferation and vascular remodelling. Importantly, we demonstrated that macitentan, an endothelin receptor antagonist, was able to reduce proliferation of VSMC from patients with biopsy proven GCA. Macitentan is a dual ET_AR/ET_BR antagonist with a high affinity to ET_AR and ET_BR. In addition, its active metabolite has an increased affinity to ET_AR and it is

known that ET_AR is the main receptor expressed on VSMC which support the vasoconstriction properties of ET-1 [34]. In addition, it has been suggested that ET_BR might either act synergistically with ET_AR but might also clear ET-1 [35].

Our works has several limits. We were able to culture VSMC from TAB of a limited number of patients. Although we limited as much as possible the numbers of passages, in order to get enough cells to perform the experiments, VSMC from patients were cultured at least for four passages, which may influence transcriptomes and proteomes of these cells. We were not able to obtain VSMC from TAB from healthy individuals, for obvious reasons, and therefore used aorta VSMC as controls. Finally, important work will be needed to analyse the signalling pathways identified as potentially involved in the increased proliferation of VSMC from patients with GCA.

In conclusion, we bring new data regarding an increased proliferation of VSMC during GCA that might contribute to the remodelling of the vessel wall and arterial obliteration. ET-1 inhibition and specifically ET_AR/ET_BR inhibition with macitentan might reverse this phenotype and offer a promising therapeutic perspective in the treatment of patients with GCA.

Acknowledgements

This work was performed within the Département Hospitalo-Universitaire (DHU) autoimmune and hormonal diseases. AR received financial support from the Société Nationale Française de Médecine Interne (SNFMI), ARMIIC (Association pour la Recherche en Médecine Interne et en Immunologie Clinique) and GPM (Groupe Pasteur Mutualité). SL received a financial support from the DRCD of Assistance Publique-Hôpitaux de Paris. We would like to thank physician from the Internal

Medicine and Ophtalmology departments of Cochin and Hotel-Dieu hospitals (Paris) and Dupuytren hospital (Limoges) who recruited patients and performed temporal artery biopsies, respectively. We would like to thank the Genomic platform (Genom'IC) and the 3P5 proteomic platform (Institut Cochin, Paris) who performed the gene chip and the 2D-DIGE experiments respectively. We thank Actelion laboratories for providing us with macitentan and its active metabolite.

REFERENCES:

1. Hunder GG, Bloch DA, Michel BA, Stevens MB, Arend WP, Calabrese LH, Edworthy SM, Fauci AS, Leavitt RY, Lie JT, et al. The American College of Rheumatology 1990 criteria for the classification of giant cell arteritis. *Arthritis Rheum.* 1990;33(8):1122-1128.

2. Gonzalez-Gay MA, Barros S, Lopez-Diaz MJ, Garcia-Porrua C, Sanchez-Andrade A, Llorca J. Giant cell arteritis: disease patterns of clinical presentation in a series of 240 patients. *Medicine (Baltimore).* 2005;84(5):269-276.

3. Coffin-Pichonnet S, Bienvenu B, Mouriaux F. [Ophthalmological complications of giant cell arteritis]. *J Fr Ophtalmol.* 2013;36(2):178-183.

4. Liozon E, Ly KH, Robert PY. [Ocular complications of giant cell arteritis]. *Rev Med Interne.* 2013;34(7):421-430.

5. Ly KH, Regent A, Tamby MC, Mouthon L. Pathogenesis of giant cell arteritis: More than just an inflammatory condition? *Autoimmun Rev.* 2010;9(10):635-645.

6. Kaiser M, Weyand CM, Bjornsson J, Goronzy JJ. Platelet-derived growth factor, intimal hyperplasia, and ischemic complications in giant cell arteritis. *Arthritis Rheum.* 1998;41(4):623-633.

7. Kaiser M, Younge B, Bjornsson J, Goronzy JJ, Weyand CM. Formation of new vasa vasorum in vasculitis. Production of angiogenic cytokines by multinucleated giant cells. *Am J Pathol.* 1999;155(3):765-774.

8. Weyand CM, Goronzy JJ. Medium- and large-vessel vasculitis. *N Engl J Med.* 2003;349(2):160-169.

9. Rodriguez-Pla A, Bosch-Gil JA, Rossello-Urgell J, Huguet-Redecilla P, Stone JH, Vilardell-Tarres M. Metalloproteinase-2 and -9 in giant cell arteritis: involvement in vascular remodeling. *Circulation.* 2005;112(2):264-269.

10. Segarra M, Garcia-Martinez A, Sanchez M, Hernandez-Rodriguez J, Lozano E, Grau JM, Cid MC. Gelatinase expression and proteolytic activity in giant-cell arteritis. *Ann Rheum Dis.* 2007;66(11):1429-1435.

11. Dimitrijevic I, Andersson C, Rissler P, Edvinsson L. Increased tissue endothelin-1 and endothelin-B receptor expression in temporal arteries from patients with giant cell arteritis. *Ophthalmology.* 2010;117(3):628-636.

12. Lozano E, Segarra M, Corbera-Bellalta M, Garcia-Martinez A, Espigol-Frigole G, Pla-Campo A, Hernandez-Rodriguez J, Cid MC. Increased expression of the endothelin system in arterial lesions from patients with giant-cell arteritis: association between elevated plasma endothelin levels and the development of ischaemic events. *Ann Rheum Dis.* 2010;69(2):434-442.

13. Pache M, Kaiser HJ, Haufschild T, Lubeck P, Flammer J. Increased endothelin-1 plasma levels in giant cell arteritis: a report on four patients. *Am J Ophthalmol.* 2002;133(1):160-162.

14. Dib H, Chafey P, Clary G, Federici C, Le Gall M, Dwyer J, Gavard J, Tamas N, Bussone G, Broussard C, Camoin L, Witko-Sarsat V, Tamby MC, Mouthon L. Proteomes of umbilical vein and microvascular endothelial cells reflect distinct biological properties and influence immune recognition. *Proteomics.* 2012;12(15-16):2547-2555.

15. Rio DC, Ares M, Jr., Hannon GJ, Nilsen TW. Purification of RNA using TRIzol (TRI reagent). *Cold Spring Harb Protoc.* 2010;2010(6):pdb prot5439.

16. Dai M, Wang P, Boyd AD, Kostov G, Athey B, Jones EG, Bunney WE, Myers RM, Speed TP, Akil H, Watson SJ, Meng F. Evolving gene/transcript definitions

significantly alter the interpretation of GeneChip data. *Nucleic Acids Res.* 2005;33(20):e175.

17. Saada S, Marget P, Fauchais AL, Lise MC, Chemin G, Sindou P, Martel C, Delpy L, Vidal E, Jaccard A, Troutaud D, Lalloue F, Jauberteau MO. Differential expression of neurotensin and specific receptors, NTSR1 and NTSR2, in normal and malignant human B lymphocytes. *J Immunol.* 2012;189(11):5293-5303.

18. Gratzner HG. Monoclonal antibody to 5-bromo- and 5-iododeoxyuridine: A new reagent for detection of DNA replication. *Science.* 1982;218(4571):474-475.

19. Edgar R, Domrachev M, Lash AE. Gene Expression Omnibus: NCBI gene expression and hybridization array data repository. *Nucleic Acids Res.* 2002;30(1):207-210.

20. Quasnichka H, Slater SC, Beeching CA, Boehm M, Sala-Newby GB, George SJ. Regulation of smooth muscle cell proliferation by beta-catenin/T-cell factor signaling involves modulation of cyclin D1 and p21 expression. *Circ Res.* 2006;99(12):1329-1337.

21. Dwivedi A, Slater SC, George SJ. MMP-9 and -12 cause N-cadherin shedding and thereby beta-catenin signalling and vascular smooth muscle cell proliferation. *Cardiovasc Res.* 2009;81(1):178-186.

22. Zhong W, Oguljahan B, Xiao Y, Nelson J, Hernandez L, Garcia-Barrio M, Francis SC. Serum and glucocorticoid-regulated kinase 1 promotes vascular smooth muscle cell proliferation via regulation of beta-catenin dynamics. *Cell Signal.* 2014.

23. Imanaka-Yoshida K, Yoshida T, Miyagawa-Tomita S. Tenascin-C in development and disease of blood vessels. *Anat Rec (Hoboken).* 2014;297(9):1747-1757.

24. Sawada Y, Onoda K, Imanaka-Yoshida K, Maruyama J, Yamamoto K, Yoshida T, Shimpo H. Tenascin-C synthesized in both donor grafts and recipients accelerates artery graft stenosis. *Cardiovasc Res.* 2007;74(3):366-376.

25. Ihida-Stansbury K, McKean DM, Lane KB, Loyd JE, Wheeler LA, Morrell NW, Jones PL. Tenascin-C is induced by mutated BMP type II receptors in familial forms of pulmonary arterial hypertension. *Am J Physiol Lung Cell Mol Physiol.* 2006;291(4):L694-702.

26. Aslan H, Pay S, Gok F, Baykal Y, Yilmaz MI, Sengul A, Aydin HI. Antiannexin V autoantibody in thrombophilic Behcet's disease. *Rheumatol Int.* 2004;24(2):77-79.

27. Tripathy NK, Sinha N, Nityanand S. Anti-annexin V antibodies in Takayasu's arteritis: prevalence and relationship with disease activity. *Clin Exp Immunol.* 2003;134(2):360-364.

28. Betapudi V. Myosin II motor proteins with different functions determine the fate of lamellipodia extension during cell spreading. *PLoS One.* 2010;5(1):e8560.

29. Satoh K, Nigro P, Matoba T, O'Dell MR, Cui Z, Shi X, Mohan A, Yan C, Abe J, Illig KA, Berk BC. Cyclophilin A enhances vascular oxidative stress and the development of angiotensin II-induced aortic aneurysms. *Nat Med.* 2009;15(6):649-656.

30. Baerlecken NT, Linnemann A, Gross WL, Moosig F, Vazquez-Rodriguez TR, Gonzalez-Gay MA, Martin J, Kotter I, Henes JC, Melchers I, Vaith P, Schmidt RE, Witte T. Association of ferritin autoantibodies with giant cell arteritis/polymyalgia rheumatica. *Ann Rheum Dis.* 2012;71(6):943-947.

31. Regent A, Ly KH, Blet A, Agard C, Puechal X, Tamas N, Le-Jeunne C, Vidal E, Guillevin L, Mouthon L. Contribution of antiferritin antibodies to diagnosis of giant cell arteritis. *Ann Rheum Dis.* 2013;72(7):1269-1270.

32. Regent A, Dib H, Ly KH, Agard C, Tamby MC, Tamas N, Weksler B, Federici C, Broussard C, Guillevin L, Mouthon L. Identification of target antigens of anti-endothelial cell and anti-vascular smooth muscle cell antibodies in patients with giant cell arteritis: a proteomic approach. *Arthritis Res Ther.* 2011;13(3):R107.

33. Veith C, Marsh LM, Wygrecka M, Rutschmann K, Seeger W, Weissmann N, Kwapiszewska G. Paxillin regulates pulmonary arterial smooth muscle cell function in pulmonary hypertension. *Am J Pathol.* 2012;181(5):1621-1633.
34. Levin ER. Endothelins. *N Engl J Med.* 1995;333(6):356-363.
35. Kelland NF, Kuc RE, McLean DL, Azfer A, Bagnall AJ, Gray GA, Gulliver-Sloan FH, Maguire JJ, Davenport AP, Kotelevtsev YV, Webb DJ. Endothelial cell-specific ETB receptor knockout: autoradiographic and histological characterisation and crucial role in the clearance of endothelin-1. *Can J Physiol Pharmacol.* 2010;88(6):644-651.
36. Shevchenko A, Loboda A, Ens W, Schraven B, Standing KG. Archived polyacrylamide gels as a resource for proteome characterization by mass spectrometry. *Electrophoresis.* 2001;22(6):1194-1203.

Figure 1. Comparison of proteomes of vascular smooth muscle cells from patients with giant cell arteritis and controls.

(A) Principal component analysis (PCA) of the protein spots differentially expressed in protein extracts from vascular smooth muscle cells (VSMC) from four patients with biopsy proven GCA (TAB^+-GCA), 4 patients with probable GCA (TAB^--GCA) and 4 patients without GCA (GCA-controls) in pH 3-11 gels by the DeCyderTM v7.0 EDA software module. Hierarchical clustering of protein spots differentially expressed in pH 3-11 gel displayed as a heat map and proportion of the variance extracted within the two first components of the PCA analysis are represented. (B) PCA analysis was performed with previous spots and addition of the protein spots of interest in the comparison of VSMC from TAB^+-GCA patients versus HAoSMC. Results of the analysis, the proportion of the variance extracted within the two first components and hierarchical clustering displayed as a heat map are shown in lower panel. The color scale goes from green (decreased protein expression) to black (no change in protein expression) and to red (increased protein expression). White color represents a spot which is not detected or not matched. (C).

GCA-controls: patients who underwent temporal artery biopsy and had a final diagnosis which was not GCA; HAoSMC: human aortic smooth muscle cell; PC: principal component; TAB^+-GCA: histology proven giant cell arteritis; TAB^--GCA: giant cell arteritis without histological evidence.

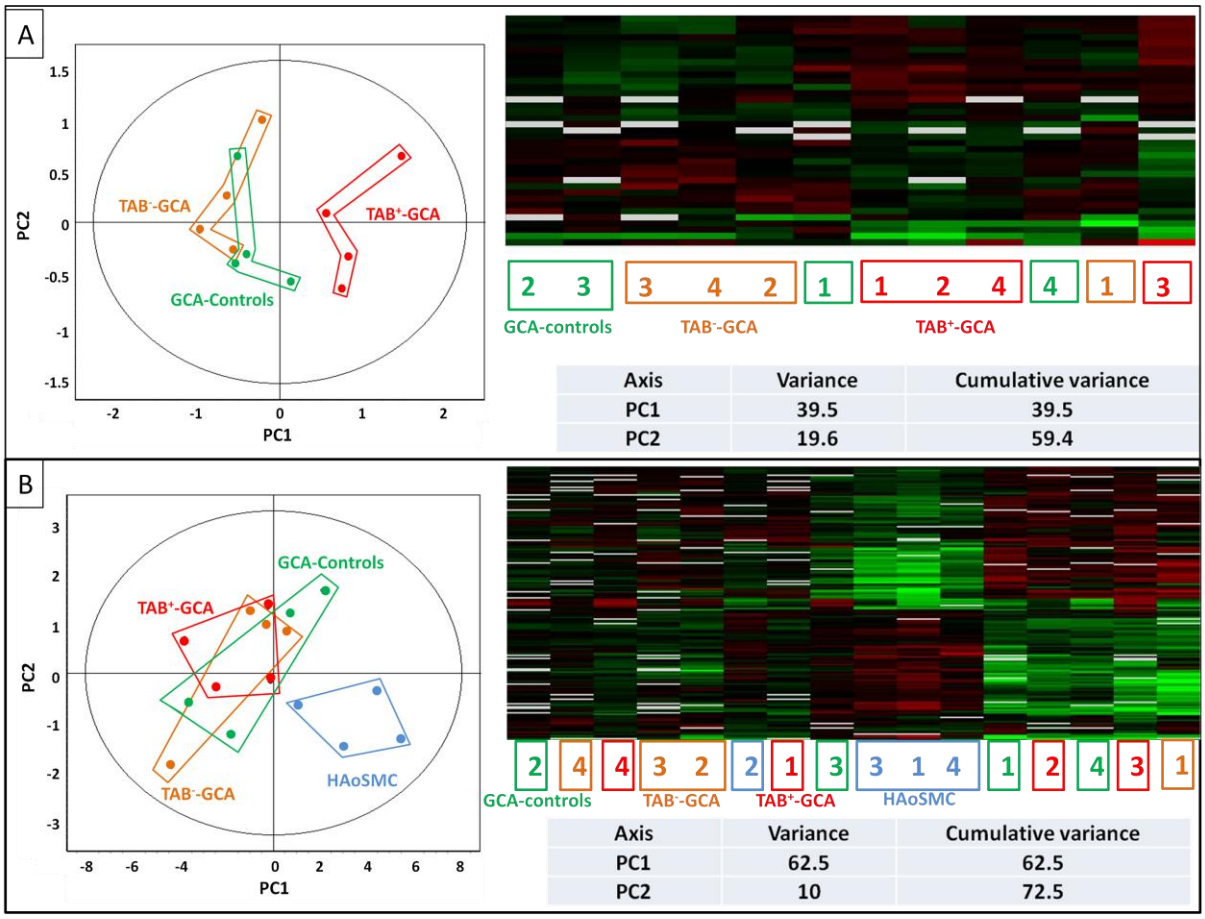

Axis	Variance	Cumulative variance
PC1	39.5	39.5
PC2	19.6	59.4

Axis	Variance	Cumulative variance
PC1	62.5	62.5
PC2	10	72.5

Figure 2. Differential expression of peptidylpropyl isomerase A in vascular smooth muscle cells from patients with giant cell arteritis and controls.

(A) 2D gel images of proteomes of VSMC of four individual donors in each group: biopsy proven GCA (TAB^+-GCA), probable GCA (TAB^--GCA), patients without GCA (GCA-controls) and normal human aortic VSMC (HAoSMC). The spot corresponding to peptidylpropyl isomerase A protein is outlined in black. (B) Peptidylpropyl isomerase A protein spots are expressed in 3 dimension view in one single donor GCA-control (upper panel) and one TAB^+-GCA (lower panel) representative protein extract. (C) Two dimension gel from a representative internal standard proteome: the selected area of the gel depicted in panel A containing the Peptidylpropyl isomerase A protein spot is delineated in blue.

HAoSMC: Human aortic smooth muscle cell; GCA-controls: patients who underwent temporal artery biopsy and had a final diagnosis which was not GCA; HAoSMC: human aortic smooth muscle cell; MW: molecular weight; pI: isoelectrofocalisation point; TAB^+-GCA: histology proven giant cell arteritis; TAB^--GCA: giant cell arteritis without histological evidence, VSMC: vascular smooth muscle cells

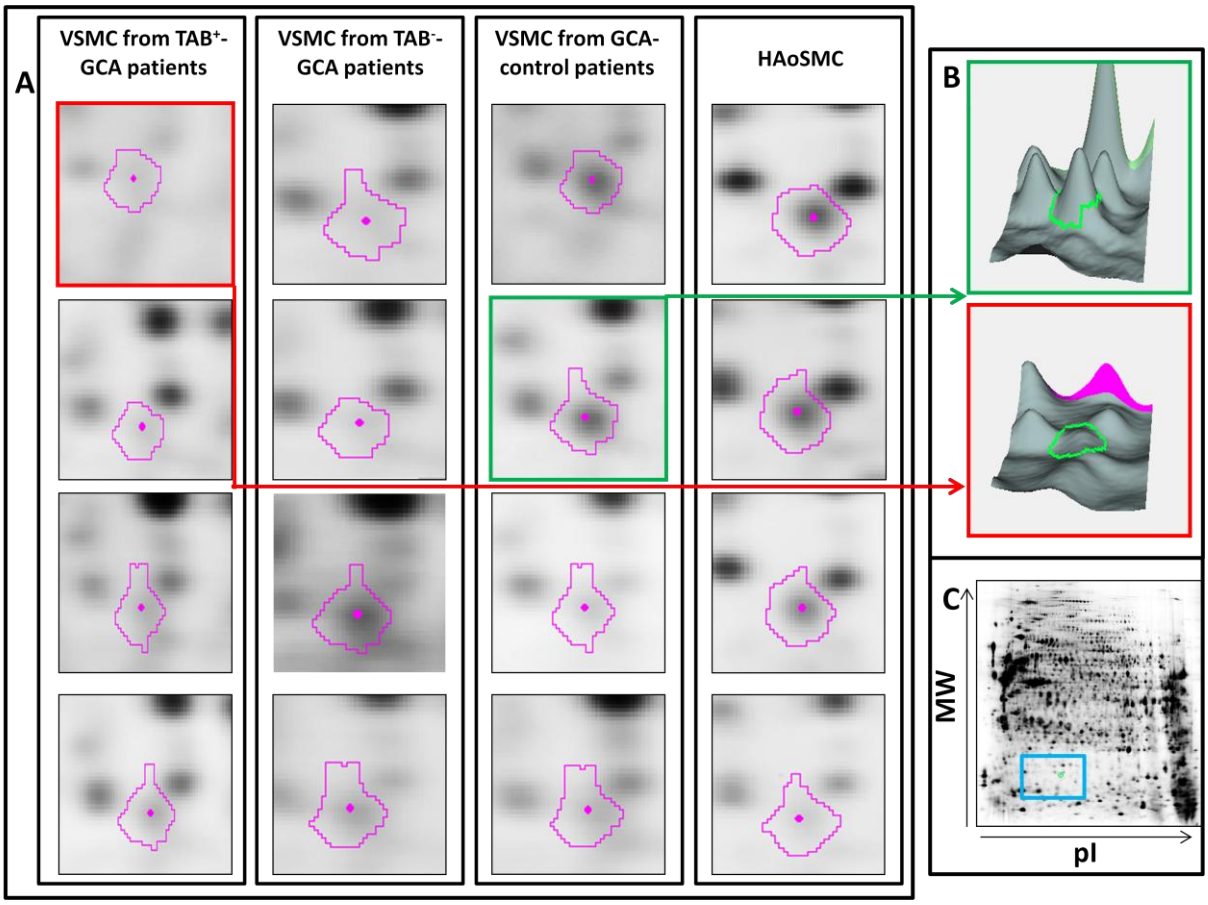
A
VSMC from TAB+-GCA patients
VSMC from TAB--GCA patients
VSMC from GCA-control patients
HAoSMC
B
C
MW
pI

Figure 3. Link between paxillin, endothelin and proteins of interest differentially expressed between VSMC from vascular smooth muscle cells from patients with giant cell arteritis and aortic smooth muscle cells

An ingenuity user-built network was generated by ingenuity pathway analysis (IPA) with proteins of interest identified in the comparison between vascular smooth muscle cells protein extract from histology proven giant cell arteritis patients and from normal aortic smooth muscle cells. Solid lines indicate direct interactions. Dashed lines indicate indirect interactions. Arrows indicate stimulation. Arrows indicate stimulation. The intensity of green and red molecule colors indicates the degree of up- or down regulation. A greater intensity of green represents a higher degree of down regulation, and a greater intensity of red represents a higher degree of up regulation. ACTB: Actin, cytoplasmic 1; ALDH18A1: Delta-1-pyrroline-5-carboxylate synthase; ALDH1B1: Aldehyde dehydrogenase X, mitochondrial; ANXA1: Annexin A1; ARPC2: Actin-related protein 2/3 complex subunit 2; CALD1: Caldesmon; CALPNS1: Calpain small subunit 1; CCT3: T-complex protein 1 subunit gamma; CKB: Creatine kinase B-type; COL1A2: Collagen alpha-2(I); COL6A2: Collagen alpha-2(VI) chain; COL6A3: Collagen alpha-3(VI); COTL1: Coactosin-like protein; CTTN: Src substrate cortactin; EDN1: endothelin 1; EEF1D: Elongation factor 1-delta; ENO1: Alpha-enolase; EZR: Ezrin; FLNA: Filamin-A; GADPH : Glyceraldehyde-3-phosphate dehydrogenase; GARS: Glycine--tRNA ligase; HNRNPA2B1: Heterogeneous nuclear ribonucleoproteins A2/B1; HSPA5: 78 kDa glucose-regulated protein; HSPA8: heat shock 70kDa protein 8; JNK: c-Jun NH(2)-terminal kinase; LMNA: Prelamin-A/C; LMNB1: Lamin-B1; MSN: Moesin; MVP: Major vault protein ; MYH9: Myosin-9; MYL6: Myosin light polypeptide 6; NF-κB: nuclear factor-kappa B; NPM1: Nucleophosmin; PAK: p21-activated kinase 1; P4HB: Protein disulfide-isomerase;

PDCD6IP: Programmed cell death 6-interacting protein; PDIA3: Protein disulfide-isomerase A3; PLC: PLOD1: Procollagen-lysine,2-oxoglutarate 5-dioxygenase 1; PXN: paxillin; RAB2A: Ras-related protein Rab-2A; RHOA: Transforming protein RhoA; ROCK: Rho associated protein kinase; RPL22: 60S ribosomal protein L22; SERPIN: Plasminogen activator inhibitor 1; SPEG: SPEG complex locus; SPTAN1: Spectrin alpha chain; TGFβ: transforming growth factor β; TPM2: Tropomyosin beta chain; TUB1A1: Tubulin alpha-1A; TUBB2A: Tubulin beta-2A chain; VIM: Vimentin; WARS: Tryptophan--tRNA ligase

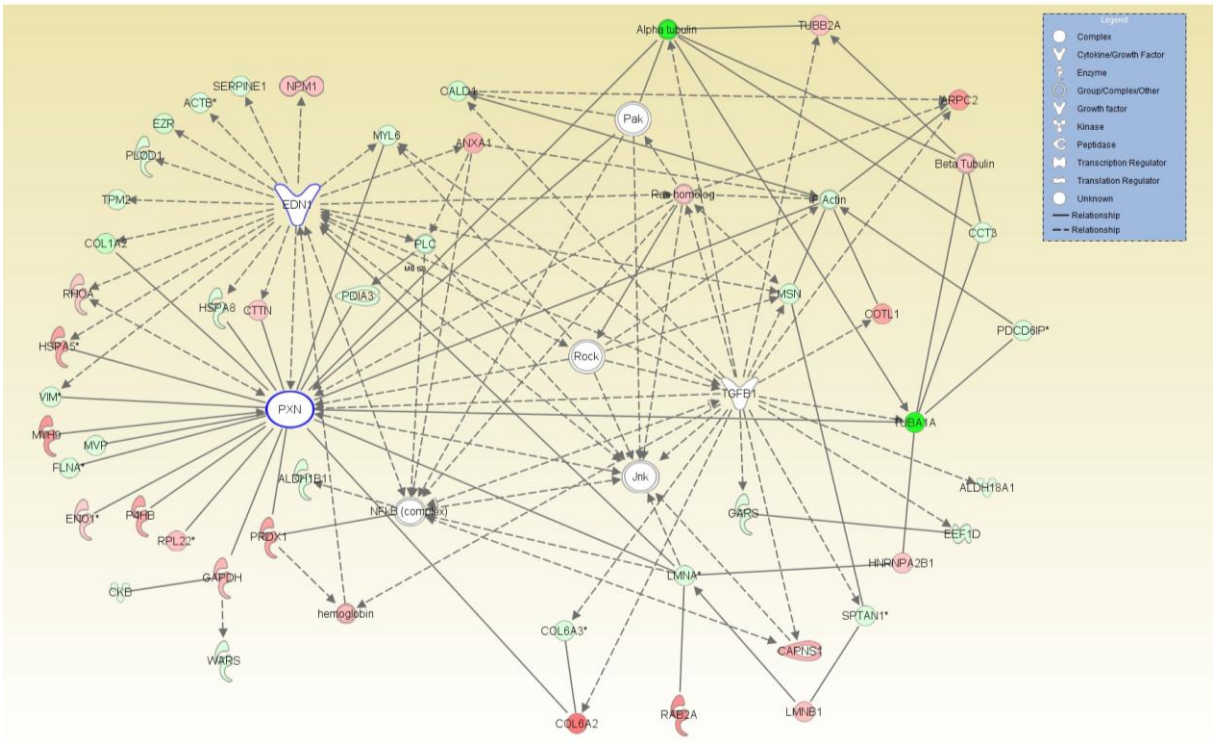

Figure 4. Gene-expression profiling in vascular smooth muscle cells from patients with giant cell arteritis and controls

(A) Hierarchical clustering of samples and genes of interest identified by a $p \leq 0.05$ and fold change ≥1.5 in at least one comparison between groups. Genes of interest are displayed as a heatmap and color scale goes from green (decreased protein expression) to black (no change in protein expression) to red (increased protein expression). (B) Diagram of genes of interest identified in the comparison of VSMC from TAB^+-VSMC patients versus GCA-controls and results extracted from ingenuity and pathway studio software regarding major functions of vascular smooth muscle cells analysis.

GCA-controls: patients who underwent temporal artery biopsy and had a final diagnosis which was not GCA; TAB^+-GCA: histology proven giant cell arteritis; TAB^--GCA: giant cell arteritis without histological evidence, VSMC: vascular smooth muscle cells

ACTG2: actin, gamma 2, smooth muscle, enteric; ACTVR1: activin A receptor, type I; ADI1: acireductone dioxygenase 1; ARMCX2: armadillo repeat containing, X-linked 2; CD46: CD46 molecule, complement regulatory protein; CITED2: Cbp/p300-interacting transactivator, with Glu/Asp-rich carboxy-terminal domain, 2; CNN2: calponin 2; COX7A1: cytochrome c oxidase subunit VIIa polypeptide 1; CTNNB1: catenin (cadherin-associated protein), beta 1, 88kDa; CXCR7: chemokine (C-X-C motif) receptor 7; DGKA: diacylglycerol kinase, alpha 80kDa; EDN-1: endothelin-1; ENTDP1: ectonucleoside triphosphate diphosphohydrolase 1; FBXO32: F-box protein 32; FST: follistatin; FTH1: ferritin, heavy polypeptide 1; GADD45A: growth arrest and DNA-damage-inducible, alpha; HMGCR: 3-hydroxy-3-methylglutaryl-CoA reductase; ITGA1: integrin, alpha 1; PEA15: phosphoprotein enriched in astrocytes

15; PIK3R3: phosphoinositide-3-kinase, regulatory subunit 3 (gamma); PIP4K2A: phosphatidylinositol-5-phosphate 4-kinase, type II, alpha; PLN: phospholamban; PODXL: podocalyxin-like; SWAP70: SWAP switching B-cell complex 70kDa subunit; TNC: tenascin; TXNIP: thioredoxin interacting protein

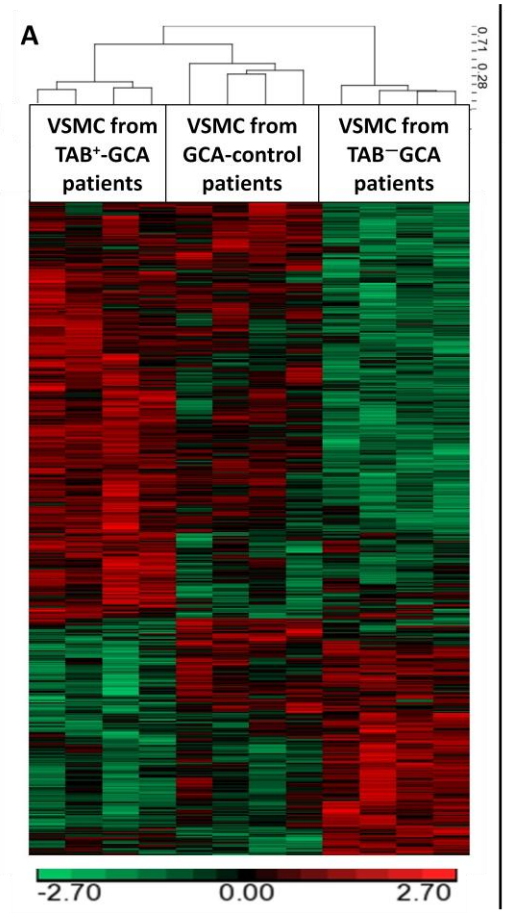

B

Analysis between VSMC from TAB⁺-GCA versus GCA-control patients

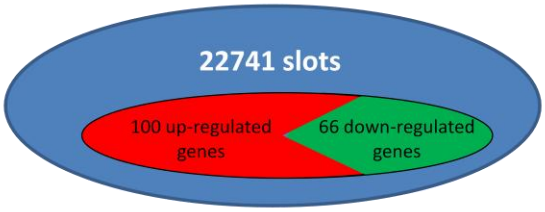

PATHWAYS	Up-regulated genes	Down-regulated genes
PROLIFERATION	PI3KR3, CTNNB1,TNC,HMGCR	
APOPTOSIS of SMC and p53 SIGNALING	PI3KR3, CTNNB1	GADD45A
CONTRACTILITY	ENTPD1, FBXO32, PLN	TXNIP, COX7A1
CELL MIGRATION	CD46, DGKA, ACTG2, ITGA1, PODXL, CTNNB1, CXCR7, ACVR1, HMGCR, ARMCX2, SNCS, TNC	PIP4K2A, CNN2, FST, TXNIP, CITED2, ADI1, FTH1, PEA15, SWAP70
CELL DIFFERENTIATION	ACVR1, CTNNB1	

Figure 5. Link between paxillin, endothelin and genes of interest differentially expressed between VSMC from patients with biopsy proven GCA and controls.

An ingenuity user-built network was generated by ingenuity pathway analysis (IPA) with identified genes showing major differences in expression between vascular smooth muscle cells (VSMC) from four patients with biopsy proven GCA (TAB^+-GCA) and 4 patients without GCA (GCA-controls). Solid lines indicate direct interactions. Dashed lines indicate indirect interactions. Arrows indicate stimulation. The intensity of green and red molecule colors indicates the degree of up- or down regulation. A greater intensity of green represents a higher degree of down regulation, and a greater intensity of red represents a higher degree of up regulation.

ACTG2: actin, gamma 2, smooth muscle, enteric; ACKR3: atypical chemokine receptor 3; CTNNB1: catenin (cadherin-associated protein), beta 1, 88kDa; DGKA: diacylglycerol kinase, alpha 80kDa; FST: follistatin; FTH1: ferritin, heavy polypeptide 1; GADD45A: growth arrest and DNA-damage-inducible, alpha; GRB2:

Growth factor receptor-bound protein 2; HIVEP1: human immunodeficiency virus type I enhancer binding protein 1; HMGCR: 3-hydroxy-3-methylglutaryl-CoA reductase; ITGA1: integrin, alpha 1; ITGA4: integrin, alpha 4; MCC: mutated in colorectal; cancers; MERTK: c-mer proto-oncogene tyrosine kinase; MEST: mesoderm specific transcript homolog (mouse); NR3C1: glucocorticoid receptor; PAX: paxillin; PCOLCE: procollagen C-endopeptidase enhancer; PEA15: phosphoprotein enriched in astrocytes 15; PIK3R3: phosphoinositide-3-kinase, regulatory subunit 3 (gamma); PLCB4: phospholipase C, beta 4; PPARγ: peroxisome proliferator-activated receptor gamma; RAB8B: RAB8B, member RAS oncogene family; RBMS2: RNA binding motif, single stranded interacting protein 2; RPS23: ribosomal protein S23; SAT1: spermidine/spermine N1-acetyltransferase 1; SMU1: smu-1 suppressor of mec-8 and

unc-52 homolog (candida); SNCA: synuclein, alpha; TNC: tenascin; UBQLN4: ubiquilin 4.

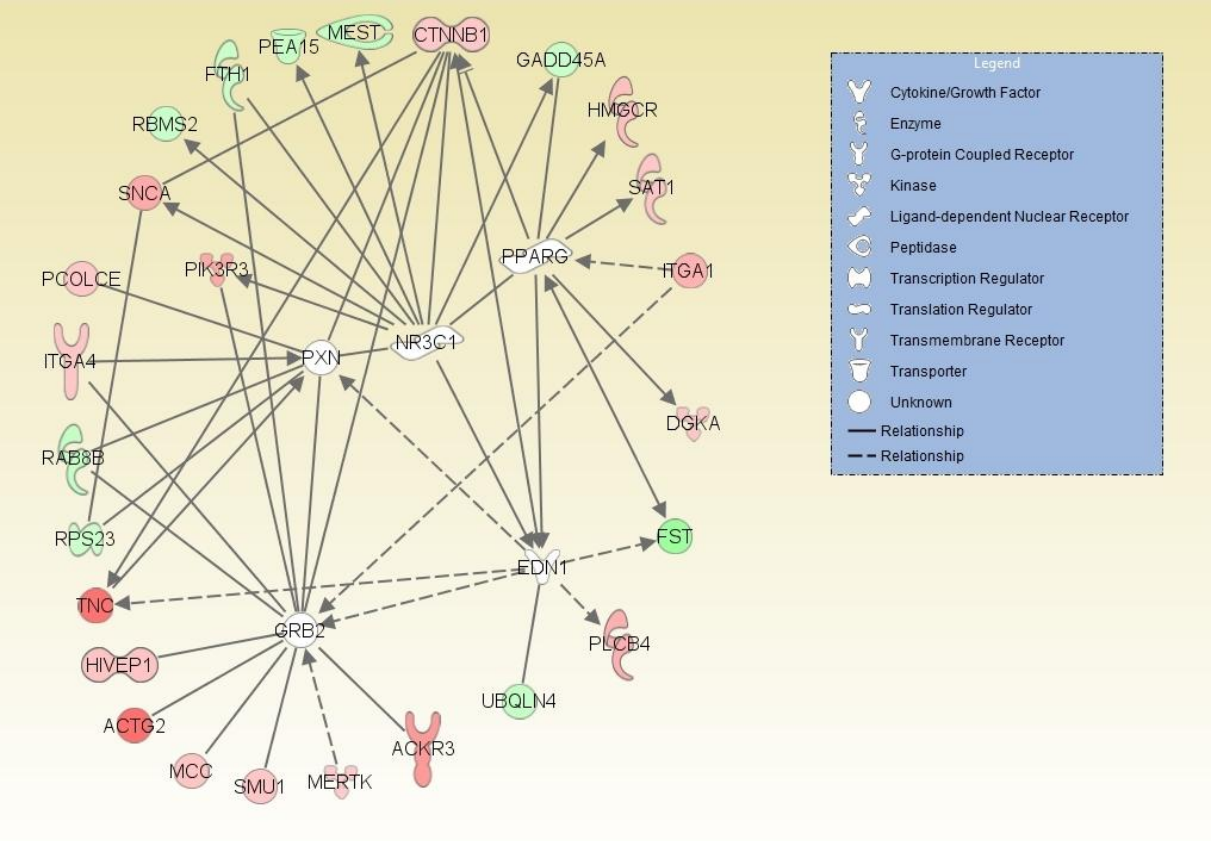

Figure 6. Protein and gene expression of endothelin 1 and its receptors ET_AR and ET_BR in temporal artery biopsy from patients with giant cell arteritis.

A. Tissue expression of endothelin-1 (ET-1), ET_AR and ET_BR by immunochemistry performed on frozen sections of temporal arteries from patients with biopsy proven GCA (n=3) (magnificence x100 and x200). B. Quantitative PCR of ET-1, ET_AR and ET_BR performed on vascular smooth muscle cells (VSMC) isolated from 6 patients with TAB^+-GCA and 6 patients without GCA (GCA-controls). Results are normalized with hypoxanthine-guanine phosphoribosyl transferase housekeeping gene and expressed as a fold change compared to VSMC from GCA-controls.

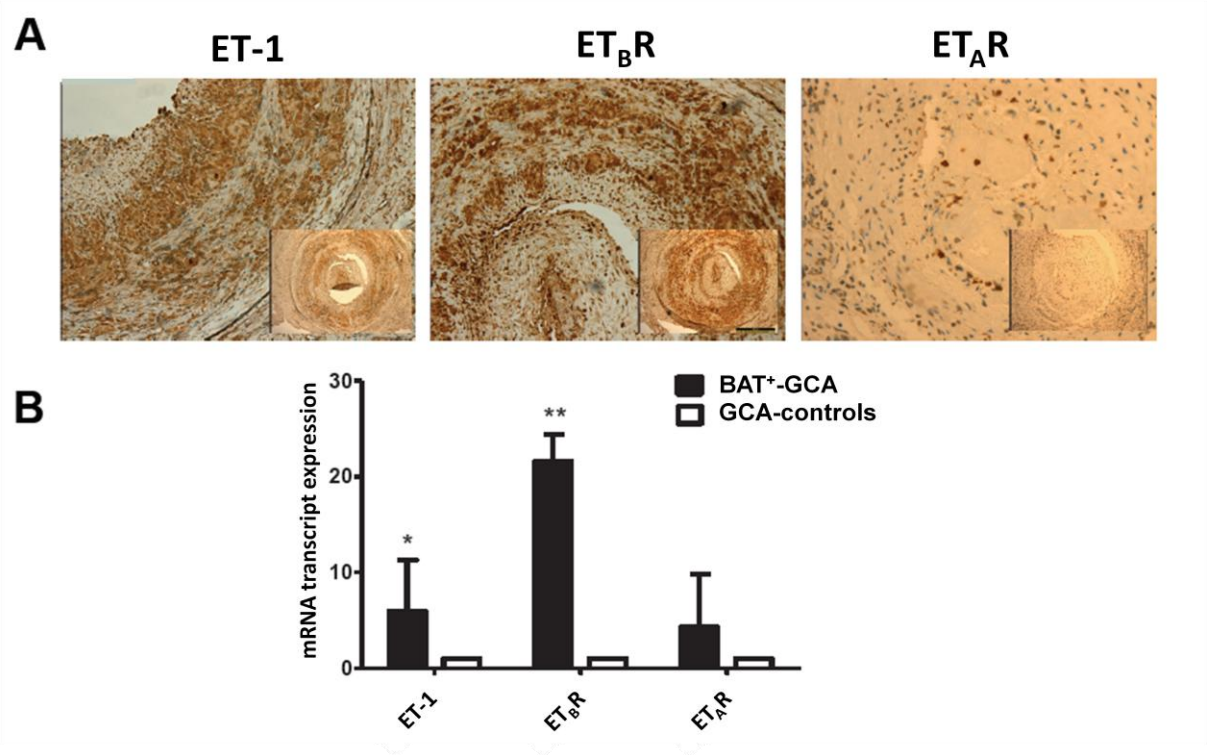

Figure 7. Effect of paxillin inhibition and endothelin receptor antagonist on the proliferation of vascular smooth muscle cells (VSMC) from patients with giant cell arteritis

Proliferation of VSMC from patients with TAB$^+$-GCA was compared to HAoSMC. Cells at the six passage were serum starved during 24 hours and then incubated during 72 hours with paxillin siRNA (A) or with/without 100mM endothelin 1, macitentan or its active metabolite (B). After incubation, proliferation was measured by BrdU incorporation during 24 hours.

ACT: active metabolite of macitentan, ET-1: endothelin 1, GCA: giant cell arteritis, HAoSMC: human aortic smooth muscle cell, MCT: macitentan, TAB: temporal artery biopsy, VSMC: vascular smooth muscle cell

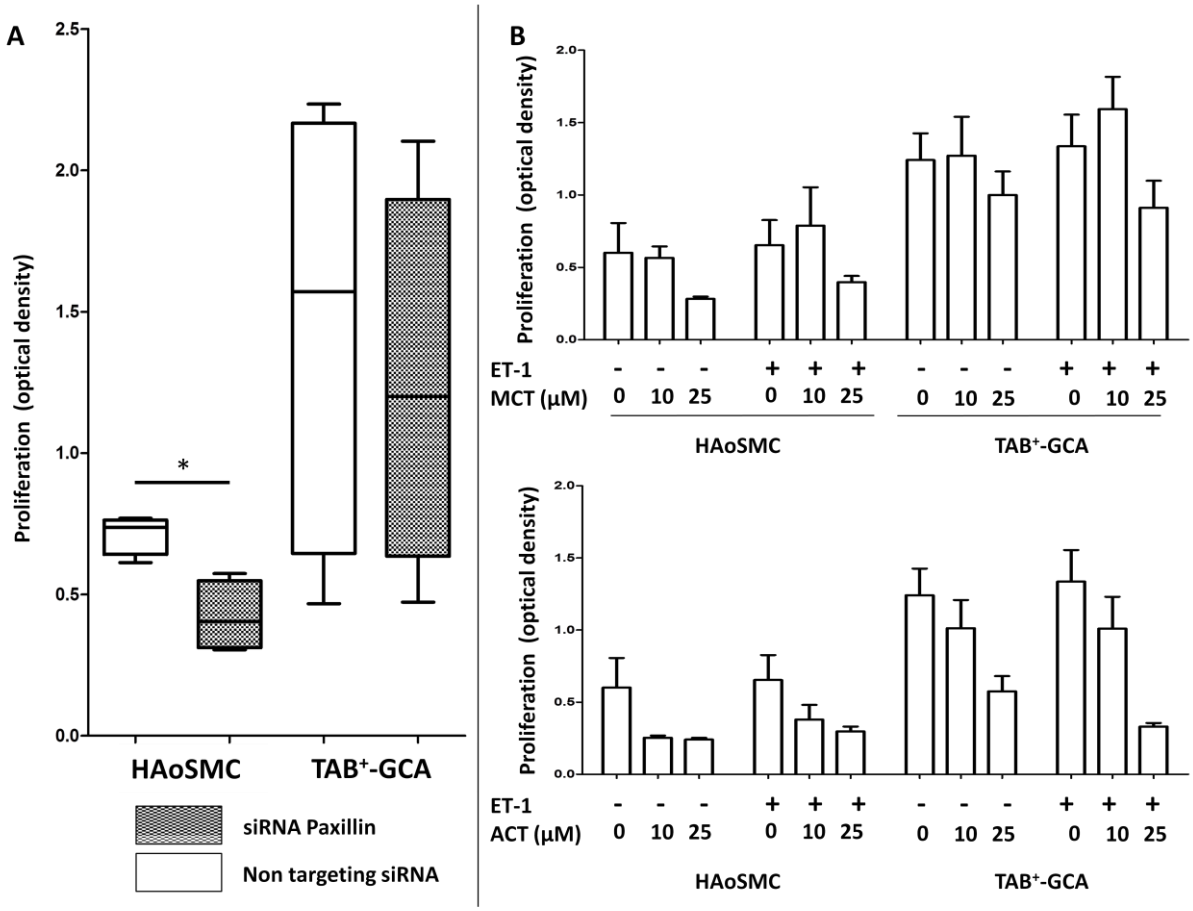

Table 1. Number of protein spots differentially expressed between smooth muscle cells from patients with giant cell arteritis and controls

	TAB^+VSMC versus Control-VSMC	TAB^+VSMC versus TAB^-VSMC	TAB^-VSMC versus Control-VSMC	TAB^+VSMC versus HAoSMC
Number of proteins differentially expressed (fold change 1.5)				
Number of proteins overexpressed	4	15	1	85
Number of proteins underexpressed	12	15	1	68
Number of proteins differentially expressed (fold change 2.0)				
Number of proteins overexpressed	1	6	1	57
Number of proteins underexpressed	4	4	0	51

Control-VSMC: vascular smooth muscle cells from temporal artery of patients who underwent temporal artery biopsy and had a final diagnosis which was not GCA; TAB^+-VSMC: vascular smooth muscle cell from temporal artery of histology proven giant cell arteritis; TAB^--GCA: vascular smooth muscle cell from temporal artery of giant cell arteritis without histological evidence, VSMC: vascular smooth muscle cells

Table 2: Proteins differentially expressed between smooth muscle cells from patients with biopsy-proven giant cell arteritis and controls (fold change ≥2.0 and p≤0.05)

SPOT	T-test	Fold change	IDENTIFIED PROTEIN	NAME	Exp pI	Exp MM	Theo pI	Theo MM	Total ion Score	Best ion Score	Number of identified peptides
1271	2.6E-02	-2.8	26S protease regulatory subunit 4	PRS4	6.6	60	5.9	49	943	96	18
1060	3.9E-02	-2.5	Phosphoenolpyruvate carboxykinase [GTP], mitochondrial	PCKGM	8.1	69	6.6	67	877	84	18
3085	2.2E-02	-2.0	Peptidyl-prolyl cis-trans isomerase A	PPIA	6.1	17	7.7	18	69	43	2
728	1.9E-02	2.0	Myosin-9 & Src substrate cortactin	MYH9 & SRC8	5.5	84	5.2 & 5.2	43 & 62	1420	113	27

Exp: experimental; MM: molecular mass; pI: isoelectrofocalisation point; Theo: theoretical. Relative quantification and statistical evaluation were carried out with DeCyderTM 2D software (GE Healthcare, version 7.0). Down or up-expressed proteins between groups were retained if protein spot fold change was larger than +1.5 or smaller than –1.5 and a Student's t-test p-value less than 0.05

Table 3: Proteins differentially expressed between vascular smooth muscle cells from patients with biopsy-proven and biopsy-negative giant cell arteritis (fold change ≥2.0 and p≤0.05)

SPOT	T-test	Fold Change	IDENTIFIED PROTEIN	NAME	Exp pI	Exp MM	Theo pI	Theo MM	Total ion Score	Best ion Score	Number of identified peptides
3300	1.3E-02	-2.5	Hemoglobin subunit alpha	HBA	8.5	14	8.7	15	64	37	2
1271	4.0E-02	-2.1	26S protease regulatory subunit 4	PRS4	6.6	60	5.9	49	943	96	18
731	3.3E-02	2.1	Myosin-9 & Src substrate cortactin	MYH9 & SRC8	5.6	84	8.8 & 5.2	354 & 62	2165 & 643	112 & 95	36 & 12
728	2.1E-02	2.2	Myosin-9 & Src substrate cortactin	MYH9 & SRC8	5.5	84	5.2 & 5.2	43 & 62	1420	113	27
829	2.3E-03	2.3	Heterogeneous nuclear ribonucleoprotein U & 78 kDa glucose-regulated	HNRPU & GRP78	4.9	79	5.8 & 5	90 & 70	390 & 168	64 & 70	9 & 3
954	2.8E-03	2.6	78 kDa glucose-regulated protein & Peptidyl-prolyl cis-trans isomerase & Stress-70 protein	GRP78 & FKB10 &GRP75	5.3	73	5 & 5.3 & 5.4	70 & 61 & 69	1690 & 1069 & 612	111 & 95 & 69	27 & 20 & 14

Exp: experimental; MM: molecular mass; pI: isoelectrofocalisation point; Theo: theoretical. Relative quantification and statistical evaluation were carried out with DeCyderTM 2D software (GE Healthcare, version 7.0). Down or up-expressed proteins between groups were retained if protein spot fold change was larger than +1.5 or smaller than –1.5 and a Student's t-test p-value less than 0.05

Table 4: Proteins differentially expressed between patients with vascular smooth muscle cells from patients with biopsy-proven giant cell arteritis and normal human aorta (fold change ≥2.0 and p≤0.05)

SPOT	T-test	Fold change	IDENTIFIED PROTEIN	NAME	Exp pI	Exp MM	Theo pI	Theo MM	Total ion Score	Best ion Score	Number of identified peptides
1349	2.0E-02	-17.2	Vimentin & Tubulin alpha-1A	VIME & TBA1A	5.3	57	5.1 & 4.9	54 & 50	2616 & 1092	116 & 95	50 & 20
240	3.6E-03	-4.3	Collagen alpha-2(I)	CO1A2	10.0	113	10.1	92	605	93	10
222	4.7E-02	-4.2	Vigilin	VIGLN	7.6	114	6.4	141	476	65	11
747	2.6E-02	-4.0	Putative pre-mRNA-splicing factor ATP-dependent RNA helicase DHX15	DHX15	8.5	84	7.1	91	663	69	14
1233	4.5E-02	-3.9	Dihydropyrimidinase-related protein 3 & Carnitine O-palmitoyltransferase 1, liver isoform &	DPYL3 & CPT1A	7.2	62	6 & 8.9	62 & 88	878 & 387	98 & 81	14 & 7
664	4.1E-02	-3.7	Elongation factor 2	EF2	7.9	88	6.4	95	1342	92	25
1060	3.6E-05	-3.5	Phosphoenolpyruvate carboxykinase [GTP], mitochondrial	PCKGM	8.1	69	6.6	67	877	84	18
826	1.5E-02	-3.4	TATA-binding protein-associated factor 2N	RBP56	8.8	80	8	62	19	57	3
860	2.2E-02	-3.4	Ezrin & Caldesmon	EZRI & CALD1	7.0	78	6 & 5.6	69 & 93	950 & 628	100 & 100	21 & 11
1420	2.7E-02	-3.2	V-type proton ATPase subunit B, brain isoform	VATB2	6.0	55	5.6	57	1498	113	23
461	4.8E-02	-3.2	Kinesin-1 heavy chain	KINH	7.0	99	6.1	110	395	89	8
640	9.5E-03	-2.9	Procollagen-lysine,2-oxoglutarate 5-dioxygenase 2	PLOD2	7.2	89	6.2	82	806	86	16
626	1.1E-02	-2.9	Programmed cell death 6-interacting protein & Procollagen-lysine,2-oxoglutarate 5-dioxygenase 2	PDC6I & PLOD2	7.1	89	6.1 & 6.2	96 & 82	1712 & 561	89 & 82	35 & 11

933	4.7E-02	-2.8	Prelamin-A/C & Moesin	LMNA & MOES	7.3	74	6.6 & 6.1	74 & 68	1594 & 1372	104 & 94	31 & 26
1967	6.7E-03	-2.6	Tropomyosin beta chain	TPM2	4.8	38	4.7	33	814	79	18
458	2.3E-02	-2.6	Kinesin-1 heavy chain	KINH	7.1	99	6.1	110	1444	100	28
522	3.8E-02	-2.6	Major vault protein & Ubiquitin-like modifier-activating enzyme 1	MVP & UBA1	5.7	96	5.3 & 6.4	99 & 95	1719 & 660	101 & 80	32 & 13
632	1.1E-02	-2.6	Programmed cell death 6-interacting protein & Procollagen-lysine,2-oxoglutarate 5-dioxygenase 2 & Filamin-A	PDC6I & PLOD2 & FLNA	7.0	89	6.1 & 6.2 & 5.7	96 & 82 & 281	917 & 567 & 662	100 & 92 &80	18 & 11 & 15
645	1.3E-02	-2.6	Procollagen-lysine,2-oxoglutarate 5-dioxygenase 2 & Filamin-A	PLOD2 & FLNA	6.8	89	6.2 & 5.7	82 & 281	783 & 581	86 & 82	15 & 12
1403	4.1E-02	-2.3	Vimentin	VIME	5.3	55	5.1	54	2111	115	40
633	3.8E-02	-2.3	Procollagen-lysine,2-oxoglutarate 5-dioxygenase 2	PLOD2	7.3	89	6.2	82	874	72	17
823	4.2E-02	-2.3	Delta-1-pyrroline-5-carboxylate synthase & Procollagen-lysine,2-oxoglutarate 5-dioxygenase 1	P5CS & PLOD1	7.5	80	6.7 & 6.5	87 & 82	993 & 398	90 & 59	19 & 10
1745	5.0E-02	-2.1	DnaJ homolog subfamily B member 11	DJB11	6.8	44	5.8	38	721	105	13
1714	2.6E-03	-2.1	Actin, cytoplasmic 1	ACTB	5.3	45	5.3	42	921	125	15
1423	4.2E-02	-2.0	Pyruvate kinase isozymes M1/M2 & Aldehyde dehydrogenase X, mitochondrial	KPYM & AL1B1	7.1	55	8.0 & 6.0	58 & 55	797 & 656	88 & 86	15 & 12
3550	2.6E-02	2.1	Hemoglobin subunit beta	HBB	4.8	11	6.8	16	201	103	7
3300	2.2E-02	2.1	Hemoglobin subunit alpha	HBA	8.5	14	8.7	15	64	37	2
2247	2.2E-02	2.2	Alpha-enolase & Proteasome activator complex subunit 3	ENOA & PSME3	6.2	31	7 & 5.7	47 & 29	379 & 365	92 & 69	6 & 7
2713	2.3E-02	2.2	Transgelin & Peptidyl-prolyl cis-trans isomerase B & Glyceraldehyde-3-phosphate dehydrogenase	TAGL & PPIB & G3P	10.2	22	8.9 & 9.3 & 8.6	22 & 20 & 36	265 & 249 & 276	72 & 73 & 76	5 & 5 & 5

2534	2.7E-02	2.4	Triosephosphate isomerase & Protein ETHE1, mitochondrial	TPIS & ETHE1	7.0	26	5.7 & 6.4	31 & 27	611 & 342	95 & 79	10 & 6
2522	1.9E-02	2.4	Annexin A1 & Cathepsin B & Inorganic pyrophosphatase	ANXA1 & CATB & IPYR	5.2	26	6.6 & 5.2 & 5.5	39 & 28 & 33	587 & 309 & 56	101 & 90 & 30	9 & 5 & 2
3433	1.6E-02	2.4	Malate dehydrogenase, cytoplasmic	MDHC	4.7	12	6.9	36	107	51	3
1361	1.9E-02	2.4	Prelamin-A/C	LMNA	8.9	57	6.6	74	1710	116	32
3464	1.6E-02	2.4	40S ribosomal protein S14	RS14	9.3	12	10.1	16	151	71	3
2555	9.4E-03	2.5	14-3-3 protein gamma & Calpain small subunit 1 & 14-3-3 protein eta	1433G & CPNS1 & 1433F	5.1	26	4.8 & 5.1 & 4.8	28 & 28 & 28	126 & 125 & 73	53 & 67 & 45	3 & 2 & 2
2343	1.9E-02	2.6	Cathepsin D	CATD	6.1	29	5.6	38	602	117	9
3193	3.3E-03	2.7	Coactosin-like protein	COTL1	5.5	15	5.5	16	364	57	9
1426	3.4E-02	2.7	Endoplasmin & Vimentin & Protein disulfide-isomerase	ENPL & VIME & PDIA1	4.8	55	4.7 & 5.1 & 4.7	90 & 54 & 55	803 & 624 & 535	102 & 76 & 87	12 & 13 & 15
3413	1.2E-02	2.8	40S ribosomal protein S3	RS3	10.4	13	9.7	27	310	68	5
2317	4.5E-02	2.9	Exosome complex component MTR3 & 78 kDa glucose-regulated protein & Proteasome subunit alpha type-1	EXOS6 & GRP78 & PSA1	7.1	30	6.1 & 5 & 6.2	28 & 70 & 30	510 & 408 & 263	103 & 65 & 81	9 & 8 & 4
3089	4.6E-02	2.9	Transgelin & Peroxiredoxin-1	TAGL & PRDX1	7.6	17	8.9 & 8.3	22 & 22	153 & 70	63 & 44	3 & 2
3312	4.3E-02	2.9	Profilin-1	PROF1	8.3	14	8.5	15	71	43	2
1611	1.1E-02	3.0	Prelamin-A/C & Fumarate hydratase, mitochondrial	LMNA & FUMH	8.0	49	6.6 & 7	74 & 50	1172 & 357	80 & 92	23 & 5
290	4.2E-02	3.1	Collagen alpha-1(VI) chain & Spectrin alpha chain,	CO6A1 & SPTA2	5.3	109	5.2 & 5.2	106 & 285	1152 & 497	110 & 67	19 & 13
1744	3.8E-02	3.1	Vimentin	VIME	4.8	44	5.1	54	1895	97	37
2438	4.0E-02	3.1	6-phosphogluconolactonase & Actin-	6PGL &	6.3	28	5.7 &	27 &	491 &	77 & 57	9 & 8

			related protein 2/3 complex subunit 2	ARPC2			6.8	34	344		
298	4.8E-02	3.2	Hypoxia up-regulated protein 1 & Collagen alpha-1(VI) chain & Myosin-9	HYOU1 & CO6A1 & MYH9	5.4	115	5.1 & 5.2 & 5.5	108 & 106 & 226	1363 & 1050 & 831	105 & 95 & 90	34 & 14 & 16
2280	3.6E-03	3.3	Cathepsin B & Alpha-soluble NSF attachment protein	CATB & SNAA	5.4	31	5.2 & 5.2	28 & 33	533 & 109	92 & 74	9 & 2
3536	3.0E-02	3.4	Profilin-1 & Guanine nucleotide-binding protein G(I)/G(S)/G(O) subunit gamma-12 & Histone H2B type 1-B	PROF1 & GBG12 & H2B1B	10.7	11	8.5 & 9.1 & 10.3	15 & 8 & 14	232 & 209 & 155	72 & 67 & 64	5 & 4 & 4
2700	4.2E-02	3.5	Aldehyde dehydrogenase, mitochondrial & Ras-related protein Rab-2A	ALDH2 & RAB2A	6.1	23	5.7 & 6.1	54 & 23	553 & 337	92 & 90	9 & 6
1115	4.9E-02	3.5	78 kDa glucose-regulated protein	GRP78	5.4	67	5	70	1362	97	21
2328	5.3E-04	3.6	Cathepsin B & Chloride intracellular channel protein 1	CATB & CLIC1	5.4	30	5.2 & 5.1	28 & 27	531 & 366	106 & 72	8 & 7
3419	1.9E-02	3.9	No identified protein		6.9	13					
294	4.8E-02	4.2	Collagen alpha-2(VI) chain	CO6A2	6.9	110	5.9	107	489	60	11
281	3.5E-02	6.3	Collagen alpha-2(VI) chain	CO6A1	6.5	110	5.2	106	792	86	15
3545	1.6E-02	6.4	Peroxiredoxin-5, mitochondrial	PRDX5	9.1	11	6.7	17	353	94	7
413	4.6E-02	7.6	Collagen alpha-3(VI)	CO6A3	7.8	101	6.2	341	721	93	15

Exp: experimental; MM: molecular mass; pI: isoelectrofocalisation point; Theo: theoretical. Relative quantification and statistical evaluation were carried out with DeCyderTM 2D software (GE Healthcare, version 7.0). Down or up-expressed proteins between groups were retained if protein spot fold change was larger than +1.5 or smaller than –1.5 and a Student's t-test p-value less than 0.05

Additional file 1: Detailed data concerning 2-D electrophoresis technique and mass spectrometry identification

Molecular analysis of vascular smooth muscle cells from patients with giant cell arteritis: targeting endothelin-1 receptor to control proliferation

Alexis Régent[1,2†], Kim Heang Ly[3,4†], Matthieu Groh[1,2], Chabha Khifer[1], Sébastien Lofek[1], Mathieu Tamby[1], Guilhem Clary[1], Philippe Chafey[1], Veronique Baud[1], Cédric Broussard[1], Christian Federici[1], François Labrousse[5], Laura Mesturoux[5], Claire Le-Jeunne[2], Elisabeth Vidal[3,4], Antoine Brezin[6], Véronique Witko-Sarsat[1], Loïc Guillevin[2], Luc Mouthon[1,2]

[†]both authors contributed equally to the work

Protein extraction

Vascular smooth muscle cells (VSMC) from patients with TAB^{+}-GCA, TAB^{-}-GCA, GCA-control and HAoSMC were used for proteomics experiments. Cells pellet (stored at -80°C) were lysed in lysis buffer (8M urea, 2M thiourea, 4% CHAPS, 60mM dithiothreitrol DTT). Then the protein extracts were clarified by ultra-centrifugation at 100.000g for 1 hour at 4°C. The separated supernatants were then treated with the 2D Clean-Up kit (GE Healthcare, Vélizy-Villacoublay, France) according to the manufacturer's instructions. The resultant dry pellets were resuspended into lysis buffer without DTT and centrifuged at 20,000g for 10 min at 4°C. Protein concentration was determined by the Quick Sart Bradford assay (Biorad, Hercules, California). Protein quantification and the quality of sample preparation were

controlled by 1D SDS-PAGE performed using Bio-Rad mini-Protean III electrophoresis system. Samples were diluted 1:1 (v/v) with 2 x SDS sample buffer and run on SDS-PAGE (T=12%) with 5µg protein per lane. The gels were visualized by staining using Bio-Safe Coomassie (Bio-Rad).

Protein labelling with CyDye DIGE fluor

DIGE Minimal labeling of protein samples was performed according to the manufacturer's instruction (GE Healthcare, Orsay, France). Briefly, samples (50µg) were labeled for 30 min on ice in the dark with 400 pmol Cy3 or Cy5 Fluor minimal dyes. Internal Standard, a pool of equal portions of each of the samples used for this study, was labeled with cy2. The reaction was stopped by adding 10 nmol lysine followed by incubation on ice for 10 min in the dark.

Two dimension in gel electrophoresis

Fifty µg of labelled samples (Cy3 or Cy5) and internal standard (Cy2) were mixed. Each mixed Cy-dye labelled protein extract (150µg) was added to rehydration buffer (8 M urea, 2 M thiourea, 2% (w/v) CHAPS, 1.2% (v/v) DeStreak Reagent (GE Healthcare), 0.5% (v/v) IPG buffer pH 3-11 NL (GE Healthcare) and bromophenol blue) in a final volume of 350µL and used to rehydrated pH 3-11NL IPG strips 18 cm (GE Healthcare) 24h at room temperature under low-viscosity paraffin oil.

Isoelectrofocusing was performed at 20°C using IPGphor3 (GE Healthcare) for a total of 40 kVh. At the end of focalisation, IPG strips were incubated consecutively for 15 min each in equilibration buffer I and II (Buffer I: 50 mM Tris-HCl (pH 6.8), 6 M urea, 2% Sodium Dodecyl Sulphate, 30% glycerol and 1% DTT; Buffer II: 50 mM Tris-HCl

(pH 6.8), 6 M urea, 2% Sodium Dodecyl Sulphate, 30% glycerol and 2.5% iodoacetamide) with gentle agitation.

Equilibrated strips were placed onto homemade polyacrylamide gels (8-18%) and overlaid with agarose solution (0.5% low-melting agarose and trace of bromophenol blue in running buffer) and electrophoresis was performed simultaneously in a Ettan-DALT II system (GE Healthcare) at 2.5W/gel at 15°C until the bromophenol blue dye reached the bottom of the gels.

Gels Analysis

Gels were scanned using a Typhoon 9400 (GE Healthcare) with a resolution set at 100µm and using optimal excitation/emission wavelength for each DIGE fluor dye (Cy2 488/520 nm; Cy3 532/580 nm; Cy5 633/670 nm). Image analysis, relative quantification and statistical evaluation and PCA (Principal Component Analysis) were carried out with DeCyderTM 2D software (GE Healthcare, version 7.0). Down or up-expressed proteins, of the different group-to-group comparisons, were retained if protein spot fold change was larger than +1.5 or smaller than –1.5 and a Student's t-test p-value less than 0.05.

For mass spectrometry analysis, 2 semi-preparative 2D-gels were prepared as analytical gels. One 2D gels loaded with 400 µg of mix containing samples of TAB^{+}-GCA, TAB^{-}-GCA, GCA-control and HAoSMC.

After electrophoresis, 2D-gels were fixed in 30% (v/v) ethanol, 2% (v/v) phosphoric acid (two changes, 30 min each), and then stained for 72h in 0.01% (w/v) Coomassie Brilliant Blue G-250, 12% (w/v) ammonium sulfate, 18% (v/v) ethanol and 2% (v/v) phosphoric acid. Spots of interest were manually excised from Coomassie blue-stained semi-preparative gels.

Protein Identification by Mass Spectrometry (MS) and Database Searching.

Spots excised from gels were placed into 96-well microtiter plates. Then, in-gel digestion was carried out with trypsin as described by Shevchenko et al. [36] with minor modifications and using for all steps a Freedom EVO 100 digester/spotter robot (Tecan, Switzerland). Spots were first destained two times with a mixture of 100 mM ammonium bicarbonate (ABC) and 50% (v/v) acetonitrile (ACN) for 45 min at 22°C and then dehydrated using 100% ACN for 15 min. Protein spots were then reduced with 25 mM ABC containing 10 mM DTT for 1 h at 60°C and then alkylated with 55 mM iodoacetamide in 25 mM ABC for 30 min in the dark at 22°C. Gel pieces were washed twice with 25 mM ABC and finally dried using 100% ACN for 10 min. Bands were finally completely dehydrated after 1 h at 60°C. Gel pieces were incubated with 13 µL of sequencing grade modified trypsin (Promega, USA; 12.5 µg/mL in 40 mM ABC with 10% ACN, pH 8.0) overnight at 40°C.

After digestion, peptides were washed with 30 µL of 25 mM ABC, dried with 100% ACN and extracted twice with a mixture of 50% ACN–5% formic acid. Extracts were dried using a vacuum centrifuge Concentrator plus (Eppendorf).

For MS and tandem Mass Spectrometry (MS/MS) analyses, peptides were dissolved in 4 µL of alpha-CHCA (2.5 mg/mL in 70% ACN–0.1% trifluoroacetic acid). One microliter and a half of each sample were spotted directly onto a MALDI plate (ABSciex, USA). Droplets were allowed to dry at room temperature. Samples analyses were performed using a MALDI TOF-TOF 4800 mass spectrometer (ABSciex). Spectra acquisition and processing were performed using the 4000 series explorer software (ABI) version 3.5.28193 in positive reflectron mode at fixed laser

fluency with a low mass gate and delayed extraction. External plate calibration was performed using 4 calibration points spotted onto the 4 corners of the plate using a mixture of five external standards (PepMix 1; LaserBio Labs, France). Peptide masses were acquired by steps of 50 spectra in the range of 900 to 4000 Da. MS spectra were summed from 500 laser shots from an Nd-YAG laser operating at 355 nm and 200 Hz. After filtering tryptic, keratin and matrix contaminant peaks up to 15 parent ions were selected for subsequent MS/MS fragmentation according to mass range, signal intensity, signal to noise ratio, and absence of neighboring masses in the MS spectrum. MS/MS spectra were acquired in 1 kV positive mode and 1000 shots were summed by steps of 50. Database searches were carried out using Mascot version 2.2 (MatrixScience, London, UK) via GPS explorer software (ABSciex) version 3.6 combining MS and MS/MS inquiries on *human* proteins from SwissProt databank (20321 sequences, March 2012, www.expasy.org).

The search parameters were as follows: carbamidomethylation as a variable modification for cysteins and oxidation as a variable modification for methionines. Up to 1 missed tryptic cleavage was tolerated and mass accuracy tolerance of 30 ppm for precursors and 0.3 Da for fragments were used for all tryptic mass searches. Positive identification was based on a Mascot score above the significance level (i.e. < 5%).The reported proteins were always those with the highest number of peptide matches. Under our identification criteria, no result was found to match to multiple members of a protein family.

For MS and MS/MS ORBITRAP analyses, analyses were realized using an Ultimate 3000 Rapid Separation Liquid Chromatographic (RSLC) system (Thermo Fisher

Scientific) online with a hybrid LTQ-Orbitrap-Velos mass spectrometer (Thermo Fisher Scientific). Briefly, peptides were loaded and washed on a C_{18} reverse phase precolumn (3 µm particle size, 100 Å pore size, 150 µm i.d., 1 cm length). The loading buffer contains 98% H_2O, 2% ACN and 0.1% TFA. Peptides were then separated on a C_{18} reverse phase resin (2 µm particle size, 100 Å pore size, 75 µm i.d., 15 cm length) with a 4 min "effective gradient" from 100% A (0.1% FA and 100% H_2O) to 50% B (80% ACN, 0.085% FA and 20% H_2O).

The Linear Trap Quadrupole Orbitrap mass spectrometer acquired data throughout the elution process and operated in a data dependent scheme with full MS scans acquired with the Orbitrap, followed by up to 20 LTQ MS/MS CID spectra on the most abundant ions detected in the MS scan. Mass spectrometer settings were: full MS (AGC: $1*10^6$, resolution: $6*10^4$, m/z range 400-2000, maximum ion injection time: 500 ms); MS/MS (AGC: $5*10^3$, maximum injection time: 50 ms, minimum signal threshold: 500, isolation width: 2Da, dynamic exclusion time setting: 15 s). The fragmentation was permitted of precursor with a charge state of 2, 3, 4 and up. For the spectral processing, the software used to generate .mgf files is Proteome discoverer 1.2. The threshold of Signal to Noise for extraction values is 3. For database searching, all the search parameters were the same as MALDI search except the precursor mass tolerance which was set to 10 ppm and the fragment mass tolerance to 0.45 Da.

Supplemental Table 1: clinical and histological characteristics of patients who underwent temporal artery biopsy and whose vascular smooth muscle cells were used for proteomic and genomic experiments

Patients	Sex	≥3 ACR criteria	Age>50 ans	Headaches	Clinical abnormal temporal artery	ESR> 50	abnormal TAB findings	Any visual symptoms	CRP (mg/L)	Positive FDG uptake
TAB$^+$GCA	F	YES	YES	NO	NO	YES	YES	NO	146	YES
	M	YES	YES	YES	NO	YES	YES	NO	144	ND
	F	YES	YES	YES	NO	YES	YES	YES	126	ND
	F	YES	YES	YES	YES	YES	YES	YES	100	ND
GCA-control	M	NO	YES	NO	NO	NO	NO	NO	37	ND
	F	NO	YES	NO	NO	NO	NO	YES	0	ND
	F	NO	YES	NO	NO	ND	NO	NO	139	ND
	F	NO	YES	NO	NO	ND	NO	NO	42	ND
TAB$^-$GCA	M	YES	YES	YES	NO	YES	NO	YES	245	ND
	F	YES	YES	YES	NO	YES	NO	NO	68	ND
	F	YES	YES	YES	NO	YES	NO	NO	147	YES
	F	YES	YES	YES	NO	YES	NO	NO	40	YES

ACR: American college of rheumatologist; CRP: C-reactive protein; ESR: erythrocyte sedimentation rate; F: female; FDG: fluorodesoxyesglucose; GCA-controls: patients who underwent temporal artery biopsy and had a final diagnosis which was not GCA; M: male, ND: not determined; TAB$^+$-GCA: histology proven giant cell arteritis; TAB$^-$-GCA: giant cell arteritis without histological evidence.

Supplemental Table 2 Differentially expressed proteins between vascular smooth muscle cells from biopsy proven giant cell arteritis and controls (fold change ≥1.5, p≤0.05)

SPOT	T-test	Fold change	IDENTIFIED PROTEIN	NAME	Exp pI	Exp MM	Theo pI	Theo MM	Total ion Score	Best ion Score	Number of identified peptides
1271	2,6E-02	**-2,8**	26S protease regulatory subunit 4	PRS4	**6,6**	**60**	**5.9**	**49**	**943**	**96**	**18**
1060	3,9E-02	**-2,5**	Phosphoenolpyruvate carboxykinase [GTP], mitochondrial	PCKGM	**8,1**	**69**	**6.6**	**67**	**877**	**84**	**18**
3085	2,2E-02	**-2,0**	Peptidyl-prolyl cis-trans isomerase A	PPIA	**6,1**	**17**	**7.7**	**18**	**69**	**43**	**2**
2923	1,4E-02	**-1,8**	Heat shock protein beta-6	HSPB6	**6,8**	**19**	**6**	**17**	**172**	**54**	**4**
2198	4,0E-02	**-1,6**	Annexin A5	ANXA5	**5,1**	**33**	**4.9**	**36**	**1136**	**128**	**17**
1848	3,3E-02	**-1,6**	Tubulin beta-2A chain & Short/branched chain specific acyl-CoA dehydrogenase, mitochondrial & Arfaptin-2	TBB2A & ACDSB & ARFP2	**6,2**	**41**	**4.8 & 5.7 & 5.7**	**50 & 44 & 38**	**680 & 475 & 167**	**90 & 94 & 85**	**12 & 9 & 3**
1352	3,2E-02	**-1,6**	D-3-phosphoglycerate dehydrogenase & Prelamin-A/C	SERA & LMNA	**7,5**	**57**	**6.3 & 6.6**	**57 & 74**	**997 & 1142**	**125 & 94**	**15 & 22**
1191	4,5E-02	**-1,5**	Vimentin & Serine/threonine-protein phosphatase 2A 65 kDa regulatory subunit A & Alpha-actinin-1 & Transitional endoplasmic reticulum ATPase	VIME & 2AAA & ACTN1 & TERA	**5,1**	**63**	**5.1 & 5 & 5.3**	**54 & 65 & 103**	**896 & 910 & 516 & 495**	**77 & 72 & 88 & 90**	**19 & 16 & 10 & 9**
903	4,0E-02	**1,5**	Peptidyl-prolyl cis-trans isomerase & Protein disulfide-isomerase A4 & 78 kDa glucose-regulated protein	FKB10 & PDIA4 & GRP78	**5,4**	**75**	**5.3 & 4.9 & 5**	**61 & 71 & 70**	**1022 & 656 & 984**	**96 & 79 & 94**	**19 & 13 & 18**
728	1,9E-02	**2,0**	Myosin-9 & Src substrate cortactin	MYH9 & SRC8	**5,5**	**84**	**5.2 & 5.2**	**43 & 62**	**1420**	**113**	**27**

Exp: experimental; MM: molecular mass; pI: isoelectrofocalisation point; Theo: theoretical. Relative quantification and statistical evaluation were carried out with DeCyderTM 2D software (GE Healthcare, version 7.0). Down or up-expressed proteins between groups were retained if protein spot fold change was larger than +1.5 or smaller than –1.5 and a Student's t-test p-value less than 0.05

Supplemental Table 3 Differentially expressed proteins between vascular smooth muscle cells from biopsy proven giant cell arteritis and from giant cell arteritis without histological evidence (fold change ≥1.5, p≤0.05)

SPOT	T-test	Fold change	IDENTIFIED PROTEIN	NAME	Exp pI	Exp MM	Theo pI	Theo MM	Total ion Score	Best ion Score	Number of identified peptides
3300	1,3E-02	**-2,5**	Hemoglobin subunit alpha	HBA	**8,5**	**14**	**8.7**	**15**	**64**	**37**	**2**
1271	4,0E-02	**-2,1**	26S protease regulatory subunit 4	PRS4	**6,6**	**60**	**5.9**	**49**	**943**	**96**	**18**
1609	4,2E-02	**-2,0**	CCA tRNA nucleotidyltransferase 1, mitochondrial & Prelamin-A/C & Alpha-enolase	TRNT1 & LMNA & ENOA	**7,6**	**49**	**6.3 & 6.6 & 7**	**45 & 74 & 47**	**379 & 814 & 374**	**58 & 83 & 92**	**9 & 16 & 5**
568	3,1E-02	**-1,9**	Ribosome-binding protein 1	RRBP1	**5,4**	**93**	**8.7**	**152**	**1947**	**107**	**34**
2923	4,2E-02	**-1,9**	Heat shock protein beta-6	HSPB6	**6,8**	**19**	**6**	**17**	**172**	**54**	**4**
1352	3,2E-02	**-1,9**	D-3-phosphoglycerate dehydrogenase & Prelamin-A/C	SERA & LMNA	**7,5**	**57**	**6.3 & 6.6**	**57 & 74**	**997 & 1142**	**125 & 94**	**15 & 22**
3028	1,7E-02	**-1,9**	Cytochrome b-5 & Polymerase I and transcript release factor	CYB5 & PTRF	**4,9**	**17**	**4.9 & 5.5**	**15 & 43**	**224 & 147**	**104 & 106**	**3 & 2**
1365	4,2E-02	**-1,7**	Glucose-6-phosphate 1-dehydrogenase & Inosine-5'-monophosphate dehydrogenase 2 & Aspartate--tRNA ligase & Annexin A11	G6PD & IMDH2 & SYDC & ANX11	**7,4**	**57**	**6.4 & 6.5 & 6.1**	**59 & 56 & 57**	**684 & 574 & 572 & 420**	**83 & 93 & 64 & 104**	**15 & 12 & 6 & 3**
1191	2,3E-02	**-1,6**	Vimentin & Serine/threonine-protein phosphatase 2A 65 kDa regulatory subunit A & Alpha-actinin-1 & Transitional endoplasmic reticulum ATPase	VIME & 2AAA & ACTN1 & TERA	**5,1**	**63**	**5.1 & 5 & 5.3**	**54 & 65 & 103**	**896 & 910 & 516 & 495**	**77 & 72 & 88 & 90**	**19 & 16 & 10 & 9**
1848	3,4E-03	**-1,6**	Tubulin beta-2A chain & Short/branched chain specific acyl-CoA dehydrogenase, mitochondrial & Arfaptin-2	TBB2A & ACDSB & ARFP2	**6,2**	**41**	**4.8 & 5.7 & 5.7**	**50 & 44 & 38**	**680 & 475 & 167**	**90 & 94 & 85**	**12 & 9 & 3**
1691	3,1E-02	**-1,5**	Actin & Collagen alpha-3(VI) chain & Spectrin alpha chain, brain	ACTB & CO6A3 & SPTA2	**5,2**	**46**	**5.3 & 6.2 & 5.2**	**42 & 341 & 285**	**830 & 632 & 566**	**105 & 85 & 90**	**13 & 12 & 11**
2638	4,3E-02	**1,5**	3-hydroxyacyl-CoA dehydrogenase type-2 & Heterogeneous nuclear ribonucleoprotein H	HCD2 & HNRH1	**7,4**	**24**	**7.9 & 5.9**	**27 & 49**	**229 & 358**	**72 & 93**	**4 & 6**
3283	4,1E-02	**1,5**	Galectin-1	LEG1	**5,2**	**14**	**5.3**	**15**	**443**	**101**	**8**

1348	4,4E-02	**1,6**	Endoplasmin & Vimentin & Protein disulfide-isomerase	ENPL & VIME & PDIA1	**4,9**	**57**	**4.7 & 5.1 & 4.7**	**90 & 54 & 55**	**1135 & 1085 & 619**	**102 & 103 & 88**	**18 & 22 & 13**
1490	4,5E-02	**1,7**	Aldehyde dehydrogenase X & Thioredoxin reductase 1, cytoplasmic	AL1B1 & TRXR1	**6,9**	**53**	**6 & 7.2**	**55 & 71**	**729 & 370**	**86 & 70**	**13 & 8**
1045	2,7E-02	**1,8**	Lamin-B1 & Peptidyl-prolyl cis-trans isomerase	LMNB1 & FKB10	**5,3**	**69**	**5.1 & 5.3**	**66 & 61**	**1619 & 811**	**112 & 94**	**30 & 15**
957	4,6E-02	**1,9**	78 kDa glucose-regulated protein & Peptidyl-prolyl cis-trans isomerase	GRP78 & FKB10	**5,4**	**73**	**5 & 5.3**	**70 & 61**	**905 & 1145**	**109 & 96**	**17 & 21**
1989	1,8E-02	**1,9**	Endoplasmin & Eukaryotic translation initiation factor 3 subunit J	ENPL & EIF3J	**4,8**	**38**	**4.7 & 4.7**	**90 & 29**	**963 & 267**	**125 & 64**	**19 & 6**
1422	3,5E-02	**1,9**	Selenium-binding protein 1 & Mitochondrial-processing peptidase subunit alpha & Pyruvate dehydrogenase protein X component, mitochondrial	SBP1 & MPPA & ODPX	**6,7**	**55**	**5.9 & 5.9 & 6**	**52 & 55 & 48**	**561 & 552 & 446**	**78 & 80 & 85**	**11 & 10 & 8**
731	3,3E-02	**2,1**	Myosin-9 & Src substrate cortactin	MYH9 & SRC8	**5,6**	**84**	**8.8 & 5.2**	**354 & 62**	**2165 & 643**	**112 & 95**	**36 & 12**
728	2,1E-02	**2,2**	Myosin-9 & Src substrate cortactin	MYH9 & SRC8	**5,5**	**84**	**5.2 & 5.2**	**43 & 62**	**1420**	**113**	**27**
829	2,3E-03	**2,3**	Heterogeneous nuclear ribonucleoprotein U & 78 kDa glucose-regulated	HNRPU & GRP78	**4,9**	**79**	**5.8 & 5**	**90 & 70**	**390 & 168**	**64 & 70**	**9 & 3**
954	2,8E-03	**2,6**	78 kDa glucose-regulated protein & Peptidyl-prolyl cis-trans isomerase & Stress-70 protein	GRP78 & FKB10 &GRP75	**5,3**	**73**	**5 & 5.3 & 5.4**	**70 & 61 & 69**	**1690 & 1069 & 612**	**111 & 95 & 69**	**27 & 20 & 14**

Exp: experimental; MM: molecular mass; pI: isoelectrofocalisation point; Theo: theoretical. Relative quantification and statistical evaluation were carried out with DeCyderTM 2D software (GE Healthcare, version 7.0). Down or up-expressed proteins between groups were retained if protein spot fold change was larger than +1.5 or smaller than –1.5 and a Student's t-test p-value less than 0.05

Supplemental Table 4 Differentially expressed proteins between vascular smooth muscle cells from giant cell arteritis without histological evidence compared to controls (fold change ≥1.5, p≤0.05)

SPOT	T-test	Fold change	IDENTIFIED PROTEIN	NAME	Exp pI	Exp MM	Theo pI	Theo MM	Total ion Score	Best ion Score	Number of identified peptides
954	**1,7E-02**	**-1,7**	78 kDa glucose-regulated protein & Peptidyl-prolyl cis-trans isomerase & Stress-70 protein	GRP78 & FKB10 &GRP75	**5,3**	**73**	**5 & 5.3 & 5.4**	**70 & 61 & 69**	**1690 & 1069 & 612**	**111 & 95 & 69**	**27 & 20 & 14**

Exp: experimental; MM: molecular mass; pI: isoelectrofocalisation point; Theo: theoretical. Relative quantification and statistical evaluation were carried out with DeCyderTM 2D software (GE Healthcare, version 7.0). Down or up-expressed proteins between groups were retained if protein spot fold change was larger than +1.5 or smaller than –1.5 and a Student's t-test p-value less than 0.05

Supplemental Table 5 Differentially expressed proteins between pulmonary artery vascular smooth muscle cells from biopsy proven giant cell arteritis compared to normal human aorta (fold change ≥1.5, p≤0.05)

SPOT	T-test	Fold change	IDENTIFIED PROTEIN	NAME	Exp pI	Exp MM	Theo pI	Theo MM	Total ion Score	Best ion Score	Number of identified peptides
1349	2,0E-02	**-17,2**	Vimentin & Tubulin alpha-1A	VIME & TBA1A	**5,3**	**57**	**5.1 & 4.9**	**54 & 50**	**2616 & 1092**	**116 & 95**	**50 & 20**
240	3,6E-03	**-4,3**	Collagen alpha-2(I)	CO1A2	**10,0**	**113**	**10.1**	**92**	**605**	**93**	**10**
222	4,7E-02	**-4,2**	Vigilin	VIGLN	**7,6**	**114**	**6.4**	**141**	**476**	**65**	**11**
747	2,6E-02	**-4,0**	Putative pre-mRNA-splicing factor ATP-dependent RNA helicase DHX15	DHX15	**8,5**	**84**	**7.1**	**91**	**663**	**69**	**14**
1233	4,5E-02	**-3,9**	Dihydropyrimidinase-related protein 3 & Carnitine O-palmitoyltransferase 1, liver isoform &	DPYL3 & CPT1A	**7,2**	**62**	**6 & 8.9**	**62 & 88**	**878 & 387**	**98 & 81**	**14 & 7**
664	4,1E-02	**-3,7**	Elongation factor 2	EF2	**7,9**	**88**	**6.4**	**95**	**1342**	**92**	**25**
1060	3,6E-05	**-3,5**	Phosphoenolpyruvate carboxykinase [GTP], mitochondrial	PCKGM	**8,1**	**69**	**6.6**	**67**	**877**	**84**	**18**
826	1,5E-02	**-3,4**	TATA-binding protein-associated factor 2N	RBP56	**8,8**	**80**	**8**	**62**	**19**	**57**	**3**
860	2,2E-02	**-3,4**	Ezrin & Caldesmon	EZRI & CALD1	**7,0**	**78**	**6 & 5.6**	**69 & 93**	**950 & 628**	**100 & 100**	**21 & 11**
1420	2,7E-02	**-3,2**	V-type proton ATPase subunit B, brain isoform	VATB2	**6,0**	**55**	**5.6**	**57**	**1498**	**113**	**23**
461	4,8E-02	**-3,2**	Kinesin-1 heavy chain	KINH	**7,0**	**99**	**6.1**	**110**	**395**	**89**	**8**
640	9,5E-03	**-2,9**	Procollagen-lysine,2-oxoglutarate 5-dioxygenase 2	PLOD2	**7,2**	**89**	**6.2**	**82**	**806**	**86**	**16**
626	1,1E-02	**-2,9**	Programmed cell death 6-interacting protein & Procollagen-lysine,2-oxoglutarate 5-dioxygenase 2	PDC6I & PLOD2	**7,1**	**89**	**6.1 & 6.2**	**96 & 82**	**1712 & 561**	**89 & 82**	**35 & 11**
933	4,7E-02	**-2,8**	Prelamin-A/C & Moesin	LMNA & MOES	**7,3**	**74**	**6.6 & 6.1**	**74 & 68**	**1594 & 1372**	**104 & 94**	**31 & 26**
1967	6,7E-03	**-2,6**	Tropomyosin beta chain	TPM2	**4,8**	**38**	**4.7**	**33**	**814**	**79**	**18**
458	2,3E-02	**-2,6**	Kinesin-1 heavy chain	KINH	**7,1**	**99**	**6.1**	**110**	**1444**	**100**	**28**
522	3,8E-02	**-2,6**	Major vault protein & Ubiquitin-like modifier-activating enzyme 1	MVP & UBA1	**5,7**	**96**	**5.3 & 6.4**	**99 & 95**	**1719 & 660**	**101 & 80**	**32 & 13**

632	1,1E-02	**-2,6**	Programmed cell death 6-interacting protein & Procollagen-lysine,2-oxoglutarate 5-dioxygenase 2 & Filamin-A	PDC6I & PLOD2 & FLNA	**7,0**	**89**	**6.1 & 6.2 & 5.7**	**96 & 82 & 281**	**917 & 567 & 662**	**100 & 92 &80**	**18 & 11 & 15**
645	1,3E-02	**-2,6**	Procollagen-lysine,2-oxoglutarate 5-dioxygenase 2 & Filamin-A	PLOD2 & FLNA	**6,8**	**89**	**6.2 & 5.7**	**82 & 281**	**783 & 581**	**86 & 82**	**15 & 12**
1403	4,1E-02	**-2,3**	Vimentin	VIME	**5,3**	**55**	**5.1**	**54**	**2111**	**115**	**40**
633	3,8E-02	**-2,3**	Procollagen-lysine,2-oxoglutarate 5-dioxygenase 2	PLOD2	**7,3**	**89**	**6.2**	**82**	**874**	**72**	**17**
823	4,2E-02	**-2,3**	Delta-1-pyrroline-5-carboxylate synthase & Procollagen-lysine,2-oxoglutarate 5-dioxygenase 1	P5CS & PLOD1	**7,5**	**80**	**6.7 & 6.5**	**87 & 82**	**993 & 398**	**90 & 59**	**19 & 10**
1745	5,0E-02	**-2,1**	DnaJ homolog subfamily B member 11	DJB11	**6,8**	**44**	**5.8**	**38**	**721**	**105**	**13**
1714	2,6E-03	**-2,1**	Actin, cytoplasmic 1	ACTB	**5,3**	**45**	**5.3**	**42**	**921**	**125**	**15**
1423	4,2E-02	**-2,0**	Pyruvate kinase isozymes M1/M2 & Aldehyde dehydrogenase X, mitochondrial	KPYM & AL1B1	**7,1**	**55**	**8.0 & 6.0**	**58 & 55**	**797 & 656**	**88 & 86**	**15 & 12**
937	3,6E-02	**-2,0**	Glycine--tRNA ligase & Prelamin-A/C	SYG & LMNA	**6,7**	**74**	**6.6 & 6.6**	**83 & 74**	**1054 & 464**	**83 & 75**	**21 & 9**
1723	4,2E-02	**-2,0**	No identified protein		**7,4**	**45**					
1051	4,9E-02	**-1,9**	Plastin-3 & Heat shock cognate 71 kDa protein	PLST & HSP7C	**5,8**	**69**	**5.4 & 5.4**	**71 & 71**	**1903 & 893**	**97 & 87**	**34 & 16**
1975	2,8E-02	**-1,9**	Apolipoprotein L2	APOL2	**7,2**	**38**	**6.3**	**37**	**332**	**84**	**6**
2858	1,2E-02	**-1,9**	Myosin regulatory light chain 12A	ML12A	**4,8**	**20**	**4.7**	**20**	**386**	**86**	**6**
1691	4,8E-03	**-1,9**	Actin & Collagen alpha-3(VI) chain & Spectrin alpha chain, brain	ACTB & CO6A3 & SPTA2	**5,2**	**46**	**5.3 & 6.2 & 5.2**	**42 & 341 & 285**	**830 & 632 & 566**	**105 & 85 & 90**	**13 & 12 & 11**
793	2,7E-02	**-1,8**	Elongation factor G, mitochondrial	EFGM	**6,9**	**80**	**5.9**	**80**	**676**	**90**	**13**
1090	1,5E-02	**-1,8**	Plastin-3 & Heat shock 70 kDA protein 1A/1B	PLST & HSP71	**6,0**	**68**	**5.4 & 5.5**	**71 & 70**	**1386 & 429**	**87 & 77**	**25 & 8**
1645	1,6E-02	**-1,7**	Vimentin & Interleukin enhancer-binding factor 2 & Myoferlin	VIME & ILF2 & MYOF	**6,7**	**47**	**5.1 & 5.2 & 5**	**54 & 43 & 83**	**465 & 780 & 746**	**66 & 79 & 92**	**11 & 15 & 13**
1229	4,5E-02	**-1,7**	T-complex protein 1 subunit gamma & Dihydropyrimidinase-related protein 3	TCPG & DPYL3	**7,0**	**62**	**6.1 & 6**	**61 & 62**	**692 & 439**	**83 & 79**	**14 & 9**
1237	4,8E-02	**-1,7**	Prolyl 4-hydroxylase subunit alpha-2 & Staphylococcal nuclease domain-containing protein 1	P4HA2 & SND1	**6,0**	**62**	**5.4 & 6.8**	**59 & 102**	**838 & 807**	**95 & 85**	**15 & 14**
1351	2,7E-	**-1,7**	Tryptophan--tRNA ligase & Protein disulfide-isomerase A3	SYWC &	**6,6**	**57**	**5.8 & 5.6**	**53 & 54**	**809 & 429 &**	**95 & 97 & 98**	**14 & 8 & 8**

	02		& Prenylcysteine oxidase 1	PDIA3 & PCYOX			**& 5.9**	**& 54**	**456**		
2042	2,2E-02	**-1,6**	Elongation factor 1-delta & Thioredoxin-like protein 1	EF1D & TXNL1	**5,1**	**36**	**4.9 & 4.8**	**31 & 32**	**606 & 267**	**100 & 77**	**9 & 5**
2204	5,0E-02	**-1,6**	Annexin A2	ANXA2	**7,7**	**37**	**7.6**	**38**	**1037**	**97**	**18**
1553	3,3E-02	**-1,5**	Alpha-enolase & Plasminogen activator inhibitor 1	ENOA & PAI1	**7,3**	**50**	**7 & 7**	**47 & 43**	**434 & 368**	**96 & 79**	**8 & 7**
3152	4,1E-02	**-1,5**	Myosin light polypeptide 6	MYL6	**4,7**	**16**	**4.6**	**17**	**683**	**85**	**12**
1687	3,6E-02	**-1,5**	Actin, cytoplasmic 1 & Creatine kinase B-type & Cathepsin D & *Lon protease homolog, mitochondria*	ACTB & KCRB & CATD & LONM	**5,8**	**46**	**5.3 & 5.4 & 5.6**	**42 & 43 & 38**	**666 & 658 & 340 & 327**	**106 & 101 & 88 & 88**	**11 & 11 & 6 & 5**
1716	2,1E-02	**1,5**	Cytochrome b-c1 complex subunit 2 & Citrate synthase & Alpha-enolase	QCR2 & CISY & ENOA	**8,5**	**46**	**7.7 & 7.4 & 7**	**47 & 49 & 47**	**432 & 332 & 529**	**95 & 68 & 97**	**8 & 8 & 7**
2434	1,1E-02	**1,5**	Adenylate kinase 2, mitochondrial	KAD2	**9,2**	**28**	**7.7**	**26**	**570**	**70**	**12**
2541	3,8E-02	**1,5**	Triosephosphate isomerase & Cytochrome b-c1 complex subunit Rieske, mitochondrial	TPIS & UCRI	**7,4**	**26**	**5.7 & 11.3**	**31 & 8**	**861 & 491**	**102 & 99**	**14 & 8**
2170	3,6E-02	**1,6**	Phosphatidylinositol transfer protein alpha isoform & Fumarylacetoacetate hydrolase domain-containing protein 2B & Dynamin-1-like protein	PIPNA & FAH2B & DNM1L	**7,3**	**33**	**6.1 & 7.6 & 6.4**	**32 & 35 & 82**	**281 & 319 & 98**	**97 & 56 & 55**	**6 & 7 & 2**
2602	2,3E-02	**1,6**	No identified protein		**7,0**	**25**					
2783	2,8E-02	**1,7**	Transforming protein RhoA & Ras-related protein Rap-1b	RHOA & RAP1B	**6,3**	**21**	**5.8 & 5.7**	**21 & 20**	**335 & 204**	**68 & 65**	**7 & 4**
2565	2,2E-02	**1,7**	Triosephosphate isomerase & Dihydropteridine reductase	TPIS & DHPR	**7,8**	**25**	**5.7 & 7.1**	**31 & 26**	**875 & 266**	**100 & 65**	**14 & 4**
2625	3,1E-02	**1,7**	Tetratricopeptide repeat protein 35 & Ras-related protein Rab-11B & Ubiquitin-conjugating enzyme E2 K & Phosphoglycerate kinase 1	TTC35 & RB11B & UBE2K & PGK1	**5,4**	**24**	**6.2 & 5.7 & 5.3**	**35 & 24 & 22**	**432 & 248 & 259 & 239**	**91 & 68 & 85 & 77**	**6 & 6 & 5 & 5**
2600	1,8E-02	**1,7**	Heterogeneous nuclear ribonucleoproteins A2/B1	ROA2	**8,4**	**25**	**9**	**37**	**463**	**100**	**8**
3066	1,9E-02	**1,7**	Ragulator complex protein LAMTOR1	LTOR1	**5,0**	**17**	**5**	**18**	**161**	**93**	**3**
728	4,8E-02	**1,7**	Myosin-9 & Src substrate cortactin	MYH9 & SRC8	**5,5**	**84**	**5.2 & 5.2**	**43 & 62**	**1420**	**113**	**27**
2352	3,0E-02	**1,7**	Glutathione S-transferase omega-1	GSTO1	**6,3**	**29**	**6.2**	**27**	**259**	**58**	**6**

3467	1,4E-02	**1,8**	10 kDa heat shock protein, mitochondrial	CH10	**9,6**	**13**	**8.9**	**11**	**294**	**115**	**6**
2991	2,4E-02	**1,9**	Nucleophosmin & Tubulin beta-2A chain	NPM & TBB2A	**4,6**	**18**	**4.6 & 4.8**	**33 & 50**	**278 & 158**	**69 & 59**	**5 & 3**
3388	2,8E-02	**1,9**	40S ribosomal protein S3	RS3	**10,7**	**13**	**9.7**	**27**	**289**	**67**	**5**
1045	5,7E-03	**1,9**	Lamin-B1 & Peptidyl-prolyl cis-trans isomerase	LMNB1 & FKB10	**5,3**	**69**	**5.1 & 5.3**	**66 & 61**	**1619 & 811**	**112 & 94**	**30 & 15**
2999	1,3E-02	**1,9**	Transgelin & Destrin	TAGL & DEST	**7,6**	**18**	**8.9 & 8.1**	**22 & 18**	**314 & 163**	**68 & 98**	**6 & 3**
2322	5,1E-03	**1,9**	Proteasome activator complex subunit 2	PSME2	**5,7**	**30**	**5.5**	**27**	**544**	**88**	**11**
3217	1,3E-02	**1,9**	*60S ribosomal protein L22*	*RL22*	**6,0**	**15**	**9.2**	**15**	**102**	**53**	**2**
2610	3,9E-02	**1,9**	NADH dehydrogenase [ubiquinone] iron-sulfur protein 8 & Actin, cytoplasmic 1 & Plasma membrane calcium-transporting ATPase 4	NDUS8 & ACTB & ATPG	**5,3**	**24**	**5.1 & 5.3 & 9**	**20 & 42 & 30**	**192 & 139 & 122**	**58 & 62 & 66**	**4 & 3 & 3**
3233	4,6E-02	**2,0**	Profilin-1 & 60S ribosomal protein L22	PROF1 & RL22	**10,0**	**15**	**8.5 & 9.2**	**15 & 15**	**151 & 102**	**77 & 58**	**3 & 2**
1641	1,5E-02	**2,0**	No identified protein		**6,5**	**47**					
3550	2,6E-02	**2,1**	Hemoglobin subunit beta	HBB	**4,8**	**11**	**6.8**	**16**	**201**	**103**	**7**
3300	2,2E-02	**2,1**	Hemoglobin subunit alpha	HBA	**8,5**	**14**	**8.7**	**15**	**64**	**37**	**2**
2247	2,2E-02	**2,2**	Alpha-enolase & Proteasome activator complex subunit 3	ENOA & PSME3	**6,2**	**31**	**7 & 5.7**	**47 & 29**	**379 & 365**	**92 & 69**	**6 & 7**
2713	2,3E-02	**2,2**	Transgelin & Peptidyl-prolyl cis-trans isomerase B & Glyceraldehyde-3-phosphate dehydrogenase	TAGL & PPIB & G3P	**10,2**	**22**	**8.9 & 9.3 & 8.6**	**22 & 20 & 36**	**265 & 249 & 276**	**72 & 73 & 76**	**5 & 5 & 5**
2534	2,7E-02	**2,4**	Triosephosphate isomerase & Protein ETHE1, mitochondrial	TPIS & ETHE1	**7,0**	**26**	**5.7 & 6.4**	**31 & 27**	**611 & 342**	**95 & 79**	**10 & 6**
2522	1,9E-02	**2,4**	Annexin A1 & Cathepsin B & Inorganic pyrophosphatase	ANXA1 & CATB & IPYR	**5,2**	**26**	**6.6 & 5.2 & 5.5**	**39 & 28 & 33**	**587 & 309 & 56**	**101 & 90 & 30**	**9 & 5 & 2**
3433	1,6E-02	**2,4**	Malate dehydrogenase, cytoplasmic	MDHC	**4,7**	**12**	**6.9**	**36**	**107**	**51**	**3**
1361	1,9E-02	**2,4**	Prelamin-A/C	LMNA	**8,9**	**57**	**6.6**	**74**	**1710**	**116**	**32**
3464	1,6E-02	**2,4**	40S ribosomal protein S14	RS14	**9,3**	**12**	**10.1**	**16**	**151**	**71**	**3**
2555	9,4E-	**2,5**	14-3-3 protein gamma & Calpain small subunit 1 & 14-3-3	1433G &	**5,1**	**26**	**4.8 & 5.1**	**28 & 28**	**126 & 125 &**	**53 & 67 & 45**	**3 & 2 & 2**

	03		protein eta	CPNS1 & 1433F			**& 4.8**	**& 28**	**73**		
2343	1,9E-02	**2,6**	Cathepsin D	CATD	**6,1**	**29**	**5.6**	**38**	**602**	**117**	**9**
3193	3,3E-03	**2,7**	Coactosin-like protein	COTL1	**5,5**	**15**	**5.5**	**16**	**364**	**57**	**9**
1426	3,4E-02	**2,7**	Endoplasmin & Vimentin & Protein disulfide-isomerase	ENPL & VIME & PDIA1	**4,8**	**55**	**4.7 & 5.1 & 4.7**	**90 & 54 & 55**	**803 & 624 & 535**	**102 & 76 & 87**	**12 & 13 & 15**
3413	1,2E-02	**2,8**	40S ribosomal protein S3	RS3	**10,4**	**13**	**9.7**	**27**	**310**	**68**	**5**
2317	4,5E-02	**2,9**	Exosome complex component MTR3 & 78 kDa glucose-regulated protein & Proteasome subunit alpha type-1	EXOS6 & GRP78 & PSA1	**7,1**	**30**	**6.1 & 5 & 6.2**	**28 & 70 & 30**	**510 & 408 & 263**	**103 & 65 & 81**	**9 & 8 & 4**
3089	4,6E-02	**2,9**	Transgelin & Peroxiredoxin-1	TAGL & PRDX1	**7,6**	**17**	**8.9 & 8.3**	**22 & 22**	**153 & 70**	**63 & 44**	**3 & 2**
3312	4,3E-02	**2,9**	Profilin-1	PROF1	**8,3**	**14**	**8.5**	**15**	**71**	**43**	**2**
1611	1,1E-02	**3,0**	Prelamin-A/C & Fumarate hydratase, mitochondrial	LMNA & FUMH	**8,0**	**49**	**6.6 & 7**	**74 & 50**	**1172 & 357**	**80 & 92**	**23 & 5**
290	4,2E-02	**3,1**	Collagen alpha-1(VI) chain & Spectrin alpha chain,	CO6A1 & SPTA2	**5,3**	**109**	**5.2 & 5.2**	**106 & 285**	**1152 & 497**	**110 & 67**	**19 & 13**
1744	3,8E-02	**3,1**	Vimentin	VIME	**4,8**	**44**	**5.1**	**54**	**1895**	**97**	**37**
2438	4,0E-02	**3,1**	6-phosphogluconolactonase & Actin-related protein 2/3 complex subunit 2	6PGL & ARPC2	**6,3**	**28**	**5.7 & 6.8**	**27 & 34**	**491 & 344**	**77 & 57**	**9 & 8**
298	4,8E-02	**3,2**	Hypoxia up-regulated protein 1 & Collagen alpha-1(VI) chain & Myosin-9	HYOU1 & CO6A1 & MYH9	**5,4**	**115**	**5.1 & 5.2 & 5.5**	**108 & 106 & 226**	**1363 & 1050 & 831**	**105 & 95 & 90**	**34 & 14 & 16**
2280	3,6E-03	**3,3**	Cathepsin B & Alpha-soluble NSF attachment protein	CATB & SNAA	**5,4**	**31**	**5.2 & 5.2**	**28 & 33**	**533 & 109**	**92 & 74**	**9 & 2**
3536	3,0E-02	**3,4**	Profilin-1 & Guanine nucleotide-binding protein G(I)/G(S)/G(O) subunit gamma-12 & Histone H2B type 1-B	PROF1 & GBG12 & H2B1B	**10,7**	**11**	**8.5 & 9.1 & 10.3**	**15 & 8 & 14**	**232 & 209 & 155**	**72 & 67 & 64**	**5 & 4 & 4**
2700	4,2E-02	**3,5**	Aldehyde dehydrogenase, mitochondrial & Ras-related protein Rab-2A	ALDH2 & RAB2A	**6,1**	**23**	**5.7 & 6.1**	**54 & 23**	**553 & 337**	**92 & 90**	**9 & 6**
1115	4,9E-02	**3,5**	78 kDa glucose-regulated protein	GRP78	**5,4**	**67**	**5**	**70**	**1362**	**97**	**21**
2328	5,3E-04	**3,6**	Cathepsin B & Chloride intracellular channel protein 1	CATB & CLIC1	**5,4**	**30**	**5.2 & 5.1**	**28 & 27**	**531 & 366**	**106 & 72**	**8 & 7**
3419	1,9E-02	**3,9**	No identified protein		**6,9**	**13**					

294	4,8E-02	**4,2**	Collagen alpha-2(VI) chain	CO6A2	**6,9**	**110**	**5.9**	**107**	**489**	**60**	**11**
281	3,5E-02	**6,3**	Collagen alpha-2(VI) chain	CO6A1	**6,5**	**110**	**5.2**	**106**	**792**	**86**	**15**
3545	1,6E-02	**6,4**	Peroxiredoxin-5, mitochondrial	PRDX5	**9,1**	**11**	**6.7**	**17**	**353**	**94**	**7**
413	4,6E-02	**7,6**	Collagen alpha-3(VI)	CO6A3	**7,8**	**101**	**6.2**	**341**	**721**	**93**	**15**

Exp: experimental; MM: molecular mass; pI: isoelectrofocalisation point; Theo: theoretical. Relative quantification and statistical evaluation were carried out with DeCyderTM 2D software (GE Healthcare, version 7.0). Down or up-expressed proteins between groups were retained if protein spot fold change was larger than +1.5 or smaller than –1.5 and a Student's t-test p-value less than 0.05

4. Discussion

4.1. Identification d'auto-anticorps au cours de l'ACG, intérêt et signification

Au cours de l'ACG, peu d'études se sont intéressées à l'immunité humorale. En effet, l'ACG est avant tout une pathologie associée à des anomalies des lymphocytes T et l'analyse histologique des BAT montre des LB épars, localisés préférentiellement au niveau adventitiel avec des plasmocytes dans seulement 7 à 24 % des cas (102). De façon intéressante, les LT subissent une expansion oligoclonale au sein de la paroi des artères temporales (95) et peuvent proliférer en présence d'extraits d'artère temporale (96). Ces éléments suggèrent l'existence d'un antigène initiateur qui pourrait déclencher une réponse immune. L'hypothèse de la responsabilité éventuelle d'un agent infectieux, si elle est très séduisante, n'a pour l'instant pas pu être démontrée et et une hypothèse alternative serait qu'un auto-antigène provenant de la paroi du vaisseau puisse initier cette réponse immune. Le fait que l'infiltrat lymphocytaire B soit modeste au sein des BAT rend peu probable l'hypothèse qu'un auto-Ac dirigé contre un antigène de la paroi vasculaire ait un rôle déterminant dans la pathogénie. Cependant, la participation des LB au processus pathologique reste possible et des auto-Ac s'ils étaient mis en évidence, pourraient éventuellement être utilisés comme des biomarqueurs, ce qui justifie cette recherche.

4.1.1. Les AECA et anti-CMLV au cours des pathologies vasculaires

Détection et rôle pathogène potentiel des AECA

Les AECA ont été rapportés chez des sujets sains et pourraient avoir des propriétés anti-inflammatoires (237). Au cours de l'ACG, les AECA ont été détectés par une méthode ELISA sur cellules fixées et leur détection était associée à une activité de la maladie (28). Cependant, ces AECA n'ont pas été retrouvés par une étude utilisant une technique d'immunofluorescence menée chez 32 patients prélevés au moment du

duagnostic d'ACG (29). Cela souligne donc l'hétérogénéité des techniques utilisées et des résultats qui en découlent. Ainsi, les AECA peuvent être détectés par ELISA cellulaire, par cytométrie en flux, par immunofluorescence indirecte sans qu'une technique de référence ne soit établie. Différents types de CE, HUVEC ou cellules de microcirculation ont été utilisés et l'hétérogénéite de leurs contenu protéique qui a été soulignée par notre équipe (238) contribue également à l'hétérogénéité des résultats obtenus et aux difficultés d'interprétation des résultats des différentes études qui ont été menées (239). Parmi les effets pathogènes des AECA qui ont été décrits, on trouve la cytotoxicité (240), l'induction d'apoptose (241) ou encore l'activation des CE (242). Par ailleurs, des cibles des AECA ont été identifiées au cours des vascularites, comme l'alpha-enolase au cours de la maladie de Behcet (243), la tropomyosine au cours de la maladie de Kawasaki (244) et la heat shoch protein-60 (HSP60) au cours de la maladie de Takayasu (245). Dans le travail présent, nous avons identifié les cibles des AECAau cours de l'ACG. Les résultats parfois contradictoires rapportés dans la littérature incitent à une analyse prudente.

Détection et rôle pathogène potentiel des Ac anti-CMLV

Des auto-Ac dirigés contre les CMLV n'avaient, à notre connaissance, jamais été rapportés auparavant chez l'homme. Dans un modèle murin de vascularite, Baiu et al. ont transféré à des souris des splénocytes après co-culture avec des CMLV de microcirculation. Les sérums des souris receveuses contenaient des Ac anti-CMLV. Le transfert de ce sérum induisait une inflammation vasculaire chez d'autres souris receveuses sauvages ou déplétées en LB alors que des souris qui n'avaient ni LB ni LT (Rag-/-) n'avaient pas de signe de vascularite. Cela suggère un rôle pathogène des Ac anti-CMLV avec une participation lymphocytaire T (246). La même équipe a rapporté par la suite que des LT $CD4^+$ activés par des CMLV pouvaient induire une

vascularite chez les souris receveuses quand bien même les souris donneuses et receveuses étaient déficientes en Ig. Dans ce modèle, qui souligne l'importance des LT $CD4^+$, l'interféron γ était nécessaire à l'initiation des lésions de vascularite chez la souris receveuse (247). Ces résultats limitent le rôle pathogène des Ac anti-CMLV rapporté précédemment.

Notre équipe a depuis rapporté l'existence d'Ac anti-CMLV dans le sérum des patients atteints d'HTAP et de ScS (160), pathologies au cours desquelles le remodelage vasculaire occupe une place importante. La reconnaissance des CMLV a été mise en évidence en immunofluorescence indirecte, et les cibles des Ac anti-CMLV ont été identifiées par immunoblot 2D. Les cibles identifiées comprenaient notamment l'α-enolase et la protéine « stress induced phosphoprotéin 1 » (STIP-1). De façon importante, il a pu être mis en évidence dans ce travail que les IgG purifiées de sérum de patients atteints de ScS et/ou d'HTAP augmentaient la contraction des CMLV comparativement aux IgG purifiées d'individus sains, attestant de leur rôle pathogène potentiel.

Logiquement, ayant identifié des Ac anti-CMLV dans le sérum de patients atteints d'ACG, nous avons voulu étudier le rôle pathogène potentiel de ces anticorps. Dans des expériences très préliminaires et qui nécessiteraient d'être répétées, nous avons étudié l'effet du sérum total sur la contraction de matrices de collagènes au sein desquelles étaient déposées des CMLV. Nous avons observé que le sérum des sujets atteints d'ACG induisait une rétraction plus rapide des matrices que le sérum de sujets contrôles. Cependant, nous n'avons pas poursuivi dans cette voie d'un rôle pathogène potentiel des auto-Ac anti-CMLV et nous avons décidé par la suite de nous concentrer sur le remodelage vasculaire et en particulier sur les CMLV. D'autres pistes auraient pu être explorées à la recherche d'un rôle pathogène de ces auto-Ac.

Ainsi, il aurait été intéressant d'étudier l'effet de ces Ac sur la prolifération de CMLV. Nous pouvons également faire l'hypothèse que ces auto-Ac pourraient avoir un effet sur la production de métalloprotéases, de collagène et d'autres composants de la matrice extra-cellulaire par les CMLV. Enfin, le surnageant des CMLV cultivées en présence d'auto-Ac pourrait avoir des propriétés pro-inflammatoires et participer à la pérennisation de l'inflammation pariétale. Cependant, pour les raisons développées par la suite, ce n'est pas dans la voie que nous avons privilégiée.

4.1.2. Analyse des auto-Ac dirigés contre les CE et les CMLV au cours de l'ACG

Dans notre étude, nous avons utilisé des extraits protéiques d'HUVEC et de CMLV immortalisées télomérase-SV40 pour identifier les cibles des anticorps anti-CE et anti-CMLV, respectivement, chez les patients atteints d'ACG. Nous avons pu identifier 30 et 19 spots spots protéiques qui étaient la cible d'auto-Ac au sein d'extraits protéiques de CE et de CMLV respectivement parmi lesquels la vinculine, la lamine et la fumarate hydratase mitochondriale ont pu être identifiées à partir des 2 extraits protéiques de CMLV et de CE. Nous avons identifié que l'annexine A5 a été identifiée comme auto-antigène cible des AECA. Des auto-Ac dirigés contre l'annexine A 5 ont déjà été identifiés dans le sérum de patients d'autres types de vascularites telles que la maladie de Takayasu (248 , 249) et la maladie de Behcet ou au cours du lupus érythémateux systémique ou de la sclérodermie systémique. L'annexine A5 a des propriétés anticoagulantes et l'idée qu'un Ac anti-annexine A5 puisse expliquer la survenue des évènements thrombotiques semble séduisante. Ainsi, des Ac dirigés contre l'annexine A5 ont été rapportés chez les patients atteints de maladie de Behcet mais ils étaient identifiés avec une fréquence similaire chez les sujets sains et n'ont pu être associés aux évènements thrombotiques (248). Plus

récemment, il a été rapporté que le titre des IgG anti-annexine A5 était significativement plus élevé dans le groupe des patients atteints de maladie de Behcet que chez les sujets contrôles avec des titres particulièrement élevés dans le groupe de patients qui présentaient des manifestations neurologiques (Neuro-Behcet) (250). Au cours du lupus erythémateux systémique, la présence d'un Ac anti-annexine A5 été associée à un risque plus élevé de thromboses veineuses et artérielles ou de pertes foetales (251) et leur présence a été associée au risque de perte foetale dans une deuxième étude (252). Par ailleurs, au cours de la ScS, 75% des patients ayant un Ac anti-annexine A5 présentaient des ischémies digitales contre 24.1% des patients n'ayant pas cet auto-Ac (253). Cependant, dans ces différentes études, le rôle physiopathologique potentiel de ces auto-Ac n'a pas été démontré. Nous avons également identifié le « far-upstream element binding protein 2 » (FUBP2) comme cible d'auto-Ac chez l'ensemble des pools de patients testés. FUBP2 se lie à une région de l'ADN appelée far upstream element (FUSE) et a un rôle d'activateur transcriptionnel du proto-oncogène c-myc qui régule la croissance et la prolifération cellulaire. Cette protéine a également été identifiée comme une cible des AECA au cours des vascularites associées aux ANCA-positives (254). Des Ac dirigés contre cette protéine ont également été identifiés en immunoblot bidimensionnel à partir d'extraits protéiques de synoviocytes de patients atteints de polyarthrite rhumatoïde mais le rôle pathogène de ces auto-Ac n'est pas connu (255).

Par ailleurs, la vinculine est une protéine du cytosquelette impliquée dans l'adhésion extra-cellulaire et les jonctions inter-cellulaires. Des modifications de la quantité de vinculine ont déjà été rapportée au cours de l'athérome (256), maladie au cours de laquelle on note un remodelage vasculaire. La lamine A et C est codée par le gène LMNA et représente un des constituants majeurs de l'architecture du noyau. Des

mutations de la lamine A et C ont été identifiées au cours de la lipodystrophie familiale partielle de Dunnigan ou au cours du syndrome progeria de Hutchinson-Gilford, maladies qui se manifestent toutes deux par une atteinte vasculaire. Des Ac anti-lamine ont été rapportés au cours du syndrome des anti-phospholipides mais leur signification reste indéterminée (257).

4.1.3. Les auto-Ac, bio-marqueurs potentiels au cours de l'ACG

La détection d'un auto-Ac peut également avoir un intérêt diagnostique ou pronostique dans l'ACG et un certain nombre de travaux ont avant tout porté sur la l'identification d'un bio-marqueur, en particulier un Ac. En effet, en l'absence biomarqueur diagnostique, nous sommes contraints à réaliser une BAT, geste relativement invasif et contraignant. De plus, il n'existe à ce jour aucun marqueur biologique qui puisse identifier les patients à risque de complication vasculaire ou de rechute. La recherche d'antigène cible à partir d'une librairie de cDNA issue de testicule humain au cours de l'ACG et de la PPR avait déjà permis d'identifier la lamine C comme un auto-antigène. Cependant, cela n'avait pas contribué à la mise au point d'un test diagnostique (104). Des Ac anti-cardiolipine ont été détectés en ELISA chez 80% des patients atteints d'ACG et 20% des sujets sains (258). Cependant, le seuil utilisé dans cette étude pose question puisque 20% des sujets sains ont des Ac anti-cardiolipines. Les Ac anti-cardiolipine ont été associés aux poussées et rechutes de la maladie (27) mais ils ne sont pas corrélés aux manifestations ischémiques (259) et leur intérêt en pratique clinique est limité. Des Ac dirigés contre la progranuline, protéine ayant une activité anti-inflammatoire, ont été détectés à partir d'un criblage d'une librairie de cDNA et leur présence a été confirmée chez 14/65 patients atteints d'ACG/PMR (111). Par ailleurs, une recherche systématique d'Ac habituellement retrouvés au cours de la maladie coeliaque a permis d'identifier des Ac anti-

transglutaminase chez 11% des patients atteints de GCA versus 1% des sujets sains (260). Cependant, l'intérêt de l'ensemble de ces auto-Ac n'a pas été démontré que ce soit au plan diagnostique ou pronostique.

Plus récemment, Baerlecken et al. ont identifié à partir de puces à protéines que des peptides de la ferritine pourraient être la cible d'auto-Ac et que ceux-ci pourraient avoir un intérêt diagnostique (30). Ils ont mis en évidence que 92% des patients ayant une ACG active avaient des Ac dirigés contre la partie N-terminale de FTH1. Le seuil de positivité était défini à partir de la courbe « receiver operating characteristic » (ROC). Cependant, dans cette étude, on pouvait noter que les groupes de patients ayant un lupus systémique, une polyarthrite rhumatoïde ou une fièvre avaient également des auto-Ac dirigés contre ce peptide (29, 3 et 16% respectivement). La chaine lourde de la ferritine et un peptide homologue du staphylocoque epidermidis ont également été testés en ELISA mais les résultats obtenus étaient moins probants qu'avec la portion N-terminale de la ferritine humaine. A partir de notre cohorte de patients suspects d'ACG, nous avons donc évalué l'intérêt diagnostique du test ELISA proposé. Nous avons mis en évidence que 72% des patients ayant une ACG avaient des Ac dirigés contre ce même peptide mais que 31% des patients suspects d'ACG ayant au final un autre diagnostic avaient également un test positif. Le seuil de positivité était défini par la moyenne de l'absorbance obtenue avec les sérums de sujets sains plus 2 déviations standard ce qui explique en partie ces résultats différents. L'intérêt de ce test à visée diagnostique n'a donc pas pu être confirmé (261).

La mise au point d'un test diagnostique aurait nécessité de confirmer les réactivités identifiées au niveau individuel par des tests ELISA sur de larges cohortes. Cependant, la mise au point d'un test diagnostique est un travail différent que nous

n'avons pas souhaité poursuivre, ce d'autant qu'une approche combinatoire serait probablement plus pertinente (par exemple vis-à-vis de la portion N-terminale de la ferritine, de la progranuline, de l'α-enolase…) ce qui complique d'autant le travail.

4.1.4. Limites de l'approche utilisée pour identifier un auto-Ac

L'identification de ces auto-anticorps par immunoblot a cependant des limites. Nous avons identifié les réactivités à partir d'extraits protéiques de CMLV issues d'artère mammaire immortalisées par le virus SV40 et d'HUVEC. Cependant, nous avons par ailleurs mis en évidence dans le laboratoire une grande hétérogénéité du contenu protéique des CE selon le vaisseau d'origine et que cette hétérogénéité pourrait influencer la reconnaissance immune (238). Ainsi, le rapport d'expression de 159 et 30 protéines différait entre les extraits protéiques d'HUVEC d'une part et de CE de microcirculation dermique et pulmonaire d'autre part respectivement. Seuls 8 spots différaient significativement entre les 2 types de CE de microcirculation. L'effet de l'acide rétinoïque, molécule identifiée comme lien potentiel entre les protéines d'intérêt, sur la tubulogenèse des CE était variable d'un type cellulaire à l'autre ce qui témoigne de propriétés biologiques différentes. Nous pouvons supposer qu'une telle spécialisation vasculaire existe également au sein des CMLV et l'hétérogénéité du phénotype des CMLV peut limiter la portée des résultats obtenus et cet élément a contribué à justifier la réalisation du travail sur l'hétérogénéité des CMLV en condition physiologique et pathologique. Par ailleurs, nous avons utilisé l'immunoblot 2D afin d'identifier les cibles des auto-Ac. Afin de pouvoir effectuer une iso-électrofocalisation, les manipulations se font avec de faibles concentrations d'agents dénaturants et cela entraîne malheureusement la perte de nombreuses protéines de membranes. Moins de 1000 spots protéiques sont marqués sur le gel de référence, ce qui est nettement inférieur au nombre total de protéines contenues dans une cellule et

témoigne de pertes lors des différentes étapes de la manipulation. Par ailleurs, c'est une technique longue et les nombreuses étapes limitent la reproductibilité des expériences et ont nécessité de grouper les sérums par 3. Afin de connaitre la réactivité à l'échelon individuel, des tests ELISA complémentaires sont donc nécessaires. Enfin, de nombreux auto-antigènes identifiés sont intra-cellulaires, ce qui pose la question de la pénétration de l'anticorps dans la cellule ou de l'expression membranaire de cet auto-antigène. De nombreuses protéines et enzymes cytoplasmiques ont déjà été identifiées à la surface cellulaire : la vimentine à la surface des macrophages (262) ou des plaquettes (263). L'α-enolase, une protéine de la glycolyse est également exprimée à la surface cellulaire ou elle a un rôle de récepteur du plasminogène (264). La pertinence des cibles identifiées reste donc à démontrer tout au moins pour un éventuel rôle pathogène.

4.1.5. La modification du répertoire, conséquence du remodelage vasculaire ?

Cette première partie permet donc de confirmer la présence d'auto-Ac dans le sérum des patients atteints d'ACG dirigés contre les CE et les CMLV. Cependant, les expériences réalisées en immunoblot 1D et 2D n'ont pas permis d'identifier une bande ou un spot ayant une réactivité forte qui soit constante chez les patients atteints d'ACG et absente chez les sujets sains. Par ailleurs, nous n'avions que peu d'argument pour travailler plus sur l'un que sur l'autre des antigènes cibles. Compte-tenu des limites précédemment décrites et de l'observation en parallèle que les CMLV de patients présentant une ACG semblaient proliférer plus vite et jusqu'à un nombre de passages plus élevé que les sujets contrôles, nous avons émis l'hypothèse que la modification du répertoire auto-immun était lié à une modification des caractéristiques des CMLV et au remodelage vasculaire et nous avons donc décider

de poursuivre l'analyse de l'ensemble des réactivités à l'aide des logiciels d'interaction moléculaire que sont Ingenuity® et Pathway Studio®. En effet les réactivités identifiées pourraient être le témoin d'une modification de la synthèse de cette protéine, de modifications post-traductionnelles, d'une présentation antigénique différente par le système immunitaire dans le contexte du remodelage vasculaire. D'autres mécanismes pourraient également intervenir dans l'apparition de ces auto-Ac tels que le mimétisme moléculaire ou l'immunisation contre un antigène extérieur. Ainsi, à partir de l'ensemble des cibles identifiées à partir des extraits protéiques de CE et de CMLV, nous avons pu identifier la molécule Growth factor receptor bound protein 2 (Grb2) comme protéine d'intérêt. Cette protéine adaptatrice de facteur de croissance facilite l'activation de la protéine Ras par les récepteurs à tyrosine kinase et elle est impliquée dans la prolifération des CMLV. La prolifération de CMLV d'aorte de rat en présence d'oligonucléotide antisense de Grb2 réduit la prolifération induite par le PDGF. Elle semble par ailleurs nécessaire au développement d'une néointima en réponse à une lésion vasculaire chez la souris (265). Ainsi, Grb2 pourrait être surexprimé et/ou activé dans les CE et les CMLV des patients atteints d'ACG et pourrait stimuler le processus de remodelage vasculaire. Par ailleurs, parmi les molécules identifiées à l'aide du logiciel Ingenuity, on trouve également le TNF-α. Il a été montre que cette cytokine était présente dans les cellules géantes et les macrophages au contact des limitantes élastiques (266). Cependant, le recrutement des macrophages se situe probablement en aval du processus pathologique (267) ce qui explique l'absence d'efficacité des essais thérapeutiques évaluant un inhibiteur du TNF (48 , 49 , 268) au cours de l'ACG. Le rôle de Grb2 dans la prolifération des CMLV reste ainsi à étudier d'autant que l'intérêt potentiel de ce facteur a été renforcé par l'étude comparative des protéomes de CMVL de patients atteints d'ACG

histologiquement prouvée, sans preuve histologique ou ayant un autre diagnostique que l'ACG.

4.2. Mise en évidence de l'hétérogénéité des CMLV en condition physiologique et pathologique.

Les pathologies vasculaires ont habituellement un tropisme vasculaire défini. Ainsi, au cours de l'HTAP, seules les artères pulmonaires sont concernées par le remodelage vasculaire. Par ailleurs, les vascularites systémiques ont été classées selon la taille des vaisseaux préférentiellement atteints. La classification de Chapel Hill sépare les vascularites des gros vaisseaux (GCA et maladie de Takayasu), des vaisseaux de moyen calibre (périartérite noueuse et maladie de Kawasaki) et des petits vaisseaux (vascularites associées aux ANCA, purpura rhumatoïde…) (269). Il est probable que la topographie des vaisseaux atteints soit liée à une spécialisation des cellules constitutives des parois artérielles. Cependant la diversité des CMLV en condition physiologique et pathologique est largement méconnue. Les études ont essentiellement porté sur la réponse à un stimulus, sur le rôle d'une protéine spécifique, de l'expression de miRNA ou de régulation épigénétique (155 , 156, 157). Ces éléments nous ont donc conduits à comparer le contenu protéique de CMLV humaines normales issues d'artères différentes (artère pulmonaire (HPASMC), aorte (HAoSMC) et artère ombilicale (HUASMC)) et d'y associer une comparaison avec des CMLV au cours de l'HTAP (PAH-SMC). En effet, cela permet à la fois d'aborder l'hétérogénéité des CMLV en contexte physiologique et d'aborder le remodelage vasculaire. Si l'HTAP et l'ACG ont des mécanismes physiopathologiques très distincts, on observe dans les deux pathologies un épaississement de la média avec constitution d'une néo-intima.

4.2.1. Analyse du protéome des CMLV humaines normales

De façon intéressante, nous avons pu mettre en évidence qu'il y avait 132 et 124 protéines différemment exprimées entre les HUASMC et les HAoSMC ou les HPASMC respectivement alors que seulement 19 étaient différemment exprimées entre HPASMC et HAoSMC (rapport d'expression ≥1,5 et p≤.0,05). Cette hétérogénéité observée entre les CMLV d'artères différentes est très nettement dépassée par celle observée entre les HPASMC et les PAH-SMC puisqu'on comptait 336 protéines différemment exprimées (rapport d'expression ≥1,5 et p≤.0,05). Au niveau protéique, nous avons identifié que la filamine et la vimentine étaient modifiées dans les HUASMC comparativement aux HPASMC ou aux HAoSMC. La filamine est capable de se lier à l'actine et participe avec la vimentine à la régulation de l'architecture cellulaire. Il a été montré que l'expression de la filamine, de la gelsoline, de la vimentine ainsi que de la vinculine étaient diminuée au sein de CMLV d'artères coronaires athéromateuses (270) et que l'expression de la vimentine ou de la calponine étaient également diminuées lors d'une dissection aortique comparativement à un vaisseau sein (136) ce qui suggère un switch entre les phénotypes contractile et synthétique. Par ailleurs, l'analyse avec Ingenuity® a montré que parmi les voies canoniques, la voie de signalisation médiée par les protéines 14-3-3 permettait de différencier les HUASMC des HPASMC ou des HAoSMC. Les protéines 14-3-3- interviennent dans la transduction du signal, dans la régulation de l'apoptose, du cycle et de la croissance cellulaire et ont souvent été retrouvées dans des conditions marquées par un remodelage vasculaire et par une dédifférentiation des CMLV avec un profil plutôt synthétique. Ainsi, au sein des CMLV, on observe une localisation de la protéine 14-3-3 ζ au niveau des cellules SMA^+ des plaques d'athérome (271). Par ailleurs, Autieri et al. ont montré que la

protéine 14-3-3 γ était phosphorylée en réponse à une stimulation par le TGF-β (272) et que son expression est augmentée au cours d'un rejet de transplant cardiaque et après lésion vasculaire chez le rat (273). De même, les isoformes de protéine 14-3-3 infiltrant des artères carotides ou cérébrales athéromateuses différent et cette variation peut être expliquée par les structures cellulaires ou extra-cellulaires environnantes (271). Ces résultats suggèrent donc que les modifications du contenu protéique pourraient être la conséquence de modulations entre les phénotypes contractiles et synthétiques entre les HUASMC et les HAoSMC et HPASMC.

4.2.2. Les CMLV dans le contexte de l'HTAP

La calponine est une protéine impliquée dans la régulation de la contraction cellulaire. Il a été montré que l'expression de la calponine était augmentée dans les HPASMC après incubation avec le micro-RNA-206 (274). Chez des souris traitées par un adénovirus contenant l'ADN complémentaire de la protéine kinase G Iα, l'expression de calponine est conservée ce qui pourrait avoir un effet favorable au cours de l'HTAP hypoxique (275). La protéine UACA (pour "Uveal autoantigen with coiled-coil domains and ankyrin repeats") a un rôle dans la régulation de l'apoptose. Cette protéine est hypo exprimée au cours du cancer non à petites cellules (276). L'hypoexpression de cette protéine au cours de l'HTAP pourrait contribuer à expliquer la prolifération accrue et la diminution de l'apoptose observée au sein des CMLV de patients atteints d'HTAP (277).

Nous avons par ailleurs mis en évidence à l'aide du logiciel Ingenuity® que les protéines différemment exprimées entre les HPASMC et les PAH-SMC appartenaient à la voie canonique de la dysfonction mitochondriale. Au cours de l'HTAP, des anomalies du métabolisme énergétique, à savoir une dépendance marquée à la glycolyse et une diminution de la consommation d'oxygène ont été mises en évidence

(189). Cet effet, appelé effet Warburg a été initialement décrit au cours du cancer et c'est un des éléments caractéristiques de l'HTAP (197). Nous apportons donc des informations nouvelles et exhaustives sur les modifications du contenu protéique des CMLV d'artérioles pulmonaires au cours de l'HTAP.

Par ailleurs, l'analyse avec le logiciel Ingenuity® de l'ensemble des protéines différemment exprimées entre HPASMC et PAH-SMC a montré que celles-ci étaient liées à la paxilline. La paxilline est une protéine qui intervient dans la signalisation intra-cellulaire (278), la migration cellulaire (279) et l'apoptose (280). L'inhibition de la prolifération des PAH-SMC que nous avons observée confirme les résultats de Veith et al.. Ils avaient mis en évidence que la paxilline avait un rôle régulateur de la croissance cellulaire au cours de l'HTAP (281). A notre connaissance, il n'existe pas d'inhibiteur de paxilline qui ait été développé à des fins thérapeutiques. Cependant, il a été montré que le sarcatinib, un inhibiteur de Src évalué au cours du cancer du sein pouvait diminuer la phosphorylation de la paxilline (282). Nous confirmons que la paxilline pourrait constituer une cible thérapeutique afin d'inhiber la prolifération des CMLV au cours de l'HTAP. Une autre protéine régulatrice STAT3 (« signal transducers and activators of transcription-3) a également été identifiée avec Ingenuity®. Cette protéine activée en réponse à des cytokines ou des facteurs de croissance active de nombreux facteurs de transcription impliqués dans la régulation de la prolifération cellulaire et de la résistance à l'apoptose. Cette molécule clé pourrait également constituer une cible thérapeutique d'avenir au cours de l'HTAP (283).

4.2.3. Implication clinique

Au cours de l'HTAP, nous avons rapporté que le sérum des patients atteints d'HTAP contenait des IgG capables d'induire la contraction de CMLV (160). La

présence de ces Ac pourrait être soit un évènement pathogène soit être la conséquence du remodelage vasculaire secondaire à la modification du contenu protéique des CMLV. Les données que nous rapportons pourraient contribuer à expliquer pourquoi certaines artères sont atteintes au cours des maladies vasculaires telles que l'ACG ou l'HTAP alors que d'autres sont épargnées. Ainsi, au cours de l'ACG, il a été mis en évidence que les DC adventitielles avaient un profil d'expression de toll like receptor (TLR) différent selon les vaisseaux et que cela pourrait être un des éléments qui explique le tropisme préférentiel de l'ACG pour l'aorte et les troncs supra-aortiques (61). La spécialisation des CMLV pourrait être un autre élément d'explication.

4.2.4. Limites de cette étude

Nous avons travaillé à partir de CMLV en culture primaire dont le phénotype est $CD90^-$ et α-SMA^+ (pour les PAH-SMC dans ce travail mais également pour les CMLV issues de BAT). Le choix de ce phénotype a été guidé par le fait que la principale « contamination » cellulaire envisagée est celle des fibroblastes qui expriment le marqueur CD90. Cependant, des travaux ont également montré que certaines CMLV pouvaient exprimer en faible proportion ce marqueur et qu'un tri cellulaire par bille magnétique ne permettait pas de s'affranchir complètement de ces cellules $CD90^+$ lors des passages successifs des CMLV en culture (284). Par ailleurs, les PAH-SMC ont été isolées à partir des vaisseaux de petit calibre alors que les HPASMC humaines normales sont isolées à partir des troncs de l'artère pulmonaire. Ce choix a été fait car l'extension distale de la muscularisation et les lésions plexiformes intéressent les petits vaisseaux (197). Cependant, cet élément pourrait en partie expliquer la différence observée entre ces 2 types cellulaires.

Dans nos manipulations, nous avons identifié 3293 spots protéiques différents et de façon similaire à l'éléctrophorèse bi-dimensionnelle que nous avions utilisés

précédemment, des protéines sont perdues à chaque étape de la manipulation jusqu'à l'identification protéique. En particulier, les protéines de membrane sont pour beaucoup absentes. Par ailleurs, nous avons utilisé la MS pour l'identification et en particulier l'orbitrap. Cette technique d'identification est très sensible ce qui permet d'obtenir une identification pour presque tous les spots prélevés. La contrepartie est la possibilité d'avoir de nombreuses protéines identifiées au sein de chaque spot sans connaître le spot majoritaire et de ne pas savoir si la modification de l'intensité d'expression doit être rapportée plutôt à l'une ou l'autre des protéines identifiées. Cela complique l'interprétation d'autant qu'une protéine donnée est parfois identifiée dans différents spots avec des variations d'expression discordantes. Les modifications post-traductionnelles ou la localisation cellulaire des protéines restent inconnues et des expériences complémentaires sont donc nécessaires à partir des protéines d'intérêt afin de confirmer cette approche globale. Par ailleurs, le travail de protéomique est avant tout descriptif et ne peut pas constituer en tant que tel une preuve du phénotype contractile que nous rapportons aux HPASMC et HAoSMC et synthétique attribué aux HUASMC. L'approche à l'aide de logiciels tels qu'Ingenuity ou Patway Studio a des limites. En effet, ces logiciels sont basés sur un recensement exhaustif de l'ensemble des interactions connues entre molécule : activation, inhibition, contrôle transcriptionnel ou régulation traductionnelle… Ce recensement ne tient pas compte du contexte physiopathologique ni du type cellulaire. Les schémas proposés par ces logiciels doivent donc être analysés de façon critique. La force de ces logiciels est d'aider à l'interprétation de quantités importantes de données. Leur faiblesse réside dans la nécessité de confirmer l'intérêt des nœuds protéiques proposés par des manipulations spécifiques. Les tests de prolifération effectués confirment la pertinence de cette approche sans pouvoir valider l'intérêt de l'ensemble des protéines

identifiées. Enfin, nous avons utilisés des groupes restreints avec quatre donneurs différents par groupe pour les manipulations de protéomique et de prolifération. La variabilité des processus biologiques observés imposent des manipulations sur des groupes plus larges afin de confirmer ces résultats.

Néanmoins, nous démontrons que les CMLV normales provenant d'artère pulmonaire, d'aorte ou d'artère ombilicale ont des profils protéiques différents ce qui pourrait refléter des propriétés physiologiques différents. Nous confirmons que la paxilline pourrait être une cible thérapeutique possible dans le traitement de l'HTAP.

4.3. Modification des caractéristiques des CMLV au cours de l'ACG : identification de pistes thérapeutiques

Malgré les progrès récents concernant la physiopathologie de l'ACG, la raison pour laquelle certains patients développent des occlusions artérielles responsables des complications visuelles reste méconnue. La participation des CMLV au remodelage vasculaire semble être cruciale. Nous apportons des données exhaustives concernant les modifications de l'expression protéique et génomique au cours de l'ACG au sein d'un groupe de patients avec une ACG prouvée histologiquement (TAB^+-ACG), un groupe de patients atteint d'ACG sans preuve histologique (TAB^--ACG) et un groupe contrôle (GCA-contrôle) pour lequel un autre diagnostique est retenu au terme des explorations.

4.3.1 Analyse comparative des protéomes et des profils d'expressions géniques

La myosine, impliquée dans le mouvement cellulaire (285) est surexprimée dans les CMLV du groupe TAB^+-GCA au niveau protéique. Nous avons également identifié que les ARN messager de la β-catenine et de la ténascine-C étaient significativement augmentés dans le groupe TAB^+-GCA comparativement au groupe

GCA-contrôle. La translocation de la β-catenine dans le noyau est associée à une expression de la cycline D1 qui induit la prolifération des CMLV (286) et il a été montré que la β-catenine médiait la prolifération des CMLV induite par les MMP9 et 12 (287) et par le PDGF (288). La ténascine-C est une protéine de la matrice extracellulaire synthétisée par les CMLV en réponse à des stimuli environnementaux. Elle régule la prolifération, la migration, la différenciation et la survie cellulaire (289). Elle pourrait réguler la prolifération des CMLV et favoriser l'hyperplasie néo-intimale de greffons artériels dans un modèle murin (290) et la ténascine C est élevée dans les formes héritables d'HTAP (195). Par ailleurs, l'expression protéique de l'annexine A5, une protéine ayant des propriétés anticoagulante, est également diminuée dans le groupe TAB^{+}-GCA comparativement au groupe GCA-control. Cependant la responsabilité des Ac dirigés contre l'annexine A5 dans les phénomènes thrombotiques au cours de la maladie de Behcet n'a pas pu être démontrée (248). Ainsi, les données protéiques et génomiques suggèrent que les CMLV au sein des lésions d'ACG pourraient avoir des capacités prolifératives accrues et nous pouvons envisager que la diminution de l'annexine A5 pourrait participer aux phénomènes thrombotiques. Ces résultats nécessitent bien sûr d'être confirmés mais pourraient aider à mieux comprendre l'occlusion qui peut survenir au sein de l'artère temporale. A l'opposé, le rôle de la Peptidyl-prolyl cis-trans isomerase A (PPIA) dans la constitution des anévrysmes aortiques a été démontré et son hypoexpression dans les CMLV des patients du groupe TAB^{+}-GCA comparativement au groupe GCA-control pourrait au contraire avoir des effets bénéfiques (291).

De façon intéressante, l'ARNm de FTH1 était diminué dans les CMLV du groupe TAB^{+}-GCA comparativement au groupe GCA–contrôles. Cela suggère une augmentation de la synthèse protéique de ferritine qui pourrait déclencher des auto-Ac

dirigés contre ce peptide même si nous avons montré que l'intérêt diagnostique de ces Ac était limité (261) (30). Cependant, la protéine FTH1 n'a pas été identifiée lors des expériences de protéomique. Cela pourrait être du à la perte de cette protéine lors des étapes de préparation des échantillons, à la difficulté de prélever ce spot pour identification du fait de sa taille ou encore à l'absence de différence au niveau du spot protéique qui ne nous aurait pas fait prélever ce spot pour identification en MS.

4.3.2. Modulation du remodelage, une cible thérapeutique innovante au cours de l'ACG

Nous avons pu identifier à l'aide du logiciel Ingenuity® que la paxilline et l'ET-1 étaient des liens entre les protéines différemment exprimées et entre les gènes différemment exprimés dans les deux approches. Il a déjà été montré que la paxilline était un régulateur de la prolifération des CMLV dans le contexte de l'HTAP (281). Cependant, dans une expérience préliminaire, nous n'avons pas réussi à identifier un rôle similaire au cours de l'ACG. L'intérêt potentiel de cette voie justifie la réalisation d'expériences complémentaires avec des groupes plus larges. Nous confirmons l'implication de l'ET-1 et de ses récepteurs dans la pathogénie de l'ACG (119). Nos données suggèrent que cibler l'ET-1 pourrait être prometteur pour inhiber la prolifération des CMLV et le remodelage. Nous avons décidé d'inhiber l'ET-1 avec du macitentan car il s'agit d'un antagonistes des récepteurs ET_AR et ET_BR et qu'il a la plus grande affinité pour ces récepteurs comparativement aux autres inhibiteurs disponibles. Par ailleurs, son métabolite actif a une activité prédominante sur l'ET_AR. Il est connu que l'ET_AR est responsable de la vasoconstriction induite par l'ET-1 (292) et que l'ET_BR pourrait avoir une action synergique ou au contraire participer à la clairance de l'ET-1 (293). Cela pourrait donc être un des éléments qui explique la supériorité du métabolite actif du macitentan dans nos expériences.

Au cours de l'HTAP, la prostacycline et les inhibiteurs de PDE5 sont également utilisés comme vaso-dilatateurs. Par analogie, nous avons testé dans une expérience très préliminaire l'effet de la prostacycline et du sildénafil sur la prolifération des CMLV d'un nombre restreint de patient. Cette approche n'a pas été concluante mais mérite cependant d'être réalisée avec un nombre plus grand d'échantillon biologique. A plus long terme, la place d'une thérapeutique qui inhiberait le remodelage de la paroi vasculaire ou favoriserait la vasodilatation reste discutable. En effet, les CMLV semblent être cibles de la réponse immune locale et il est peu probable qu'elles soient l'élément initiateur de la réponse inflammatoire (par le biais de la présentation antigénique ou par leurs capacités sécrétoires par exemple). La place des inhibiteurs du remodelage vasculaire serait donc la prévention des évènements thrombotiques survenant après introduction de la corticothérapie. Cependant, la cécité qui découle de la thrombose artérielle est peu fréquente et devient rare après l'introduction de la corticothérapie ce qui rend difficile un essai thérapeutique.

4.3.3. Forces et faiblesses de cette étude

A notre connaissance, à ce jour, aucune autre équipe ne peut se prévaloir de travailler sur des CMLV cultivées à partir de BAT. Ainsi, l'équipe de M. Cid travaille à partir de cellules cultivées sur un support Matrigel. Il s'agit d'une membrane basale soluble développée afin de favoriser la croissance des CE (294). Par ailleurs, l'utilisation de la SMA et du collagène de type 1 et 3 comme marqueur de CMLV laisse à penser que des fibroblastes pourraient contaminer la culture (122). L'utilisation dans nos expériences de cellules cultivées sans matrigel et n'exprimant pas le CD90 en immunofluorescence nous rend confiant sur le fait que nous avons bien travaillé sur des CMLV. Par ailleurs, cette méthode de caractérisation est identique à celle utilisée par le laboratoire auprès duquel nous nous sommes procuré

les cellules humaines normales ce qui permet des comparaisons plus fiables. Cependant, la taille du prélèvement obtenu au moment de la BAT fait que la culture n'est que rarement positive et que la quantité de CMLV disponible pour les expériences est limitée. Notre décision d'exiger des cellules dont le phénotype a été contrôlé avec une pureté de 90% environ a également contribué à réduire le nombre d'échantillons disponibles. Une autre limite est liée au fait que la corticothérapie est parfois débutée avant la réalisation de la BAT. Bien que la durée soit brève, on ne peut pas éliminer que les résultats puissent être partiellement biaisés par cette thérapeutique. Lozano et al. ont montré une modification du système de l'ET-1 après une corticothérapie de 8 jours en moyenne. Ainsi, alors que l'ET-1 n'était pas significativement diminuée, l'expression de l'ET_AR était diminuée et revenait à des valeurs similaires aux sujets sains (119). Nous aurions pu également effectuer un extrait protéique total à partir du fragment de BAT ou à partir de la media après dissection mécanique. Cela aurait permis de s'affranchir de la modification phénotypique qui survient en culture. En effet, les CMLV en culture prolifèrent et migrent. Elles ont donc un phénotype synthétique ce qui va modifier leur contenu protéique. Par ailleurs, afin d'avoir un matériel protéique suffisant, nous avons effectué les extraits protéiques au $4^{ème}$ passage. Cela participe également à cette dédifférenciation qui survient en culture et modifie donc d'autant les résultats (158). Ce choix a été fait car l'objectif final était celui de moduler les propriétés des CMLV afin de prévenir le remodelage. Il était donc nécessaire d'avoir des CMLV en culture. La difficulté de la culture et le nombre de prélèvements reçus ne nous permettaient pas d'utiliser l'ensemble du prélèvement pour la protéomique et la génomique et l'exiguité des fragments de BAT ne permettait pas d'envisager les 2 approches à partir d'un unique prélèvement (extraction initiale et CMLV en culture).

Enfin, nous avions identifiés Grb2 comme une protéine d'intérêt faisant le lien entre les antigènes cibles des auto-Ac au cours de l'ACG. Nous identifions à nouveau Grb2 à partir des gènes différemment exprimés entre les CMLV du groupe TAB^{+}-GCA et le groupe GCA-control. Cela renforce donc l'intérêt de cibler cette molécule dans de futures recherches.

5. Conclusion et perspectives

Au total, nous avons identifié les cibles antigéniques des auto-Ac au cours de l'ACG à partir d'extraits protéiques de CE et de CMLV. Nous avons ainsi pu identifier que la vinculine, la lamine A/C ou l'annexine 5 étaient des cibles spécifiques des auto-anticorps. Le rôle pathogène de ces auto-anticorps n'est pas établi. Cependant, l'identification de Grb2 comme lien potentiel entre les cibles d'auto-Ac au cours de l'ACG d'une part et entre les gènes différemment exprimés entre les CMVL de patients atteints d'ACG et de patients contrôle d'autre part nous encourage à poursuivre ces résultats avec une approche de remodelage vasculaire.

Nous avons étudié les caractéristiques et la diversité des CMLV en condition physiologique, au cours de l'HTAP et au cours de l'ACG. Nous avons identifié des différences importantes entre les protéomes de CMLV de différentes origines. Alors qu'un nombre limité de différences est observé entre HPASMC et HAoSMC, les protéomes de ces deux groupes diffèrent nettement de celui des HUASMC. Les PAH-SMC surexpriment la calponine et l'UACA respectivement impliquées dans la contraction cellulaire et la régulation de l'apoptose. Les protéines d'intérêt entre PAH-SMC et HPASMC interagissent avec la paxilline et son inhibition par un siRNA a permis une diminution des capacités prolifératives des PAH-SMC. Ces résultats, confirmant par certains aspects ceux obtenus par une autre équipe, pourraient ouvrir des perspectives thérapeutiques nouvelles dans l'HTAP.

Enfin, par des approches transcriptomique et protéomique, nous avons identifié au cours de l'ACG, des molécules comme la β-caténine, la ténascine C et la myosine impliquées dans la contraction et la prolifération des CMLV. Leur expression majorée au sein des lésions d'artérite temporale pourrait contribuer au remodelage vasculaire observé au cours de cette maladie. La paxilline et ET-1, en interaction avec de nombreuses protéines d'intérêt, ont été identifiées comme des cibles thérapeutiques

potentielles au cours de l'ACG. Après avoir confirmé l'augmentation d'expression de l'ET-1 et de ses récepteurs dans les BAT de patients, nous avons montré que le macitentan permet de réduire la prolifération des CMLV de patients atteints d'ACG. Ces données, qui devront être confirmées en étudiant un groupe plus large de patients, ouvrent des perspectives thérapeutiques nouvelles dans le traitement de l'ACG et la prévention des complications vasculaires au cours de cette maladie. Enfin, l'étude du remodelage artériel et de la place des CMLV au cours de l'ACG est facilitée par les connaissances issues de l'HTAP. La comparaison prudente de ces pathologies permet d'élaborer de multiples hypothèses sur les facteurs de prédisposition ou les mécanismes qui participent au remodelage vasculaire et à l'occlusion artérielle au cours de l'ACG. Le matériel dont nous disposons permet d'envisager de poursuivre ce travail exploratoire.

6. Références bibliographiques

1. Hunder GG, Bloch DA, Michel BA, Stevens MB, Arend WP, Calabrese LH, et al. The American College of Rheumatology 1990 criteria for the classification of giant cell arteritis. Arthritis Rheum. 1990 Aug;33(8):1122-8.
2. Bloch DA, Michel BA, Hunder GG, McShane DJ, Arend WP, Calabrese LH, et al. The American College of Rheumatology 1990 criteria for the classification of vasculitis. Patients and methods. Arthritis Rheum. 1990 Aug;33(8):1068-73.
3. Hunder GG. Epidemiology of giant-cell arteritis. Cleve Clin J Med. 2002;69 Suppl 2:SII79-82.
4. Baldursson O, Steinsson K, Bjornsson J, Lie JT. Giant cell arteritis in Iceland. An epidemiologic and histopathologic analysis. Arthritis Rheum. 1994 Jul;37(7):1007-12.
5. Haugeberg G, Paulsen PQ, Bie RB. Temporal arteritis in Vest Agder County in southern Norway: incidence and clinical findings. J Rheumatol. 2000 Nov;27(11):2624-7.
6. Lawrence RC, Felson DT, Helmick CG, Arnold LM, Choi H, Deyo RA, et al. Estimates of the prevalence of arthritis and other rheumatic conditions in the United States. Part II. Arthritis Rheum. 2008 Jan;58(1):26-35.
7. Reinhold-Keller E, Zeidler A, Gutfleisch J, Peter HH, Raspe HH, Gross WL. Giant cell arteritis is more prevalent in urban than in rural populations: results of an epidemiological study of primary systemic vasculitides in Germany. Rheumatology (Oxford). 2000 Dec;39(12):1396-402.
8. Kobayashi S, Yano T, Matsumoto Y, Numano F, Nakajima N, Yasuda K, et al. Clinical and epidemiologic analysis of giant cell (temporal) arteritis from a nationwide survey in 1998 in Japan: the first government-supported nationwide survey. Arthritis Rheum. 2003 Aug 15;49(4):594-8.
9. Cha DM, Lee T, Choe G, Yang HK, Hwang JM. Silent giant cell arteritis in an elderly Korean woman. Korean J Ophthalmol. 2013 Jun;27(3):224-7.
10. Duhaut P, Pinede L, Demolombe-Rague S, Loire R, Seydoux D, Ninet J, et al. Giant cell arteritis and cardiovascular risk factors: a multicenter, prospective case-control study. Groupe de Recherche sur l'Arterite a Cellules Geantes. Arthritis Rheum. 1998 Nov;41(11):1960-5.
11. Larsson K, Mellstrom D, Nordborg E, Oden A. Early menopause, low body mass index, and smoking are independent risk factors for developing giant cell arteritis. Ann Rheum Dis. 2006 Apr;65(4):529-32.
12. Salvarani C, Gabriel SE, O'Fallon WM, Hunder GG. The incidence of giant cell arteritis in Olmsted County, Minnesota: apparent fluctuations in a cyclic pattern. Ann Intern Med. 1995 Aug 1;123(3):192-4.
13. Gonzalez-Gay MA, Miranda-Filloy JA, Lopez-Diaz MJ, Perez-Alvarez R, Gonzalez-Juanatey C, Sanchez-Andrade A, et al. Giant cell arteritis in northwestern Spain: a 25-year epidemiologic study. Medicine (Baltimore). 2007 Mar;86(2):61-8.
14. Liozon F. [Horton's disease]. Ann Med Interne (Paris). 1989;140(2):122-41.
15. Gonzalez-Gay MA, Barros S, Lopez-Diaz MJ, Garcia-Porrua C, Sanchez-Andrade A, Llorca J. Giant cell arteritis: disease patterns of clinical presentation in a series of 240 patients. Medicine (Baltimore). 2005 Sep;84(5):269-76.
16. Salvarani C, Hunder GG. Musculoskeletal manifestations in a population-based cohort of patients with giant cell arteritis. Arthritis Rheum. 1999 Jun;42(6):1259-66.
17. Liozon E, Ly KH, Robert PY. [Ocular complications of giant cell arteritis]. Rev Med Interne. 2013 Jul;34(7):421-30.

18. Cid MC, Font C, Oristrell J, de la Sierra A, Coll-Vinent B, Lopez-Soto A, et al. Association between strong inflammatory response and low risk of developing visual loss and other cranial ischemic complications in giant cell (temporal) arteritis. Arthritis Rheum. 1998 Jan;41(1):26-32.
19. Lobato-Berezo A, Alcalde-Villar M, Imbernon-Moya A, Martinez-Perez M, Aguilar-Martinez A, Collado-Ramos P. Tongue necrosis: An unusual clinical presentation of giant cell arteritis. Arthritis Rheumatol. 2014 Jun 30.
20. Samson M, Jacquin A, Audia S, Daubail B, Devilliers H, Petrella T, et al. Stroke associated with giant cell arteritis: a population-based study. J Neurol Neurosurg Psychiatry. 2014 Apr 29.
21. Ferroir JP, Cocheton JJ, Roland J, Chatelet F. [Horton's disease. Coronary localization causing fatal myocardial infarction]. Ann Med Interne (Paris). 1982;133(8):569-72.
22. Ghaffar SA, Todd PM. Scalp necrosis secondary to giant-cell arteritis. Clin Exp Dermatol. 2010 Apr;35(3):e40-1.
23. Lin LW, Wang SS, Shun CT. Myocardial infarction due to giant cell arteritis: a case report and literature review. Kaohsiung J Med Sci. 2007 Apr;23(4):195-8.
24. Smetana GW, Shmerling RH. Does this patient have temporal arteritis? JAMA. 2002 Jan 2;287(1):92-101.
25. Coffin-Pichonnet S, Bienvenu B, Mouriaux F. [Ophthalmological complications of giant cell arteritis]. J Fr Ophtalmol. 2013 Feb;36(2):178-83.
26. Agard C, Barrier JH, Dupas B, Ponge T, Mahr A, Fradet G, et al. Aortic involvement in recent-onset giant cell (temporal) arteritis: a case-control prospective study using helical aortic computed tomodensitometric scan. Arthritis Rheum. 2008 May 15;59(5):670-6.
27. Liozon E, Roblot P, Paire D, Loustaud V, Liozon F, Vidal E, et al. Anticardiolipin antibody levels predict flares and relapses in patients with giant-cell (temporal) arteritis. A longitudinal study of 58 biopsy-proven cases. Rheumatology (Oxford). 2000 Oct;39(10):1089-94.
28. Navarro M, Cervera R, Font J, Reverter JC, Monteagudo J, Escolar G, et al. Anti-endothelial cell antibodies in systemic autoimmune diseases: prevalence and clinical significance. Lupus. 1997;6(6):521-6.
29. Amor-Dorado JC, Garcia-Porrua C, Gonzalez-Gay MA. Anti-endothelial cell antibodies and biopsy-proven temporal arteritis. Lupus. 2002;11(2):134.
30. Baerlecken NT, Linnemann A, Gross WL, Moosig F, Vazquez-Rodriguez TR, Gonzalez-Gay MA, et al. Association of ferritin autoantibodies with giant cell arteritis/polymyalgia rheumatica. Ann Rheum Dis. 2012 Jun;71(6):943-7.
31. Genereau T, Lortholary O, Pottier MA, Michon-Pasturel U, Ponge T, de Wazieres B, et al. Temporal artery biopsy: a diagnostic tool for systemic necrotizing vasculitis. French Vasculitis Study Group. Arthritis Rheum. 1999 Dec;42(12):2674-81.
32. Mahr A, Saba M, Kambouchner M, Polivka M, Baudrimont M, Brocheriou I, et al. Temporal artery biopsy for diagnosing giant cell arteritis: the longer, the better? Ann Rheum Dis. 2006 Jun;65(6):826-8.
33. Breuer GS, Nesher R, Nesher G. Effect of biopsy length on the rate of positive temporal artery biopsies. Clin Exp Rheumatol. 2009 Jan-Feb;27(1 Suppl 52):S10-3.
34. Boyev LR, Miller NR, Green WR. Efficacy of unilateral versus bilateral temporal artery biopsies for the diagnosis of giant cell arteritis. Am J Ophthalmol. 1999 Aug;128(2):211-5.

35. Achkar AA, Lie JT, Hunder GG, O'Fallon WM, Gabriel SE. How does previous corticosteroid treatment affect the biopsy findings in giant cell (temporal) arteritis? Ann Intern Med. 1994 Jun 15;120(12):987-92.
36. Hall S, Persellin S, Lie JT, O'Brien PC, Kurland LT, Hunder GG. The therapeutic impact of temporal artery biopsy. Lancet. 1983 Nov 26;2(8361):1217-20.
37. Karassa FB, Matsagas MI, Schmidt WA, Ioannidis JP. Meta-analysis: test performance of ultrasonography for giant-cell arteritis. Ann Intern Med. 2005 Mar 1;142(5):359-69.
38. Maldini C, Depinay-Dhellemmes C, Tra TT, Chauveau M, Allanore Y, Gossec L, et al. Limited value of temporal artery ultrasonography examinations for diagnosis of giant cell arteritis: analysis of 77 subjects. J Rheumatol. 2010 Nov;37(11):2326-30.
39. Blockmans D, de Ceuninck L, Vanderschueren S, Knockaert D, Mortelmans L, Bobbaers H. Repetitive 18F-fluorodeoxyglucose positron emission tomography in giant cell arteritis: a prospective study of 35 patients. Arthritis Rheum. 2006 Feb 15;55(1):131-7.
40. Jover JA, Hernandez-Garcia C, Morado IC, Vargas E, Banares A, Fernandez-Gutierrez B. Combined treatment of giant-cell arteritis with methotrexate and prednisone. a randomized, double-blind, placebo-controlled trial. Ann Intern Med. 2001 Jan 16;134(2):106-14.
41. Spiera RF, Mitnick HJ, Kupersmith M, Richmond M, Spiera H, Peterson MG, et al. A prospective, double-blind, randomized, placebo controlled trial of methotrexate in the treatment of giant cell arteritis (GCA). Clin Exp Rheumatol. 2001 Sep-Oct;19(5):495-501.
42. Hoffman GS, Cid MC, Hellmann DB, Guillevin L, Stone JH, Schousboe J, et al. A multicenter, randomized, double-blind, placebo-controlled trial of adjuvant methotrexate treatment for giant cell arteritis. Arthritis Rheum. 2002 May;46(5):1309-18.
43. Mahr AD, Jover JA, Spiera RF, Hernandez-Garcia C, Fernandez-Gutierrez B, Lavalley MP, et al. Adjunctive methotrexate for treatment of giant cell arteritis: an individual patient data meta-analysis. Arthritis Rheum. 2007 Aug;56(8):2789-97.
44. de Boysson H, Boutemy J, Creveuil C, Ollivier Y, Letellier P, Pagnoux C, et al. Is there a place for cyclophosphamide in the treatment of giant-cell arteritis? A case series and systematic review. Semin Arthritis Rheum. 2013 Aug;43(1):105-12.
45. De Silva M, Hazleman BL. Azathioprine in giant cell arteritis/polymyalgia rheumatica: a double-blind study. Ann Rheum Dis. 1986 Feb;45(2):136-8.
46. Liozon F, Vidal E, Barrier J. Does dapsone have a role in the treatment of temporal arteritis with regard to efficacy and toxicity? Clin Exp Rheumatol. 1993 Nov-Dec;11(6):694-5.
47. Sailler L, Pugnet G, Bienvenu B. [Treatment of giant cell arteritis]. Rev Med Interne. 2013 Jul;34(7):431-7.
48. Hoffman GS, Cid MC, Rendt-Zagar KE, Merkel PA, Weyand CM, Stone JH, et al. Infliximab for maintenance of glucocorticosteroid-induced remission of giant cell arteritis: a randomized trial. Ann Intern Med. 2007 May 1;146(9):621-30.
49. Seror R, Baron G, Hachulla E, Debandt M, Larroche C, Puechal X, et al. Adalimumab for steroid sparing in patients with giant-cell arteritis: results of a multicentre randomised controlled trial. Ann Rheum Dis. 2013 Jul 29.
50. Ly KH, Stirnemann J, Liozon E, Michel M, Fain O, Fauchais AL. Interleukin-1 blockade in refractory giant cell arteritis. Joint Bone Spine. 2014 Jan;81(1):76-8.

51. Seitz M, Reichenbach S, Bonel HM, Adler S, Wermelinger F, Villiger PM. Rapid induction of remission in large vessel vasculitis by IL-6 blockade. A case series. Swiss Med Wkly. 2011;141:w13156.
52. Le Page L, Duhaut P, Seydoux D, Bosshard S, Ecochard R, Abbas F, et al. [Incidence of cardiovascular events in giant cell arteritis: preliminary results of a prospective double cohort study (GRACG)]. Rev Med Interne. 2006 Feb;27(2):98-105.
53. Proven A, Gabriel SE, Orces C, O'Fallon WM, Hunder GG. Glucocorticoid therapy in giant cell arteritis: duration and adverse outcomes. Arthritis Rheum. 2003 Oct 15;49(5):703-8.
54. Jamilloux Y, Liozon E, Pugnet G, Nadalon S, Heang Ly K, Dumonteil S, et al. Recovery of adrenal function after long-term glucocorticoid therapy for giant cell arteritis: a cohort study. PLoS One. 2013;8(7):e68713.
55. Evans JM, O'Fallon WM, Hunder GG. Increased incidence of aortic aneurysm and dissection in giant cell (temporal) arteritis. A population-based study. Ann Intern Med. 1995 Apr 1;122(7):502-7.
56. Blockmans D, Coudyzer W, Vanderschueren S, Stroobants S, Loeckx D, Heye S, et al. Relationship between fluorodeoxyglucose uptake in the large vessels and late aortic diameter in giant cell arteritis. Rheumatology (Oxford). 2008 Aug;47(8):1179-84.
57. Mackie SL, Hensor EM, Morgan AW, Pease CT. Should I send my patient with previous giant cell arteritis for imaging of the thoracic aorta? A systematic literature review and meta-analysis. Ann Rheum Dis. 2014 Jan;73(1):143-8.
58. Nesher G, Sonnenblick M, Friedlander Y. Analysis of steroid related complications and mortality in temporal arteritis: a 15-year survey of 43 patients. J Rheumatol. 1994 Jul;21(7):1283-6.
59. Ly KH, Regent A, Tamby MC, Mouthon L. Pathogenesis of giant cell arteritis: More than just an inflammatory condition? Autoimmun Rev. 2010 Aug;9(10):635-45.
60. Brack A, Rittner HL, Younge BR, Kaltschmidt C, Weyand CM, Goronzy JJ. Glucocorticoid-mediated repression of cytokine gene transcription in human arteritis-SCID chimeras. J Clin Invest. 1997 Jun 15;99(12):2842-50.
61. Pryshchep O, Ma-Krupa W, Younge BR, Goronzy JJ, Weyand CM. Vessel-specific Toll-like receptor profiles in human medium and large arteries. Circulation. 2008 Sep 16;118(12):1276-84.
62. Ma-Krupa W, Jeon MS, Spoerl S, Tedder TF, Goronzy JJ, Weyand CM. Activation of arterial wall dendritic cells and breakdown of self-tolerance in giant cell arteritis. J Exp Med. 2004 Jan 19;199(2):173-83.
63. Raptis L, Pappas G, Akritidis N. Horton's three sisters: familial clustering of temporal arteritis. Clin Rheumatol. 2007 Nov;26(11):1997-8.
64. Gonzalez-Gay MA, Garcia-Porrua C, Hajeer AH, Dababneh A, Ollier WE. HLA-DRB1*04 may be a marker of severity in giant cell arteritis. Ann Rheum Dis. 2000 Jul;59(7):574-5.
65. Rauzy O, Fort M, Nourhashemi F, Alric L, Juchet H, Ecoiffier M, et al. Relation between HLA DRB1 alleles and corticosteroid resistance in giant cell arteritis. Ann Rheum Dis. 1998 Jun;57(6):380-2.
66. Gonzalez-Gay MA, Rueda B, Vilchez JR, Lopez-Nevot MA, Robledo G, Ruiz MP, et al. Contribution of MHC class I region to genetic susceptibility for giant cell arteritis. Rheumatology (Oxford). 2007 Mar;46(3):431-4.
67. Mattey DL, Hajeer AH, Dababneh A, Thomson W, Gonzalez-Gay MA, Garcia-Porrua C, et al. Association of giant cell arteritis and polymyalgia rheumatica

with different tumor necrosis factor microsatellite polymorphisms. Arthritis Rheum. 2000 Aug;43(8):1749-55.
68. Amoli MM, Gonzalez-Gay MA, Zeggini E, Salway F, Garcia-Porrua C, Ollier WE. Epistatic interactions between HLA-DRB1 and interleukin 4, but not interferon-gamma, increase susceptibility to giant cell arteritis. J Rheumatol. 2004 Dec;31(12):2413-7.
69. Amoli MM, Salway F, Zeggini E, Ollier WE, Gonzalez-Gay MA. MCP-1 gene haplotype association in biopsy proven giant cell arteritis. J Rheumatol. 2005 Mar;32(3):507-10.
70. Boiardi L, Casali B, Farnetti E, Pipitone N, Nicoli D, Macchioni P, et al. Interleukin-10 promoter polymorphisms in giant cell arteritis. Arthritis Rheum. 2006 Dec;54(12):4011-7.
71. Rodriguez-Pla A, Beaty TH, Savino PJ, Eagle RC, Jr., Seo P, Soloski MJ. Association of a nonsynonymous single-nucleotide polymorphism of matrix metalloproteinase 9 with giant cell arteritis. Arthritis Rheum. 2008 Jun;58(6):1849-53.
72. Palomino-Morales RJ, Vazquez-Rodriguez TR, Torres O, Morado IC, Castaneda S, Miranda-Filloy JA, et al. Association between IL-18 gene polymorphisms and biopsy-proven giant cell arteritis. Arthritis Res Ther. 2010;12(2):R51.
73. Enjuanes A, Benavente Y, Hernandez-Rodriguez J, Queralt C, Yague J, Jares P, et al. Association of NOS2 and potential effect of VEGF, IL6, CCL2 and IL1RN polymorphisms and haplotypes on susceptibility to GCA--a simultaneous study of 130 potentially functional SNPs in 14 candidate genes. Rheumatology (Oxford). 2012 May;51(5):841-51.
74. Song GG, Choi SJ, Ji JD, Lee YH. Toll-like receptor polymorphisms and vasculitis susceptibility: meta-analysis and systematic review. Mol Biol Rep. 2013 Feb;40(2):1315-23.
75. Serrano A, Carmona FD, Castaneda S, Solans R, Hernandez-Rodriguez J, Cid MC, et al. Evidence of association of the NLRP1 gene with giant cell arteritis. Ann Rheum Dis. 2013 Apr;72(4):628-30.
76. Marquez A, Hernandez-Rodriguez J, Cid MC, Solans R, Castaneda S, Fernandez-Contreras ME, et al. Influence of the IL17A locus in giant cell arteritis susceptibility. Ann Rheum Dis. 2014 Jun 11.
77. Gonzalez-Gay MA, Hajeer AH, Dababneh A, Garcia-Porrua C, Amoli MM, Llorca J, et al. Interferon-gamma gene microsatellite polymorphisms in patients with biopsy-proven giant cell arteritis and isolated polymyalgia rheumatica. Clin Exp Rheumatol. 2004;22(6 Suppl 36):S18-20.
78. Rodriguez-Rodriguez L, Castaneda S, Vazquez-Rodriguez TR, Morado IC, Gomez-Vaquero C, Mari-Alfonso B, et al. Role of the rs6822844 gene polymorphism at the IL2-IL21 region in biopsy-proven giant cell arteritis. Clin Exp Rheumatol. 2011 Jan-Feb;29(1 Suppl 64):S12-6.
79. Weyand CM, Schonberger J, Oppitz U, Hunder NN, Hicok KC, Goronzy JJ. Distinct vascular lesions in giant cell arteritis share identical T cell clonotypes. J Exp Med. 1994 Mar 1;179(3):951-60.
80. Martinez-Taboada VM, Goronzy JJ, Weyand CM. Clonally expanded CD8 T cells in patients with polymyalgia rheumatica and giant cell arteritis. Clin Immunol Immunopathol. 1996 Jun;79(3):263-70.

81. Gabriel SE, Espy M, Erdman DD, Bjornsson J, Smith TF, Hunder GG. The role of parvovirus B19 in the pathogenesis of giant cell arteritis: a preliminary evaluation. Arthritis Rheum. 1999 Jun;42(6):1255-8.
82. Alvarez-Lafuente R, Fernandez-Gutierrez B, Jover JA, Judez E, Loza E, Clemente D, et al. Human parvovirus B19, varicella zoster virus, and human herpes virus 6 in temporal artery biopsy specimens of patients with giant cell arteritis: analysis with quantitative real time polymerase chain reaction. Ann Rheum Dis. 2005 May;64(5):780-2.
83. Powers JF, Bedri S, Hussein S, Salomon RN, Tischler AS. High prevalence of herpes simplex virus DNA in temporal arteritis biopsy specimens. Am J Clin Pathol. 2005 Feb;123(2):261-4.
84. Helweg-Larsen J, Tarp B, Obel N, Baslund B. No evidence of parvovirus B19, Chlamydia pneumoniae or human herpes virus infection in temporal artery biopsies in patients with giant cell arteritis. Rheumatology (Oxford). 2002 Apr;41(4):445-9.
85. Cankovic M, Zarbo RJ. Failure to detect human herpes simplex virus, cytomegalovirus, and Epstein-Barr virus viral genomes in giant cell arteritis biopsy specimens by real-time quantitative polymerase chain reaction. Cardiovasc Pathol. 2006 Sep-Oct;15(5):280-6.
86. Cooper RJ, D'Arcy S, Kirby M, Al-Buhtori M, Rahman MJ, Proctor L, et al. Infection and temporal arteritis: a PCR-based study to detect pathogens in temporal artery biopsy specimens. J Med Virol. 2008 Mar;80(3):501-5.
87. Nordborg C, Nordborg E, Petursdottir V, LaGuardia J, Mahalingam R, Wellish M, et al. Search for varicella zoster virus in giant cell arteritis. Ann Neurol. 1998 Sep;44(3):413-4.
88. Duhaut P, Bosshard S, Calvet A, Pinede L, Demolombe-Rague S, Dumontet C, et al. Giant cell arteritis, polymyalgia rheumatica, and viral hypotheses: a multicenter, prospective case-control study. Groupe de Recherche sur l'Arterite a Cellules Geantes. J Rheumatol. 1999 Feb;26(2):361-9.
89. Wagner AD, Gerard HC, Fresemann T, Schmidt WA, Gromnica-Ihle E, Hudson AP, et al. Detection of Chlamydia pneumoniae in giant cell vasculitis and correlation with the topographic arrangement of tissue-infiltrating dendritic cells. Arthritis Rheum. 2000 Jul;43(7):1543-51.
90. Njau F, Ness T, Wittkop U, Pancratz T, Eickhoff M, Hudson AP, et al. No correlation between giant cell arteritis and Chlamydia pneumoniae infection: investigation of 189 patients by standard and improved PCR methods. J Clin Microbiol. 2009 Jun;47(6):1899-901.
91. Haugeberg G, Bie R, Nordbo SA. Chlamydia pneumoniae not detected in temporal artery biopsies from patients with temporal arteritis. Scand J Rheumatol. 2000;29(2):127-8.
92. Koening CL, Katz BJ, Hernandez-Rodriguez J, Corbera-Bellalta M, Cid MC, Schweizer PS, et al. Identification of a Burkholderia -Like Strain From Temporal Arteries of Subjects with Giant Cell Arteritis. Arthrtis Rheum. 2012;64(10):S373.
93. Weyand CM, Goronzy JJ. Medium- and large-vessel vasculitis. N Engl J Med. 2003 Jul 10;349(2):160-9.
94. Samson M, Bonnotte B. [Giant-cell arteritis pathogenesis]. Presse Med. 2013 Oct;41(10):937-47.
95. Grunewald J, Andersson R, Rydberg L, Gigliotti D, Schaufelberger C, Hansson GK, et al. CD4+ and CD8+ T cell expansions using selected TCR V and J gene segments at the onset of giant cell arteritis. Arthritis Rheum. 1994 Aug;37(8):1221-7.

96. Martinez-Taboada V, Hunder NN, Hunder GG, Weyand CM, Goronzy JJ. Recognition of tissue residing antigen by T cells in vasculitic lesions of giant cell arteritis. J Mol Med (Berl). 1996 Nov;74(11):695-703.
97. Piggott K, Biousse V, Newman NJ, Goronzy JJ, Weyand CM. Vascular damage in giant cell arteritis. Autoimmunity. 2009 Nov;42(7):596-604.
98. Deng J, Younge BR, Olshen RA, Goronzy JJ, Weyand CM. Th17 and Th1 T-cell responses in giant cell arteritis. Circulation. 2010 Feb 23;121(7):906-15.
99. Samson M, Audia S, Fraszczak J, Trad M, Ornetti P, Lakomy D, et al. Th1 and Th17 lymphocytes expressing CD161 are implicated in giant cell arteritis and polymyalgia rheumatica pathogenesis. Arthritis Rheum. 2012 Nov;64(11):3788-98.
100. Terrier B, Geri G, Chaara W, Allenbach Y, Rosenzwajg M, Costedoat-Chalumeau N, et al. Interleukin-21 modulates Th1 and Th17 responses in giant cell arteritis. Arthritis Rheum. 2012 Jun;64(6):2001-11.
101. Piggott K, Deng J, Warrington K, Younge B, Kubo JT, Desai M, et al. Blocking the NOTCH pathway inhibits vascular inflammation in large-vessel vasculitis. Circulation. 2011 Jan 25;123(3):309-18.
102. Chatelain D, Duhaut P, Schmidt J, Loire R, Bosshard S, Guernou M, et al. Pathological features of temporal arteries in patients with giant cell arteritis presenting with permanent visual loss. Ann Rheum Dis. 2009 Jan;68(1):84-8.
103. van der Geest KS, Abdulahad WH, Chalan P, Rutgers A, Horst G, Huitema MG, et al. Disturbed B cell homeostasis in newly diagnosed giant cell arteritis and polymyalgia rheumatica. Arthritis Rheumatol. 2014 Jul;66(7):1927-38.
104. Schmits R, Kubuschok B, Schuster S, Preuss KD, Pfreundschuh M. Analysis of the B cell repertoire against autoantigens in patients with giant cell arteritis and polymyalgia rheumatica. Clin Exp Immunol. 2002 Feb;127(2):379-85.
105. Liozon E, Roussel V, Roblot P, Liozon F, Preud'Homme JL, Loustaud V, et al. Absence of anti-beta2 glycoprotein I antibodies in giant cell arteritis: a study of 45 biopsy-proven cases. Br J Rheumatol. 1998 Oct;37(10):1129-31.
106. Duhaut P, Berruyer M, Pinede L, Demolombe-Rague S, Loire R, Seydoux D, et al. Anticardiolipin antibodies and giant cell arteritis: a prospective, multicenter case-control study. Groupe de Recherche sur l'Arterite a Cellules Geantes. Arthritis Rheum. 1998 Apr;41(4):701-9.
107. Cid MC, Cervera R, Font J, Lopez-Soto A, Pallares L, Navarro M, et al. Late thrombotic events in patients with temporal arteritis and anticardiolipin antibodies. Clin Exp Rheumatol. 1990 Jul-Aug;8(4):359-63.
108. Espinosa G, Tassies D, Font J, Munoz-Rodriguez FJ, Cervera R, Ordinas A, et al. Antiphospholipid antibodies and thrombophilic factors in giant cell arteritis. Semin Arthritis Rheum. 2001 Aug;31(1):12-20.
109. Lopez-Hoyos M, Alvarez L, Ruiz Soto M, Blanco R, Jose Bartolome M, Martinez-Taboada VM. Serum levels of antibodies to Chlamydia pneumoniae and human HSP60 in giant cell arteritis patients. Clin Exp Rheumatol. 2008 Nov-Dec;26(6):1107-10.
110. Grosse K, Schmidt RE, Witte T, Baerlecken NT. Epitope mapping of antibodies against ferritin heavy chain in giant cell arteritis and polymyalgia rheumatica. Scand J Rheumatol. 2013;42(3):215-9.
111. Thurner L, Preuss KD, Fadle N, Regitz E, Klemm P, Zaks M, et al. Progranulin antibodies in autoimmune diseases. J Autoimmun. 2013 May;42:29-38.
112. Cid MC, Hoffman MP, Hernandez-Rodriguez J, Segarra M, Elkin M, Sanchez M, et al. Association between increased CCL2 (MCP-1) expression in lesions and

persistence of disease activity in giant-cell arteritis. Rheumatology (Oxford). 2006 Nov;45(11):1356-63.
113. Rittner HL, Hafner V, Klimiuk PA, Szweda LI, Goronzy JJ, Weyand CM. Aldose reductase functions as a detoxification system for lipid peroxidation products in vasculitis. J Clin Invest. 1999 Apr;103(7):1007-13.
114. Kaiser M, Younge B, Bjornsson J, Goronzy JJ, Weyand CM. Formation of new vasa vasorum in vasculitis. Production of angiogenic cytokines by multinucleated giant cells. Am J Pathol. 1999 Sep;155(3):765-74.
115. Kaiser M, Weyand CM, Bjornsson J, Goronzy JJ. Platelet-derived growth factor, intimal hyperplasia, and ischemic complications in giant cell arteritis. Arthritis Rheum. 1998 Apr;41(4):623-33.
116. Borkowski A, Younge BR, Szweda L, Mock B, Bjornsson J, Moeller K, et al. Reactive nitrogen intermediates in giant cell arteritis: selective nitration of neocapillaries. Am J Pathol. 2002 Jul;161(1):115-23.
117. Segarra M, Garcia-Martinez A, Sanchez M, Hernandez-Rodriguez J, Lozano E, Grau JM, et al. Gelatinase expression and proteolytic activity in giant-cell arteritis. Ann Rheum Dis. 2007 Nov;66(11):1429-35.
118. Rodriguez-Pla A, Bosch-Gil JA, Rossello-Urgell J, Huguet-Redecilla P, Stone JH, Vilardell-Tarres M. Metalloproteinase-2 and -9 in giant cell arteritis: involvement in vascular remodeling. Circulation. 2005 Jul 12;112(2):264-9.
119. Lozano E, Segarra M, Corbera-Bellalta M, Garcia-Martinez A, Espigol-Frigole G, Pla-Campo A, et al. Increased expression of the endothelin system in arterial lesions from patients with giant-cell arteritis: association between elevated plasma endothelin levels and the development of ischaemic events. Ann Rheum Dis. 2010 Feb;69(2):434-42.
120. Cid MC, Cebrian M, Font C, Coll-Vinent B, Hernandez-Rodriguez J, Esparza J, et al. Cell adhesion molecules in the development of inflammatory infiltrates in giant cell arteritis: inflammation-induced angiogenesis as the preferential site of leukocyte-endothelial cell interactions. Arthritis Rheum. 2000 Jan;43(1):184-94.
121. Cid MC, Hernandez-Rodriguez J, Esteban MJ, Cebrian M, Gho YS, Font C, et al. Tissue and serum angiogenic activity is associated with low prevalence of ischemic complications in patients with giant-cell arteritis. Circulation. 2002 Sep 24;106(13):1664-71.
122. Owens GK, Kumar MS, Wamhoff BR. Molecular regulation of vascular smooth muscle cell differentiation in development and disease. Physiol Rev. 2004 Jul;84(3):767-801.
123. Woodcock-Mitchell J, Mitchell JJ, Low RB, Kieny M, Sengel P, Rubbia L, et al. Alpha-smooth muscle actin is transiently expressed in embryonic rat cardiac and skeletal muscles. Differentiation. 1988 Dec;39(3):161-6.
124. Sartore S, Chiavegato A, Faggin E, Franch R, Puato M, Ausoni S, et al. Contribution of adventitial fibroblasts to neointima formation and vascular remodeling: from innocent bystander to active participant. Circ Res. 2001 Dec 7;89(12):1111-21.
125. Arciniegas E, Sutton AB, Allen TD, Schor AM. Transforming growth factor beta 1 promotes the differentiation of endothelial cells into smooth muscle-like cells in vitro. J Cell Sci. 1992 Oct;103 (Pt 2):521-9.
126. Cintorino M, Vindigni C, Del Vecchio MT, Tosi P, Frezzotti R, Hadjistilianou T, et al. Expression of actin isoforms and intermediate filament proteins in childhood orbital rhabdomyosarcomas. J Submicrosc Cytol Pathol. 1989 Jul;21(3):409-19.

127. Frid MG, Moiseeva EP, Stenmark KR. Multiple phenotypically distinct smooth muscle cell populations exist in the adult and developing bovine pulmonary arterial media in vivo. Circ Res. 1994 Oct;75(4):669-81.
128. Bochaton-Piallat ML, Clowes AW, Clowes MM, Fischer JW, Redard M, Gabbiani F, et al. Cultured arterial smooth muscle cells maintain distinct phenotypes when implanted into carotid artery. Arterioscler Thromb Vasc Biol. 2001 Jun;21(6):949-54.
129. Etchevers HC, Vincent C, Le Douarin NM, Couly GF. The cephalic neural crest provides pericytes and smooth muscle cells to all blood vessels of the face and forebrain. Development. 2001 Apr;128(7):1059-68.
130. Majesky MW. Developmental basis of vascular smooth muscle diversity. Arterioscler Thromb Vasc Biol. 2007 Jun;27(6):1248-58.
131. Wasteson P, Johansson BR, Jukkola T, Breuer S, Akyurek LM, Partanen J, et al. Developmental origin of smooth muscle cells in the descending aorta in mice. Development. 2008 May;135(10):1823-32.
132. Arciniegas E, Ponce L, Hartt Y, Graterol A, Carlini RG. Intimal thickening involves transdifferentiation of embryonic endothelial cells. Anat Rec. 2000 Jan 1;258(1):47-57.
133. Kumar AH, Metharom P, Schmeckpeper J, Weiss S, Martin K, Caplice NM. Bone marrow-derived CX3CR1 progenitors contribute to neointimal smooth muscle cells via fractalkine CX3CR1 interaction. FASEB J. 2014 Jan;24(1):81-92.
134. Rensen SS, Doevendans PA, van Eys GJ. Regulation and characteristics of vascular smooth muscle cell phenotypic diversity. Neth Heart J. 2007;15(3):100-8.
135. Ailawadi G, Moehle CW, Pei H, Walton SP, Yang Z, Kron IL, et al. Smooth muscle phenotypic modulation is an early event in aortic aneurysms. J Thorac Cardiovasc Surg. 2009 Dec;138(6):1392-9.
136. Zhang J, Wang L, Fu W, Wang C, Guo D, Jiang J, et al. Smooth muscle cell phenotypic diversity between dissected and unaffected thoracic aortic media. J Cardiovasc Surg (Torino). 2013 Aug;54(4):511-21.
137. O'Brien ER, Alpers CE, Stewart DK, Ferguson M, Tran N, Gordon D, et al. Proliferation in primary and restenotic coronary atherectomy tissue. Implications for antiproliferative therapy. Circ Res. 1993 Aug;73(2):223-31.
138. Kim HR, Appel S, Vetterkind S, Gangopadhyay SS, Morgan KG. Smooth muscle signalling pathways in health and disease. J Cell Mol Med. 2008 Dec;12(6A):2165-80.
139. Newby AC. Molecular and cell biology of native coronary and vein-graft atherosclerosis: regulation of plaque stability and vessel-wall remodelling by growth factors and cell-extracellular matrix interactions. Coron Artery Dis. 1997 Mar-Apr;8(3-4):213-24.
140. Chen Y, Kelm RJ, Jr., Budd RC, Sobel BE, Schneider DJ. Inhibition of apoptosis and caspase-3 in vascular smooth muscle cells by plasminogen activator inhibitor type-1. J Cell Biochem. 2004 May 1;92(1):178-88.
141. Blanc-Brude OP, Yu J, Simosa H, Conte MS, Sessa WC, Altieri DC. Inhibitor of apoptosis protein survivin regulates vascular injury. Nat Med. 2002 Sep;8(9):987-94.
142. Schmidt A, Lorkowski S, Seidler D, Breithardt G, Buddecke E. TGF-beta1 generates a specific multicomponent extracellular matrix in human coronary SMC. Eur J Clin Invest. 2006 Jul;36(7):473-82.
143. Wagenseil JE, Mecham RP. Vascular extracellular matrix and arterial mechanics. Physiol Rev. 2009 Jul;89(3):957-89.

144. Vozzi F, Bianchi F, Ahluwalia A, Domenici C. Hydrostatic pressure and shear stress affect endothelin-1 and nitric oxide release by endothelial cells in bioreactors. Biotechnol J. 2014 Jan;9(1):146-54.
145. Hirschi KK, Rohovsky SA, Beck LH, Smith SR, D'Amore PA. Endothelial cells modulate the proliferation of mural cell precursors via platelet-derived growth factor-BB and heterotypic cell contact. Circ Res. 1999 Feb 19;84(3):298-305.
146. Ehrenreich H, Anderson RW, Fox CH, Rieckmann P, Hoffman GS, Travis WD, et al. Endothelins, peptides with potent vasoactive properties, are produced by human macrophages. J Exp Med. 1990 Dec 1;172(6):1741-8.
147. Carey DJ. Control of growth and differentiation of vascular cells by extracellular matrix proteins. Annu Rev Physiol. 1991;53:161-77.
148. Dinbergs ID, Brown L, Edelman ER. Cellular response to transforming growth factor-beta1 and basic fibroblast growth factor depends on release kinetics and extracellular matrix interactions. J Biol Chem. 1996 Nov 22;271(47):29822-9.
149. Auge N, Maupas-Schwalm F, Elbaz M, Thiers JC, Waysbort A, Itohara S, et al. Role for matrix metalloproteinase-2 in oxidized low-density lipoprotein-induced activation of the sphingomyelin/ceramide pathway and smooth muscle cell proliferation. Circulation. 2004 Aug 3;110(5):571-8.
150. Chamley JH, Campbell GR, Burnstock G. Dedifferentiation, redifferentiation and bundle formation of smooth muscle cells in tissue culture: the influence of cell number and nerve fibres. J Embryol Exp Morphol. 1974 Oct;32(2):297-323.
151. Owens GK, Vernon SM, Madsen CS. Molecular regulation of smooth muscle cell differentiation. J Hypertens Suppl. 1996 Dec;14(5):S55-64.
152. Su B, Mitra S, Gregg H, Flavahan S, Chotani MA, Clark KR, et al. Redox regulation of vascular smooth muscle cell differentiation. Circ Res. 2001 Jul 6;89(1):39-46.
153. Raines EW. PDGF and cardiovascular disease. Cytokine Growth Factor Rev. 2004 Aug;15(4):237-54.
154. Bjorkerud S. Effects of transforming growth factor-beta 1 on human arterial smooth muscle cells in vitro. Arterioscler Thromb. 1991 Jul-Aug;11(4):892-902.
155. Werth D, Grassi G, Konjer N, Dapas B, Farra R, Giansante C, et al. Proliferation of human primary vascular smooth muscle cells depends on serum response factor. Eur J Cell Biol. 2010 Feb-Mar;89(2-3):216-24.
156. Liu R, Leslie KL, Martin KA. Epigenetic regulation of smooth muscle cell plasticity. Biochim Biophys Acta. 2014 Jun 15.
157. Madrigal-Matute J, Rotllan N, Aranda JF, Fernandez-Hernando C. MicroRNAs and atherosclerosis. Curr Atheroscler Rep. 2013 May;15(5):322.
158. Dinardo CL, Venturini G, Omae SV, Zhou EH, da Motta-Leal-Filho JM, Dariolli R, et al. Vascular smooth muscle cells exhibit a progressive loss of rigidity with serial culture passaging. Biorheology. 2012;49(5-6):365-73.
159. Weksler BB, Subileau EA, Perriere N, Charneau P, Holloway K, Leveque M, et al. Blood-brain barrier-specific properties of a human adult brain endothelial cell line. FASEB J. 2005 Nov;19(13):1872-4.
160. Bussone G, Tamby MC, Calzas C, Kherbeck N, Sahbatou Y, Sanson C, et al. IgG from patients with pulmonary arterial hypertension and/or systemic sclerosis binds to vascular smooth muscle cells and induces cell contraction. Ann Rheum Dis. 2012 Apr;71(4):596-605.
161. Eberhard A, Kahlert S, Goede V, Hemmerlein B, Plate KH, Augustin HG. Heterogeneity of angiogenesis and blood vessel maturation in human tumors:

implications for antiangiogenic tumor therapies. Cancer Res. 2000 Mar 1;60(5):1388-93.
162. Tarbell JM, Simon SI, Curry FR. Mechanosensing at the vascular interface. Annu Rev Biomed Eng. 2014 Jul 11;16:505-32.
163. Intengan HD, Schiffrin EL. Structure and mechanical properties of resistance arteries in hypertension: role of adhesion molecules and extracellular matrix determinants. Hypertension. 2000 Sep;36(3):312-8.
164. Pietra GG, Edwards WD, Kay JM, Rich S, Kernis J, Schloo B, et al. Histopathology of primary pulmonary hypertension. A qualitative and quantitative study of pulmonary blood vessels from 58 patients in the National Heart, Lung, and Blood Institute, Primary Pulmonary Hypertension Registry. Circulation. 1989 Nov;80(5):1198-206.
165. Mouthon L, Mehrenberger M, Teixeira L, Fakhouri F, Berezne A, Guillevin L, et al. Endothelin-1 expression in scleroderma renal crisis. Hum Pathol. 2011 Jan;42(1):95-102.
166. Sakao S, Taraseviciene-Stewart L, Cool CD, Tada Y, Kasahara Y, Kurosu K, et al. VEGF-R blockade causes endothelial cell apoptosis, expansion of surviving CD34+ precursor cells and transdifferentiation to smooth muscle-like and neuronal-like cells. FASEB J. 2007 Nov;21(13):3640-52.
167. Short M, Nemenoff RA, Zawada WM, Stenmark KR, Das M. Hypoxia induces differentiation of pulmonary artery adventitial fibroblasts into myofibroblasts. Am J Physiol Cell Physiol. 2004 Feb;286(2):C416-25.
168. Yuan W, Liu W, Li J, Li X, Sun X, Xu F, et al. Effects of BMSCs interactions with adventitial fibroblasts in transdifferentiation and ultrastructure processes. Int J Clin Exp Pathol. 2014;7(7):3957-65.
169. Lin CH, Lilly B. Endothelial Cells Direct Mesenchymal Stem Cells Toward a Smooth Muscle Cell Fate. Stem Cells Dev. 2014 Jul 14.
170. Satomi-Kobayashi S, Kinugasa M, Kobayashi R, Hatakeyama K, Kurogane Y, Ishida T, et al. Osteoblast-like differentiation of cultured human coronary artery smooth muscle cells by bone morphogenetic protein endothelial cell precursor-derived regulator (BMPER). J Biol Chem. 2012 Aug 31;287(36):30336-45.
171. Humbert M, Sitbon O, Chaouat A, Bertocchi M, Habib G, Gressin V, et al. Survival in patients with idiopathic, familial, and anorexigen-associated pulmonary arterial hypertension in the modern management era. Circulation. 2010 Jul 13;122(2):156-63.
172. Humbert M, Sitbon O, Chaouat A, Bertocchi M, Habib G, Gressin V, et al. Pulmonary arterial hypertension in France: results from a national registry. Am J Respir Crit Care Med. 2006 May 1;173(9):1023-30.
173. Simonneau G, Gatzoulis MA, Adatia I, Celermajer D, Denton C, Ghofrani A, et al. Updated clinical classification of pulmonary hypertension. J Am Coll Cardiol. 2013 Dec 24;62(25 Suppl):D34-41.
174. D'Alonzo GE, Barst RJ, Ayres SM, Bergofsky EH, Brundage BH, Detre KM, et al. Survival in patients with primary pulmonary hypertension. Results from a national prospective registry. Ann Intern Med. 1991 Sep 1;115(5):343-9.
175. Harrison RE, Flanagan JA, Sankelo M, Abdalla SA, Rowell J, Machado RD, et al. Molecular and functional analysis identifies ALK-1 as the predominant cause of pulmonary hypertension related to hereditary haemorrhagic telangiectasia. J Med Genet. 2003 Dec;40(12):865-71.
176. Chaouat A, Coulet F, Favre C, Simonneau G, Weitzenblum E, Soubrier F, et al. Endoglin germline mutation in a patient with hereditary haemorrhagic

telangiectasia and dexfenfluramine associated pulmonary arterial hypertension. Thorax. 2004 May;59(5):446-8.
177. Machado RD, Eickelberg O, Elliott CG, Geraci MW, Hanaoka M, Loyd JE, et al. Genetics and genomics of pulmonary arterial hypertension. J Am Coll Cardiol. 2009 Jun 30;54(1 Suppl):S32-42.
178. Nasim MT, Ogo T, Ahmed M, Randall R, Chowdhury HM, Snape KM, et al. Molecular genetic characterization of SMAD signaling molecules in pulmonary arterial hypertension. Hum Mutat. 2011 Dec;32(12):1385-9.
179. Austin ED, Ma L, LeDuc C, Berman Rosenzweig E, Borczuk A, Phillips JA, 3rd, et al. Whole exome sequencing to identify a novel gene (caveolin-1) associated with human pulmonary arterial hypertension. Circ Cardiovasc Genet. 2012 Jun;5(3):336-43.
180. Ma L, Roman-Campos D, Austin ED, Eyries M, Sampson KS, Soubrier F, et al. A novel channelopathy in pulmonary arterial hypertension. N Engl J Med. 2013 Jul 25;369(4):351-61.
181. Soubrier F, Chung WK, Machado R, Grunig E, Aldred M, Geraci M, et al. Genetics and genomics of pulmonary arterial hypertension. J Am Coll Cardiol. 2013 Dec 24;62(25 Suppl):D13-21.
182. Rabinovitch M, Bothwell T, Hayakawa BN, Williams WG, Trusler GA, Rowe RD, et al. Pulmonary artery endothelial abnormalities in patients with congenital heart defects and pulmonary hypertension. A correlation of light with scanning electron microscopy and transmission electron microscopy. Lab Invest. 1986 Dec;55(6):632-53.
183. Lee SD, Shroyer KR, Markham NE, Cool CD, Voelkel NF, Tuder RM. Monoclonal endothelial cell proliferation is present in primary but not secondary pulmonary hypertension. J Clin Invest. 1998 Mar 1;101(5):927-34.
184. Yeager ME, Halley GR, Golpon HA, Voelkel NF, Tuder RM. Microsatellite instability of endothelial cell growth and apoptosis genes within plexiform lesions in primary pulmonary hypertension. Circ Res. 2001 Jan 19;88(1):E2-E11.
185. Aldred MA, Comhair SA, Varella-Garcia M, Asosingh K, Xu W, Noon GP, et al. Somatic chromosome abnormalities in the lungs of patients with pulmonary arterial hypertension. Am J Respir Crit Care Med. 2010 Nov 1;182(9):1153-60.
186. Guignabert C, Tu L, Le Hiress M, Ricard N, Sattler C, Seferian A, et al. Pathogenesis of pulmonary arterial hypertension: lessons from cancer. Eur Respir Rev. 2013 Dec;22(130):543-51.
187. Tu L, Dewachter L, Gore B, Fadel E, Dartevelle P, Simonneau G, et al. Autocrine fibroblast growth factor-2 signaling contributes to altered endothelial phenotype in pulmonary hypertension. Am J Respir Cell Mol Biol. 2011 Aug;45(2):311-22.
188. Teichert-Kuliszewska K, Kutryk MJ, Kuliszewski MA, Karoubi G, Courtman DW, Zucco L, et al. Bone morphogenetic protein receptor-2 signaling promotes pulmonary arterial endothelial cell survival: implications for loss-of-function mutations in the pathogenesis of pulmonary hypertension. Circ Res. 2006 Feb 3;98(2):209-17.
189. Xu W, Koeck T, Lara AR, Neumann D, DiFilippo FP, Koo M, et al. Alterations of cellular bioenergetics in pulmonary artery endothelial cells. Proc Natl Acad Sci U S A. 2007 Jan 23;104(4):1342-7.
190. Dewachter L, Adnot S, Fadel E, Humbert M, Maitre B, Barlier-Mur AM, et al. Angiopoietin/Tie2 pathway influences smooth muscle hyperplasia in idiopathic pulmonary hypertension. Am J Respir Crit Care Med. 2006 Nov 1;174(9):1025-33.

191. Xu W, Kaneko FT, Zheng S, Comhair SA, Janocha AJ, Goggans T, et al. Increased arginase II and decreased NO synthesis in endothelial cells of patients with pulmonary arterial hypertension. FASEB J. 2004 Nov;18(14):1746-8.
192. Liu Y, Li M, Warburton RR, Hill NS, Fanburg BL. The 5-HT transporter transactivates the PDGFbeta receptor in pulmonary artery smooth muscle cells. FASEB J. 2007 Sep;21(11):2725-34.
193. Lawrie A, Spiekerkoetter E, Martinez EC, Ambartsumian N, Sheward WJ, MacLean MR, et al. Interdependent serotonin transporter and receptor pathways regulate S100A4/Mts1, a gene associated with pulmonary vascular disease. Circ Res. 2005 Aug 5;97(3):227-35.
194. Hansmann G, de Jesus Perez VA, Alastalo TP, Alvira CM, Guignabert C, Bekker JM, et al. An antiproliferative BMP-2/PPARgamma/apoE axis in human and murine SMCs and its role in pulmonary hypertension. J Clin Invest. 2008 May;118(5):1846-57.
195. Ihida-Stansbury K, McKean DM, Lane KB, Loyd JE, Wheeler LA, Morrell NW, et al. Tenascin-C is induced by mutated BMP type II receptors in familial forms of pulmonary arterial hypertension. Am J Physiol Lung Cell Mol Physiol. 2006 Oct;291(4):L694-702.
196. Lawrie A, Waterman E, Southwood M, Evans D, Suntharalingam J, Francis S, et al. Evidence of a role for osteoprotegerin in the pathogenesis of pulmonary arterial hypertension. Am J Pathol. 2008 Jan;172(1):256-64.
197. Rabinovitch M. Molecular pathogenesis of pulmonary arterial hypertension. J Clin Invest. 2012 Dec 3;122(12):4306-13.
198. Jones PL, Cowan KN, Rabinovitch M. Tenascin-C, proliferation and subendothelial fibronectin in progressive pulmonary vascular disease. Am J Pathol. 1997 Apr;150(4):1349-60.
199. Thompson K, Rabinovitch M. Exogenous leukocyte and endogenous elastases can mediate mitogenic activity in pulmonary artery smooth muscle cells by release of extracellular-matrix bound basic fibroblast growth factor. J Cell Physiol. 1996 Mar;166(3):495-505.
200. Cowan KN, Heilbut A, Humpl T, Lam C, Ito S, Rabinovitch M. Complete reversal of fatal pulmonary hypertension in rats by a serine elastase inhibitor. Nat Med. 2000 Jun;6(6):698-702.
201. Frid MG, Brunetti JA, Burke DL, Carpenter TC, Davie NJ, Reeves JT, et al. Hypoxia-induced pulmonary vascular remodeling requires recruitment of circulating mesenchymal precursors of a monocyte/macrophage lineage. Am J Pathol. 2006 Feb;168(2):659-69.
202. Humbert M, Monti G, Brenot F, Sitbon O, Portier A, Grangeot-Keros L, et al. Increased interleukin-1 and interleukin-6 serum concentrations in severe primary pulmonary hypertension. Am J Respir Crit Care Med. 1995 May;151(5):1628-31.
203. Tamby MC, Chanseaud Y, Humbert M, Fermanian J, Guilpain P, Garcia-de-la-Pena-Lefebvre P, et al. Anti-endothelial cell antibodies in idiopathic and systemic sclerosis associated pulmonary arterial hypertension. Thorax. 2005 Sep;60(9):765-72.
204. Tamby MC, Humbert M, Guilpain P, Servettaz A, Dupin N, Christner JJ, et al. Antibodies to fibroblasts in idiopathic and scleroderma-associated pulmonary hypertension. Eur Respir J. 2006 Oct;28(4):799-807.
205. Perros F, Dorfmuller P, Montani D, Hammad H, Waelput W, Girerd B, et al. Pulmonary lymphoid neogenesis in idiopathic pulmonary arterial hypertension. Am J Respir Crit Care Med. 2012 Feb 1;185(3):311-21.

206. Barst RJ, Rubin LJ, Long WA, McGoon MD, Rich S, Badesch DB, et al. A comparison of continuous intravenous epoprostenol (prostacyclin) with conventional therapy for primary pulmonary hypertension. N Engl J Med. 1996 Feb 1;334(5):296-301.
207. Simonneau G, Torbicki A, Hoeper MM, Delcroix M, Karlocai K, Galie N, et al. Selexipag: an oral, selective prostacyclin receptor agonist for the treatment of pulmonary arterial hypertension. Eur Respir J. 2012 Oct;40(4):874-80.
208. Channick RN, Simonneau G, Sitbon O, Robbins IM, Frost A, Tapson VF, et al. Effects of the dual endothelin-receptor antagonist bosentan in patients with pulmonary hypertension: a randomised placebo-controlled study. Lancet. 2001 Oct 6;358(9288):1119-23.
209. Galie N, Badesch D, Oudiz R, Simonneau G, McGoon MD, Keogh AM, et al. Ambrisentan therapy for pulmonary arterial hypertension. J Am Coll Cardiol. 2005 Aug 2;46(3):529-35.
210. Pulido T, Adzerikho I, Channick RN, Delcroix M, Galie N, Ghofrani HA, et al. Macitentan and morbidity and mortality in pulmonary arterial hypertension. N Engl J Med. 2013 Aug 29;369(9):809-18.
211. Galie N, Brundage BH, Ghofrani HA, Oudiz RJ, Simonneau G, Safdar Z, et al. Tadalafil therapy for pulmonary arterial hypertension. Circulation. 2009 Jun 9;119(22):2894-903.
212. Galie N, Ghofrani HA, Torbicki A, Barst RJ, Rubin LJ, Badesch D, et al. Sildenafil citrate therapy for pulmonary arterial hypertension. N Engl J Med. 2005 Nov 17;353(20):2148-57.
213. Ghofrani HA, Galie N, Grimminger F, Grunig E, Humbert M, Jing ZC, et al. Riociguat for the treatment of pulmonary arterial hypertension. N Engl J Med. 2013 Jul 25;369(4):330-40.
214. O'Callaghan DS, Savale L, Montani D, Jais X, Sitbon O, Simonneau G, et al. Treatment of pulmonary arterial hypertension with targeted therapies. Nat Rev Cardiol. 2013 Sep;8(9):526-38.
215. Inoue A, Yanagisawa M, Kimura S, Kasuya Y, Miyauchi T, Goto K, et al. The human endothelin family: three structurally and pharmacologically distinct isopeptides predicted by three separate genes. Proc Natl Acad Sci U S A. 1989 Apr;86(8):2863-7.
216. Dong F, Zhang X, Wold LE, Ren Q, Zhang Z, Ren J. Endothelin-1 enhances oxidative stress, cell proliferation and reduces apoptosis in human umbilical vein endothelial cells: role of ETB receptor, NADPH oxidase and caveolin-1. Br J Pharmacol. 2005 Jun;145(3):323-33.
217. Haynes WG, Strachan FE, Webb DJ. Endothelin ETA and ETB receptors cause vasoconstriction of human resistance and capacitance vessels in vivo. Circulation. 1995 Aug 1;92(3):357-63.
218. Komuro I, Kurihara H, Sugiyama T, Yoshizumi M, Takaku F, Yazaki Y. Endothelin stimulates c-fos and c-myc expression and proliferation of vascular smooth muscle cells. FEBS Lett. 1988 Oct 10;238(2):249-52.
219. Ohlstein EH, Arleth A, Bryan H, Elliott JD, Sung CP. The selective endothelin ETA receptor antagonist BQ123 antagonizes endothelin-1-mediated mitogenesis. Eur J Pharmacol. 1992 Apr 10;225(4):347-50.
220. Meoli DF, White RJ. Endothelin-1 induces pulmonary but not aortic smooth muscle cell migration by activating ERK1/2 MAP kinase. Can J Physiol Pharmacol. 2010 Aug;88(8):830-9.

221. Lerman A, Edwards BS, Hallett JW, Heublein DM, Sandberg SM, Burnett JC, Jr. Circulating and tissue endothelin immunoreactivity in advanced atherosclerosis. N Engl J Med. 1991 Oct 3;325(14):997-1001.
222. Imai T, Hirata Y, Emori T, Yanagisawa M, Masaki T, Marumo F. Induction of endothelin-1 gene by angiotensin and vasopressin in endothelial cells. Hypertension. 1992 Jun;19(6 Pt 2):753-7.
223. Matsuura A, Yamochi W, Hirata K, Kawashima S, Yokoyama M. Stimulatory interaction between vascular endothelial growth factor and endothelin-1 on each gene expression. Hypertension. 1998 Jul;32(1):89-95.
224. Luscher TF, Barton M. Endothelins and endothelin receptor antagonists: therapeutic considerations for a novel class of cardiovascular drugs. Circulation. 2000 Nov 7;102(19):2434-40.
225. Haller H, Schaberg T, Lindschau C, Lode H, Distler A. Endothelin increases [Ca2+]i, protein phosphorylation, and O2-. production in human alveolar macrophages. Am J Physiol. 1991 Dec;261(6 Pt 1):L478-84.
226. Lopez Farre A, Riesco A, Espinosa G, Digiuni E, Cernadas MR, Alvarez V, et al. Effect of endothelin-1 on neutrophil adhesion to endothelial cells and perfused heart. Circulation. 1993 Sep;88(3):1166-71.
227. Knofler R, Urano T, Malyszko J, Takada Y, Takada A. In vitro effect of endothelin-1 on collagen, and ADP-induced aggregation in human whole blood and platelet rich plasma. Thromb Res. 1995 Jan 1;77(1):69-78.
228. Agui T, Xin X, Cai Y, Sakai T, Matsumoto K. Stimulation of interleukin-6 production by endothelin in rat bone marrow-derived stromal cells. Blood. 1994 Oct 15;84(8):2531-8.
229. Ruetten H, Thiemermann C. Endothelin-1 stimulates the biosynthesis of tumour necrosis factor in macrophages: ET-receptors, signal transduction and inhibition by dexamethasone. J Physiol Pharmacol. 1997 Dec;48(4):675-88.
230. Peifley KA, Winkles JA. Angiotensin II and endothelin-1 increase fibroblast growth factor-2 mRNA expression in vascular smooth muscle cells. Biochem Biophys Res Commun. 1998 Jan 6;242(1):202-8.
231. Yang Z, Krasnici N, Luscher TF. Endothelin-1 potentiates human smooth muscle cell growth to PDGF: effects of ETA and ETB receptor blockade. Circulation. 1999 Jul 6;100(1):5-8.
232. Dimitrijevic I, Andersson C, Rissler P, Edvinsson L. Increased tissue endothelin-1 and endothelin-B receptor expression in temporal arteries from patients with giant cell arteritis. Ophthalmology. 2010 Mar;117(3):628-36.
233. Pache M, Kaiser HJ, Haufschild T, Lubeck P, Flammer J. Increased endothelin-1 plasma levels in giant cell arteritis: a report on four patients. Am J Ophthalmol. 2002 Jan;133(1):160-2.
234. Garcia de la Pena-Lefebvre P, Chanseaud Y, Tamby MC, Reinbolt J, Batteux F, Allanore Y, et al. IgG reactivity with a 100-kDa tissue and endothelial cell antigen identified as topoisomerase 1 distinguishes between limited and diffuse systemic sclerosis patients. Clin Immunol. 2004 Jun;111(3):241-51.
235. Shevchenko A, Wilm M, Vorm O, Mann M. Mass spectrometric sequencing of proteins silver-stained polyacrylamide gels. Anal Chem. 1996 Mar 1;68(5):850-8.
236. Perkins DN, Pappin DJ, Creasy DM, Cottrell JS. Probability-based protein identification by searching sequence databases using mass spectrometry data. Electrophoresis. 1999 Dec;20(18):3551-67.

237. Ronda N, Leonardi S, Orlandini G, Gatti R, Bellosta S, Bernini F, et al. Natural anti-endothelial cell antibodies (AECA). J Autoimmun. 1999 Aug;13(1):121-7.
238. Dib H, Chafey P, Clary G, Federici C, Le Gall M, Dwyer J, et al. Proteomes of umbilical vein and microvascular endothelial cells reflect distinct biological properties and influence immune recognition. Proteomics. 2012 Aug;12(15-16):2547-55.
239. Revelen R, D'Arbonneau F, Guillevin L, Bordron A, Youinou P, Dueymes M. Comparison of cell-ELISA, flow cytometry and Western blotting for the detection of antiendothelial cell antibodies. Clin Exp Rheumatol. 2002 Jan-Feb;20(1):19-26.
240. Mayet WJ, Schwarting A, Meyer zum Buschenfelde KH. Cytotoxic effects of antibodies to proteinase 3 (C-ANCA) on human endothelial cells. Clin Exp Immunol. 1994 Sep;97(3):458-65.
241. Nakamura N, Shidara Y, Kawaguchi N, Azuma C, Mitsuda N, Onishi S, et al. Lupus anticoagulant autoantibody induces apoptosis in umbilical vein endothelial cells: involvement of annexin V. Biochem Biophys Res Commun. 1994 Dec 15;205(2):1488-93.
242. Muller Kobold AC, van Wijk RT, Franssen CF, Molema G, Kallenberg CG, Tervaert JW. In vitro up-regulation of E-selectin and induction of interleukin-6 in endothelial cells by autoantibodies in Wegener's granulomatosis and microscopic polyangiitis. Clin Exp Rheumatol. 1999 Jul-Aug;17(4):433-40.
243. Lee KH, Chung HS, Kim HS, Oh SH, Ha MK, Baik JH, et al. Human alpha-enolase from endothelial cells as a target antigen of anti-endothelial cell antibody in Behcet's disease. Arthritis Rheum. 2003 Jul;48(7):2025-35.
244. Kaneko M, Ono T, Matsubara T, Yamamoto Y, Ikeda H, Yoshiki T, et al. Serological identification of endothelial antigens predominantly recognized in Kawasaki disease patients by recombinant expression cloning. Microbiol Immunol. 2004;48(9):703-11.
245. Chauhan SK, Tripathy NK, Nityanand S. Antigenic targets and pathogenicity of anti-aortic endothelial cell antibodies in Takayasu arteritis. Arthritis Rheum. 2006 Jul;54(7):2326-33.
246. Baiu DC, Barger B, Sandor M, Fabry Z, Hart MN. Autoantibodies to vascular smooth muscle are pathogenic for vasculitis. Am J Pathol. 2005 Jun;166(6):1851-60.
247. Baiu DC, Sandor M, Hart M. CD4+ T cells sensitized by vascular smooth muscle induce vasculitis, and interferon gamma is critical for the initiation of vascular pathology. Am J Pathol. 2010 Dec;177(6):3215-23.
248. Aslan H, Pay S, Gok F, Baykal Y, Yilmaz MI, Sengul A, et al. Antiannexin V autoantibody in thrombophilic Behcet's disease. Rheumatol Int. 2004 Mar;24(2):77-9.
249. Tripathy NK, Sinha N, Nityanand S. Anti-annexin V antibodies in Takayasu's arteritis: prevalence and relationship with disease activity. Clin Exp Immunol. 2003 Nov;134(2):360-4.
250. Gheita TA, Samir H, Hussein H. Anti-annexin V antibodies in neuro-Behcet patients: clinical significance and relation to disease activity. Int J Rheum Dis. 2012 Oct;15(5):e124-6.
251. Kaburaki J, Kuwana M, Yamamoto M, Kawai S, Ikeda Y. Clinical significance of anti-annexin V antibodies in patients with systemic lupus erythematosus. Am J Hematol. 1997 Mar;54(3):209-13.
252. Nojima J, Kuratsune H, Suehisa E, Futsukaichi Y, Yamanishi H, Machii T, et al. Association between the prevalence of antibodies to beta(2)-glycoprotein I, prothrombin, protein C, protein S, and annexin V in patients with systemic lupus

erythematosus and thrombotic and thrombocytopenic complications. Clin Chem. 2001 Jun;47(6):1008-15.
253. Sugiura K, Muro Y. Anti-annexin V antibodies and digital ischemia in patients with scleroderma. J Rheumatol. 1999 Oct;26(10):2168-72.
254. Regent A, Lofek S, Dib H, Bussone G, Tamas N, Federici C, et al. Identification of target antigens of anti-endothelial cell antibodies in patients with anti-neutrophil cytoplasmic antibody-associated vasculitides: a proteomic approach. Clin Immunol. 2014 Jul;153(1):123-35.
255. Goeb V, Thomas-L'Otellier M, Daveau R, Charlionet R, Fardellone P, Le Loet X, et al. Candidate autoantigens identified by mass spectrometry in early rheumatoid arthritis are chaperones and citrullinated glycolytic enzymes. Arthritis Res Ther. 2009;11(2):R38.
256. Glukhova MA, Kabakov AE, Frid MG, Ornatsky OI, Belkin AM, Mukhin DN, et al. Modulation of human aorta smooth muscle cell phenotype: a study of muscle-specific variants of vinculin, caldesmon, and actin expression. Proc Natl Acad Sci U S A. 1988 Dec;85(24):9542-6.
257. Hill C, Roberts-Thomson P, Pollard A, Gillis D, Kirkham B. Clinical associations of anti-lamin autoantibodies. Aust N Z J Med. 1996 Apr;26(2):162-6.
258. Espinoza LR, Jara LJ, Silveira LH, Martinez-Osuna P, Zwolinska JB, Kneer C, et al. Anticardiolipin antibodies in polymyalgia rheumatica-giant cell arteritis: association with severe vascular complications. Am J Med. 1991 Apr;90(4):474-8.
259. Hulin C, Hachulla E, Michon-Pasturel U, Hatron PY, Masy E, Gillot JM, et al. [Prevalence of antiphospholipid antibodies in Horton's disease and in polymyalgia rheumatica]. Rev Med Interne. 1999 Aug;20(8):659-63.
260. Shor DB, Orbach H, Boaz M, Altman A, Anaya JM, Bizzaro N, et al. Gastrointestinal-associated autoantibodies in different autoimmune diseases. Am J Clin Exp Immunol. 2012;1(1):49-55.
261. Regent A, Ly KH, Blet A, Agard C, Puechal X, Tamas N, et al. Contribution of antiferritin antibodies to diagnosis of giant cell arteritis. Ann Rheum Dis. 2013 Jul;72(7):1269-70.
262. Mor-Vaknin N, Punturieri A, Sitwala K, Markovitz DM. Vimentin is secreted by activated macrophages. Nat Cell Biol. 2003 Jan;5(1):59-63.
263. Podor TJ, Singh D, Chindemi P, Foulon DM, McKelvie R, Weitz JI, et al. Vimentin exposed on activated platelets and platelet microparticles localizes vitronectin and plasminogen activator inhibitor complexes on their surface. J Biol Chem. 2002 Mar 1;277(9):7529-39.
264. Wygrecka M, Marsh LM, Morty RE, Henneke I, Guenther A, Lohmeyer J, et al. Enolase-1 promotes plasminogen-mediated recruitment of monocytes to the acutely inflamed lung. Blood. 2009 May 28;113(22):5588-98.
265. Zhang S, Ren J, Khan MF, Cheng AM, Abendschein D, Muslin AJ. Grb2 is required for the development of neointima in response to vascular injury. Arterioscler Thromb Vasc Biol. 2003 Oct 1;23(10):1788-93.
266. Field M, Cook A, Gallagher G. Immuno-localisation of tumour necrosis factor and its receptors in temporal arteritis. Rheumatol Int. 1997;17(3):113-8.
267. Samson M, Audia S, Janikashvili N, Bonnotte B. Is TNF-alpha really involved in giant cell arteritis pathogenesis? Ann Rheum Dis. 2014 Jan;73(1):e1.
268. Martinez-Taboada VM, Rodriguez-Valverde V, Carreno L, Lopez-Longo J, Figueroa M, Belzunegui J, et al. A double-blind placebo controlled trial of etanercept in patients with giant cell arteritis and corticosteroid side effects. Ann Rheum Dis. 2008 May;67(5):625-30.

269. Jennette JC, Falk RJ, Bacon PA, Basu N, Cid MC, Ferrario F, et al. 2012 revised International Chapel Hill Consensus Conference Nomenclature of Vasculitides. Arthritis Rheum. 2013 Jan;65(1):1-11.
270. de la Cuesta F, Zubiri I, Maroto AS, Posada M, Padial LR, Vivanco F, et al. Deregulation of smooth muscle cell cytoskeleton within the human atherosclerotic coronary media layer. J Proteomics. 2013 Apr 26;82:155-65.
271. Umahara T, Uchihara T, Koyama S, Hashimoto T, Akimoto J, Haraoka J, et al. Isoform-specific immunolocalization of 14-3-3 proteins in atherosclerotic lesions of human carotid and main cerebral arteries. J Neurol Sci. 2012 Jun 15;317(1-2):106-11.
272. Autieri MV, Carbone CJ. 14-3-3Gamma interacts with and is phosphorylated by multiple protein kinase C isoforms in PDGF-stimulated human vascular smooth muscle cells. DNA Cell Biol. 1999 Jul;18(7):555-64.
273. Autieri MV. Inducible expression of the signal transduction protein 14-3-3gamma in injured arteries and stimulated human vascular smooth muscle cells. Exp Mol Pathol. 2004 Apr;76(2):99-107.
274. Jalali S, Ramanathan GK, Parthasarathy PT, Aljubran S, Galam L, Yunus A, et al. Mir-206 regulates pulmonary artery smooth muscle cell proliferation and differentiation. PLoS One. 2012;7(10):e46808.
275. Yi B, Cui J, Ning JN, Wang GS, Qian GS, Lu KZ. Over-expression of PKGIalpha inhibits hypoxia-induced proliferation, Akt activation, and phenotype modulation of human PASMCs: the role of phenotype modulation of PASMCs in pulmonary vascular remodeling. Gene. 2012 Jan 25;492(2):354-60.
276. Moravcikova E, Krepela E, Prochazka J, Rousalova I, Cermak J, Benkova K. Down-regulated expression of apoptosis-associated genes APIP and UACA in non-small cell lung carcinoma. Int J Oncol. 2012 Jun;40(6):2111-21.
277. Nasim MT, Ogo T, Chowdhury HM, Zhao L, Chen CN, Rhodes C, et al. BMPR-II deficiency elicits pro-proliferative and anti-apoptotic responses through the activation of TGFbeta-TAK1-MAPK pathways in PAH. Hum Mol Genet. 2012 Jun 1;21(11):2548-58.
278. Tumbarello DA, Brown MC, Turner CE. The paxillin LD motifs. FEBS Lett. 2002 Feb 20;513(1):114-8.
279. Petit V, Boyer B, Lentz D, Turner CE, Thiery JP, Valles AM. Phosphorylation of tyrosine residues 31 and 118 on paxillin regulates cell migration through an association with CRK in NBT-II cells. J Cell Biol. 2000 Mar 6;148(5):957-70.
280. Chay KO, Park SS, Mushinski JF. Linkage of caspase-mediated degradation of paxillin to apoptosis in Ba/F3 murine pro-B lymphocytes. J Biol Chem. 2002 Apr 26;277(17):14521-9.
281. Veith C, Marsh LM, Wygrecka M, Rutschmann K, Seeger W, Weissmann N, et al. Paxillin regulates pulmonary arterial smooth muscle cell function in pulmonary hypertension. Am J Pathol. 20012 Nov;181(5):1621-33.
282. Jones RJ, Young O, Renshaw L, Jacobs V, Fennell M, Marshall A, et al. Src inhibitors in early breast cancer: a methodology, feasibility and variability study. Breast Cancer Res Treat. 2009 Mar;114(2):211-21.
283. Paulin R, Meloche J, Bonnet S. STAT3 signaling in pulmonary arterial hypertension. JAKSTAT. 2012 Oct 1;1(4):223-33.
284. Kisselbach L, Merges M, Bossie A, Boyd A. CD90 Expression on human primary cells and elimination of contaminating fibroblasts from cell cultures. Cytotechnology. 2009 Jan;59(1):31-44.

285. Betapudi V. Myosin II motor proteins with different functions determine the fate of lamellipodia extension during cell spreading. PLoS One. 2010;5(1):e8560.
286. Quasnichka H, Slater SC, Beeching CA, Boehm M, Sala-Newby GB, George SJ. Regulation of smooth muscle cell proliferation by beta-catenin/T-cell factor signaling involves modulation of cyclin D1 and p21 expression. Circ Res. 2006 Dec 8;99(12):1329-37.
287. Dwivedi A, Slater SC, George SJ. MMP-9 and -12 cause N-cadherin shedding and thereby beta-catenin signalling and vascular smooth muscle cell proliferation. Cardiovasc Res. 2009 Jan 1;81(1):178-86.
288. Zhong W, Oguljahan B, Xiao Y, Nelson J, Hernandez L, Garcia-Barrio M, et al. Serum and glucocorticoid-regulated kinase 1 promotes vascular smooth muscle cell proliferation via regulation of beta-catenin dynamics. Cell Signal. 2014 Aug 22.
289. Imanaka-Yoshida K, Yoshida T, Miyagawa-Tomita S. Tenascin-C in development and disease of blood vessels. Anat Rec (Hoboken). 2014 Sep;297(9):1747-57.
290. Sawada Y, Onoda K, Imanaka-Yoshida K, Maruyama J, Yamamoto K, Yoshida T, et al. Tenascin-C synthesized in both donor grafts and recipients accelerates artery graft stenosis. Cardiovasc Res. 2007 Jun 1;74(3):366-76.
291. Satoh K, Nigro P, Matoba T, O'Dell MR, Cui Z, Shi X, et al. Cyclophilin A enhances vascular oxidative stress and the development of angiotensin II-induced aortic aneurysms. Nat Med. 2009 Jun;15(6):649-56.
292. Levin ER. Endothelins. N Engl J Med. 1995 Aug 10;333(6):356-63.
293. Kelland NF, Kuc RE, McLean DL, Azfer A, Bagnall AJ, Gray GA, et al. Endothelial cell-specific ETB receptor knockout: autoradiographic and histological characterisation and crucial role in the clearance of endothelin-1. Can J Physiol Pharmacol. 2010 Jun;88(6):644-51.
294. Lozano E, Segarra M, Garcia-Martinez A, Hernandez-Rodriguez J, Cid MC. Imatinib mesylate inhibits in vitro and ex vivo biological responses related to vascular occlusion in giant cell arteritis. Ann Rheum Dis. 2008 Nov;67(11):1581-8.

7. Annexes

Autoimmunity Reviews 9 (2010) 635–645

Contents lists available at ScienceDirect

Autoimmunity Reviews

journal homepage: www.elsevier.com/locate/autrev

Review

Pathogenesis of giant cell arteritis: More than just an inflammatory condition?

Kim-Heang Ly [a,b], Alexis Régent [a,c], Mathieu C. Tamby [a], Luc Mouthon [a,c,*]

[a] Université Paris Descartes, Institut Cochin, INSERM U1016, Paris, France
[b] Service de Médecine Interne A, CHU Dupuytren, Limoges, France
[c] Université Paris Descartes, Faculté de Médecine, Pôle de Médecine Interne, Centre de référence pour les vascularites nécrosantes et la sclérodermie systémique, hôpital Cochin, Assistance Publique-Hôpitaux de Paris, Paris, France

ARTICLE INFO

Article history:
Received 2 May 2010
Accepted 3 May 2010
Available online 8 May 2010

Keywords:
Giant cell arteritis
Pathogenesis
Inflammation
T lymphocytes
Remodeling

ABSTRACT

Giant cell arteritis (GCA) is characterized by intimal hyperplasia and luminal obstruction leading to ischemic manifestations involving extra-cranial branches of carotid arteries and aorta. Histopathological lesions involve all layers of the arterial wall and are associated with multinucleated giant cells, fragmented internal elastic lamina and polymorphic cellular infiltrates, including T lymphocytes and macrophages. The pathophysiology of GCA is still poorly understood. After dendritic cell activation, $CD4^+$ T lymphocytes, T helper 1 (Th1) cells, produce interferon γ and modulate macrophage activation and functions, and Th17 cells produce interleukin 17 (IL-17), which can induce cytokine production by macrophages and fibroblasts. Macrophages in the adventitia produce pro-inflammatory cytokines such as IL-1, IL-6 and tumor necrosis factor α. These cytokines promote arterial wall and systemic inflammation. Questions remain regarding the nature of the antigen(s) triggering dendritic cell activation and the mechanisms underlying vascular remodeling. Here we review recent advances in the pathogenesis of GCA, with emphasis on the interactions between cells of the immune system and components of the vessel wall, including vascular smooth muscle cells and endothelial cells, leading to vascular remodeling. Finally, we propose new areas of investigation that could help understand the triggering factors and key pathogenic events in GCA.

Contents

1. Introduction . . . 636
2. Age, sex, ethnicity and cardiovascular risk factors . . . 636
3. Interaction between innate and adaptive immune system . . . 636
4. Vascular injury and vascular remodeling. . . . 638
5. Potential role of endothelial cells . . . 638
6. Genetic background . . . 639
7. Viral and bacterial triggering factors. . . . 639
8. Perturbations of the humoral immune system . . . 639
9. Is GCA an autoinflammatory disease? . . . 641
10. Summary . . . 641

Abbreviations: aCL, anticardiolipin antibody; AECA, anti-endothelial cells antibody; BL, B lymphocytes; CCL, Chemokine (C–C motif) ligand; CCR, Chemokine (C–C motif) receptor; CD, cluster of differentiation; CMV, Cytomegalovirus; *Cp, Chlamydia pneumoniae*; CRP, C-reactive protein; DC, dendritic cell; EC, endothelial cell; eNOS, endothelial nitric oxide synthase; ESR, erythrocyte sedimentation rate; ICAM, intracellular adhesion molecule; IFN-γ, interferon-γ; IgG, immunoglobulin G; IL, interleukin; IL-1R1, Interleukin 1 receptor, type I; IL-1Ra, Interleukin 1 receptor antagonist; IL-1r1, Interleukin 1 receptor, type I gene; IL-1rn, Interleukin 1 receptor antagonist gene; GCA, giant cell arteritis; HHV, Human herpes virus; HLA, human leucocyte antigen; HPVB19, human parvovirus B19; HSP, heat shock protein; HSV, herpes simplex virus; LPS, lipopolysaccharide; MALDI TOF/TOF, matrix-assisted laser desorption/ionization time-of-flight/time-of-flight; MCP-1, monocyte chemoattractant protein 1; MHC, major histocompatibility complex; MICA, MHC class I chain-related gene A; MMP, matrix metalloproteinases; MPO, myeloperoxidase; PDGF, platelet-derived growth factor; RNI, reactive nitrogen intermediates; ROS, reactive oxygen species; SCID, severe combined immunodeficiency; TAB, temporal artery biopsy; TIR, Toll-interleukin-1 receptor; Th, T helper lymphocyte; TGF-β1, transforming growth factor β1; TL, T lymphocyte; TLR, toll-like receptor; TNF-α, tumor necrosis factor-α; VEGF, vascular endothelial growth factor; VSMC, vascular smooth muscle cell; VZV, varicella zoster virus.

* Corresponding author. Inserm U1016, Pavillon Gustave Roussy, 4e étage, Université Paris Descartes, 8 rue Méchain, 75014, Paris, France. Tel.: +33 1 44 41 25 44; fax: +33 1 44 41 25 46.
E-mail address: luc.mouthon@cch.aphp.fr (L. Mouthon).

1568-9972/$ – see front matter © 2010 Elsevier B.V. All rights reserved.
doi:10.1016/j.autrev.2010.05.002

Conflict of interest . . . 642
Take-home messages . . . 642
Acknowledgements . . . 642
References . . . 642

1. Introduction

Giant cell arteritis (GCA) is a large-vessel vasculitis. This condition occurs exclusively in patients older than 50 years, mainly among people older than 70 years [1]. Women are affected in two-thirds of the cases. Most of the epidemiologic studies have focused on the incidence of GCA, estimated to be 10–29/100 000 at-risk persons and increasing with advancing age [1,2]. The prevalence of GCA in people over 50 years old has been reported to vary between 278/100 000 in Olmsted County, Minnesota, USA [3], 25/100 000 in Germany [4], and 1.47/100 000 in Japan [5].

GCA specifically involves the aorta and external carotid arteries and their branches, with intimal hyperplasia and luminal obstruction leading to ischemic manifestations such as temporal headaches, jaw claudication, scalp tenderness and temporal artery involvement [6,7]. Visual loss, which may occur as a consequence of acute anterior ischemic optic neuritis, central retinal artery occlusion or retro-bulbar optic neuritis, represents the most severe complication [8,9]. In about 50% of patients with GCA, polymyalgia rheumatica develops and is responsible for hip and shoulder inflammation [10]. Most patients with GCA present signs of systemic inflammation, including weight loss, fatigue and fever, together with increased erythrocyte sedimentation rate (ESR) and C-reactive protein (CRP) level [11]. No specific biological marker of GCA has been identified, and the diagnosis is usually established by temporal artery biopsy (TAB) [12]. Corticosteroids are the mainstay of GCA treatment [13,14]. Histopathological lesions involve the 3 layers of the arterial wall and are associated with multinucleated giant cells resulting from the fusion of macrophages, fragmented internal elastic lamina and polymorphic cellular infiltrates, including T lymphocytes (TLs) and macrophages [15]. Several studies provided evidence that adventitial dendritic cells (DCs) are activated by an unknown stimulus that might be a microbial antigen (viral or bacterial) or an autoantigen [16]. These DCs, once activated, selectively activate antigen-specific TLs, which release interferon γ (IFN-γ) and regulate macrophage function and differentiation. Macrophages produce interleukin 1 (IL-1), IL-6 and tumor necrosis factor α (TNF-α); promote inflammation in the arterial wall; and initiate vascular remodeling through the release of cytokines, growth factors, reactive oxygen species (ROS) and matrix metalloproteinases (MMPs), which contribute to tissue injury and intimal hyperplasia [17]. However, the key mechanisms involved in vascular remodeling that lead to luminal occlusion remain unidentified in GCA. Among other factors contributing to vascular remodeling, endothelial cells (ECs), under the influence of cytokines or growth factors produced by macrophages, might also promote neoangiogenesis. In addition, newly formed ECs are involved in local inflammation by producing pro-inflammatory cytokines and expressing adhesion molecules that allow for the recruitment of TLs [18]. Finally, despite the lack of data regarding the implication of humoral immunity in GCA, several studies provided evidence of autoantibodies in CGA [19,20].

In this review, we provide an overview of recent breakthroughs in the pathogenesis of GCA and emphasize interactions between the main components of the immune system and the different compartments of the vessel wall, including ECs and vascular smooth muscle cells (VSMCs) that may lead to vascular remodeling.

2. Age, sex, ethnicity and cardiovascular risk factors

The incidence of GCA is higher in Caucasians than in African Americans in the USA [21,22], Arabs [23] or Asians [5,24]. Thus, GCA occurs most commonly in European and American Caucasians. Moreover, there is a north to south gradient between the Arctic Circle and Tropic of Cancer, with the highest rates in Northern Europeans [25–27] and North Americans [28,29] and lowest rates in Southern Europeans [30,31] and South Americans [32]. GCA occurs exclusively in people older than 50 years, with the highest rates among patients older than 70 years. The mean age at diagnosis of GCA is about 73 years throughout the world, regardless of country [5,26,27,29–31,33,34]. In these studies, females seem to be at greater risk than males, with a ratio of females to males ranging from 1.7:1 to 3.8:1 [5,26,27,29,33,34]; parity and the age of menopause may be factors [35,36]. Finally, a number of factors such as cardiovascular risk factors and smoking, particularly in women, have been reported to be associated with increased risk of GCA (odds ratio 4.5 and 6.5, respectively) [36,37].

3. Interaction between innate and adaptive immune system

Temporal arteries from patients with GCA are infiltrated by multinucleated giant cells located in the vicinity of fragmented internal elastic lamina, $CD4^+$ TLs and macrophages organized in granulomas; $CD8^+$ TLs and neutrophils are scarce in this area [38] (Fig. 1). All layers of the arterial wall are affected, which corresponds to panarteritis with segmentary lesions. Medial and intimal layers are avascular, which, together with a high velocity of blood flow probably preventing cell adhesion, helps explain that the primary injury of GCA pathogenesis would probably be located in the adventitia, a layer that contains *vasa vasorum*. TLs and macrophages might access the arterial wall through the capillary network to allow for vascularization of medium- and large-vessel arteries. Therefore, the adventitia layer provides the arterial wall with oxygen and nutrients and regulates vascular inflammation and immune recognition through indigenous embedded DCs [39,40]. Immature and quiescent DCs are present in the adventitia of temporal arteries from healthy individuals and probably act as arterial wall sentinels. These cells express S100 and chemokine (C–C motif) receptor 6 (CCR6) but not the co-stimulatory molecules and cell surface markers CD83 or CD86, which indicates their resting state. Finally, DCs express at their surface a number of components of the innate immune system such as TLR that recognize pathogen-associated molecular patterns such as lipopolysaccharide (LPS). Transcripts of TLR2 and TLR4 have been detected in noninflamed temporal arteries from control individuals [41]. In a mouse animal model with severe combined immunodeficiency (SCID) engrafted with temporal arteries from TABs of patients with unconfirmed GCA, intravenous injection of LPS, 7-10 days after implantation, led to DC activation, whereas arterial grafts harvested 48 h later expressed transcripts of CD83. Mice implanted with temporal arteries from patients with biopsy-proven GCA received an anti-CD83 monoclonal antibody, which abrogated vasculitis in arterial grafts harvested 1 week later. The density of TL infiltrates and IFN-γ and IL-1β transcript levels were decreased and granulomatous microstructures were destroyed, which suggest that DCs are critical antigen-presenting cells in GCA [40]. Normally, activated DCs migrate to the lymph nodes, where they can trigger the adaptive immune response; however, in patients with GCA, activated DCs remain in the arterial wall [42]. Activation of ECs and DCs precedes the recruitment of $CD4^+$ TLs and are ligand specific. TLR4 ligands induce transmural panarteritis, whereas TLR5 ligands cause adventitial perivascular infiltrates. Adventitial DCs produce IL-6 and IL-18 and express CD86,

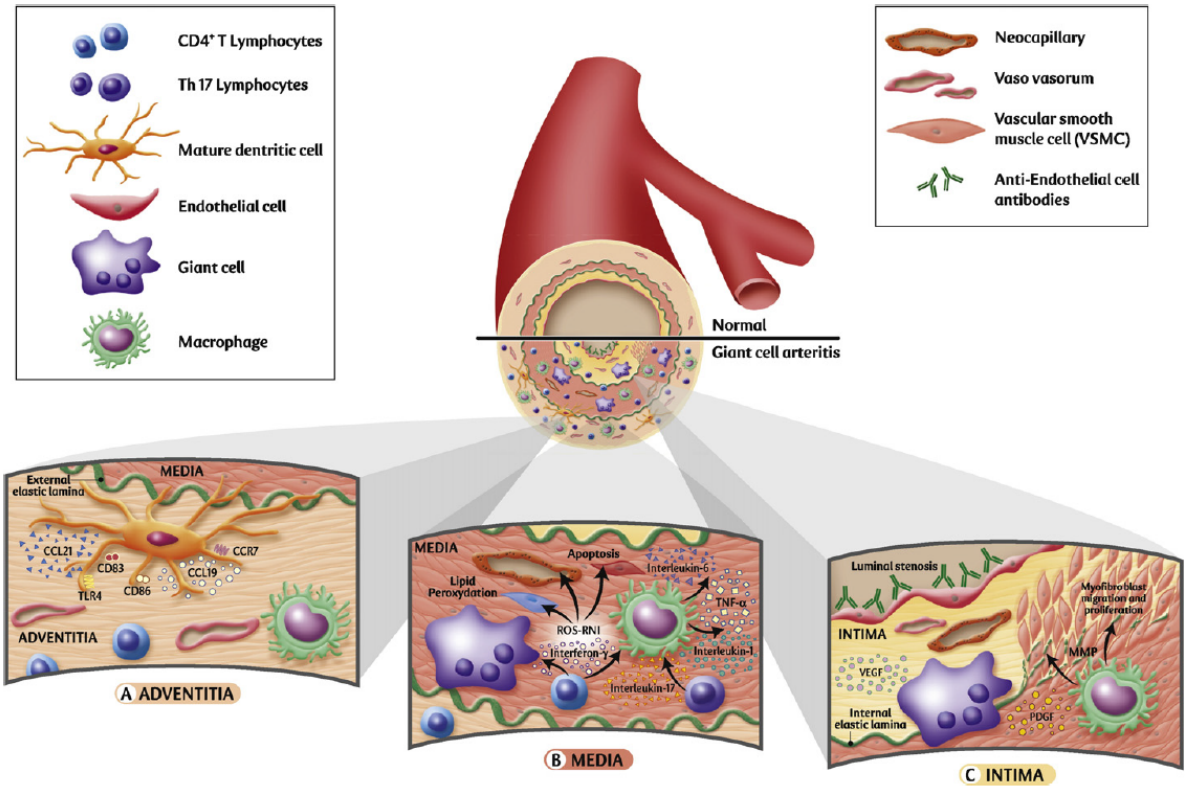

Fig. 1. Pathophysiology of GCA. (A) DCs are present in the adventitia, and at their surface, they express a number of components of the innate immune system such as TLR that recognize pathogen-associated molecular patterns. After activation by an unknown stimulus, mature DCs express CD83 or CD86, a co-receptor required for their interaction with TLs. They also produce CCR7 and homing chemokines such as CCL18, CCL19, CCL20 and CCL21 and their receptors. CCR7 binds CCL19 and CCL21 in an autocrine mechanism that contributes to DCs being trapped in the arterial wall. Thus, DCs may act as antigen-presenting cells, recruiting and activating $CD4^+$ TLs and infiltrating the external elastic lamina and the intima-media junction. (B) TLs undergo clonal expansion. Most are IFN-γ-producing Th1 TLs, which promote recruitment and activation of macrophages. However, IL-17-producing TLs, Th17 cells, which can induce pro-inflammatory cytokine production by macrophages, are also present in small proportions. Activated macrophages produce pro-inflammatory cytokines such as TNF-α, IL-1, and IL-6, thus promoting local and systemic inflammation. They can fuse, form giant cells and participate in the formation of granulomas, which are located close to the internal elastic lamina, at the intima-media junction. Giant cells and medial macrophages release ROS and RNI, which contribute to VSMC and EC lipid peroxidation and apoptosis. (C) These cells also express MMPs, PDGF and VEGF, which leads to the destruction of the internal elastic lamina, the pathological hallmark of GCA and vascular remodeling, with proliferation and migration of medial myofibroblasts and neoangiogenesis. These last events contribute to intimal hyperplasia and luminal stenosis. The role of anti-EC in the pathogenesis of GCA remains poorly understood. Abbreviations: CCL: chemokine (C–C motif) ligand, CCR: chemokine (C–C motif) receptor, CD: cluster of differentiation, DCs: dendritic cells, ECs: endothelial cells, IFN-γ: interferon-γ, IL: interleukin, GCA: giant cell arteritis, MMP: matrix metalloproteinases, PDGF: platelet-derived growth factor, RNI: reactive nitrogen intermediates, ROS: reactive oxygen species, Th1: T helper 1 cells, TL: T lymphocytes, TLR: Toll-like receptor, TNF-α: tumor necrosis factor-α, VEGF: vascular endothelial growth factor, VSMCs: vascular smooth muscle cells.

CD83 and CCR7, as well as homing chemokines such as chemokine C–C motif ligand (CCL) 18, CCL19, CCL20 and CCL21 and their specific receptors. CCR7 binds CCL19 and CCL21 in an autocrine mechanism, which probably contributes to the activation of DCs trapped in the arterial wall [42]. Thus, activated DCs may act as antigen-presenting cells and activate $CD4^+$ TLs after TLR4 ligation and upregulation of CCL20 and infiltrate the external elastic lamina and intima-media junction. TLs localized in vascular infiltrates from patients with GCA undergo clonal expansion [43], proliferate in the presence of protein extracts of temporal arteries from these patients [44], and secrete Th1 cytokines, mainly IFN-γ and IL-2. TLs expressing the same specificity were detected in different localizations of temporal arteries but not peripheral blood [45]. In a SCID mouse model with grafted fragments of temporal arteries from patients with GCA, treatment with a T cell-depleting antiserum led to a marked decrease in pro-inflammatory cytokine production and a regression of inflammatory infiltrates in implanted arteries [46]. In addition to Th1 and Th2 cells, which are characterized by different cytokine profiles and distinct effector functions, a third subset of TLs has been described: Th17 cells preferentially produce IL-17 but not IFN-γ or IL-4. Th17 TLs are known to clear specific types of infectious organisms and induce inflammation. Most parenchymal cells, including fibroblasts and macrophages, express IL-17 receptors. Signaling through these receptors can induce macrophages and fibroblasts to release proinflammatory cytokines such as TNF-α, IL-6 and IL-1 [47]. The role of functionally relevant TL subsets was recently studied in peripheral blood and TABs from patients with GCA [48]. Among $CD4^+$ T cells, the proportion of circulating IFN-γ-producing Th1 and IL-17-producing Th17 cells was 20.6% and 2.2%, on average, respectively, in untreated GCA-patients, versus 11.8% and less than 0.59%, respectively, in healthy controls. In 34 patients who received 16.7 mg/d prednisone, on average, the proportion of circulating IL-17-producing Th17 cells was decreased to 0.46%, whereas that (18.4%) of circulating Th1 cells remained unchanged. This result was confirmed at the cytokine level: before corticosteroid therapy, circulating IL-17 and IFN-γ protein levels were both elevated, whereas after therapy, the level of circulating IL-17 but not IFN-γ was suppressed at the transcriptional level. Total transcript levels of IL-17 and IFN-γ were high in temporal artery extracts from untreated patients with GCA, but control samples were

negative for both. Analysis of monocytes/macrophages in peripheral blood and in temporal arteries provided evidence for the glucocorticoid-mediated suppression of Th17-promoting cytokines (IL-1β, IL-6, and IL-23) and the sparing of Th1-promoting cytokines (IL-12). In the model of SCID mice engrafted with normal human arteries, LPS or saline, as a control, was injected 1 week post-grafting, and after 24 h, TL cell lines established from the blood of GCA patients were adoptively transferred. Chimeras were treated with dexamethasone or saline, and temporal arteries were explanted. Glucocorticoids inhibited mRNA production of IL-17 but not IFN-γ, and the density of IL-17 TLs was markedly diminished in the vessel wall, as seen on immunohistochemistry. These data support the concept that many of the acute manifestations of GCA are mediated by IL-17. However, further studies of the effects of Th1- and Th17-dependent processes in this condition are needed [48].

$CD4^+$ TL-producing IFN-γ represents only 2% to 4% of tissue-infiltrating TLs and aggregates in the adventitial layer, close to resident DCs [45,49]. IFN-γ promotes recruitment and activation of macrophages, which infiltrate the arterial wall via the *vasa vasorum*. IFN-γ synthesis and release is induced by IL-12 and IL-18 produced by DCs [50,51]. Macrophages present in the adventitia produce pro-inflammatory cytokines such as TNF-α, IL-1, and IL-6, thus promoting local and systemic inflammation. IL-6 induces an increase in CRP level and ESR, which are associated with disease severity [52]. In temporal artery media, macrophages activated by IFN-γ can fuse, form giant cells and participate in granuloma formation [53]. These granulomas, composed of $CD4^+$ TLs, macrophages and giant cells, are preferentially located close to the internal elastic lamina, at the intima-media junction.

4. Vascular injury and vascular remodeling

During the course of GCA, luminal occlusion may occur as a consequence of intimal hyperplasia. In temporal arteries from patients with GCA, medial layer destruction results from the combined effect of several factors, including the production of reactive oxygen species (ROS), reactive nitrogen intermediates (RNIs) and MMPs (Fig. 1). MMPs are proteolytic enzymes and can destroy cellular matrix proteins including elastin. MMP-2 and MMP-9 are both detected in inflamed temporal arteries in patients with GCA and are involved in the digestion of the internal elastic lamina [53,54]. Maximal expression and activity of both MMP-2 and MMP-9 were documented in granulomatous areas surrounding the internal elastic lamina [55]. However, only MMP-9 seems to contribute to the destruction of the internal elastic lamina [56]. Interestingly, VSMCs and myofibroblasts of the media and intima layers can also produce these MMPs. The release of ROS leads to lipid peroxidation of membrane phospholipids of VSMCs and infiltrating mononuclear cells [57]. The combination of ROS, RNIs and MMPs contributes to the induction of VSMC and mononuclear cell apoptosis and destruction of the internal elastic lamina, the pathological hallmark of GCA. These events are offset by at least 2 protective factors. Aldose reductase, a ketoreductase that limits lipid peroxidation of the phospholipid membrane, is detected in macrophages, TLs and VSMCs in areas of arterial wall destruction in patients with GCA. Aldose reductase expression is associated with 4-hydroxy-2-nonenal adducts, a downstream product of lipid peroxidation detected in VSMCs and tissue-infiltrating cells, in close vicinity to giant cells and macrophages. Inhibition of aldose reductase activity by Sorbinil and Zopolrestat augments 4-hydroxynonenal formation and increases the number of apoptotic cells in the arterial wall [58].

Furthermore, growth factors such as platelet-derived growth factor (PDGF) and VEGF are expressed with tissue injury in inflamed arteries of patients with GCA for protecting the arterial wall. These growth factors are involved in intimal hyperplasia and neoangiogenesis, respectively, and PDGF stimulates VSMC migration from the media to the intima after arterial injury [59,60]. Interestingly, medial cells of noninflamed arteries express low levels of PDGF-A and PDGF-B, whereas the expression of both is high in all layers in temporal arteries of patients with GCA, except the intima [61]. PDGF is mainly released by macrophages, and giant cells present at the intima-media junction, near the internal elastic lamina, but also by activated VSMCs and ECs located around the vascular lumen. High expression of PDGF is associated with intimal hyperplasia, and ischemic complications, including jaw claudication, ocular and central nervous system ischemia, seem to occur more frequently in patients with evidence of intimal proliferation. In normal arteries, the *vasa vasorum* is restricted to the adventitia. In inflamed arteries of patients with GCA, neocapillaries are detected in both the media and the intima. This neovascularization is associated with intimal hyperplasia, internal elastic lamina fragmentation and VEGF production by macrophages and giant cells at the intima-media junction [62]. Thus, neoangiogenesis probably plays a dual role in GCA: a primary hypoxia compensation role and a secondary proinflammatory role. By producing a number of chemokines, newly formed vessels can contribute to increase TLs and macrophage recruitment and maintain and perpetuate the inflammatory process. In summary, GCA vascular remodeling corresponds to a maladaptative response that contributes to intimal hyperplasia and vascular lumen occlusion.

The origin of myofibroblasts contributing to intimal hyperplasia remains controversial. These cells could derive from medial VSMCs. Thus, in the normal condition, VSMCs express a differentiated contractile phenotype, whereas in atherosclerotic lesions or in an animal model of vascular injury, VSMCs can dedifferentiate, proliferate and migrate from the media to the intima layer, thus contributing to intimal hyperplasia after PDGF-mediated activation [63]. Furthermore, VSMCs can acquire a secretory phenotype, producing urokinase and tissue-type plasminogen activator, as was reported in a murine model of injured carotid artery [64], and/or MMPs that facilitate their migration through the arterial wall and contribute to the dissolution of matrix proteins, as was observed in GCA [56]. Thus, VSMCs can help maintain local inflammation and intimal hyperplasia by producing ROS and extracellular matrix proteins.

Alternatively, myofibroblasts could derive from adventitial cells, as was reported in animal models of atherosclerosis or angioplasty-induced restenosis [65–70]. In these models, adventitial fibroblasts can differentiate and migrate to the intima, thus contributing to intimal hyperplasia. Furthermore, it is now accepted that nearly half of the neointimal cells originate from proliferating adventitial cells [71]. Thus, adventitial fibroblasts can acquire myofibroblast characteristics with the expression of α-smooth muscle actin and the production of collagen, extracellular matrix and growth factors such as transforming growth factor-β1 (TGF-β1). The autocrine induction of TGF-β1 in adventitial fibroblasts induces the differentiation of fibroblasts to myofibroblasts, thus allowing their migration to the intimal layer [72]. Evidence of a critical role of TGF-β1 in this setting has been obtained in the balloon angioplasty rat model, where blocking of TGF-β receptor II is associated with reduced post-angioplasty restenosis, with decreased remodelling and collagen content [73].

In addition, adventitial progenitor cells may differentiate into functional VSMCs or myofibroblasts that could contribute to intimal hyperplasia [74,75]. Finally, intimal myofibroblasts could derive from circulating progenitor cells, which was found to contribute to enhanced neointimal formation in an experimental model of vein grafting in pig [76].

In conclusion, further studies are needed to improve our understanding of the mechanisms underlying vascular remodeling in GCA, to prevent the occurrence of ischemic events.

5. Potential role of endothelial cells

ECs are important because they form a barrier between blood and tissues and play a crucial role in the regulation of vasomotor,

haemostatic, angiogenetic and inflammatory processes. EC dysfunction appears to increase with age [77]. In patients with GCA, EC dysfunction is associated with increased production of cytokines [52] and growth factors [62] by TLs and macrophages, thus favouring a neovascularization process. In these patients, ECs represent a passive target of macrophages and TL products and react in response to these stimulations by producing cytokines and expressing adhesion molecules [18], thus contributing to the recruitment of TLs. Constitutive (platelet EC adhesion molecule 1, intracellular adhesion molecule 1 [ICAM-1], ICAM-2 and P-selectin) and inducible (E-selectin and vascular cell adhesion molecule 1) expression of leukocytes and EC adhesion molecules by adventitial micro-vessels and neo-vessels were shown within inflammatory infiltrates in TABs from patients with GCA [86]. Moreover, soluble ICAM-1 plasma concentrations were found to be associated with disease activity in patients with GCA [87]. EC dysfunction has been studied in GCA by use of tubular constructs with or without an endothelial monolayer. In this model, amplification of the immune response was documented in terms of DC recruitment and TL activation associated with the endothelial layer [78]. Thus, ECs probably play an important role in the pathophysiology of GCA by interacting with components of the immune system and maintaining local inflammation [79].

6. Genetic background

A genetic predisposition to GCA has been suggested from reports of cases in first-degree relatives and monozygotic twins [80–84]. A number of factors have been suspected to increase the risk of GCA, including haplotypes of human leukocyte antigen (HLA) classes I and II, particularly the HLA-DRB1*04 haplotype, and gene polymorphisms for adhesion molecules, cytokines, chemokines or growth factors (Table 1). An association of HLA-DRB1*04 haplotype and risk of ocular involvement [85,86] or resistance to corticosteroids [87,88] has been suggested.

The G/R 241 polymorphism of ICAM-1 was found to be associated with GCA susceptibility [89]. However, this result was not confirmed in another study [90]. Other case-control studies have examined a number of gene polymorphisms and their association with disease susceptibility (Table 2). Most of these studies (18/21) were performed on the same cohort of GCA patients, and other results are from a Southern Europe cohort. Unfortunately, none of the studies of the 2 cohorts included a replication cohort. The genes related to GCA susceptibility, at least for one polymorphism, that have been investigated include IL-4, IL-10, monocyte chemoattractant protein 1 (MCP-1), myeloperoxidase (MPO), cluster of differentiation 24 (CD24), major histocompatibility complex (MHC) class I chain-related gene A (MICA), HLA-B, MMP-9, Toll-like receptor (TLR)-4 and Fc gamma receptors IIA and IIIA. Finally, conflicting results were obtained for 3 polymorphisms for TNF-α, vascular endothelial growth factor (VEGF), and endothelial nitric oxide synthase (eNOS) evaluated in 2 independent cohorts [91–95]. Overall, only a limited number of genes—eNOS, MMP-9 and TLR4—might be good candidates in this setting. Further studies in different ethnic groups and continents are necessary to strengthen these results and improve our understanding of the pathogenesis of GCA.

Table 1
HLA haplotypes in patients with GCA.

Author, year [Ref]	Patients with biopsy-proven GCA/controls	Methods used	Association with GCA	P	OR or RR
Kemp et al. [136]	88/3164	MLCA	HLA B8	0.041	ND
Hansen et al. [137]	35/219	MLCA	HLA A31	< 0.05	RR: 3.09
			HLA B40	< 0.01	RR: 3
			HLA Cw3	< 0.001	RR: 5.65
			HLA DR4	< 0.01	RR: 2.7
Cid et al. [138]	65/200	MLCA	HLA DR4	< 0.05	ND
Salvarani et al. [30]	20/242	MLCA	HLA DR4	NS	ND
Bignon et al. [139]	88/146	PCR	HLA DR4	< 0.001	ND
Richardson et al. [140]	43/243	MLCA	HLADR4	NS	ND
Weyand et al. [141]	52/72	PCR	HLA DRB1*04	0.0001	ND
Combe et al. [142]	42/1609	PCR	HLA DRB1*04	0.0005	OR: 3.1
Rauzy et al. [87]	41/384	PCR	HLA DRB1*04	<0.001	ND
Jacobsen et al. [143]	65/193	PCR	HLA DRB1*04	0.01	ND
Dabaneh et al. [144]	53/145	PCR	HLA DRB1* 0401	NA	NA
Weyand et al. [88]	42/63	PCR	HLA DRB1*0401	0.03	ND
Martinez-Taboada, et al. [145]	44/99	PCR	HLA-DRB1* 0401	0.02	OR: 3.1
			HLA-DRB1* 0404	0.04	OR: 3.5

GCA: giant cell arteritis; HLA: human leucocyte antigen; MLCA: microlymphocytotoxicity assay; NA: not available; ND: not done; NS: not significant; OR: odds ratio; PCR: polymerase chain reaction; RR: relative risk.

7. Viral and bacterial triggering factors

A number of case-control studies have investigated the potential role of viruses and/or bacteria in the pathogenesis of GCA. Most of the studies aimed at detecting viral and/or bacterial DNA by PCR, together with, in some studies, immunohistochemistry or *in situ* hybridization in TABs from patients with GCA (Table 3). A large number of pathogens have been investigated (Table 3), but no association was found with human herpes virus (HHV)-6, HHV-7, varicella zoster virus or Epstein–Barr virus [96–100]. An association of cytomegalovirus with GCA was found by *in situ* hybridization [101], which was not confirmed by PCR in 5 other studies [97,98,100,102,103]. Herpes simplex virus DNA was detected in TABs from patients with GCA [104]. However, the study sample was small, and 6 other studies failed to confirm this result in larger samples [96–98,100,103,105]. Human parvovirus B19 (HPVB19) DNA was found in 7 of 13 biopsy-positive and 4 of 37 biopsy-negative GCA cases [102]. This result was confirmed in a larger study [99]. However, 4 other studies failed to detect HPVB19 in TABs from patients with GCA [100]. Finally, Duhaut et al. [104] using serological tests, reported higher titers of immunoglobulin M directed against human parainfluenzae virus 1 in patients with biopsy-proven GCA than in age-matched healthy controls. To our knowledge, no confirmative study was performed at the DNA level.

The only bacterium investigated in this setting has been *Chlamydia pneumoniae* (*Cp*). DNA of *Cp* was detected in TABs from patients with GCA, with an adventitial layer localization [39]. However the same group [106] and 4 others failed to confirm these results [97,100,107,108].

Overall, despite the large number of studies conducted so far, no infectious agent has been clearly identified to be associated with GCA, which does not favor the hypothesis that an infectious antigen could trigger the disease process, activate DCs and initiate vascular inflammation. However, these results do not rule out the implication of an external antigen but might favor the concept of an immune response directed toward an autoantigen at this stage of the disease process.

8. Perturbations of the humoral immune system

Not surprisingly, few studies have focused on perturbations of the humoral immune system in patients with GCA. Few B lymphocytes (BLs) are detected in TABs from patients with GCA [38,109]. When present, BLs are mainly found in the adventitial layer [109]. Moreover, plasmocytes can be found in the adventitia in 7% to 24% of TABs from patients with GCA and have been reported to be more frequently detected in patients with permanent visual loss [110]. An explanation for the presence of plasmocytes in the adventitia might be an infectious agent initiating vascular inflammation. However, as stated before, a number of studies failed to identify an infectious agent, either virus or bacteria, in the arterial wall by immunohistochemistry

Table 2
Case-control studies investigating gene polymorphisms and susceptibility to GCA.

Author, year [ref]	Patients with biopsy-proven GCA/controls	Genes analyzed	Investigated alleles, haplotypes or variants	Association with GCA	p	Odds ratio
Gonzalez-Gay et al. [146]	57/128	IL-1A, IL-1B,TNF-α	IL-1A (+4845) IL-1B (+3954; -511) IL-1RN intron 2 VNTR TNF-α (-308)	N		
Mattey et al. [91]	62/147	TNF microsatellite markers (a–d)	TNFa2 allele	Y	0.003	2.5
			TNFa10 allele	Y	0.02	0.3
Gonzalez-Gay et al. [147]	62/124	IL-6	IL-6 promoter : -174 G/C	Y	0.03	2.3
Salvarani et al. [148]	126/112	IL-6	IL-6 promoter : -174 G/C	N		
Gonzalez-Gay et al. [149]	50/129	INF-γ	INF-γ microsatellite Dinucleotide CA repeat (alleles 1 to 7), intron 1	N		
Amoli et al. [150]	82/102	INF-γ: Intron 3: SNP1 (rs1861494), SNP2 (rs1861493), SNP3 (rs2069718) -IL-4: Exon 1: SNP1 (rs2070874). Intron 2: SNP2 (rs2227284), SNP3 (rs2227282), SNP4 (rs2243266), SNP5 (rs2243267)	SNP2*T allele T-T-C-A-C IL-4	Y Y	0.0001 0.02	4.2 2
Boiardi et al. [151]	140/200	IL-10 promoter: -592 C/A -1082 G/A	A592 allele (A/A or C/A) A/G 1082	Y N	0.004	2
Rueda et al. [152]	103/226	IL-10 promoter: -592 C/A -1082 G/A	A592 allele (A/A or C/A) A/G 1082	Y N	0.004	2
Amoli et al. [153]	83/122	MIF	MIF gene promoter -173 G/C	N		
Amoli et al. [154]	79/99	MCP-1	Haplotype C–C Haplotype T–T	Y Y	0.03 0.05	2.09
Boiardi et al. [92]	92/200	VEGF	936 C/T C634 and I	N Y	0.025	1.9
Rueda et al. [93]	103/226	VEGF	634 G–>C 1154 G–>A	N N		
Amoli et al. [94]	57/117	ENOS	C/1/T C/1/G	Y Y	0.04 0.02	1.8 0.3
Salvarani et al. [155]	91/133	ENOS	TAAA Glu/Asp(298)	Y Y	0.007 0.0002	1.98 3.3
Gonzalez-Gay et al. [95]	103/198	ENOS	CCTTT	N		
Rodriguez-Pla et al. [156]	30/23	MMP-9	rs2250889 G allelle	Y	0.009	
Palomino-Morales et al. [157]	210/678	TLR-4	+896 G allele	Y	0.01	1.65
Rueda et al. [158]	120/195	CD24	rs3838646 TG/del rs8743	Y Y	0.01 0.001	1.94 6
Gonzalez-Gay et al. [159]	99/229	PTPN22	PTPN22 gene 1858C(R)T 94ins/delATTG	N		
Martin et al. [160]	96/204	NF-kB1	NF-kB1 promoter	N		
Palomino-Morales et al. [161]	212/678	STAT-4	rs7574865	N		
Torres et al. [162]	220/410	TRAF1/C5	rs10818488 and rs2900180	N		
Torres et al. [163]	220/520	IRF-5	rs2004640 and CGGGG insertion/deletion	N		
Morgan et al. [164]	85/132	FcγR	FCGR2A-131RR FCGR3A-158F	Y Y	0.02 0.03	2.10 3.09
Gonzalez-Gay et al. [165]	98/225	MICA HLA-B	A5 allele HLA-B*15 allele	Y Y	0.0005 0.04	2.2 2.7
Salvarani et al. [166]	156/235	MPO	463 G allele	Y	0.0002	2
Palomino-Morales et al. [167]	125/234	CRP	rs1417938, rs1800947, rs1205, and rs3093059	N		
Gonzalez-Gay et al. [168]	62/147	CRH	CRH A1,A2,alleles B1,B2 alleles	N		

* :number of TAB in patients with GCA. CD24: cluster of differentiation 24; CRH: corticotrophin-releasing hormone; CRP: C-reactive protein; eNOS: endothelial nitric oxide synthase; FcγR: Fc gamma receptor; GCA: giant cell arteritis; HLA-B: human leucocyte antigen B; IRF5: interferon regulatory factor 5; IL-1A: interleukin 1A; IL-1B: interleukin 1B; IL-4: Interleukin 4; IL-6: interleukin 6 ; Interleukin 10; MIF: macrophage migration inhibitory factor; MCP-1: monocyte chemoattractant protein 1; MICA: MHC class I chain-related gene A; MMP-9: matrix metalloproteinase 9; MPO: myeloperoxidase; NF-kB1: nuclear factor of k-light polypeptide gene enhancer in B cells; PTPN22: protein tyrosine phosphatase, non-receptor type 22; STAT 4: signal transducer and activator of transcription 4; TNF-α: tumor necrosis factor alpha; TLR-4: Toll-like receptor 4; TRAF1/C5: tumour necrosis factor receptor-associated factor 1/complement component 5; VEGF: vascular endothelial growth factor.

or PCR (Table 3). An alternative hypothesis is an autoantigen, eventually present in the arterial wall, triggering a specific immune response in GCA. Screening antigens in a cDNA library derived from normal human testis revealed high-intensity serum immunoglobulin G (IgG) reactivity directed against a number of ubiquitous autoantigens, including human lamin C, cytokeratin and mitochondrial cytochrome oxidase subunit II in patients with GCA [19].

Among other autoantigens, anticardiolipin antibodies (aCLs) were detected in 20% to 50% of patients with GCA [111–113]; anti-β2 glycoprotein I antibodies were not detected in this condition [114]. aCLs were detected at a low range [111,113], were not associated with increased risk of ischemic events [111,112,115] and disappeared after 3 months of corticosteroid treatment [113,116].

Anti-EC antibodies (AECAs) have been detected in 33% of patients with GCA [117]. AECAs can be detected in healthy individuals [118] and in a number of systemic autoimmune diseases [119] and therefore are not disease specific [120]. We used a 2-D immunoblotting technique and mass spectrometry (MALDI-TOF-TOF) with human umbilical vein ECs as the source of protein antigens and identified that serum IgG from patients with GCA reacted with a number of EC autoantigens, including lamin A/C, voltage-dependent anion-selective channel protein 2 and annexin V [121]. Interestingly, in other

Table 3
Case-control studies investigating the potential association between microbial agents and GCA.

Author, year [ref]	Number of TABs	Number of patients with biopsy-proven GCA	Methods used	Results of viral and bacterial DNA or proteins investigated								P
				HSV	*VZV*	*EBV*	*CMV*	*HHV6*	*HPIV 1*	*PB 19*	*C.p*	
Fest et al. [101]	174	38	Serology ISH	ND	ND	ND	+	ND	ND	ND	ND	0.03
Nordborg et al. [96]	10	10	IHC PCR	−	−	ND	ND	ND	ND	ND	ND	−
Gabriel et al. [102]	50	13	PCR	ND	ND	ND	−	ND	ND	+	ND	0.0013
Duhaut et al. [105]	305	159	Serology	−	ND	−	ND	ND	+	ND	ND	0.00005
Wagner et al. [39]	27	9 (14)*	IHC PCR	ND	ND	ND	ND	ND	ND	ND	+	ND
Haugeberg et al. [107]	20	12	Nested PCR	ND	ND	ND	ND	ND	ND	ND	−	−
Salvarani et al. [169]	83	31	Nested PCR	ND	ND	ND	ND	ND	ND	−	ND	−
Regan et al. [108]	180	79	PCR	ND	ND	ND	ND	ND	ND	ND	−	−
Helweg-Larsen et al. [97]	30	13	PCR	−	−	−	−	−	ND	−	−	−
Kennedy et al. [170]	22	15	ISH ISPCR	ND	−	ND	ND	ND	ND	ND	ND	−
Rodriguez-Pla et al. [98]	147	50	IHC PCR	−	−	−	−	−	ND	−	ND	−
Powers et al. [104]	39	24	HS PCR	+	ND	ND	ND	ND	ND	ND	ND	0.027
Alvarez et al. [99]	113	57	QPCR	ND	−	ND	ND	−	ND	+	ND	0.007
Cankovic et al. [103]	41	35	QPCR	−	ND	−	−	ND	ND	ND	ND	−
Cooper et al. [100]	104	37	PCR Nested PCR	−	−	−	−	−	ND	−	−	−
Njau et al. [106]	224	115	TETR-PCR Nested PCR	ND	ND	ND	ND	ND	ND	ND	−	−

*:number of TAB in patients with GCA. CP: *Chlamydia pneumoniae*; CMV: cytomegalovirus; EBV: Epstein-Barr virus; HHV6: human herpes virus 6; HPIV 1: human parainfluenzae 1 virus; HPVB19: human parvovirus B19; HSV: herpes simplex virus; ISH: *in situ* hybridization; IHC: immunohistochemical analysis; ND: not done; PCR: polymerase chain reaction, QPCR: quantitative real-time PCR, TETR-PCR: touchdown enzyme time-release PCR; TAB: temporal artery biopsy; VZV: varicella zoster virus.
−: no statistically significant difference between patients with biopsy-proven GCA and controls.
+: statistically significant difference between patients with biopsy-proven GCA and controls.

conditions, a number of target antigens of AECA identified include heat shock proteins (HSPs) in atherosclerosis [122,123]. Interestingly, HSP60 [124] and HSP70 [125] are ligands of TLR4 in DCs, ECs and macrophages, which might be of interest in GCA. AECAs were found associated with disease activity in patients with vasculitis, including anti-neutrophil cytoplasmic antibody-associated vasculitis, Takayasu's arteritis and GCA [117]. Although AECAs have been shown to induce EC apoptosis in patients with systemic sclerosis, the potential pathogenic role of AECAs in GCA has not yet been documented, and further investigations are needed.

9. Is GCA an autoinflammatory disease?

Autoinflammatory diseases are characterized by seemingly unprovoked episodes of inflammation and absence of high-titer autoantibodies or antigen-specific T cells. Their pathogenesis implies the presence of myeloid effector cells and germline molecules of innate immunity. The concept was proposed more than 10 years ago with the identification of mutations in a number of genes associated with hereditary periodic fever syndromes. Recently, Masters et al. proposed an updated classification based on molecular insights and 6 categories of autoinflammatory diseases, including IL-1β activation disorders (inflammasomopathies) [126]. A number of complex/acquired conditions classified in this latter group include gout, pseudogout, fibrosing disorders, type 2 diabetes mellitus and Schnitzler syndrome. In all these conditions, dysfunction of inflammasome complexes is responsible for IL-1β production by monocytes, thus leading to local and systemic inflammation [126].

Although the major inflammatory cytokine involved in the pathogenesis of GCA is IL-6, IL-1 also plays an important role. Circulating levels of IL-1 were increased in patients with GCA [127,128], and the IL-1β transcript level was found higher in TABs from GCA patients with a strong inflammatory response, which suggests more local than systemic inflammation. The intracytoplasmic domains of Toll-IL-1 receptor (TIR), present in TLR, and IL-1 receptor (IL-1R1) show a high degree of homology. Thus, IL-1 and TLR ligands can both induce indistinguishable inflammatory responses such as the induction of type 2 cyclooxygenase, increased expression of adhesion molecules, or synthesis of nitric oxide. IL-1α and IL-1β share a natural antagonist protein called IL-1R antagonist (IL-1Ra), which is a competitive protein for binding their widely distributed common receptor, IL-1R1 [129]. IL-1Ra, along with IL-1, is produced by monocytes and macrophages after exposure to a proinflammatory stimulus and is also produced after activation of ECs and/or VSMCs and at a low level in many tissues [130,131].

Data suggesting that GCA could be classified with autoinflammatory syndromes have been obtained in mouse models. Mice deficient in IL-1Ra (*Il1rn*−/− mice) show psoriasiform skin lesions [132], polyarthritis mimicking rheumatoid arthritis [133] and arteritis [134]. Interestingly, histopathological lesions in *Il1rn*−/− mice are similar to those observed in GCA, and the aortas of these mice are infiltrated with DCs, macrophages and INF-γ-producing $CD4^+$ TLs. However, a major difference with GCA is the absence of giant cells in aortic lesions. Conversely, EC activation is not evidenced. When *Il1rn*−/− mice were bred with mice deficient or not in IL-1r1 gene, aortic root lesions developed in Il1rn−/−/Il1r1+/+ mice but not IL-1rn−/−/IL-1r1−/− mice which suggests an essential role for a high level of IL-1 as a mediator of the disease process [135].

In conclusion, GCA shares with autoinflammatory diseases the major implication of innate immunity and IL-1 function disturbances. In this setting, IL-1 blockade might be of interest and would be helpful to document the classification of GCA among inflammasomopathies.

10. Summary

Significant advances have been made in understanding the pathogenesis of GCA. Macrophages, giant cells and granulomas are responsible for tissue injury with a destruction of the internal elastic lamina, which is the hallmark of this disease. Recent studies highlighted the crucial role of adventitial DCs and their interaction

with TLs in the initiation of the pathophysiological process. Pro-inflammatory cytokines involved in arterial lesions and clinical manifestations, including TNF-α, IL-6 and IL-1 expression, could represent therapeutic targets, although the efficacy of anti-TNF-α monoclonal antibodies is controversial in this condition. In response to vascular injury, the development of intimal hyperplasia leads to vascular remodeling and luminal occlusion. A better understanding of vascular remodeling mechanisms involving VSMCs, ECs and adventitial fibroblasts could lead to the development of specific therapy and the prevention of ischemic complications.

Conflict of interest

LM received consulting fees from Actelion, Pfizer, GSK, Lilly, LFB Biotechnologies and CSL Behring. The other authors declare no conflict of interest.

Take-home messages

- Intimal hyperplasia, which results from tissue injury and growth factor synthesis, leads to luminal occlusion by proliferation and migration of medial myofibroblasts.
- Understanding the remodeling of vascular mechanisms in patients with GCA could help provide specific treatment to prevent ischemic events.
- Macrophages are recruited and activated by IFN-γ produced by T cells, producing giant cells and granuloma formation and leading to arterial wall injury through the production of cytokines, MMPs, ROS and RNIs.
- Macrophages in the adventitia produce pro-inflammatory cytokines such as IL-1, IL-6 and TNF-α. Early events in the immunogical response are based on interactions between the innate and adaptative immune system involving DCs and TLs.
- Genetic and environmental risk factors of GCA include an HLA-DRB1*04 haplotype and age older than 50 years. However, to date, no infectious agent has been clearly associated with GCA.

Acknowledgements

KHL received financial support from Limoges Hospital. AR received financial support from the Agence Régionale de Santé Champagne-Ardennes. MCT received financial support from Pfizer. We thank Monisokha Ly for her help in drawing the figure.

References

[1] Hunder GG. Epidemiology of giant-cell arteritis. Cleve Clin J Med 2002;69(Suppl 2): SII79–82.
[2] Gonzalez-Gay MA, Vazquez-Rodriguez TR, Lopez-Diaz MJ, Miranda-Filloy JA, Gonzalez-Juanatey C, Martin J, et al. Epidemiology of giant cell arteritis and polymyalgia rheumatica. Arthritis Rheum 2009;61:1454–61.
[3] Lawrence RC, Felson DT, Helmick CG, Arnold LM, Choi H, Deyo RA, et al. Estimates of the prevalence of arthritis and other rheumatic conditions in the United States. Part II. Arthritis Rheum 2008;58:26–35.
[4] Reinhold-Keller E, Zeidler A, Gutfleisch J, Peter HH, Raspe HH, Gross WL. Giant cell arteritis is more prevalent in urban than in rural populations: results of an epidemiological study of primary systemic vasculitides in Germany. Rheumatology (Oxford) 2000;39:1396–402.
[5] Kobayashi S, Yano T, Matsumoto Y, Numano F, Nakajima N, Yasuda K, et al. Clinical and epidemiologic analysis of giant cell (temporal) arteritis from a nationwide survey in 1998 in Japan: the first government-supported nationwide survey. Arthritis Rheum 2003;49:594–8.
[6] Liozon F. Horton's disease. Ann Med Interne (Paris) 1989;140:122–41.
[7] Gonzalez-Gay MA, Barros S, Lopez-Diaz MJ, Garcia-Porrua C, Sanchez-Andrade A, Llorca J. Giant cell arteritis: disease patterns of clinical presentation in a series of 240 patients. Medicine (Baltimore) 2005;84:269–76.
[8] Aiello PD, Trautmann JC, McPhee TJ, Kunselman AR, Hunder GG. Visual prognosis in giant cell arteritis. Ophthalmology 1993;100:550–5.
[9] Liozon E, Herrmann F, Ly K, Robert PY, Loustaud V, Soria P, et al. Risk factors for visual loss in giant cell (temporal) arteritis: a prospective study of 174 patients. Am J Med 2001;111:211–7.
[10] Salvarani C, Hunder GG. Musculoskeletal manifestations in a population-based cohort of patients with giant cell arteritis. Arthritis Rheum 1999;42:1259–66.
[11] Gonzalez-Gay MA, Lopez-Diaz MJ, Barros S, Garcia-Porrua C, Sanchez-Andrade A, Paz-Carreira J, et al. Giant cell arteritis: laboratory tests at the time of diagnosis in a series of 240 patients. Medicine (Baltimore) 2005;84:277–90.
[12] Myklebust G, Gran JT. A prospective study of 287 patients with polymyalgia rheumatica and temporal arteritis: clinical and laboratory manifestations at onset of disease and at the time of diagnosis. Br J Rheumatol 1996;35:1161–8.
[13] Hunder GG, Sheps SG, Allen GL, Joyce JW. Daily and alternate-day corticosteroid regimens in treatment of giant cell arteritis: comparison in a prospective study. Ann Intern Med 1975;82:613–8.
[14] Andersson R, Malmvall BE, Bengtsson BA. Long-term corticosteroid treatment in giant cell arteritis. Acta Med Scand 1986;220:465–9.
[15] Lie JT. Illustrated histopathologic classification criteria for selected vasculitis syndromes. American College of Rheumatology Subcommittee on Classification of Vasculitis. Arthritis Rheum 1990;33:1074–87.
[16] Duhaut P, Bosshard S, Ducroix JP. Is giant cell arteritis an infectious disease? Biological and epidemiological evidence. Presse Méd 2004;33:1403–8.
[17] Weyand CM, Goronzy JJ. Medium- and large-vessel vasculitis. N Engl J Med 2003;349:160–9.
[18] Cid MC, Hernandez-Rodriguez J, Esteban MJ, Cebrian M, Gho YS, Font C, et al. Tissue and serum angiogenic activity is associated with low prevalence of ischemic complications in patients with giant-cell arteritis. Circulation 2002;106:1664–71.
[19] Schmits R, Kubuschok B, Schuster S, Preuss KD, Pfreundschuh M. Analysis of the B cell repertoire against autoantigens in patients with giant cell arteritis and polymyalgia rheumatica. Clin Exp Immunol 2002;127:379–85.
[20] Baiu DC, Barger B, Sandor M, Fabry Z, Hart MN. Autoantibodies to vascular smooth muscle are pathogenic for vasculitis. Am J Pathol 2005;166:1851–60.
[21] Liu NH, LaBree LD, Feldon SE, Rao NA. The epidemiology of giant cell arteritis: a 12-year retrospective study. Ophthalmology 2001;108:1145–9.
[22] Bielory L, Ogunkoya A, Frohman LP. Temporal arteritis in blacks. Am J Med 1989;86:707–8.
[23] Chaudhry IA, Shamsi FA, Elzaridi E, Arat YO, Bosley TM, Riley FC. Epidemiology of giant-cell arteritis in an Arab population: a 22-year study. Br J Ophthalmol 2007;91:715–8.
[24] Hu Z, Yang Q, Zeng S, Li J, Wu X, Cao L, et al. Giant cell arteritis in China: a prospective investigation. Angiology 2002;53:457–63.
[25] Nordborg E, Bengtsson BA. Epidemiology of biopsy-proven giant cell arteritis (GCA). J Intern Med 1990;227:233–6.
[26] Haugeberg G, Paulsen PQ, Bie RB. Temporal arteritis in Vest Agder County in southern Norway: incidence and clinical findings. J Rheumatol 2000;27:2624–7.
[27] Baldursson O, Steinsson K, Bjornsson J, Lie JT. Giant cell arteritis in Iceland. An epidemiologic and histopathologic analysis. Arthritis Rheum 1994;37:1007–12.
[28] Machado EB, Michet CJ, Ballard DJ, Hunder GG, Beard CM, Chu CP, et al. Trends in incidence and clinical presentation of temporal arteritis in Olmsted County, Minnesota, 1950–1985. Arthritis Rheum 1988;31:745–9.
[29] Salvarani C, Crowson CS, O'Fallon WM, Hunder GG, Gabriel SE. Reappraisal of the epidemiology of giant cell arteritis in Olmsted County, Minnesota, over a fifty-year period. Arthritis Rheum 2004;51:264–8.
[30] Salvarani C, Macchioni P, Zizzi F, Mantovani W, Rossi F, Castri C, et al. Epidemiologic and immunogenetic aspects of polymyalgia rheumatica and giant cell arteritis in northern Italy. Arthritis Rheum 1991;34:351–6.
[31] Gonzalez-Gay MA, Miranda-Filloy JA, Lopez-Diaz MJ, Perez-Alvarez R, Gonzalez-Juanatey C, Sanchez-Andrade A, et al. Giant cell arteritis in northwestern Spain: a 25-year epidemiologic study. Medicine (Baltimore) 2007;86:61–8.
[32] Smith CA, Fidler WJ, Pinals RS. The epidemiology of giant cell arteritis. Report of a ten-year study in Shelby County, Tennessee. Arthritis Rheum 1983;26:1214–9.
[33] Ramstead CL, Patel AD. Giant cell arteritis in a neuro-ophthalmology clinic in Saskatoon, 1998–2003. Can J Ophthalmol 2007;42:295–8.
[34] Smeeth L, Cook C, Hall AJ. Incidence of diagnosed polymyalgia rheumatica and temporal arteritis in the United Kingdom, 1990–2001. Ann Rheum Dis 2006;65: 1093–8.
[35] Duhaut P, Pinede L, Demolombe-Rague S, Dumontet C, Ninet J, Seydoux D, et al. Giant cell arteritis and polymyalgia rheumatica: are pregnancies a protective factor? A prospective, multicentre case-control study. GRACG (Groupe de Recherche sur l'Arterite a Cellules Geantes). Rheumatology (Oxford) 1999;38:118–23.
[36] Larsson K, Mellstrom D, Nordborg E, Oden A. Early menopause, low body mass index, and smoking are independent risk factors for developing giant cell arteritis. Ann Rheum Dis 2006;65:529–32.
[37] Duhaut P, Pinede L, Demolombe-Rague S, Loire R, Seydoux D, Ninet J, et al. Giant cell arteritis and cardiovascular risk factors: a multicenter, prospective case-control study. Groupe de Recherche sur l'Arterite a Cellules Geantes. Arthritis Rheum 1998;41:1960–5.
[38] Banks PM, Cohen MD, Ginsburg WW, Hunder GG. Immunohistologic and cytochemical studies of temporal arteritis. Arthritis Rheum 1983;26:1201–7.
[39] Wagner AD, Gerard HC, Fresemann T, Schmidt WA, Gromnica-Ihle E, Hudson AP, et al. Detection of Chlamydia pneumoniae in giant cell vasculitis and correlation with the topographic arrangement of tissue-infiltrating dendritic cells. Arthritis Rheum 2000;43:1543–51.
[40] Ma-Krupa W, Jeon MS, Spoerl S, Tedder TF, Goronzy JJ, Weyand CM. Activation of arterial wall dendritic cells and breakdown of self-tolerance in giant cell arteritis. J Exp Med 2004;199:173–83.
[41] Pryshchep O, Ma-Krupa W, Younge BR, Goronzy JJ, Weyand CM. Vessel-specific Toll-like receptor profiles in human medium and large arteries. Circulation 2008;118:1276–84.
[42] Krupa WM, Dewan M, Jeon MS, Kurtin PJ, Younge BR, Goronzy JJ, et al. Trapping of misdirected dendritic cells in the granulomatous lesions of giant cell arteritis. Am J Pathol 2002;161:1815–23.

[43] Grunewald J, Andersson R, Rydberg L, Gigliotti D, Schaufelberger C, Hansson GK, et al. CD4+ and CD8+ T cell expansions using selected TCR V and J gene segments at the onset of giant cell arteritis. Arthritis Rheum 1994;37:1221–7.
[44] Martinez-Taboada V, Hunder NN, Hunder GG, Weyand CM, Goronzy JJ. Recognition of tissue residing antigen by T cells in vasculitic lesions of giant cell arteritis. J Mol Med 1996;74:695–703.
[45] Weyand CM, Hicok KC, Hunder GG, Goronzy JJ. Tissue cytokine patterns in patients with polymyalgia rheumatica and giant cell arteritis. Ann Intern Med 1994;121:484–91.
[46] Brack A, Geisler A, Martinez-Taboada VM, Younge BR, Goronzy JJ, Weyand CM. Giant cell vasculitis is a T cell-dependent disease. Mol Med 1997;3:530–43.
[47] Miossec P, Korn T, Kuchroo VK. Interleukin-17 and type 17 helper T cells. N Engl J Med 2009;361:888–98.
[48] Deng J, Younge BR, Olshen RA, Goronzy JJ, Weyand CM. Th17 and Th1 T-cell responses in giant cell arteritis. Circulation 2010;121:906–15.
[49] Wagner AD, Bjornsson J, Bartley GB, Goronzy JJ, Weyand CM. Interferon-gamma-producing T cells in giant cell vasculitis represent a minority of tissue-infiltrating cells and are located distant from the site of pathology. Am J Pathol 1996;148:1925–33.
[50] McColl SR. Chemokines and dendritic cells: a crucial alliance. Immunol Cell Biol 2002;80:489–96.
[51] Medzhitov R. Toll-like receptors and innate immunity. Nat Rev Immunol 2001;1:135–45.
[52] Roche NE, Fulbright JW, Wagner AD, Hunder GG, Goronzy JJ, Weyand CM. Correlation of interleukin-6 production and disease activity in polymyalgia rheumatica and giant cell arteritis. Arthritis Rheum 1993;36:1286–94.
[53] Weyand CM, Wagner AD, Bjornsson J, Goronzy JJ. Correlation of the topographical arrangement and the functional pattern of tissue-infiltrating macrophages in giant cell arteritis. J Clin Invest 1996;98:1642–9.
[54] Nikkari ST, Hoyhtya M, Isola J, Nikkari T. Macrophages contain 92-kd gelatinase (MMP-9) at the site of degenerated internal elastic lamina in temporal arteritis. Am J Pathol 1996;149:1427–33.
[55] Segarra M, Garcia-Martinez A, Sanchez M, Hernandez-Rodriguez J, Lozano E, Grau JM, et al. Gelatinase expression and proteolytic activity in giant-cell arteritis. Ann Rheum Dis 2007;66:1429–35.
[56] Rodriguez-Pla A, Bosch-Gil JA, Rossello-Urgell J, Huguet-Redecilla P, Stone JH, Vilardell-Tarres M. Metalloproteinase-2 and -9 in giant cell arteritis: involvement in vascular remodeling. Circulation 2005;112:264–9.
[57] Rittner HL, Kaiser M, Brack A, Szweda LI, Goronzy JJ, Weyand CM. Tissue-destructive macrophages in giant cell arteritis. Circ Res 1999;84:1050–8.
[58] Rittner HL, Hafner V, Klimiuk PA, Szweda LI, Goronzy JJ, Weyand CM. Aldose reductase functions as a detoxification system for lipid peroxidation products in vasculitis. J Clin Invest 1999;103:1007–13.
[59] Fingerle J, Johnson R, Clowes AW, Majesky MW, Reidy MA. Role of platelets in smooth muscle cell proliferation and migration after vascular injury in rat carotid artery. Proc Natl Acad Sci U S A 1989;86:8412–6.
[60] Ferns GA, Raines EW, Sprugel KH, Motani AS, Reidy MA, Ross R. Inhibition of neointimal smooth muscle accumulation after angioplasty by an antibody to PDGF. Science 1991;253:1129–32.
[61] Kaiser M, Weyand CM, Bjornsson J, Goronzy JJ. Platelet-derived growth factor, intimal hyperplasia, and ischemic complications in giant cell arteritis. Arthritis Rheum 1998;41:623–33.
[62] Kaiser M, Younge B, Bjornsson J, Goronzy JJ, Weyand CM. Formation of new vasa vasorum in vasculitis. Production of angiogenic cytokines by multinucleated giant cells. Am J Pathol 1999;155:765–74.
[63] Owens GK, Kumar MS, Wamhoff BR. Molecular regulation of vascular smooth muscle cell differentiation in development and disease. Physiol Rev 2004;84:767–801.
[64] Clowes AW, Clowes MM, Au YP, Reidy MA, Belin D. Smooth muscle cells express urokinase during mitogenesis and tissue-type plasminogen activator during migration in injured rat carotid artery. Circ Res 1990;67:61–7.
[65] Xu F, Ji J, Li L, Chen R, Hu WC. Adventitial fibroblasts are activated in the early stages of atherosclerosis in the apolipoprotein E knockout mouse. Biochem Biophys Res Commun 2007;352:681–8.
[66] Shi Y, O'Brien JE, Fard A, Mannion JD, Wang D, Zalewski A. Adventitial myofibroblasts contribute to neointimal formation in injured porcine coronary arteries. Circulation 1996;94:1655–64.
[67] Li G, Chen SJ, Oparil S, Chen YF, Thompson JA. Direct in vivo evidence demonstrating neointimal migration of adventitial fibroblasts after balloon injury of rat carotid arteries. Circulation 2000;101:1362–5.
[68] Zalewski A, Shi Y. Vascular myofibroblasts. Lessons from coronary repair and remodeling. Arterioscler Thromb Vasc Biol 1997;17:417–22.
[69] Shi Y, O'Brien Jr JE, Mannion JD, Morrison RC, Chung W, Fard A, et al. Remodeling of autologous saphenous vein grafts. The role of perivascular myofibroblasts. Circulation 1997;95:2684–93.
[70] Siow RC, Mallawaarachchi CM, Weissberg PL. Migration of adventitial myofibroblasts following vascular balloon injury: insights from in vivo gene transfer to rat carotid arteries. Cardiovasc Res 2003;59:212–21.
[71] Wilcox JN, Waksman R, King SB, Scott NA. The role of the adventitia in the arterial response to angioplasty: the effect of intravascular radiation. Int J Radiat Oncol Biol Phys 1996;36:789–96.
[72] Shi Y, O'Brien Jr JE, Fard A, Zalewski A. Transforming growth factor-beta 1 expression and myofibroblast formation during arterial repair. Arterioscler Thromb Vasc Biol 1996;16:1298–305.
[73] Smith JD, Bryant SR, Couper LL, Vary CP, Gotwals PJ, Koteliansky VE, et al. Soluble transforming growth factor-beta type II receptor inhibits negative remodeling, fibroblast transdifferentiation, and intimal lesion formation but not endothelial growth. Circ Res 1999;84:1212–22.
[74] Xu Q. The impact of progenitor cells in atherosclerosis. Nat Clin Pract Cardiovasc Med 2006;3:94–101.
[75] Hu Y, Zhang Z, Torsney E, Afzal AR, Davison F, Metzler B, et al. Abundant progenitor cells in the adventitia contribute to atherosclerosis of vein grafts in ApoE-deficient mice. J Clin Invest 2004;113:1258–65.
[76] Rotmans JI, Heyligers JM, Verhagen HJ, Velema E, Nagtegaal MM, de Kleijn DP, et al. In vivo cell seeding with anti-CD34 antibodies successfully accelerates endothelialization but stimulates intimal hyperplasia in porcine arteriovenous expanded polytetrafluoroethylene grafts. Circulation 2005;112:12–8.
[77] Folkow B, Svanborg A. Physiology of cardiovascular aging. Physiol Rev 1993;73:725–64.
[78] Han JW, Shimada K, Ma-Krupa W, Johnson TL, Nerem RM, Goronzy JJ, et al. Vessel wall-embedded dendritic cells induce T-cell autoreactivity and initiate vascular inflammation. Circ Res 2008;102:546–53.
[79] Tobon GJ, Alard JE, Youinou P, Jamin C. Are autoantibodies triggering endothelial cell apoptosis really pathogenic? Autoimmun Rev 2009;8:605–10.
[80] Kemp A. Monozygotic twins with temporal arteritis and ophthalmic arteritis. Acta Ophthalmol (Copenh) 1977;55:183–90.
[81] Wernick R, Davey M, Bonafede P. Familial giant cell arteritis: report of an HLA-typed sibling pair and a review of the literature. Clin Exp Rheumatol 1994;12:63–6.
[82] Fietta P, Manganelli P, Zanetti A, Neri TM. Familial giant cell arteritis and polymyalgia rheumatica: aggregation in 2 families. J Rheumatol 2002;29:1551–5.
[83] Raptis L, Pappas G, Akritidis N. Horton's three sisters: familial clustering of temporal arteritis. Clin Rheumatol 2007;26:1997–8.
[84] Liozon E, Ouattara B, Rhaiem K, Ly K, Bezanahary H, Loustaud V, et al. Familial aggregation in giant cell arteritis and polymyalgia rheumatica: a comprehensive literature review including 4 new families. Clin Exp Rheumatol 2009;27:S89–94.
[85] Gonzalez-Gay MA, Garcia-Porrua C, Hajeer AH, Dababneh A, Ollier WE. HLA-DRB1*04 may be a marker of severity in giant cell arteritis. Ann Rheum Dis 2000;59:574–5.
[86] Gonzalez-Gay MA, Garcia-Porrua C, Llorca J, Hajeer AH, Branas F, Dababneh A, et al. Visual manifestations of giant cell arteritis. Trends and clinical spectrum in 161 patients. Medicine (Baltimore) 2000;79:283–92.
[87] Rauzy O, Fort M, Nourhashemi F, Alric L, Juchet H, Ecoiffier M, et al. Relation between HLA DRB1 alleles and corticosteroid resistance in giant cell arteritis. Ann Rheum Dis 1998;57:380–2.
[88] Weyand CM, Hicok KC, Hunder GG, Goronzy JJ. The HLA-DRB1 locus as a genetic component in giant cell arteritis. Mapping of a disease-linked sequence motif to the antigen binding site of the HLA-DR molecule. J Clin Invest 1992;90:2355–61.
[89] Salvarani C, Casali B, Boiardi L, Ranzi A, Macchioni P, Nicoli D, et al. Intercellular adhesion molecule 1 gene polymorphisms in polymyalgia rheumatica/giant cell arteritis: association with disease risk and severity. J Rheumatol 2000;27:1215–21.
[90] Amoli MM, Shelley E, Mattey DL, Garcia-Porrua C, Thomson W, Hajeer AH, et al. Lack of association between intercellular adhesion molecule-1 gene polymorphisms and giant cell arteritis. J Rheumatol 2001;28:1600–4.
[91] Mattey DL, Hajeer AH, Dababneh A, Thomson W, Gonzalez-Gay MA, Garcia-Porrua C, et al. Association of giant cell arteritis and polymyalgia rheumatica with different tumor necrosis factor microsatellite polymorphisms. Arthritis Rheum 2000;43:1749–55.
[92] Boiardi L, Casali B, Nicoli D, Farnetti E, Chen Q, Macchioni P, et al. Vascular endothelial growth factor gene polymorphisms in giant cell arteritis. J Rheumatol 2003;30:2160–4.
[93] Rueda B, Lopez-Nevot MA, Lopez-Diaz MJ, Garcia-Porrua C, Martin J, Gonzalez-Gay MA. A functional variant of vascular endothelial growth factor is associated with severe ischemic complications in giant cell arteritis. J Rheumatol 2005;32:1737–41.
[94] Amoli MM, Garcia-Porrua C, Llorca J, Ollier WE, Gonzalez-Gay MA. Endothelial nitric oxide synthase haplotype associations in biopsy-proven giant cell arteritis. J Rheumatol 2003;30:2019–22.
[95] Gonzalez-Gay MA, Oliver J, Sanchez E, Garcia-Porrua C, Paco L, Lopez-Nevot MA, et al. Association of a functional inducible nitric oxide synthase promoter variant with susceptibility to biopsy-proven giant cell arteritis. J Rheumatol 2005;32:2178–82.
[96] Nordborg C, Nordborg E, Petursdottir V, LaGuardia J, Mahalingam R, Wellish M, et al. Search for varicella zoster virus in giant cell arteritis. Ann Neurol 1998;44:413–4.
[97] Helweg-Larsen J, Tarp B, Obel N, Baslund B. No evidence of parvovirus B19, Chlamydia pneumoniae or human herpes virus infection in temporal artery biopsies in patients with giant cell arteritis. Rheumatology (Oxford) 2002;41:445–9.
[98] Rodriguez-Pla A, Bosch-Gil JA, Echevarria-Mayo JE, Rossello-Urgell J, Solans-Laque R, Huguet-Redecilla P, et al. No detection of parvovirus B19 or herpesvirus DNA in giant cell arteritis. J Clin Virol 2004;31:11–5.
[99] Alvarez-Lafuente R, Fernandez-Gutierrez B, Jover JA, Judez E, Loza E, Clemente D, et al. Human parvovirus B19, varicella zoster virus, and human herpes virus 6 in temporal artery biopsy specimens of patients with giant cell arteritis: analysis with quantitative real time polymerase chain reaction. Ann Rheum Dis 2005;64:780–2.
[100] Cooper RJ, D'Arcy S, Kirby M, Al-Buhtori M, Rahman MJ, Proctor L, et al. Infection and temporal arteritis: a PCR-based study to detect pathogens in temporal artery biopsy specimens. J Med Virol 2008;80:501–5.
[101] Fest T, Mougin C, Dupond JL. Giant cell arteritis. Ann Intern Med 1996;124:927–8.
[102] Gabriel SE, Espy M, Erdman DD, Bjornsson J, Smith TF, Hunder GG. The role of parvovirus B19 in the pathogenesis of giant cell arteritis: a preliminary evaluation. Arthritis Rheum 1999;42:1255–8.
[103] Cankovic M, Zarbo RJ. Failure to detect human herpes simplex virus, cytomegalovirus, and Epstein–Barr virus viral genomes in giant cell arteritis biopsy specimens by real-time quantitative polymerase chain reaction. Cardiovasc Pathol 2006;15:280–6.

[104] Powers JF, Bedri S, Hussein S, Salomon RN, Tischler AS. High prevalence of herpes simplex virus DNA in temporal arteritis biopsy specimens. Am J Clin Pathol 2005;123:261–4.
[105] Duhaut P, Bosshard S, Calvet A, Pinede L, Demolombe-Rague S, Dumontet C, et al. Giant cell arteritis, polymyalgia rheumatica, and viral hypotheses: a multicenter, prospective case-control study. Groupe de Recherche sur l'Arterite a Cellules Geantes. J Rheumatol 1999;26:361–9.
[106] Njau F, Ness T, Wittkop U, Pancratz T, Eickhoff M, Hudson AP, et al. No correlation between giant cell arteritis and Chlamydia pneumoniae infection: investigation of 189 patients by standard and improved PCR methods. J Clin Microbiol 2009;47:1899–901.
[107] Haugeberg G, Bie R, Nordbo SA. Chlamydia pneumoniae not detected in temporal artery biopsies from patients with temporal arteritis. Scand J Rheumatol 2000;29:127–8.
[108] Regan MJ, Wood BJ, Hsieh YH, Theodore ML, Quinn TC, Hellmann DB, et al. Temporal arteritis and Chlamydia pneumoniae: failure to detect the organism by polymerase chain reaction in ninety cases and ninety controls. Arthritis Rheum 2002;46:1056–60.
[109] Lavignac C, Jauberteau-Marchan MO, Liozon E, Vidal E, Catanzano G, Liozon F. Immunohistochemical study of lesions in Horton's temporal arteritis before and during corticotherapy. Rev Méd Interne 1996;17:814–20.
[110] Chatelain D, Duhaut P, Schmidt J, Loire R, Bosshard S, Guernou M, et al. Pathological features of temporal arteries in patients with giant cell arteritis presenting with permanent visual loss. Ann Rheum Dis 2009;68:84–8.
[111] Liozon E, Roblot P, Paire D, Loustaud V, Liozon F, Vidal E, et al. Anticardiolipin antibody levels predict flares and relapses in patients with giant-cell (temporal) arteritis. A longitudinal study of 58 biopsy-proven cases. Rheumatology (Oxford) 2000;39:1089–94.
[112] Duhaut P, Berruyer M, Pinede L, Demolombe-Rague S, Loire R, Seydoux D, et al. Anticardiolipin antibodies and giant cell arteritis: a prospective, multicenter case-control study. Groupe de Recherche sur l'Arterite a Cellules Geantes. Arthritis Rheum 1998;41:701–9.
[113] Manna R, Latteri M, Cristiano G, Todaro L, Scuderi F, Gasbarrini G. Anticardiolipin antibodies in giant cell arteritis and polymyalgia rheumatica: a study of 40 cases. Br J Rheumatol 1998;37:208–10.
[114] Liozon E, Roussel V, Roblot P, Liozon F, Preud'Homme JL, Loustaud V, et al. Absence of anti-beta2 glycoprotein I antibodies in giant cell arteritis: a study of 45 biopsy-proven cases. Br J Rheumatol 1998;37:1129–31.
[115] Cid MC, Cervera R, Font J, Lopez-Soto A, Pallares L, Navarro M, et al. Late thrombotic events in patients with temporal arteritis and anticardiolipin antibodies. Clin Exp Rheumatol 1990;8:359–63.
[116] Liozon F, Jauberteau-Marchan MO, Boutros-Toni F, Barrier JH, Dupond JL, Roblot P, et al. Anticardiolipin antibodies and Horton disease. Ann Med Interne (Paris) 1995;146:541–7.
[117] Navarro M, Cervera R, Font J, Reverter JC, Monteagudo J, Escolar G, et al. Anti-endothelial cell antibodies in systemic autoimmune diseases: prevalence and clinical significance. Lupus 1997;6:521–6.
[118] Servettaz A, Guilpain P, Tamas N, Kaveri SV, Camoin L, Mouthon L. Natural anti-endothelial cell antibodies. Autoimmun Rev 2008;7:426–30.
[119] Domiciano DS, Carvalho JF, Shoenfeld Y. Pathogenic role of anti-endothelial cell antibodies in autoimmune rheumatic diseases. Lupus 2009;18:1233–8.
[120] Guilpain P, Mouthon L. Antiendothelial cells autoantibodies in vasculitis-associated systemic diseases. Clin Rev Allergy Immunol 2008;35:59–65.
[121] Regent A, Dib H, Agard C, Camoin L, Weksler B, Broussard C, et al. Identification of target antigens of anti-endothelial-cell and anti-vascular-smooth-muscle-cell antibodies in patients with giant cell arteritis: a proteomic approach [abstract]. Arthritis Rheum 2009;60:186.
[122] Wick G, Knoflach M, Xu Q. Autoimmune and inflammatory mechanisms in atherosclerosis. Annu Rev Immunol 2004;22:361–403.
[123] Rajaiah R, Moudgil KD. Heat-shock proteins can promote as well as regulate autoimmunity. Autoimmun Rev 2009;8:388–93.
[124] Ohashi K, Burkart V, Flohe S, Kolb H. Cutting edge: heat shock protein 60 is a putative endogenous ligand of the toll-like receptor-4 complex. J Immunol 2000;164:558–61.
[125] Asea A, Rehli M, Kabingu E, Boch JA, Bare O, Auron PE, et al. Novel signal transduction pathway utilized by extracellular HSP70: role of toll-like receptor (TLR) 2 and TLR4. J Biol Chem 2002;277:15028–34.
[126] Masters SL, Simon A, Aksentijevich I, Kastner DL. Horror autoinflammaticus: the molecular pathophysiology of autoinflammatory disease (*). Annu Rev Immunol 2009;27:621–68.
[127] Hernandez-Rodriguez J, Segarra M, Vilardell C, Sanchez M, Garcia-Martinez A, Esteban MJ, et al. Elevated production of interleukin-6 is associated with a lower incidence of disease-related ischemic events in patients with giant-cell arteritis: angiogenic activity of interleukin-6 as a potential protective mechanism. Circulation 2003;107:2428–34.
[128] Pountain G, Hazleman B, Cawston TE. Circulating levels of IL-1beta, IL-6 and soluble IL-2 receptor in polymyalgia rheumatica and giant cell arteritis and rheumatoid arthritis. Br J Rheumatol 1998;37:797–8.
[129] Dinarello CA. Immunological and inflammatory functions of the interleukin-1 family. Annu Rev Immunol 2009;27:519–50.
[130] Beasley D, McGuiggin ME, Dinarello CA. Human vascular smooth muscle cells produce an intracellular form of interleukin-1 receptor antagonist. Am J Physiol 1995;269:C961–8.
[131] Dewberry R, Holden H, Crossman D, Francis S. Interleukin-1 receptor antagonist expression in human endothelial cells and atherosclerosis. Arterioscler Thromb Vasc Biol 2000;20:2394–400.
[132] Shepherd J, Little MC, Nicklin MJ. Psoriasis-like cutaneous inflammation in mice lacking interleukin-1 receptor antagonist. J Invest Dermatol 2004;122:665–9.
[133] Horai R, Saijo S, Tanioka H, Nakae S, Sudo K, Okahara A, et al. Development of chronic inflammatory arthropathy resembling rheumatoid arthritis in interleukin 1 receptor antagonist-deficient mice. J Exp Med 2000;191:313–20.
[134] Nicklin MJ, Hughes DE, Barton JL, Ure JM, Duff GW. Arterial inflammation in mice lacking the interleukin 1 receptor antagonist gene. J Exp Med 2000;191:303–12.
[135] Shepherd J, Nicklin MJ. Elastic-vessel arteritis in interleukin-1 receptor antagonist-deficient mice involves effector Th1 cells and requires interleukin-1 receptor. Circulation 2005;111:3135–40.
[136] Kemp A, Marner K, Nissen SH, Heyn J, Kissmeyer-Nielsen F. HLA antigens in cases of giant cell arteritis. Acta Ophthalmol (Copenh) 1980;58:1000–4.
[137] Hansen JA, Healey LA, Wilske KR. Association between giant cell (temporal) arteritis and HLA-Cw3. Hum Immunol 1985;13:193–8.
[138] Cid MC, Ercilla G, Vilaseca J, Sanmarti R, Villalta J, Ingelmo M, et al. Polymyalgia rheumatica: a syndrome associated with HLA-DR4 antigen. Arthritis Rheum 1988;31:678–82.
[139] Bignon JD, Barrier J, Soulillou JP, Martin P, Grolleau JY. HLA DR4 and giant cell arteritis. Tissue Antigens 1984;24:60–2.
[140] Richardson JE, Gladman DD, Fam A, Keystone EC. HLA-DR4 in giant cell arteritis: association with polymyalgia rheumatica syndrome. Arthritis Rheum 1987;30:1293–7.
[141] Weyand CM, Hunder NN, Hicok KC, Hunder GG, Goronzy JJ. HLA-DRB1 alleles in polymyalgia rheumatica, giant cell arteritis, and rheumatoid arthritis. Arthritis Rheum 1994;37:514–20.
[142] Combe B, Sany J, Le Quellec A, Clot J, Eliaou JF. Distribution of HLA-DRB1 alleles of patients with polymyalgia rheumatica and giant cell arteritis in a Mediterranean population. J Rheumatol 1998;25:94–8.
[143] Jacobsen S, Baslund B, Madsen HO, Tvede N, Svejgaard A, Garred P. Mannose-binding lectin variant alleles and HLA-DR4 alleles are associated with giant cell arteritis. J Rheumatol 2002;29:2148–53.
[144] Dababneh A, Gonzalez-Gay MA, Garcia-Porrua C, Hajeer A, Thomson W, Ollier W. Giant cell arteritis and polymyalgia rheumatica can be differentiated by distinct patterns of HLA class II association. J Rheumatol 1998;25:2140–5.
[145] Martinez-Taboda VM, Bartolome MJ, Lopez-Hoyos M, Blanco R, Mata C, Calvo J, et al. HLA-DRB1 allele distribution in polymyalgia rheumatica and giant cell arteritis: influence on clinical subgroups and prognosis. Semin Arthritis Rheum 2004;34:454–64.
[146] Gonzalez-Gay MA, Di Giovine FS, Silvestri T, Amoli MM, Garcia-Porrua C, Thomson W, et al. Lack of association between IL-1 cluster and TNF-alpha gene polymorphisms and giant cell arteritis. Clin Exp Rheumatol 2002;20:431.
[147] Gonzalez-Gay MA, Hajeer AH, Dababneh A, Garcia-Porrua C, Mattey DL, Amoli MM, et al. IL-6 promoter polymorphism at position -174 modulates the phenotypic expression of polymyalgia rheumatica in biopsy-proven giant cell arteritis. Clin Exp Rheumatol 2002;20:179–84.
[148] Salvarani C, Casali B, Farnetti E, Pipitone N, Nicoli D, Macchioni P, et al. Interleukin-6 promoter polymorphism at position -174 in giant cell arteritis. J Rheumatol 2005;32:2173–7.
[149] Gonzalez-Gay MA, Hajeer AH, Dababneh A, Garcia-Porrua C, Amoli MM, Llorca J, et al. Interferon-gamma gene microsatellite polymorphisms in patients with biopsy-proven giant cell arteritis and isolated polymyalgia rheumatica. Clin Exp Rheumatol 2004;22:S18–20.
[150] Amoli MM, Gonzalez-Gay MA, Zeggini E, Salway F, Garcia-Porrua C, Ollier WE. Epistatic interactions between HLA-DRB1 and interleukin 4, but not interferon-gamma, increase susceptibility to giant cell arteritis. J Rheumatol 2004;31:2413–7.
[151] Boiardi L, Casali B, Farnetti E, Pipitone N, Nicoli D, Macchioni P, et al. Interleukin-10 promoter polymorphisms in giant cell arteritis. Arthritis Rheum 2006;54:4011–7.
[152] Rueda B, Roibas B, Martin J, Gonzalez-Gay MA. Influence of interleukin 10 promoter polymorphisms in susceptibility to giant cell arteritis in Northwestern Spain. J Rheumatol 2007;34:1535–9.
[153] Amoli MM, Garcia-Porrua C, Ollier WE, Gonzalez-Gay MA. Lack of association between macrophage migration inhibitory factor gene polymorphism and giant cell arteritis. J Rheumatol 2005;32:74–6.
[154] Amoli MM, Salway F, Zeggini E, Ollier WE, Gonzalez-Gay MA. MCP-1 gene haplotype association in biopsy proven giant cell arteritis. J Rheumatol 2005;32:507–10.
[155] Salvarani C, Casali B, Nicoli D, Farnetti E, Macchioni P, Catanoso MG, et al. Endothelial nitric oxide synthase gene polymorphisms in giant cell arteritis. Arthritis Rheum 2003;48:3219–23.
[156] Rodriguez-Pla A, Beaty TH, Savino PJ, Eagle Jr RC, Seo P, Soloski MJ. Association of a nonsynonymous single-nucleotide polymorphism of matrix metalloproteinase 9 with giant cell arteritis. Arthritis Rheum 2008;58:1849–53.
[157] Palomino-Morales R, Torres O, Vazquez-Rodriguez TR, Morado IC, Castaneda S, Callejas-Rubio JL, et al. Association between toll-like receptor 4 gene polymorphism and biopsy-proven giant cell arteritis. J Rheumatol 2009;36:1501–6.
[158] Rueda B, Miranda-Filloy JA, Martin J, Gonzalez-Gay MA. Association of CD24 gene polymorphisms with susceptibility to biopsy-proven giant cell arteritis. J Rheumatol 2008;35:850–4.
[159] Gonzalez-Gay MA, Oliver J, Orozco G, Garcia-Porrua C, Lopez-Nevot MA, Martin J. Lack of association of a functional single nucleotide polymorphism of PTPN22, encoding lymphoid protein phosphatase, with susceptibility to biopsy-proven giant cell arteritis. J Rheumatol 2005;32:1510–2.
[160] Martin J, Perez-Armengol C, Miranda-Filloy JA, Vilchez JR, Lopez-Nevot MA, Garcia-Porrua C, et al. Lack of association of a functional -94ins/delATTG NFKB1

promoter polymorphism with susceptibility and clinical expression of biopsy-proven giant cell arteritis in northwest Spain. J Rheumatol 2006;33:285–8.
[161] Palomino-Morales R, Vazquez-Rodriguez TR, Morado IC, Castaneda S, Ortego-Centeno N, Miranda-Filloy JA, et al. Lack of association between STAT4 gene polymorphism and biopsy-proven giant cell arteritis. J Rheumatol 2009;36:1021–5.
[162] Torres O, Palomino-Morales R, Vazquez-Rodriguez TR, Castaneda S, Morado IC, Miranda-Filloy JA, et al. Lack of association between TRAF1/C5 gene polymorphisms and biopsy-proven giant cell arteritis. J Rheumatol 2010;37:131–5.
[163] Torres O, Palomino-Morales R, Vazquez-Rodriguez TR, Castaneda S, Morado IC, Miranda-Filloy JA, et al. Lack of association between IRF5 gene polymorphisms and biopsy-proven giant cell arteritis. J Rheumatol 2010;37:136–40.
[164] Morgan AW, Robinson JI, Barrett JH, Martin J, Walker A, Babbage SJ, et al. Association of FCGR2A and FCGR2A–FCGR3A haplotypes with susceptibility to giant cell arteritis. Arthritis Res Ther 2006;8:R109.
[165] Gonzalez-Gay MA, Rueda B, Vilchez JR, Lopez-Nevot MA, Robledo G, Ruiz MP, et al. Contribution of MHC class I region to genetic susceptibility for giant cell arteritis. Rheumatology (Oxford) 2007;46:431–4.
[166] Salvarani C, Casali B, Farnetti E, Pipitone N, Nicoli D, Macchioni PL, et al. 463 G/A myeloperoxidase promoter polymorphism in giant cell arteritis. Ann Rheum Dis 2008;67:485–8.
[167] Palomino-Morales R, Vazquez-Rodriguez TR, Miranda-Filloy JA, Martin J, Gonzalez-Gay MA. C-reactive protein gene polymorphisms in biopsy-proven giant cell arteritis from Northwestern Spain. J Rheumatol 2009;36:341–6.
[168] Gonzalez-Gay MA, Hajeer AH, Dababneh A, Garcia-Porrua C, Amoli MM, Thomson W, et al. Corticotropin releasing hormone promoter polymorphisms in giant cell arteritis and polymyalgia rheumatica. Clin Exp Rheumatol 2002;20:133–8.
[169] Salvarani C, Farnetti E, Casali B, Nicoli D, Wenlan L, Bajocchi G, et al. Detection of parvovirus B19 DNA by polymerase chain reaction in giant cell arteritis: a case-control study. Arthritis Rheum 2002;46:3099–101.
[170] Kennedy PG, Grinfeld E, Esiri MM. Absence of detection of varicella-zoster virus DNA in temporal artery biopsies obtained from patients with giant cell arteritis. J Neurol Sci 2003;215:27–9.

Activation profile of Toll-like receptors of peripheral blood lymphocytes in patients with systemic lupus erythematosus

Systemic lupus erythematosus (SLE) is a systemic autoimmune disease associated with aberrant activation of T and B lymphocytes for the production of inflammatory cytokines and autoreactive antibodies. Animal studies of SLE have indicated that Toll-like receptors (TLR) are important in the pathogenesis of murine lupus. In the present study **Wong CK. et al. (Clin Exp Immunol 2010; 159: 11–22)**, investigated the differential protein expressions of TLR-1-9 of monocytes and different lymphocyte subsets (using flow cytometry) from patients with SLE and normal controls. The expression of intracellular TLRs (TLR-3, -8, -9) and extracellular TLRs (TLR-1, -2, -4, -5, -6) were elevated in monocytes, CD4+ and CD8+ T lymphocytes and B lymphocytes of SLE patients compared to control subjects (all $p<0.001$). Moreover, cell surface expression of TLR-4 on CD4+ and CD8+ T lymphocytes, and TLR-6 on B lymphocytes, were correlated positively with SLE disease activity index (SLEDAI) (TLR-4 on CD4+ and CD8+ T cells: $r=0.536$, $p=0.04$; $r=0.713$, $p=0.003$; TLR-6 in B lymphocytes: $r=0.572$, $p=0.026$). In concordance with the above results, there is an observable increased relative induction (%) of inflammatory cytokine interleukin (IL)-1 beta, IL-6, IL-10, and IL-12, chemokines CCL2, CXCL8, CCL5 and CXCL10 from peripheral blood mononuclear cells (PBMC) upon differential stimulation by PolyIC (TLR-3 ligand), LPS (TLR-4 ligand), peptidoglycan (TLR-2 ligand) flagellin (TLR-5 ligand) R837 (TLR-7 ligand) and CpG DNA (TLR-9 ligand) in SLE patients compared to controls. These results suggest that the innate immune response for extracellular pathogens and self-originated DNA plays immunopathological roles via TLR activation in SLE.

B cell depletion in diffuse progressive systemic sclerosis: safety, skin score modification and IL-6 modulation in an up to thirty-six months follow-up open-label trial

An over-expression of CD19 has been shown in B cells of systemic sclerosis (SSc) and B cells are thought to contribute to the induction of skin fibrosis in the tight skin mouse model. The aim here, **Bosello S. et al. (Arthritis Res Ther 2010; 12: R54)** was to define the outcome on safety and the change in skin score after rituximab therapy in SSc patients and to correlate the clinical characteristics with the levels of interleukin (IL)-6 and with the immune cell infiltrate detected by immunohistochemistry. Nine patients with SSc with mean age 40.9 ± 11.1 years were treated with anti-CD20, Ig at time 0 and after 14 days. Skin biopsy was performed at baseline and during the follow-up. B-cell activating factor (BAFF) and IL-6 levels were also determined at the follow-up times. After six months, patients presented a median decrease of the skin score of 43.3% (range 21.1–64.0%), and a decrease in disease activity index and disease severity index. IL-6 levels decreased permanently during the follow up. After treatment, a complete depletion of peripheral blood B cells observed in all but 2 patients. Only 3 patients presented CD20 positive cells in the biopsy of the involved skin at baseline. Thus, anti-CD20 treatment has been well tolerated and SSc patients experienced an improvement of the skin score and of clinical symptoms. The clear fall in IL-6 levels could contribute to the skin fibrosis improvement, while the presence of B cells in the skin seems to be irrelevant with respect to the outcome after B cell depletion.

Critical role of IRF-5 in regulation B-cell differentiation

IFN-regulatory factor 5 (IRF-5), a member of the IRF family, is a transcription factor that has a key role in the induction of the antiviral and inflammatory response. When compared with C57BL/6 mice. IRF5-/- mice show higher susceptibility to viral infection and decreased serum levels of type I IFN and the inflammatory cytokines IL-6 and TNF-alpha. Here, **Lien C. et al. (Proc Natl Acad Sci USA 2010 107: 4664–8)** demonstrate that IRF-5 is involved in B-cell maturation and the stimulation of Blimp-1 expression. The IRF5-/- mice develop an age-related splenomegaly, associated with a dramatic accumulation of CD19+B220- B cells and a disruption of normal splenic architecture. Splenic B cells from IRF5-/- mice also exhibited a decreased level of plasma cells. The CD19+ IRF-/- B cells show a defect in Toll-like receptor (TLR) 7- and TLR- induced IL-6 production, and the aged IRF5-/- have decreased serum levels of natural antibodies; however, the antigen-specific IgG1 primary response was already dependent in IRF-5 in young mice, although the IgM response was not. Analysis of the profile of transcription factors associated with plasma cell differentiation shows down-regulation of Blimp-1 expression, a master regulator of plasma cell differentiation, which can be reconstituted with ectopic IRF-5. IRF-5 stimulates transcription of the Prdml gene encoding Blimp-1 and binds to the IRF site in the Prdml promoter. Collectively, these results reveal that the age-related splenomegaly in IRF5-/- mice is associated with an accumulation of CD19+B220- B cells with impaired functions and show the role of IRF-5 in the direct regulation of the plasma cell commitment factor Blimp-1 and in B-cell terminal differentiation.

Contribution of antiferritin antibodies to diagnosis of giant cell arteritis

Establishing the diagnosis of giant cell arteritis (GCA) may be challenging. In the absence of validated biological marker[1] and despite imaging technique contribution,[2] the diagnosis of GCA currently relies on temporal artery biopsy (TAB). Autoantibodies have been identified in GCA[3–6] and recently, Baerlecken *et al*[7] detected IgG antibodies directed against a peptide of the human ferritin heavy chain (FTH1) in 92% of untreated GCA and polymyalgia rheumatica at first diagnosis versus 1% of healthy controls (HC).

In order to evaluate the diagnosis value of these antibodies, we tested sera from 122 consecutive patients suspected of GCA at the time of TAB. Based on the American College of Rheumatology (ACR) criteria,[8] 40 patients had biopsy-proven GCA (TAB^+GCA), 29 patients had biopsy-negative GCA (TAB^-GCA), 47 patients received another diagnosis than GCA (GCA controls) and 6 patients had polymyalgia rheumatica (collection dc-2010–1079). Sera from 40 healthy blood donors were used as HCs. All patients and controls gave signed informed consent. The study was approved by the ethics committee of Cochin hospital.

Detection of antibodies targeting 19–45 FTH1 amino acids was performed as described.[7] Continuous variables were compared using Mann-Whitney test. Correlations were determined by Spearman's correlation coefficient.

Clinical and biological characteristics of the 122 patients are depicted in table 1. The positive likelihood ratios of visual symptoms, headaches, jaw claudication and erythrocyte sedimentation rate ≥50 mm were 1.24, 2.25, 4.44 and 1.53, respectively. Median and mean time of corticosteroid treatment before TAB were 0 day and 3.9 days, respectively.

With a threshold of the mean for HCs+2 SDs, anti-FTH1 antibodies were identified in 72.5%, 41.3%, 31.9% and 2.5% of patients with TAB^+GCA, TAB^-GCA, GCA controls and HC, respectively (figure 1). In patients who never received corticosteroids before blood sampling and TAB, 18/22 (82%) TAB^+GCA patients were positive for anti-FTH1 antibodies versus 13/38 (34%) GCA controls.

The positive and negative predictive values of anti-FTH1 antibodies were 71.9% and 56.9%, respectively, for patients with GCA (TAB^+ or TAB^-) and a threshold of the mean for HC+2 SDs. Positive and negative likelihood ratios were 1.96 and 0.58, respectively. In patients with GCA, erythrocyte sedimentation rate and C reactive protein (CRP) level were higher ($p=0.003$ and $p=0.01$, respectively) and haemoglobin concentration was lower ($p=0.01$) in those with anti-FTH1 antibodies than those without anti-FTH1 antibodies with no difference in visual impairment. Anti-FTH1 antibody titres significantly correlated with CRP level (Spearman r=0.32, 95% CI 0.14 to 0.47, $p=0.0004$).

Thus, 72.5% of patients with proven GCA showed IgG reactivities towards anti-FTH1 antibody (82% of those who never received corticosteroids before blood sampling), which is lower than the 92% patients with active GCA reported by Baerlecken

Table 1 Clinical and biological characteristics of 122 patients undergoing temporal artery biopsy (TAB) for suspected giant cell arteritis (GCA)

	Total population (n=122)	TAB^+GCA (n=40)	TAB^-GCA (n=29)	GCA control (n=47)	PMR (n=6)
Age (mean±SD)	74.6±9.5	76.7±7.6	71.6±8.2	75±11.2	71±9.4
Female sex, no. (%)	79 (64.7)	26 (65)	21 (72)	27 (57)	5 (83)
Symptoms, no. (%) of patients					
Headache	67 (55)	30 (75)	20 (69)	14 (30)	3 (50)
Scalp tenderness	39 (32)	20 (50)	12 (41)	6 (13)	1 (17)
Jaw claudication	27 (22)	16 (40)	7 (24)	3 (6)	1 (17)
Abnormal temporal artery (tender and/or absent pulse)	27 (22)	18 (45)	5 (17)	4 (8)	0 (0)
Any visual sign	21 (17)	8 (20)	5 (17)	8 (17)	0 (0)
Polymyalgia rheumatica	36 (29)	9 (22)	11 (38)	10 (21)	6 (100)
Biology, mean±SD					
Erythrocyte sedimentation rate (1st hour) (mm)*	69±31	77.1±26	73.4±31.4	59.2±32.8	47±41.9
C reactive protein level (mg/l)	71±73.8	101.6±79.3	65.0±69.3	53.9±67.6	30.3±37.9
Leucocyte count (/mm^3)	9100±3700	9800±3800	9300±3200	8500±3900	8200±2000
Haemoglobin level (g/dl)	11.9±1.8	11.9±1.7	11.8±1.6	11.9±2.0	12.0±1.8
Platelet count (*10^3/mm^3)	370±150	420±150	370±120	320±150	320±110

*Available in 93 patients.
PMR, polymyalgia rheumatica.

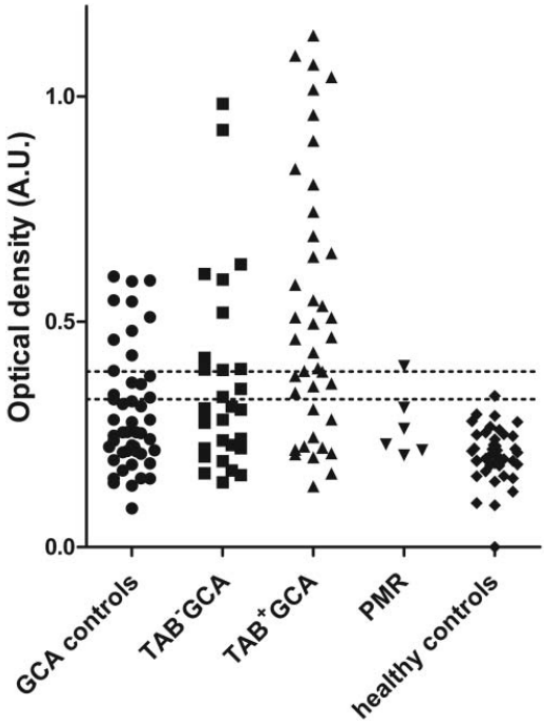

Figure 1 Antibodies against the N-terminal 19–45 amino acids of human ferritin heavy chain (FTH1) in patients undergoing temporal artery biopsy (TAB) by final diagnosis: biopsy-proven giant cell arteritis (GCA) (TAB+GCA), biopsy-negative GCA (TAB-GCA), polymyalgia rheumatica, diagnosis other than GCA (GCA controls) and healthy controls (HC). Data are presented as optical density at 450 nm (OD450) with subtraction of the background OD450 (KPL coating solution). Each dot represents the reactivity of one serum sample. Dashed lines indicate +2 and +3 SDs above the mean value for HC. Samples were considered positive with OD > the mean + 2 SDs of the value for HC.

et al[7] Positive likelihood ratio for anti-FTH1 antibodies by ELISA (1.96), was in the same range than clinical findings as previously reported.[9]

In the GCA control group, 31.9% of patients showed anti-FTH1 antibody positivity (34% of those who never received corticosteroids before blood sampling). Therefore, the contribution of anti-FTH1 antibodies to the diagnosis of GCA is probably limited. In addition, we failed to correlate antibody positivity with any clinical symptom.

Alexis Régent,[1,2] Kim Heang Ly,[3,4] Aurélie Blet,[1] Christian Agard,[5] Xavier Puéchal,[1,2] Nicolas Tamas,[1] Claire Le-Jeunne,[6] Elisabeth Vidal,[3,4] Loïc Guillevin,[2] Luc Mouthon[1,2]

[1]Institut Cochin, INSERM U1016, CNRS UMR 8104, Université Paris Descartes, Paris, France
[2]Pôle de Médecine Interne, Centre de Référence pour les vascularites nécrosantes et la sclérodermie systémique, Hôpital Cochin, Assistance Publique Hôpitaux de Paris (AP-HP), Paris, France
[3]Service de Médecine Interne A, CHU Dupuytren, Limoges, France
[4]Laboratoire d'immunologie, EA3842, Faculté de médecine, Limoges, France
[5]Service de Médecine Interne, Hôpital Hôtel Dieu, Nantes, France
[6]Service de Médecine Interne, Hôpital Hôtel Dieu, AP-HP, Paris, France

Correspondence to Dr Alexis Régent, Service de Médecine Interne, Hôpital Cochin, 27 rue du faubourg Saint-Jacques, 75679 Paris, Cedex 14, France; alexisregent@hotmail.com

Acknowledgements AR received financial support from the Société Nationale Française de Médecine Interne (SNFMI), Association pour la Recherche en Médecine Interne et en Immunologie Clinique (ARMIIC) and Groupe Pasteur Mutualité (GPM). We thank CSL Behring for financial support.

Contributors AR designed the experiments, carried out the ELISA experiments, analysed the results and drafted the manuscript. KHL provided sera from patients, participated in the analysis of the results and edited the manuscript. AB carried out ELISA experiments with AR and edited the manuscript.CA provided sera from patients, participated in the analysis of the results and edited the manuscript. XP participated in the study design and edited the manuscript. NT carried out ELISA experiments with AR and edited the manuscript. CLJ provided sera from patients, participated in the analysis of the results and edited the manuscript. EV provided sera from patients, participated in the analysis of the results and edited the manuscript. LG provided sera from patients, participated in the study design and analysis of the results and also edited the manuscript. LM provided sera from patients, designed the experiments, analysed the results and drafted the manuscript.

Competing interests AR and LM have applied for a patent for a diagnostic test of vasculitic disorders including giant cell arteritis (US 20120088257).

Ethics approval The ethics committee of Cochin hospital.

Provenance and peer review Not commissioned; externally peer reviewed.

Accepted 17 March 2013
Published Online First 10 April 2013

Ann Rheum Dis 2013;**72**:1269–1270. doi:10.1136/annrheumdis-2012-202963

REFERENCES

1. **Ly KH,** Regent A, Tamby MC, *et al*. Pathogenesis of giant cell arteritis: more than just an inflammatory condition? *Autoimmun Rev* 2010;**9**:635–45.
2. **Blockmans D,** Bley T, Schmidt W. Imaging for large-vessel vasculitis. *Curr Opin Rheumatol* 2009;**21**:19–28.
3. **Amor-Dorado JC,** Garcia-Porrua C, Gonzalez-Gay MA. Anti-endothelial cell antibodies and biopsy-proven temporal arteritis. *Lupus* 2002;**11**:134.
4. **Navarro M,** Cervera R, Font J, *et al*. Anti-endothelial cell antibodies in systemic autoimmune diseases: prevalence and clinical significance. *Lupus* 1997;**6**:521–6.
5. **Regent A,** Dib H, Ly KH, *et al*. Identification of target antigens of anti-endothelial cell and anti-vascular smooth muscle cell antibodies in patients with giant cell arteritis: a proteomic approach. *Arthritis Res Ther* 2011;**13**:R107.
6. **Liozon E,** Roblot P, Paire D, *et al*. Anticardiolipin antibody levels predict flares and relapses in patients with giant-cell (temporal) arteritis. A longitudinal study of 58 biopsy-proven cases. *Rheumatology (Oxford)* 2000;**39**:1089–94.
7. **Baerlecken NT,** Linnemann A, Gross WL, *et al*. Association of ferritin autoantibodies with giant cell arteritis/polymyalgia rheumatica. *Ann Rheum Dis* 2012;**71**:943–7.
8. **Hunder GG,** Bloch DA, Michel BA, *et al*. The American College of Rheumatology 1990 criteria for the classification of giant cell arteritis. *Arthritis Rheum* 1990;**33**:1122–8.
9. **Smetana GW,** Shmerling RH. Does this patient have temporal arteritis? *JAMA* 2002;**287**:92–101.

Neurotrophins are involved in vascular remodeling of giant cell arteritis

En révision dans Arthritis Research Therapy

Kim Heang Ly[1,2], Alexis Régent[3,4], Elsa Molina[1], Sofiane Saada[1], Philippe Sindou[1], Claire Le-Jeunne[5], Antoine Brezin[6], Véronique Witko-Sarsat[1], François Labrousse[7], Pierre-Yves Robert[8], Philippe Bertin[9], Jean-Louis Bourges[6], Anne-Laure Fauchais[1,2], Elisabeth Vidal[2], Luc Mouthon[3,4] Marie-Odile Jauberteau[1]

[1]Laboratoire d'immunologie, EA3842, Faculté de médecine, Limoges, France

[2]Service de Médecine Interne A, CHU Dupuytren, Limoges, France

[3]Institut Cochin, INSERM U1016, CNRS UMR 8104, Université Paris Descartes, Paris, France

[4]Service de Médecine Interne, Centre de Référence pour les vascularites nécrosantes et la sclérodermie systémique, Hôpital Cochin, Assistance Publique Hôpitaux de Paris (AP-HP), Paris, France

[5]Service de Médecine Interne, hôpital Hôtel Dieu, AP-HP, Paris, France

[6]Centre d'ophtalmologie HUPC Cochin Hôtel-Dieu, Université Sorbonne Paris Cité, Faculté de médecine Paris Descartes, AP-HP, Paris, France

[7]Service d'Anatomie pathologique, CHU Dupuytren, Limoges, France

[8]Service d'Ophtalmologie, CHU Dupuytren, Limoges, France

[9]Service de Rhumatologie, CHU Dupuytren, Limoges, France

Corresponding author:

Dr Kim Heang Ly

Service de Médecine Interne A, CHU Dupuytren

2 avenue Martin Luther King, 87042 Limoges cedex, France

Tel:+ 335 55 05 67 77

Fax:+335 55 05 66 50

Email: kim.ly@chu-limoges.fr

Abstract

Objectives: Giant cell arteritis (GCA) is characterized by intimal hyperplasia leading to ischemic manifestations that involve large vessels. Neurotrophins (NTs) and their receptors (NTRs) are protein factors for growth, differentiation and survival of neurons. They are also involved in the migration of vascular smooth muscle cells (VSMCs). Our aim was to investigate whether NTs and NTRs are involved in vascular remodeling of GCA.

Methods: We included consecutive patients who underwent a temporal-artery biopsy for suspected GCA. We developed an enzymatic digestion method to obtain VSMCs from smooth muscle cells in GCA patients and controls. Neurotrophin protein and gene expression and functional assays were studied from these VSMC. Neurotrophin expression was also analysed by immunohistochemistry in GCA patients and controls.

Results: Whereas temporal arteries of both GCA patients (n=22) and controls (*n*=21) expressed nerve-growth factor (NGF), brain-derived neurotrophic factor (BDNF), tropomyosin receptor kinase B (TrkB) and sortilin, immunostaining was more intense in GCA patients, especially in the media and intima, while neurotrophin-3 (NT-3) and P75 receptor ($P75^{NTR}$) were only detected in TA from GCA patients. Expression of TrkB, a BDNF receptor, was higher in GCA patients with ischemic complications. Serum NGF was significantly higher in GCA patients (*n*=28) *vs* controls (*n*=48), whereas no significant difference was found for BDNF and NT-3. NGF enhanced GCA-derived temporal-artery VSMCs proliferation and BDNF facilitated migration of temporal-artery VSMCs in patients with GCA compared to controls.

Conclusion: Our results suggest that NTs and NTRs are involved in vascular remodeling of GCA. In GCA-derived temporal-artery VSMC, NGF promoted proliferation and BDNF enhanced migration by binding to TrkB and $p75^{NTR}$ receptors. Further experiments are needed on a larger number of VSMC samples to confirm these results.

Keywords: giant cell arteritis, neurotrophins, vasculitis, vascular remodelling.

Introduction

Giant cell arteritis (GCA) is a primary vasculitis involving aorta and its extra- and intra-cranial branches. Histopathological findings show cellular infiltrates, internal elastic lamina disruption and intimal hyperplasia, leading to luminal stenosis. Macrophages and giant cells produce platelet-derived growth factor (PDGF), which stimulates migration of vascular smooth muscle cells (VSMCs) from the media to the intima to initiate intimal hyperplasia. However, several mechanisms involved in vascular remodeling of GCA still remain unclear [1].

Neurotrophins (NTs) are growth factors, initially described in the nervous system and now include vascular cells [2]. Three NTs and their receptors (NTRs) are well investigated. They include the nerve growth factor (NGF), brain-derived neurotrophic factor (BDNF) and neurotrophin-3 (NT-3), the selective tropomyosin receptor kinase (Trk), TrkA for NGF, TrkB for BDNF and TrkC for NT-3, a non-selective receptor $p75^{NTR}$ and a co-receptor, which is usually associated with $p75^{NTR}$, called sortilin. In the cardiovascular system, NTs and NTRs are involved in cardiovascular development, blood-vessel growth, VSMCs and cardiomyocyte functions [2]. NTs and NTRs are detected *in vivo* and *in vitro* in endothelial cells and human aortic VSMC donors and in rats [3]. In addition, NGF promotes similar VSMC migration as PDGFs, but not their proliferation [3, 4]. Moreover, NGF and BDNF and their two specific Trk receptors are involved in aortic intimal hyperplasia induced by balloon angioplasty in rats [3], while activation of $p75^{NTR}$ by NGF, NT-3 and, to a lesser extent, BDNF, induce VSMC apoptosis [5].

Using temporal artery VSMCs (TASMCs) obtained prospectively from suspected GCA patients, we hypothesized that NTs and NTRs are involved in the pathogenesis of GCA, especially in the vascular remodeling stage.

Methods

Patients

We prospectively enrolled patients who had undergone a temporal-artery biopsy for suspected GCA at Limoges and Paris (Cochin and Hotel-Dieu) university hospitals, since January 2010. GCA diagnosis was established according to ACR criteria [6]. Patients with a negative temporal-artery biopsy without clinical diagnosis of arteritis were defined as controls. All subjects gave their informed consent prior to participation and the study was approved by the Ethics Committee of the Cochin University of Paris (collection dc-2010-1079). Clinical and biological data are shown in Table 1.

Cell culture

TASMCs were isolated from segments of 5–10 mm of temporal artery (TA) after removal of adventitia and enzymatic digestion of media with 500 U/mL of type-I collagenase in 5 mL of DMEM Glutamax II (Gibco, Grand Island, New York, USA). Cultures were performed, as previously described [7], in Smooth Muscle Cell Basal Medium (PromoCell, Heidelberg, Germany) supplemented with FCS (5%), insulin (5 µg/mL), FGF-2 (2 ng/mL), epidermal growth factor (0.5 ng/ml) and streptomycin/penicillin (1%) at 37°C in 5% CO_2

Cultures contained 90% VSMC cells expressing α-smooth-muscle actin (Sigma-Aldrich, Saint-Louis, Missouri, USA), without CD-90 fibroblastic

staining (Dianova, Hamburg, Germany) (supplemental data figure 1). TASMCs were used for the experiments between passages 3 and 8. The cells were studied for NTs and NTRs expression at protein and transcriptional levels and in proliferation and migration assays. GCA-derived TASMC used for western blotting, Real-Time PCR analysis and functional assays were obtained from patients with positive TAB for GCA.

Immunohistochemistry

Immunohistochemistry was performed on paraffin-embedded sections of TA deparaffinised in 22 biopsy-proven GCA patients according to previous described criteria [8] and 21 controls with rabbit anti-NGF, -BDNF, -NT-3, -TrkA, -TrkB, -TrkC, -$p75^{NTR}$ and goat anti-sortilin antibodies (Ab) (Santa Cruz, Heidelberg, Germany) at 1:100 and anti-CD3 Ab for T lymphocytes (1/400; Dako Glostrup, Denmark). Sections of TA were rehydrated and subjected to steam-heat antigen retrieval in citrate buffer in a microwave oven (750 W). Endogenous peroxidases were inhibited with 5% H_2O_2 in methanol and non-specific sites were blocked with PBS-3% bovine serum albumin. The primary Ab as above were incubated at a 1/100 dilution overnight at 4°C and revealed with the anti-rabbit HRP Envision™ (Dako). After counterstaining, the slides were studied with a Leica microscope (×200 magnification). Immunostaining was scored using a staining index based on the percentage of positive cells. To perform semi-quantitative measurement of immunostaining, we chose three representative area of temporal artery (×200 magnification) to count staining cells that expressed myofibroblast or VSMC phenotype (*i.e*, elongated cells). The mean of positive cell percentage of these three

measurements for each patient or control was used to determine immunostaining intensity. The results were expressed as the mean of three independent quantifications made by two different observers.

Western blotting

Western Blotting was performed as previously described [9] with rabbit anti-NGF, -BDNF, -NT-3, -TrkA, -TrkB, -$p75^{NTR}$ and goat anti-sortilin Ab (Santa Cruz) or anti-TrkC (R&D Systems, Minneapolis, Minnesota, USA) at 1/200 dilution. Signaling activation was studied by using rabbit anti-Akt and -phospho-Akt Ab and -phospho-Erk1/2 and mouse anti-Erk1/2 Ab (at 1/1000 dilution; R&D Systems). Proteins (50 µg/lane) obtained from whole-cell lysates of TASMCs using lysis buffer [9] were separated on 10–12% SDS-polyacrylamide gels (Invitrogen, Carlsbad, California, USA) and transferred onto PVDF membranes (Millipore, Billerica, Massachusetts, USA). After saturation (5% nonfat dry milk, 0.1% Tween in PBS), Ab were incubated overnight at 4°C, and revealed after 1 h incubation at RT with anti-rabbit or -goat Ig-HRP-conjugated Ab (Santa Cruz, dilution 1/1000) by chemiluminescence (ECL reagent; Amersham Little Chalfont, UK). Protein-loading control was performed with anti-actin Ab (Santa Cruz, 1/10,000). Western blots were scanned using a bioimaging system (Genesnap; Syngene, Cambridge, UK).

RNA extraction, Reverse Transcription and Real-Time PCR assays

Total RNAs were extracted with Qiagen RNeasy Isolation Kit (Qiagen, Venlo, Netherlands), treated with RNase-free DNase I (Qiagen), and quantified by

NanoDrop (ND-1000) spectrophotometer (NanoDrop, Wilmington, Delaware, USA). The RNA quality was evaluated on Agilent 2100 bioanalyzer using the RNA 6000 Labchip kit (Agilent Technologies, Palo Alto, California, USA). cDNA synthesis was performed with a High-Capacity cDNA Reverse Transcription Kit (Applied Biosystems, Carlsbad, California, USA), as recommended by the manufacturer. Real-time PCR was performed by predesigned primer/probe TaqMan gene expression assays (Applied) and normalized to HPRT housekeeping gene (Supplemental data). Experiments were assessed in triplicate in at least using TaqMan Fast-Univ Master Mix (Applied) using an Applied Biosystems StepOnePlus Real-Time PCR System and analyzed by a StepOne Software v2.2.2 with a two-step PCR protocol as previously described [9] .The comparative ΔCt method was used for relative quantification of gene expression on duplicate of each reaction.

Cell viability, proliferation and chemoinvasion assays

Cell viability, proliferation and migration assays were studied using exogenous NGF (Alomone Labs, Jerusalem, Israel), recombinant human BDNF (Promega, Madison, Wisconcin, USA), or PDGF-AB (R&D Systems, Minneapolis, Minnesota, USA), alone or both with K252a, a pharmacological Trk inhibitor (Alomone), ANA-12 (100 μM), a specific TrkB inhibitor, acting without altering TrkA and TrkC functions (Tocris, Bristol, UK) [10] or an anti-$p75^{NTR}$ antagonist Ab (Alomone).

Cell viability of TASMCs was assessed using the colorimetric XTT assay (Cell Proliferation Kit II, XTT Roche, Basel, Switzerland) according to the

manufacturer's instructions. A range of concentrations was evaluated for each of the conditions studied. Efficient concentrations were defined as follows: NGF (10 ng/mL), BDNF (200 ng/mL), K252a Trk inhibitor (100 ng/mL), ANA-12 (100 µM), anti-$p75^{NTR}$ antagonist Ab (10 mg/mL) and PDGF (40 ng/mL), which was used as a positive control [11] (supplemental data).

Cell proliferation was determined by incorporation of BrdU (Cell Signaling, Danvers, Massachusetts, USA) according to the manufacturer's instructions. Assays were studied using recombinant human NGF (10 ng/mL), recombinant human BDNF (200 ng/mL), or recombinant human PDGF-AB (40 ng/mL), alone or both with K252a Trk inhibitor (100 ng/mL), or ANA-12 specific TrkB inhibitor (100 µM) or an anti-$p75^{NTR}$ antagonist Ab (10 mg/mL). Efficient concentrations of exogenous NTs, PDGF and NTR inhibitors were determined with XTT assay (Cell Proliferation Kit II, XTT Roche, Basel, Switzerland) (supplemental data figure 2). Cells were seeded in 96-well plates (5,000 cells/well) and maintained in DMEM-free serum medium during 48h before stimulation. Proliferation assays were performed after 1, 3 and 4 days of TASMC incubation with NT or NTR inhibitors, or both.

Chemoinvasion assay

The Boyden chamber method was performed in a BD Biocoat Matrigel Invasion Chambers (BD Biosciences, Franklin Lakes, New jersey, USA) with an 8-µm pore-size membrane for the chemoinvasion assay. Experiments were performed in duplicate in at least two independent experiments. Serum-starved TASMCs were seeded (1×10^5 cells/well) in 500 µL of serum-free

DMEM into the upper chamber of the membrane-embedded insert during 48h before stimulation. DMEM containing either 10% FCS alone or NGF, BDNF or PDGF at the concentrations defined above were placed in the lower chamber and the cells were incubated for 24 or 48 h at 37°C/5% CO_2. After incubation, the lower chamber was treated with 50 µM calcein AM fluorescent dye for 30 min at 37°C/5% CO_2. Non-invading cells in the upper part of the insert were carefully removed. Then, 8 µl of Calcein AM fluorescent dye (BD Biosciences) was added for 15 min to the lower chamber. Non-invading cells in the upper part of the insert were carefully removed. The migration of TASMCs to the lower part was quantified by fluorescent counting spectrophotometry at 488 nm (Berthold, Bad Wildbad, Germany) and images were obtained using a fluorescence microscope M2FLIII (Leica, Wetzlar, Germany).

Measurement of sera and supernatant neurotrophin secretion

Cell-culture medium was collected and centrifuged for 30 min at 3000 g in Vivaspin columns (Millipore, Billerica, Massachusetts, USA). Concentrations of NGF, BDNF and NT-3 in TASMC supernatant and 1:100 diluted sera from GCA patients and controls were measured using ELISA kits according to the manufacturer's instructions (NGF or BDNF or NT-3 EmaxH ELISA, Promega).

Statistical analysis

Results were expressed as their means ± standard errors of the mean (SEM) of at least three independent experiments. Statistical analyses were performed using Student's t-test; a *p*-value <0.05 was considered statistically

significant. Asterisks in figures indicate statistically significant differences: *p<0.05, ** p<0.01, ***p<0.001.

Results

Neurotrophins are overexpressed in temporal arteries from patients with GCA compared to controls

Temporal arteries (TAs) from 22 GCA patients and 21 controls expressed NGF, BDNF, TrkB and sortilin, whereas TrkA and TrkC were not detected in any studied TAs (Figure 1A). However, significant differences in the intensity and location of staining were observed between GCA patients and controls. Indeed, NGF expression was more intense in the adventitia (76.2 +/- 19 *vs* 35.4 +/- 22%, p=0.002) and the media (59.6 +/- 25% *vs* 26 +/- 22%, p=0.004), respectively. BDNF was markedly expressed in the media (82 +/- 21 *vs* 26.5 +/- 27%, p<0.0001) and the intima (78 +/- 20 *vs* 36 ± 27%, p=0.0007), respectively. Concerning sortilin, expression was prominent in the adventitia (31 ± 28 *vs* 2 ± 4%, p=0.003) and the intima (41 ± 14 *vs* 27 ± 14%, p=0.02), respectively (Figure 1B). Interestingly, only GCA arteries strongly expressed NT-3 and $P75^{NTR}$ in all artery layers (Figure 1A).

By contrast, T lymphocytes (anti-CD3+) staining was localized in the media intima junction.

To search for a relationship between these expressions and the course of the disease, we evaluated the staining of NTs and NTRs in association with the clinical parameters of the 22 GCA patients (Table 1).

TrkB is overexpressed in temporal arteries of GCA patients with ischemic complications

Strikingly, only GCA patients with ischemic events (stroke, amaurosis or permanent visual loss) (n=9) had significant overexpression of TrkB in the

media (p=0.04) and intima (p=0.015), compared to GCA patients without ischemia (n=13) (Figure 1C). No difference in expression of NTs and NTRs was found in the TAs of GCA patients regarding other clinical characteristics or inflammatory biomarkers. Moreover, we did not find any difference in immunostaining of NTs and NTRs between GCA patients who received corticosteroids before a temporal-artery biopsy (n=14) and untreated patients (n=8).

Considering these differences in the expression of NTs and NTRs on *ex vivo* TAs in GCA patients, we achieved primary cultures for six TAs from biopsy-proven GCA patients and from 10 suspected GCA patients who had normal histological TAs as controls.

Expression of neurotrophins and receptors in TASMCs from the temporal arteries of GCA patients and controls

Protein expression was assessed by western blotting in proteins extracted from the TASMCs of GCA patients and controls (Figure 2A). Whereas NGF, BDNF, TrkB, TrkC, $p75^{NTR}$ and sortilin were detected in TASMCs from patients and controls, proteins for TrkA receptor were not detected in cells from either of these groups. In contrast, NT-3 protein was only detected in GCA and not in control cells. Exploration of signaling pathways at baseline showed that phospho-Akt is predominantly detected in GCA-derived TASMCs than control. The ratio of phospho-Akt/ Akt/ actin is significantly higher in GCA cells patients in comparison to patients controls ($p = 0.033$) (Figure 2B) whereas no difference was found for ERK 1/2 and phospho-ERK 1/2. In parallel, we have confirmed by RT-PCR that the corresponding mRNAs for

NGF, BDNF, TrkB (truncated 95 length) and $p75^{NTR}$ were present but not those for TrkA, as expected (Figure 2B). However, some discrepancies were noted between protein and mRNA expressions. This was evidenced for NT-3 mRNA, which was detected in all sampled cells from patients and controls, and feebly for the TrkC transcript. Therefore, a quantitative RT-PCR was performed to determine the differences between transcript expression of NT and NTR genes in cells from patients and controls.

While BDNF, NGF and NT-3 mRNA were expressed, those of NT-3, TrkB, TrkC and sortilin were overexpressed (increase by fivefold) in TASMCs from GCA patients compared to controls, but the difference was not significant (Figure 2C). Thus, because NGF and BDNF and their receptors were detected in TASMCs from GCA and control patients, the functional effects of these two NTs were evaluated in cultured cells from TAs from the two groups and compared with PDGF as a positive control.

Proliferation effects of NT and NT-receptor blockers in GCA patients

NGF promoted proliferation of TASMCs from GCA patients compared to controls (p=0.025) similarly to FCS (p=0.012) and PGDF (p=0.023) by day 1. BDNF tended to enhance cell proliferation by day 1 especially in TASMCs from GCA patients (*p*=0.052). Proliferation effects with NTs, FCS 10% and PDGF tended to disappear by day 3 (Figure 3B) and day 4 (additional data) with no difference between two groups. Addition of K252a, ANA-12 or anti-$p75^{NTR}$ Ab prior NTs did not induce a significant difference between two groups.

Because especially NGF and to a lesser extent BDNF induced proliferation in TASMCs from GCA patients compared to controls, we searched for the potential effect of NTs in TASMC migration in Matrigel chambers to determine whether NTs are involved in intimal hyperplasia as shown by immunohistochemistry.

BDNF activates TASMC migration in GCA patients but not in controls

Comparison of TASMC invasion in GCA and control patients demonstrated that TASMCs from GCA patients were significantly able to migrate in the presence of exogenous BDNF compared to those from controls (p=0.012) after a 24-h exposure (Figure 4). In contrast, no effect was shown for exogenous NGF whatever the status of TASMCs in patients or controls. Interestingly, only cells from GCA patients were able to significantly invade Matrigel chambers in the presence of 10% FCS (p = 0.0175, compared to cells from controls) as was also observed for exogenous PDGF (p<0.0001 *vs* cell migration in controls). Strikingly, neither BDNF nor PDGF induced migration of TASMCs in controls. Migration of TASMCs in GCA patients was only detected after a 24-h exposure and disappeared after 48 h of incubation (data not shown).

Because NTs are expressed in TAs and in VSMCs of GCA patients, we looked for secretions by TASMC cells in cultures and the sera.

NGF concentration was higher in the sera and in TASMC culture-supernatants from GCA patients

NGF sera concentrations were significantly higher in GCA patients compared to controls (177 +/- 67.6 *vs* 145.5 +/- 66 pg/mL, *p*=0.04) (Figure 5A) whereas no difference was found for BDNF (Figure 5A) or NT-3 (data not shown). There was no correlation between NGF, BDNF or NT-3 level and ischemic events or inflammatory syndrome. NGF and BDNF secretion was measured in cell supernatants. NGF levels tended to be higher in TASMCs from GCA patients (*p*= 0.06) (Figure 5B) whereas no difference was detected for BDNF and NT-3 supernatants (data not shown).

Discussion

Despite substantial improvement in understanding the pathophysiologic features of GCA, some mechanisms still remain unclear, especially in relation to vascular remodeling. Herein, we report on the expression and functions of NTs and their receptors, which are potentially involved in vascular remodeling in GCA. It is worth noting that NGF, BDNF and sortilin are significantly overexpressed in different histological layers of TAs in GCA patients compared to those of controls. In addition, TrkB staining was significantly higher in the TAs of GCA patients with a cranial ischemic event. TrkA and TrkC were not detected in patients or controls, whereas NT-3 and $p75^{NTR}$ were enhanced only in GCA patients. These data dealt with mRNA and protein expression of NTs and NTRs in TASMCs from GCA patients and controls. Enhanced TrkB transcription was observed in GCA cells whereas those of TrkA and TrkC were feebly detected.

The expressions of NGF, BDNF and sortilin in the TAs of GCA patients could be related to other inflammatory disorders associated with localized expression of NTs. Indeed, NGF is expressed in endothelial cells and keratinocytes in patients with psoriasis [12], and NGF and BDNF are present in the inflamed joints of patients with rheumatoid arthritis [13, 14]. Interestingly, constitutive NGF expression and release in both human and mouse articular chondrocytes is enhanced by Il-1β [15]. Likewise, NTs are detected in other bronchial smooth-muscle cells during asthma [16] or sarcoidosis [17] and their relationship with inflammatory cytokines, IL-1β and IFN-γ has been established by the induction of NGF, and BDNF mRNA expression and secretion in cell-culture supernatants [18, 19]. Hence, the

overexpression of NTs and their receptors in TAs from GCA patients could be, in part, related to the presence of pro-inflammatory cytokines in all layers of the inflamed arterial wall. Moreover, it has been demonstrated that ischemia contributes to the overexpression of some NTs and their related receptors, as we have shown with the increased TrkB expression in GCA patients with a cranial ischemic event. Indeed, in experimental arterial injury that leads to ischemia, enhanced expression of NGF, BDNF and their specific receptors has been described [3]. Furthermore, in a murine experimental model of atherosclerosis, the TrkB receptor is overexpressed in neointimal VSMC cells whereas decreased TrkB expression reduces atherosclerotic lesions [20].

Moreover, sortilin expression is enhanced in the adventitia and intima of TAs from GCA patients. This data could be correlated with intimal TrkB overexpression, as sortilin acts as an intracellular protein transporter for immature NTs [21] and controls the regulation of BDNF trafficking and release [22]. Such a function could be related to BDNF and sortilin overexpression in TAs from GCA patients. In addition, sortilin is also a co-receptor for $p75^{NTR}$**,** which was only observed in the TAs of GCA patients. $P75^{NTR}$ is mostly absent in healthy conditions: its expression is enhanced by pathologic conditions such as diabetes or atherosclerosis [3, 5, 23].

Serum NGF levels are significantly enhanced in GCA patients, but not BDNF or NT-3. Such elevated NGF levels have been previously reported in inflammatory diseases such as Sjögren syndrome [24].

The proliferation effects of NTs are well described in smooth muscle cells other than VSMCs, especially for NGF and BDNF [25-28]. In our study NGF promoted proliferation in GCA-derived TASMCs similarly to PDGF.

Because TrkA was not detected in TASMCs, this effect probably took place through $p75^{NTR}$ activation as already described in brain tumor-initiating cells [29]. BDNF induced GCA-derived TASMCs proliferation in a lesser extent than NGF. This effect, well reported in SMC in pulmonary hypertension [27] is not significant probably because our small number samples. In GCA patients we have demonstrated that BDNF promote TASMCs migration rather than their proliferation. Because both TrkB and BDNF were prominently expressed in the same areas of GCA temporal arteries, it is probable that BDNF activates TASMCs migration from TAs of patients through its interaction with TrkB. Our data are consistent with previous studies on the effects of VSMCs on NTs. [3, 4, 30]. Indeed, BDNF-related migration was comparable to that observed with PDGF, as described previously, [4] and was more consistent than that observed with NGF.

Exploration of signalling pathways in our study showed that PI3/Akt pathway seemed to be more activated than ERK1/2 pathway in GCA patients compared to controls. Though PI3/Akt signalling pathway can be activated by TNF-α in human smooth muscle cells [31] or IL-1β in rat brain astrocytes [32], our results is consistent with BDNF-induced migration in human chondrosarcoma [33] through a transducing signal involving TrkB.

Taken together, our results provide new insights regarding the involvement of NTs and NTRs in the vascular remodeling of GCA pathogenesis. Their overexpression in TAs from GCA patients could facilitate VSMC migration from media to intima, thus contributing to intimal hyperplasia. However, further studies are needed to elucidate the signaling pathways that

allow VSMC migration in order to define new therapeutic approaches for patients with GCA.

Abbreviations

Ab: antibody; ACR: American College of Rheumatology; Akt: protein kinase B; BDNF: brain-derived neurotrophic factor; ELISA: enzyme-linked immunosorbent assay; ERK: extracellular signal-regulated kinase; FCS: foetal calf serum; FGF: fibroblast growth factor; GCA: giant cell arteritis; HC: healthy control; NGF: nerve growth factor; NT: neurotrophin; NTR: neurotrophin receptor; NT-3: neurotrophin-3; TA: temporal artery; TASMC: temporal artery VSMC; Trk: tropomyosin receptor kinase; PCR: polymerase chain reaction; PDGF: platelet-derived growth factor; RT: reverse transcriptase; TNF-α : tumor necrosis factor α ;VSMC: vascular smooth muscle cell.

Competing interests: The authors declare that they have no competing interests.

Acknowledgements: AR received financial support from the Direction Régionale et Départementale de Champagne-Ardennes et de la Marne and the Société Nationale Française de Médecine Interne (SNFMI) and SS from Conseil Régional du Limousin.

Author contribution: KHL carried out the design of the study, cell culture, immunohistochemistry, western blotting, molecular, ELISA, proliferation and migration assays, analysed the results and drafted the manuscript. AR participated to cell culture, immunoassays and drafted the manuscript. EM participated in immunohistochemistry and molecular experiments and edited the manuscript. SS participated in molecular experiments and edited the

manuscript. PS participated in immunohistochemistry analysis. CLJ, VWS, PB, ALF and EV provided sera patients and participated in the acquisition of clinical and biological data. AB, PYR and JLB provided temporal arteries. FL participated in the acquisition and analysis of immunohistochemistry data. LM provided sera and participated in the drafting of the manuscript. MOJ carried out the design of the study with KHL, designed the experiments, analysed the results and drafted the manuscript. All authors read and approved the final manuscript.

References

1. **Ly KH, Regent A, Tamby MC, Mouthon L: Pathogenesis of giant cell arteritis: More than just an inflammatory condition? *Autoimmun Rev* 2010, 9(10):635-645.**
2. **Caporali A, Emanueli C: Cardiovascular actions of neurotrophins. *Physiol Rev* 2009, 89(1):279-308.**
3. **Donovan MJ, Miranda RC, Kraemer R, McCaffrey TA, Tessarollo L, Mahadeo D, Sharif S, Kaplan DR, Tsoulfas P, Parada L *et al*: Neurotrophin and neurotrophin receptors in vascular smooth muscle cells. Regulation of expression in response to injury. *Am J Pathol* 1995, 147(2):309-324.**
4. **Kraemer R, Nguyen H, March KL, Hempstead B: NGF activates similar intracellular signaling pathways in vascular smooth muscle cells as PDGF-BB but elicits different biological responses. *Arterioscler Thromb Vasc Biol* 1999, 19(4):1041-1050.**
5. **Wang S, Bray P, McCaffrey T, March K, Hempstead BL, Kraemer R: p75(NTR) mediates neurotrophin-induced apoptosis of vascular smooth muscle cells. *Am J Pathol* 2000, 157(4):1247-1258.**
6. **Hunder GG, Bloch DA, Michel BA, Stevens MB, Arend WP, Calabrese LH, Edworthy SM, Fauci AS, Leavitt RY, Lie JT *et al*: The American College of Rheumatology 1990 criteria for the classification of giant cell arteritis. *Arthritis Rheum* 1990, 33(8):1122-1128.**
7. **Regent A, Dib H, Ly KH, Agard C, Tamby MC, Tamas N, Weksler B, Federici C, Broussard C, Guillevin L *et al*: Identification of target antigens of anti-endothelial cell and anti-vascular smooth muscle cell antibodies in patients with giant cell arteritis: a proteomic approach. *Arthritis Res Ther* 2011, 13(3):R107.**
8. **Emilie D, Liozon E, Crevon MC, Lavignac C, Portier A, Liozon F, Galanaud P: Production of interleukin 6 by granulomas of giant cell arteritis. *Hum Immunol* 1994, 39(1):17-24.**
9. **Saada S, Marget P, Fauchais AL, Lise MC, Chemin G, Sindou P, Martel C, Delpy L, Vidal E, Jaccard A *et al*: Differential expression of neurotensin and specific receptors, NTSR1 and NTSR2, in normal and malignant human B lymphocytes. *Journal of immunology* 2012, 189(11):5293-5303.**
10. **Cazorla M, Premont J, Mann A, Girard N, Kellendonk C, Rognan D: Identification of a low-molecular weight TrkB antagonist with anxiolytic and antidepressant activity in mice. *J Clin Invest* 2011, 121(5):1846-1857.**
11. **Benjamin CW, Jones DA: Platelet-derived growth factor stimulates growth factor receptor binding protein-2 association with Shc in vascular smooth muscle cells. *J Biol Chem* 1994, 269(49):30911-30916.**
12. **Raychaudhuri SP, Raychaudhuri SK: Role of NGF and neurogenic inflammation in the pathogenesis of psoriasis. *Prog Brain Res* 2004, 146:433-437.**
13. **Barthel C, Yeremenko N, Jacobs R, Schmidt RE, Bernateck M, Zeidler H, Tak PP, Baeten D, Rihl M: Nerve growth factor and receptor expression in rheumatoid arthritis and spondyloarthritis. *Arthritis Res Ther* 2009, 11(3):R82.**
14. **Klein K, Aeschlimann A, Jordan S, Gay R, Gay S, Sprott H: ATP induced brain-derived neurotrophic factor expression and release from osteoarthritis synovial fibroblasts is mediated by purinergic receptor P2X4. *PloS one* 2012, 7(5):e36693.**
15. **Pecchi E, Priam S, Gosset M, Pigenet A, Sudre L, Laiguillon MC, Berenbaum F, Houard X: Induction of nerve growth factor expression and release by mechanical and inflammatory stimuli in chondrocytes: possible involvement in osteoarthritis pain. *Arthritis Res Ther* 2014, 16(1):R16.**
16. **Braun A, Lommatzsch M, Lewin GR, Virchow JC, Renz H: Neurotrophins: a link between airway inflammation and airway smooth muscle contractility in asthma? *Int Arch Allergy Immunol* 1999, 118(2-4):163-165.**

17. **Dagnell C, Grunewald J, Kramar M, Haugom-Olsen H, Elmberger GP, Eklund A, Olgart Hoglund C: Neurotrophins and neurotrophin receptors in pulmonary sarcoidosis - granulomas as a source of expression. *Respir Res* 2010, 11:156.**
18. **Kemi C, Grunewald J, Eklund A, Hoglund CO: Differential regulation of neurotrophin expression in human bronchial smooth muscle cells. *Respir Res* 2006, 7:18.**
19. **Freund V, Pons F, Joly V, Mathieu E, Martinet N, Frossard N: Upregulation of nerve growth factor expression by human airway smooth muscle cells in inflammatory conditions. *Eur Respir J* 2002, 20(2):458-463.**
20. **Kraemer R, Baker PJ, Kent KC, Ye Y, Han JJ, Tejada R, Silane M, Upmacis R, Deeb R, Chen Y *et al*: Decreased neurotrophin TrkB receptor expression reduces lesion size in the apolipoprotein E-null mutant mouse. *Circulation* 2005, 112(23):3644-3653.**
21. **Nykjaer A, Willnow TE: Sortilin: a receptor to regulate neuronal viability and function. *Trends Neurosci* 2012, 35(4):261-270.**
22. **Evans SF, Irmady K, Ostrow K, Kim T, Nykjaer A, Saftig P, Blobel C, Hempstead BL: Neuronal brain-derived neurotrophic factor is synthesized in excess, with levels regulated by sortilin-mediated trafficking and lysosomal degradation. *J Biol Chem* 2011, 286(34):29556-29567.**
23. **Salis MB, Graiani G, Desortes E, Caldwell RB, Madeddu P, Emanueli C: Nerve growth factor supplementation reverses the impairment, induced by Type 1 diabetes, of hindlimb post-ischaemic recovery in mice. *Diabetologia* 2004, 47(6):1055-1063.**
24. **Fauchais AL, Boumediene A, Lalloue F, Gondran G, Loustaud-Ratti V, Vidal E, Jauberteau MO: Brain-derived neurotrophic factor and nerve growth factor correlate with T-cell activation in primary Sjogren's syndrome. *Scand J Rheumatol* 2009, 38(1):50-57.**
25. **Freund-Michel V, Bertrand C, Frossard N: TrkA signalling pathways in human airway smooth muscle cell proliferation. *Cellular signalling* 2006, 18(5):621-627.**
26. **Stawowy P, Marcinkiewicz J, Graf K, Seidah N, Chretien M, Fleck E, Marcinkiewicz M: Selective expression of the proprotein convertases furin, pc5, and pc7 in proliferating vascular smooth muscle cells of the rat aorta in vitro. *J Histochem Cytochem* 2001, 49(3):323-332.**
27. **Kwapiszewska G, Chwalek K, Marsh LM, Wygrecka M, Wilhelm J, Best J, Egemnazarov B, Weisel FC, Osswald SL, Schermuly RT *et al*: BDNF/TrkB signaling augments smooth muscle cell proliferation in pulmonary hypertension. *Am J Pathol* 2012, 181(6):2018-2029.**
28. **Aravamudan B, Thompson M, Pabelick C, Prakash YS: Brain-derived neurotrophic factor induces proliferation of human airway smooth muscle cells. *J Cell Mol Med* 2012, 16(4):812-823.**
29. **Forsyth PA, Krishna N, Lawn S, Valadez JG, Qu X, Fenstermacher DA, Fournier M, Potthast L, Chinnaiyan P, Gibney GT *et al*: p75 neurotrophin receptor cleavage by alpha- and gamma-secretases is required for neurotrophin-mediated proliferation of brain tumor-initiating cells. *J Biol Chem* 2014, 289(12):8067-8085.**
30. **Urban D, Lorenz J, Meyborg H, Ghosh S, Kintscher U, Kaufmann J, Fleck E, Kappert K, Stawowy P: Proprotein convertase furin enhances survival and migration of vascular smooth muscle cells via processing of pro-nerve growth factor. *J Biochem* 2013, 153(2):197-207.**
31. **Lee CW, Lin CC, Lin WN, Liang KC, Luo SF, Wu CB, Wang SW, Yang CM: TNF-alpha induces MMP-9 expression via activation of Src/EGFR, PDGFR/PI3K/Akt cascade and promotion of NF-kappaB/p300 binding in human tracheal smooth muscle cells. *American journal of physiology Lung cellular and molecular physiology* 2007, 292(3):L799-812.**

32. Wu CY, Hsieh HL, Sun CC, Tseng CP, Yang CM: IL-1 beta induces proMMP-9 expression via c-Src-dependent PDGFR/PI3K/Akt/p300 cascade in rat brain astrocytes. *Journal of neurochemistry* 2008, 105(4):1499-1512.

33. Lin CY, Chen HJ, Li TM, Fong YC, Liu SC, Chen PC, Tang CH: beta5 integrin up-regulation in brain-derived neurotrophic factor promotes cell motility in human chondrosarcoma. *PloS one* 2013, 8(7):e67990.

Figure 1: (A). Immunostaining of NTs and their receptors and T lymphocytes (CD3+) in temporal arteries from GCA patients (*n*=22) compared to controls (*n*=21). Panels are representative examples of immunohistological images (x50 and x200). **(B)**. Panels are measurements of significant NT immunostaining intensities. Results are shown as mean values and standard errors of the mean (SEM). **(C)**. TrkB immunostaining in GCA patients with or without ischaemic complications. Immunoreactivity to TrkB in the media and intima of TAs in GCA patients with (*n*=8) or without (*n*=13) ischaemic complications. (*$p<0.05$,** $p<0.01$, ***$p<0.001$).

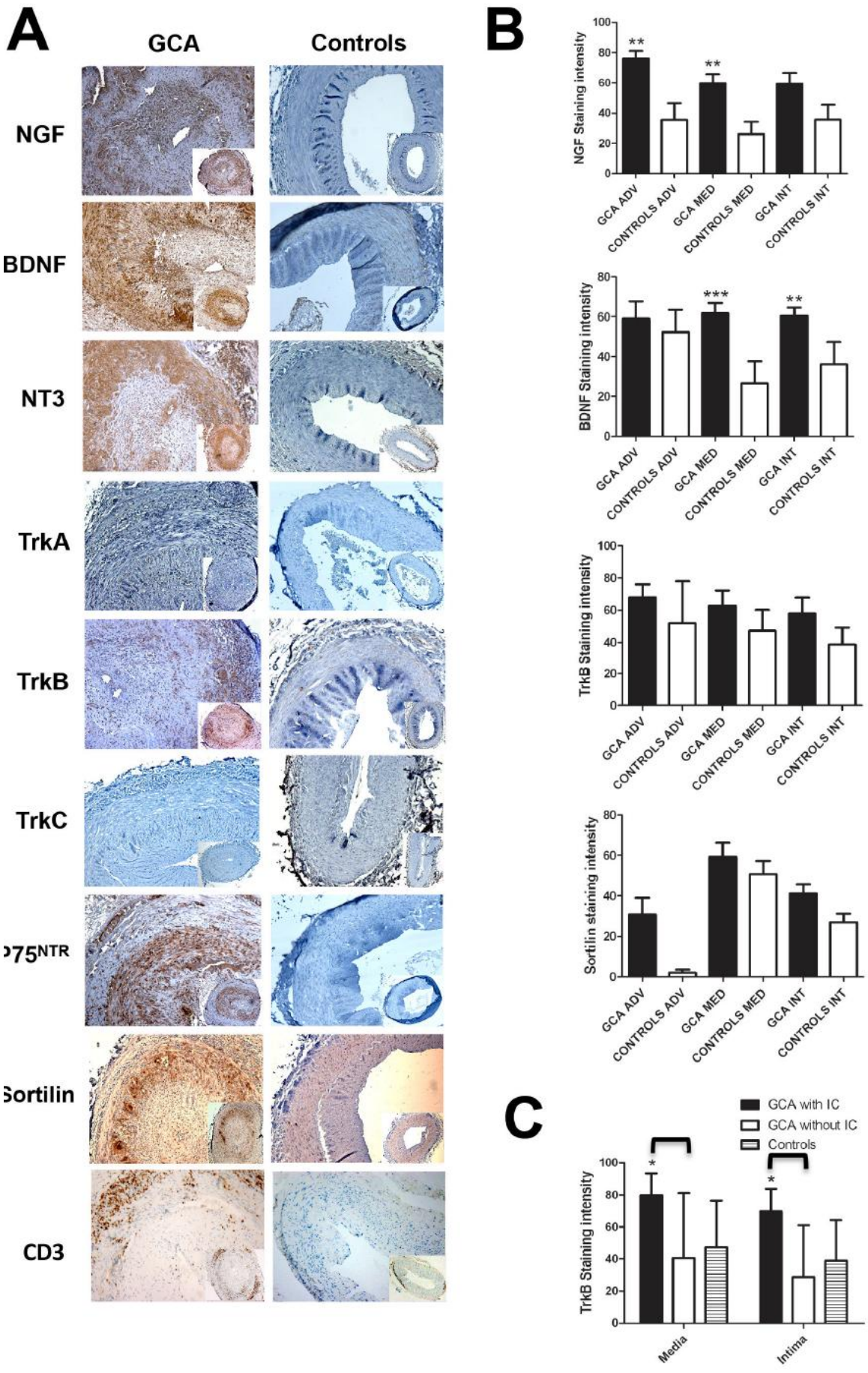
A
GCA
Controls
NGF
BDNF
NT3
TrkA
TrkB
TrkC
p75NTR
Sortilin
CD3
B
NGF Staining intensity
BDNF Staining intensity
TrkB Staining intensity
Sortilin staining intensity
GCA ADV
CONTROLS ADV
GCA MED
CONTROLS MED
GCA INT
CONTROLS INT
C
GCA with IC
GCA without IC
Controls
TrkB Staining intensity
Media
Intima

Figure 2: Western-blot (WB) analysis of GCA patients (*n*=6) and controls (*n*=4) TASMC lysates for NTs and NT-receptors **(A)** and for Akt, phospho-Akt, ERK 1/2 and phosphor ERK 1/2 **(B).** Panels are representative examples of western-blot analysis. **(C)** Transcription of NTs and NT-receptors by TASMCs from GCA patients (*n*=6) and controls (*n*=6) cultured with 10% FCS. The neuroblastoma cell line SH-SY-5Y (S) was used as a positive control. Constitutively expressed GAPDH is a control of PCR efficiency. Panels are representative examples of the transcription assay. NC: negative control. **(D)** qRT-PCR analysis of NT and NT-receptor expression in TASMC cultures from GCA patients (*n*=6) and controls (*n*=6), normalized to *HPRT* gene expression.

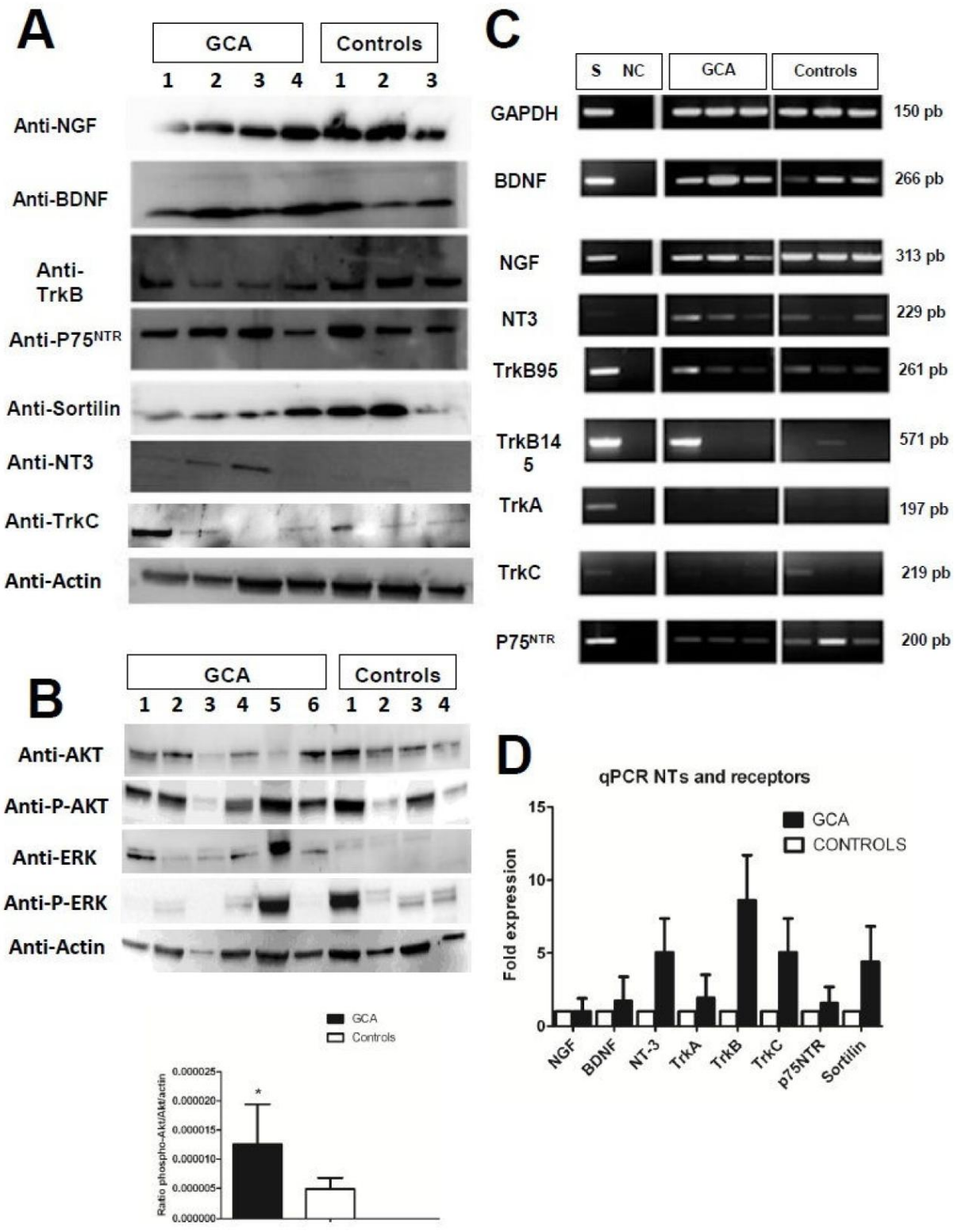
A
GCA
Controls
1 2 3 4 1 2 3
Anti-NGF
Anti-BDNF
Anti-TrkB
Anti-P75NTR
Anti-Sortilin
Anti-NT3
Anti-TrkC
Anti-Actin
B
GCA
Controls
1 2 3 4 5 6 1 2 3 4
Anti-AKT
Anti-P-AKT
Anti-ERK
Anti-P-ERK
Anti-Actin
GCA
Controls
Ratio phospho-Akt/Akt/actin
0.000025
0.000020
0.000015
0.000010
0.000005
0.000000
*
C
S NC
GCA
Controls
GAPDH
150 pb
BDNF
266 pb
NGF
313 pb
NT3
229 pb
TrkB95
261 pb
TrkB145
571 pb
TrkA
197 pb
TrkC
219 pb
P75NTR
200 pb
D
qPCR NTs and receptors
GCA
CONTROLS
Fold expression
15
10
5
0
NGF
BDNF
NT-3
TrkA
TrkB
TrkC
p75NTR
Sortilin

Figure 3: Effects of NTs and the inhibitors of Trk (K252a), TrkB (ANA-12) and $P75^{NTR}$ (antiP75) on TASMC proliferation in GCA patients and controls.

Proliferation assay performed with a BrdU assay on days 1 **(A)** and 3**(B)** respectively, in serum-starved TASMC incubated with NT or NT-receptor inhibitors, or a combination of NT and NT-inhibitor receptors, in GCA patients (*n*=6) and controls (*n*=10). In all figures, bars represent the mean of three experiments with their SEMs. K252a: specific Trk receptor inhibitor; ANA-12: a specific TrkB receptor inhibitor; antiP75: $p75^{NTR}$ Ab inhibitor; N (NGF) or B (BDNF) +K (K252a) or anti-$p75^{NTR}$: NGF or BDNF are added at the same time with the specific inhibitor. Three independent assays were performed and cells were seeded in triplicate for each cell line (**p*<0.05,** *p*<0.01, ****p*<0.001).

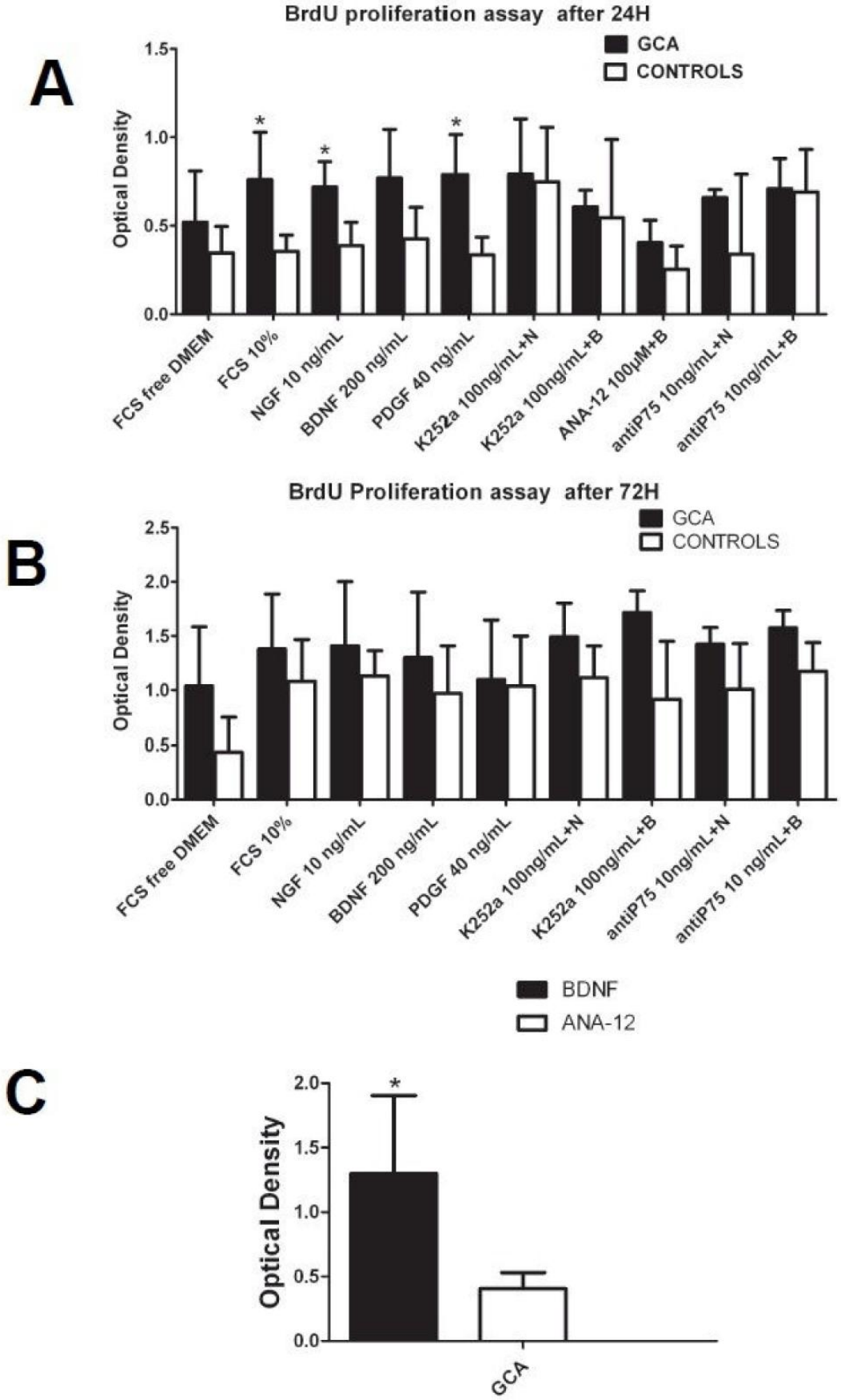
A
BrdU proliferation assay after 24H
GCA
CONTROLS
Optical Density
1.5
1.0
0.5
0.0
*
*
*
FCS free DMEM
FCS 10%
NGF 10 ng/mL
BDNF 200 ng/mL
PDGF 40 ng/mL
K252a 100ng/mL+N
K252a 100ng/mL+B
ANA-12 100µM+B
antiP75 10ng/mL+N
antiP75 10ng/mL+B
B
BrdU Proliferation assay after 72H
GCA
CONTROLS
Optical Density
2.5
2.0
1.5
1.0
0.5
0.0
FCS free DMEM
FCS 10%
NGF 10 ng/mL
BDNF 200 ng/mL
PDGF 40 ng/mL
K252a 100ng/mL+N
K252a 100ng/mL+B
antiP75 10ng/mL+N
antiP75 10 ng/mL+B
BDNF
ANA-12
C
Optical Density
2.0
1.5
1.0
0.5
0.0
*
GCA

Figure 4: Migration assay of TASMC with NGF and BDNF.

Migration assays were performed with TASMCs from GCA patients (*n*=6) and controls (*n*=6) incubated in the upper chamber with serum-free DMEM during 48h whereas NGF (10 ng/mL), BDNF (200 ng/mL), PDGF (40 ng/mL) or 10% FCS were added in the lower chamber during 24 h. Two independent assays were performed and cells were seeded in duplicate for each cell line.

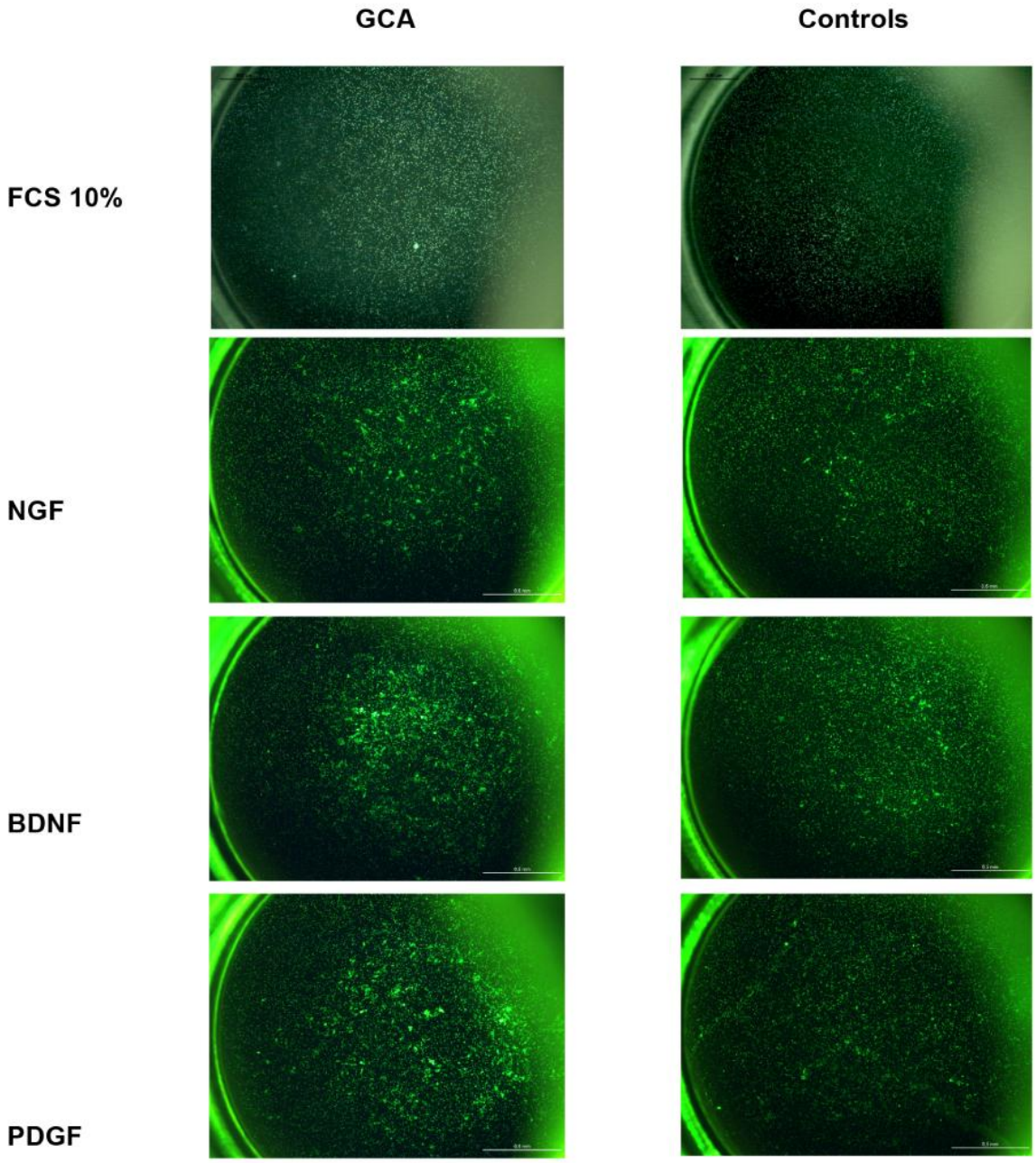
GCA
Controls
FCS 10%
NGF
BDNF
PDGF

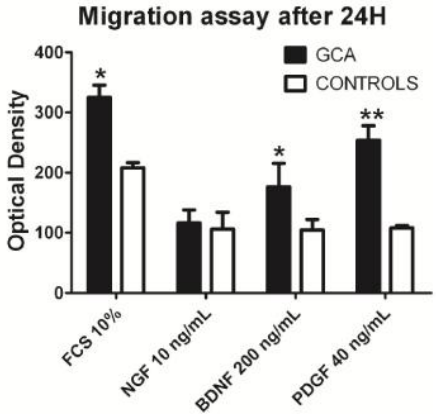
Migration assay after 24H
GCA
CONTROLS
Optical Density
400
300
200
100
0
*
**
*
FCS 10%
NGF 10 ng/mL
BDNF 200 ng/mL
PDGF 40 ng/mL

Figure 5: Sera and supernatant concentrations of NGF and BDNF: **(A)** NGF and BDNF sera concentrations from patients with GCA (*n*=30) compared to controls (*n*=48) with a sera dilution of 1:100. **(B)** NGF TASMC related-supernatant concentration from GCA patients (*n*=8) compared to controls (*n*=8). Supernatants were collected when VSMC reached 80% confluence, between passages 3 and 5. Experiments were performed in duplicate, with three independent ELISA assays and data are presented as pg/mL.

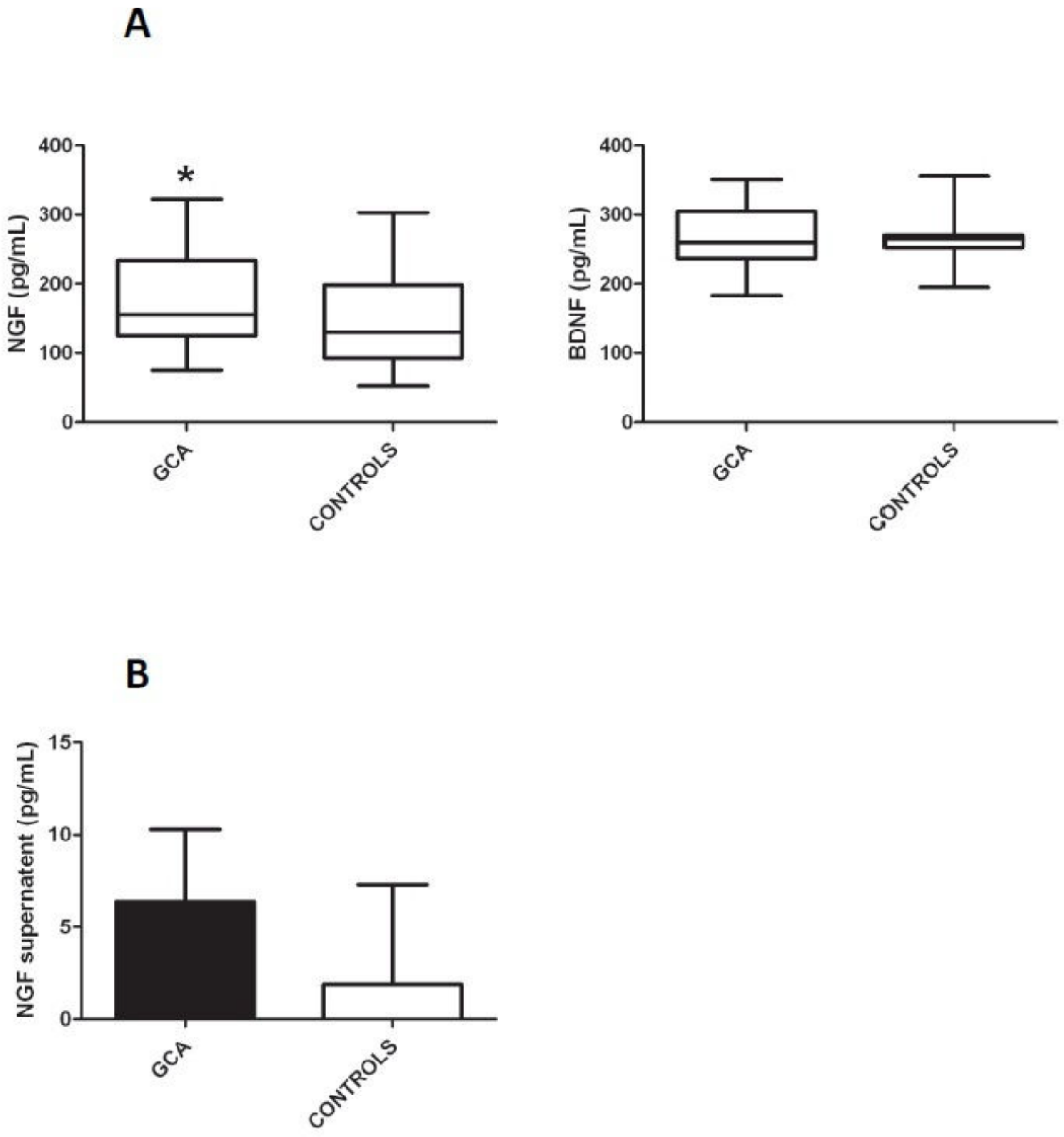

Table 1 Clinical and biological findings in the study cohort patients with GCA

Clinical characteristics			
	GCA patients (Plasma study) N (%)	**GCA patients (IHC study) N (%)**	**GCA patients (Cohort study) N (%)**
No of patients	30	22	42
General characteristics			
Age in years, median (range)	77 (60-92)	80.7 (73-89)	76.3 (60-92)
Sex, women/men	23/7	14/8	30/12
Systemic manifestations	15 (50)	17 (77)	33 (78.5)
Fever	9 (30)	4 (18)	13 (31)
Weight loss	15 (50)	12 (54.5)	20 (47.6)
Cranial symptoms	21 (70)	14 (63.6)	31 (73.8)
Headache	21 (70)	14 (63.6)	31 (73.8)
Jaw claudication	15 (50)	11 (50)	19 (45.2)
Scalp tenderness	14 (46.6)	12 (54.5)	21 (50)
Abnormal temporal arteries*	13 (43)	7 (32)	7 (16.6)
Cranial ischaemic events	9 (30)	8 (36)	11(26)
Permanent visual loss	1 (3)	3 (13.6)	2 (4.7)
Amaurosis fugax	6 (20)	8 (36)	11 (26)
Stroke	2 (6.6)	1 (4.5)	3 (7)
Polymyalgia rheumatica	7 (23)	7 (32)	10 (24)

*Abnormal temporal arteries at physical examination (painful, swollen, indurated and/or with decreased or absent pulsation)

Biological findings	**Mean ±SD**	**Mean ±SD**	**Mean ±SD**
Erythrocyte sedimentation rate (mm/h)	85.8+/-25	84+/-28	77.8+/-26
C-Reactive Protein (mg/L)	102.2+/-70.3	92.6+/-66	86.2+/-78
Platelet count (x 10^9/L)	476+/-157	484+/-162	448+/-150
Haemoglobin (g/L)	11.5+/-1.6	12.2+/-1.4	11.8+/-1.7

Supplemental methods

Reagents

Immunohistochemistry and western blotting were performed with rabbit anti-NGF, -BDNF, -NT-3, -TrkA, -TrkB, -TrkC, -$p75^{NTR}$ and goat anti-sortilin antibodies (Ab) (Santa Cruz, Heidelberg, Germany) at 1:100 for immunohistochemistry and 1:200 for western-blotting dilutions. Proliferation and migration assays were studied using exogenous NGF (Alomone Labs, Jerusalem, Israel), recombinant human BDNF (Promega, Madison, Wisconcin, USA), or PDGF (R&D Systems, Minneapolis, Minnesota, USA), alone or both with K252a, a pharmacological Trk inhibitor (Alomone), or an anti-$p75^{NTR}$ antagonist Ab (Alomone).

Cell culture

Cultures of TASMCs were performed in Smooth Muscle Cell Basal Medium (PromoCell, Heidelberg, Germany) supplemented with FCS (5%), insulin (5 µg/mL), basic fibroblast growth factor (2 ng/mL), epidermal growth factor (0.5 ng/ml) and streptomycin/penicillin (1%) at 37°C in 5% CO_2.

Western blotting

Proteins (50 µg/lane) obtained from whole-cell lysates of TASMCs using lysis buffer 7 were separated on 10–12% SDS-polyacrylamide gels (Invitrogen, Carlsbad, California, USA) and transferred onto PVDF membranes (Millipore, Billerica, Massachusetts, USA). After saturation (5% nonfat dry milk, 0.1% Tween in PBS), rabbit anti-NGF, -BDNF, -NT-3, -TrkA, -TrkB, -TrkC, -p75NTR and goat anti-sortilin antibodies (Ab) (Santa Cruz, Heidelberg, Germany) were used at 1/200 dilution, incubated overnight at 4°C, and revealed after 1 h incubation at RT with anti-rabbit or goat Ig-HRP-conjugated Ab (Santa Cruz, dilution 1/1000) by chemiluminescence (ECL reagent; Amersham Little Chalfont, UK). Protein-loading control was performed with anti-actin Ab (Santa Cruz, 1/10,000). Western blots were scanned using a bioimaging system (Genesnap; Syngene, Cambridge, UK).

Immunohistochemistry

Immunohistochemistry was performed on paraffin-embedded sections of TA deparaffinised, rehydrated and subjected to steam-heat antigen retrieval in citrate buffer in a microwave oven (750 W). Endogenous peroxidases were inhibited with 5% H_2O_2 in methanol and non-specific sites were blocked with PBS-3% bovine serum albumin. The primary Ab as above were incubated at a 1/100 dilution overnight at 4°C and revealed with the anti-rabbit HRP Envision™ (Dako, Glostrup, Denmark). After counterstaining, the slides were studied with a Leica microscope (×200 magnification). Immunostaining was scored using a staining index based on the percentage of positive cells. The results were expressed as the mean of three independent quantifications made by two different observers.

Cell viability and proliferation assay

Cell viability of TASMCs was assessed using the colorimetric XTT assay (Cell Proliferation Kit II, XTT Roche, Basel, Switzerland) according to the manufacturer's instructions. A range of concentrations was evaluated for each of the conditions studied. Efficient concentrations were defined as follows: NGF (10 ng/mL), BDNF (200 ng/mL), K252a Trk inhibitor (100 ng/mL), anti-$p75^{NTR}$ antagonist Ab (10 mg/mL) and PDGF (40 ng/mL), which was used as a positive control.

Table 1: Primers used in qPCR and RT-PCR studies

Genes	Accession number	qPCR Primers (3'6FAM-MGBNFQ5')	RT-PCR primers	Length (bp)	TM (°C)
NGF	NM_002506.2	Hs01113193_m1	**F:** ATACAGGCGGAACCACACTC **R:** TGCTCCTGTGAGTCCTGTTG	**313**	**58**
BDNF	NM_001143810	Hs.00380947_m1	**F:**TACTTTGGTTGCATGAAGGCTCC **R:**ACTTGACTACTGAGCATCACCCTG	**266**	**58**
NT-3	NM_001102654	Hs00267375_s1	**F:** TGGCATCCAAGGTAACAACA **R:** GGTGTCCATTGCAATCACTG	**229**	**58**
TrkA	NM_002507	Hs01021011_m1	**F:** TCAACAAATGTGGACGGAGA **R:** GTGGTGAACACAGGCATCAC	**197**	**58**
TrkB	NM_001018064.1	Hs.01093096_m1	**TrkB145** **F:** AGGGCAACCCGCCCACGGAA **R:** GGATCGGTCTGGGGAAAAG	**571**	**62**
			TrkB 95 **F:**GTTTCATAAGATCCCACTGGA **R:**TGCTGCTTAGCTGCCTGAGAG	**261**	**58**
TrkC	NM_001243101	Hs00176797_m1	**F:** ACTTCCGTCAGGGACACAAC **R:** CCTCCCTCTGGAAATCCTTC	**219**	**58**
$p75^{NTR}$	NM_002507	Hs.00609976_m1	**F:** GTGGGACAGAGTCTGGGTGT **R:** AAGGAGGGGAGGTGATAGGA	**200**	**58**
Sortilin	NM_002959	Hs.00907094_m1	**F:** GCTGGTCACAGTCGTAGCAG **R:** TTAGTGTGGGAGGCTGTGTC	**150**	**60**
GAPDH			**F:**GGGTGGAATCATATTGGAACATG **R:** GTCGGAGTCAACGGATTTGG	**150**	**58**
HPRT	NM_000194	Hs.02800695_m1			

F: Forward, R: Reverse

Supplemental data

Figure 1

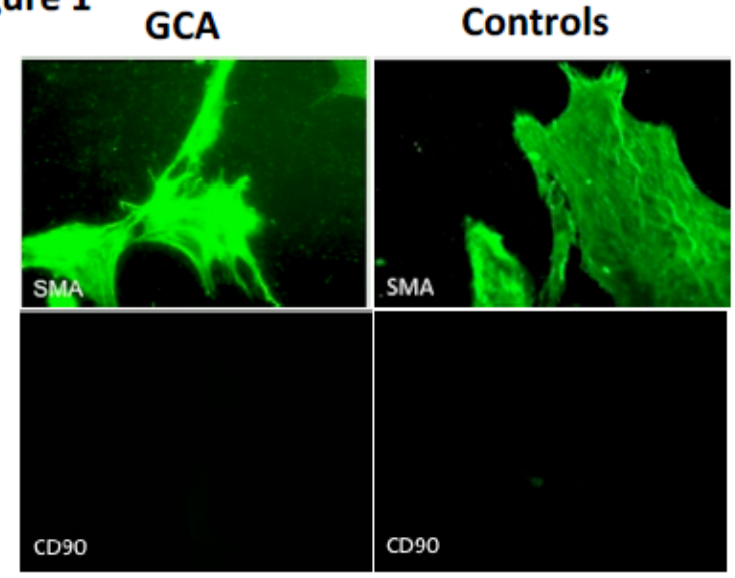

Figure 1 : VSMC phenotype in immunocytochemistry assay. GCA patients (n=6) and controls (n=10) TASMC used for experiments exhibit positive SMA staining and negative CD90 staining.
Panels are representatives examples of immunocytochemsitry images. SMA: α smooth actin, CD90: fibroblast marker

Figure 2

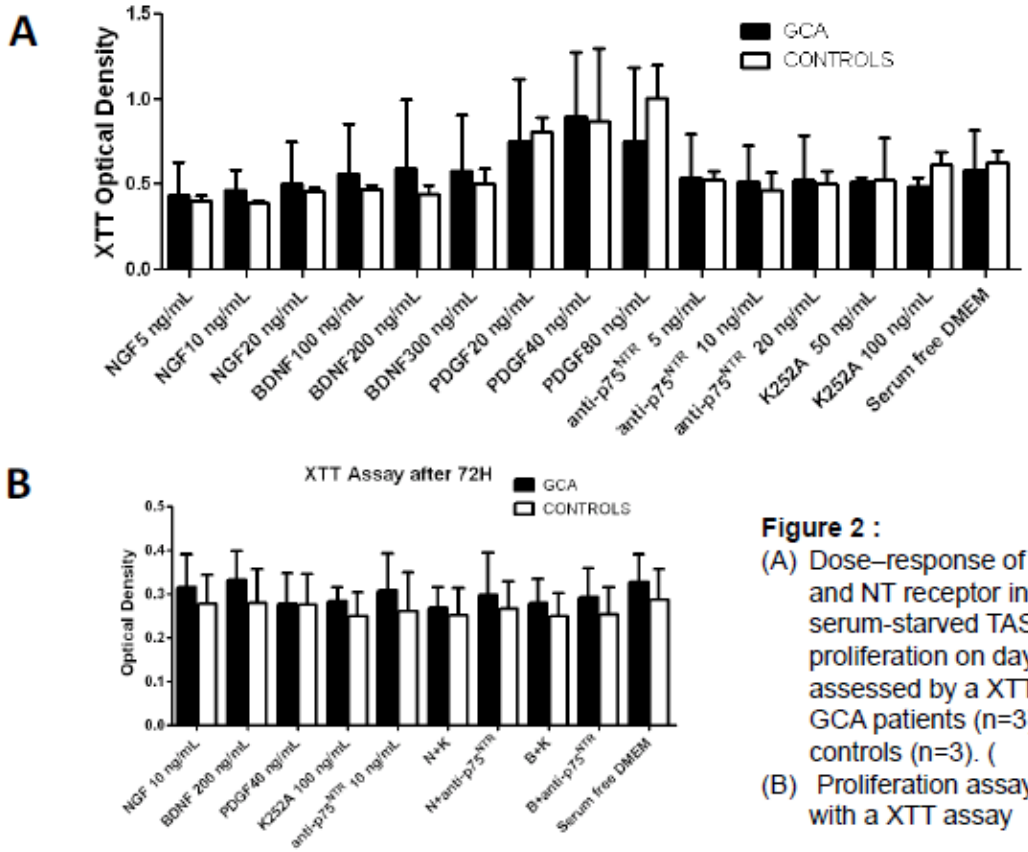

Figure 2 :
(A) Dose–response of NGF, BDNF and NT receptor inhibitors on serum-starved TASMC proliferation on day 3 assessed by a XTT assay in GCA patients (n=3) and controls (n=3). (
(B) Proliferation assay performed with a XTT assay

Figure 3

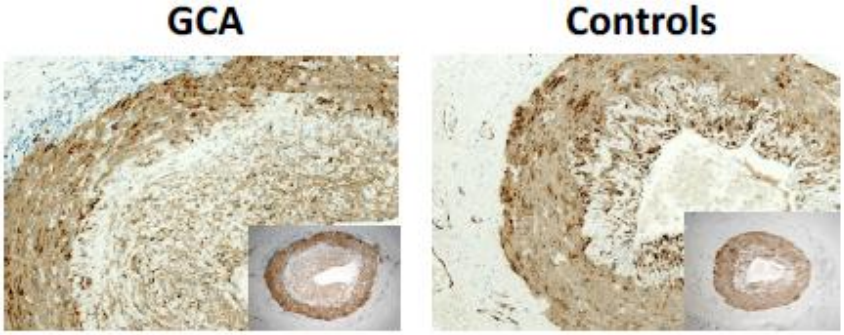

Figure 3 : Immunostaining of actin in temporal arteries from GCA patients (*n*=22) compared to controls (*n*=21). Panels are representative examples of immunohistological images (x50 and x200)

Figure 4

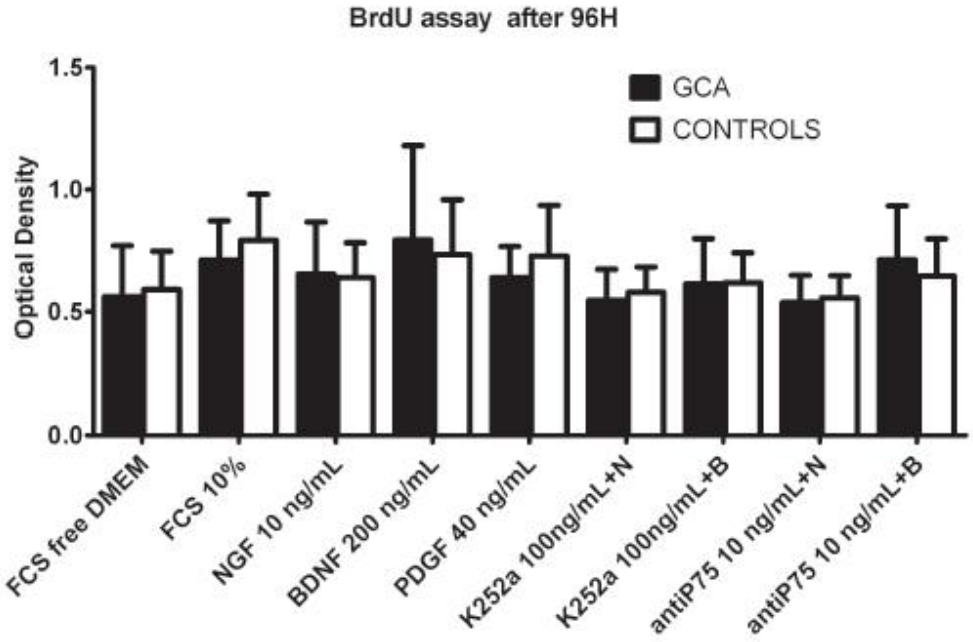

Figure 4: Effects of NTs and the inhibitors of Trk (K252a), Tr:kB (ANA-12) and $P75^{NTR}$ (antiP75) on TASMC proliferation in GCA patients and controls. Proliferation assay performed with a BrdU assay on days 4 in serum-starved TASMC incubated with NT or NT-receptor inhibitors, or a combination of NT and NT-inhibitor receptors, in GCA patients (*n*=6) and controls (*n*=10).

Clinical Immunology (2014) 153, 123–135

available at www.sciencedirect.com

Clinical Immunology

www.elsevier.com/locate/yclim

Identification of target antigens of anti-endothelial cell antibodies in patients with anti-neutrophil cytoplasmic antibody-associated vasculitides: A proteomic approach

Alexis Régent[a,b], Sébastien Lofek[a,1], Hanadi Dib[a,1], Guillaume Bussone[b], Nicolas Tamas[a], Christian Federici[a,c], Cédric Broussard[a,c], Loïc Guillevin[a,b], Luc Mouthon[a,b,*]

[a] *Institut Cochin, INSERM U1016, CNRS UMR 8104, Université Paris Descartes, 22 rue Méchain, 75014 Paris, France*
[b] *Pôle de Médecine Interne, Centre de Référence pour les vascularites nécrosantes et la sclérodermie systémique, Hôpital Cochin, Assistance Publique-Hôpitaux de Paris, 27 rue du Faubourg Saint-Jacques, F-75679 Paris Cedex 14, France*
[c] *Plate-forme Protéomique 3P5, Université Paris Descartes, Sorbonne Paris Cité, 22 rue Méchain, 75014 Paris, France*

Received 29 August 2013; accepted with revision 31 March 2014
Available online 12 April 2014

KEYWORDS
Anti-neutrophil cytoplasmic antibodies;
Autoantibodies;
Human umbilical vein endothelial cell;
Vasculitides;
Lamin;
Erk

Abstract Anti-endothelial cell antibodies (AECAs) have been reported to cause endothelial cell dysfunction, but their specific targets have never been identified in anti-neutrophil cytoplasmic antibody (ANCA)-associated vasculitides (AAVs). Proteins from human umbilical vein endothelial cells (HUVECs) were separated by 2-dimensional electrophoresis (2-DE). 2-D immunoblots were used to compare serum IgG reactivities from 30 patients with AAV and 12 healthy controls (HCs). Proteins identified as target antigens by MALDI- TOF-TOF mass spectrometry included lamin A/C, vimentin, α-enolase, far upstream binding protein 2 (FUBP2) and protein disulfide-isomerase A3 precursor (PDIA3). Antibodies targeting lamin A, vimentin, α-enolase, FUBP2 and PDIA3 were identified in 57.1%, 64.3%, 35.7%, 50% and 0% of patients with microscopic polyangiitis and 8%, 3.3%, 7.2%, 0% and 6.7% of HCs respectively. IgG from patients with microscopic polyangiitis had stronger reactivity against HUVEC than other groups and HCs and induced stronger Erk phosphorylation in HUVECs than IgG from HCs.

* Corresponding author at: INSERM U1016, CNRS UMR 8104, 8 rue Mechain, 75014 Paris, France. Fax: +33 1 44 41 25 46.
E-mail addresses: alexisregent@hotmail.com (A. Régent), sebastien.lofek@gmail.com (S. Lofek), hanadi_dib@hotmail.fr (H. Dib), guillaume.bussone@cch.aphp.fr (G. Bussone), nicolas.tamas@parisdescartes.fr (N. Tamas), christian.federici@inserm.fr (C. Federici), cedric.broussard@inserm.fr (C. Broussard), loic.guillevin@cch.aphp.fr (L. Guillevin), luc.mouthon@cch.aphp.fr (L. Mouthon).
[1] Both authors contributed equally to the work.

http://dx.doi.org/10.1016/j.clim.2014.03.020
1521-6616/

1. Introduction

Granulomatosis with polyangiitis (GPA) (formerly Wegener's granulomatosis), eosinophilic granulomatosis with polyangiitis (EGPA) (formerly Churg-Strauss syndrome) and microscopic polyangiitis (MPA) are pauci-immune necrotizing vasculitides of small-sized vessels associated with anti-neutrophil cytoplasmic antibodies (ANCAs). The immunofluorescence pattern distinguishes cytoplasmic ANCA, which usually targets proteinase 3 (PR3), and perinuclear ANCA, targeting myeloperoxydase (MPO). The spectrum of ANCA-associated vasculitides (AAVs) is wide, and the main clinical manifestations involve the eye, nose, throat, lung, kidney, skin, muscle, joints and peripheral nervous system [1].

In vitro, ANCAs trigger the activation, degranulation and apoptosis of neutrophils, which then cause endothelial cell (EC) damage [2]. Thus, evidence has been obtained for the pathogenic role of ANCAs in vitro and in vivo, mostly involving anti-MPO antibodies, although other mechanisms including B-cell and T-cell activations and granuloma formation occur during AAVs [3]. Recent advances have been made in the treatment of AAVs with the demonstration in 2 prospective randomized studies that rituximab, a chimeric anti-CD20 monoclonal antibody targeting B cells, is as effective as oral and/or intravenous cyclophosphamide [4,5], which emphasizes the pathogenic role of B cells and auto-antibodies.

Interestingly, not all patients with AAVs have detectable ANCAs, and other autoantibodies are probably involved in these conditions. Thus, anti-EC antibodies (AECAs), described in other conditions such as systemic lupus erythematosus [6], systemic sclerosis and pulmonary arterial hypertension [7], have been detected in patients with AAVs. Although the pathogenic role of AECAs remains controversial [8], AECAs have been reported to induce the expression of vascular adhesion protein 1 and major histocompatibility complex (MHC) class I-related antigen A [9] and mediate antibody-dependent cellular cytotoxicity in AAVs [10]. A few target antigens of AECAs have been identified in patients with AAVs and include PR3 and MPO, which may be adsorbed at the surface of ECs. To uncover the target antigens of these AECAs in patients with AAVs, we used 2-D electrophoresis (2-DE), then immunoblotting with proteins of HUVECs and identified proteins involved in cytoskeleton, cell energy metabolism, and other key cellular pathways. Importantly, these target antigens are linked to transforming growth factor β (TGF-β) and the mitogen associated protein kinase (MAPK) family. We confirmed by ELISA tests that α-enolase, vimentin, lamin A and far upstream binding protein 2 (FUBP2) were target antigens of AECAS. Finally, we demonstrated that purified serum IgG from patients with MPA induced stronger Erk phosphorylation than IgG from healthy controls (HCs).

2. Methods

2.1. Patient sera

Sera were obtained from 46 patients with AAVs, including 15 with GPA, 14 with MPA and 17 with EGPA fulfilling the classification criteria of the American College of Rheumatology and/or the Chapel Hill nomenclature [11]. Disease activity was evaluated by the Birmingham vasculitis activity score (BVAS). Vasculitides was considered active with BVAS ≥ 3 [12]. Sera from 30 patients including 12 with GPA, 9 with EGPA and 9 with PMA were used for proteomic experiments. Twenty five patients had active vasculitides, as assessed by BVAS ≥ 3 and mean disease duration 65 months (range 0–240 months), and 18 patients had detectable ANCAs targeting PR3 or MPO at the time of blood sampling (Additional File 1).

For proteomic experiments, sera were pooled by groups of 3 according to disease type and/or disease activity. Thus, we tested 10 pools of sera from patients: 4 pools from patients with GPA, 3 from patients with MPA, and 3 from patients with EGPA. A pool of sera from 12 HCs was used as a control. All patients and healthy controls gave a written informed consent. Sera were collected with approval of the ethics committee of the "groupe hospitalier Pitié-Salpêtrière" and the study conforms to the principles outlined in the Declaration of Helsinki.

2.2. Cell culture

HUVECs were isolated by digestion of freshly obtained umbilical cords and cultured with microvascular EC growth medium (Promocell, Heidelberg, Germany) as previously described [7,13,14]. Cells at passage 2 were harvested for protein extraction. Immunofluorescence assays were performed at the 3rd passage in multiple chamber slides (Millipore, Billerica, MA, USA).

2.3. Indirect immunofluorescence

Endohelial cells were fixed with 4% paraformaldehyde, washed with phosphate buffer saline (PBS), incubated with sera from patients or healthy controls at a 1:100 dilution for 1 h 30 min at room temperature and finally washed twice with PBS. A goat anti-human IgG secondary antibody conjugated with FITC (Invitrogen, Carlsbad, CA, USA) was then added for 1 h at room temperature. Slides were mounted with a mounting medium containing 4′,6′-diamidino-2-phenylindole (Vector Laboratories, Burlingame, CA, USA) and cells visualized under a Zeiss Axio Observer.Z1 microscope equipped for fluorescence (Carl Zeiss, Oberkochen, Germany). All slides from each single experiment were visualized at the same time of exposure. Corrected total cell fluorescence (CTCF) was obtained with Image J and corresponds to cell fluorescence corrected by background noise.

2.4. 2-D immunoblotting

2.4.1. Protein extracts

HUVECs were stored at −80 °C in 1 mM phenylmethanesulfonylfluoride (PMSF) and protease inhibitors (Complete Mini, Roche Diagnostics, Meylan, France). Protein extraction was performed as described [15] and detailed in the Additional File 2. Briefly, cells were suspended at 10^6/ml in a sample solution extraction kit (Kit 3; Bio-Rad, Hercules, CA, USA). Cells were sonicated and the supernatant was collected after ultracentrifugation (Ultracentrifuge Optima L90K; Beckman Coulter, Fullerton, CA, USA) at 150,000 *g* for 25 min at 4 °C.

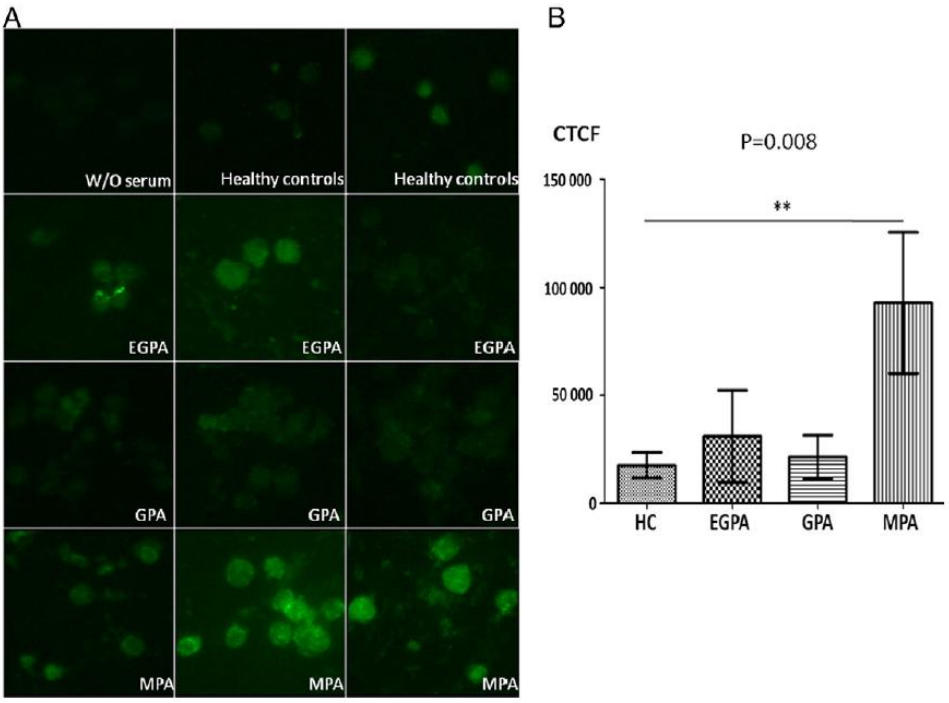

Figure 1 Immunofluorescence on unpermeabilized HUVEC with serum from patients with ANCA associated vasculitides and healthy controls. Representative immunofluorescence obtained from 2 healthy controls (HCs), 3 patients with GPA, 3 with EGPA and 3 with MPA in addition to the negative control (without any serum) is shown in panel A. Corrected total cell fluorescence of HUVECs with serum from 5 patients each with MPA, GPA, EGPA and 5 HCs is depicted in panel B (mean ± standard derivation). Comparison was performed with a Mann–Whitney test. CTCF: corrected total cell fluorescence.

Protein quantification involved the Lowry method [16]. The supernatant was aliquoted and stored at −80 °C.

2.4.2. 2-DE

2-DE, immunoblotting, and protein identification by mass spectrometry (MS) were performed as previously reported [17,18] and detailed in the Additional File 2. The experimental design is detailed in Additional File 3.

2.5. Modelling with ingenuity pathway analysis

To gain insight into the biological pathways and networks significantly represented in our proteomic datasets, we used ingenuity pathway analysis (IPA; Ingenuity Systems, Redwood City, CA, USA). IPA selects "focus proteins" for generating biological networks. Focus proteins are proteins from datasets that are mapped to corresponding gene objects in the Ingenuity Pathway Knowledgebase (IPKB) and are known to interact with other proteins from published, peer-reviewed content in the IPKB. From these interactions, IPA builds networks with a size of no more than 35 genes or proteins. A *P*-value for each network is calculated according to the fit of the user's set of significant genes/proteins. IPA computes a score for each network from the *P*-value that indicates the likelihood of the focus proteins in a network being found together due to chance. We selected only networks with score ≥ 2, with $P < 0.01$ of not being generated by chance. Biological functions were assigned to each network by the use of annotations from scientific literature and stored in the IPKB. Fisher exact test was used to calculate the *P*-value determining the probability of each biological function/disease or pathway being assigned by chance. We used $P \leq 0.05$ to select highly significant biological functions and pathways represented in our proteomic datasets. The build function of IPA allows for generating pathways that can complete the data analysis by showing interactions of identified proteins with a specific group of molecules.

2.6. ELISA

We coated 96-well plates (Maxisorb, Nunc, Denmark) with 6 μg/mL for lamin A (Abcam, Cambridge, UK), 5 μg/ml for vimentin (Tebu-bio, Le Perray-en-Yvelines, France), 4 μg/ml for FUBP2 (Tebu-bio), 4 μg/ml for phophodiesterase A3 precursor (PDIA3) (Abcam) and 4 μg/mL for α-enolase in bicarbonate buffer overnight at 4 °C. Plates were then saturated with PBS and 1% bovine serum albumin (BSA) for 1 h at room temperature. Sera diluted with PBS (1:100) were incubated for 60 min at room temperature and washed 3 times with PBS. Plates were then incubated with 1/1000 mouse anti-human AP-conjugated secondary antibody (Rockland, MA, USA) for 30 min at room temperature and washed 3 times with PBS. Optical density (OD) was read with an ELISA reader. A positive test was defined by the mean OD of healthy control + 2 or 3 standard deviations.

Table 1 Mass spectrometry data of HUVEC specific target antigens in patients with granulomatosis with polyangiitis.

ID	Identification	Swiss Prot accession no.	Estimated/ theoretical pI	Estimated/ theoretical MW (kDa)	Total ion score	Best ion score	No. of unique identified peptides [a]
363	Far upstream element-binding protein 2	FUBP2_HUMAN	7.4/6.8	96/73	389/79	64/33	10/3
421	No identified protein		6.3/	86/			
429	No identified protein		6.7/	85/			
430	No identified protein		6.8/	85/			
438	Caldesmon	CALD1_HUMAN	6.6/5.6	83/93	123	66	2
461	Lamin-A/C	LMNA_HUMAN	7.3/6.6	80/74	573	82	11
	Semaphorin-4D precursor	SEM4D_HUMAN	7.3/8.3	80/96	44	29	2
472	No identified protein		6.6/	79/			
473	No identified protein		6.7/	80/			
631	No identified protein		6.9/	71/			
646	Lamin-A/C	LMNA_HUMAN	7.0/6.6	70/74	223/604	49/87	7/13
703	No identified protein		5.9/	65			
768	No identified protein		7.9/	60			
784	No identified protein		7.3	59			
791	No identified protein		6.4/	58/			
809	Protein disulfide-isomerase A3 precursor	PDIA3_HUMAN	6.1/6.0	56/57	778/97	105/ 37	11/3
814	Protein disulfide-isomerase A3 precursor	PDIA3_HUMAN	6.0/6.0	56/57	278	63	6
831	T-complex protein 1 subunit beta	TCPB_HUMAN	6.8/6.0	55/57	797	117	10
	Cytosol aminopeptidase	AMPL_HUMAN	6.8/8.0	55/56	253	64	6
908	Alpha-enolase	ENOA_HUMAN	8.3/7.0	50/47	450/34	143/ 18	7/2
946	Alpha-enolase	ENOA_HUMAN	7.0/7.0	50/47	175	73	4
950	Tripeptidyl-peptidase 1 precursor	TPP1_HUMAN	6.4/6.0	50/61	79	34	3
971	26S protease regulatory subunit 7	PRS7_HUMAN	6.6/5.7	50/49	93	31	4
997	26S protease regulatory subunit 8	PRS8_HUMAN	7.7/7.1	49/46	321	75	7
1013	No identified protein		8.3/	49/			
1116	No identified protein		6.9/	43/			
1134	Poly(rC)-binding protein 1	PCBP1_HUMAN	7.4/6.7	42/37	331	95	9
1138	Sialic acid synthase	SIAS_HUMAN	7.0/6.3	42/40	161	67	4
1142	26S proteasome non-ATPase regulatory subunit 7	PSD7_HUMAN	6.8/6.3	42/37	122	57	4
1189	Heterogeneous nuclear ribonucleoprotein A/B	ROAA_HUMAN	7.0/8.2	39/36	62	32	2
1214	PDZ and LIM domain protein 1	PDLI1_HUMAN	7.4/6.6	37/36	87/269	62/62	2/5
1249	60S acidic ribosomal protein P0	RLA0_HUMAN	6.0/5.7	37/34	20/55	20/39	1/2
	Glyceraldehyde-3-phosphate dehydrogenase	G3P_HUMAN	6.1/8.6	37/36	128	85	2
1404	Proteasome subunit alpha type-1	PSA1_HUMAN	6.8/6.2	31/30	128	71	3
1415	Ran-specific GTPase-activating protein	RANG_HUMAN	5.6/5.2	30/23	28	28	1 [b]
2123	No identified protein		9.3/	33/			

ID: identity; kDa: kilodalton; MW: molecular weight.

[a] Number of unique identified peptides in MS/MS and MS + MS/MS searches.
[b] Identification spectrum is given in Additional File 7.

2.7. ERK1/2 immunoblotting

IgG from patients and healthy controls were purified with protein G sepharose beads. At passage 3, HUVECs were incubated for 10 min with 0.1 mg/mL purified serum IgG from patients with MPA and HCs and without any serum. Protein extraction and 1D electrophoresis were performed as described by Regent et al. [15]. After migration in a 12% polyacrylamide gel, proteins were transferred to PVDF (Immobilon-P) membrane (Millipore, Bedford, MA) for 40 min. Membranes were blocked with 0.1% tween–5% milk–PBS solution for 1 h. Blotting was performed with rabbit anti-human-Erk1/2

Table 2 Mass spectrometry data of HUVEC specific target antigens in patients with microscopic polyangiitis.

ID	Identification	Swiss Prot accession no.	Estimated/ theoretical pI	Estimated/ theoretical MW (kDa)	Total ion score	Best ion score	No. of unique identified peptides[a]
518	78 kDa glucose-regulated protein precursor	GRP78_HUMAN	5.4/5.1	75/72	1210/ 952	144/ 128	13/11
550	No identified protein		6.0/	75			
570	No identified protein		5.9/	75			
740	Vimentin	VIME_HUMAN	5.7/5.1	61/54	277/ 234	66/97	7/3
	Heterogeneous nuclear ribonucleoprotein K	HNRPK_HUMAN	5.7/5.4	61/51	225	69	5
	Desmin	DESM_HUMAN	5.7/5.2	61/54	57	32	2
	60 kDa heat shock protein, mitochondrial precursor	CH60_HUMAN	5.7/5.7	61/54	948	208	9
	T-complex protein 1 subunit epsilon	TCPE_HUMAN	5.8/5.5	61/60	238/ 305	77/82	6/8
797	Protein disulfide-isomerase A3 precursor	PDIA3_HUMAN	6.3/6.0	57/57	773/ 712	143/ 121	10/10

ID: Identity; kDa: kilodalton; MW: molecular weight.

[a] Number of unique identified peptides in MS/MS and in MS + MS/MS searches.

Table 3 Mass spectrometry data of HUVEC specific target antigens in patients with eosinophilic granulomatosis with polyangiitis.

ID	Identification	Swiss Prot accession no.	Estimated/ theoretical pI	Estimated/ theoretical MW (kDa)	Total ion score	Best ion score	No. of unique identified peptides[a]
391	No identified protein		5.4/	90/			
461	Lamin-A/C	LMNA_HUMAN	7.3/6.6	80/74	573	82	11
	Semaphorin-4D precursor	SEM4D_HUMAN	7.3/8.3	80/96	44	29	2
570	No identified protein		5.9/	75/			
631	No identified protein		6.9/	71/			
646	Lamin-A/C	LMNA_HUMAN	7.0/6.6	70/74	223/ 604	49/87	7/13
713	Stress-induced-phosphoprotein 1	STIP1_HUMAN	6.6/6.4	64/63	67	41	2
803	Nicotinamide phosphoribosyltransferase	NAMPT_HUMAN	7.6/6.7	57/55	172	53	5
814	Protein disulfide-isomerase A3 precursor	PDIA3_HUMAN	6.0/6.0	56/57	278	63	6
944	No identified protein		7.5/	48/			
1054	No identified protein		8.2/	46/			
1055	No identified protein		9.2/	46/			
1277	No identified protein		6.3/	37/			
1492	Endoplasmic reticulum protein ERp29 precursor	ERP29_HUMAN	6.6/6.8	28/29	331	83	5
1603	No identified protein		6.8/	25/			
1652	No identified protein		8.3/	22/			
2124	No identified protein		9.1/	37/			
2153	Lamin-A/C	LMNA_HUMAN	7.5/6.6	70/74	202	53	6
	Heterogeneous nuclear ribonucleoprotein L	HNRPL_HUMAN	7.5/6.7	70/60	52	36	2

ID: identity; kDa: kilodalton; MW: molecular weight.

[a] Number of unique identified peptides in MS/MS and in MS + MS/MS searches.

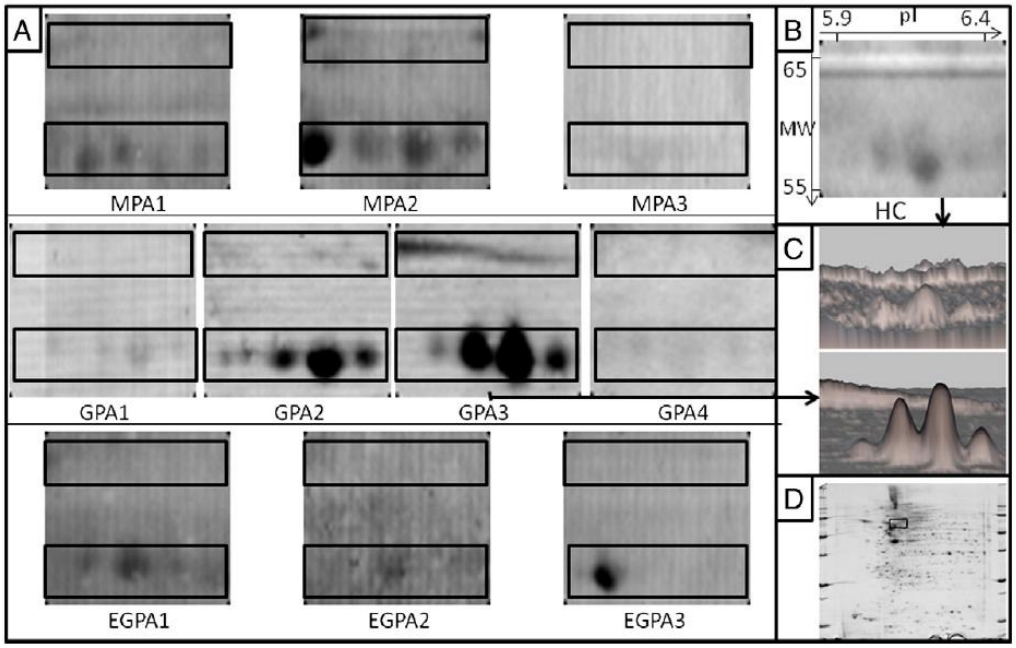

Figure 2 Serum IgG reactivity to protein disulfide-isomerase A3 precursor in sera for patients with ANCA-associated vasculitides. Protein extracts were obtained from human umbilical vein endothelial cells (HUVECs) and protein disulfide-isomerase A3 precursor (PDIA3) was identified in different protein spots (within the 2 rectangles). (A) IgG reactivity to PDIA3 in 3 different pools of sera from patients with microscopic polyangiitis (MPA1 to 3), 4 from patients with granulomatosis with polyangiitis (GPA1 to 4) and 3 from patients with eosinophilic granulomatosis with polyangiitis (EGPA1 to 3) and (B) one pool from 12 healthy controls (HCs). (C) PDIA3 spots expressed in 3-D view for one representative serum pool for patients (bottom) and the HC pool (top). (D) HUVEC proteome showing the localization of PDIA3 spots in A.

antibodies (Cell Signaling Technology, Danvers, MA) diluted 1/2000 and rabbit anti-human-P-ERK1/2 antibodies (Cell Signaling Technology) diluted 1/1000 and rabbit anti-human anti-vinculin antibodies (Sigma-Aldrich, St Louis, MO) diluted 1/2000 at 4 °C overnight. After a washing step, mouse anti-rabbit secondary antibodies (Sigma-Aldrich) diluted 1/2500 were incubated for 60 min at room temperature. Reactivity was revealed by enhanced chemoluminescence.

2.8. Statistical analysis

For indirect immunofluorescence experiments, corrected total cell fluorescence was compared between 5 representative patients in each group with a Mann–Whitney test. For Elisa tests, comparison between patients and controls was realized with a two side Fisher's exact test.

3. Results

3.1. Indirect immunofluorescence

Using indirect immunofluorescence on unpermeabilized HUVECs, we observed that AECAs from patients with AAVs bind to the cell membranes with stronger reactivity than healthy controls. Despite individual variation, the intensity of immunofluorescence was more important in the case of patients with MPA than in the case of patients with GPA or EGPA (Fig. 1 and Additional File 4).

3.2. Target antigen identification

HUVEC proteins were separated on 2-DE (immobilized pH gradient 3–10; 7–18% polyacrylamide gel electrophoresis); 888 distinct protein spots were detected on silver nitrate staining. Most of the protein spots were detected at pI 4.5–8 and 15–100 kDa. A total of 878 ± 196 spots were successfully transferred onto polyvinylidene fluoride membranes.

Serum IgG antibodies recognized 85 protein spots in the sera pool for the 12 HCs and a mean of 134 ± 65 different protein spots in the pools from patients with AAVs. Most of the spots were recognized in one pool for each group. We thus focused on proteins recognized in at least 3 of 4 pools for patients with GPA and 2 of 3 pools for patients with MPA or EGPA and not by HCs. We identified 33 different protein spots, corresponding to 20 distinct proteins, including lamin A/C and α − enolase, in at least 3 of 4 sera pools for patients with GPA (Table 1) but only 5 different protein spots, corresponding to 7 distinct proteins, in 2 of 3 sera pools for patients with MPA (Table 2). In addition, we identified 17 protein spots, corresponding to 8 distinct proteins, in sera pools for patients with EGPA (Table 3). Most of the 330 spots recognized by sera pools from patients with AAVs were recognized by only a few pools. At least 6 of 10 pools recognized

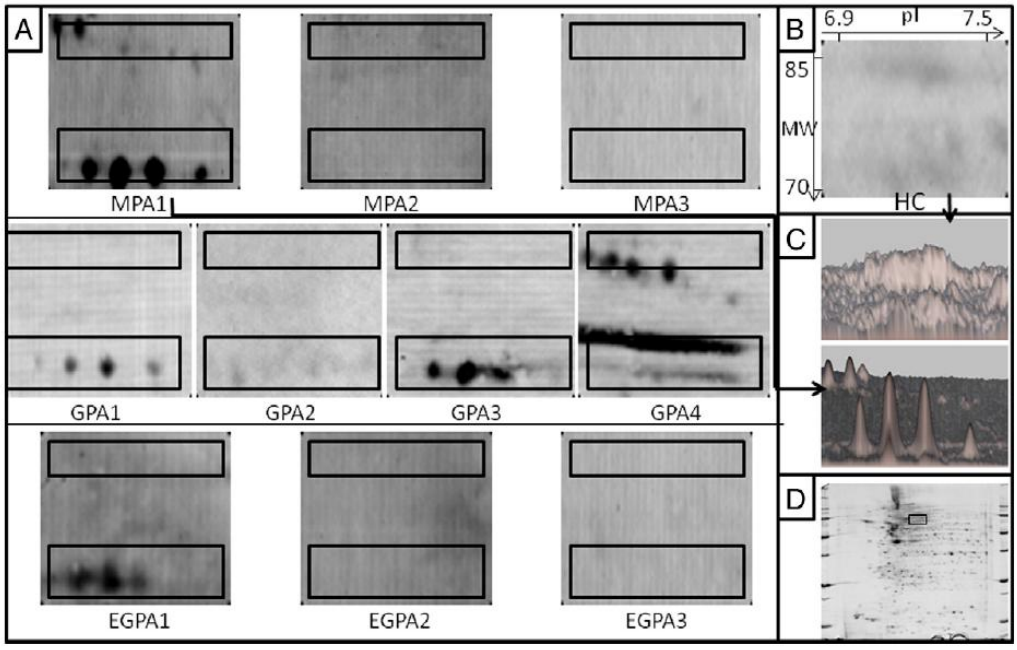

Figure 3 Serum IgG reactivity to lamin A/C in sera from patients with ANCA associated vasculitides. Protein extract was from HUVECs. Lamin A/C was identified in different protein spots (within the 2 rectangles). (A) IgG reactivity to lamin A/C in 3 different pools of sera from patients with microscopic polyangiitis (MPA1 to 3), 4 from patients with granulomatosis with polyangiitis (GPA1 to 4) and 3 from patients with eosinophilic granulomatosis with polyangiitis (EGPA1 to 3) and (B) one pool from 12 healthy controls (HCs). (C) Lamin spots in 3-D view for one representative serum pool of patients (bottom) and the HC pool (top). (D) Proteome of HUVECs showing the localization of lamin A/C spots in A.

10 different spots; identified proteins included lamin A/C and protein disulfide-isomerase A3 precursor (Additional file 5). These proteins were identified in several protein spots and reactivity against protein disulfide-isomerase A3 precursor and lamin A/C is depicted in Figs. 2 and 3, respectively.

3.3. Ingenuity pathway analysis

Lists of HUVEC antigens identified as targets of IgG in sera from patients with AAVs were analyzed by IPA. Interestingly, TGF-β and members of the MAPK family, including JUN, extracellular signal-regulated kinase 1/2 and p38MAPK, were associated with a large number of target antigens of AECAs. A simplified network is in Fig. 4 and the merged network of the three networks generated by IPA analysis is in Additional File 6.

3.4. ELISA

Antibodies targeting lamin A, vimentin, α-enolase, FUBP2 and PDIA3 were identified in 26.7%, 26.1%, 34.9%, 23.9% and 2.2% of patients with ANCA associated vasculitis versus 8%, 3.3%, 7.2%, 0% and 6.7% of HCs respectively. Interestingly, patients with MPA had stronger reactivity against tested antigens than other groups and HCs. Detailed results of ELISA tests are depicted in Table 4 and Fig. 5 and comparison of ELISA results with immunofluorescence assay is in Additional File 4.

3.5. Erk 1/2 activation

In order to confirm the role of IgG AECAs in the activation of MAPK pathway, we incubated HUVEC with IgG purified from the serum of patients with MPA and HCs. Interestingly, as depicted in Fig. 6, we could confirm that IgG from patients with MPA induced increased Erk1/2 phosphorylation compared to IgG from HCs.

4. Discussion

Here, we report on the identification of target antigens of AECAs in patients with AAVs by 2-D immunoblotting and MS. The identified antigens are involved in cytoskeleton organization, energy production and cell metabolism. Among others, target antigens of AECAs include lamin A/C, α-enolase, far upstream binding protein 2 and vinculin and we confirm the presence of auto-antibodies targeting these antigens with ELISA in patients with AAVs as compared to healthy controls. Patient IgG binds to unpermeabilized HUVECs in IF experiments with a variable intensity among individuals in a group and among groups. Interestingly patients with MPA expressed the strongest reactivity either in IF or ELISA experiments. This result is probably important since MPA seems more and more to be distinguished from GPA and EGPA, particularly regarding the specificity of autoantibodies and their potential role in the pathogenesis [19]. In addition, we could confirm that purified

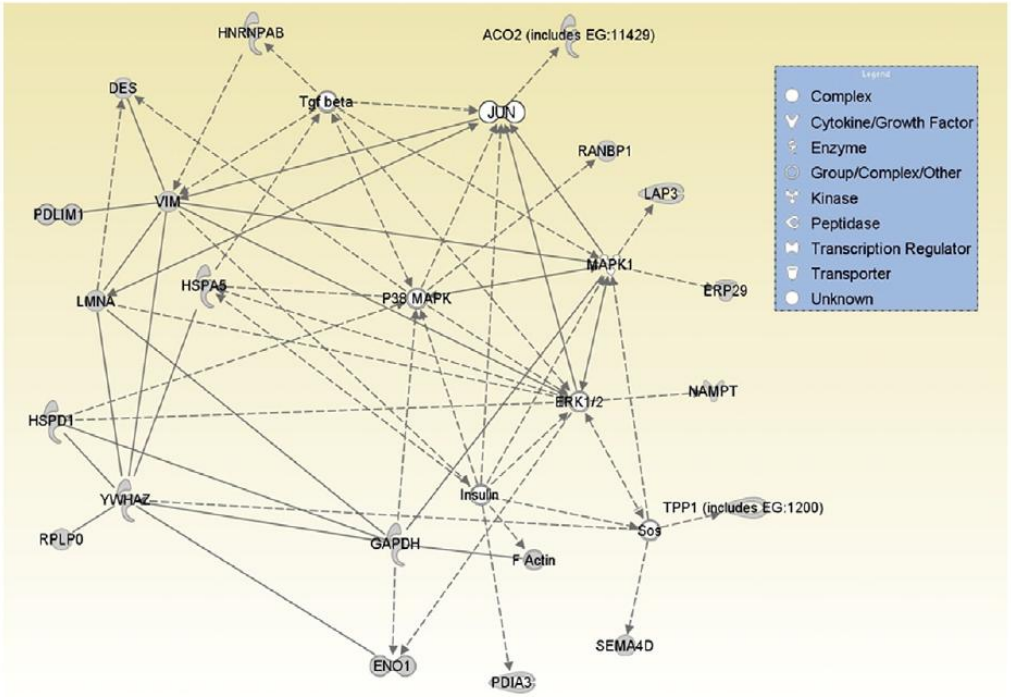

Figure 4 Simplified pathway generated by ingenuity pathway analysis with proteins identified as specific target antigens. Solid lines indicate direct interactions. Dashed lines indicate indirect interactions. Arrows indicate stimulation. Mass spectrometry-identified proteins are in gray. DES: desmin; ENO1: enolase 1, (alpha); ERP29: endoplasmic reticulum protein 29; ERK1/2: extracellular signal-regulated kinase 1/2; GAPDH: glyceraldehyde-3-phosphate dehydrogenase; HNRNPAB: heterogeneous nuclear ribonucleoprotein A/B; HSPA5: heat shock 70 kDa protein 5 (glucose-regulated protein, 78 kDa); HSPD1: heat shock 60 kDa protein 1 (chaperonin); LAP3: leucine aminopeptidase 3; LMNA: lamin A/C; MAPK1: mitogen-activated protein kinase 1; NAMPT: nicotinamide phosphoribosyltransferase; p38MAPK: p38 mitogen-activated protein kinase; PDIA3: protein disulfide-isomerase family A, member 3; PDLIM1: PDZ and LIM domain 1; RANBP1: RAN binding protein 1; RPLP0: ribosomal protein, large, P0; SEMA4D: sema domain, immunoglobulin domain (Ig), transmembrane domain (TM) and short cytoplasmic domain, (semaphorin) 4D; SOS: son of sevenless; TGF-β: transforming growth factor β; TPP1: tripeptidyl peptidase I; VIM: vimentin; YWHAZ: tyrosine 3-monooxygenase/tryptophan 5-monooxygenase activation protein, zeta polypeptide.

serum IgG from patients with MPA induced stronger Erk phosphorylation in HUVECs than IgG from HCs. Our results support the idea that different pathophysiological processes occur during MPA, GPA and EGPA and encourage to split up MPA from other AAV groups as recently suggested by our group [19].

Using indirect immunofluorescence, Navarro et al. showed that 33% to 56% of patients with systemic vasculitides had detectable AECAs, which were associated with disease activity [20]. Use of 1D immunoblots or immunoprecipitation with HUVEC protein extracts revealed specific bands with systemic vasculitides [21,22]. However, only a few antigens were previously identified, including tropomyosin in patients with Kawasaki disease [23] and α-enolase in patients with Behçet disease [24]. In addition, Mayet et al. showed that AECAs could encompass anti-PR3 ANCAs [25], which suggests synthesis of PR3 by ECs. Using sera from patients with various vasculitis types, including AAVs, Karasawa et al. identified peroxyredoxine 2 as one of the targets of AECAs [26]. In this study, anti-peroxyredoxine 2 autoantibodies were detected more frequently in large- than small-vessel vasculitis. Thus, to our knowledge, no study has focused on the identification of target antigens of AECAs in patients with AAVs.

We uncovered lamin A/C and protein disulfide-isomerase A3 precursor in sera pools from patients with AAVs. Lamin A/C belongs to intermediate filaments and participates in nucleus architecture. Patients with mutations in the LMNA gene (Hutchinson-Gilford progeria syndrome) often show a vascular involvement [27]. Autoantibodies against lamin A/C are detected in the serum of patients with auto-immune hepatitis and primary biliary cirrhosis. More recently, we identified lamin A/C as a target of auto-antibodies in vascular diseases such as giant cell arteritis [15], systemic sclerosis [28,17] and pulmonary arterial hypertension [7]. Whether the occurrence of these antibodies is related to the cause or consequence of the vascular pathological process needs further investigation.

Protein disulfide-isomerase A3 precursor is a subunit of the transporters associated with antigen processing (TAP) complex. Interestingly, TAP complex is involved in antigen loading on MHC class I complex, and TAP1 or 2 deficiency [29] is responsible for a bare lymphocyte syndrome. In rare situations,

Table 4 Serum IgG reactivities directed against five target autoantigens in patients with ANCA associated vasculitides.

	α-Enolase (%)	Lamin A (%)	Vimentin (%)	FUBP-2 (%)	PDIA3 (%)
HC					
2 SD	7.2	8	3.3	0	6,7
3 SD	0	0	3.3	0	3,3
EGPA					
2 SD	29.4	12.5	29.4*	11.8	5,9
3 SD	11.8	0	17.6	5.9	0
GPA					
2 SD	13.3	6.7	6.7	13.3	0
3 SD	13.3	6.7	6.7	6.7	0
MPA					
2 SD	57.1***	64.3***	35.7*	50***	0
3 SD	35.7 **	42.8***	35.7*	42.9***	0
AAV					
2 SD	34.9*	26.7	26.1*	23.9**	2.2
3 SD	20.9*	15.6*	19.5	17.4*	0

HC: healthy controls; GPA: granulomatosis with polyangiitis; EGPA: eosinophilic granulomatosis with polyangiitis; AAV: ANCA associated vasculitis; FUBP-2: far upstream binding protein 2; MPA: microscopic polyangiitis; PDIA3: phosphodiesterase A3 precursor; SD: standard deviation.
*$P < 0.05$; **$P < 0.01$; ***$P < 0.001$ (comparison of each group with the control group).

TAP mutation causes lung disease, sinusitis, and skin lesions mimicking GPA [30].

By using IPA, we found that most of HUVEC proteins specifically recognized as target antigens by IgG in sera from patients with AAVs interacted with the MAPK family and TGF-β. TGF-β is a multifunctional peptide that regulates proliferation, differentiation, apoptosis, and migration in many cell types. Alteration of TGF-β signaling has been implicated in the pathophysiologic features of several vascular disorders, including Marfan and Loeys Dietz syndromes and Kawasaki disease [31,32]. In the immune system, TGF-β modulates the balance of pro-inflammatory and anti-inflammatory T cells through a complex set of interactions. In addition, the pro-inflammatory phenotype of ECs may be induced by the MAPK pathway [33]. Thus, the IPA network constituted by HUVEC target antigens could be due to EC activation during AAVs.

Circulating ECs and endothelial micro-particles are linked with endothelial damage and vasculitis in patients with AAVs [34]. However, the immunogenicity remains poorly documented and the origin of AECAs is unknown. AECAs may induce a pro-inflammatory phenotype of ECs by increasing the expression of E-selectin or intercellular adhesion molecule. The phenotype might result from activating a MAPK cascade. Indeed, activation of Erk by AECA has already been reported by Lee et al. during Behçet's disease [33]. The precise mechanism of Erk activation and the consequence on HUVECs activation should be more extensively studied. In addition, AECAs could confer EC cytotoxicity by inducing complement activation or antibody-dependent cell cytotoxicity [25], even though these results remain debated [8]. Finally, AECAs could induce apoptosis by targeting heat shock protein 60 at the cell surface of ECs [35].

The combined use of 2-DE and immunoblotting offers an interesting approach to identify target antigens of autoantibodies. However, our work has several limitations. We found fewer than 1000 protein spots stained in the reference gel, which is less than the total number of proteins contained in these cells. Therefore, a number of proteins were probably lost at each step of the technique, depending on their pI, molecular weight, sub-cellular localization and/or abundance in the cell. In addition, not all protein spots were identified by MS. ECs are known to display a heterogeneous functional and phenotypic profile depending on the anatomic origin and/or vessel type [14]. However, the technique does not allow for multiple antigen sources and we thus decided to describe target antigens of AECAs using a HUVEC proteome. In addition, most of the identified antigens are ubiquitous protein and thus not endothelial cell specific. Finally, we used sera pooled for sets of 3 patients because this number was sufficiently low to allow for detecting strong reactivity that would be detected in the serum of a single individual. However, we cannot rule out that a low-intensity reactivity specific to a given individual might not be detected by this pooling approach.

5. Conclusion

We provide a list of the HUVEC antigens targeted by AECAs in patients with AAVs and confirm reactivity by ELISA in four of them. Interestingly, AECA might be pathogenic, since IgG from patients with microscopic polyangiitis induces stronger Erk phosphorylation in HUVECs than IgG from HCs.

Supplementary data to this article can be found online at http://dx.doi.org/10.1016/j.clim.2014.03.020.

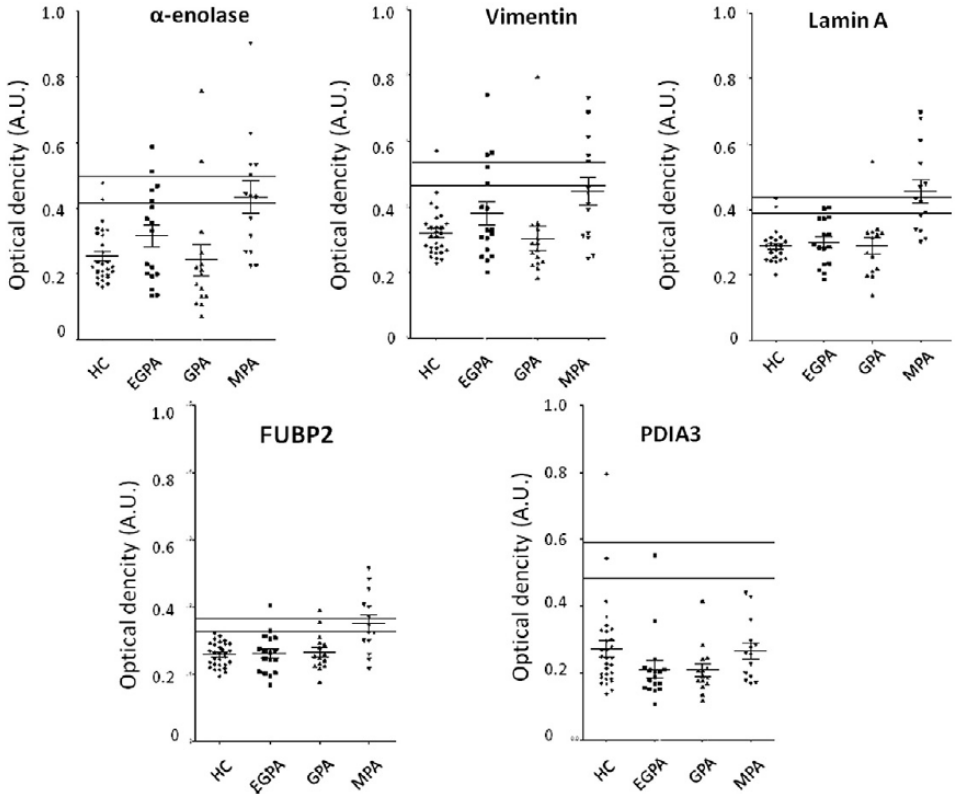

Figure 5 Antibody reactivity directed against 5 target autoantigens in patients with ANCA associated vasculitides. Serum IgG reactivities of healthy controls (HC) (●), patients with eosinophilic granulomatosis with polyangiitis (EGPA) (■), granulomatosis with polyangiitis (GPA) (▲) and microscopic polyangiitis (MPA) (▼) were tested with ELISA against alpha-enolase, protein disulfide-isomerase A3 (PDIA3), lamin A, vimentin and far upstream binding protein 2 (FUBP2). Each individual is represented by a single dot. Intensity of reactivity is quantified by optical density measured in arbitrary units (AU).

Abbreviations

2-DE	two dimensional electrophoresis
AAV	ANCA-associated vasculitides
ABC	ammonium bicarbonate
ACN	acetonitrile
ANCA	anti-neutrophil cytoplasmic antibody
DTT	dithiotreitol
EC	endothelial cell
EGPA	eosinophilic granulomatosis with polyangiitis
ERK	extracellular signal-regulated kinase
FCS	fetal calf serum
FUBP2	far upstream binding protein 2
GPA	granulomatosis with polyangiitis
HC	healthy control
HUVEC	human umbilical vein endothelial cell
IPA	ingenuity pathway analysis
IPG	immobilized pH gradient
IPKB	Ingenuity Pathway Knowledgebase
MAPK	mitogen-activated protein kinase
MHC	major histocompatibility complex
MPA	microscopic polyangiitis
MPO	myeloperoxydase
MS	mass spectrometry
PBS	Phosphate buffer saline
PDIA3	Protein disulfide-isomerase A3 precursor
PMSF	phenylmethanesulfonylfluoride
PR3	proteinase 3
SDS	sodium dodecyl sulfate
TAP	transporter associated with antigen processing
TGF-β	transforming growth factor-β

Conflict of interest statement

AR, HD and LM have applied for a patent relating to the content of the manuscript (Patent "Procédé de diagnostic d'une vascularite", FR0951205).

Author contribution

AR carried out the immunoblotting and proteomic experiments, analyzed the results and drafted the manuscript. SL performed the ELISA experiments, the IF experiments and Erk immunoblotting. HD carried out immunoblotting and proteomic experiments with AR, participated in the analysis

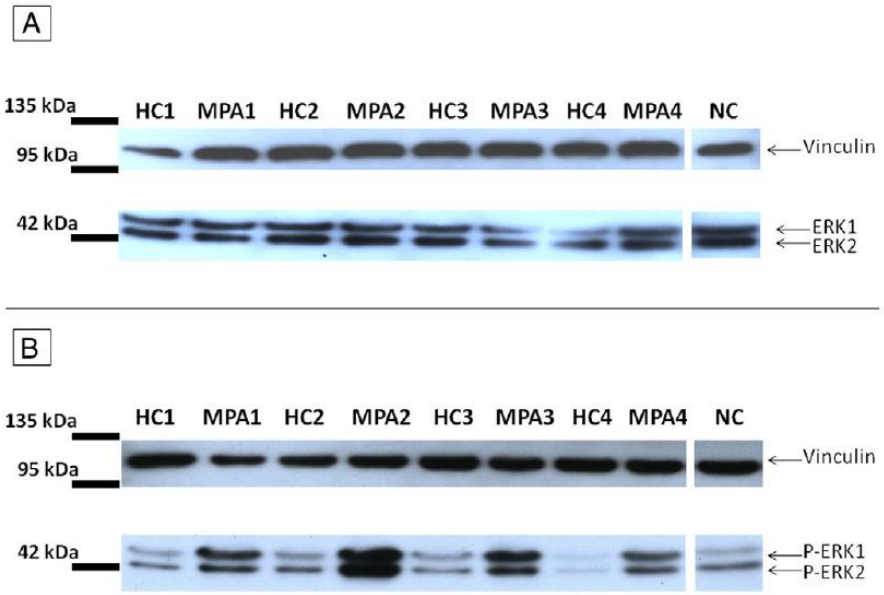

Figure 6 Erk 1/2 activation in HUVEC induced by purified serum IgG from patients with MPA and healthy controls. HUVECs were stimulated during 10 min with purified IgG isolated in serum from 4 patients with microscopic polyangiitis and 4 healthy controls. Negative control was obtained without any serum. Immunoblots were performed with anti-vinculin and anti-Erk1/2 antibody (Panel A) and anti-vinculin and anti-P-Erk1/2 specific antibodies (Panel B). Reactivity was revealed by enhanced chemoluminescence. HC: healthy control, MPA: microscopic polyangiitis, NC: negative control (without any serum).

of the results and edited the manuscript. GB participated in the analysis of the results and in the drafting of the manuscript. NT participated in the analysis of the results and edited the manuscript. CF performed ingenuity pathway analysis, participated in the analysis of the results and edited the manuscript. CB performed proteomic analysis, participated in the analysis of the results and edited the manuscript. LG provided sera from patients, participated in the study design and analysis of the results and also edited the manuscript. LM provided sera from patients, designed the experiments, analyzed the results and drafted the manuscript. All authors read and approved the final manuscript.

Acknowledgments

AR received financial support from the SNFMI (Société Nationale Française de Médecine Interne), ARMIIC (Association pour la Recherche en Médecine Interne et en Immunologie Clinique) and GPM (Groupe Pasteur Mutualité). SL received a financial support from the DRCD of Assistance Publique-Hôpitaux de Paris. HD received a financial support from AMPLI (Avenir Mutualiste des Professions Libérales & Indépendantes). We also thank CSL Behring for financial support.

None of the funding bodies had a role in the design, collection, analysis or interpretation of the data, writing the manuscript and the decision to submit the manuscript for publication.

References

[1] A. Mahr, S. Katsahian, H. Varet, L. Guillevin, E.C. Hagen, P. Hoglund, P.A. Merkel, C. Pagnoux, N. Rasmussen, K. Westman, D. R. Jayne, Revisiting the classification of clinical phenotypes of anti-neutrophil cytoplasmic antibody-associated vasculitis: a cluster analysis, Ann. Rheum. Dis. 72 (2013) 1003–1010.

[2] V. Witko-Sarsat, S. Daniel, L.H. Noel, L. Mouthon, Neutrophils and B lymphocytes in ANCA-associated vasculitis, APMIS Suppl. (2009) 27–31.

[3] L. Mouthon, A. Millet, A. Regent, M. Pederzoli-Ribeil, V. Witko-Sarsat, Pathophysiology of ANCA-associated vasculitides, Presse Med. 41 (2012) 996–1003.

[4] J.H. Stone, P.A. Merkel, R. Spiera, P. Seo, C.A. Langford, G.S. Hoffman, C.G. Kallenberg, E.W. St Clair, A. Turkiewicz, N.K. Tchao, L. Webber, L. Ding, L.P. Sejismundo, K. Mieras, D. Weitzenkamp, D. Ikle, V. Seyfert-Margolis, M. Mueller, P. Brunetta, N.B. Allen, F.C. Fervenza, D. Geetha, K.A. Keogh, E.Y. Kissin, P.A. Monach, T. Peikert, C. Stegeman, S.R. Ytterberg, U. Specks, Rituximab versus cyclophosphamide for ANCA-associated vasculitis, N. Engl. J. Med. 363 (2010) 221–232.

[5] R.B. Jones, J.W. Tervaert, T. Hauser, R. Luqmani, M.D. Morgan, C.A. Peh, C.O. Savage, M. Segelmark, V. Tesar, P. van Paassen, D. Walsh, M. Walsh, K. Westman, D.R. Jayne, Rituximab versus cyclophosphamide in ANCA-associated renal vasculitis, N. Engl. J. Med. 363 (2010) 211–220.

[6] D. Carvalho, C.O. Savage, D. Isenberg, J.D. Pearson, IgG anti-endothelial cell autoantibodies from patients with systemic lupus erythematosus or systemic vasculitis stimulate the release of two endothelial cell-derived mediators, which enhance adhesion molecule expression and leukocyte adhesion in an autocrine manner, Arthritis Rheum. 42 (1999) 631–640.

[7] H. Dib, M.C. Tamby, G. Bussone, A. Regent, A. Berezne, C. Lafine, C. Broussard, G. Simonneau, L. Guillevin, V. Witko-Sarsat, M. Humbert, L. Mouthon, Targets of anti-endothelial cell antibodies in pulmonary hypertension and scleroderma, Eur. Respir. J. 39 (2012) 1405-14.
[8] N. Del Papa, L. Guidali, M. Sironi, Y. Shoenfeld, A. Mantovani, A. Tincani, G. Balestrieri, A. Radice, R.A. Sinico, P.L. Meroni, Anti-endothelial cell IgG antibodies from patients with Wegener's granulomatosis bind to human endothelial cells in vitro and induce adhesion molecule expression and cytokine secretion, Arthritis Rheum. 39 (1996) 758–766.
[9] C. Holmen, E. Elsheikh, M. Christensson, J. Liu, A.S. Johansson, A. R. Qureshi, S. Jalkanen, S. Sumitran-Holgersson, Anti endothelial cell autoantibodies selectively activate SAPK/JNK signalling in Wegener's granulomatosis, J. Am. Soc. Nephrol. 18 (2007) 2497–2508.
[10] C.O. Savage, B.E. Pottinger, G. Gaskin, C.M. Lockwood, C.D. Pusey, J.D. Pearson, Vascular damage in Wegener's granulomatosis and microscopic polyarteritis: presence of anti-endothelial cell antibodies and their relation to anti-neutrophil cytoplasm antibodies, Clin. Exp. Immunol. 85 (1991) 14–19.
[11] J.C. Jennette, R.J. Falk, K. Andrassy, P.A. Bacon, J. Churg, W. L. Gross, E.C. Hagen, G.S. Hoffman, G.G. Hunder, C.G. Kallenberg, et al., Nomenclature of systemic vasculitides. Proposal of an international consensus conference, Arthritis Rheum. 37 (1994) 187–192.
[12] R.A. Luqmani, P.A. Bacon, R.J. Moots, B.A. Janssen, A. Pall, P. Emery, C. Savage, D. Adu, Birmingham vasculitis activity score (BVAS) in systemic necrotizing vasculitis, QJM 87 (1994) 671–678.
[13] M.C. Tamby, Y. Chanseaud, M. Humbert, J. Fermanian, P. Guilpain, P. Garcia-de-la-Pena-Lefebvre, S. Brunet, A. Servettaz, B. Weill, G. Simonneau, L. Guillevin, M.C. Boissier, L. Mouthon, Anti-endothelial cell antibodies in idiopathic and systemic sclerosis associated pulmonary arterial hypertension, Thorax 60 (2005) 765–772.
[14] H. Dib, P. Chafey, G. Clary, C. Federici, M. Le Gall, J. Dwyer, J. Gavard, N. Tamas, G. Bussone, C. Broussard, L. Camoin, V. Witko-Sarsat, M.C. Tamby, L. Mouthon, Proteomes of umbilical vein and microvascular endothelial cells reflect distinct biological properties and influence immune recognition, Proteomics 12 (2012) 2547–2555.
[15] A. Regent, H. Dib, K.H. Ly, C. Agard, M.C. Tamby, N. Tamas, B. Weksler, C. Federici, C. Broussard, L. Guillevin, L. Mouthon, Identification of target antigens of anti-endothelial cell and anti-vascular smooth muscle cell antibodies in patients with giant cell arteritis: a proteomic approach, Arthritis Res. Ther. 13 (2011) R107.
[16] O.H. Lowry, N.J. Rosebrough, A.L. Farr, R.J. Randall, Protein measurement with the Folin phenol reagent, J. Biol. Chem. 193 (1951) 265–275.
[17] G. Bussone, H. Dib, J.D. Dimitrov, L. Camoin, C. Broussard, N. Tamas, L. Guillevin, S.V. Kaveri, L. Mouthon, Identification of target antigens of self-reactive IgG in intravenous immunoglobulin preparations, Proteomics 9 (2009) 2253–2262.
[18] G. Bussone, M.C. Tamby, C. Calzas, N. Kherbeck, Y. Sahbatou, C. Sanson, K. Ghazal, H. Dib, B.B. Weksler, C. Broussard, F. Verrecchia, A. Yaici, V. Witko-Sarsat, G. Simonneau, L. Guillevin, M. Humbert, L. Mouthon, IgG from patients with pulmonary arterial hypertension and/or systemic sclerosis binds to vascular smooth muscle cells and induces cell contraction, Ann. Rheum. Dis. 71 (2012) 596–605.
[19] A. Millet, M. Pederzoli-Ribeil, L. Guillevin, V. Witko-Sarsat, L. Mouthon, Anti-neutrophil cytoplasmic antibody-associated vasculitides: is it time to split up the group? Ann. Rheum. Dis. 72 (2013) 1273-9.
[20] M. Navarro, R. Cervera, J. Font, J.C. Reverter, J. Monteagudo, G. Escolar, A. Lopez-Soto, A. Ordinas, M. Ingelmo, Anti-endothelial cell antibodies in systemic autoimmune diseases: prevalence and clinical significance, Lupus 6 (1997) 521–526.
[21] Y. Chanseaud, P. Garcia de la Pena-Lefebvre, P. Guilpain, A. Mahr, M.C. Tamby, M. Uzan, L. Guillevin, M.C. Boissier, L. Mouthon, IgM and IgG autoantibodies from microscopic polyangiitis patients but not those with other small- and medium-sized vessel vasculitides recognize multiple endothelial cell antigens, Clin. Immunol. 109 (2003) 165–178.
[22] N. Del Papa, G. Conforti, D. Gambini, L. La Rosa, A. Tincani, D. D'Cruz, M. Khamashta, G.R. Hughes, G. Balestrieri, P.L. Meroni, Characterization of the endothelial surface proteins recognized by anti-endothelial antibodies in primary and secondary autoimmune vasculitis, Clin. Immunol. Immunopathol. 70 (1994) 211–216.
[23] M. Kaneko, T. Ono, T. Matsubara, Y. Yamamoto, H. Ikeda, T. Yoshiki, S. Furukawa, E. Nakayama, Serological identification of endothelial antigens predominantly recognized in Kawasaki disease patients by recombinant expression cloning, Microbiol. Immunol. 48 (2004) 703–711.
[24] K.H. Lee, H.S. Chung, H.S. Kim, S.H. Oh, M.K. Ha, J.H. Baik, S. Lee, D. Bang, Human alpha-enolase from endothelial cells as a target antigen of anti-endothelial cell antibody in Behcet's disease, Arthritis Rheum. 48 (2003) 2025–2035.
[25] W.J. Mayet, A. Schwarting, K.H. Meyer zum Buschenfelde, Cytotoxic effects of antibodies to proteinase 3 (C-ANCA) on human endothelial cells, Clin. Exp. Immunol. 97 (1994) 458–465.
[26] R. Karasawa, M.S. Kurokawa, K. Yudoh, K. Masuko, S. Ozaki, T. Kato, Peroxiredoxin 2 is a novel autoantigen for anti-endothelial cell antibodies in systemic vasculitis, Clin. Exp. Immunol. 161 (2010) 459–470.
[27] M. Eriksson, W.T. Brown, L.B. Gordon, M.W. Glynn, J. Singer, L. Scott, M.R. Erdos, C.M. Robbins, T.Y. Moses, P. Berglund, A. Dutra, E. Pak, S. Durkin, A.B. Csoka, M. Boehnke, T.W. Glover, F.S. Collins, Recurrent de novo point mutations in lamin A cause Hutchinson-Gilford progeria syndrome, Nature 423 (2003) 293–298.
[28] G. Bussone, H. Dib, M.C. Tamby, C. Broussard, C. Federici, G. Woimant, L. Camoin, L. Guillevin, L. Mouthon, Identification of new autoantibody specificities directed at proteins involved in the transforming growth factor beta pathway in patients with systemic sclerosis, Arthritis Res. Ther. 13 (2011) R74.
[29] H. de la Salle, D. Hanau, D. Fricker, A. Urlacher, A. Kelly, J. Salamero, S.H. Powis, L. Donato, H. Bausinger, M. Laforet, et al., Homozygous human TAP peptide transporter mutation in HLA class I deficiency, Science 265 (1994) 237–241.
[30] A. Villa-Forte, H. de la Salle, D. Fricker, F. Hentges, J. Zimmer, HLA class I deficiency syndrome mimicking Wegener's granulomatosis, Arthritis Rheum. 58 (2008) 2579–2582.
[31] C. Shimizu, S. Jain, S. Davila, M.L. Hibberd, K.O. Lin, D. Molkara, J.R. Frazer, S. Sun, A.L. Baker, J.W. Newburger, A.H. Rowley, S.T. Shulman, D. Burgner, W.B. Breunis, T.W. Kuijpers, V.J. Wright, M. Levin, H. Eleftherohorinou, L. Coin, S.J. Popper, D.A. Relman, W. Fury, C. Lin, S. Mellis, A.H. Tremoulet, J.C. Burns, Transforming growth factor-beta signaling pathway in patients with Kawasaki disease, Circ. Cardiovasc. Genet. 4 (2011) 16–25.
[32] B.L. Loeys, J. Chen, E.R. Neptune, D.P. Judge, M. Podowski, T. Holm, J. Meyers, C.C. Leitch, N. Katsanis, N. Sharifi, F.L. Xu, L. A. Myers, P.J. Spevak, D.E. Cameron, J. De Backer, J. Hellemans, Y. Chen, E.C. Davis, C.L. Webb, W. Kress, P. Coucke, D.B. Rifkin, A.M. De Paepe, H.C. Dietz, A syndrome of altered cardiovascular, craniofacial, neurocognitive and skeletal development caused by mutations in TGFBR1 or TGFBR2, Nat. Genet. 37 (2005) 275–281.
[33] K.H. Lee, H.J. Cho, H.S. Kim, W.J. Lee, S. Lee, D. Bang, Activation of extracellular signal regulated kinase 1/2 in human dermal microvascular endothelial cells stimulated by

anti-endothelial cell antibodies in sera of patients with Behcet's disease, J. Dermatol. Sci. 30 (2002) 63–72.
[34] M. Haubitz, A. Dhaygude, A. Woywodt, Mechanisms and markers of vascular damage in ANCA-associated vasculitis, Autoimmunity 42 (2009) 605–614.
[35] C. Jamin, C. Dugue, J.E. Alard, S. Jousse, A. Saraux, L. Guillevin, J.C. Piette, P. Youinou, Induction of endothelial cell apoptosis by the binding of anti-endothelial cell antibodies to Hsp60 in vasculitis-associated systemic autoimmune diseases, Arthritis Rheum. 52 (2005) 4028–4038.

Supplemental Table 1: Clinical presentation of the 30 patients with ANCA-associated vasculitides at the time of blood sampling

Pool	Patient	Age	Disease duration (months)	Previous treatment	Current treatment	Previous features during the course of AAVs	Clinical features at the time of blood sampling	ANCA (p, c, u)	ELISA target
MPA 1	P1	56	0	None	Pred	None	J, PN	P	MPO
	P2	69	24	Pred	Pred	K	K	p	MPO
	P3	53	8	None	Pred, CYC	PN, H, K, L	K	p	MPO
MPA 2	P4	71	0	None	Pred	None	S, K	u	u
	P5	62	0	None	Pred	None	S, J, K, B	none	none
	P6	84	120	Pred	Pred	S, J, PN	S, J, PN	none	none
MPA 3	P7	63	0	None	Pred	None	S, K, PN, J	none	none
	P8	71	2	None	Pred	S, K	S, K	u	u
	P9	49	0	None	Pred	None	J, S	none	none
EGPA 1	P10	57	138	CYC, Pred	Pred	L, S, PN	PN, S, L	c	PR3
	P11	57	0	None	None	None	J, S, ENT, L, PN, B	none	none
	P12	88	0	None	Pred	None	L, PN, S, K	p	MPO
EGPA 2	P13	46	5	Pred, CYC	Pred, CYC	L, H, PN	L	none	none
	P14	62	0	None	Pred	L	L, H, B, ENT, PN	none	none
	P15	61	3	Pred	Pred	L, PN, S, H	L, PN, S, H	none	none
EGPA 3	P16	27	24	Pred	Pred	L, PN, H	L	none	none
	P17	74	41	Pred, CYC	Pred	ENT, L, H	L	none	none
	P18	42	52	Pred, CYC, AZA	Pred, CYC	ENT, S, K, J, B, L, PN	PN, L, J	p	MPO
GPA 1	P19	34	58	Pred, Ritux, CYC, AZA, MTX	CYC	J, ENT, L	remision	c	PR3
	P20	63	41	Pred, IVIg, CYC	Pred	J, ENT, K, E	remission	c	PR3
	P21	69	101	AZA, CYC, Pred	Pred	J, L, K, S	PN, L, R	c	PR3
GPA 2	P22	47	240	Pred, CYC, Ritux, MMF	Pred, LEF	ENT, J, K, L	ENT	c	PR3
	P23	52	36	CYC, AZA, Pred	CYC, Pred	ENT, L, E	ENT, L	c	PR3
	P24	64	156	CYC, MTX, AZA, Pred	Pred, MTX	PN, L, S, J	remission	c	PR3
GPA 3	P25	84	144	MTX, CYC, Pred	CYC, Pred	PN, S, K, ENT, J	ENT, K	c	PR3
	P26	62	155	CYC, AZA, SUL, MMF, Pred, INFL	Pred, INFL, AZA	ENT, B	ENT, B	p	PR3
	P27	36	65	MTX, Ritux, Pred	Pred	ENT, L, J	remission	c	PR3
GPA 4	P28	78	150	Pred, CYC, AZA	Pred, AZA	ENT, L K, E, H	remission	c	PR3
	P29	61	143	Pred, CYC, AZA	none	L, ENT, K, E, J, ENT	ENT, L, K	c	PR3
	P30	49	248	CYC, MTX, ETA, IgIV, Pred	MTX, AZA, Pred	J, E, ENT, K,	J	c	PR3

AAV: ANCA-associated vasculitides, EGPA: eosinophilic granulomatosis with polyangiitis, GPA: granulomatosis with polyangiitis, MPA: microscopic polyangiitis
B: bowel; E: eye; ENT: ear, nose, throat; H: heart;J: joint; K: kidney; L: lung; PN: peripheral neuropathy; S: skin
AZA: azathioprine; CYC: cyclophosphamide; ETA: etanercept; INFL: infliximab; IVIg: intravenous immunoglobulin; LEF: leflunomide; MMF: mofetil mycofenolate; MTX: methotrexate; Pred: prednisone; Ritux: rituximab; SUL: sulfasalazine
c: cytoplasmic; p perinuclear; u: unknown
MPO: myeloperoxydase, PR3 proteinase 3

Supplemental Figure 1: Experimental design for screening anti-human umbilical vein endothelial cell antibodies and identifying their target autoantigens. Proteins were extracted from human umbilical vein endothelial cells (HUVECs) and separated on 2-D gels. One gel was stained with ammonia silver nitrate and used as a reference gel, and other proteins were transferred onto PVDF membranes. IgG reactivity in pooled sera sets from 3 patients each with AAVs and pooled sera from 12 healthy blood donors were immunoblotted at 1:100 dilution and scanned with a densitometer. The 2-D immunoblots were stained with colloidal gold for visualization of the transferred proteins. Analysis of the images of the 2-D immunoblots before and after colloidal gold staining and in comparison to the reference gel involved image analysis software. Protein spots recognized by IgG antibodies in serum pools for more than 3 of 4 pools (GPA), 2 of 3 pools (PAM, EGPA) and not in the healthy control pool and in 6 of 10 pools (AAV altogether) and were digested before mass spectrometry. Database searching involved MASCOT 2.2 software

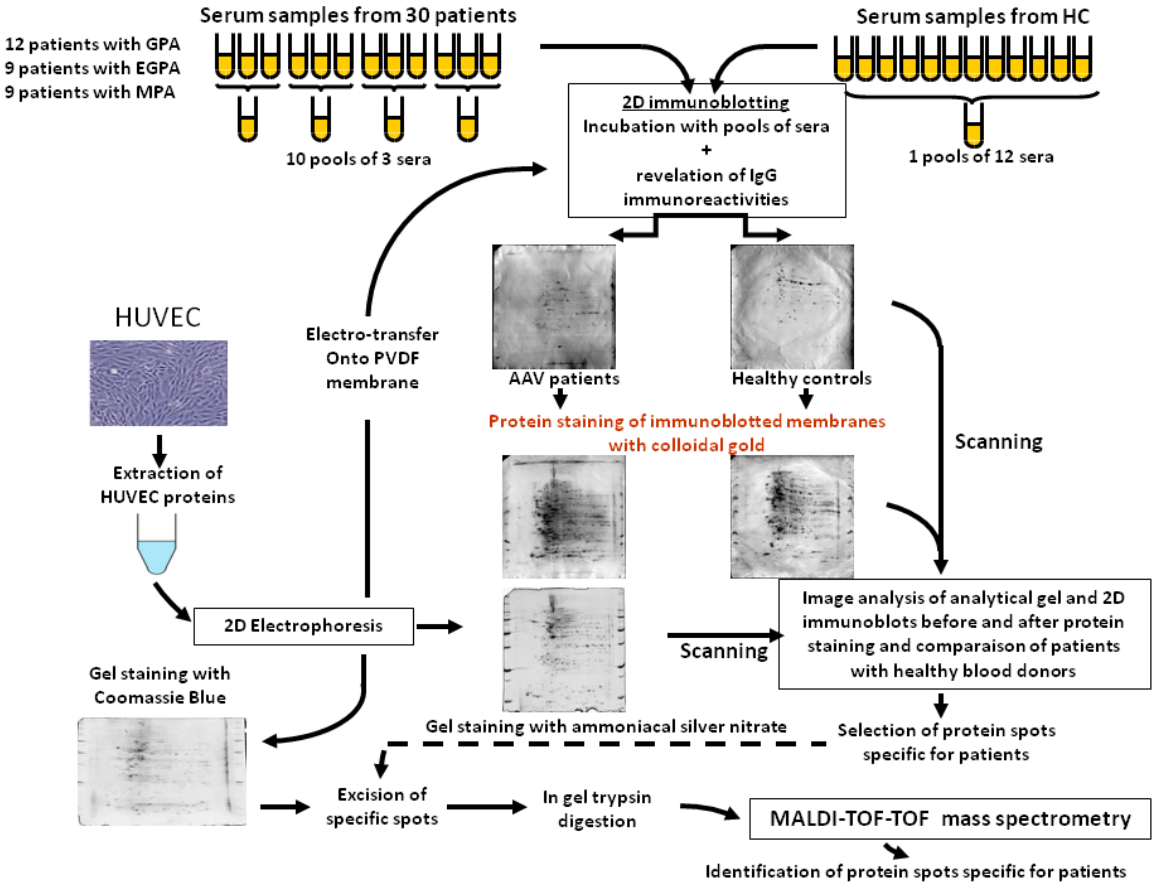

<u>Supplemental figure 2</u>: Antibody reactivity directed against alpha-enolase, protein disulfide-isomerase A3 (PDIA3), lamin A, vimentin and far upstream binding protein (FUBP) 2 in individual patients with ANCA associated vasculitides. HC: healthy controls; EGPA: eosinophilic granulomatosis with polyangiitis; GPA: granulomatosis with polyangiitis; MPA: microscopic polyangiitis; PDIA3: protein disulfide isomerase A3, FUBP-2: far upstream binding protein 2; SD: standard deviation. In white: no serum reactivity, in light gray: serum reactivity between 2 and SD, in dark gray: serum reactivity above 3 SD. IF: Immunofluorescence, weak, medium or strong fluorescence is symbolized respectively by one, two or three stars, absence of fluorescence is symbolized by a lack of star.

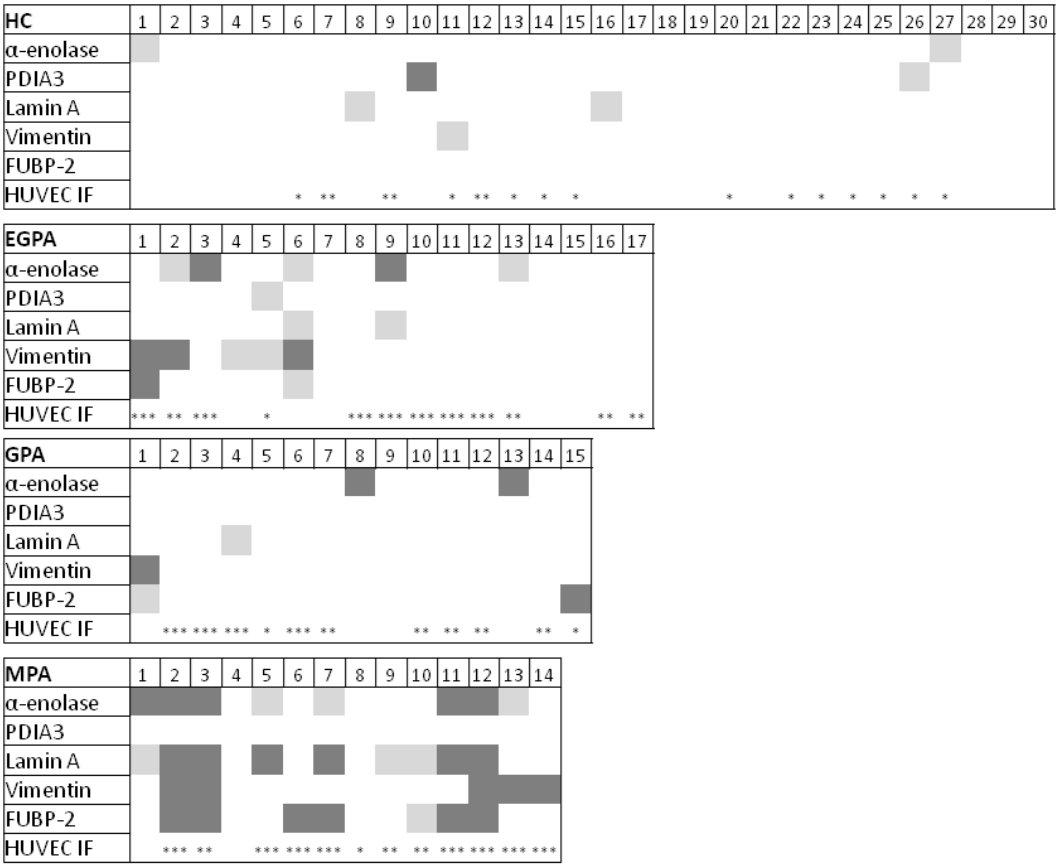

<u>Supplemental Table 2:</u> Mass spectrometry data of HUVEC target antigens in patients with ANCA-associated vasculitides.

ID	Identification	Swiss Prot accession no.	Estimated / Theoretical pI	Estimated / Theoretical MW (kDa)	Total ion score	Best ion score	No. of unique identified peptides (a)
570	No identified protein		6.0/	75/			
583	Heat shock cognate 71 kDa protein	HSP7C_HUMAN	6.2/5.4	75/71	736	116	10
584	Heat shock cognate 71 kDa protein	HSP7C_HUMAN	6.1/5.4	75/71	589	97	9
	78 kDa glucose-regulated protein precursor	GRP78_HUMAN	6.1/5.1	75/72	99		3
619	Lamin-A/C	LMNA_HUMAN	7.2/6.6	71/74	19 / 565	19 / 85	1 / 13
646	Lamin-A/C	LMNA_HUMAN	7.0/6.6	70/74	223 / 604	49 / 87	7 / 13
802	Protein disulfide-isomerase A3 precursor	PDIA3_HUMAN	6.2/6.0	56/57	863 / 1112	125 / 165	12 / 12
814	Protein disulfide-isomerase A3 precursor	PDIA3_HUMAN	6.0/6.0	56/57	278	63	6
917	Alpha-enolase	ENOA_HUMAN	7.5/7.0	50/47	841 / 901	161 / 188	12 / 11
973	No identified protein		7.9/	50/			
1076	Actin, cytoplasmic 2	ACTG_HUMAN	5.6/5.3	45/42	540 / 555	125 / 140	9 / 6
	ANKRD26-like family C member 1A	A26CB_HUMAN	5.6/5.9	45/121	260	116	4

ID: Identity; kDa: Kilo dalton; MW: Molecular weight

(a) number of unique identified peptides in MS/MS and MS+MS/MS searches

Supplemental Figure 3: Merged network generated by ingenuity pathway analysis with proteins identified as specific target antigens. Solid lines indicate direct interactions. Dashed lines indicate indirect interactions. Arrows indicate stimulation. Mass spectrometry-identified proteins are in gray. ACO2: aconitase 2, mitochondrial; ACTG1: actin, gamma 1; CALD1: caldesmon 1; CCT2: chaperonin containing TCP1, subunit 2 (beta); CCT5: chaperonin containing TCP1, subunit 5 (epsilon); DES: desmin; ENO1: enolase 1, (alpha); ERK1/2: extracellular signal-regulated kinases1/2; ERP29: endoplasmic reticulum protein 29; 34 GAPDH: glyceraldehyde-3-phosphate dehydrogenase; HNRNPAB: heterogeneous nuclear ribonucleoprotein A/B; HNRNPD: heterogeneous nuclear ribonucleoprotein D; HNRNPK: heterogeneous nuclear ribonucleoprotein K; HNRNPL: heterogeneous nuclear ribonucleoprotein L; HSP90AB1: heat shock protein 90 kDa alpha (cytosolic), class B member 1; HSPA1L: heat shock 70 kDa protein 1-like; HSPA2: heat shock 70 kDa protein 2; HSPA5: heat shock 70 kDa protein 5 (glucose-regulated protein, 78 kDa); HSPD1: heat shock 60 kDa protein 1 (chaperonin); KHSRP: KH-type splicing regulatory protein; KRT1: keratin 1; LAP3: leucine aminopeptidase 3; LMNA: lamin A/C; MAPK1: mitogen-activated protein kinase 1; NAMPT: nicotinamide phosphoribosyltransferase; NANS: N-acetylneuraminic acid synthase; p38MAPK: p38 mitogen-activated protein kinase; PCBP1: poly(rC) binding protein 1; PDIA3: protein disulfide-isomerase family A, member 3; PDLIM1: PDZ and LIM domain 1; PSMA1: proteasome (prosome, macropain) subunit, alpha type, 1; PSMC2: proteasome (prosome, macropain) 26S subunit, ATPase, 2; PSMC5: proteasome (prosome, macropain) 26S subunit, ATPase, 5; PSMD7: proteasome (prosome, macropain) 26S subunit, non-ATPase, 7; RANBP1: RAN binding protein 1; RPLP0: ribosomal protein, large, P0; SEMA4D: sema domain, immunoglobulin domain (Ig), transmembrane domain (TM) and short cytoplasmic domain, (semaphorin) 4D; SOS: son of sevenless; SRSF1: serine/arginine-rich splicing factor 1; STIP1: stress-induced-phosphoprotein 1; TGF-β: transforming growth factor β; TPP1: tripeptidyl peptidase I; TUBA1B: tubulin, alpha 1b; VCP: valosin containing protein; VIM: vimentin; YWHAZ: tyrosine 3-monooxygenase/tryptophan 5-monooxygenase activation protein, zeta polypeptide.

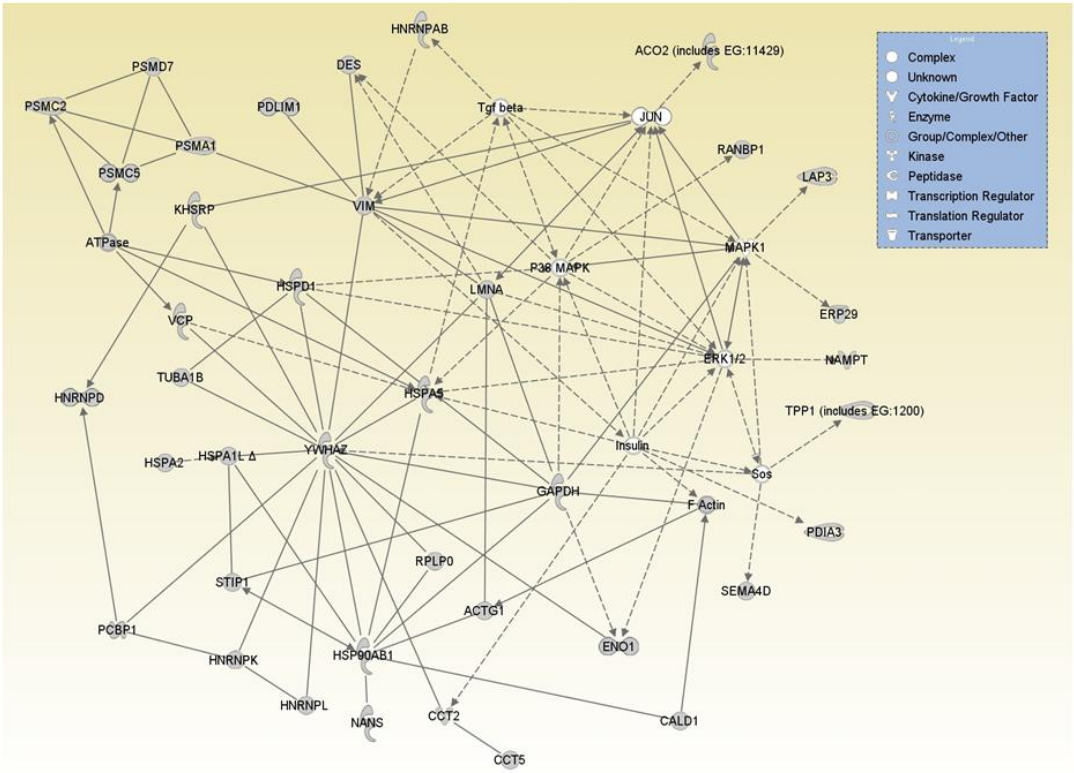

Supplemental file 2: Mass spectrometry data of target antigens recognized by only one peptide.

Precursor 1335.63Da MS/MS results (Ran-specific GTPase-activating protein - Homo sapiens)

Mascot Search Results

Match to: **RANG_HUMAN** Score: **28**

Ran-specific GTPase-activating protein - Homo sapiens (Human)

Matched peptides shown in **Bold Red**

1 MAAAKDTHED HDTSTENTDE SNHDPQFEPI VSLPEQEIKT LEEDEEELFK
51 MRAKLFR**FAS ENDLPEWK**ER GTGDVKLLKH KEKGAIRLLM RRDKTLKICA
101 NHYITPMMEL KPNAGSDRAW VWNTHADFAD ECPKPELLAI RFLNAENAQK
151 FKTKFEECRK EIEEREKKAG SGKNDHAEKV AEKLEALSVK EETKEDAEEK
201 Q

Start - End	Observed	Mr(expt)	Mr(calc)	ppm	Miss	Sequence	
58 - 68	1335.630	1334.623	1334.614	6	0	R.FASENDLPEWK.E	(Ions score 28)

MS/MS Fragmentation of **FASENDLPEWK**

Found in **RANG_HUMAN**, Ran-specific GTPase-activating protein - Homo sapiens (Human)

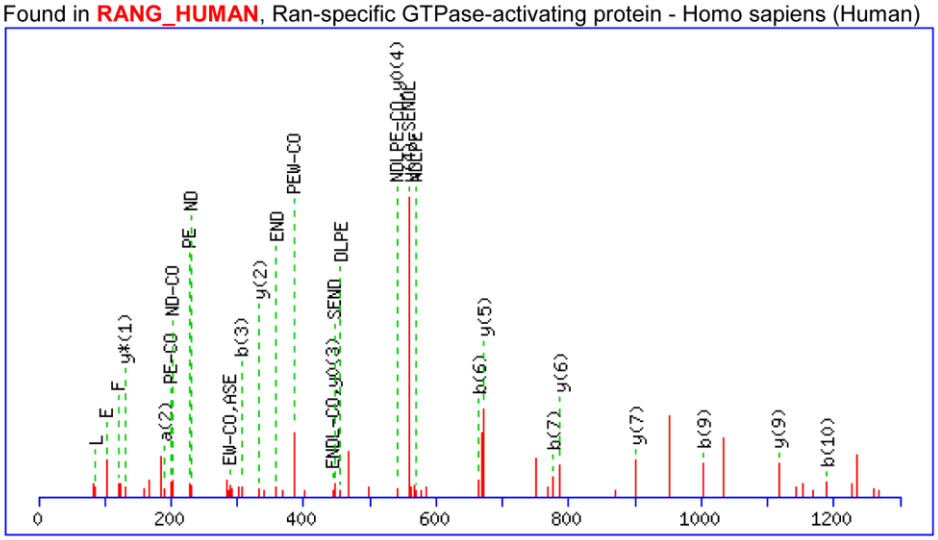

#	b	Seq.	y	#
1	148.076	F		11
2	219.113	A	1188.553	10
3	306.145	S	1117.516	9
4	435.187	E	1030.484	8
5	549.23	N	901.441	7
6	664.257	D	787.398	6
7	777.341	L	672.372	5
8	874.394	P	559.287	4
9	1003.437	E	462.235	3
10	1189.516	W	333.192	2
11		K	147.113	1

ARTICLE IN PRESS YCLIM-07339; No. of page: 1; 4C:

Clinical Immunology (2014) xx, xxx

available at www.sciencedirect.com

Clinical Immunology

www.elsevier.com/locate/yclim

LETTER TO THE EDITOR

Reply to "Anti-endothelial cell antibodies in patients with AAV: The relationship with ANCA? Comment on: Identification of target antigens of anti-endothelial cell antibodies in patients with anti-neutrophil cytoplasmic antibody-associated vasculitides: A proteomic approach" by Shen-Ju Gou, Ping Fu

We thank Dr Gou SJ and Fu P for their comment regarding our work on the identification of target antigens of anti-endothelial cell antibodies in patients with anti-neutrophil cytoplasmic antibody (ANCA)-associated vasculitides [1]. Since the target of ANCA, myeloperoxidase (MPO) is not expressed by endothelial cells [2], and the biological effect on endothelial cells of IgG purified from the serum of patients with anti-MPO ANCA is probably the consequence of the binding to another antigen that is present in endothelial cells. Then we can argue either that anti-MPO ANCA binds to other antigens that are expressed at the cell surface and shares common epitope with MPO or that other autoantibodies than ANCA are responsible for this effect.

It was previously reported that polyclonal IgG purified from the serum of a rabbit immunized with recombinant mouse MPO induced an up-regulation of adhesion molecules on mouse glomerular endothelial cells [3]. Injected to mice, this polyclonal IgG could significantly increase the number of neutrophils infiltrating glomeruli. In this model, it was proposed that moesin, which could share an epitope with MPO, could be recognized by anti-MPO antibodies leading to endothelial cell activation [4].

In our work, using a 2-dimensional immunoblotting technique, we investigated the targets of AECA in patients with ANCA associated vasculitis. In this work, we did not identify moesin as a target of AECA in HUVEC. In fact our aim was not to demonstrate that ANCA could bind to other antigens than MPO or proteinase 3, but just to identify other antibodies in addition to ANCA that could participate in the pathogenic process in ANCA associated vasculitis. We looked for protein sequence homology between MPO and the target antigens that were identified in patients with MPA by basic local alignment search tool (pBLAST, NCBI). It revealed that common protein sequences of four amino acids were found between vimentin and MPO and of 3 amino acids between other target antigens except one and MPO. This could be enough in order to explain cross-reactivity, even though it doesn't take into account conformational epitope [5]. We agree that we cannot rule out that part of the biological effect that we observed with purified IgG was obtained through ANCA binding at the cell surface. In order to assess this hypothesis, additional experiments with ANCA depleted purified IgG and anti-MPO ANCA would have been required. AECA have been identified in a large number of diseases and reported to bind to diverse target antigens. Thus, alternatively, ANCA and AECA could be distinct autoantibodies, and AECA could contribute to explain the occurrence of vasculitis in ANCA-negative patients and potentially participate in the pathogenic process in ANCA-positive patients.

References

[1] A. Regent, S. Lofek, H. Dib, G. Bussone, N. Tamas, C. Federici, C. Broussard, L. Guillevin, L. Mouthon, Identification of target antigens of anti-endothelial cell antibodies in patients with anti-neutrophil cytoplasmic antibody-associated vasculitides: a proteomic approach, Clin. Immunol. 153 (2014) 123–135.

[2] W.F. Pendergraft, D.A. Alcorta, M. Segelmark, J.J. Yang, R. Tuttle, J.C. Jennette, R.J. Falk, G.A. Preston, ANCA antigens, proteinase 3 and myeloperoxidase, are not expressed in endothelial cells, Kidney Int. 57 (2000) 1981–1990.

[3] T. Nagao, M. Matsumura, A. Mabuchi, A. Ishida-Okawara, O. Koshio, T. Nakayama, H. Minamitani, K. Suzuki, Up-regulation of adhesion molecule expression in glomerular endothelial cells by anti-myeloperoxidase antibody, Nephrol. Dial. Transplant. 22 (2007) 77–87.

[4] T. Nagao, K. Suzuki, K. Utsunomiya, M. Matsumura, K. Saiga, P.C. Wang, H. Minamitani, Y. Aratani, T. Nakayama, Direct activation of glomerular endothelial cells by anti-moesin activity of anti-myeloperoxidase antibody, Nephrol. Dial. Transplant. 26 (2011) 2752–2760.

[5] Y. El-Manzalawy, D. Dobbs, V. Honavar, Predicting linear B-cell epitopes using string kernels, J. Mol. Recognit. 21 (2008) 243–255.

Alexis Regent
Luc Mouthon
Institut Cochin, INSERM U1016, CNRS UMR 8104, Université Paris Descartes, 22 rue Méchain, 75014 Paris, France
Pôle de Médecine Interne, Centre de Référence pour les vascularites nécrosantes et la sclérodermie systémique, Hôpital Cochin, Assistance Publique-Hôpitaux de Paris, 27 rue du Faubourg Saint-Jacques, F-75679 Paris Cedex 14, France

27 July 2014

http://dx.doi.org/10.1016/j.clim.2014.07.009
1521-6616

Résumé

Rationnel : L'artérite à cellules géantes (ACG) est une vascularite primitive des gros vaisseaux dont le diagnostic repose sur la mise en évidence d'un infiltrat inflammatoire et de cellules géantes à la biopsie d'artère temporale (BAT). On note également un remodelage de la paroi vasculaire lié à une prolifération des cellules musculaires lisses vasculaires (CMLV) pouvant aboutir à une occlusion artérielle.

Objectif : Caractériser les auto-anticorps dirigés contre les cellules endothéliales (CE) et les CMLV au cours de l'ACG et préciser le rôle des CMLV dans le remodelage pariétal.

Méthodes : La recherche d'auto-anticorps a reposé sur un immunoblot 2D couplé à la spectrométrie de masse. Les protéomes des CMLV d'artère ombilicale, d'artère pulmonaire et d'aorte humaines normales a été comparés par protéomique différentielle (2D-DIGE). Nous avons utilisé la 2D-DIGE et des puces d'expression pan-génomiques pour comparer les CMLV issues de BAT de patients suspects d'ACG (avec un diagnostic final d'ACG ou non), afin d'identifier les mécanismes contribuant à la prolifération des CMLV.

Résultats : Chez 15 patients atteints d'ACG, nous avons notamment identifié la lamine, la vinculine et l'annexine A5 comme cible des auto-anticorps anti-CMLV. Les antigènes cibles identifiés sont liés à Grb2, une protéine adaptatrice impliquée dans la prolifération des CMLV. Nous avons mis en évidence des protéomes différents au sein des CMLV humaines normales selon leur origine vasculaire et avons principalement identifié des protéines du cytosquelette et du métabolisme énergétique.A partir des CMLV isolées des BAT et à l'aide d'Ingenuity®, nous avons identifié l'endothéline 1 (ET-1) et la paxilline comme des molécules impliquées dans le remodelage vasculaire. En immunohistochimie et par qPCR, nous avons confirmé l'expression de l'ET-1 et de ses récepteurs ET_AR et ET_BR au sein des artères temporales de patients atteints d'ACG. Enfin, nous avons inhibé la prolifération des CMLV avec du macitentan, un inhibiteur d'ET_AR et en particulier avec son métabolite actif, mais pas avec d'autres inhibiteurs des récepteurs de l'ET-1.

Conclusion : Nous avons identifié chez les patients atteints d'ACG des anticorps anti-CMLV dont le rôle pathogéne potentiel reste à définir. Les différences protéiques observées à partir des CMLV humaines normales pourraient correspondre à des phénotypes différents. A partir d'un matériel biologique unique, nous avons pu montrer que la prolifération excessive des CMLV au cours de l'ACG pouvait être inhibée par le macitentan ce qui permet d'envisager un usage thérapeutique de cette molécule.

Abstract

Background : Giant cell arteritis (GCA) is a large vessel vasculitis and its diagnosis usually relies on the identification of an inflammatory infiltrate made of mononuclear cells and giant cells upon temporal artery biopsy. There is also a remodeling process in the arterial wall due to an excessive proliferation of vascular smooth muscle cells (VSMC) which can sometimes lead to arterial occlusion.

Purpose: Identify auto-antibodies targeting either endothelial cells (EC) and/or VSMC during GCA and better understand the role of VSMC in the remodeling process.

Methods : Auto-antibodies were detected by a 2-dimensionnal immunoblot and their target antigens were identified by mass spectrometry. Proteoms of umbilical artery, pulmonary artery and aorta VSMC were compared by 2 dimension differential in gel electrophoresis (2D-DIGE). In order to identify mechanisms involved in VSMC proliferation in GCA, we used both 2D-DIGE and pan genomic chips in order to compare VSMC isolated at the time of temporal artery biopsy (TAB) from patients with a final diagnosis of GCA or another diagnosis.

Results : In 15 patients with GCA, we identified lamin, vinculin and Annexin A5 as target antigens of anti-VSMC antibodies. Target antigens were linked with Grb2, an adaptator protein involved in VSMC proliferation. Normal VSMC originating from different vascular beds have differ in protein contents with differential expression of cytoskeleton and energy metabolism proteins. We compared VSMC from TAB with Ingenuity software and identified endothelin-1 (ET-1) and paxillin as proteins involved in vessel remodeling. We confirmed by immunohistichemistry and qPCR that ET-1 and its receptor ET_AR and ET_BR were expressed in temporal arteries from patients with GCA. Last, we reduced VSMC proliferation with Macitentan, an ET_AR and ET_BR antagonist and significantly inhibited VSMC proliferation with its active metabolite whereas other ET-1 inhibitors had no effect.

Conclusion : We identified anti-VSMC auto-antibodies in patients with GCA. Their pathogenic role remains to be determined. Normal VSMC from different vascular locations differ in protein content which might reflect different phenotypes and different properties. The escessive proliferation of VSMC from patients with GCA was inhibited by Macitentan. This drug might constitute a future therapeutic option.